

UNIVERSAL  
LIBRARY

**OU\_160720**

UNIVERSAL  
LIBRARY



**OSMANIA UNIVERSITY LIBRARY**

Call No. 548.8  
L76D  
Author Lipson, H.  
Title Determination of crystal structure  
by H. Lipson & W. Cochran. 1957  
This book should be returned on or before the date last marked below.









# THE CRYSTALLINE STATE

VOL. III

THE DETERMINATION  
OF CRYSTAL STRUCTURES



THE CRYSTALLINE STATE. VOL. III

Editor: SIR LAWRENCE BRAGG

---

THE DETERMINATION  
OF  
CRYSTAL STRUCTURES

By

H. LIPSON

D.SC., M.A., F.INST.P., F.R.S.

PROFESSOR OF PHYSICS

MANCHESTER COLLEGE OF SCIENCE AND TECHNOLOGY

and

W. COCHRAN

M.A., PH.D.

LECTURER IN PHYSICS IN THE UNIVERSITY OF CAMBRIDGE

LONDON

G. BELL AND SONS LTD

1957

COPYRIGHT © 1957 BY  
G. BELL AND SONS LTD

*First published 1953*  
*Second edition 1957*

PRINTED IN GREAT BRITAIN BY ROBERT MACLEHOSE AND CO. LTD  
THE UNIVERSITY PRESS, GLASGOW

## PREFACE

The scope of this book is quite simply defined; we have tried to cover the subject of crystal-structure determination from the stage at which a set of structure amplitudes has been obtained to the final accurate positioning of the atoms. Some of the steps—such as the calculation of structure factors and the summation of Fourier series—are routine ones, and are described first, but the last five chapters are concerned with the more difficult problems of the derivation of atomic positions, and in these chapters we have attempted to preserve some degree of logical order in the treatment. Nevertheless, we have emphasized throughout the book that each problem requires individual treatment, and that no single sequence of methods is likely to prove universally successful.

Two main classes of reader have been kept in mind—the beginner who has to find his way through the various procedures that he is expected to carry out, and the more advanced worker who wishes to have a résumé of the possible approaches to his own problem. To assist both these classes of reader, we have, throughout the book, adopted the principle of giving practical examples of the processes described; often these examples consist of a simple one designed to bring out the essential points and a more complicated one from an actual research project. In this way, we hope that we have preserved a sense of reality in the subjects treated.

It has been found necessary to give a considerable number of cross references in the book, and in order to make these as straightforward as possible, some departures from normal practice have been introduced. In addition to the decimal classification of sections, all figures, tables and equations bear the number of the page on which they appear, so that, for example, equation 10.3 is the third equation on page 10 and fig. 25 (ii) is the second figure on page 25 (figures appearing as half-tone illustrations on Plates bear the number of the page which the Plate faces). The author index and bibliography are combined, so that the page on which a particular reference occurs can easily be found. Finally, space groups are designated by their numbers in the 1952 International Tables together with their Hermann-Mauguin symbols. It is hoped that this will become standard practice.

We wish to acknowledge the help and advice we have received from many of our friends and colleagues. Professor Sir Lawrence Bragg, the editor of this series, has spent a great deal of effort and time in moulding the book into shape, and his patience and wisdom have left their mark on most of the contents. Professor Kathleen Lonsdale and Dr. Dorothy Hodgkin have also given us considerable advice, and Dr. C. A. Taylor has been extremely helpful in checking manuscripts and

proofs. Finally, we wish to record our gratitude to our first mentor in this most fascinating subject—Dr. C. A. Beevers.

The acknowledgments would not be complete without reference to the helpful co-operation of the publishers, and particularly of Mr. A. W. Ready, who discussed with us so patiently some of our more unorthodox ideas.

H.L.  
W.C.

June 1953

## ACKNOWLEDGEMENTS

The authors wish to acknowledge with thanks permission to reproduce diagrams from the following journals :

Acta Crystallographica (figs. 63, 98, 116, 123, 129i, 132, 137, 178, 179, 185i, 185ii, 190ii, 232, 236, 237, 269, 304, 305i, 305ii, 325).

Zeitschrift für Kristallographie (figs. 61, 66, 67, 68i, 68ii, 69, 126, 176ii).

Proceedings of the Royal Society (figs. 105, 176i, 196, 212, 215).

Nature (figs. 108, 109, 219, 242).

Journal of the Chemical Society (figs. 139, 182, 183, 209).

Comptes rendus (figs. 187, 188, 189).

Journal of the American Chemical Society (figs. 191, 192, 194i).

Philosophical Magazine (fig. 214).

Proceedings of the Physical Society (fig. 229).

British Journal of Applied Physics (fig. 230).

Journal of Chemical Physics (fig. 181).

Research (fig. 129ii).

Acknowledgement to the authors is made in the figure legends or in the nearby text.

Thanks are similarly due to the following publishers and authors :

Messrs. Macmillan & Co. Ltd. for permission to reproduce Fig. 8 from *The Interpretation of X-Ray Diffraction Photographs* by N. F. M. Henry, H. Lipson and W. A. Wooster, and figs. 118 and 119 from *Crystals and Practical Crystal Measurement* by A. E. H. Tutton.

The Oxford University Press for permission to reproduce figs. 71 and 114 from *Chemical Crystallography* by C. W. Bunn.

The Princeton University Press for permission to reproduce figs. 204 and 222 from *The X-Ray Crystallographic Investigation of the Structure of Penicillin* by D. Crowfoot, C. W. Bunn, B. W. Rogers-Low and A. Turner Jones.



# CONTENTS

CHAPTER	PAGE
1. X-RAY OPTICS . . . . .	1
2. DETERMINATION AND USE OF SPACE GROUPS . . . . .	21
3. CALCULATION OF STRUCTURE FACTORS . . . . .	54
4. SUMMATION OF FOURIER SERIES . . . . .	76
5. TRIAL-AND-ERROR METHODS . . . . .	110
6. THE USE OF THE PATTERSON FUNCTION . . . . .	150
7. FOURIER METHODS . . . . .	199
8. DIRECT METHODS . . . . .	246
9. THE ACCURACY OF A CRYSTAL-STRUCTURE DETERMINATION . . . . .	277
APPENDIX	
I. TABLES OF WAVE-LENGTHS IN ANGSTROM UNITS . . . . .	314
II. RADII OF THE ELEMENTS . . . . .	315
III. TRANSFORMATION OF AXES AND ATOMIC PARAMETERS . . . . .	316
IV. ARRANGEMENT OF SPACE-GROUP DATA IN THE INTERNATIONAL TABLES (1935) . . . . .	318
V. ARRANGEMENT OF SPACE-GROUP DATA IN THE INTERNATIONAL TABLES (1952) . . . . .	319
VI. STRUCTURE-FACTOR MACHINES AND DEVICES . . . . .	320
VII. $\cos 2\pi x$ AND $\sin 2\pi x$ . . . . .	323
VIII. FOURIER MACHINES . . . . .	325
IX. STANDARDIZATION OF CRYSTAL-STRUCTURE MODELS . . . . .	327
REFERENCES AND NAME INDEX . . . . .	329
INDEX OF SUBJECTS . . . . .	341



## CHAPTER 1

### X-RAY OPTICS

#### 1. INTRODUCTION

The principles used in the determination of crystal structures are essentially those of physical optics. The complexity of the various formulae that arise may tend to disguise this fact, but this complexity occurs only because interest has shifted from the study of objects of known structure, such as diffraction gratings, to that of objects of unknown structure, such as crystals. If we wished to know the structure of a diffraction grating in as much detail as we wish to know the structure of a crystal, most of the problems in crystal-structure determination would appear; the only complications missing would be those due to the three-dimensional nature of crystals.

The importance of a proper appreciation of these optical principles has been emphasized by the devotion of Volume II of this series to the subject; the fundamental equations of X-ray crystallography have been derived in this volume and definitions of all the important concepts have been given. In order that this present volume shall be complete in itself, it is proposed to give an outline of the theory in this chapter also, although for the more complete statement the reader is referred to Volume II.

Opportunity is also taken in the present volume to introduce some concepts that are not discussed in Volume II, but which are becoming of increasing importance. Chief amongst these is the Fourier transform,\* which, in addition to providing an elegant basis for the presentation of diffraction theory, is proving to be of great practical value in crystal-structure determination.

The general aim of this chapter is the derivation of the fundamental relationships between X-ray diffraction patterns and atomic arrangements. Several approaches are used. The first—the most common one—is based upon the lattice of a crystal, the dimensions of this lattice deciding completely the conditions necessary for the production of diffracted beams; these conditions can be expressed either as Bragg's law, or, more generally, in terms of the reciprocal lattice.

These concepts, however, give no information about the intensity scattered in any one diffracted beam, as this depends upon the atomic arrangement. The theory must be modified for two reasons: first, atoms have finite sizes and also, because of their heat motion, are displaced, at any one instant, from their mean positions in the crystal; and secondly, in practically all crystals the atomic centres do not lie

\* An Appendix on this subject is to be included in the next edition of Vol. II.

upon one set of lattice points. The former effect can be allowed for, leaving the latter as the particular interest of this book; the results are expressed as the structure-factor equation, which gives that factor in the expression for the intensity of a diffracted beam which depends upon the positions of the atomic centres.

The second approach is a modification of the first. A crystal is considered as a continuous distribution of electron density, reaching maxima at the atomic centres and falling off asymptotically to zero in the space between atoms. This distribution is triply periodic since it repeats in each unit cell, and we shall show that its Fourier components are the structure factors of the various orders of diffraction.

This approach has made possible the determination of structures with unit cells containing large numbers of atoms. It is not, however, self-sufficient because the structure factors cannot be observed experimentally; the phases of the scattered beams are involved, but knowledge of these phases is lost in the process of recording the intensities. To state the difficulty mathematically, we may regard each structure factor as a complex quantity of which we are able to observe only the amplitude. This quantity is called the structure amplitude.

The third approach makes use only of these structure amplitudes. If a Fourier series is summed with the squares of the structure amplitudes as coefficients, the function obtained is related in a simple way to the electron density. This function—the Patterson function—can therefore be used as an aid to structure determination, but unfortunately its relation to the electron density, while simple in principle, in practice becomes excessively complicated when the number of atoms in the unit cell is large; no complete success in interpreting the Patterson function of a crystal can therefore be guaranteed.

The final approach is radically different from the others; instead of considering first the periodicity of the crystal and then inserting real atoms, we consider the scattering by a group of atoms and introduce the periodicity by placing other groups of atoms periodically separated from the first. The function representing the amplitude and phase of the radiation scattered by a group of atoms in a particular direction is the Fourier Transform of the group. The addition of other periodically arranged groups of atoms causes the transform to be observed only at the points of the reciprocal lattice.

The value of this approach is that it allows use to be made of knowledge of relative atomic positions in a molecule, even if the positions of the atoms in the unit cell are unknown. The Fourier transform of the molecule can be evaluated, and the orientation of the molecule in the unit cell can, in principle, be determined by orienting the transform with respect to the reciprocal lattice until a fit with the observed structure amplitudes is obtained.

The chapter concludes with a discussion of the relation between X-ray and light diffraction. This is included in order to emphasize

the optical principles mentioned in the opening paragraph of this section; while these principles have been fully stated in the approaches already discussed, the optical approach may cause them to be more readily appreciated. In addition, it has played some part in suggesting new methods of determining crystal structures, and may well play a still larger part in the future.

## 2. DIFFRACTION BY A CRYSTAL

**2.1 X-ray diffraction by a lattice of electrons.** Crystals are composed of groups of atoms repeated at regular intervals, with the same orientation, in three dimensions. For certain purposes it is sufficient to regard each group of atoms as replaced by a representative point, and the collection of points so formed is the *space lattice* or *lattice* of the crystal (Volume I, p. 3). The word 'lattice' thus has a very definite meaning and should not be used in any other way; in particular, it should not be used to signify the complete atomic arrangement.

The lattice is important because it provides a basis for the theory of X-ray diffraction by the complete crystal: in the same way as the angles of diffraction produced by a diffraction grating depend only upon the spacing, so the angles of diffraction produced by a crystal depend only upon the dimensions of the lattice; the finer details of construction are not involved.

In order to invest the lattice with the power to diffract X-rays it is necessary to give it some material existence. We shall therefore assume that each lattice point is the site of an electron. Then the positions of the electrons can be specified by the ends of vectors  $\mathbf{r}$  such that

$$= u\mathbf{a} + v\mathbf{b} + w\mathbf{c} \quad (3)$$

where  $\mathbf{a}$ ,  $\mathbf{b}$  and  $\mathbf{c}$  are the primitive translations of the lattice (the *lattice constants* or *lattice parameters*) and  $u$ ,  $v$  and  $w$  are integers.

Consider a parallel beam of X-rays of wave-length  $\lambda$  falling on the lattice in a direction defined by the vector  $\mathbf{s}_0$ ; in Volume II  $\mathbf{s}_0$  is taken

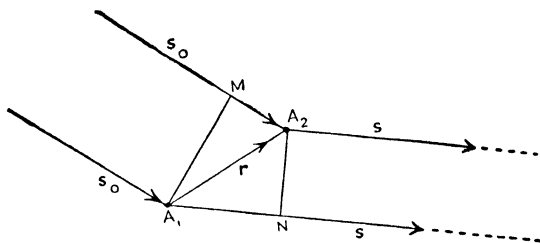


FIG. 3. Scattering from two lattice points

to be a unit vector, but some simplicity results if the magnitude of  $\mathbf{s}_0$  is taken as  $1/\lambda$ . The electrons are set into vibration and so act as sources of secondary radiation, and in order to find the total effect

of the combination of these secondary waves it is necessary to consider the phase differences between the waves scattered in any particular direction.

Suppose we choose a direction defined by the vector  $\mathbf{s}$  which also has modulus  $1/\lambda$ . Let  $A_1$  and  $A_2$  (fig. 3) be two lattice points separated by a vector distance  $\mathbf{r}$ ,  $A_1M$  and  $A_2N$  being lines drawn in an incident and diffracted wave front respectively. Then the path difference between the two scattered waves is

$$\begin{aligned} A_1N - A_2M &= \lambda(\mathbf{r} \cdot \mathbf{s} - \mathbf{r} \cdot \mathbf{s}_0) \\ &= \lambda \mathbf{r} \cdot \mathbf{S} \end{aligned} \quad (4.1)$$

where

$$\mathbf{S} = \mathbf{s} - \mathbf{s}_0.$$

In order that the waves scattered by  $A_1$  and  $A_2$  shall be in phase, this path difference should be equal to a whole number of waves, and thus  $\mathbf{r} \cdot \mathbf{S}$  must be equal to an integral number.

Thus

$$(u\mathbf{a} + v\mathbf{b} + w\mathbf{c}) \cdot \mathbf{S} = \text{integer}.$$

Since this equation must be true when  $u$ ,  $v$  and  $w$  change by integral values, it follows that each of the products separately must be integral; that is, since  $u$ ,  $v$  and  $w$  are already integral,

$$\left. \begin{aligned} \mathbf{a} \cdot \mathbf{S} &= h \\ \mathbf{b} \cdot \mathbf{S} &= k \\ \mathbf{c} \cdot \mathbf{S} &= l \end{aligned} \right\} \quad (4.2)$$

where  $h$ ,  $k$  and  $l$  are integers. These equations are known as Laue's equations.

When Laue's equations are simultaneously satisfied, a diffracted beam of maximum intensity will be produced. The numbers  $h$ ,  $k$  and  $l$  specify the 'order' of diffraction, in the same way that single numbers specify the orders of diffraction from a one-dimensional grating.

The mathematical form of Laue's equations made them unsuitable at first for the interpretation of experimental results, and it was not until W. L. Bragg (1913) placed them on a physical basis that it was possible to make use of them, both to interpret X-ray spectra and to determine the structure of crystals.

**2.2 Bragg's Law.** Essentially, Bragg's contribution was to identify the integers  $h$ ,  $k$  and  $l$  with the Miller indices (Volume I, p. 7) of the lattice planes. He was then able to reduce the problem to a one-dimensional one, and the method of attack so derived proved to be extremely fruitful. Its importance cannot be over-estimated, but as more difficult problems of crystal-structure determination have arisen, methods have had to become more general, and it is probably true to say that we are now back in the stage of direct use of Laue's equations. But whether this stage would have been reached had it not been for Bragg's equation is doubtful.

The connexion between Bragg's law and Laue's equations is brought out by rewriting the latter in the following form:

$$\frac{\mathbf{a}}{h} \cdot \mathbf{S} = 1,$$

$$\frac{\mathbf{b}}{k} \cdot \mathbf{S} = 1,$$

$$\frac{\mathbf{c}}{l} \cdot \mathbf{S} = 1.$$

Subtraction of the first two equations gives

$$\left( \frac{\mathbf{a}}{h} - \frac{\mathbf{b}}{k} \right) \cdot \mathbf{S} = 0,$$

which means that the vector  $\mathbf{S}$  is perpendicular to the vector  $\mathbf{a}/h - \mathbf{b}/k$ . From fig. 5 (a) it can be seen that the latter is in the plane of Miller

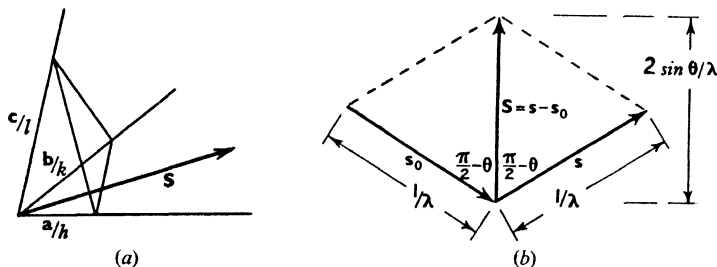


FIG. 5. (a) Relationship between the vector  $\mathbf{S}$  and the plane  $(hkl)$ .  
(b) Relationship between the vectors  $\mathbf{s}_0$ ,  $\mathbf{s}$ , and  $\mathbf{S}$

indices  $hkl$ . Similarly, it can be shown that  $\mathbf{S}$  is perpendicular to the vector  $\mathbf{a}/h - \mathbf{c}/l$ , which is also a vector in the plane  $hkl$ . Thus  $\mathbf{S}$  is perpendicular to this plane. But  $\mathbf{S}$  is a vector in the direction of the bisector of the incident and diffracted beam, since the moduli of  $\mathbf{s}$  and  $\mathbf{s}_0$  are equal (fig. 5 (b)); thus this bisector is identified with the normal to the  $hkl$  plane—the first step in the proof of Bragg's law and the justification for the concept of each diffraction as a 'reflexion' of the rays from lattice planes.

To make the law quantitative we have to introduce the spacing  $d$  of the planes  $hkl$ ; this is the perpendicular distance of the plane from the origin (fig. 5 (a)) and is the projection of  $\mathbf{a}/h$ ,  $\mathbf{b}/k$  or  $\mathbf{c}/l$  on the vector  $\mathbf{S}$ ; that is

$$d = \frac{\frac{\mathbf{a}}{h} \cdot \mathbf{S}}{|\mathbf{S}|}.$$

But  $\frac{\mathbf{a}}{h} \cdot \mathbf{S} = 1$  (equ. 4.2) and  $|\mathbf{S}| = \frac{2 \sin \theta}{\lambda}$  (fig. 5 (b)).

$$\begin{array}{ll} \text{Thus} & d = \lambda/2 \sin \theta \\ \text{or} & \lambda = 2d \sin \theta. \end{array} \quad (6)$$

The quantity  $n$  that usually appears in Bragg's equation is now absorbed in the integers  $hkl$ . Indices of diffraction, unlike Miller indices of planes, can have a common factor; if  $n$  is this common factor the spacing corresponding to indices  $nh, nk, nl$  is regarded as  $1/n$ th of the spacing corresponding to indices  $hkl$ .

If it is thought that this proof of Bragg's law is rather tortuous it must be pointed out that the present chapter is not directed towards this proof but towards the formulae that are to be used in later chapters. Moreover, many of the so-called proofs of Bragg's law are deceptively simple and lack the completeness of the proof given by Bragg himself (Volume I, p. 13).

**2.3. Reciprocal lattice.** Bragg's equation may be regarded as the result of a physical method of solving Laue's equations. Mathematical methods lead to a different form of solution, and this is most neatly expressed by the *reciprocal lattice*. These methods are directed towards finding values of  $S$  that are solutions of the equations.

The first equation is equivalent to the statement that the projection of  $S$  on  $\mathbf{a}$  is constant for a fixed value of  $h$ ; that is, the ends of the vectors  $S$  lie on a plane perpendicular to  $\mathbf{a}$ . If  $h$  is zero, the plane passes through the origin; if  $h$  is unity, the plane makes a certain intercept on  $\mathbf{a}$ ; if  $h=2$ , it makes double the intercept; and so on. In other words, a set of planes of constant spacing is set up, each plane of the set corresponding to a particular value of  $h$ . In a similar way a set of equidistant planes perpendicular to  $\mathbf{b}$  will be set up, each plane corresponding to a particular value of  $k$ ; and a further set of planes perpendicular to  $\mathbf{c}$  will correspond to different values of  $l$ . The intersections of these planes represent the end points of vectors that satisfy the three Laue equations simultaneously, and so give the required solutions. These sets of planes define a lattice of points—the reciprocal lattice. The unit cell of this lattice is defined by three vectors, which are usually called  $\mathbf{a}^*$ ,  $\mathbf{b}^*$  and  $\mathbf{c}^*$ , and each point in the lattice is defined by the three numbers  $h, k$  and  $l$ .

To find the reciprocal-lattice vectors, we make use of the fact that each is formed by the intersection of two planes perpendicular to two axes, and thus that  $\mathbf{a}^*$ , for example, is perpendicular to  $\mathbf{b}$  and  $\mathbf{c}$ . Thus  $\mathbf{a}^*$  must be representable as  $p(\mathbf{b} \times \mathbf{c})$ , where  $p$  is a constant to be determined. We thus have the three equations

$$\mathbf{a}^* = p(\mathbf{b} \times \mathbf{c}),$$

$$\mathbf{b}^* = q(\mathbf{c} \times \mathbf{a}),$$

$$\mathbf{c}^* = r(\mathbf{a} \times \mathbf{b}),$$

where  $p, q$  and  $r$  are constants.



$$\begin{aligned}\text{Then} \quad \mathbf{S} &= h\mathbf{a}^* + k\mathbf{b}^* + l\mathbf{c}^* \\ &= hp(\mathbf{b} \times \mathbf{c}) + kq(\mathbf{c} \times \mathbf{a}) + lr(\mathbf{a} \times \mathbf{b}).\end{aligned}$$

$$\begin{aligned}\text{But} \quad h &= \mathbf{a} \cdot \mathbf{S} \\ &= \mathbf{a} \cdot \{hp(\mathbf{b} \times \mathbf{c}) + kq(\mathbf{c} \times \mathbf{a}) + lr(\mathbf{a} \times \mathbf{b})\} \\ &= h\mathbf{pa} \cdot \mathbf{b} \times \mathbf{c}\end{aligned}$$

since  $\mathbf{a} \cdot \mathbf{c} \times \mathbf{a}$  and  $\mathbf{a} \cdot \mathbf{a} \times \mathbf{b} = 0$ .

$$\text{Therefore} \quad l = \mathbf{pa} \cdot \mathbf{b} \times \mathbf{c}$$

$$\begin{aligned}\text{or} \quad p &= \frac{1}{\mathbf{a} \cdot \mathbf{b} \times \mathbf{c}} \\ \text{Similarly} \quad q &= \frac{1}{\mathbf{b} \cdot \mathbf{c} \times \mathbf{a}} \\ \text{and} \quad r &= \frac{1}{\mathbf{c} \cdot \mathbf{a} \times \mathbf{b}}.\end{aligned} \quad \left. \vphantom{\begin{aligned} p \\ q \\ r \end{aligned}} \right\} (7.1)$$

It will be noted that  $p$ ,  $q$  and  $r$  are all equal since  $\mathbf{a} \cdot \mathbf{b} \times \mathbf{c}$ ,  $\mathbf{b} \cdot \mathbf{c} \times \mathbf{a}$  and  $\mathbf{c} \cdot \mathbf{a} \times \mathbf{b}$  are all representations of the volume  $V$  of the unit cell of the space lattice.

$$\begin{aligned}\text{Thus} \quad p &= q = r = 1/V, \\ \text{and}\end{aligned}$$

$$\begin{aligned}\mathbf{a}^* &= \mathbf{b} \times \mathbf{c}/V, \\ \mathbf{b}^* &= \mathbf{c} \times \mathbf{a}/V, \\ \mathbf{c}^* &= \mathbf{a} \times \mathbf{b}/V.\end{aligned} \quad \left. \vphantom{\begin{aligned} \mathbf{a}^* \\ \mathbf{b}^* \\ \mathbf{c}^* \end{aligned}} \right\} (7.2)$$

These are the simplest expressions for the reciprocal-lattice vectors, but for purposes of computation they have to be expressed in terms of  $\mathbf{a}$ ,  $\mathbf{b}$  and  $\mathbf{c}$  and the interaxial angles  $\alpha$ ,  $\beta$  and  $\gamma$ ; the required expressions can be found in the International Tables (1952). For some purposes, particularly when it is necessary to make use of the reciprocal lattice in the interpretation of X-ray photographs, it is usual to define the reciprocal-lattice vectors as, for example,  $\mathbf{a}^* = \lambda \mathbf{b} \times \mathbf{c}/V$ . It will be noted that this replacement does not affect the relative values of  $\mathbf{a}^*$ ,  $\mathbf{b}^*$  and  $\mathbf{c}^*$ , and produces quantities that are characteristic both of the crystal and of the process of diffraction.

The reciprocal lattice is important in almost all branches of X-ray diffraction; its use in the interpretation of X-ray photographs is particularly valuable. In this book its particular importance lies in the part it plays in the optics of X-ray diffraction, as described in section 1.4.2. In this connexion the space between the reciprocal-lattice points becomes as important as the points themselves. It is customary to call the space in which the reciprocal lattice is plotted 'reciprocal space', and it may either be dimensionless, if  $\lambda$  is introduced into the expressions for the reciprocal-lattice constants, or of dimensions  $\text{length}^{-1}$  if  $\lambda$  is not introduced.

**2.4. Atomic scattering factor.** In section 1.2.1 the scattering units were assumed to be electrons in order that their linear dimensions could be neglected in comparison with the space-lattice dimensions, and, incidentally, in comparison with the wave-length of the X-rays; under these conditions the scattering by a single electron is independent of angle apart from any effects of polarization of the radiation. In atoms, however, the electrons occupy a finite volume and the phase differences between rays scattered from different points in this volume have to be taken into account.

For small angles of diffraction these phase differences are small and therefore the amplitude of scattering by an atom can be taken as the sum of the amplitudes of the scattering by its individual electrons. If, therefore, the electrons at the lattice points are replaced by an atom of atomic number  $Z$ , then the expression for the amplitude of the scattered beam must be multiplied by  $Z$ . As the angle of diffraction increases, however, the phase differences become larger, and thus the scattered beam becomes weaker; that is, the factor becomes less than  $Z$ . The factor is called the *atomic scattering factor*,  $f$ , and if the atom is assumed to have spherical symmetry the atomic scattering factor is constant for a given angle of diffraction. The curve of scattering factor against  $(\sin \theta)/\lambda$  is called the *scattering-factor curve* or  *$f$  curve* (fig. 8). The calculation of these curves for the different atoms is described in Volume II, Chapter III.

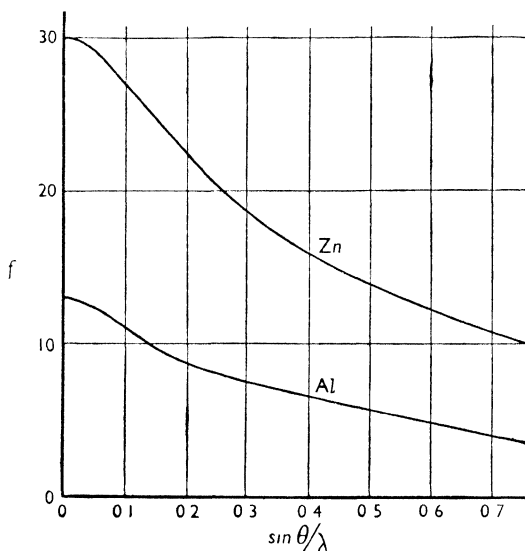


FIG. 8. Typical curves of atomic scattering factor

**2.5 Temperature factor.** The electron densities in atoms are independent of temperature for all ordinary temperatures, provided that there is no change in the state of ionisation; it might therefore be supposed that temperature should have no effect on the intensities of X-ray reflexions. This would be so if the atoms were scattering independently, as in a gas; but in a crystal the atoms are not scattering independently and it is necessary to see how this fact affects the total scattering.

At all temperatures, including absolute zero, atoms have a finite amplitude of oscillation. The frequency of this oscillation (about  $10^{13}$  per second) is so much smaller than the frequency of X-rays (about  $10^{18}$  per second) that, to a train of X-ray waves, the atoms would appear to be stationary, but displaced from their true positions in the lattice. Thus, in producing a given X-ray reflexion, atoms in neighbouring unit cells, which should scatter in phase, will scatter slightly out of phase, the total effect being apparently to reduce the scattering factor of the atom by an amount which increases with angle. If the displacements of neighbouring atoms are not disconnected, unusual diffraction effects are produced; these are the so-called 'diffuse reflexions'. But if the displacements are considered to be entirely random, the form of the variation of scattering factor with angle can be worked out with certain assumptions about the nature of the atomic vibrations. The result is that, if the atomic scattering factor discussed in the previous section is called  $f_0$ , the factor  $f$  to be used in practice is  $f_0 \exp(-B \sin^2 \theta / \lambda^2)$  where  $\theta$  is the Bragg angle and  $B$  is a constant.

This constant is related to the mean square displacement  $\bar{u}^2$  of the atoms from their mean positions; the relationship is (Volume II, p. 193)

$$B = 8\pi^2 \bar{u}^2.$$

This equation is not, however, particularly helpful because the evaluation of  $\bar{u}^2$  from the measurable physical properties of a crystal is not easy; in Volume II (p. 219) an expression involving the characteristic temperature is given. Even this applies only to simple structures, and, in general,  $B$  is different for the different atoms in a structure, and also varies with direction. Such effects have usually to be ignored, and  $B$  treated as an empirical constant derivable from measurements of the intensities of the X-ray reflexions from a crystal.

**2.6. Diffraction by a crystal with atoms in general positions.** We have now arrived at a stage at which the theory is physically significant; the crystal is one in which atoms of finite size are located with their mean positions at lattice points. Some crystals actually have this simple structure. But most crystals are much more complicated; they can be represented only by placing within each unit cell of the lattice a certain arrangement of atoms. We may still regard any one set of corresponding atoms in the different unit cells as lying upon a

lattice, and thus a crystal with  $N$  atoms in the unit cell can be regarded as based upon  $N$  identical interpenetrating lattices. The equations already deduced are still obeyed by each separate lattice of atoms, and therefore by the complete crystal; but the rays scattered by the different lattices will differ in phase according to their separations. Thus, if there is a large number of atoms in the unit cell, complicated relationships may be expected between the intensities of the various orders of diffraction.

Suppose that the unit cell of a crystal contains  $N$  atoms, situated at points  $x_n, y_n, z_n$ . These quantities are best considered as co-ordinates with respect to the axes of the lattice, their magnitudes being equal to fractions of the lattice dimensions (fig. 10). (If the co-ordinates are

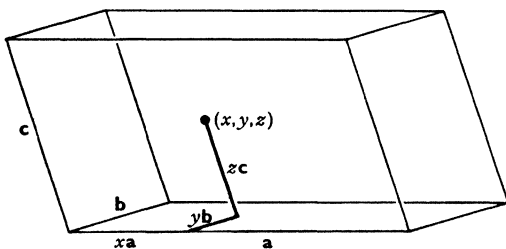


FIG. 10. Structural parameters  $x, y, z$

taken as actual distances, as is sometimes preferable, quantities such as  $x/a$  appear in the formulae and result in rather cumbersome expressions.) The position of the  $n$ th atom in the unit cell can thus be represented by the vector  $\mathbf{r}_n$ , where

$$\mathbf{r}_n = x_n \mathbf{a} + y_n \mathbf{b} + z_n \mathbf{c}. \quad (10.1)$$

The path difference between the waves scattered by these atoms and those that would be scattered by a set of atoms at the points of the lattice that define the origins of the unit cells is, by analogy with equation 4.1,  $\lambda \mathbf{r}_n \cdot \mathbf{S}$ . Thus the expression for the complete wave scattered by the  $n$ th lattice contains a term  $f_n \exp \frac{2\pi i}{\lambda} \lambda \mathbf{r}_n \cdot \mathbf{S}$ , or  $f_n \exp 2\pi i \mathbf{r}_n \cdot \mathbf{S}$ , where  $f_n$  is the scattering factor of the  $n$ th atom. Thus the expression for the complete wave scattered by the crystal would contain a term

$$F = \sum_{n=1}^N f_n \exp 2\pi i \mathbf{r}_n \cdot \mathbf{S}. \quad (10.2)$$

Substituting the value of  $\mathbf{r}_n$  from equation 10.1, we have

$$\begin{aligned} F &= \sum_{n=1}^N f_n \exp 2\pi i (x_n \mathbf{a} \cdot \mathbf{S} + y_n \mathbf{b} \cdot \mathbf{S} + z_n \mathbf{c} \cdot \mathbf{S}) \\ &= \sum_{n=1}^N f_n \exp 2\pi i (hx_n + ky_n + lz_n) \end{aligned} \quad (10.3)$$

(from Laue's equations 4.2). This is the most important expression in crystal-structure determination. The quantity  $F$  is a function of  $h, k$  and  $l$ , and is called the *Structure Factor*; its modulus is called the *Structure Amplitude* and is defined as the ratio of the amplitude of the radiation scattered in the order  $h, k, l$  by the contents of one unit cell to that scattered by a single electron under the same conditions (Lonsdale, 1936). It will thus be seen that  $|F|$  is a pure number—a number of electrons.\*

The complex form of the expression for the structure factor merely means that the phase of the scattered wave is not simply related to that of the incident wave. The phase, however, is not an observable quantity, the only observable quantity being the intensity, which is proportional to  $|F|^2$ . Then, if  $F$  be put equal to  $A' + iB'$ ,

$$\left. \begin{aligned} A' &= \sum_n f_n \cos 2\pi(hx_n + ky_n + lz_n) \\ B' &= \sum_n f_n \sin 2\pi(hx_n + ky_n + lz_n) \end{aligned} \right\} \quad (11.1)$$

and

$$F^2 = A'^2 + B'^2.$$

These are the equations that have to be used in practice. They will be discussed in more detail in Chapter III.

A more fundamental interpretation of the structure-factor equation is possible, for the reduction of a structure to a set of point atoms with variable scattering factors is essentially artificial. This reduction is avoided by considering each element of volume of the unit cell separately. Thus if  $\rho(x, y, z)$  is the electron density at the point  $(x, y, z)$ , the amount of scattering matter in the volume element  $Vdxdydz$  is  $\rho Vdxdydz$ , and the structure-factor equation is

$$F(hkl) = \int_{x=0}^1 \int_{y=0}^1 \int_{z=0}^1 V\rho(x, y, z) \exp 2\pi i(hx + ky + lz) dxdydz \quad (11.2)$$

Although this equation is not used for calculating structure factors, it is necessary in the development of the theory which follows in the succeeding sections.

### 3. APPLICATIONS OF FOURIER SERIES

**3.1. Representation of a crystal by a Fourier series.** Since a crystal is periodic in three dimensions, it can be represented by a three-dimensional Fourier series. This concept is most simply expressed by allotting to each Fourier coefficient  $C$  three integral indices  $h', k'$  and  $l'$ , these symbols being chosen because they have a simple relation to the indices  $h, k, l$  of the X-ray reflexions. Thus we have

$$\rho(x, y, z) = \sum_{h'} \sum_{k'} \sum_{l'=-\infty}^{\infty} C(h', k', l') \exp 2\pi i(h'x + k'y + l'z).$$

\* It will be noted that the use of the expression 'Structure Amplitude' is the same as that in Volume I (p. 96) but not the same as that in Volume II (p. 28).

This value for the electron density can be inserted in equation 11.2, and thus

$$F(hkl) = \int_0^1 \int_0^1 \int_0^1 \sum_{h'} \sum_{k'} \sum_{l'} C(h', k', l') \exp 2\pi i(h'x + k'y + l'z) \exp 2\pi i(hx + ky + lz) V dx dy dz. \quad (12.1)$$

The exponential functions are both periodic and the integral of their product over a single complete period is zero in general; only if  $h = -h'$ ,  $k = -k'$ ,  $l = -l'$  is it not zero, since the periodicity disappears. Under these conditions

$$F(hkl) = \int_0^1 \int_0^1 \int_0^1 C(h'k'l') V dx dy dz.$$

(The summations disappear since there is only one term to consider.)

$$\text{Therefore} \quad F(hkl) = C(\bar{h}\bar{k}\bar{l})V. \quad (12.2)$$

In other words, the Fourier coefficients  $C$  are directly related to the corresponding structure factors, and

$$\rho(x, y, z) = \frac{1}{V} \sum_h \sum_k \sum_{l=-\infty}^{\infty} F(hkl) \exp \{ -2\pi i(hx + ky + lz) \}. \quad (12.3)$$

It may seem from this that the process of determining crystal structures is entirely straightforward: from experimental observation of intensities the values of the structure amplitudes are deduced; the Fourier coefficients are calculated; the series is summed; and the result is a representation of the crystal structure. It should not even be necessary to have absolute values of the structure amplitudes; relative values should give a recognizable representation.

That this is not possible appears when we consider the nature of the structure factor; as we have seen in section 1.2.6, the structure factor is complex, and from the intensity we can derive only the modulus. But equations 12.2 and 12.3 are absolute;  $C$  and  $F$  are related in phase as well as in magnitude and so, in general, the process of crystal-structure determination cannot be carried out by direct means. If it could be, it would not be necessary to write the rest of this book, since it is entirely concerned with methods of overcoming the particular difficulty of lack of knowledge of the relative phases of the diffracted beams.

**3.2 Patterson's Fourier series.** An attempt to evade the difficulty mentioned in the last section was made by Patterson (1935a). Instead of the structure factors, he used the squares of the moduli as Fourier coefficients; these quantities are directly related to the observed intensities and so they can always be measured. He showed that the resulting synthesis was related in a simple way to the crystal structure, and could give direct evidence about atomic positions with no pre-

liminary assumptions. It can rarely be used to work out complete structures, but in some projects it has played a major role in producing the final solution.

Patterson defines a function  $P(u, v, w)$  such that

$$P(u, v, w) = V \int_0^1 \int_0^1 \int_0^1 \rho(x, y, z) \rho(x+u, y+v, z+w) dx dy dz. \quad (13.1)$$

If we substitute in this expression the values for the electron densities given by equation 12.3 we arrive at the equation

$$P(u, v, w) = \frac{1}{V} \int_0^1 \int_0^1 \int_0^1 \sum_h \sum_k \sum_l \sum_{h'} \sum_{k'} \sum_{l'} \sum_{-\infty}^{\infty} F(hkl) \exp \{ -2\pi i(hx + ky + lz) \} \\ \times F(h'k'l') \exp \{ -2\pi i(h'x + k'y + l'z) \} \exp \{ -2\pi i(h'u + k'v + l'w) \} dx dy dz.$$

For the reasons that apply to equation 12.1, the right-hand side is zero unless  $h = -h'$ ,  $k = -k'$ ,  $l = -l'$ ; when this condition applies,

$$P(u, v, w) = \frac{1}{V} \sum_h \sum_k \sum_{l=-\infty}^{\infty} F(hkl) F(\bar{h}\bar{k}\bar{l}) \exp \{ -2\pi i(h'u + k'v + l'w) \}.$$

From equation 10.3 we note that  $F(hkl)$  and  $F(\bar{h}\bar{k}\bar{l})$  are complex conjugates and so

$$P(u, v, w) = \frac{1}{V} \sum_h \sum_k \sum_{l=-\infty}^{\infty} |F(hkl)|^2 \exp 2\pi i(hu + kv + lw). \quad (13.2)$$

As stated above, the quantities  $|F|^2$ —the squares of the structure amplitudes—are directly derivable from the X-ray intensities, and so the series can be summed without ambiguity. What, then, is the physical significance of the summation?

Suppose that fig. 13 represents a crystal structure projected on to a plane, the electron density being finite within the circles and zero elsewhere. From any point  $(x, y)$  in the unit cell draw a vector with components  $u$  and  $v$ . In general, it is probable that the electron density is zero at each end of the line, and so the product will be zero. Even if we choose one end to lie within a circle, it is probable that the other end will not, and so the product will still be zero; thus it might be expected that there should be a high probability that the total summation for all points  $(x, y)$  will be zero.

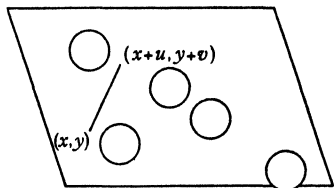


FIG. 13. Basis of theory of the Patterson synthesis

Under what conditions will the product not be zero? Obviously, when we deliberately choose  $u$  and  $v$  to be such that they represent the components of a vector whose ends lie within circles; in other

words, the Patterson summation will be finite only for values of  $u$  and  $v$  that represent vectors joining two atoms. This is the importance of the Patterson series: it gives information about interatomic distances, but not about atomic positions.

It is improbable that a given vector, whatever its position in the unit cell, always has one end or the other at a point of zero electron density, and thus the Patterson summation rarely has zero value for a reasonably complicated crystal. This can be seen more clearly by regarding the Patterson summation, for given values of  $u$  and  $v$ , as the product of the structure with its counterpart displaced by components  $u$  and  $v$ . This process is illustrated, for the same structure and vector displacement as in fig. 13; the regions where positive electron densities overlap are indicated. It can readily be visualized that, even for a structure as simple as this, it would be difficult to find values of  $u$  and  $v$  for which there was no overlapping at all.

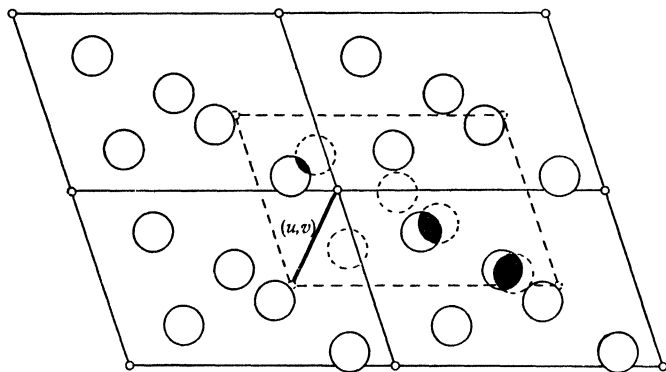


FIG. 14. Alternative explanation of Patterson function. One unit cell (broken lines) is superimposed on four displaced unit cells (full lines); the extent of overlap is shown by the black regions

In principle (Wrinch, 1939), atomic positions are derivable from complete knowledge of interatomic vectors. Theory, however, requires that the knowledge be presented in the form of distances between point atoms, whereas, in practice, one obtains only the information with respect to atoms of finite size. In other words, Patterson syntheses consist of collections of more-or-less broad and unresolved peaks, and no general method of deducing atomic positions has yet been put forward that will work in any but the simplest crystals. Nevertheless, the Patterson method has been extensively used to give information that could not be obtained in any other way, and its various uses will be described in Chapter 6.

That the quantity  $P(u, v, w)$  is real for all values of  $u, v, w$  can be shown by collecting together the coefficients in pairs,  $hkl$  and  $\bar{h}\bar{k}\bar{l}$ .



Then

$$\begin{aligned} P(u, v, w) &= \frac{1}{2V} \sum \sum \sum_{-\infty}^{\infty} |F(hkl)|^2 \exp \{ -2\pi i(hu + kv + lw) \} \\ &\quad + |F(\bar{h}\bar{k}\bar{l})|^2 \exp \{ 2\pi i(hu + kv + lw) \} \\ &= \frac{1}{2V} \sum \sum \sum_{-\infty}^{\infty} |F(hkl)|^2 [\exp \{ -2\pi i(hu + kv + lw) \} \\ &\quad + \exp \{ 2\pi i(hu + kv + lw) \}] \end{aligned}$$

since  $|F(\bar{h}\bar{k}\bar{l})| = |F(hkl)|$ .

$$\text{Thus} \quad P(u, v, w) = \frac{1}{V} \sum \sum \sum_{-\infty}^{\infty} |F(hkl)|^2 \cos 2\pi(hu + kv + lw) \quad (15)$$

which is real for all values of  $u, v$  and  $w$ .

Equation 15 gives the form in which the Patterson summation is usually expressed.

**3.3. Fourier transforms.** There is another method of treating the problem of diffraction by a crystal: instead of starting with the lattice and then introducing atoms into the unit cell, we may consider the unit-cell contents first and then see how the diffraction pattern is affected by the juxtaposition of other unit cells in regular array. For simplicity we may still refer the positions of the atoms to the crystallographic axes, although obviously these axes have no particular significance when we are dealing with a non-periodic object.

The atoms in the unit cell are represented by co-ordinates  $(x_n, y_n, z_n)$  and by scattering factors  $f_n$ . The equation (10.2)

$$F = \sum_{n=1}^N f_n \exp 2\pi i \mathbf{r}_n \cdot \mathbf{S}$$

still applies, but now it represents the complete scattering from the set of atoms. The vector  $\mathbf{S}$  may assume any value, not merely the discrete values given by Laue's equations (4.2); in other words,  $F$  can be evaluated at any point in reciprocal space. The function  $F$  is called the Fourier transform of the set of atoms, and it is worth while giving it a separate symbol; following Wrinch (1946), we shall call it  $G$ . The structure factors are the values, at the reciprocal-lattice points, of the Fourier transform of one unit cell.

The effect of placing two units at a distance apart of  $\mathbf{a}$  is to multiply the Fourier transform by a set of sinusoidal fringes of separation  $\mathbf{a}^{-1}$ .<sup>\*</sup> If a large number of units is placed regularly in line, then the fringes become extremely sharp, so that in effect the Fourier transform is observed only in planes given by  $\mathbf{S} \cdot \mathbf{a} = h$ , where  $h$  is an integer; this is the first Laue equation. The placing of the units in three-dimensional array causes the Fourier transform to be observed only in the intersections of the three sets of planes corresponding to the three Laue conditions. These intersections form the reciprocal lattice. We see

<sup>\*</sup>  $\mathbf{a}^{-1}$  is a vector in the same direction as  $\mathbf{a}$  and with modulus  $1/|\mathbf{a}|$ .

then that the reciprocal lattice, with weights attached to each point proportional to the structure factor, is a complete representation of the diffraction pattern of the crystal.

The simplest illustration of this idea is given by considering a crystal with only one atom per unit cell. The structure amplitude of any reflexion is then equal to the scattering factor of the atom at the corresponding angle, and hence it follows that the  $f$ -curve of an atom, regarded as spherically distributed in reciprocal space, is the Fourier transform of that atom.

For purposes of calculation, the Fourier transform of a set of atoms may be expressed as

$$G = \sum f_n \exp \{2\pi i(hx_n + ky_n + lz_n)\}$$

where  $h$ ,  $k$  and  $l$  may have non-integral values. The details of the contents of the unit cell are contained in the Fourier transform, and we have seen that the process of stacking these unit cells in orderly array allows us to measure the amplitude of the Fourier transform at discrete points only; this is a considerable loss, for if we could observe the whole of the transform the work of the determination of crystal structures would be considerably simplified. On the other hand, if we had one unit only, the diffraction pattern would be too weak to be observed, and if we had a number in irregular array, unless the units were all parallel, the diffraction pattern would be almost a hopeless jumble. We have therefore to be satisfied that the crystalline regularity leads to certain advantages, and to counteract the disadvantages as best we may.

#### 4. COMPARISON OF X-RAY AND LIGHT DIFFRACTION

**4.1. Introduction.** The mathematical sections of this chapter are necessary in order to establish the formulae that are required in practice. Nevertheless, it is not intended to imply that a knowledge of the derivation of these formulae is a sufficient basis for one who is embarking upon the determination of crystal structures; X-ray diffraction is a physical phenomenon and an understanding of the underlying physical principles is of value in following some of the more recent developments in the subject (Preston, 1944).

The simplest way of appreciating these principles is to compare them with the known effects of light diffraction. It is, of course, not possible to produce a three-dimensional grating, but most of the general principles discussed in the preceding sections can be illustrated by effects that occur with one-dimensional and two-dimensional gratings.

**4.2. Theory of the diffraction grating.** The general equation for the diffraction grating is

$$n\lambda = d(\sin \phi + \sin \theta_n)$$



# PLATE I

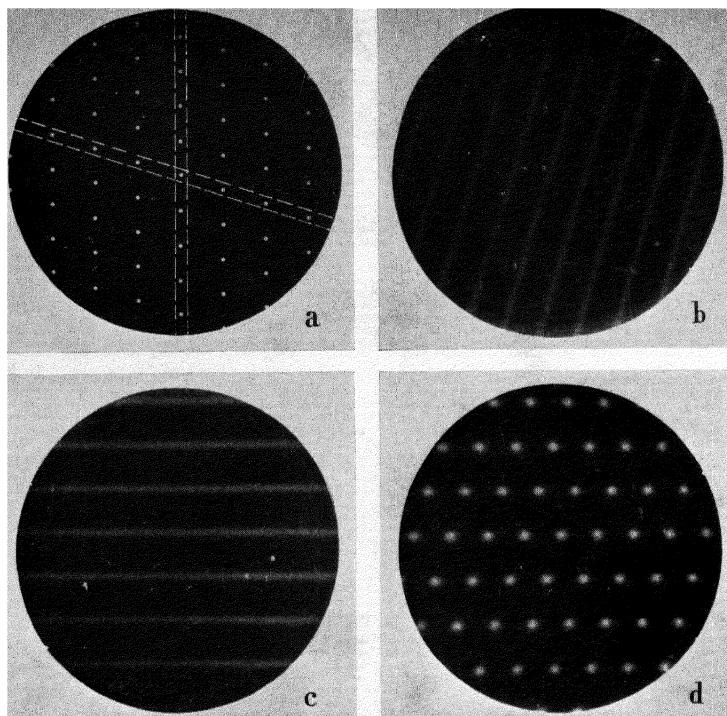


FIG. 17 (i)

- (a) Two-dimensional array of holes, showing two basic linear elements between broken lines
- (b) Fringes formed by one element, corresponding to first Laue equation
- (c) Fringes formed by second element, corresponding to second Laue equation
- (d) Diffraction pattern of (a), showing maxima only where fringes in (b) and (c) intersect

where  $\phi$  is the angle of incidence and  $\theta_n$  is the angle of diffraction. For normal incidence,  $\phi = 0$ , but if the grating is used in the position for minimum deviation of the  $n$ th order,  $\phi = \theta_n$  and the equation reduces to

$$n\lambda = 2d \sin \theta_n.$$

This is analogous to Bragg's equation (6).

For a one-dimensional diffraction grating, the order of diffraction is specified by a single number  $n$ , whereas for a two-dimensional grating two numbers are required. Such a grating can be made by first drilling a line of holes; this will behave as a diffraction grating producing orders of diffraction whose separation is inversely proportional to the spacing of the holes, as shown in Fig. 17 (i) (b). The two-dimensional grating may now be made by drilling similar sets of holes at equal distances apart; considering each set of holes as an element of a diffraction grating, we see that orders of diffraction are again formed perpendicular to the line of separation Fig. 17 (i) (c). Orders of diffraction from the two-dimensional grating are observed only where the two sets of orders intersect, and so we have a lattice of diffraction spots produced. This lattice of spots is analogous to the reciprocal lattice (section 1.2.3).

If a grating is badly ruled various optical effects are produced, depending on the nature of the imperfection. If the error in the position of any one line is independent of the positions of neighbouring lines, the effect is, to a first approximation, equivalent to the effect of temperature on a crystal (section 1.2.5); the grating can be considered as composed of broadened elements, and the orders of diffraction, particularly the higher ones, are reduced in intensity. If the displacements of the elements of the grating are not independent, then further diffraction effects occur that give rise to 'diffuse reflexions' (Vol. II, Chapter V).

The reason for the reduction in intensity can be seen by considering a diffraction grating of which the elements are narrow slits. As shown in textbooks on physical optics (e.g. Jenkins and White 1950, p. 327),

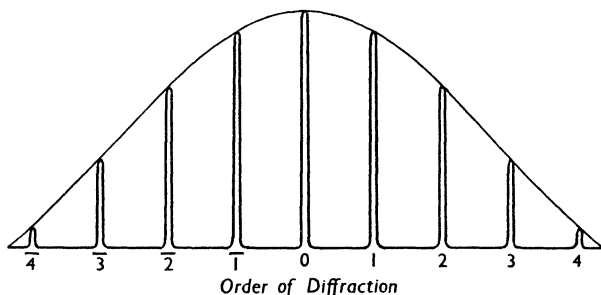


FIG. 17 (ii). Amplitudes of orders of diffraction from grating of fine slits

the amplitude of a particular order of diffraction is governed by the amplitude diffracted in the same direction by the single element; the envelope of the ordinates representing the amplitude of the orders of diffraction is the curve representing the diffraction pattern of the single element. This curve is shown in fig. 17 (ii). If the spacing is large compared with the width of the slit, all the orders of diffraction are largely confined to a region near to the central maximum; otherwise they will be spaced farther out (fig. 18), and so will be reduced in intensity.

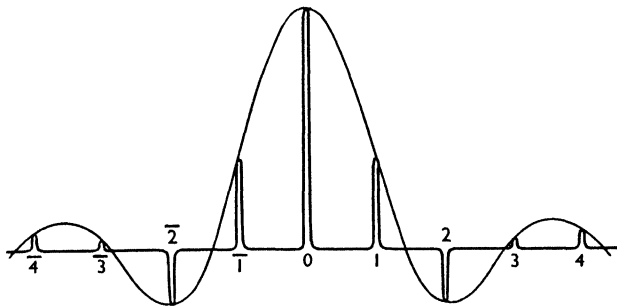


FIG. 18. Amplitudes of orders of diffraction from grating of coarse slits

This effect corresponds to the decrease in intensity due to the finite sizes of atoms (section 1.2.4), and it will be noted that the central part of the curve in fig. 18 is similar in general outline to the curve in fig. 8; the lack of sharp outline of an atom, however, removes the negative regions shown in the former figure, but it will be noted that there is no *a priori* reason why the scattering factor of an atom should not be negative at certain angles.

The function showing the amplitude and phase of the beam diffracted in any direction by an object is the Fourier transform of the object; the Fourier transform of a crystal is the weighted reciprocal lattice, and the Fourier transform of the weighted reciprocal lattice is the crystal. Fig. 18 shows the Fourier transform of a single slit, and the superposition of the orders of diffraction on the diffraction pattern of the single slit is exactly analogous to the superposition of the reciprocal lattice on the Fourier transform of the unit-cell contents (section 1.3.3.).

**4.3. Abbe's theory of image formation.** The process of Fourier synthesis of electron density can be explained simply in terms of Abbe's theory of image formation (Vol. I, p. 230, and Vol. II, p. 390). Abbe pointed out that image formation by a lens consisted of two parts—scattering by the object and re-combination of the scattered light by a lens.

If we choose a diffraction grating as an object and illuminate it normally by a narrow beam of light, then the scattered beams are confined to particular directions given by the grating equation

$$n\lambda = d \sin \theta_n. \quad (19.1)$$

In fig. 19*a*, two orders of diffraction,  $\pm n$ , are shown as single lines,

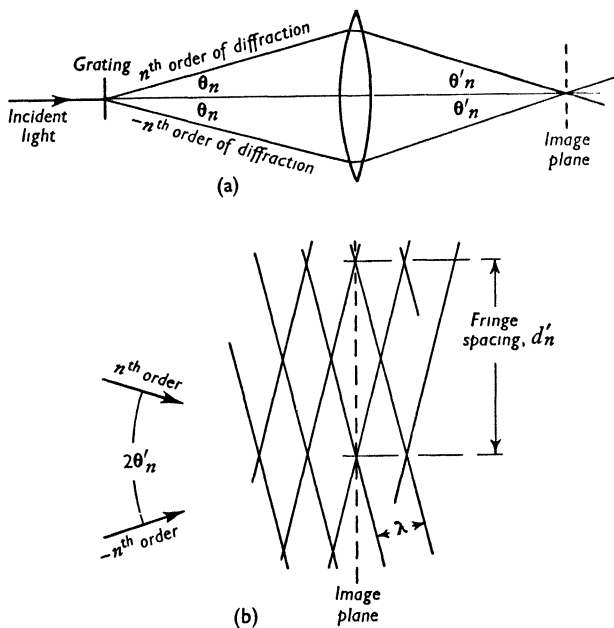


FIG. 19 (*a, b*). Production of one fringe component in the image of a diffraction grating

and these meet, after refraction by the lens, at an angle of  $2\theta'_n$ . If we represent these beams by the crests at any particular instant, as shown in fig. 19*b*, it will be seen that, in the image plane, diffraction fringes are formed with separation  $d'_n$  where

$$d'_n = \lambda / \sin \theta'_n. \quad (19.2)$$

Now, to a first approximation,  $\sin \theta_n / \sin \theta'_n$  is a constant and equal to the magnification  $m$  produced by the lens. Therefore

$$\begin{aligned} d'_n &= m\lambda / \sin \theta_n \\ &= md/n \quad (\text{from equation } 19.1). \end{aligned}$$

From this equation we can see how the image of the diffraction

grating is built up. The zero order of diffraction gives an infinite value for  $d'_0$ ; that is, there is no variation in intensity. The first orders give fringes of spacing  $md$ , that is, a true magnified image of the spacing, but with an intensity distribution independent of the shape of the grating element. The second orders produce fringes that modify the fringes formed by the first orders, and give a closer approximation to the truth. The addition of fringes produced by further orders adds to the detail, but the representation cannot be perfect so long as some orders of diffraction of appreciable intensity are not included.

This description of image formation applies only to one-dimensional gratings; it can readily be extended to two dimensions, but not to three. In two dimensions, each pair of diffracted beams symmetrically related with respect to the origin combines to form a set of fringes, whose sum gives the total effect from all the diffracted beams. These fringes, which differ both in spacing and orientation, are equivalent to the Fourier components (section 1.3.1) that are used to produce an image of a crystal structure by computation. (The process cannot be extended to three dimensions because a three-dimensional grating does not give all its orders of diffraction simultaneously (section 1.2.1); this is one reason why the image of only one plane of an object can be formed at any one time.)

An accurate image cannot be formed with X-rays because there is no known way of deflecting the X-rays scattered by a crystal in such a way that they can produce an interference pattern; a 'lens' accurate to a fraction of a wave-length would be required. Nevertheless, the ideas just discussed are not merely of academic interest; they have been fruitful in suggesting new approaches to problems in X-ray diffraction (Bragg 1939, 1944) and these will be discussed in more detail in Chapters 3, 4 and 7.



## CHAPTER 2

# DETERMINATION AND USE OF SPACE GROUPS

### 1. IMPORTANCE OF SYMMETRY

In the theory outlined in Chapter 1, the unit cell of a crystal was supposed to contain  $N$  independent atoms, the positions of which were defined by  $3N$  structural parameters. A crystal of such general type is, however, rare; most crystals show some symmetry, and, since this depends upon the way in which the atoms are arranged in the crystal, *a priori* knowledge of the symmetry of the atomic arrangement can be a very useful aid to structure determination. To begin with, when symmetry is present, the number of independent parameters is less than the value  $3N$ , but frequently the information gained is much more helpful than this; certain sets of atoms in a crystal structure may be fixed by only one or two parameters, and, in extreme cases, some atoms can be precisely located from symmetry considerations alone.

Thus the determination of the full symmetry of a crystal structure is now regarded as a necessary preliminary to the determination of the atomic positions, and the present chapter is concerned with describing the accepted procedures for determining, as unequivocally as possible, the symmetry of a given crystal structure. The basic principles have been dealt with in Chapter V of Volume I. The present account, therefore, includes only a general review of these basic principles, and is chiefly concerned with describing in detail the various steps that may be taken in the deduction of the symmetry of a crystal structure.

### 2. EXTERNAL SYMMETRY OF CRYSTALS

**2.1. Types of symmetry.** A body is said to be symmetrical when it can be divided into parts that are related to each other in certain ways. The operation of transferring one part to the position of a symmetrically related part is termed a *symmetry operation*, the result of which is to leave the final state of the body indistinguishable from its original state. In general, successive application of the symmetry operation must ultimately bring the body actually into its original state again.

An infinite number of symmetry operations is possible. For example, a regular polygon of  $n$  sides will appear identical if turned through an angle of  $2\pi/n$ , and is said to have an  *$n$ -fold axis of rotation*. The possibilities in crystals are limited however, because the symmetry has to conform with that possible in an extended lattice, as can be seen by considering a two-dimensional lattice of dimensions  $a$  and  $b$  and

angle  $\gamma$  (fig. 22 (i)). By making  $a=b$  and ascribing various values to  $\gamma$ , lattices of different symmetry may be obtained; for example if  $\gamma=\pi/2$ , the lattice has four-fold symmetry and if  $\gamma=\pi/3$  it has six-fold symmetry. Now, the angle of the general lattice may be taken as  $\pi-\gamma$  instead of  $\gamma$ ; the choice of one value or the other is arbitrary. Thus, in order that a lattice with higher than two-fold symmetry should be produced, both  $\gamma$  and  $\pi-\gamma$  must be submultiples of  $2\pi$ . That is

$$\gamma = 2\pi/n$$

and

$$\pi - \gamma = 2\pi/m$$

where  $n$  and  $m$  are integers. Thus

$$\begin{aligned} m &= \frac{2\pi}{\pi - \frac{2\pi}{n}} \\ &= \frac{2}{1 - 2/n} \end{aligned}$$

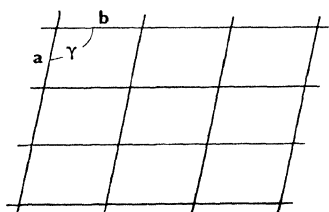


FIG. 22 (i). Two-dimensional lattice

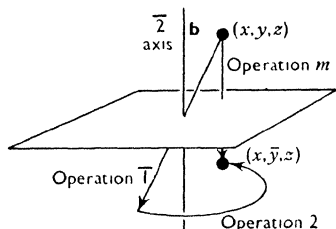


FIG. 22 (ii). Equivalence of  $\bar{2}$  and  $m$

By trial we find that the only values of  $n$  that satisfy this condition are 1, 2, 3, 4 and 6, and these numbers are used to represent the corresponding axes of rotation. The symbol 1 represents the *identical operation*, since it merely expresses the fact that a body turned through an angle of  $2\pi$  will be coincident with itself.

The other important type of symmetry is that represented by inversion, and is possessed by a body which is such that any line drawn through a certain point within it intersects the surface at equal distances on either side of the point; the point is known as a *centre of inversion* or *centre of symmetry*. The operation of inversion combined with that of rotation produces a type of symmetry element known as an *inversion axis*; these axes are represented by the symbols  $\bar{1}$ ,  $\bar{2}$ ,  $\bar{3}$ ,  $\bar{4}$  and  $\bar{6}$ . Obviously  $\bar{1}$  is the operation of inversion itself. From fig. 22 (ii) we see that  $\bar{2}$  is equivalent to reflexion across a plane, and this is so important that it is given a special symbol,  $m$ .

The rotation axes and inversion axes are all the symmetries possible in the external form of a crystal.

**2.2. Lattice symmetry.** All lattices are centro-symmetrical, and thus the presence of a centre of symmetry does not introduce any relations between the lattice constants. A crystal with only this property is said to belong to the *triclinic system*, and such a crystal may have the symmetry represented by 1 or  $\bar{1}$ .

If a crystal has a two-fold axis, then a prominent row of lattice points will be associated with this direction; otherwise, if the points lay slightly off, the axis would produce another set of points at a slight angle to the first set. This axis is conventionally taken to be  $b$  (although occasionally it is taken to be  $c$ ). Then it follows that the other two axes,  $a$  and  $c$ , must be perpendicular to  $b$ , since, by the same reasoning, if they were not perpendicular to  $b$ , two more axes would be produced. It can be shown in the same way that if a crystal has a reflexion plane,  $m$ , one of the axes can be taken perpendicular to the plane and the other two must then lie in the plane. Therefore if we find that the crystal lattice has one axis perpendicular to the other two we suspect that it has either a two-fold axis, a mirror plane, or a two-fold axis perpendicular to a mirror plane, denoted by the symbol  $2/m$ . Such crystals are said to belong to the *monoclinic system*.

The symmetry  $2/m$  is the only one of the three possibilities in the monoclinic system which is centro-symmetrical. Thus, since all lattices are centro-symmetrical, the lattice of a monoclinic crystal must have symmetry  $2/m$ ; nevertheless, the atomic arrangement in such a crystal may have symmetry  $2$ ,  $m$  or  $2/m$ , and these subdivisions of a crystal system are known as *point groups* (Phillips, 1946, p. 235). Each crystal system contains a number of point groups, lists being given in standard works such as the International Tables (1952).

**2.3. Analytical representation of symmetry elements.** The operation of a symmetry element can be represented by the position to which a point in the general position  $(x, y, z)$  (section 1.2.6) would be moved by the operation. Thus from fig. 23 we see that the operation of a two-fold axis along  $b$  can be represented by the points  $(x, y, z)$  and  $(\bar{x}, y, \bar{z})$ , and from fig. 22 (ii) we see that reflexion in a mirror plane perpendicular to  $b$  can be represented by the points  $(x, y, z)$  and  $(x, \bar{y}, z)$ . Consequently, the symmetry  $2/m$  can be expressed by the four points  $(x, y, z)$   $(\bar{x}, y, \bar{z})$   $(x, \bar{y}, z)$  and  $(\bar{x}, \bar{y}, \bar{z})$ . But this set of points has also a centre of symmetry and, amongst the many utilities of this representation, this property of showing the existence of further symmetry elements in a combination is particularly important.

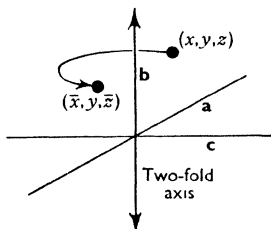


FIG. 23. Equivalent points produced by a two-fold axis

## 3. SYMMETRY OF CRYSTAL STRUCTURES

**3.1. Screw axes and glide planes.** In an extended array of atoms, types of symmetry are possible other than rotation and inversion axes: in addition to considering the relationship between atoms in the same unit cell, we can also consider the relationship between atoms in different unit cells. That is, we can consider symmetry operations whose continued application brings an atom not into self

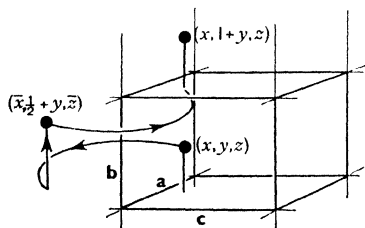


FIG. 24. Two successive operations of screw axis. The points  $(x, y, z)$  and  $(x, 1+y, z)$  are similar points in neighbouring unit cells

coincidence, but into coincidence with an atom in a neighbouring unit cell. For example, the following symmetry operation is possible—first, rotation of an angle  $\pi$  about an axis parallel to one of the crystallographic axes, followed by translation of half the length of the cell edge. This is called a *two-fold screw axis*. As shown in fig. 24, the repeated operation brings the point considered into

coincidence with the corresponding one in the next unit cell, as contrasted with the two operations of a two-fold rotation axis which brings the point into coincidence with itself.

Many other such symmetry elements are possible; a complete list is given in the International Tables (1952). It will be noted that they can be classed as axes—screw axes—or planes—*glide planes*. Glide planes represent reflexion across the plane plus translation in a direction parallel to the plane. In the monoclinic system the plane of the glide is usually perpendicular to  $b$ , but in other systems the orientation of the plane is specified by the position of the symbol in the complete representation of the symmetry, as described in Vol. I (p. 87).

**3.2. Non-primitive lattices.** So far we have assumed that there is only one sort of plane of symmetry or one sort of axis of symmetry in any given direction. In the monoclinic system, for example, we have seen that the symmetry can be either 2,  $m$  or  $2/m$  (section 2.2.2). Such symmetry elements will produce other symmetry elements of the same sort. For example, it can be seen from fig. 25 (i) that two-fold axes along the edges of the unit cell produce two-fold axes along lines in between. Similarly, mirror planes in opposite faces of the unit cell must be interleaved by other mirror planes.

It is therefore possible to introduce further symmetry elements, subject only to the rule that the operation of symmetry element upon symmetry element produces a self-consistent system. Thus, as shown in fig. 25 (ii), two-fold screw axes can be placed between two-fold rotation

axes, and glide planes can be placed between mirror planes. The symmetry operations may then be expressed as  $2+2_1$ , and  $m+a$ ,

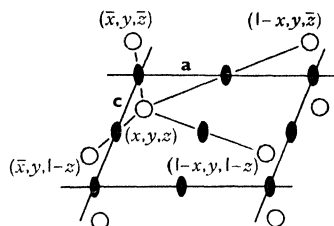


FIG. 25 (i). Two-fold axes lying half-way between two-fold axes along edges of unit cells

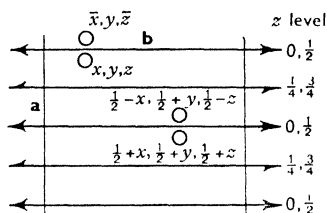


FIG. 25 (ii). Screw axes placed between rotation axes. The screw axes could also be placed at levels 0 and  $\frac{1}{2}$

respectively. This process cannot be continued further for no type of symmetry operation can, for example, turn a screw axis into a rotation axis.

Where does this process lead? Consider the operations  $2+2_1$ , combined in the particular way shown in fig. 25 (ii). Operation 2 leads to equivalent points  $x, y, z$  and  $\bar{x}, y, \bar{z}$ , and the operation  $2_1$  leads to further points  $\frac{1}{2}-x, \frac{1}{2}+y, \frac{1}{2}-z$ , and  $\frac{1}{2}+x, \frac{1}{2}+y, \frac{1}{2}+z$ . The last one is important; it can be regarded as derived from the original point by a simple translation of  $\frac{1}{2}(\mathbf{a}+\mathbf{b}+\mathbf{c})$ . In other words, whatever set of atoms is placed around the origin, an exactly similar set of atoms, similarly oriented, is produced by the symmetry around the point  $\frac{1}{2}, \frac{1}{2}, \frac{1}{2}$ —the centre of the unit cell. Now from the definition of the lattice (section 1.2.1), we see that all the lattice points are produced by simple translation. Therefore this process of combining symmetry elements has led to new lattice points in between the original ones.

This concept can, of course, be evaded by rechoosing the axes of the lattice, as shown in fig. 25 (iii), but such a choice no longer brings out clearly the relationship of the lattice to the symmetry. It is therefore customary to retain the original axes and to admit the possibility of non-primitive lattices—that is, lattices with points at positions other than the corners of the unit cells. The lattice produced by combining two-fold rotation and screw axes in this way is called a body-centred lattice, and is represented by the symbol I. The possible lattices are shown in fig. 48 of Volume I.

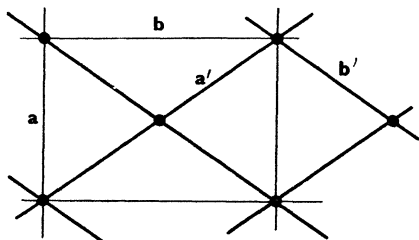
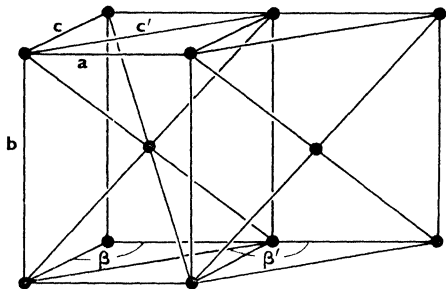


FIG. 25 (iii). Re-choice of axes to produce primitive cell from centred cell

Some of the lattices are not essentially different from each other. From fig. 26 we can see that in the monoclinic system the lattice I



can be regarded as A, with the retention of the convention of axes—that **b** should be perpendicular to the plane of symmetry and **a** and **c** should lie in this plane. In fact, in this system the lattice A is equivalent to both C and F.

FIG. 26. Transformation of I lattice into A by re-  
choice of c axis

of symmetry elements that is consistent with an infinitely extended, regularly repeating pattern. In specifying a space group it is not necessary to specify the complete collection of symmetry elements; those that can be derived from the others may be omitted. Thus the symbol 2 represents a space group, for we know (section 2.3.2) that the placing of rotation axes along one set of parallel edges of a unit cell leads to other rotation axes.

On this basis, therefore, we should expect the scheme of derivation of the thirteen space groups of the monoclinic system to have some form such as that set out in table 26, in which the space groups are denoted both by their symmetry elements and by their Hermann-Mauguin symbols.

TABLE 26

The Monoclinic Space Groups

Point Group 2		Point Group <i>m</i>		Point Group 2/ <i>m</i>	
2 2 <sub>1</sub>	P2	<i>m</i>	P <i>m</i>	2/ <i>m</i>	P2/ <i>m</i>
	P2 <sub>1</sub>	<i>c</i>	P <i>c</i>	2 <sub>1</sub> / <i>m</i>	P2 <sub>1</sub> / <i>m</i>
		( <i>a</i> , <i>n</i> )	(P <i>a</i> , P <i>n</i> )	2/ <i>c</i>	P2/ <i>c</i>
2+2 <sub>1</sub>	C2	<i>m</i> + <i>a</i>	C <i>m</i>	(2/ <i>a</i> , 2/ <i>n</i> )	(P2/ <i>a</i> , P2/ <i>n</i> )
		( <i>m</i> + <i>c</i> , <i>m</i> + <i>n</i> )	(A <i>m</i> , I <i>m</i> )	2 <sub>1</sub> / <i>c</i>	P2 <sub>1</sub> / <i>c</i>
		<i>c</i> + <i>n</i>	C <i>c</i>	(2 <sub>1</sub> / <i>a</i> , 2 <sub>1</sub> / <i>n</i> )	(P2 <sub>1</sub> / <i>a</i> , P2 <sub>1</sub> / <i>n</i> )
		( <i>a</i> + <i>c</i> , <i>a</i> + <i>n</i> )	(I <i>a</i> , A <i>a</i> )	2/ <i>m</i> + <i>a</i>	C2/ <i>m</i>
				(2/ <i>m</i> + <i>c</i> , 2/ <i>m</i> + <i>n</i> )	(A2/ <i>m</i> , I2/ <i>m</i> )
				2/ <i>c</i> + <i>n</i>	C2/ <i>c</i>
				(2/ <i>a</i> + <i>c</i> , 2/ <i>a</i> + <i>n</i> )	(I2/ <i>a</i> , A2/ <i>a</i> )

Thus the symbol 2 is sufficient to describe the space group that has only two-fold rotation axes, but the Hermann-Mauguin notation gives

also the lattice symbol  $P$ . The advantage of this notation can be seen by considering combinations of symmetry elements; thus if mirror planes  $m$  are interleaved with glide planes  $a$ , a C-face-centred lattice is produced, and the resulting space-group symbol  $Cm$  is more informative than the symmetry notation  $m + a$ .

The number of combinations of the symmetry elements  $2$ ,  $2_1$ ,  $m$ ,  $a$ ,  $c$ ,  $n$ , is much greater than thirteen, but several different combinations produce equivalent symmetries; some of the alternative space-group symbols are shown in brackets in table 26, the symmetry elements differing only in their orientations with respect to the chosen crystal axes. In particular, new space groups do not arise when the four symmetry elements,  $2$ ,  $2_1$ ,  $m$  and a glide plane, are combined.

Most space groups can be represented in several different ways, and, in dealing with an unknown crystal, it is possible that the original choice of axes will not result in a space-group symbol the same as one in the International Tables. For this reason, tables of space groups are usually accompanied by another table giving the symbols that are equivalent to each other (Volume I, Appendix VI).

This introduction to the theory of space groups has attempted no more than to lay the groundwork for a more complete study. It has dealt only with the triclinic and monoclinic systems, and the difficulties in the systems of higher symmetry, particularly in the cubic system, have not even been hinted at. A complete study could be attempted only in a book devoted solely to space-group theory, such as that written by Hilton (1906), which deals with the derivation of the 230 space groups.

#### 4. DETERMINATION OF SPACE GROUPS

**4.1. *Determination of crystal system.*** The classical method of finding the system to which a particular crystal belongs is to examine the arrangement of its faces (Phillips, 1946, Chapter 5). The normals to these faces are located with reference to arbitrary axes, and a stereographic projection is plotted; if the symmetry is not obvious from the projection, the orientation of the projection can be changed until symmetrical relationships are observed.

If this method is used, it is essential that several crystals should be measured, and they should have well-formed plane faces. This condition cannot always be obeyed, but effectively the same process can be carried through with X-rays. The more usual method, however, is to detect symmetry elements directly on X-ray photographs; if a fragment is found to be a single crystal, it is not difficult, by trial and error, to adjust it so that it gives straight layer lines, and then a plane of symmetry may make itself obvious. If there is no plane of symmetry, the crystal is triclinic; if a plane of symmetry is found, the crystal is at least monoclinic, and further examination with the crystal rotating about different axes should help to identify precisely the

system to which a crystal belongs. Laue photographs may also be used to show more clearly symmetry elements that may be present.

If reasonably flat plates can be obtained, examination with the polarizing microscope should decide whether the crystal is cubic, uniaxial (hexagonal, trigonal or tetragonal) or biaxial (orthorhombic, monoclinic or triclinic) (Hartshorne and Stuart, 1950). A preliminary examination of this sort can be extremely useful as a guide to the application of the other methods.

**4.2. Determination of crystal class.** It is next necessary to allocate the crystal to the correct class within the system. The classical method of examination of the faces can be used, but it has an important limitation—faces of special form are not always sufficient to fix the true symmetry. For example, crystals of alum usually show only faces of the forms  $\{100\}$ ,  $\{110\}$  and  $\{111\}$ , and these would indicate the highest symmetry of the cubic system,  $m\bar{3}m$ . Nevertheless the symmetry is only  $m\bar{3}$ , and this can be found from crystals that have faces of the form  $\{hk0\}$ ; thus crystals with unusual faces are particularly important.

Because of this limitation, there is sometimes a tendency for too high a symmetry to be assigned to a crystal. For example,  $\text{BeSO}_4 \cdot 4\text{H}_2\text{O}$  was stated by Fricke and Havestadt (1928) to belong to the crystal class  $D_4^h$  or  $C_4^h$  ( $4/mmm$  or  $4/m$ ), but it was ultimately found that the only possible structure was based on a space group in the crystal class  $D_2^d(42m)$  (Beevers and Lipson, 1932).

The data from the external form of the crystal should therefore be supplemented by the information obtained from other methods (Phillips, 1946, p. 151). For example, etch figures may give the true symmetry even if general faces are not developed on a crystal, and the presence of optical activity and piezo- and pyro-electricity will show the absence of a centre of symmetry. Such tests, however, are not always conclusive because the absence of these two effects does not necessarily indicate that centro-symmetry is present.

The symmetry of X-ray diffraction photographs is not, in itself, necessarily sufficient to establish the class of a crystal; it can place the crystal only into one of eleven groups, called *Laue groups*. This is so because all X-ray diffraction patterns must indicate a centre of symmetry, in that the reflexion  $hkl$  has the same intensity as the reflexion  $\bar{h}\bar{k}\bar{l}$  (Friedel's law). All triclinic crystals therefore fall into the same Laue group  $\bar{1}$ , and all monoclinic crystals into the same Laue group  $2/m$ .

The X-ray diffraction pattern of a crystal does, however, contain other information about the true symmetry, and, if this information can be extracted, the space group, with a few exceptions, can be determined unequivocally. The methods of procedure are described in section 2.4.5.

It will thus be seen that the determination of the class of a crystal



presents certain difficulties which may not be resolvable. Fortunately, however, although logic would suggest that the crystal class should be determined as a prelude to the space group, it may happen that the step can be circumvented. As shown in the next section, the systematic absences of X-ray reflexions, necessary for space-group determination, may also fix the crystal class, and, even if this is not so, it is sometimes possible to show that certain crystal classes are not possible on structural grounds (Bradley and Thewlis, 1926). If this cannot be done, the class of highest symmetry may be tried first, and if no acceptable structure can be based upon it, lower symmetry may be tried (Bradley and Lu, 1937). Possibilities such as these should be considered, and certainly the X-ray investigator should not be discouraged from further effort by failure to fix a crystal class unambiguously.

**4.3. Systematic absence of X-ray reflexions.** The structure amplitude of a particular reflexion depends upon the atomic parameters, and, of course, it may be extremely small—so small that no reflexion corresponding to the particular indices can be observed. In general, such absent reflexions are randomly distributed amongst the possible indices, but sometimes they are systematically distributed, and are called *systematic absences* or *extinctions*.

We can see how this phenomenon arises by considering the expression for the structure factor

$$F(hkl) = \sum_n f_n \exp 2\pi i(hx_n + ky_n + lz_n). \quad (29.1)$$

The summation has to be taken over all the atoms in the unit cell, and if there are no relations between the atomic co-ordinates the expression cannot be simplified. But, as we have seen in section 2.1, there often *is* some relation between the atomic positions, and then equation 29.1 can be simplified by collecting into a group those atoms that form a related set; the summation may then be made over the number of groups.

For example, consider a space group with the lattice C. We know that for each point  $xyz$  there must be another at  $\frac{1}{2} + x, \frac{1}{2} + y, z$ . Then if we sum over these pairs of atoms, we have

$$\begin{aligned} F(hkl) &= \sum_{n=1}^{N/2} f_n [\exp \{2\pi i(hx_n + ky_n + lz_n)\} \\ &\quad + \exp \{2\pi i(hx_n + ky_n + lz_n + \tfrac{1}{2}h + \tfrac{1}{2}k)\}] \\ &= \sum_{n=1}^{N/2} f_n \left[ \exp \{2\pi i(hx_n + ky_n + lz_n)\} \left\{ 1 + \exp \left( 2\pi i \frac{h+k}{2} \right) \right\} \right] \end{aligned} \quad (29.2)$$

The last factor can have only two values; if  $h+k$  is even it is two and if  $h+k$  is odd it is zero. Thus if  $h+k$  is odd the result must be zero whatever the values of  $x_n, y_n$  and  $z_n$ . Conversely, if we find that no reflexion is observed for which  $h+k$  is odd, we may deduce that the

lattice of the crystal investigated is C. Rules for the other lattices may be deduced in a similar way.

Suppose next that the crystal has a glide plane,  $c$ , passing through the origin and parallel to the plane (010). Then the atoms may be grouped in pairs with co-ordinates  $xyz$ , and  $x, \bar{y}, \frac{1}{2} + z$ . If we take the atoms in pairs, the expression for the structure factor becomes

$$F(hkl) = \sum_{n=1}^{N/2} f_n [\exp \{2\pi i(hx_n + ky_n + lz_n)\} + \exp \{2\pi i(hx_n - ky_n + lz_n + \frac{1}{2}l)\}]. \quad (30.1)$$

This expression cannot be further simplified as equation 29.2 can, because the arguments of the exponentials are now dissimilar in that the sign of one term is different in the two. But if  $k$  were zero, the arguments would differ only by  $\pi l$ , and thus the expression would contain a factor, corresponding to the last factor in equation 29.2,

$$1 + \exp 2\pi i l / 2.$$

This expression is zero if  $l$  is odd, and therefore any reflexions that satisfy *both* the rules—that  $k$  should be zero and  $l$  should be odd—will be absent. This is the characteristic of the glide plane. General rules for other glide planes may be deduced in a similar way.

The final type of systematic absence is that which is connected with screw axes. If there is a two-fold screw axis along  $b$ , the equivalent points are  $x, y, z$  and  $\bar{x}, \frac{1}{2} + y, \bar{z}$ , and the expression for  $F$  is

$$F(hkl) = \sum_{n=1}^{N/2} f_n [\exp \{2\pi i(hx_n + ky_n + lz_n)\} + \exp \{2\pi i(-hx_n + ky_n - lz_n + \frac{1}{2}k)\}]. \quad (30.2)$$

By comparing this with equation 30.1, we see that if *both*  $h$  and  $l$  are zero, the expression will contain a factor

$$1 + \exp 2\pi i k / 2,$$

and this will be zero if  $k$  is odd. Therefore two-fold screw axes lead to the absence of reflexions for which two indices are zero and one is odd.

**4.4. An experimental difficulty—double reflexions.** Occasionally reflexions are observed on X-ray photographs which seem to be at variance with the symmetry indications of the other reflexions; for example, a reflexion 010 may be observed although all the others of type  $hk0$  with  $k$  odd are absent. Such a reflexion should certainly be queried before arriving at the conclusion that the crystal has only an approximate glide plane.

One way in which spurious spots can arise has been pointed out by Renninger (1937): X-rays which have been reflected from one set of lattice planes may be reflected from another set of planes which happen, by chance, to be in the correct orientation; when this hap-



With a reasonably complicated crystal this effect must occur quite frequently, but in general double reflexions are extremely weak, and so are inappreciable. Occasionally, however, the reflexions  $h_1k_1l_1$  and  $h_2k_2l_2$  may both be reasonably strong, and then the intensity of the doubly reflected beam will add to that of the reflexion  $h_1+h_2, k_1+k_2, l_1+l_2$ , producing perhaps some of the experimental errors that experience has shown can never be entirely eliminated. But here we are more concerned with spurious reflexions that occur in conditions which the true space group will not allow.

The effect cannot produce any uncertainty of lattice; as we have seen in section 2.4.3, the lattice type is determined by systematic absences of reflexions of general type, and the sums of the indices must obey the same rules. For example, if the lattice is body-centred, the sum of the indices of any reflexion must be even, and therefore the sums of the indices of two separate reflexions must also be even. But the effect can interfere with the detection of glide planes and screw axes; for example, we may observe a spurious reflexion 010, formed by reflexion from the two sets of planes 111 and 101, neither of which is forbidden by a  $b$  glide plane or a screw axis parallel to  $b$ . Collin and Lipscomb (1949) describe the observation of a spurious 302 reflexion from a crystal for which all the other reflexions indicated space group No. 62,  $Pbnm$ ; this turned out to be the double reflexion from the planes 221 and  $\bar{1}21$ .

A glide plane produces so many systematic absences that the presence of one non-conforming reflexion would be immediately suspect; the danger is much greater with screw axes, for which the number of systematic absences is fewer. The double reflexions can, however, be recognized by their shapes; since they are formed by the reflexion of truly parallel rays, they are much sharper than ordinary spots, and so cannot easily be mistaken for them. If an observed spot is suspected to be of this type, a check should be made to see if it could be formed by the simultaneous passage of the sphere of reflexion through two reciprocal-lattice points corresponding to strong reflexions; this check must, of course, be carried out in three dimensions.

**4.5. Intensity statistics.** The determination of space groups by means of systematically absent reflexions is, as we have seen, incomplete in that it frequently fails to distinguish between space groups in a given crystal system. While the ambiguity has not in fact proved to be a serious obstacle in the determination of crystal structures, a clear and unequivocal determination of the space group at the outset of a structure investigation may well lead to more rapid and certain progress, and the statement by Buerger (1946, 1950 *a, g*) that the X-ray intensities themselves should provide information in addition to that given by the systematically absent reflexions, is therefore of importance.

Buerger's approach to the problem was made through the theory of the interpretation of the Patterson synthesis (section 1.3.2). If we accept the conclusion that a particular Patterson synthesis corresponds to one and only one atomic arrangement—a conclusion that is discussed further in sections 5.6.2 and 6.3.1—then the symmetry of this atomic arrangement must also be inherent in the Patterson synthesis and hence in the diffracted intensities; Buerger thus considers the characteristic features that different symmetry elements should impress upon Patterson syntheses.

The reasoning is best explained by means of an example. If a structure contains an  $a$  glide plane through the origin parallel to (010), all the atoms must be related in pairs with co-ordinates  $(x, y, z)$  and  $(\frac{1}{2} + x, \bar{y}, z)$ , and thus the Patterson synthesis will show peaks at points  $(\frac{1}{2}, 2y, 0)$ . There will be other peaks in general positions due to atoms not related by this symmetry element, but along the line  $x = \frac{1}{2}, z = 0$ , we should expect an excess of peaks, and if this excess can be detected it gives confirmation of the existence of the glide plane.

Such glide planes are, however, more definitely detected from systematic absences, but the importance of the reasoning is that it applies to symmetry elements, such as mirror planes, which do not lead to systematic absences. If a structure has a mirror plane through the origin parallel to (010), the equivalent points are  $(x, y, z)$  and  $(x, \bar{y}, z)$  and thus in the Patterson synthesis there will be an excess of peaks in the line  $x = 0, z = 0$ ; if this excess can be detected, it gives confirmation of the existence of a mirror plane which may not be detectable by other means.

The effect of screw axes is more general. A screw axis through the origin along the  $b$  axis gives equivalent points  $(x, y, z)$  and  $(\bar{x}, \frac{1}{2} + y, \bar{z})$ , and consequently in the Patterson synthesis gives excess of peaks in the plane  $y = \frac{1}{2}$ . The characteristic of a two-fold rotation axis is excess of peaks in the plane  $y = 0$ , and, again, this axis may not be detectable by any other means.

These principles do not, however, apply to the centre of symmetry, since the Patterson peaks representing vectors between related atoms have co-ordinates  $(2x, 2y, 2z)$ , which are quite general. Nevertheless, a distinction still exists between the Patterson syntheses of centrosymmetrical and non-centrosymmetrical structures, for, as Buerger points out, peaks in the former representing vectors between unrelated atoms must occur in pairs, while in the latter they do not. This point is illustrated in fig. 34, which shows the representations of the vectors produced by centrosymmetrical and non-centrosymmetrical arrangements of six points; in the former the Patterson peaks are larger and fewer than in the latter. Thus, other things being equal, we should expect a non-centrosymmetrical structure to give a more even and featureless Patterson synthesis than a centrosymmetrical structure would give.

To make use of these principles, three-dimensional syntheses are necessary, and thus a great deal of computational work must be undertaken. From general principles, however, we might expect that

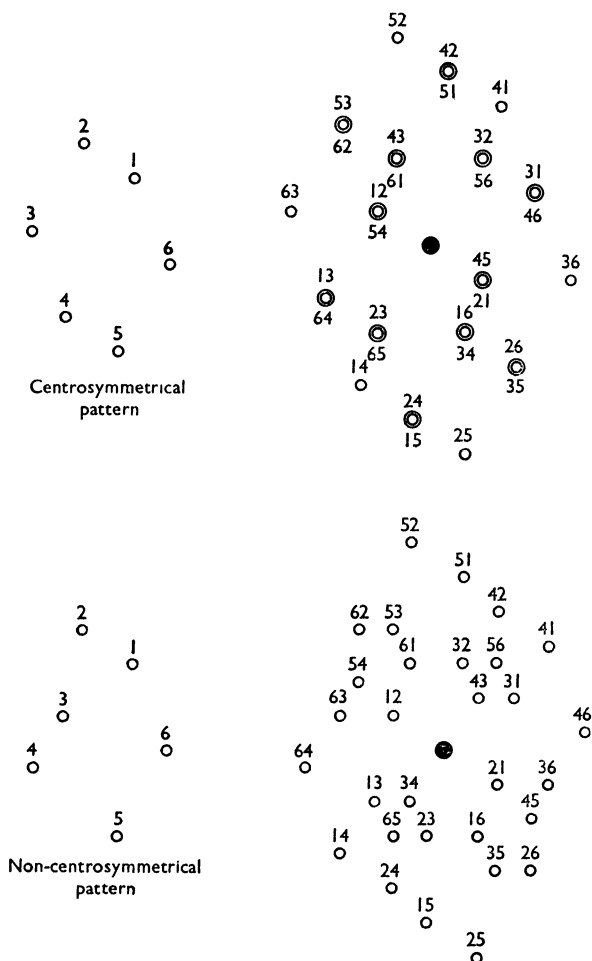


FIG. 34. Representations of vectors produced by centrosymmetrical and non-centrosymmetrical patterns of points. The black spots represent the zero vectors, and the double circles represent overlapping vectors

the computations should not be necessary; the information sought is contained within the set of diffracted beams, and thus other methods might be available for extracting it.

This was shown to be so by Wilson (1949), who has considered the problem in terms of the distribution of intensities from a crystal containing a reasonably large number of approximately equal atoms. For crystals with the same total number of similar atoms per unit cell the same total intensity of radiation should be scattered, and the same distribution of intensities in the various orders of diffraction should occur, although, of course, they will be differently arranged amongst the individual orders of diffraction. Thus we may define a quantity  $P(I)$ , where  $P(I) dI$  is the proportion of intensities  $I$  ( $=FF^*$ ) which have values lying between  $I$  and  $I+dI$ . Wilson shows that if the crystal has no symmetry

$$P(I) = \frac{\exp \left\{ -I / \sum_{j=1}^N f_j^2 \right\}}{\sum_{j=1}^N f_j^2}, \quad (35.1)$$

where the summation is taken over all the atoms in the unit cell. If, however, the crystal has a centre of symmetry, it is simpler to consider the distribution of structure amplitudes:

$$P(F) = \frac{\exp \left\{ -|F|^2 / 2 \sum_{j=1}^N f_j^2 \right\}}{(2\pi \sum_{j=1}^N f_j^2)^{\frac{1}{2}}}. \quad (35.2)$$

These results are equivalent to the properties of Patterson syntheses stated by Buerger, but the fact that they are quantitative makes them of greater use. Thus Wilson has shown that, for a non-centrosymmetrical crystal, the mean value of the structure amplitudes is greater than that for a centrosymmetrical crystal; he has deduced that the ratio of the square of the mean structure amplitude to the mean intensity should have the values  $\pi/4 = 0.785$  and  $2/\pi = 0.637$  for the two types of crystal respectively.

The distinction between the values 0.785 and 0.637 should be readily detectable, but nevertheless there may be some reluctance to base a space-group determination on a single item of evidence; the evidence for systematic absences, for example, is accepted only when a reasonably large number of reflexions is considered. In order to make the method more convincing, therefore, Howells, Phillips and Rogers (1950) have devised a way of verifying the complete intensity distribution. They show that the fractions  $N(z)$  of reflexions whose intensities are equal to or less than a fraction  $z$  of the local average are given, for a non-centrosymmetrical crystal, by the function

$$N(z) = 1 - \exp(-z)$$

and for a centrosymmetrical crystal by the function

$$N(z) = \operatorname{erf}(\frac{1}{2}z)^{\frac{1}{2}},$$

where the symbol 'erf' represents the error function (Jahnke and Emde, 1933). These two functions, which are plotted in fig. 36 and which

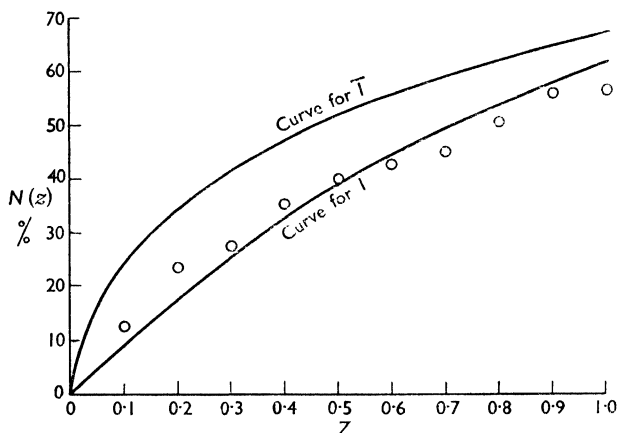


FIG. 36. Distribution for metatoluidine dihydrochloride, compared with theoretical curves for  $I$  and  $\bar{I}$

are tabulated below up to  $z=1$ , differ appreciably from each other, particularly at lower values of  $z$ .

TABLE 36

Values, in percentages, of the two functions representing  $N(z)$

	0.0	0.1	0.2	0.3	0.4	0.5	0.6	0.7	0.8	0.9	1.0
$1 - \exp(-z)$	0.00	9.52	18.13	25.92	32.97	39.35	45.12	50.34	55.07	59.34	63.21
$\text{erf}(\frac{1}{2}z)^2$	0.00	24.81	34.53	41.87	47.38	52.05	56.14	59.72	62.89	65.72	68.33

An extremely important practical point arises from the investigations of Howells, Phillips and Rogers; in assessing the reliability of these methods they discovered that they could often be applied satisfactorily to *zones* of reflexions. There are reasons why this was not to be expected: first, the number of reflexions in a zone is so much smaller than the number of general reflexions that statistical methods might not be applicable; and in projections of structures on to planes, overlapping of atoms might lead to departures from the general distributions upon which the theory rests. These considerations were shown to be unimportant, and clear verification of the space groups of several crystals was demonstrated.

The possibility of confining the calculations to zones of intensities means, of course, that they can be carried out without excessive labour. In addition, however, it leads to the detection of symmetry elements



by noting whether they have the effect of producing a 'centric' distribution of intensities (that due to a centrosymmetrical structure) or an 'acentric' distribution. For example, a two-fold axis in a structure produces a centric distribution in the reciprocal-lattice section perpendicular to the axis, but not in any other section; a mirror plane gives only acentric distributions. Thus we may distinguish between the space groups  $Pm$ ,  $P2$  and  $P2/m$  by considering the section  $h0l$ , and one other, such as  $hk0$ : for  $Pm$  the two sections are acentric; for  $P2$ , the section  $h0l$  is centric and  $hk0$  is acentric; and for  $P2/m$  both sections are centric. It will therefore be seen that the method is of extreme importance in filling in a gap left by the methods described in section 2.4.3.

Before actual examples of use are given, one important practical point must be emphasized. The theoretical results apply only to the distribution of intensities produced by a 'random' collection of atoms; they do not apply to any systematic variations produced, for example, by the fall in scattering factors (section 1.2.4) or by temperature (section 1.2.5). Intensities should therefore be compared only with others having about the same value of  $\theta$ . If, however, the ranges of  $\theta$  are narrow, each will contain too small a number of reflexions for the theory to apply: thus some discretion must be used in deciding what subdivisions to adopt, and the following example will give some idea of a working compromise.

Metatolidine dihydrochloride (Fowweather and Hargreaves, 1950) was known to be monoclinic, but systematic absences showed only the lattice  $I$ ; consequently the space group could be either No. 8,  $Im$ ; No. 5,  $I2$ ; or No. 12,  $I2/m$ . The structure finally adopted had the space group  $I2$ , but Howells, Phillips and Rogers (1949) showed that this space group could have been deduced from the intensity data alone. The table of values of intensities  $I(0kl)$ , derived by squaring the values of  $|F_0|$  given by Fowweather and Hargreaves, is shown below.

These may be divided into, say, five sets with ranges of  $0.2$  in  $\sin \theta$ , but this procedure would not be satisfactory, for the lower ranges would not contain enough reflexions for the theory to be properly applicable. Therefore it is better to take larger ranges at low values of  $\theta$ , and this is reasonable because scattering-factors and the temperature factor do not vary rapidly for such values. Also, for theoretical reasons, the reflexions of lowest angle should be omitted. A reasonable choice of subdivision is indicated in table 38, the full lines separating the reflexions into the four ranges of  $\sin \theta$ ,  $0-0.2$ ,  $0.2-0.6$ ,  $0.6-0.8$ ,  $0.8-1.0$ . The first range is disregarded, and the other three—1, 2 and 3—contain 35, 30 and 31 reflexions respectively.

Though these are the numbers of reflexions shown in the table, they are not the numbers of reflexions in the corresponding sections of the reciprocal lattice; only one quadrant is shown, and in taking averages the whole section must be taken into account. This may be

TABLE 38

Values of  $I = |F_0|^2$  for metatolidine dihydrochloride

$l$	$k$							
	0	1	2	3	4	5	6	7
0			2500		841		1521	
1		1296		144		100		144
2	49		2209		1369		400	
3		64		256		16		0
4	169		1444		529		25	
5		784		144		361		169
6	729		400		144		49	
7		1521		1225		441		256
8	625		324		0		25	
9		841		1024		324		64
10	169		484		361		100	
11		256		225		144		64
12	2809		1444		400		484	
13		841		121		81		64
14	1024		784		841		324	
15		441		16		256		
16	256		841		576		49	
17		100		16		121		
18	36		225		16		16	
19		676		324		400		
20	0		324		169			
21		784		484		100		
22	4		49		25			
23		361		529		121		
24	16		196		36			
25		256		49				
26	169		100		25			
27		9		36				
28	121		121					
29		49						

achieved most simply by allotting a weight of  $\frac{1}{2}$  to any reflexions  $0k0$  and  $00l$ , but, of course, this procedure must be modified according to the symmetry of the reciprocal-lattice section.

The mean value of  $I$  for range 1 is  $22383/(27 + 8/2) = 722$ . Thus the value of  $N(0.1)$  is obtained by counting the number of reflexions with  $I$  less than 72; there are only two— $0.4.8$  and  $0.0.18$ —and thus the number is  $1\frac{1}{2}$ , the value of  $N(0.1)$  being  $1\frac{1}{2}/31 = 0.048$ . (It is advisable to mark those reflexions that have been dealt with, so that, when the value of  $N(1.0)$  has been deduced, it may be confirmed that all those with  $I$  less than 722 have been included.) To find the values of  $N(0.2)$  we count the number of reflexions with  $I$  equal to or less than 144; there are  $6\frac{1}{2}$ , and thus  $N(0.2)$  is 0.21. The complete set of results derived in this way for the three ranges is given in table 39.

TABLE 39

Values of  $N(z)$ , in percentages, for the  $0kl$  reflexions of metatolidine dihydrochloride

Range	$z$									
	0.1	0.2	0.3	0.4	0.5	0.6	0.7	0.8	0.9	1.0
I	4.8	21.0	22.5	33.9	37.1	43.5	50.0	53.1	54.8	54.8
II	25.8	34.0	37.5	41.1	41.1	44.7	44.7	48.3	51.9	51.9
III	6.7	16.7	23.3	33.3	43.3	43.3	43.3	53.3	65.0	65.0
Mean	12.4	23.9	27.8	36.1	40.5	43.8	46.0	51.6	57.2	57.2

As shown in fig. 36, these values lie close to the values for an acentric zone, and thus the space group is not  $I2/m$ . The corresponding values for the  $h0l$  reflexions show that this zone has a centric distribution, and thus the space group is  $I2$ .

In principle, the method can also be applied to reflexions with two indices zero; a mirror plane perpendicular to  $b$ , for example, should cause only the  $0k0$  reflexions to have a centric distribution. In general, however, such rows do not contain enough reflexions for statistical theory to be applicable, but, as was shown earlier in this section, other evidence should be available for detecting such symmetry elements; certain parts of the Patterson syntheses should show concentrations of peaks, and these concentrations should be traceable to intensity variations in the reciprocal lattice.

Wilson (1950a) has explained the occurrence of this effect in a particularly simple way. He points out that if, for example, a crystal possesses a mirror plane of symmetry perpendicular to the  $b$  axis in the projection of the structure on the  $(010)$  plane the atoms will overlap in pairs; thus the scattering for the  $h0l$  reflexions will simulate that due to half the number of atoms (provided that none is in a special position) each with twice the scattering factor. Thus the local intensity average (see section 5.5.3), instead of being

$$\sum_{j=1}^N f_j^2$$

will be

$$\sum_{j=1}^{N/2} (2f_j)^2$$

which has a value twice as great as the former expression. Thus the local intensity average for the  $h0l$  reflexions should be twice as great as for the general  $hkl$  reflexions.

Rotation axes lead to similar results for 'central rows' of reflexions—reflexions that are represented by reciprocal-lattice points lying on lines passing through the origin of the reciprocal lattice. Thus a

two-fold axis parallel to  $b$  should cause the  $0k0$  reflexions to be, on the average, twice as strong as the more general reflexions. The same considerations can also be applied to glide planes and screw axes, but, since these symmetry elements are definitely detectable from systematic absences, there is no need to make use of statistical results.

These methods of detecting symmetry elements are of greatest use when three-dimensional data are available, but even in two dimensions they can lead to useful conclusions. For example, we may consider the data contained in table 38, assuming that the space group has not yet been decided upon. If the space group were  $I2$ , we should expect the  $0k0$  reflexions to be stronger than the average; if the space group were  $Im$ , we should expect the  $00l$  reflexions, as special cases of the  $h0l$  reflexions, to be stronger than the average; and if the space group were  $I2/m$ , we should expect both these features to exist. In fact, it is almost immediately obvious that only the  $0k0$  reflexions are outstanding, in agreement with the earlier deduction that the space group is  $I2$ .

It is perhaps wise to make a quantitative investigation of the effect, and this should be performed by taking averages over given ranges of  $\theta$ . The results for the  $0kl$  reflexions of metatolidine dihydrochloride are shown in table 40.

TABLE 40

Comparison of the values of  $\langle I(0kl) \rangle$  and  $\langle I(00l) \rangle$  with general intensity averages

Range of $\sin \theta$	$\langle I(0kl) \rangle$	$\langle I(0k0) \rangle$	$\langle I(00l) \rangle$
0.2—0.6	722	1620	820
0.6—0.8	318	1521	7
0.8—1.0	141	—	145

Although the numbers of  $0k0$  and  $00l$  reflexions are too small to provide data of statistical significance, the conclusions previously drawn are seen to be quite clearly supported.

From these examples, it will be seen that intensity statistics can be extremely valuable in supplementing the information given by systematic absences. For successful application of the methods, however, certain conditions must obtain; the data must be reasonably accurate and must not suffer from systematic errors, such as those due to extinction (section 5.5.3) and absorption. The detection of centrosymmetry, depending as it does upon the survey of large numbers of reflexions, is least likely to be affected by such errors, but, as we can see from the example in the last paragraph, the detection of other symmetry elements may depend more critically on only a few reflexions.

Absorption, which can affect systematically a row of reflexions if plate-like crystals are used, is particularly serious, and care should be taken to use crystals whose sections are not far from circular.

Moreover, the methods obviously apply only to crystals containing a reasonably large number of atoms in general positions. They would therefore not be expected to apply to simple structures with small unit cells, to structures containing a small number of predominant atoms (although the chlorine atoms in metatoluidine dihydrochloride do not seem to be deleterious), or to crystals in which some of the atoms are in special positions (section 2.6.2). But in spite of these difficulties, the methods have been shown to be useful, and are well worth trying even for crystals which would not seem to come completely within the range of their application.

**4.6. Summary.** The sequence of operations for determining space groups by means of the principles described in this chapter are as follows. First reflexions of general type  $hkl$  are considered; if any of these are systematically absent the lattice is non-primitive. Then reflexions with one zero index are considered; systematic absences amongst these give information about glide planes. Finally, reflexions with two zero indices give information about screw axes. For the uniaxial and cubic systems, other types of reflexions, as indicated in the International Tables, must be examined as well.

These rules must be used strictly in order, as systematic absences which are special cases of more general absences are not significant. For example, the absence of reflexions  $0k0$  with  $k$  odd does not necessarily signify a screw axis if a glide plane is present which causes the absence of reflexions  $hk0$  with  $h+k$  odd.

Sometimes systematic absences allow a space group to be determined uniquely, because they are characteristic of only one space group in a crystal system; for instance, if a monoclinic crystal gives no reflexions  $h0l$  with  $h$  odd, and no reflexions  $0k0$  with  $k$  odd, the space group is No. 14,  $P2_1/a$ . If, however, the systematic absences are only  $0k0$  with  $k$  odd, the space group may be either No. 4,  $P2_1$  or No. 11,  $P2_1/m$ . Statistical methods should then be tried. The latter space group would be indicated by a centric distribution of all intensities, which may be most simply tested by the principal sections, whereas for the former space group only the  $h0l$  section would be centric. Furthermore, the presence of a mirror plane would be indicated by enhancement of the  $h0l$  reflexions with respect to the general reflexions, or again, more simply but perhaps less clearly, by the enhancement of the  $h00$  or  $00l$  reflexions with respect to the  $hk0$  or  $0kl$  reflexions.

There are still some space groups which cannot be distinguished by these methods. Apart from the obvious ones, such as Nos. 76 and 78,  $P4_1$  and  $P4_3$ , there are pairs such as Nos. 23 and 24,  $I222$  and  $I2_12_12_1$ .

In the latter space group the lattice absences mask the absences due to the space group, and this happens also for the pair of space groups Nos. 197 and 199,  $I2_3$  and  $I2_13$  (Rogers, 1950). Crystals with these space groups are fortunately rare, but if the problem of distinguishing between them is encountered, it would be necessary to find which of them was capable of providing the basis for a satisfactory structure (section 2.4.2).

## 5. SPACE-GROUP REPRESENTATIONS

**5.1. General equivalent points.** A space group may be represented in two ways—as a collection of symmetry elements, each with its location in the unit cell precisely indicated, or as a collection of points arranged so that it possesses these symmetries. These points are obtained by applying the various symmetry operations to a point in a general position  $x, y, z$  in the unit cell; the collection of points, which is such that if any operation is applied to any point no new point is produced, is called a set of *general equivalent points*.

The representation of a symmetry element by a set of symmetrically related points (section 2.2.3) is most simply illustrated by space group No. 2,  $P\bar{1}$ . If the centre of symmetry is taken to be at the origin (since the origin can be taken as any position it is preferable to place it at a centre of symmetry), the equivalent points are  $x, y, z$  and  $\bar{x}, \bar{y}, \bar{z}$ . It so happens that these are the general equivalent points in the space group, but this is not necessarily so; as shown in fig. 25 (i), a single symmetry element repeated by the lattice translations will produce other symmetry elements, and these may in turn produce further equivalent points in the same unit cell. In the space group  $P\bar{1}$ , the point  $1-x, \bar{y}, \bar{z}$  is related to the point  $\bar{x}, \bar{y}, \bar{z}$  by translation  $a$ . But it is also related to the point  $x, y, z$  by a centre of symmetry at  $\frac{1}{2}, 0, 0$ , and if we consider all the points related by lattice translations to the points  $xyz$  and  $\bar{x}\bar{y}\bar{z}$  we find that there are centres of symmetry at the points  $000, \frac{1}{2}00, 0\frac{1}{2}0, 00\frac{1}{2}, 0\frac{1}{2}\frac{1}{2}, \frac{1}{2}0\frac{1}{2}, \frac{1}{2}\frac{1}{2}0, \frac{1}{2}\frac{1}{2}\frac{1}{2}$ . These centres of symmetry are called *non-equivalent symmetry elements* because they are not themselves related by any symmetry elements in the unit cell. They do not in this case lead to any further equivalent points and thus the points  $x, y, z$  and  $\bar{x}, \bar{y}, \bar{z}$  form the complete set of general equivalent points for the space group  $P\bar{1}$ .

Consider a more complicated space group, No. 64,  $Cmca$ . The symbol tells us that this has a C-face-centred lattice, a mirror plane parallel to (100), a glide plane parallel to (010) with translation  $\frac{1}{2}c$  and a glide plane parallel to (001) with translation  $\frac{1}{2}a$ . To find the complete set of symmetry elements, we first draw a diagram showing the elements given (fig. 43a) and another (fig. 43b) showing the four points that result from the operation of these elements on a general point  $x, y, z$ . The directions of the axes are drawn to agree with the

International Tables—**a** downwards in the plane of the paper, **b** to the right, and **c** upwards from the plane of the paper. The origin is arbitrary.

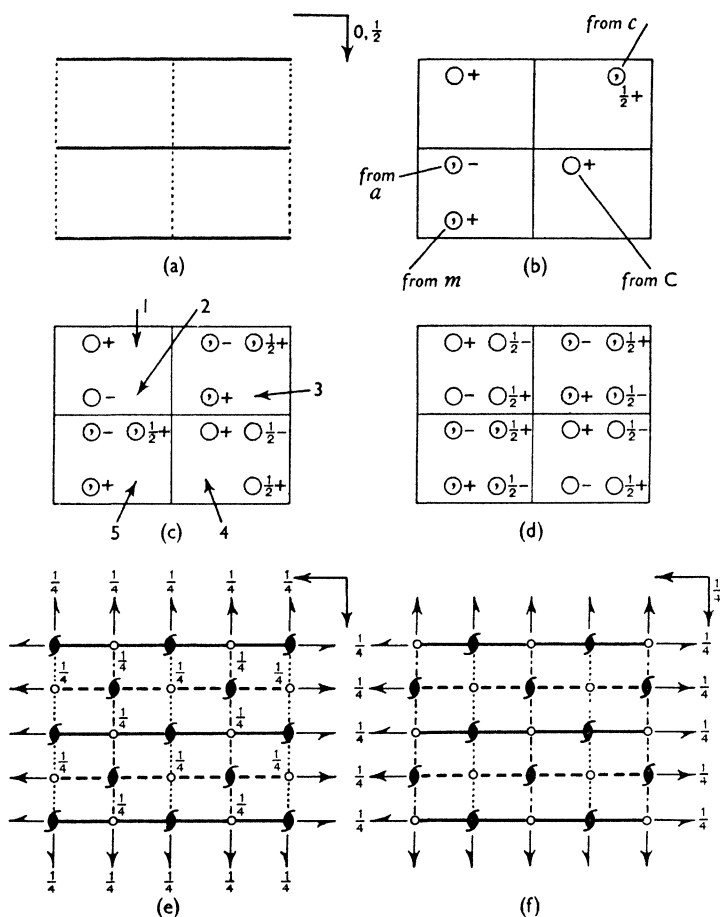


FIG. 43. Development of representation of space group No. 64 *Cmca*. (a) Basic symmetry elements. (b) Points related by basic symmetry elements to point  $(x, y, z)$ . (c) Points related by basic symmetry elements to points shown in (b). (d) Complete set of equivalent points. (e) Symmetry elements deduced from (d). (f) Diagram of symmetry elements from International Tables

trary, and it is simplest to place it at the point of intersection of the three planes of symmetry.

The points equivalent to  $(x, y, z)$  are then:

From operation C  $\frac{1}{2} + x, \frac{1}{2} + y, z$ ;

From operation  $m$   $\bar{x}, y, z$ ;

From operation  $c$   $x, \bar{y}, \frac{1}{2} + z$ ;

From operation  $a$   $\frac{1}{2} + x, y, \bar{z}$ .

The five points are shown in fig. 43*b*.

These points obviously do not satisfy the symmetry elements producing them, and the operations have to be repeated on each point in turn until no new points are produced. The next step is to apply each element in turn to each of the points in the list above except, of course, that produced by its own operation; thus:

C  $(\frac{1}{2} - x, \frac{1}{2} + y, z), (\frac{1}{2} + x, \frac{1}{2} - y, \frac{1}{2} + z), (x, \frac{1}{2} + y, \bar{z})$ ;

$m$   $(\frac{1}{2} - x, \frac{1}{2} + y, z), (\bar{x}, \bar{y}, \frac{1}{2} + z), (\frac{1}{2} - x, y, \bar{z})$ ;

$c$   $(\frac{1}{2} + x, \frac{1}{2} - y, \frac{1}{2} + z), (\bar{x}, \bar{y}, \frac{1}{2} + z), (\frac{1}{2} + x, \bar{y}, \frac{1}{2} - z)$ ;

$a$   $(x, \frac{1}{2} + y, \bar{z}), (\frac{1}{2} - x, y, \bar{z}), (\frac{1}{2} + x, \bar{y}, \frac{1}{2} - z)$ .

It will be noted that these are not all different; they are equal in pairs, since the operations C and  $m$ , for example, must lead to the same point as the operations  $m$  and C.

Plotting these points together with the original five we obtain fig. 43*c*. This figure is still unsymmetrical, and the same operation should be repeated with the eleven points found. This process, although mechanical, is rather lengthy, and it can be avoided by guesswork. In fig. 43*c* gaps in the diagram are indicated by numbered arrows. Arrow (1) indicates that a point should occur at  $(x, \frac{1}{2} - y, ?)$ ; such a point can be derived from the operation C on  $(\frac{1}{2} + x, \bar{y}, \frac{1}{2} - z)$ , which gives  $(x, \frac{1}{2} - y, \frac{1}{2} - z)$ . By similar reasoning, we arrive at the points

(2)  $\frac{1}{2} - x, \frac{1}{2} - y, \frac{1}{2} + z$ , by operation C from  $(\bar{x}, \bar{y}, \frac{1}{2} + z)$ ;

(3)  $(\frac{1}{2} - x, \bar{y}, \frac{1}{2} - z)$  by operation  $m$  from  $(\frac{1}{2} + x, \bar{y}, \frac{1}{2} - z)$ ;

(4)  $(\bar{x}, \frac{1}{2} + y, \bar{z})$  by operation C from  $(\frac{1}{2} - x, y, \bar{z})$ ;

(5)  $(\bar{x}, \frac{1}{2} - y, \frac{1}{2} - z)$  by operation  $m$  from  $(x, \frac{1}{2} - y, \frac{1}{2} - z)$ .

These points could have been derived from other points by means of other symmetry operations, but, in general, operations that do not involve translations are more easily visualized than screw axes and glide planes.

The complete set of equivalent points for the space group No. 64,  $Cmca$ , is as follows:

$(0, 0, 0; \frac{1}{2}, \frac{1}{2}, 0) +$

$x, y, z; \bar{x}, y, z; x, \bar{y}, \frac{1}{2} + z; \bar{x}, \bar{y}, \frac{1}{2} + z;$

$x, \frac{1}{2} + y, \bar{z}; \bar{x}, \frac{1}{2} + y, \bar{z}; x, \frac{1}{2} - y, \frac{1}{2} - z; \bar{x}, \frac{1}{2} - y, \frac{1}{2} - z.$

The points thus found are shown in fig. 43*d*. (In accordance with the convention used in the International Tables those points which



are enantiomorphous to the original point are marked with commas.) It does not follow that this collection is complete; this is proved by applying the symmetry elements to any point, when no further new points are produced. Moreover, the number of points—16—is that to be expected from the four symbols of the space group, each of which produces a doubling of the number of points. (This is not an invariable rule: in the space group No. 16, P222, for example, the three two-fold axes produce only four general equivalent points, not eight.)

5.2. *Symmetry representation.* From the general equivalent points it is possible to find further symmetry elements. It is difficult to do this systematically and experience of where to look for such elements is invaluable. For *Cmca* the complete diagram of symmetry elements derived from the general equivalent positions is shown in fig. 43e. This figure differs from that given in the International Tables (fig. 43f); the difference will be discussed later (section 3.1.1).

## 6. APPLICATION TO STRUCTURE DETERMINATION

6.1. *Structural parameters.* The equivalent points are, from the crystal-structure point of view, the more important mode of representation of a space group, since a structure can be defined by placing atoms at various equivalent positions in the space group found; the problem of finding a crystal structure resolves itself, once the space group has been found, into the determination of the parameters,  $x_n, y_n, z_n$ , that define particular sets of atomic positions. Thus if a crystal with space group *Cmca* contained 16 similar atoms, it would be probable that these atoms would be on a set of general equivalent positions, and they would be defined by three parameters—called *structural parameters*—instead of the 48 that would be required if each atom in the unit cell were considered separately. If there were 32 atoms, they could be divided into two sets of 16, and thus they would be defined by six structural parameters.

6.2. *Special equivalent positions.* Suppose however that the number of atoms is less than 16, or that it is not a multiple of 16; is it possible to fit such numbers of atoms into the unit cell? It is sometimes possible; in addition to the general equivalent positions there are also special equivalent positions which are fewer in number, but which have the same space-group symmetry. These special positions arise when the co-ordinates chosen for the generation of equivalent points lie on certain types of symmetry element. For example, in the space group  $P\bar{1}$ , suppose we had started with the point  $\frac{1}{2}, \frac{1}{2}, 0$  and had applied the symmetry operation to this; we should have found that no more points would have been produced in the unit cell. Thus it is possible to place an odd number of atoms in this unit cell provided that one atom is placed *at* a centre of symmetry.

Let us see what this implies in the more complicated space group No. 64, *Cmca*. In fig. 43e all the symmetry elements have been derived; which ones lead to special positions? The glide planes and screw axes cannot, because they involve a translation; the only symmetry elements that can lead to special positions are those that do not involve translations—the centre of symmetry, the mirror plane, the rotation axes and the inversion axes. The necessity for knowing whether such symmetry elements are present justifies the work involved in finding the complete symmetry representation of the space group; the Hermann-Mauguin symbol gives only a minimum of information and is sufficient only for classification. In the symbol *Cmca* the mirror plane appears directly but only the complete representation of the space group shows the other symmetry elements that lead to special positions—the centres of symmetry and the two-fold axes.

A method of finding the special positions is to consider a point on an appropriate symmetry element and to substitute the values of  $x$ ,  $y$  and  $z$  in the expressions for the general equivalent points. We may first consider the mirror plane at  $x=0$ ; that is, we take our original point as  $(0, y, z)$ . The sixteen equivalent points are then:

$$\begin{aligned} & (0, 0, 0; \frac{1}{2}, \frac{1}{2}, 0) + \\ & 0, y, z; 0, y, z; 0, \bar{y}, \frac{1}{2} + z; 0, \bar{y}, \frac{1}{2} + z; \\ & 0, \frac{1}{2} + y, \bar{z}; 0, \frac{1}{2} + y, \bar{z}; 0, \frac{1}{2} - y, \frac{1}{2} - z; 0, \frac{1}{2} - y, \frac{1}{2} - z. \end{aligned}$$

That the operation has been correctly performed is shown by the facts that the co-ordinates now appear in pairs and that there are only eight equivalent points, not sixteen.

In a similar way the other special positions may be found. All the symmetry elements must be considered; it is not sufficient to consider only one mirror plane, unless the special positions it produces include also those produced by the other at  $x=\frac{1}{2}$ . This is so in *Cmca*, because the special positions listed above include some with  $x=\frac{1}{2}$ . If we consider the two-fold axes, however, we find that they are in two sets: (i) at  $x=\frac{1}{4}, z=0$ ;  $x=\frac{3}{4}, z=0$ ;  $x=\frac{1}{4}, z=\frac{1}{2}$ ;  $x=\frac{3}{4}, z=\frac{1}{2}$ ; and (ii) at  $y=\frac{1}{4}, z=\frac{1}{4}$ ;  $y=\frac{3}{4}, z=\frac{3}{4}$ ;  $y=\frac{1}{4}, z=\frac{3}{4}$ ;  $y=\frac{3}{4}, z=\frac{1}{4}$ . Substituting the first values,  $x=\frac{1}{4}, z=0$ , in the expressions for the general equivalent points gives the following set of equivalent positions:

$$\begin{array}{cccc} \frac{1}{4}, y, 0, & \frac{3}{4}, \frac{1}{2} + y, 0, & \frac{3}{4}, y, 0, & \frac{1}{4}, \bar{y}, \frac{1}{2} \\ \frac{1}{4}, \frac{1}{2} + y, 0, & \frac{3}{4}, \frac{1}{2} - y, \frac{1}{2}, & \frac{3}{4}, \bar{y}, \frac{1}{2}, & \frac{1}{4}, \frac{1}{2} - y, \frac{1}{2}. \end{array}$$

It will be noted that these include the positions on all the axes parallel to  $b$ , and so there is no need to consider these separately. In a similar way it can be shown that the two-fold axes parallel to  $a$  lead to only one set of special positions.

This is not so with the centres of symmetry. That at  $\frac{1}{4}, 0, 0$  leads to the following special positions:

$$\frac{1}{4}, 0, 0, \quad \frac{3}{4}, \frac{1}{2}, 0, \quad \frac{3}{4}, 0, 0, \quad \frac{1}{4}, 0, \frac{1}{2}, \quad \frac{1}{4}, \frac{1}{2}, 0, \quad \frac{3}{4}, \frac{1}{2}, \frac{1}{2}, \quad 0, \frac{3}{4}, \frac{1}{2}, \quad \frac{1}{4}, \frac{1}{2}, \frac{1}{2};$$

these are half of the total number of centres. One of those not included is at  $0, \frac{1}{4}, \frac{1}{4}$ . This produces the special positions:

$$0, \frac{1}{4}, \frac{1}{4}, \quad \frac{1}{2}, \frac{3}{4}, \frac{1}{4}, \quad 0, \frac{3}{4}, \frac{3}{4}, \quad \frac{1}{2}, \frac{1}{4}, \frac{3}{4}.$$

There are thus four still remaining, and these can be found to be another equivalent set:

$$\frac{1}{2}, \frac{1}{4}, \frac{1}{4}, \quad 0, \frac{3}{4}, \frac{1}{4}, \quad \frac{1}{2}, \frac{3}{4}, \frac{3}{4}, \quad 0, \frac{1}{4}, \frac{3}{4}.$$

That there should be two types of centres of symmetry is obvious, since eight lie on the intersections of mirror planes and two-fold axes and the others do not; but it is not obvious that the former divide into two non-equivalent sets of four each.

6.3. *The placing of atoms on general and special positions.* To summarize the results, we have found two sets of four equivalent points, on centres of symmetry; four sets of eight equivalent points, on centres of symmetry, on mirror planes, and on two sets of two-fold axes; and one set of sixteen equivalent points. By making use of the special positions it is possible to introduce numbers of atoms in multiples of four into the unit cell. For example, suppose there are 28 to be fixed; the simplest way of placing them is to put 16 in general positions, 8 in eight-fold special positions, and 4 on four equivalent centres of symmetry. In practice, it is better to apportion the atoms on the positions of smaller multiplicity first, in this case on the centres of symmetry. At first sight, it may seem that there are two possibilities, corresponding to the two sets of four special positions; this however is not so, as both sets have exactly the same environment of symmetry elements, and they differ only in choice of origin. Once a set of atoms has been placed, however, the origin of the structure is fixed, and further atoms must be placed on their correct symmetry elements even if there are others with similar environments. The choice cannot of course be made from space-group considerations only.

## 7. PRACTICAL EXAMPLES

7.1. *Alum,  $KAl(SO_4)_2 \cdot 12H_2O$ .* Potassium aluminium alum is cubic, the unit cell containing  $4\{KAl(SO_4)_2 \cdot 12H_2O\}$ ; the only systematic absences are  $0kl$  with  $k$  odd,  $h0l$  with  $l$  odd, and  $hk0$  with  $h$  odd, which show that the space group is No. 205,  $Pa\bar{3}$ . The data for this space group are as follows.

24: (d)  $xyz$ ;  $zxy$ ;  $yzx$ ;

$$\frac{1}{2} + x, \frac{1}{2} - y, \bar{z}; \frac{1}{2} + z, \frac{1}{2} - x, \bar{y}; \frac{1}{2} + y, \frac{1}{2} - z, \bar{x};$$

$$\bar{x}, \frac{1}{2} + y, \frac{1}{2} - z; \bar{z}, \frac{1}{2} + x, \frac{1}{2} - y; \bar{y}, \frac{1}{2} + z, \frac{1}{2} - x;$$

$$\frac{1}{2} - x, \bar{y}, \frac{1}{2} + z; \frac{1}{2} - z, \bar{x}, \frac{1}{2} + y; \frac{1}{2} - y, \bar{z}, \frac{1}{2} + x;$$

$$\bar{x}\bar{y}\bar{z}; \bar{z}\bar{x}\bar{y}; \bar{y}\bar{z}\bar{x};$$

$$\frac{1}{2} - x, \frac{1}{2} + y, z; \frac{1}{2} - z, \frac{1}{2} + x, y; \frac{1}{2} - y, \frac{1}{2} + z, x;$$

$$x, \frac{1}{2} - y, \frac{1}{2} + z; z, \frac{1}{2} - x, \frac{1}{2} + y; y, \frac{1}{2} - z, \frac{1}{2} + x;$$

$$\frac{1}{2} + x, y, \frac{1}{2} - z; \frac{1}{2} + z, x, \frac{1}{2} - y; \frac{1}{2} + y, z, \frac{1}{2} - x.$$

8: (c)  $xxx$ ;  $\frac{1}{2} + x, \frac{1}{2} - x, \bar{x}$ ;  $\bar{x}, \frac{1}{2} + x, \frac{1}{2} - x$ ;  $\frac{1}{2} - x, \bar{x}, \frac{1}{2} + x$ ;

$$\bar{x}\bar{x}\bar{x}; \frac{1}{2} - x, \frac{1}{2} + x, x; x, \frac{1}{2} - x, \frac{1}{2} + x; \frac{1}{2} + x, x, \frac{1}{2} - x.$$

4: (a)  $000$ ;  $0\frac{1}{2}\frac{1}{2}$ ;  $\frac{1}{2}0\frac{1}{2}$ ;  $\frac{1}{2}\frac{1}{2}0$ . (b)  $\frac{1}{2}\frac{1}{2}\frac{1}{2}$ ;  $\frac{1}{2}00$ ;  $0\frac{1}{2}0$ ;  $00\frac{1}{2}$ .

The unit cell contains four potassium atoms, four aluminium atoms, eight sulphur atoms, thirty-two oxygen atoms and forty-eight water molecules. We attempt to locate the smaller numbers of atoms first, since the positions of these should be more definite. Thus the potassium atoms must occupy (a) or (b) positions. But there is no essential difference between one of the (a) positions (e.g. 0, 0, 0) and one of the (b) positions (e.g.  $\frac{1}{2}$ , 0, 0); they have the same environment of symmetry elements. Thus we may choose either to start with, but having made our choice we have not the same liberty of action for other atoms. We therefore choose to put the potassium atoms in the (a) positions.

The four aluminium atoms must occupy the other four-fold positions, (b). Thus both the sets of metal atoms are fixed solely by space-group considerations.

The eight sulphur atoms must occupy (c) positions—the only eight-fold ones—since all the four-fold positions are occupied. The sulphur atoms are not, however, definitely located in the unit cell, since their positions depend upon a parameter  $x$  about which we have so far no information.

The thirty-two oxygen atoms cannot all be equivalent since there is no set of thirty-two equivalent points; they must therefore be placed on twenty-four general positions (d) and eight special positions (c), or on four different sets of special positions (c). The fact that the (c) positions have already been chosen for the sulphur atoms is immaterial; any number of atoms can be placed upon the same set of positions provided that at least one variable parameter is involved. For the same reason, four sets of special positions could be chosen for the oxygen atoms, although this possibility is unlikely. Similarly, it is unlikely that the forty-eight water molecules will make use of the (c) positions; they probably lie on two sets of general positions (d).

The most probable arrangement of atoms is thus:

(i) K and Al on fixed special positions (a) and (b),

(ii) S on special positions (c) with one parameter,

- (iii) O on one set of special positions (c) with one parameter and on one set of general positions (d) with three parameters,
- (iv) H<sub>2</sub>O on two sets of general positions (d) with six parameters.

Thus the position of the ninety-six atoms (excluding hydrogen) in the unit cell are determined by only eleven parameters—a striking instance of the usefulness of space-group theory. This of course is exceptional; for crystals of lower symmetry it is rare to have as great a gain in simplicity; but it is quite usual, even in monoclinic crystals, for space-group theory to lead immediately to important results.

7.2. *Potassium mercury chloride, K<sub>2</sub>HgCl<sub>4</sub>·H<sub>2</sub>O.* An example of lack of definiteness in the space-group information is given by potassium mercury chloride, K<sub>2</sub>HgCl<sub>4</sub>·H<sub>2</sub>O, which belongs to space group No. 55, *Pbam* (MacGillavry, de Wilde and Bijvoet, 1938). This space group has the following sets of equivalent points:

- 2: (a) 000;  $\frac{1}{2}\frac{1}{2}0$ . (b)  $00\frac{1}{2}$ ;  $\frac{1}{2}\frac{1}{2}\frac{1}{2}$ . (c)  $0\frac{1}{2}0$ ;  $\frac{1}{2}00$ . (d)  $0\frac{1}{2}\frac{1}{2}$ ;  $\frac{1}{2}0\frac{1}{2}$ .  
 4: (e) 00z; etc. (f)  $0\frac{1}{2}z$ ; etc. (g) xy0; etc. (h)  $xy\frac{1}{2}$ ; etc.  
 8: (i) xyz; etc.

Since the unit cell contains K<sub>8</sub>Hg<sub>4</sub>Cl<sub>16</sub>·4H<sub>2</sub>O, numerous possibilities arise for placing the atoms, and it is advisable to deal first with the smallest groups. Thus the mercury atoms may lie upon sets of positions (e) or (g), or upon any pairs of sets (a), (b), (c) and (d); there is no need to consider the sets (f) and (h) because these are equivalent to the sets (e) and (g) respectively, with a change of origin. Similar considerations apply to the water molecules, except that the four sets (e), (f), (g) and (h) must now be considered, since any arbitrariness in origin vanishes when some atoms have been fixed. Moreover, of course, the water molecules cannot occupy positions already occupied by the mercury atoms, but this fact does not preclude the placing of both on positions such as (e) which involve a variable parameter; this is permissible so long as the values of z are different.

The potassium atoms can be accommodated on the general positions (i) or upon combinations of special positions. Still more possibilities arise for the chlorine atoms. So many combinations are possible that the assignment cannot be considered systematically; methods of trial-and-error, as described in Chapter 5, have to be used, and the heaviness of the mercury atom (section 5.5.2) makes the problem not too difficult. The structure actually contains atoms in the following positions:

Hg on (e),  
 H<sub>2</sub>O on (f),  
 K on (g) + (h),  
 Cl on (g) + (h) + (i).

**7.3. The Spinel structures.** That the theory of space groups applies to crystals is now taken as a matter of course. It is nevertheless remarkable that a theory worked out completely before the discovery of X-ray diffraction should apply so precisely in practice. That exceptions occur should not be regarded as remarkable—the remarkable fact is that exceptions are so rare! Rigid application of space-group theory should always be the first step in crystal-structure determination, but the fact should be borne in mind that there are crystals which to some extent disregard the theory or make use of it in unexpected ways.

The reason for this is that natural systems tend to disorder (the second law of thermodynamics), and the extreme degree of order found in crystals is exceptional; if possible some disorder will creep in. Normally this is negligible, but occasionally it may not be; cobalt (Edwards and Lipson, 1942) is so irregular that its structure is not even based on a lattice and this produces a broadening of some of the X-ray reflexions; but other crystals, such as some that are isomorphous with spinel, behave in a much more subtle manner.

Spinel is a mineral of composition  $\text{MgAl}_2\text{O}_4$ , and is isomorphous with a number of other compounds of similar formula, such as  $\text{MnCr}_2\text{O}_4$  and  $\text{CuFe}_2\text{O}_4$ . The space group is No. 227,  $Fd3m$ , and the unit cell contains  $8(\text{MgAl}_2\text{O}_4)$ .

In this space group there are 192 general equivalent positions; all the atoms are thus in special positions and we need not consider any sets of multiplicity higher than 32. The equivalent positions to be considered are as follows:

$$\begin{aligned}
 & (000; 0 \frac{1}{2} \frac{1}{2}; \frac{1}{2} 0 \frac{1}{2}; \frac{1}{2} \frac{1}{2} 0) + \\
 8: & (a) 000; \frac{1}{4} \frac{1}{4} \frac{1}{4}; \quad 8: (b) \frac{1}{2} \frac{1}{2} \frac{1}{2}; \frac{3}{4} \frac{3}{4} \frac{3}{4}. \\
 16: & (c) \frac{1}{8} \frac{1}{8} \frac{1}{8}; \frac{1}{8} \frac{3}{8} \frac{3}{8}; \frac{3}{8} \frac{1}{8} \frac{3}{8}; \frac{3}{8} \frac{3}{8} \frac{1}{8}. \\
 16: & (d) \frac{5}{8} \frac{5}{8} \frac{5}{8}; \frac{5}{8} \frac{7}{8} \frac{7}{8}; \frac{7}{8} \frac{5}{8} \frac{7}{8}; \frac{7}{8} \frac{7}{8} \frac{5}{8}. \\
 32: & (e) xxx; x\bar{x}\bar{x}; \frac{1}{4} - x, \frac{1}{4} - x, \frac{1}{4} - x; \frac{1}{4} - x, \frac{1}{4} + x, \frac{1}{4} + x; \\
 & \quad \bar{x}x\bar{x}; \bar{x}\bar{x}x; \frac{1}{4} + x, \frac{1}{4} - x, \frac{1}{4} + x; \frac{1}{4} + x, \frac{1}{4} + x, \frac{1}{4} - x.
 \end{aligned}$$

The eight magnesium atoms should occupy either (a) or (b) positions; since the origin is arbitrary, it does not matter which are chosen and so we may put them on the (a) positions. The sixteen aluminium atoms can then occupy either the (c) or (d) positions; they cannot make use of the eight-fold positions since one of these sets is occupied by magnesium atoms. The oxygen atoms can occupy (e) positions with one variable parameter, to be determined.

These principles are obeyed, and the complete structure is defined in the following way:

$$\begin{aligned}
 & 8 \text{ Mg in } (a), \\
 & 16 \text{ Al in } (d), \\
 & 32 \text{ O in } (e) \text{ with } x = \frac{3}{8} \text{ (approximately)}.
 \end{aligned}$$

But certain compounds, such as  $\text{MgFe}_2\text{O}_4$ , do not fit into this scheme. They belong to the cubic system; X-ray photographs show that they have a face-centred lattice F; and the unit cell contains  $8(\text{MgFe}_2\text{O}_4)$ . Yet no structure based on the above principles will fit in with the X-ray data, and Barth and Posnjak (1932) have shown that the following sets of positions are occupied:

- 8 Fe on (a),
- 8 Fe + 8 Mg statistically distributed on (d),
- 32 O on (e) with  $x = \cdot 390$ .

Thus the structure is essentially similar to that of spinel, but the space-group rules are not obeyed except in a statistical way.

7.4. *Analcite*,  $\text{NaAlSi}_2\text{O}_6 \cdot \text{H}_2\text{O}$ . Analcite provides an instance of a much greater departure from space-group principles. It is cubic, the space group being No. 230,  $Ia3d$ , and the unit cell containing  $16(\text{NaAlSi}_2\text{O}_6 \cdot \text{H}_2\text{O})$ . The space group has the following sets of equivalent positions:

- 16: (a) 000; etc. (b)  $\frac{1}{8} \frac{1}{8} \frac{1}{8}$ ; etc.
- 24: (c)  $\frac{1}{8} 0 \frac{1}{4}$ ; etc. (d)  $\frac{3}{8} 0 \frac{1}{4}$ ; etc.
- 32: (e) xxx; etc.
- 48: (f)  $x 0 \frac{1}{4}$ ; etc. (g)  $\frac{1}{8}, x, \frac{1}{4} - x$ ; etc.
- 96: (h) xyz; etc.

It will be noted that it is impossible to place the atoms in the unit cell in accordance with this scheme, because if the sodium and aluminium atoms occupy positions (a) and (b) there are no sixteen-fold positions left for the water molecules. There is, however, no difficulty in placing the silicon atoms in (e) and the oxygen atoms in (h).

In fact, the following structure is found (Taylor, 1930). The silicon and aluminium atoms together distribute themselves at random on the 48-fold positions (g); the water molecules occupy positions (b); the oxygen atoms occupy positions (h); and the sodium atoms, instead of occupying positions (a), distribute themselves so that on the average two-thirds of an atom occupies each of the 24-fold positions (c). The complete specification of the structure is:

- 48 (Si, Al) on (g) with  $x = 0.661$ .
- 16 Na statistically distributed on (c).
- 96 O on (h) with  $x = 0.111, y = 0.131, z = 0.722$ .
- 16  $\text{H}_2\text{O}$  on (b).

This structure accounts adequately for all the X-ray intensities.

A way of evading this difficulty is suggested by Kästner (1931). The structure is regarded as merely pseudo-cubic, and lower symmetries

are considered. The tetragonal space group No. 142,  $I4_1/acd$ , has most of the systematic absences of the cubic space group  $Ia3d$  and so an attempt may be made to fit the structure into this space group. The following sets of equivalent positions exist:

- 8: (a) 000; etc. (b)  $00\frac{1}{2}$ ; etc.  
 16: (c)  $0\frac{1}{4}\frac{1}{8}$ ; etc. (d) 00z; etc. (e)  $\frac{1}{4}x\frac{1}{8}$ ; etc. (f)  $xx\frac{1}{4}$ ; etc.  
 32: (g)  $xyz$ ; etc.

There are thus many ways of placing the atoms in the unit cell, and Kästner states that the following specification gives a structure closely resembling the cubic one:

- 16 Na on (e) with  $x=0.625$ .  
 16 A on (f) with  $x=0.339$ .  
 32 Si on (g) with  $x=0.125$ ,  $y=0.411$ ,  $z=0.224$ .  
 32 O on (g) with  $x=0.119$ ,  $y=0.111$ ,  $z=0.653$ .  
 32 O on (g) with  $x=0.131$ ,  $y=0.472$ ,  $z=0.736$ .  
 32 O on (g) with  $x=0.278$ ,  $y=0.139$ ,  $z=0.756$ .  
 16  $H_2O$  on (f) with  $x=0.125$ .

If this is the true structure, space-group principles are not violated. Nevertheless, readiness to contemplate the possibility of violation led Taylor to essentially the correct structure whereas a more pedantic approach might have been less fruitful.

Problems of this sort are rare. Space-group theory works very well for almost all crystals, but, if difficulties are met with in its application, the possibilities of an unorthodox approach—such as the placing of two-thirds of a sodium atom on each of 24 equivalent positions—should not be ignored.

## 8. PLANE GROUPS

8.1. *Two-dimensional symmetry operations.* Although crystals are three-dimensional, it is often necessary to consider projections of crystal structures on planes, and then only symmetry elements operating in two dimensions arise. The arrangements of these symmetry elements that produce a regularly repeating pattern are called plane groups, by analogy with the term space group.

The symmetry operations must necessarily be those that do not require the movement of the representative point out of the plane considered; thus only rotation axes, mirror planes and glide planes, all perpendicular to the plane, are possible. These may be represented by the symbols 1, 2, 3, 4, 6,  $m$  and  $g$ . Two-dimensional lattices are denoted by small letters, and only two need be considered— $p$  and  $c$ .

8.2. *Two-dimensional systems.* The presence of these various symmetry elements leads to relationships between the two axes, which we may



call  $a$  and  $b$ , and so provides a means of classification of projections of crystal structures into systems. These relationships are tabulated below:

Relationships		System	Plane groups
$a \neq b$	$\gamma \neq 90^\circ$	Oblique	1. <i>p1</i> ; 2. <i>p2</i> .
$a \neq b$	$\gamma = 90^\circ$	Rectangular	3. <i>pm</i> ; 4. <i>pg</i> ; 5. <i>cm</i> ; 6. <i>pmm</i> ; 7. <i>pmg</i> ; 8. <i>pgg</i> ; 9. <i>cmm</i> .
$a = b$	$\gamma = 90^\circ$	Square	10. <i>p4</i> ; 11. <i>p4m</i> ; 12. <i>p4g</i> .
$a = b$	$\gamma = 120^\circ$	Hexagonal	13. <i>p3</i> ; 14. <i>p3m1</i> ; 15. <i>p31m</i> ; 16. <i>p6</i> ; 17. <i>p6m</i> .

It will be noted that the number of systems is only four; projections of monoclinic crystals fall into one or other of the first two systems, the distinction between the trigonal and hexagonal systems—never a clear one even in three dimensions—disappears completely, and there is no system corresponding to the cubic. This last fact follows, of course, because the characteristic of the cubic system is the set of three-fold axes inclined to the crystallographic axes; these cannot have any equivalent in two dimensions. It might be thought that, since the projections of a cubic structure on the cube faces have  $a = b$  and  $\gamma = 90^\circ$ , such projections must belong to the square system. This is not so; the plane groups in this system all have four-fold axes of symmetry, and two cubic point groups, 23 and  $m\bar{3}$ , do not have this symmetry. Thus the projections of crystals which have these point groups belong to the rectangular system, and the equality of the lengths of the sides of the unit cell must, from the point of view of the two-dimensional representation, be regarded as fortuitous.

Complete descriptions of the 17 plane groups are given in the International Tables (1952).

8.3. *Uses of plane groups.* Since a great deal of crystal-structure work is confined to two dimensions, plane groups would appear to have important uses, and they do, for example, provide a basis for the classification of structure-factor formulae (Bragg and Lipson, 1936). Patterson (1935*b*) considered them to be of great value in interpreting  $|F|^2$  projections (Chapter 6). Nevertheless, they do not appear to have been greatly used: most workers refer to the space group only, since it is unique for a particular crystal; the three projections parallel to the axes of a monoclinic crystal may belong to three different plane groups, which does not make for simplicity. Moreover, for plane groups, it is sometimes necessary to subdivide the axes, and even to choose new axes, as for the projection of a centred tetragonal cell. It is therefore not surprising that the theory of plane groups has not achieved great prominence in the field of crystal-structure determination.

## CHAPTER 3

### CALCULATION OF STRUCTURE FACTORS

#### 1. STRUCTURE-FACTOR FORMULAE

1.1 *Formulae for different space groups.* The expression for the structure factor derived in Chapter 1 (equation 10.3),

$$F(hkl) = \sum_{n=1}^N f_n \exp 2\pi i(hx_n + ky_n + lz_n),$$

is valid for any space group. In Chapter 2, however, we have seen that the atomic positions in the unit cell are usually symmetrically related, and important simplifications of equation 10.3 can be made by collecting the atoms together in their equivalent groups (section 2.5.1). An expression may be derived for one such group, and then the summation need only be made over the number of groups, which is necessarily smaller than the number of atoms.

The simplest illustration is provided by the space group  $P\bar{1}$ . For each atom at the point  $x, y, z$  there is a corresponding atom at the point  $\bar{x}, \bar{y}, \bar{z}$ . The contribution of these two atoms to the structure factor is

$$f \exp \{2\pi i(hx + ky + lz)\} + f \exp \{-2\pi i(hx + ky + lz)\} \\ = 2f \cos 2\pi(hx + ky + lz).$$

Thus if we wish to calculate structure factors for a crystal with space group  $P\bar{1}$ , the expression used is

$$F(hkl) = 2 \sum_{n=1}^{N/2} f_n \cos 2\pi(hx_n + ky_n + lz_n), \quad (54.1)$$

the summation now being made over half the unit cell; any atom related to an atom already considered is not included in the summation.

The simplification introduced by collecting equivalent atoms together is not always so marked. Consider, for example, space group No. 3,  $P2$ , with a two-fold axis along  $b$ . The equivalent points are  $x, y, z$  and  $\bar{x}, y, \bar{z}$ . The contribution to the structure factor of atoms at these two points is

$$f \exp \{2\pi i(hx + ky + lz)\} + f \exp \{2\pi i(-hx + ky - lz)\} \\ = 2f \exp \{2\pi iky\} \cos 2\pi(hx + lz). \quad (54.2)$$

Thus the contribution of the two atoms is again reduced to a single expression, but it is more complicated than that in equation 54.1.

Moreover, it will be noted that the expression 54.1 is real, whereas

the expression 54.2 is complex. Since the only symmetry involved in the derivation of 54.1 is the centre of symmetry at the origin, it must follow that it is this property which causes the structure factor to be real. If the space group has no centre of symmetry, or if the centre of symmetry is not at the origin, the structure factor will not be real for all values of  $h$ ,  $k$  and  $l$ , although it may be so for special values of these indices. For example, in space group No. 3,  $P2_1$ , the structure factor is shown by equation 54.2 to be real if  $k = 0$ . Use can be made of such relationships, as will be shown in Chapter 7.

The importance of having real structure factors is such that, wherever possible, the origin of co-ordinates in a space group is placed at a centre of symmetry. This explains why the symmetry representation of the space group  $Cmca$  in section 2.5.2 appears to differ from that in the International Tables; in these tables the origin is taken at a centre of symmetry, whereas the deduction of the representation made in section 2.5.2 happened to put this centre of symmetry at  $(0\frac{1}{4}\frac{1}{4})$ . The equivalent points, of course, also differ from those given in the International Tables.

For purposes of computation, expressions such as 54.2 have to be resolved into real and imaginary parts.

$$\begin{aligned} 2f \exp \{2\pi iky\} \cos 2\pi(hx + lz) \\ = 2f \cos 2\pi ky \cos 2\pi(hx + lz) + i2f \sin 2\pi ky \cos 2\pi(hx + lz). \end{aligned}$$

Thus the two quantities  $A'$  and  $B'$  of equation 11.1 are

$$\left. \begin{aligned} A' &= 2 \sum f \cos 2\pi ky \cos 2\pi(hx + lz), \\ B' &= 2 \sum f \sin 2\pi ky \cos 2\pi(hx + lz). \end{aligned} \right\} \quad (55)$$

The corresponding expressions for the 230 space groups are given in the International Tables (1952). In these tables, the summation sign and the symbol for the scattering factor are omitted, and the resulting expressions are termed simply  $A$  and  $B$ .

1.2. *Formulae for different classes of reflexion.* Expressions such as those in 54.1 and 55 can be evaluated for different values of  $x$ ,  $y$  and  $z$ , and  $h$ ,  $k$  and  $l$ . For some space groups, however, it may so happen that further simplification can be introduced by separating the reflexions into various classes with indices having various properties; this is so when the space group contains screw axes and glide planes.

We may see this by considering the space group No. 4,  $P2_1$ , of which the general equivalent points are  $x, y, z$  and  $\bar{x}, \frac{1}{2} + y, \bar{z}$ . Then

$$A = \cos 2\pi(hx + ky + lz) + \cos 2\pi(-hx + ky - lz + \frac{1}{2}k).$$

If  $k$  is even this reduces to

$$A = 2 \cos 2\pi ky \cos 2\pi(hx + lz),$$

and if  $k$  is odd, it reduces to

$$\begin{aligned} A &= \cos 2\pi(hx + ky + lz) - \cos 2\pi(hx - ky + lz) \\ &= -2 \sin 2\pi ky \sin 2\pi(hx + lz). \end{aligned} \quad (56.1)$$

In a similar way, for even values of  $k$ ,  $B$  reduces to

$$B = 2 \sin 2\pi ky \cos 2\pi(hx + lz),$$

and for odd values of  $k$ , to

$$B = 2 \cos 2\pi ky \sin 2\pi(hx + lz).$$

} (56.2)

For systematic calculation these separate formulae are much more useful than the general expressions given in the International Tables (1935), and for this reason they have been published in a separate volume by Lonsdale (1936). They are also included in the International Tables (1952). Nevertheless it is recommended that the expressions for each space group should be worked out as required, Lonsdale's tables or the International Tables being used as a check.

**1.3. Formulae for atoms in special positions.** The formulae in the International Tables and in Lonsdale's tables are for atoms in general equivalent positions, but they can readily be adapted for atoms in special positions. The adaptation, however, does not consist merely in the substitution, in the general formula, of the values of  $x$ ,  $y$  and  $z$  representative of the special positions; the multiplicity of these special positions is also involved. The general rule is that the contribution of an atom in a special position has to be multiplied by the ratio of the multiplicity of the set of special positions (section 2.6.2) to that of the set of general positions. Thus for a structure with space group No. 2,  $P\bar{1}$ , containing an atom of scattering factor  $f$  in the position 000, and  $2N$  other atoms of scattering factor  $f_n$  in general positions  $(x_n, y_n, z_n)$ , the expression for the structure factor is

$$F = f + 2 \sum_{n=1}^N f_n \cos 2\pi(hx_n + ky_n + lz_n). \quad (56.3)$$

In the more complicated space groups many more possibilities may arise. For example, in space group No. 64,  $Cmca$ , with a centre of symmetry at the origin, the following sets of equivalent positions occur:

- 4: (a) 000; etc.      (b)  $\frac{1}{2}$ 00; etc.  
 8: (c)  $\frac{1}{4}\frac{1}{4}$ 0; etc.      (d)  $x$ 00; etc.  
     (e)  $\frac{1}{4}y\frac{1}{4}$ ; etc.      (f) 0 $yz$ ; etc.  
 16: (g)  $xyz$ ; etc.

In order to find the contributions given by atoms in each of these seven sets, we consider the formulae in Lonsdale's tables. For  $h+k$  even,  $k+l$  even,

$$A = 16 \cos 2\pi hx \cos 2\pi ky \cos 2\pi lz.$$

Application of the rule just stated leads to the following expressions for the contributions of atoms in the various sets of equivalent positions:

$$\begin{array}{ll}
 (a) \ A = 16 \times \frac{4}{16} & = 4 \\
 (b) \ A = 16 \cos \pi h \times \frac{4}{16} & = 4 \cos \pi h \\
 (c) \ A = 16 \cos \pi h/2 \cdot \cos \pi k/2 \times \frac{8}{16} & = 8 \cos \pi h/2 \cos \pi k/2 \\
 (d) \ A = 16 \cos 2\pi hx \times \frac{8}{16} & = 8 \cos 2\pi hx \\
 (e) \ A = 16 \cos \pi h/2 \cdot \cos 2\pi ky \cdot \cos \pi l/2 \times \frac{8}{16} & = 8 \cos \pi h/2 \cos 2\pi ky \cdot \cos \pi l/2 \\
 (f) \ A = 16 \cos 2\pi ky \cdot \cos 2\pi lz \times \frac{8}{16} & = 8 \cos 2\pi ky \cos 2\pi lz
 \end{array}
 \left. \vphantom{\begin{array}{l} (a) \\ (b) \\ (c) \\ (d) \\ (e) \\ (f) \end{array}} \right\}$$

Expressions such as these are not yet tabulated for the different space groups, and indeed it is hardly necessary that they should be so, since they are easily derived from the general formulae.

**1.4. Space-group absences from structure-factor formulae.** The systematic absences of the space-groups are deducible from the structure-factor formulae, and this provides a way of checking these formulae: the structure factor should be zero for the indices corresponding to absent reflexions, independently of particular values of  $x$ ,  $y$  and  $z$ . Zero values arise, for example, if the structure-factor formula contains a sine term which is zero if a certain index or combination of indices is zero.

The formulae for space group No. 2,  $P\bar{1}$  are

$$\begin{aligned}
 A &= 2 \cos 2\pi(hx + ky + lz), \\
 B &= 0.
 \end{aligned}$$

and this, since it does not include a sine term, is not zero for any particular combination of indices; correspondingly, there are no systematic absences for this space group. For the space group  $P2_1$  however, equations 56.1 and 56.2 include sine terms that lead to the following results:

$$\begin{array}{ll}
 \text{For } k \text{ even,} & B = 0 \text{ if } k = 0, \\
 \text{and for } k \text{ odd,} & A = 0 \text{ if } h = l = 0 \text{ (} k \text{ cannot, of course, be zero),} \\
 \text{and} & B = 0 \text{ if } h = l = 0.
 \end{array}$$

Thus we see that the only combinations of indices that lead to zero values for *both*  $A$  and  $B$  are that  $k$  should be odd, and  $h$  and  $l$  both zero; this is the set of absent reflexions that characterize the screw axis.

The fact that  $B$  is zero for certain reflexions while  $A$  is not is also important. In space group No. 4,  $P2_1$ ,  $B$  is zero for all reflexions with  $k = 0$ , and this means that, although the space group has not a centre of symmetry, the projection of the structure on the plane (010) has such a centre. This symmetry is, of course, the projection of the screw

axis on the (010) plane. The presence of centres of symmetry in projections can be very useful; in space group No. 19,  $P2_12_12_1$ , for example, the three projections parallel to the axes each have centrosymmetry, and so the structure factors for the three principal zones can all be real. They will not be real, however, if the same origin is maintained for each projection, since the three screw axes do not intersect, but the gain in putting the origin at a centre of symmetry is so great that it is worth while choosing a different origin for each of the projections (section 3.1.1).

## 2. SYSTEMATIC METHODS OF CALCULATION

2.1. *Layout of calculations.* In calculating a set of intensities, systematic methods can save a great deal of time, and planning the operation in advance will be found well worth while. Naturally each worker will devise or adopt methods best suited to his own inclinations, and the following procedure should be regarded only as a guide for the beginner, to be altered, or perhaps completely discarded, as he gains greater experience.

The procedure is best described by means of an actual example. Table 59 shows some calculations of structure factors for the compound cryolite,  $\text{Na}_3\text{AlF}_6$  (Náray-Szabó and Sasvari, 1938), which belongs to the space group No. 14,  $P2_1/n$ , with atoms in the following positions:

2Al in (a)  $0, 0, 0; \frac{1}{2}, \frac{1}{2}, \frac{1}{2}$ .

2Na in (b)  $0, 0, \frac{1}{2}; \frac{1}{2}, \frac{1}{2}, 0$ .

4Na in (c)  $x, y, z; \bar{x}, \bar{y}, \bar{z}; \frac{1}{2}+x, \frac{1}{2}-y, \frac{1}{2}+z; \frac{1}{2}-x, \frac{1}{2}+y, \frac{1}{2}-z$ ,  
with  $x=0.50, y=-0.055, z=0.24$ .

12F in (c) with  $x_1=0.065, y_1=0.06, z_1=0.22$ ,  
 $x_2=-0.29, y_2=0.16, z_2=0.03$ ,  
 $x_3=0.15, y_3=0.28, z_3=-0.06$ .

For this space group, the structure-factor formulae fall into two classes, and the sets of indices should be divided into these two sets—those with  $h+k+l$  even and those with  $h+k+l$  odd. The formulae are

$$A = 4 \cos 2\pi(hx + lz) \cos 2\pi ky \text{ for } h+k+l \text{ even}$$

$$\text{and } A = -4 \sin 2\pi(hx + lz) \sin 2\pi ky \text{ for } h+k+l \text{ odd.}$$

Since the space group has a centre of symmetry at the origin,  $B=0$  for all reflexions.

Table 59 shows the calculations for fifteen reflexions with  $h+k+l$  even, the complete structure-factor equation being

$$F(hkl) = 2f_{\text{Al}} + 2(-1)^l f_{\text{Na}} + 4f_{\text{Na}} \cos 2\pi(hx + lz) \cos 2\pi ky \\ + 4f_{\text{F}} \sum_{n=1}^3 \cos 2\pi(hx_n + lz_n) \cos 2\pi ky_n.$$

TABLE 59  
Calculation of structure factors for Cryolite,  $\text{Na}_3\text{AlF}_6$

$hk0$	cos			cos			cos			cos			cos			cos			$\sum_1^3$ Prod.	F con- trib.	F ( $hk0$ )
	$2f_{\text{Al}}$	$2f_{\text{Na}}$	$4f_{\text{Na}}$	$2\pi hx$	$2\pi ky$	Prod.	$4f_{\text{F}}$	$2\pi hx_1$	$2\pi ky_1$	Prod. <sub>1</sub>	$2\pi hx_2$	$2\pi ky_2$	Prod. <sub>2</sub>	$2\pi hx_3$	$2\pi ky_3$	Prod. <sub>3</sub>					
200	18.5	16.9	33.8	1.000	1.000	1.000	26.0	0.684	1.000	0.684	0.876	1.000	0.876	0.309	1.000	0.309	0.501	13.0	56.2		
400	14.0	11.5	23.0	1.000	1.000	1.000	14.5	0.063	1.000	0.063	0.536	1.000	0.536	0.809	1.000	0.809	0.336	4.7	43.8		
600	10.0	7.2	14.4	1.000	1.000	1.000	9.5	0.770	1.000	0.770	0.063	1.000	0.063	0.809	1.000	0.809	0.024	0.2	31.4		
110	20.7	18.5	37.0	1.000	0.941	0.941	29.5	0.918	0.930	0.854	0.249	0.536	0.133	0.588	0.187	0.110	0.611	18.0	22.4		
310	15.7	13.7	27.4	1.000	0.941	0.941	19.0	0.339	0.930	0.315	0.684	0.536	0.367	0.951	0.187	0.178	0.860	16.3	19.9		
510	11.7	8.8	17.6	1.000	0.941	0.941	11.5	0.454	0.930	0.422	0.951	0.536	0.510	0.000	0.187	0.000	0.932	10.7	6.8		
710	8.2	5.8	11.6	1.000	0.941	0.941	8.0	0.960	0.930	0.893	0.982	0.536	0.526	0.951	0.187	0.178	0.545	4.4	1.3		
020	18.7	17.0	34.0	1.000	0.770	0.770	26.0	1.000	0.729	0.729	1.000	0.426	0.426	1.000	0.930	0.930	0.627	16.3	45.6		
220	16.5	14.8	29.6	1.000	0.770	0.770	21.0	0.684	0.729	0.498	0.876	0.426	0.369	0.309	0.930	0.287	1.154	24.3	78.4		
420	13.0	10.3	20.6	1.000	0.770	0.770	13.0	0.063	0.729	0.046	0.536	0.426	0.228	0.809	0.930	0.752	0.478	6.2	45.4		
620	8.7	6.2	12.4	1.000	0.770	0.770	8.5	0.770	0.729	0.561	0.063	0.426	0.027	0.809	0.930	0.752	1.286	10.9	13.5		
130	15.9	13.9	27.8	1.000	0.509	0.509	14.1	0.918	0.426	0.391	0.249	0.992	0.247	0.588	0.536	0.315	0.953	18.1	33.8		
330	13.5	11.0	22.0	1.000	0.509	0.509	11.2	0.339	0.426	0.144	0.684	0.992	0.679	0.951	0.536	0.510	1.045	14.6	1.3		
530	10.4	7.5	15.0	1.000	0.509	0.509	7.6	0.454	0.426	0.193	0.951	0.992	0.944	0.000	0.536	0.000	0.751	7.5	17.8		
730	7.4	5.4	10.8	1.000	0.509	0.509	5.5	0.960	0.426	0.409	0.982	0.992	0.974	0.951	0.536	0.510	0.873	6.5	0.8		
1	2	3	4	5	6	7	8	9	10	11	12	13	14	15	16	17	18	19	20		

The columns are numbered in sequence, and the numbers below certain columns show how the quantities in them are derived. The quantities in heavy type are the contributions to the structure factor.

The corresponding equation for reflexions with  $h+k+l$  odd is

$$F(hkl) = 4f_{\text{Na}} \sin 2\pi(hx + lz) \sin 2ky + 4f_{\text{F}} \sum_{n=1}^3 \sin 2\pi(hx_n + lz_n) \sin 2\pi ky_n,$$

the contributions from the atoms in special positions being zero.

Although this table is self-explanatory, the sources of the numerical values included in it require some discussion, as the speed of calculation can be greatly reduced by failure to adopt reasonable methods of deriving them.

**2.2. Cosine and sine tables.** One possible way of determining the values of the cosines that appear in table 59 is to express  $2\pi x$  as an angle, to multiply this angle by the corresponding indices, and to look up the cosine values in ordinary trigonometrical tables. This can be rather a lengthy operation, particularly when angles greater than  $\pi/2$  are involved, and the tables of  $\cos 2\pi x$  and  $\sin 2\pi x$  in the International Tables (1935) (p. 546) are more useful. In these tables  $x$  is given at intervals of 0.001, up to 0.250, and corresponding values of  $\cos 2\pi x$  are given to four significant figures. By ingenious doubling, the table is completed up to  $x=1.000$ , and sine values can also be derived: nevertheless, ease of consultation has been subordinated to space-saving, and great care has to be taken that the wrong sign is not selected. A rather simpler table, in steps of only 0.005, is given in Appendix VIII; this should be sufficient for at least the preliminary stages of crystal analysis. For more general work the tables of Buerger (1941b) should be used.

**2.3. Atomic scattering factors.** As explained in section 1.2.4, values of scattering factors have been derived theoretically and have been recorded as functions of  $\sin \theta/\lambda$ ; tables are given in Appendix IV in Volume I and these are used in table 59. To make use of these values they should be plotted against  $\sin \theta$  for the radiation used and a smooth curve drawn through the points; the scattering factor for any particular value of  $\sin \theta$  can then be obtained from this graph.

For some of the lighter elements a degree of choice is offered for the scattering factors derived theoretically, in that the values have been calculated for different degrees of ionization. For example, neutral sodium has eleven electrons, but ionized sodium has only ten. The odd electron, however, is in the outer part of the atom and so its contribution to the scattering factor falls off rapidly; the difference between the two scattering factors is not appreciable above  $\sin \theta/\lambda=0.2$ . Even so, with large unit cells many reflexions may occur below this value.

It is probably unwise, however, to make use of the data precisely; it is unlikely that all the valency electrons from a positively ionized atom are detached from it. Thus, in  $\text{CuSO}_4 \cdot 5\text{H}_2\text{O}$ , the sulphur atom could lose six electrons and so would, at zero value of  $\theta$ , have a scattering factor as low as 10; but Beevers and Lipson (1934) found that the



sulphur atom contained 15 electrons. The best procedure, therefore, seems to be to use the values for the unionized atoms, but to examine the results for the low-angle reflexions critically to see if the agreement between calculated and observed intensities could be improved by taking ionization into account.

**2.4. Temperature factor.** If absolute values of the intensities have been determined experimentally it should be found that for the low-angle reflexions reasonable agreement is obtained with the scattering factors discussed in the last section, but that, as the angle increases, the calculated values gradually become systematically greater than the observed ones. This is due, of course, to the effect of temperature, which has not been taken into account in computing the atomic scattering factors (section 1.2.5). It can be taken into account by multiplying the scattering factors by a quantity  $\exp(-B \sin^2 \theta / \lambda^2)$ , but the value of  $B$  will not in general be known. Some estimate of its value can be found from the comparison of the calculated and observed intensities. Thus, if  $I_o$  is the observed value and  $I_c$  the calculated value of an intensity of reflexion, we have that

$$I_o = I_c \exp(-2B \sin^2 \theta / \lambda^2)$$

$$\text{or} \quad \log \frac{I_o}{I_c} = -2B \sin^2 \theta / \lambda^2. \quad (61)$$

Thus, if the logarithms of the ratios of the observed and calculated intensities are plotted against  $\sin^2 \theta / \lambda^2$ , the slope of the graph should give the value of  $B$ . Fig. 61, from the results of Bradley and Lu (1937)

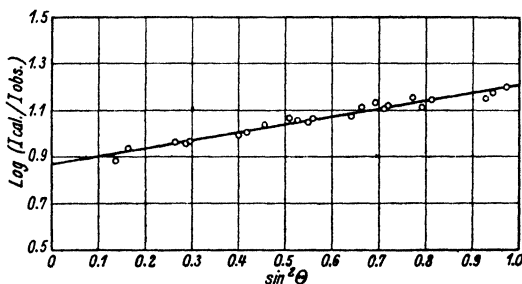


FIG. 61. Derivation of temperature constant for  $\text{Cr}_2\text{Al}$  (Bradley and Lu, 1937)

for  $\text{Cr}_2\text{Al}$ , provides an example of the determination of  $B$  in this way.

A knowledge of the value of  $B$  before the structure is even approximately known would, however, be more useful, and this knowledge can be derived by a method due to Wilson (1942). Wilson makes use of the fact, referred to later (section 5.5.3), that the mean value of  $|F|^2$  is equal to the value of  $\sum f^2$  at a particular value of  $\theta$ . Thus by dividing

the reflexions into groups covering narrow ranges of  $\theta$ , the  $f$  curve could be directly derived. It is more usual, however, to assume the theoretical form of  $f$  curve, and to use Wilson's method to derive the constant B; this is necessary when the crystal contains atoms of different scattering factors which may vary differently with  $\theta$ .

The method can be illustrated by means of the data contained in table 38, the ranges of  $\sin \theta$  being divided more finely, as shown by the broken lines, than was required in section 2.4.5. The mean values for the intensities are shown in the following table, together with the other data which are needed.

TABLE 62  
Deduction of value of temperature constant B for  
metatolidine dihydrochloride,  $C_{14}H_{16}N_2 \cdot 2HCl$

$\langle \sin \theta \rangle$	$\langle \sin^2 \theta / \lambda^2 \rangle$	$\langle I \rangle$	$\langle f_0^2 \rangle$	$\langle I \rangle / \langle f_0^2 \rangle$	$\ln \{ \langle I \rangle / \langle f_0^2 \rangle \}$
·30	·04	875	20·8	42	3·74
·50	·10	612	13·2	46	3·83
·65	·18	315	9·9	32	3·47
·75	·24	263	8·6	31	3·43
·85	·30	204	7·4	28	3·32
·95	·38	77	6·8	11	2·40

The value of  $\langle f_0^2 \rangle$  is taken as the mean of the squares of the scattering factors of carbon, nitrogen and chlorine weighted in the proportions 7 : 1 : 1.

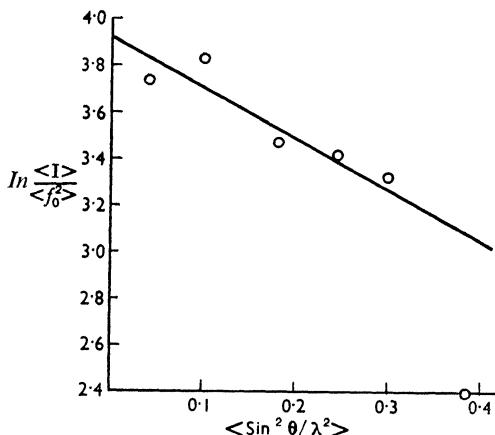


FIG. 62. Graph for finding the temperature factor for metatolidine dihydrochloride. (The last point is unreliable and has been ignored)

To find the value of  $B$ , the logarithms of the values of  $\langle I \rangle / \langle f_0^2 \rangle$  are plotted against  $\sin^2 \theta / \lambda^2$  as shown in fig. 62; the slope of the graph gives the value of  $2B$ .

Although this procedure is reasonably satisfactory for giving the values of scattering factors, some workers may prefer to use empirical scattering factors, such as those given by Robertson (1935*c*) for carbon. Since these scattering factors already include the effects of temperature, they should be much closer approximations than the values of  $f_0$ . But they should be used with caution, since they may not apply accurately to the particular crystal under examination. The more objective procedure just outlined would seem to be preferable.

**2.5. Unitary scattering factors.** Scattering factors of atoms all have maximum values equal to the atomic numbers at zero angle of scattering, and fall off asymptotically to zero at large angles. The rate of fall-off differs from atom to atom; as described in Appendix IV of Volume I, the scattering-factor curves of atoms with Thomas-Fermi electron distributions, and with atomic numbers greater than about 55 (caesium), are similar only if plotted on different scales of  $\sin \theta / \lambda$ . The extent of the similarity of the various  $f$ -curves has been discussed by Harker and Kasper (1948), who have produced the diagram shown in fig. 63 in

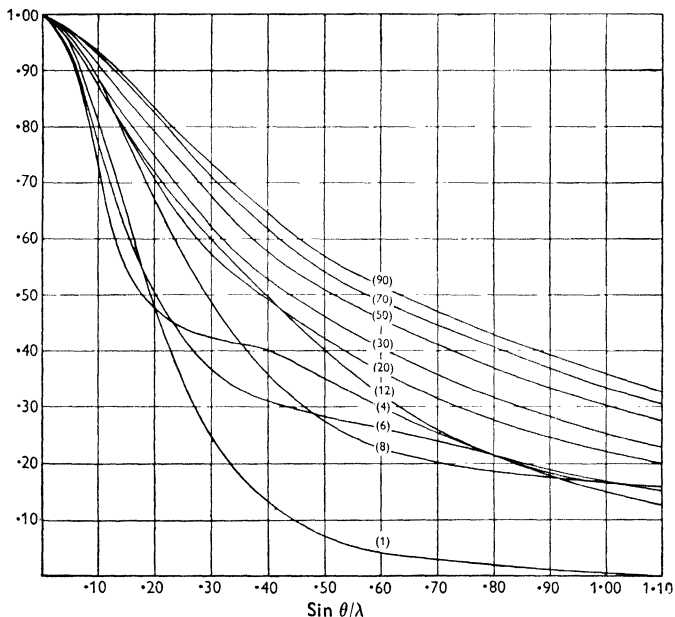


FIG. 63. Unitary scattering factors for atoms whose atomic numbers are shown in parentheses (Harker and Kasper, 1948)

which the  $f$ -curves are shown normalized to have unit value at  $\sin \theta/\lambda = 0$ ; it will be observed that the curves vary erratically in the region of low atomic numbers, but that they gradually become more regular as the atomic numbers increase.

The ordinates of the curves shown in fig. 63 are known as unitary scattering factors, and are represented by the symbol  $\hat{f}_0$ . If the effect of temperature is also taken into account, the symbol is  $\hat{f}$  (' $f$  cap' or ' $f$  hat').

If a crystal contains a number of atoms of similar atomic number, the  $\hat{f}$  curves will be rather similar, and a fair degree of accuracy can be achieved by assuming that they are exactly equal. This simplifies the calculations to a great extent, and is necessary for some of the methods of structure-factor calculation described in Appendix VI; the device should not be used, however, when results of the highest accuracy are required.

*2.6. Adaptation to projections of low symmetry.* When the function  $\cos 2\pi(hx + ky)$  is involved, the methods described in section 3.2.1 can be used if this expression is put into the form  $\cos 2\pi hx \cos 2\pi ky - \sin 2\pi hx \sin 2\pi ky$ . The work involved is not thereby doubled, as may be supposed, because the same set of calculations will serve for both the  $hk0$  and  $\bar{h}k0$  reflexions, the only difference being the change in sign of the second part of the expression. Thus, if this method is used, the  $hk0$  and  $\bar{h}k0$  reflexions should be placed in neighbouring positions in the tables of calculations.

If the direct evaluation of  $\cos 2\pi(hx + ky)$  is preferred, the reflexions should again be grouped in sets with constant  $h$  (or  $k$ ). The value of  $hx$  can be set on a calculating machine and successive multiples of  $y$  added to it (or subtracted for the  $\bar{h}k0$  reflexions); the values of  $\cos 2\pi(hx + ky)$  can then be read from tables without the necessity of transferring the value of  $hx + ky$  to the tables of calculations.

*2.7. Adaptation to projections of higher symmetry.* For symmetries higher than orthorhombic, more complicated expressions arise. For example, in some tetragonal space groups, such as No. 89,  $P4_{22}$ , the expression  $\cos 2\pi hx \cos 2\pi ky + \cos 2\pi kx \cos 2\pi hy$  appears; these two parts must, of course, be treated separately, although they are concerned with only one equivalent set of atoms. More complicated expressions can also appear; for example, the space group No. 92,  $P4_2 2_1 2$ , introduces, for reflexions with  $2h + 2k + l = 4n + 1$ , the expression

$$\begin{aligned} & -\cos \pi(h+k)(x+y) \sin \pi(h-k)(x-y) \sin 2\pi lz \\ & + \sin \pi(h-k)(x+y) \cos \pi(h+k)(x-y) \cos 2\pi lz. \end{aligned}$$

This can best be evaluated in terms of the quantities  $(h+k)/2$  and  $(h-k)/2$ , but this does not apply to reflexions for which  $2h + 2k + l$  is

even. Similar considerations apply to certain hexagonal space groups such as No. 178, P6<sub>1</sub>22.

In the cubic system there are either three, six or twelve products in the expressions for A or B, and these have to be treated separately by calculation. Nevertheless, the expressions are not complicated and appear much less formidable than some that occur in hexagonal space groups.

**2.8. Fourier methods.** The similarity of equation 10.3, which gives the structure factor in terms of the atomic arrangement, and equation 12.3, which gives the electron density in terms of the structure factors, suggests that Fourier methods can be used for computing both electron densities and structure factors. In fact, the Fourier transform of a crystal is its weighted reciprocal lattice, and thus a set of structure factors is merely the Fourier transform of the electron density (section 1.3.3). In practice, therefore, in order to calculate a zone of structure factors, the appropriate electron-density projection must be first expressed as a set of numbers on a regular mesh, these numbers then being used as Fourier coefficients in one of the ways to be described in the next chapter; the sum of the series then gives the required structure factors. This subject will be considered in more detail in sections 4.3.6 and 4.3.7.

### 3. METHODS FOR ISOLATED REFLEXIONS

**3.1. Introduction.** The methods described in the preceding sections are suitable only when a complete two-dimensional or three-dimensional set of structure factors has to be calculated. This, however, is often not required; in the initial stages of the determination of a crystal structure it is more important to establish the correctness or otherwise of a few reflexions, and for this purpose only a few, perhaps unrelated, structure factors need be calculated. In these circumstances each structure factor has to be tackled individually; extreme accuracy is less important than reliability and rapidity, and consequently methods have to be adapted to provide these properties. Calculation can still, of course, be used, but several suggestions have been made which seem to offer more possibilities of easing the work of the initial stages of a structure determination.

**3.2 Structure-factor graphs.** Since in the initial stages we can confine our attention to any chosen reflexions, it is natural to choose those that are most easily calculated, that is, those with one or two indices zero. The latter limitation is usually too severe, and so practically all structure work begins with consideration of intensities with one index zero.

For such reflexions, in the systems of lower symmetry, only two co-ordinates are involved in the structure-factor formulae, and thus it is

possible to evaluate the expression at all points within the unit cell and express these values on a two-dimensional diagram; the contribution to the structure factor of any atom can then be found by multiplying the value of the expression at the atomic position by the atomic scattering factor.

Bragg and Lipson (1936) have suggested that the representation of the structure factor should take the form of contours of constant value, and they proposed that these diagrams should be called structure-factor graphs. Although there are many different formulae to be dealt with, and the graphs would not be of value unless a considerable number of sets of indices were available, the difficulties are not as formidable as might be expected. As we have seen in section 2.8.2, there are only 17 plane groups and therefore the number of separate formulae to be considered is much smaller than the number required for the 230 space groups. The production of structure-factor graphs for limited ranges of indices is therefore quite practicable. The unit cell may, of course, be considered as a square, since the structure factors depend only upon the parameters and not upon the unit-cell dimensions.

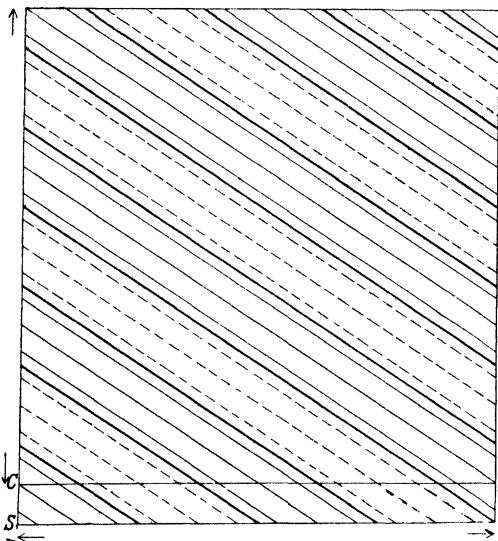


FIG. 66. Graph of  $\cos 2\pi(2x + 3y)$  and  $\sin 2\pi(2x + 3y)$  with contours drawn at 1.0 and 0.5 (thin full lines), 0 (thick lines), and 0.5 and 1.0 (thin broken lines) (Bragg and Lipson, 1936)

It was originally thought by Bragg and Lipson that the structure-factor graphs would be of greatest use for crystals of high symmetry, where the structure-factor formulae (section 3.1.1) are of greatest complexity. It has turned out, however, that they have been of much

greater use for crystals of low symmetry, merely because such crystals occur most frequently. All triclinic, monoclinic and orthorhombic crystals, and projections on the prism faces of tetragonal and hexagonal crystals, are covered by expressions of the type  $\cos 2\pi(hx + ky)$  and  $\cos 2\pi hx \cos 2\pi ky$ .

The graphs can be prepared either by calculation of the shapes of the contours or by evaluation of the function at specific points in the unit cell and drawing the contours by graphical interpolation. For the function  $\cos 2\pi(hx + ky)$  the former method is used; obviously a constant value of  $\cos 2\pi(hx + ky)$  corresponds to a constant value of  $hx + ky$  and so the contours are straight lines of equation  $hx + ky = \text{constant}$ , that is, straight lines of slope  $-k/h$ . An example—the structure-factor graphs for the reflexion 230—is shown in fig. 66.

Although the preparation of graphs for the function  $\cos 2\pi hx \cos 2\pi ky$  is rather more difficult, general principles can again be used. The function is zero when  $hx$  or  $ky$  is equal to  $\frac{1}{4}, \frac{3}{4}, \frac{5}{4}, \dots$ , and thus the unit cell will be divided into sub-cells by straight contours corresponding to zero—nodal lines, as they may be called. Within the various sub-cells, the contours have similar shapes, and so only one sub-cell need be evaluated. Moreover, the contours can be derived from the

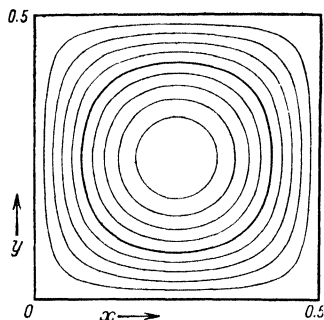


FIG. 67. Graph of contours of basic function  $\sin 2\pi x \sin 2\pi y$  (Bragg and Lipson, 1936)

contours for the basic expression  $\cos 2\pi x \cos 2\pi y$ , which are based on a square sub-cell; for the reflexion  $hk0$  these contours are compressed parallel to the  $a$  direction by a factor  $h$  and parallel to the  $b$  direction by a factor  $k$ .

The basic contours are shown in fig. 67, and their modification for the reflexion 230 is shown in fig. 68 (i). Negative contours are shown by broken lines, but other methods of differentiation, such as colouring, may also be used.

The same graphs may be used for cosine and sine functions by a simple translation of the origin. In fig. 66 the letter  $C$  indicates the origin for the cosine function and the letter  $S$  that for the sine function,

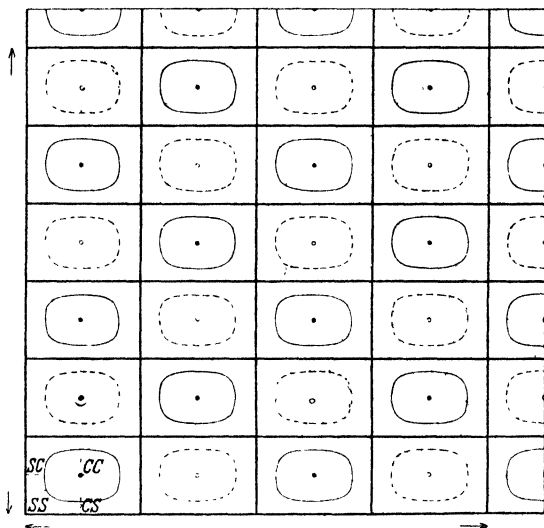


FIG. 68(i). Graph of function  $\cos_{\sin} 4\pi x \times \cos_{\sin} 6\pi y$ , with contours drawn at 1.0 (black spots), 0.5 (thin full lines), 0 (thick lines) 0.5 (thin broken lines) and 1.0 (small circles). The arrows indicate the cell dimensions (Bragg and Lipson, 1936)

and in fig. 68 (i) the four points CC, SC, CS and SS have similar meanings. In addition each graph may be used for the reflexion  $kh0$  also by turning it through  $90^\circ$ .

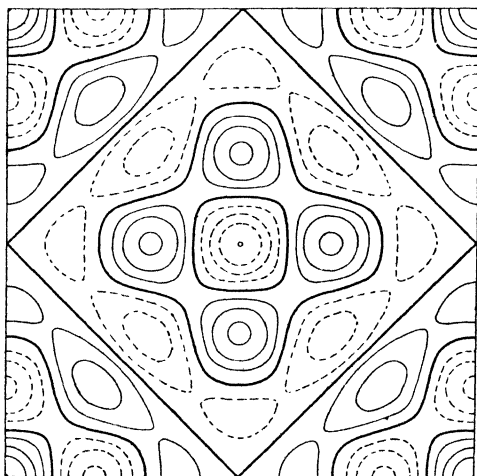


FIG. 68 (ii). A tetragonal 230 structure-factor graph (Bragg and Lipson, 1936)



For projections of higher symmetry the graphs, as shown in figs. 68(ii) and 69, become more complicated; methods of preparing some of them have been described by Beevers and Lipson (1938). In using such graphs, only those points within the asymmetric unit of pattern need be inserted, special positions being allowed for as described in section 3.1.3. This may not always mean that only non-equivalent points need be considered; as Chrobak (1937) points out, if there are symmetry elements inclined obliquely to the plane of projection, all three parameters  $x$ ,  $y$  and  $z$  may be involved and these cannot possibly be represented by a point with two co-ordinates. For example, the triad axes of the cubic system produce equivalent points with relationships of the type  $xyz$ ,  $yzx$ ,  $zxy$ , and in two dimensions these would have to be represented

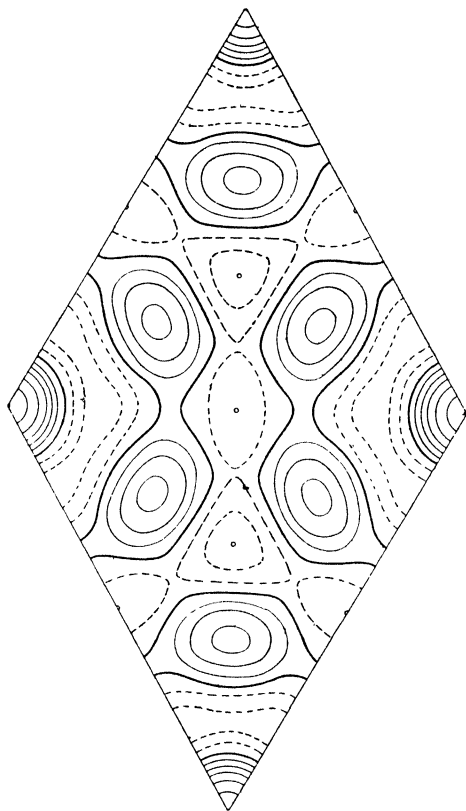


FIG. 69. A hexagonal 1230 structure-factor graph (Bragg and Lipson, 1936)

by the three points  $xy$ ,  $yz$ ,  $zx$ . For this reason, the structure-factor graphs for some of the cubic systems do not reduce to those for the basal plane of the tetragonal system, as might be expected; for example, the graphs for the space group No. 195,  $P2_13$ , reduce to those for the plane group  $pmm$  (cf. section 2.8.2).

For rough work, the graphs are most simply used by plotting the atomic co-ordinates on tracing paper and placing them successively over the different graphs. This is illustrated in figs. 70(a) and (b), which show the evaluation of two of the structure factors included in table 59. For accurate work, variation in the dimensions of the paper on which the graphs are drawn must be allowed for and Bunn (1945)

describes how this may be done for the function  $\cos 2\pi(hx + ky)$ ; for other functions this limitation renders it improbable that high accuracy can be obtained with the graphs.

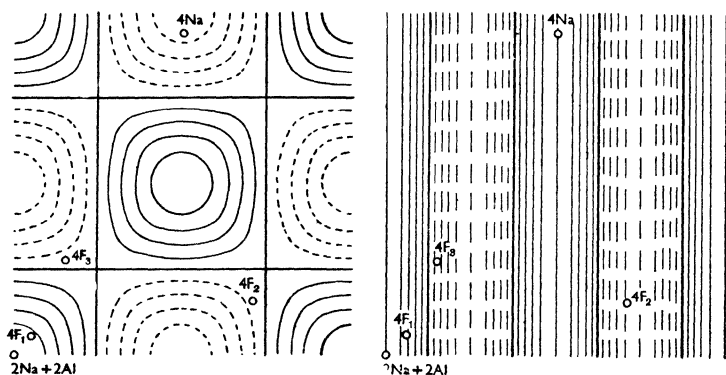


FIG. 70 (a) 110 and (b) 200 structure-factor graph for cryolite, showing positions of atoms. The thick lines are zero contours and the broken lines are negative

A further use of the graphs becomes manifest from figs. 70(a) and (b). It will be noted that certain atoms lie in regions where their contribution to the structure factor changes slowly, whereas other atoms lie on quite steep slopes. Thus, if the agreement between observed and calculated intensity is unsatisfactory, it is obvious which atoms should be moved and in which way. For example, if we wish to increase the intensity of the 200 reflexion the  $F_1$  or the  $F_3$  atoms must be moved to positions with smaller  $x$  parameters; both these sets of atoms lie on steep gradients. A slight change in the positions of the general sodium atoms would be useless, since these lie on maxima; and giving  $F_2$  a larger  $x$  parameter would have a small effect, since this atom lies near a minimum. Consideration of a number of graphs for different reflexions can give useful evidence about possible atomic shifts, as described by Bunn (1945, p. 268).

**3.3. Use of structure-factor graphs for general intensities.** Although the structure-factor graphs were devised for reflexions with one index zero, they can be used also for general reflexions. Suppose, for example, that the structure-factor formula is  $\cos 2\pi hx \cos 2\pi ky \cos 2\pi lz$ . For  $l=1$ , we may write down the value of  $\cos 2\pi z$  against the position of each atom in the projection, and when the value of  $\cos 2\pi hx \cos 2\pi ky$  is read from the chart it can be multiplied by  $\cos 2\pi z$  on a slide rule, the product being entered directly in the table. A separate diagram is thus needed for each value of  $l$  and for the different structure-factor expressions that involve changes in the function of  $lz$ .

3.4. *Figure fields.* Certain difficulties occur in the use of structure-factor graphs, particularly near maxima and minima, where the gradients are changing rapidly; here interpolation becomes rather difficult, and Beevers and Lipson (1938) have suggested that what they call 'figure fields' would be more useful. These are structure-factor graphs which are represented by the values of the functions at specific points in the unit cell. (For certain plane groups calculation of these values is a necessary preliminary to the construction of the graphs.) An interval of division of the cell must be chosen, and if the atomic positions are always represented as multiples of this unit of division, the contributions of the atoms to the structure factor can be read off directly without interpolation. Beevers and Lipson have prepared such figure fields for some hexagonal plane groups, but it would appear that a treatment of lower symmetries would be far more useful.

#### 4. OPTICAL METHODS

4.1. *Fly's eye.* The preceding sections have given a general account of the methods of evaluating structure factors. It must be borne in mind, however, that essentially we are merely deriving the diffraction pattern of the crystal; the reciprocal lattice gives the geometrical conditions governing the various orders of diffraction and the structure factors lead to their relative intensities. In other words, we have to do by calculation what the crystal does naturally, and if we could make a model to diffract X-rays there would be no need for calculation.

This is obviously impracticable; the wave-length of X-rays is much too short. But we might perhaps use another radiation, whose wave-length is long enough to make practicable the construction of models of corresponding size. The advantages of visible light are obvious, but even with this radiation the wave-length is so small that considerable difficulties arise in its use. These difficulties have been largely overcome in a device suggested by W. L. Bragg (1944) and described in detail by Bunn (1945, p. 271); it is known as the 'Fly's Eye', because it forms a large number of images of a single object instead of the single image that the human eye forms on the retina.

The apparatus is suitable only for dealing with zones of intensities. These intensities depend on the projection of the structure on a plane, and the fly's-eye apparatus is a device for preparing a set of images, regularly spaced in two dimensions, corresponding to the projections of the contents of neighbouring unit cells. These images are produced by a set of regularly spaced pin-holes, which is made by photographing a drawing consisting of a square array of 625 black spots, of about 2 mm. diameter, separated by a distance of about 2 cm.; the negative (fig. 71)

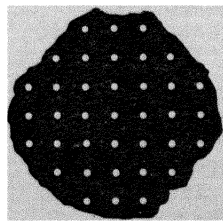


FIG. 71. Portion of multiple pin-hole camera (fly's eye) (Bunn, 1945)

is then the set of apertures required. It is convenient if the holes cover a square of about 1 cm. side; the large reduction required can best be obtained in two stages and this is convenient since the final image has black spots on a transparent background from which reproductions may be taken.

The set of apertures is placed at a distance of about 1 mm. from, and accurately parallel to, a photographic plate. If the device is exposed to a point source of light at a distance of about a metre, after development the plate will be found to contain a set of black spots regularly spaced. If, before development, the lamp is moved to another position and the plate exposed again, two sets of regularly spaced spots will be produced. The ratio of the separation of the spots to the spacing of the orifices can easily be controlled, and thus, by exposing the plate to the source moved successively to several different positions, patterns of high degree of complexity may be produced, the detail being limited either by the fineness of the orifices in the fly's eye, or by diffraction effects if these orifices are made too small.

Atomic arrangements can be simulated by moving the source to various positions to give spots with the correct parameters with respect to the sides of the square unit cell; an example is shown in fig. 72. Atoms of different scattering factors can be simulated by exposing the plate for different periods of time. In this way a diffraction grating is produced with 625 elements each representing the projection of the contents of one unit cell. The diffraction pattern of this grating should therefore represent the X-ray diffraction pattern of the crystal.

The spacing of the grating is about 0.04 cm., and thus light of wavelength  $5 \times 10^{-5}$  cm. would be diffracted through angles of a few minutes of arc; special apparatus is therefore needed for viewing the diffraction pattern. The grating must be placed in a parallel beam of light which Bunn obtains by means of a microscope with a substage lens, illuminated by a point source of monochromatic light. The microscope is focused to give an image of the point source, and, when the grating is placed on the stage, its diffraction pattern is seen in the microscope; as an example, the diffraction pattern of the grating shown in fig. 72 is also reproduced.

This device is extremely useful for testing large numbers of structures; the operation of testing a hypothetical structure can be carried out in less than an hour, and if many structures are to be tried, the rate is considerably faster than one per hour, since different parts of the operations can be carried out simultaneously.

The grating has black spots on a transparent background. This is disadvantageous, since the zero order of diffraction is outstandingly strong, and may 'swamp' the neighbouring orders which are, of course, particularly important. This difficulty may be overcome by reversing the grating, so that it consists of transparent spots on an opaque background; by Babinet's theorem (Drude, 1929, p. 221) the

# PLATE II

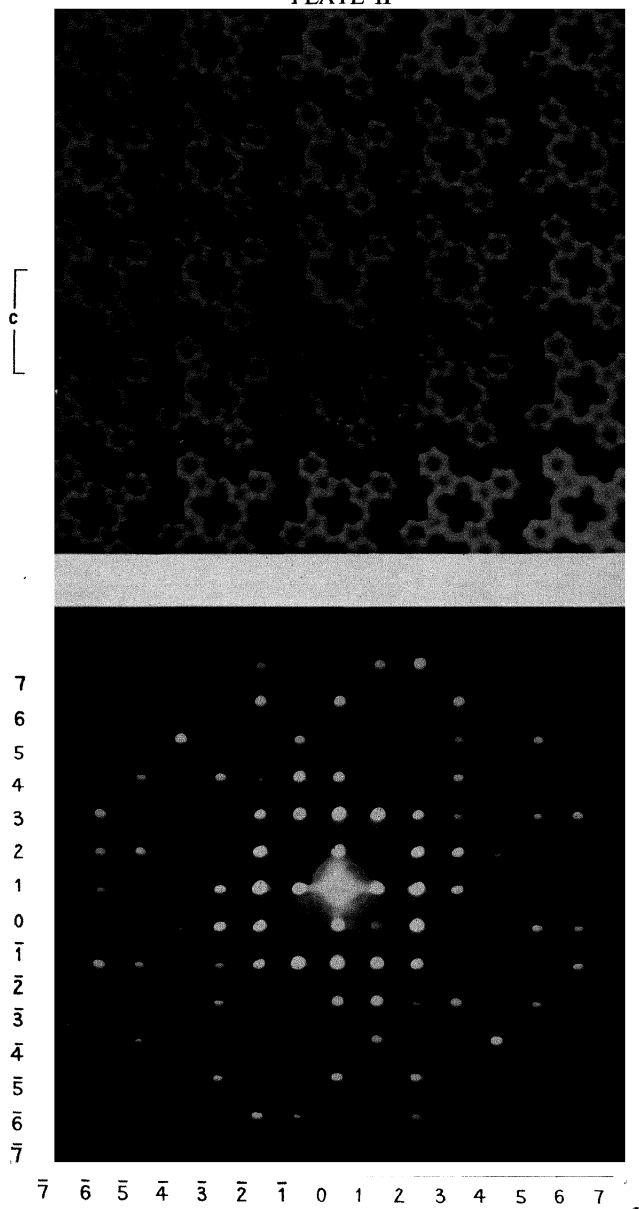


FIG. 72. *Above* : Pattern representing projection of phthalocyanine crystal on (010). *Below* : Optical diffraction pattern (Bunn, 1945)



diffraction pattern is still the same except at zero angle. Alternatively, instead of forming the grating by means of a moving lamp, a uniformly illuminated screen with black circles on it may be used (Bragg and Stokes, 1945). The grating will then be directly in the form required, and the procedure for making it is rather simpler.

Improvement in the diffraction pattern may be obtained by placing the grating between two optically flat glass plates, with oil of refractive index 1.5 in the interstices. This procedure will eliminate possible errors due to unevenness in the emulsion of the grating, which would produce irregular phase differences in the diffracted light.

Hanson and Lipson (1952*a*) have suggested a further simplification; they show that even with only four unit cells an adequate representation of the reciprocal lattice is obtained, although the spots are, of course, rather large. The atomic positions in the four unit cells take the form of holes in an opaque card, and thus the photographic processes preliminary to the production of the diffraction pattern are dispensed with; the time for testing a structure is thus reduced to a few minutes. The method has been used successfully in the determination of the structure of *p*-di-isocyanobenzene (Hulme, 1952), the comparison of the optical diffraction pattern and the weighted reciprocal lattice being shown in fig. 74(i).

When the atoms in the structure are nearly all of equal weight, the fly's-eye method works well, and was used with great success by Bunn and Turner-Jones for establishing the structure of sodium benzyl penicillin (Crowfoot, et al., 1949). As can be seen in fig. 72 the spots representing the atoms are rather blurred, and their scattering factors seem to resemble remarkably closely the scattering factors of true atoms. When a wide range of atoms is involved, however, difficulties arise in simulating their scattering factors: a longer exposure not only produces more developable silver grains in the emulsion, but also spreads them over a larger area; the scattering factor thus falls off more rapidly for the heavier atoms, in contrast to true scattering factors (section 3.2.3). Thus the accuracy is greatly reduced, particularly for the higher orders.

Bragg and Stokes (1945) have suggested an improvement that can overcome this difficulty and, indeed, is more closely analogous to the fly's eye in that it uses a set of small lenses rather than pin-hole orifices. The lenses are made by pressing a steel ball into a copper block, and making a replica of the resulting impressions by pressing hot perspex on to it. The result is a series of small lenses embossed on the surface of the perspex. If care is taken to see that the depressions on the mould are all of equal depth, and that the other surface of the perspex is flat, then the principal foci of the perspex lenses are all in one plane, and a lamp at a reasonable distance away will give a series of sharp images in this plane (Stokes, 1946).

The fact that the images are now focused enables certain refinements

to be introduced. For example, an atom may be represented by a ring instead of a spot. The advantage of this is that atomic scattering factors may be accurately simulated: a light atom may be represented by a ring of large radius and small thickness, so that the amount of light transmitted is small, but the scattering also falls off rapidly with angle; and a heavy atom may be represented by a thick ring of small radius (De Vos, 1948). Of course, such representations are not perfectly accurate, and better approximations could be obtained by series of rings, but in view of the lack of accuracy in our knowledge of scattering factors the representation by single rings is probably good enough for many purposes.

In practice, unless the projection of the unit cell is square, atoms have to be represented by ellipses. De Vos produced these ellipses by cutting them from black paper and laying them on an illuminated screen, as suggested by Bragg and Stokes. The grating produced then consists of transparent ellipses on a black background (fig. 74(ii)).

This more elaborate form of the apparatus has certain disadvantages. First, the dimensions of the ellipses have to be calculated in advance, from the shapes of the unit cells and the variation of scattering factors with angle. Secondly, since it is hardly practicable to prepare the set of lenses with spacing less than 1 mm., the resultant grating covers a large area and so the spectra cannot be viewed in a microscope; a special apparatus (Bragg and Lipson, 1943) has to be used. Thus, on the whole, it would appear to be better to make use of the simpler device first, unless it is definitely known that the inaccuracies it introduces make the results of little value.

**4.2. *Fourier-transform method.*** It was explained in section 1.4.2. that the structure amplitude of a particular reflexion is proportional to the amplitude of the radiation scattered at the same angle by a single unit of pattern with the same orientation as the units in the crystal. In fact, the process of calculating structure factors is essentially the 'sampling' of the scattering of the unit of pattern at specific points—the reciprocal-lattice points. If the unit is of known dimensions, its scattering factor can be calculated, and the relative values of the structure amplitudes of the various reflexions can be found by superimposing the reciprocal lattice on to this scattering factor and observing the values at the reciprocal lattice points; if these values do not agree with those observed, then other orientations of the reciprocal lattice can be tried until a match is found.

There are many difficulties in the way of application of the method. First, the scattering factor of the unit is a complicated function; it does not fall off gradually to zero as the scattering factor of a single atom does, and the variation is different in different directions. In other words, it is three-dimensional, the dimensions being the same as those of the reciprocal lattice. Secondly, the method can obviously be used



# PLATE III

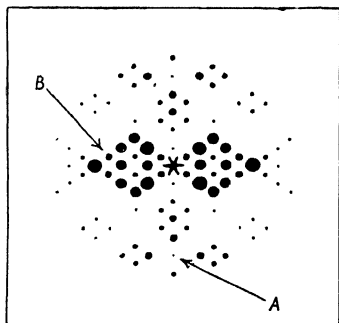
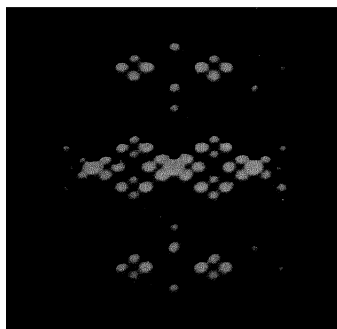


FIG. 74 (i). Comparison of optical diffraction pattern from mask representing four unit cells of para-diisocyanobenzene and weighted reciprocal lattice. A and B are points lying on small and large gradients, respectively (Hanson & Lipson, 1952a)

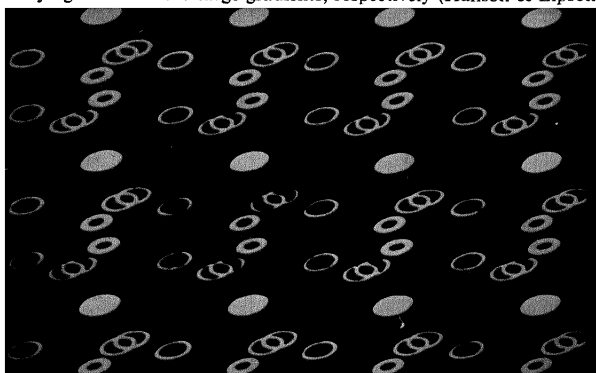


FIG. 74 (ii). Pattern representing projection of diopside crystal on (010). The white ellipses represent superimposed Ca and Mg atoms, the thick elliptical rings represent Si atoms, and the thin elliptical rings represent O atoms (De Vos, 1948)

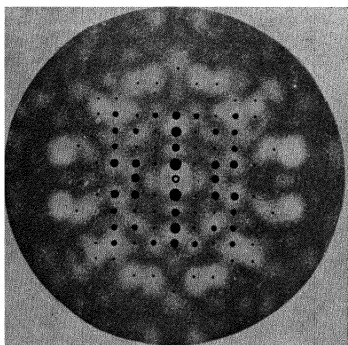


FIG. 74 (iii). Optical transform of unit cell of naphthalene structure projected on (100). The black spots superimposed represent the weighted reciprocal lattice, the area of each spot being approximately proportional to the structure amplitude (Lipson and Taylor, 1951)



only in two dimensions, and, although this simplifies the calculations, it means that the orientation with respect to the plane chosen for projection has to be assumed (Knott, 1940; Wrinch, 1946). Thirdly, in order that the scattering factor—the Fourier transform—should be of practical use, its value must be calculated at points much closer together than the reciprocal-lattice points. The work of calculating a set of structure factors for a zone of a reasonably complicated structure is considerable, and a ten-fold multiplication of the work, which would still give only a third of the interval between the reciprocal lattice points, is not to be lightly contemplated.

This third difficulty is the most serious, and if the method is to come into general use, methods of evaluating the scattering factors other than by calculation must be devised. Bragg (1944) has suggested using light. A card may be punched with holes representing the atomic positions in the projection of the unit and the diffraction pattern in parallel light—the Fraunhofer diffraction pattern—represents the required Fourier transform. This may be photographed, and a reciprocal-lattice section, drawn to the corresponding scale, can be superimposed upon it and rotated about the common origin until the required relationships between the various intensities are found. Examples of the use of this process are given in figs. 74(iii) and 238.

The device has great potentialities. The time of testing a proposed structure is limited mainly by the making of the diffracting mask, and different orientations in the plane of projection can be tried out extremely rapidly. Different masks can be made to represent different dispositions of atoms, or to represent different orientations of a molecule, and the method, as applied by Lipson and Taylor (1951), would seem to be extremely well suited to the trial-and-error methods of structure determination described in Chapter 5. A further discussion of the method is also given in Chapter 7.

## CHAPTER 4

### SUMMATION OF FOURIER SERIES

#### 1. GENERAL FORMULAE

##### 1.1 Elimination of complex quantities. Equation (12.3)

$$\rho(x, y, z) = \frac{1}{V} \sum \sum \sum F(hkl) \exp \{ -2\pi i(hx + ky + lz) \}$$

is not suitable for quantitative evaluation of electron densities since it contains complex quantities; these quantities must therefore be resolved into their real and imaginary parts. The process of resolution may be described most simply by considering a single term only— $F(hkl) \exp \{ -2\pi i(hx + ky + lz) \}$ , which can be expressed as

$$\{A'(hkl) + iB'(hkl)\} \{ \cos 2\pi(hx + ky + lz) - i \sin 2\pi(hx + ky + lz) \},$$

where  $A'$  and  $B'$  are the two components of  $F$  (section 1.2.6). We may now combine this expression with that for the conjugate term ( $\bar{h}\bar{k}\bar{l}$ ), which gives:

$$\begin{aligned} & \{A'(hkl) + iB'(hkl)\} \{ \cos 2\pi(hx + ky + lz) - i \sin 2\pi(hx + ky + lz) \} \\ & + \{A'(\bar{h}\bar{k}\bar{l}) + iB'(\bar{h}\bar{k}\bar{l})\} \{ \cos 2\pi(hx + ky + lz) + i \sin 2\pi(hx + ky + lz) \} \\ & = 2A'(hkl) \cos 2\pi(hx + ky + lz) + 2B'(hkl) \sin 2\pi(hx + ky + lz), \quad (76.1) \end{aligned}$$

since  $A'(\bar{h}\bar{k}\bar{l}) = A'(hkl)$  and  $B'(\bar{h}\bar{k}\bar{l}) = -B'(hkl)$ . This expression is suitable for numerical calculation, if all the values of  $A'(hkl)$  and  $B'(hkl)$  are known.

In performing the summation, it must be remembered that the expression does not apply to the term 000, which has no conjugate (or more strictly, is its own conjugate). Thus the factor 2 in expression 76.1 has to be omitted for this term only, and the expression for the electron density is

$$\rho(x, y, z) = \frac{1}{V} \left[ F(000) + 2 \sum_{h=0}^{\infty} \sum_{k=-\infty}^{\infty} \sum_{l=-\infty}^{\infty} A'(hkl) \cos 2\pi(hx + ky + lz) + B'(hkl) \sin 2\pi(hx + ky + lz) \right], \quad (76.2)$$

the summation being taken over only half the complete reciprocal lattice, excluding the term for which  $h=k=l=0$ .

Equation 76.2 gives the general expression from which all others are derived, and it is probably the best form for evaluation. It can, however, be expressed more simply if a phase angle  $\alpha$  is introduced (section 1.3.1); this angle is defined by the equations

$$\left. \begin{aligned} \tan \alpha(hkl) &= B'(hkl)/A'(hkl), \\ \text{whence} \quad A'(hkl) &= |F(hkl)| \cos \alpha(hkl), \\ \text{and} \quad B'(hkl) &= |F(hkl)| \sin \alpha(hkl). \end{aligned} \right\} \quad (76.3)$$

Equation 76.2 becomes

$$\rho(x, y, z) = \frac{1}{V} \left[ F(000) + 2 \sum_{h=0}^{\infty} \sum_{k=-\infty}^{\infty} \sum_{l=-\infty}^{\infty} |F(hkl)| \cos \{2\pi(hx + ky + lz) - \alpha(hkl)\} \right]. \quad (77)$$

**1.2. Formulae for different space groups.** Although equation 77.1 holds generally for all crystals, some simplification in its application may be obtained by making use of any symmetry that the reciprocal lattice might possess. For example, if a crystal has a centre of symmetry at the origin,  $F(hkl) = F(\bar{h}\bar{k}\bar{l})$ ; the structure factors are therefore all real (section 3.1.1) and the expression for the electron density becomes

$$\rho(x, y, z) = \frac{1}{V} \left[ F(000) + 2 \sum_{h=0}^{\infty} \sum_{k=-\infty}^{\infty} \sum_{l=-\infty}^{\infty} F(hkl) \cos 2\pi(hx + ky + lz) \right].$$

Corresponding results follow from the presence of other types of symmetry elements; for example, if the crystal has a two-fold axis along the  $b$  axis (space group No. 3,  $P2_1$ ), the relationship between the structure factors is that  $F(hkl) = F(\bar{h}k\bar{l})$ ; thus if we combine the terms  $F(hkl)$ ,  $F(\bar{h}k\bar{l})$ ,  $F(h\bar{k}l)$  and  $F(\bar{h}k\bar{l})$  we obtain

$$\rho(x, y, z) = \frac{1}{V} \left[ F(000) + 2 \sum \sum \sum |F(hkl)| \cos \{2\pi(hx + ky + lz) - \alpha(hkl)\} + |F(\bar{h}k\bar{l})| \cos \{2\pi(-hx + ky - lz) - \alpha(\bar{h}k\bar{l})\} \right],$$

the summation not including the term  $F(000)$ .

Because of the relationship between the structure factors,  $|F(hkl)| = |F(\bar{h}k\bar{l})|$  and  $\alpha(hkl) = \alpha(\bar{h}k\bar{l})$ , and thus the separate terms in the summation are

$$4|F(hkl)| \cos 2\pi(hx + lz) \cos \{2\pi ky - \alpha(hkl)\}.$$

This result will not however apply to the terms  $F(0k0)$  and  $F(h0l)$ , since there are not four of them to make a set. The complete expression for the electron density therefore includes the expressions  $F(000)$ ,

$$2 \sum_{k=1}^{\infty} |F(0k0)| \cos \{2\pi ky - \alpha(0k0)\}$$

and 
$$2 \sum_{h=0}^{\infty} \sum_{l=-\infty}^{\infty} F(h0l) \cos 2\pi(hx + lz),$$

the general triple summation not including these terms, and the double summation not including the term  $F(000)$ .

An extra complication arises for space groups that contain screw axes and glide planes. In the space group No. 11,  $P2_1/m$ , for example, the structure-factor formulae are

$$A = 4 \cos 2\pi(hx + lz) \cos 2\pi ky, \quad B = 0, \text{ if } k \text{ is even,}$$

and 
$$A = -4 \sin 2\pi(hx + lz) \sin 2\pi ky, \quad B = 0, \text{ if } k \text{ is odd.}$$

Thus the relationships between the structure factors are different for these two classes of reflexion; for those with  $k$  even, the relationships are  $F(hkl) = F(h\bar{k}l) = F(\bar{h}kl) = F(\bar{h}\bar{k}l)$ , while for those with  $k$  odd the relationships are  $F(hkl) = -F(h\bar{k}l) = -F(\bar{h}kl) = F(\bar{h}\bar{k}l)$ . The summation for the terms with  $k$  even is thus different from the summation for terms with  $k$  odd, which contains expressions such as:

$$\begin{aligned} & F(hkl) \cos 2\pi(hx + ky + lz) + F(\bar{h}\bar{k}l) \cos 2\pi(-hx + ky - lz) \\ &= F(hkl) \cos 2\pi(hx + ky + lz) - F(hkl) \cos 2\pi(-hx + ky - lz) \\ &= -2F(hkl) \sin 2\pi(hx + lz) \sin 2\pi ky. \end{aligned}$$

The expression for the electron density then includes the general terms

$$4 \sum_{-\infty}^{+\infty} \sum_{\frac{1}{2}}^{\infty} \sum_0^{\infty} F(hkl) \cos 2\pi(hx + lz) \cos 2\pi ky,$$

( $k$  even)

$$\text{and} \quad -4 \sum_{-\infty}^{+\infty} \sum_1^{\infty} \sum_0^{\infty} F(hkl) \sin 2\pi(hx + lz) \sin 2\pi ky, \quad (78.1)$$

( $k$  odd)

the multiplicities of the special terms  $F(000)$ ,  $F(0k0)$  and  $F(h0l)$  being the same as those set out on page 77. (It will be noted that, since this space group has a centre of symmetry, we can specify the structure factors themselves, not merely their moduli.)

In other space groups still more subdivisions may have to be made. A complete list of the formulae is given by Lonsdale (1936), but the mode of description is not quite the same as that adopted in this book; the special reflexions, such as  $0k0$ , are not listed separately, but, on the other hand, reflexions with the same numerical indices but different signs *are* listed separately. For example, in the triclinic space groups separate summations are given for the terms  $hkl$ ,  $\bar{h}kl$ ,  $h\bar{k}l$ , and  $h\bar{k}\bar{l}$ , the summation in each case being from zero to infinity. It is important to realize, if Lonsdale's tables are used, that special terms— $F(000)$  always and others sometimes—have different numerical factors from those listed, as explained in the introduction to the tables.

In the International Tables (1952) the expression for the electron density in terms of the general structure factors only is given. For the space group No. 11,  $P2_1/m$ , the expression is

$$\begin{aligned} \rho(\text{XYZ}) = & \frac{4}{V_c} \left\{ \sum_0^{\infty} \sum_0^{\infty} \sum_0^{l=2n} [F(hkl) \cos 2\pi(hX + kY) \right. \\ & + F(\bar{h}kl) \cos 2\pi(-hX + kY)] \cos 2\pi lZ - \sum_0^{\infty} \sum_0^{\infty} \sum_0^{l=2n+1} [F(hkl) \sin 2\pi(hX + kY) \\ & + F(\bar{h}kl) \sin 2\pi(-hX + kY)] \sin 2\pi lZ \}. \end{aligned} \quad (78.2)$$

It will be noted that the coordinates (XYZ) of a general point in the unit cell are printed differently from the coordinates (xyz) representing an atomic position. In this book, no differentiation has been made.

1.3. *Projections on to planes and lines.* The summation of series such as 77.1 and 78 involves a great deal of work; not only are the calculations themselves tedious, but the labour of obtaining the coefficients from the observed X-ray reflexions is also great, since *all* the reflexions observable have to be considered. A considerable reduction in the amount of work can be achieved by considering the projection of a structure on to a plane (Bragg, 1929a). The information obtained is less than that given by three-dimensional summations, but the work is curtailed by such a large factor that for some time only two-dimensional methods were considered practicable; even at present three-dimensional methods are used only to establish detail of considerable importance.

The electron density projected on to a point (x, y) in the (001) face of the unit cell is given by the equation:

$$\begin{aligned}\rho(x, y) &= \int_0^1 \rho(x, y, z) c \, dz \\ &= \frac{c}{V} \int_0^1 \sum \sum \sum F(hkl) \exp \{ -2\pi i(hx + ky + lz) \} \, dz \\ &= \frac{1}{A_c} \sum \sum \sum F(hkl) \exp \{ -2\pi i(hx + ky) \} \int_0^1 \exp \{ -2\pi ilz \} \, dz,\end{aligned}$$

where  $A_c$  is the area of the projection of the unit cell. Since  $\exp 2\pi ilz = \cos 2\pi lz + i \sin 2\pi lz$ , the integral is zero for all values of  $l$  except zero; when  $l$  is zero, the integral is unity and the equation becomes:

$$\rho(x, y) = \frac{1}{A_c} \sum_h \sum_k F(hk0) \exp \{ -2\pi i(hx + ky) \}. \quad (79)$$

We see therefore that the projected electron density can be obtained from the data given by a single zone of X-ray reflexions.

Similar equations apply to projections on other faces of the unit cell, and the same theory may be applied to oblique planes also; in general, if we make use of that section of the reciprocal lattice for which  $ph + qk + rl = 0$ , we obtain the electron density projected on the plane ( $pqr$ ). Naturally the most information will be obtained when the period of repetition in the direction of the projection is small, and this will usually happen when the electron density is projected along one of the crystallographic axes. But exceptional cases may arise when this is not so, and other directions of projection should then be considered; centred lattices, in particular, can lead to such conditions. For example, if a crystal has a lattice C, a Fourier series with the values of  $F(hhl)$  as coefficients will give the electron density projected on the plane ( $1\bar{1}0$ ).

An atom at the point  $x, y, z$  will project exactly at the same position as an atom at  $\frac{1}{2} + x, \frac{1}{2} + y, z$ , and thus, in effect, the period of repetition in the direction of projection is  $\frac{1}{2}(a^2 + b^2)^{\frac{1}{2}}$ ; this may be less than  $a$  or  $b$  separately.

Electron densities can also be projected on to lines. For the projection on to a cell edge we have

$$\begin{aligned}\rho(x) &= \int_0^1 \rho(x, y) b \, dy \\ &= \frac{bc}{V} \sum_h \sum_k F(hk0) \exp \{ -2\pi i h x \} \int_0^1 \exp \{ -2\pi i k y \} \, dy \\ &= \frac{bc}{V} \sum_h F(h00) \exp \{ -2\pi i h x \},\end{aligned}\quad (80)$$

since the integral is zero unless  $k = 0$ . To evaluate  $\rho(x)$  we need to know only the structure factors of a set of orders from a single set of planes, but, of course, the information is of much less value.

**1.4. Partial three-dimensional summations.** Two-dimensional projection has, so far, proved to be the most popular method of application of Fourier synthesis; the work involved in obtaining the data for and summing a three-dimensional series is so great that, as stated in the previous section, it is reserved for the most important problems. A compromise, however, may be arrived at; information may be obtained from a knowledge of the data contained in the complete observable reciprocal lattice without the necessity for the complete summation of the three-dimensional series. For example, a single section at a constant value of one parameter may be chosen, or a particular line in the unit cell along which two-dimensional summations indicate that there is a high electron density.

In addition to these possibilities, Booth (1945c) has suggested two others. The first is the projection of the contents of the unit cell lying between two planes, say  $z = z_1$  and  $z = z_2$  (the bounded projection). If interest lies in the  $x$  and  $y$  parameters of atoms that are known to lie between these two planes, there is no need to confine attention to the precise planes in which these atoms lie.

Let us call the density projected in this way  $\rho_{12}(x, y)$ . Then

$$\begin{aligned}\rho_{12}(x, y) &= \int_{z_1}^{z_2} \rho(x, y, z) c \, dz \\ &= \frac{c}{V} \int_{z_1}^{z_2} \sum_h \sum_k \sum_l F(hkl) \exp \{ -2\pi i (hx + ky + lz) \} \, dz \\ &= \frac{1}{A_c} \sum_h \sum_k \sum_l \frac{F(hkl)}{-2\pi i l} [\exp \{ -2\pi i (hx + ky + lz_2) \} \\ &\quad - \exp \{ -2\pi i (hx + ky + lz_1) \}]\end{aligned}$$



$$\begin{aligned}
&= \frac{1}{A_c} \sum \sum \sum \frac{F(hkl)}{2\pi l} [\sin 2\pi(hx + ky + lz_2) \\
&\quad + i \cos 2\pi(hx + ky + lz_2) - \sin 2\pi(hx + ky + lz_1) \\
&\quad - i \cos 2\pi(hx + ky + lz_1)] \\
&= \frac{1}{A_c} \sum \sum \sum \frac{F(hkl)}{2\pi l} \left[ 2 \cos 2\pi \left( hx + ky + l \frac{z_2 + z_1}{2} \right) \sin \pi l(z_2 - z_1) \right. \\
&\quad \left. - 2i \sin 2\pi \left( hx + ky + l \frac{z_2 + z_1}{2} \right) \sin \pi l(z_2 - z_1) \right] \\
&= \frac{1}{A_c} \sum \sum \sum \frac{F(hkl)}{\pi l} \sin \pi l(z_2 - z_1) \\
&\quad \left\{ - \exp 2\pi i \left( hx + ky + l \frac{z_2 + z_1}{2} \right) \right\}.
\end{aligned}$$

By methods similar to those used in section 4.1.1, this expression can be shown to be equal to

$$\frac{1}{A_c} \sum \sum \sum \frac{F(hkl)}{\pi l} \sin \pi l(z_2 - z_1) \cos 2\pi \left\{ hx + ky + l \frac{z_2 + z_1}{2} - \alpha(hkl) \right\}, \quad (81.1)$$

the summation now being taken over half the reciprocal lattice.

The summation may be made by combining the quantity  $l(z_2 + z_1)/2$  with  $\alpha(hkl)$ , and then proceeding in the way described in section 4.1.1—that is, the A and B parts of the coefficients should be calculated. For a crystal with a centre of symmetry the summation may be expressed as

$$\begin{aligned}
\frac{1}{A_c} \sum \sum \sum \left[ \frac{F(hkl) \sin \pi l(z_2 - z_1) \cos \pi l(z_2 + z_1)}{\pi l} \cos 2\pi(hx + ky) \right. \\
\left. - \frac{F(hkl) \sin \pi l(z_2 - z_1) \sin \pi l(z_2 + z_1)}{\pi l} \sin 2\pi(hx + ky) \right]. \quad (81.2)
\end{aligned}$$

The quantities  $F(hkl)$  have therefore to be multiplied by factors that, for given values of  $z_2$  and  $z_1$ , are functions of  $l$  only, and can therefore be evaluated separately for the few different values of  $l$  to be considered. The new coefficients having been obtained, the summation follows the ordinary lines of a two-dimensional summation.

It will be noted that, though the computational work is not large, all the values of  $F(hkl)$  have to be known, and thus the labour of interpretation of photographs and derivation of structure factors is still as large as for a complete three-dimensional synthesis. In special cases, this labour can be reduced to some extent. For example, if we wish to project the contents of half the unit cell,  $z_2 - z_1 = \frac{1}{2}$ , and thus the value of  $\sin \pi l(z_2 - z_1)$  is zero if  $l$  is even; consequently, the reflexions with  $l$  even, but not zero, need not be measured. If  $l$  is zero, the quantity  $\{\sin \pi l(z_2 - z_1)\}/\pi l$  is equal to  $z_2 - z_1$  and so the terms with  $l$  zero do not disappear when  $z_2 - z_1 = \frac{1}{2}$ .

Booth (1945c) has also shown how it is possible to add together the electron densities in several parallel sections by methods that are no more tedious than those for a single section. This operation would be useful if one required, say, the  $x$  and  $y$  parameters of several different atoms whose  $z$  parameters were already known; the parameters must, of course, be known approximately as the result gives no indication of which  $x$  and  $y$  parameters are associated with a particular  $z$  parameter.

## 2. REDUCTION OF FORMULAE FOR SYSTEMATIC CALCULATION

2.1. *General principles for three-dimensional summations.* We have seen in section 4.1.1 how the expression for the electron density in a crystal can be reduced to include real quantities only; but there still remains the practical problem of performing the summation. Equation 76.2, despite its apparently greater complexity, forms a better starting point than equation 77.1, since it does not contain the quantities  $\alpha(hkl)$ , which may have any value between  $0^\circ$  and  $360^\circ$ . Nevertheless, equation 76.2 still includes the terms  $\cos 2\pi(hx + ky + lz)$  and  $\sin 2\pi(hx + ky + lz)$ , and thus each index cannot be considered separately, as they could be if terms such as  $\cos 2\pi hx \cos 2\pi ky \cos 2\pi lz$  occurred. This difficulty can be overcome by expanding  $\cos 2\pi(hx + ky + lz)$  and  $\sin 2\pi(hx + ky + lz)$  into the forms:

$$\begin{aligned}\cos 2\pi(hx + ky + lz) &= \cos 2\pi hx \cos 2\pi ky \cos 2\pi lz - \cos 2\pi hx \sin 2\pi ky \sin 2\pi lz \\ &\quad - \sin 2\pi hx \cos 2\pi ky \sin 2\pi lz - \sin 2\pi hx \sin 2\pi ky \cos 2\pi lz \\ \text{and } \sin 2\pi(hx + ky + lz) &= \sin 2\pi hx \cos 2\pi ky \cos 2\pi lz \\ &\quad + \cos 2\pi hx \sin 2\pi ky \cos 2\pi lz + \cos 2\pi hx \cos 2\pi ky \sin 2\pi lz \\ &\quad - \sin 2\pi hx \sin 2\pi ky \sin 2\pi lz.\end{aligned}$$

The disadvantage of expanding each single term into four is offset by the fact that the calculations need to be carried out for only one eighth of the unit cell; the separate terms can be changed in sign appropriately to provide the electron densities at the points  $(x, y, z)$ ,  $(\bar{x}, y, z)$ ,  $(x, \bar{y}, z)$ ,  $(x, y, \bar{z})$ ,  $(x, \bar{y}, \bar{z})$ ,  $(\bar{x}, y, \bar{z})$ ,  $(\bar{x}, \bar{y}, z)$  and  $(\bar{x}, \bar{y}, \bar{z})$ .

The advantage of expressing the separate terms as triple products is brought out by considering the problem in detail. The general case of a crystal with no symmetry has been discussed by Goodwin and Hardy (1938), but the principles can be explained rather more simply by considering terms of the form  $F(hkl) \cos 2\pi hx \cos 2\pi ky \cos 2\pi lz$ , which arise in the orthorhombic system. The summation can be written as

$$\sum_l \left\{ \sum_k \left\{ \sum_h F(hkl) \cos 2\pi hx \right\} \cos 2\pi ky \right\} \cos 2\pi lz.$$

The expression between the braces is a one-dimensional series, and can be summed for particular values of  $k$  and  $l$ , the ordinates of the curve so obtained representing values of each summation for particular values of  $x$ ; by completing the summations for the various groups of

reflexions with given values of  $k$  and  $l$  we obtain quantities that are characteristic of certain values of  $x$ ,  $k$  and  $l$ : let us call them  $C(x, k, l)$ .

The summation now is

$$\sum_l [\sum_k C(x, k, l) \cos 2\pi ky] \cos 2\pi lz.$$

We can now divide the values of  $C(x, k, l)$  into sets with constant  $l$ , and again perform separate one-dimensional summations, each ordinate of which now is a quantity characteristic of a particular value of  $x$ ,  $y$  and  $l$ : let us call it  $C(x, y, l)$ . The final summation is then

$$\sum_l C(x, y, l) \cos 2\pi lz.$$

In this way the process of summing a three-dimensional series has been reduced to a succession of one-dimensional summations.

Because of the complexity of the rigorous expressions involved in the complete process of three-dimensional Fourier synthesis, the rest of this chapter will be mainly concerned with two-dimensional methods; these methods bring out the essential principles involved, and can easily be extended to three dimensions if required.

*2.2. General principles for two-dimensional summations.* We have seen from equations 76.1 and 76.2 that the general expression for the electron density projected on to a plane contains terms such as

$$A'(hk0) \cos 2\pi(hx + ky) + B'(hk0) \sin 2\pi(hx + ky),$$

which can be written as

$$\begin{aligned} & A'(hk0) \cos 2\pi hx \cos 2\pi ky - A'(hk0) \sin 2\pi hx \sin 2\pi ky \\ & + B'(hk0) \sin 2\pi hx \cos 2\pi ky + B'(hk0) \cos 2\pi hx \sin 2\pi ky. \end{aligned} \quad (83.1)$$

This expression, it will be remembered, was obtained by combining the two terms  $(hk0)$  and  $(\bar{h}\bar{k}0)$ ; the corresponding expression for the terms  $(\bar{h}k0)$  and  $(h\bar{k}0)$  is

$$\begin{aligned} & A'(\bar{h}k0) \cos 2\pi hx \cos 2\pi ky + A'(\bar{h}k0) \sin 2\pi hx \sin 2\pi ky \\ & - B'(\bar{h}k0) \sin 2\pi hx \cos 2\pi ky + B'(\bar{h}k0) \cos 2\pi hx \sin 2\pi ky. \end{aligned} \quad (83.2)$$

If we combine expressions 83.1 and 83.2 we obtain

$$\begin{aligned} & [A'(hk0) + A'(\bar{h}k0)] \cos 2\pi hx \cos 2\pi ky \\ & - [A'(hk0) - A'(\bar{h}k0)] \sin 2\pi hx \sin 2\pi ky \\ & + [B'(hk0) - B'(\bar{h}k0)] \sin 2\pi hx \cos 2\pi ky \\ & + [B'(hk0) + B'(\bar{h}k0)] \cos 2\pi hx \sin 2\pi ky. \end{aligned} \quad (83.3)$$

The advantage of this form of expression has been described in the previous section: that is, it is possible to combine terms with the same value of one index, say  $k$ .

If we write

$$A_1 = A'(hk0) + A'(\bar{h}k0), \quad A_2 = A'(hk0) - A'(\bar{h}k0),$$

$$B_1 = B'(hk0) + B'(\bar{h}k0) \text{ and } B_2 = B'(hk0) - B'(\bar{h}k0),$$

expression 83.3 can be written as

$$(A_1 \cos 2\pi hx + B_2 \sin 2\pi hx) \cos 2\pi ky \\ - (A_2 \sin 2\pi hx - B_1 \cos 2\pi hx) \sin 2\pi ky.$$

The summation may then be expressed as

$$\sum_k \left[ \sum_h A_1(hk0) \cos 2\pi hx + B_2(hk0) \sin 2\pi hx \right] \cos 2\pi ky \\ - \sum_k \left[ \sum_h A_2(hk0) \sin 2\pi hx - B_1(hk0) \cos 2\pi hx \right] \sin 2\pi ky.$$

The expressions in square brackets may be evaluated in preliminary tables which give the coefficients to be used in the final summations. In other words, we evaluate the expressions in the square brackets for groups of reflexions with a given value of  $k$ , and the result is a series of ordinates at particular values of  $x$ ; we may therefore call the quantities obtained  $C(k, x)$ . Similarly, the quantities obtained from the other brackets may be called  $S(k, x)$ . The final summation is then

$$\sum_k [C(k, x) \cos 2\pi ky - S(k, x) \sin 2\pi ky].$$

It will be noted that, since we have taken the terms together in groups of four, with all possible changes of sign, the summation must be taken over positive values of the indices only. Moreover, the considerations mentioned in section 4.1.2 concerning the special terms such as  $h00$  also apply, and the precise expression for the electron density is

$$\rho(x, y) = \frac{1}{A_c} \left[ F(000) + 2 \sum_{h=1}^{\infty} \{A'(h00) \cos 2\pi hx + B'(h00) \sin 2\pi hx\} \right. \\ + 2 \sum_{k=1}^{\infty} \{A'(0k0) \cos 2\pi ky + B'(0k0) \sin 2\pi ky\} \\ + 2 \sum_{k=1}^{\infty} \left\{ \sum_{h=1}^{\infty} (A_1(hk0) \cos 2\pi hx + B_2(hk0) \sin 2\pi hx) \right\} \cos 2\pi ky \\ \left. - 2 \sum_{k=1}^{\infty} \left\{ \sum_{h=1}^{\infty} (A_2(hk0) \sin 2\pi hx - B_1(hk0) \cos 2\pi hx) \right\} \sin 2\pi ky \right]. \quad (84)$$

**2.3. Two-dimensional summations for the space group  $P\bar{1}$ .** The space group No. 2,  $P\bar{1}$ , is particularly important because, as we have seen in section 3.1.1, the structure factors are real and there are thus only two possibilities to consider—that a particular  $F$  is positive or negative. In

addition, since the coefficients of a Patterson series (section 1.3.2) are all real, the method of summation can always be based upon the methods devised for the space group  $P\bar{1}$ .

The summations are simpler for this space group because the imaginary components of the structure factors are zero, and thus  $A'(hk0) = F(hk0)$ . The expression for the electron density is therefore

$$\rho(x, y) = \frac{1}{A_c} \left[ F(000) + 2 \sum_{h=1}^{\infty} F(h00) \cos 2\pi hx + 2 \sum_{k=1}^{\infty} F(0k0) \cos 2\pi ky \right. \\ \left. + 2 \sum_{h=1}^{\infty} \left\{ \sum_{k=1}^{\infty} \{F(hk0) + F(\bar{h}k0)\} \cos 2\pi hx \right\} \cos 2\pi ky \right. \\ \left. - 2 \sum_{h=1}^{\infty} \left\{ \sum_{k=1}^{\infty} \{F(hk0) - F(\bar{h}k0)\} \sin 2\pi hx \right\} \sin 2\pi ky \right]. \quad (85)$$

TABLE 85

Values of  $F(hk0)$  for  $\text{CuSO}_4 \cdot 5\text{H}_2\text{O}$

$$F(hk0) = F(\bar{h}\bar{k}0)$$

	<i>h</i>																
	$\bar{8}$	7	$\bar{6}$	5	$\bar{4}$	3	$\bar{2}$	1	0	1	2	3	4	5	6	7	8
0	8	11	12	0	28	0	33	26	129	26	33	0	28	0	12	11	8
1		11	0	20	0	21	$\bar{18}$	30	0	18	10	19	$\bar{10}$	0	0	0	
2		0	0	0	0	21	0	$\bar{17}$	12	32	17	$\bar{7}$	10	0	9	0	
3		0	0	18	7	26	20	23	11	50	17	18	7	16	6	8	
4		0	18	13	26	8	27	17	0	0	17	10	8	0	10		
5		0	0	0	0	12	0	0	$\bar{14}$	11	$\bar{15}$	0	$\bar{10}$	0	0		
<i>k</i> 6		0	0	0	7	0	16	0	12	14	15	0	9	0	0		
7		7	0	13	9	19	15	21	15	18	0	19	7	15			
8		0	10	0	0	0	16	$\bar{8}$	12	0	11	0	0	0			
9			0	0	0	0	$\bar{11}$	0	0	0	0	7	0				
10			8	0	12	0	14	7	16	0	10	0	12				
11				13	0	12	0	17	0	8	0	7					
12				0	0	0	0	0	0	0	0						
13					0	0	0	11	0	7							

2.4. *Adaptation to other space groups.* It is obvious that relationships between the structure factors may simplify the equations 84 and 85 still further. The space groups considered in section 4.1.2 provide examples of this simplification. In the space group No. 3,  $P2$ ,  $F(hk0) = F(\bar{h}k0)$ , which means that  $A'(hk0) = A'(\bar{h}k0)$  and  $B'(hk0) = B'(\bar{h}k0)$ .

Since also we have the general relationships  $A'(hk0) = A'(\bar{h}\bar{k}0)$  and  $B'(hk0) = -B'(\bar{h}\bar{k}0)$ ,

$$A_1(hk0) = 2A'(hk0), \quad A_2 = 0,$$

$$B_1(hk0) = 2B'(hk0), \text{ and } B_2 = 0;$$

the insertion of these values in equation 84 then gives an equation that is equivalent to that in the International Tables (1952) for this space group.

In the space group No. 11,  $P2_1/m$ , which has a centre of symmetry, the  $B$ 's are zero, and in addition there are the following relations between the structure factors:

$$F(hk0) = F(h\bar{k}0) \text{ if } k \text{ is even,}$$

and

$$F(hk0) = -F(h\bar{k}0) \text{ if } k \text{ is odd.}$$

If we substitute these relationships in equation 85 we arrive at a relationship equivalent to equation 78.2 with  $l$  equal to zero.

*2.5. Illustration of the method of two-dimensional summation.* The principles outlined in the preceding sections are perhaps best understood by reference to an actual example. The data shown in table 85 are those given by Beevers and Lipson (1934) for  $\text{CuSO}_4 \cdot 5\text{H}_2\text{O}$ . The crystal has a centre of symmetry so that all the structure factors are

TABLE 86  
Values of  $2A_1 = 2[F(hk0) + F(\bar{h}\bar{k}0)]$

		<i>h</i>								
		0	1	2	3	4	5	6	7	8
<i>k</i>	0	129	52	66	0	56	0	24	22	16
	2	24	98	34	56	20	0	18	0	
	4	0	34	88	36	68	26	56	0	
	6	24	28	62	0	32	0	0	0	
	8	24	16	54	0	0	0	20	0	
	10	32	14	48	0	48	0	16		
	12	0	0	0	0	0	0			
<i>k</i>	1	0	96	16	80	20	40	0	22	
	3	22	146	6	88	28	68	12	16	
	5	28	22	30	24	20	0	0	0	
	7	30	78	30	76	32	56	0	14	
	9	0	0	22	14	0	0	0		
	11	0	50	0	38	0	26			
	13	0	36	0	0	0				

TABLE 87

Values of  $2A_2 = 2[F(hk0) - F(\bar{h}\bar{k}0)]$ 

	<i>h</i>								
	0	1	2	3	4	5	6	7	8
0	0	0	0	0	0	0	0	0	0
2	0	30	34	28	20	0	18	0	
4	0	34	20	4	36	26	16	0	
<i>k</i> 6	0	28	2	0	4	0	0	0	
8	0	16	10	0	0	0	20	0	
10	0	14	8	0	0	0	16		
12	0	0	0	0	0	0			
1	0	24	56	4	20	40	0	22	
3	0	54	74	16	0	4	12	16	
5	0	22	30	24	20	0	0	0	
<i>k</i> 7	0	6	30	0	4	4	0	14	
9	0	0	22	14	0	0	0		
11	0	18	0	10	0	26			
13	0	8	0	0	0				

real; otherwise, two tables would have been needed—one for the A parts of the structure factors and one for the B parts. In addition, since  $F(hk0)$  and  $F(\bar{h}\bar{k}0)$  are equal only half the reciprocal lattice need be shown.

The next step is to prepare tables of values of  $2A_1$ , which is equal to  $2[F(hk0) + F(\bar{h}\bar{k}0)]$ , and of  $2A_2$ , which is equal to  $2[F(hk0) - F(\bar{h}\bar{k}0)]$ . The relative weights of the various coefficients, as expressed in equations such as 84, are obtained by including only the single value of  $F(000)$ , of  $A_1(h00)$ , of  $A_2(h00)$ , of  $A_1(0k0)$ , and of  $A_2(0k0)$ ; the general rule is that such special quantities should be included only in the ratio of the number of times they appear in the reciprocal lattice. The resulting quantities are shown in tables 86 and 87.

It is now necessary to compute values of the function  $2 \sum_n A_1 \cos 2\pi hx$  and  $2 \sum_n A_2 \sin 2\pi hx$ . There is, of course, no reason why these quantities should be summed first; the summations can be made equally well by taking the  $k$  summations first. In this case, there is some advantage in so doing: the indices  $k$  cover a larger range (up to 13) than do the indices  $h$  (up to 8); thus by making the summations first with respect to  $k$  the larger range of index is confined to the preliminary tables, and the final tables, which are much more extensive, include only the smaller range of index.

In order to effect the summations numerically, ordinates at particular values of the parameter  $y$  have to be determined, and a decision has to be made concerning the intervals into which the projection should be divided. Ideally, the interval of division should be very small, but the work of computation increases as the size of the interval decreases. On the other hand, if the interval is made large to reduce the work of computation, some detail may be lost in the final projection. It is therefore necessary to consider with some care what fineness of interval forms a reasonable compromise between these two considerations.

*2.6. Interval of division of projection.* The argument that leads to a suitable interval of division is essentially physical. As we have seen in section 1.3.1, Fourier methods provide a mathematical way of deriving the image of a crystal structure, and the detail shown in this image is limited by the resolving power of the optical instrument used to derive it. For ordinary optical instruments the limit of resolution is given by the expression  $0.6\lambda/\sin \theta_m$ , where  $\lambda$  is the wave-length of the radiation and  $\theta_m$  is the maximum angle which the rays entering the entrance pupil of the instrument make with the axis.

It is shown in Volume II (p. 400) that the limit of resolution of the X-ray goniometer is  $0.6\lambda/2 \sin \theta_m$ , where  $\theta_m$  is the maximum Bragg angle observed (Bragg and West, 1930). For  $\text{CuK}\alpha$  radiation, of wave-length  $1.5 \text{ \AA}$ , the value is about  $0.45 \text{ \AA}$  if all reflexions with Bragg angles up to  $\pi/2$  are observed. In order to make sure that the electron-density peaks are reasonably well defined it is necessary that the interval of division should be considerably less than this; if, for example, we had made the interval equal to  $0.45 \text{ \AA}$ , it would have been possible for the dip between two barely resolved atoms to have been omitted completely. For results obtained with  $\text{CuK}\alpha$  radiation with  $\theta_m \simeq \pi/2$ , we may say that an interval of division of, at most,  $0.2 \text{ \AA}$  is necessary. For  $\text{CuSO}_4 \cdot 5\text{H}_2\text{O}$ , the  $b$  edge of the unit cell ( $10.7 \text{ \AA}$ ) should be divided into about 50 parts, and the  $a$  edge ( $6.1 \text{ \AA}$ ) into about 30 parts.

It is more directly useful to express the interval of division in terms of the highest indices used, since then both  $\lambda$  and  $\theta$  are taken into consideration. Suppose we assume that the interval is to be about 0.4 of the limit of resolution, that is, about  $0.12\lambda/\sin \theta_m$ . Then the number  $n$  of intervals along a cell edge,  $a$ , is given by the equation

$$n = \frac{a \sin \theta_m}{0.12\lambda}.$$

The highest observable index,  $h_m$ , is given by the equation

$$h_m = \frac{2a \sin \theta_m}{\lambda}.$$



Therefore  $n$  is equal to  $4h_m$ . That is, the number of intervals into which a cell edge should be divided should be at least four times the highest corresponding index. For the projection of  $\text{CuSO}_4 \cdot 5\text{H}_2\text{O}$ , for which the highest indices are  $h_m = 8$  and  $k_m = 13$ , the cell edges should be divided into 32 and 52 parts respectively, in reasonable agreement with the previous deduction.

It is, of course, inconvenient to adopt different values of subdivision for each crystal, and convention has now settled upon particular values which are related to the numbers used in angular measure. The most common number of parts is 60, corresponding to an interval of  $6^\circ$  in a complete period of  $360^\circ$ . For small cell edges, of the order of  $6 \text{ \AA}$ ,  $12^\circ$  may be used, and for larger cell edges of the order of  $20\text{--}30 \text{ \AA}$ ,  $3^\circ$  subdivision is now common. Still finer subdivisions of about  $1^\circ$  have also been suggested.

Emphasis must be laid upon the fact that these rules give only the minimum number of parts into which the cell edges should be divided; fig. 89, from an actual Fourier synthesis (table 94), shows how this

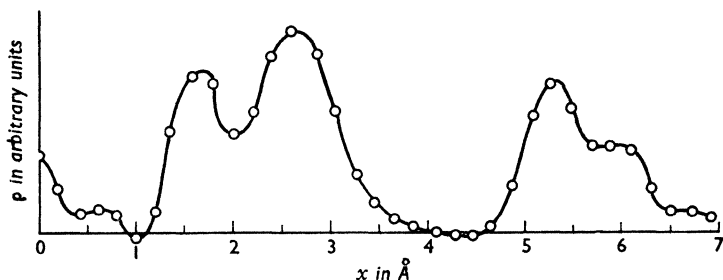


FIG. 89. Electron density along line in  $\text{CuSO}_4 \cdot 5\text{H}_2\text{O}$ , calculated at intervals of  $0.203 \text{ \AA}$  ( $x/30$ ). This subdivision is rather coarse, and, although it ensures that no peaks are missed, some of them, such as that near  $1.7 \text{ \AA}$ , are rather poorly defined.

fineness gives only a barely acceptable definition of the peaks. For work of the highest accuracy we have too little margin of safety, and a finer subdivision should be used. Mathematically, also, the results are hardly satisfactory; for the highest index, 8, with a subdivision of  $12^\circ$ , the sine curve is represented by points  $96^\circ$  apart—hardly an acceptable substitute for a sine curve! Nevertheless, it has been found in practice that the rules given work reasonably well; an interesting discussion of the matter will be found following a paper by Beevers (1939).

### 3. METHODS OF COMPUTATION

**3.1. Beevers-Lipson strips.** The most popular devices used for Fourier summations consist of strips of card upon which are printed numbers

representing the ordinates of the various terms to be included. The simplest of such sets of strips is that produced by Lipson and Beevers (1936). In these strips, two variables are incorporated, one representing the amplitude of the term and the other representing the index: the amplitudes are recorded on separate strips in steps of unity from 1 to 99, the negative values, from -1 to -99, being recorded on the backs; there is one set of such strips for each index from 0 to 20 for the cosine terms and 1 to 20 for the sine terms.

The values of the ordinates for each term are recorded on the strip at intervals of  $6^\circ$ , each ordinate being given to the nearest digit, as shown in fig. 90(i). In this figure a cosine and a sine strip are shown, the

76	C	7	76	56	8	45	74	66	23	31	69	72	38	16	61	76	51	0
19	S	6	0	11	18	18	11	0	11	18	18	11	0	11	18	18	11	0

FIG. 90 (i). Two Beevers-Lipson strips

sequence of symbols at the left-hand side representing the amplitude, cosine (C) or sine (S), and index. The total number of strips is approximately 4000.

It will be noted that, although the interval of division is  $6^\circ$ , the indices exceed the maximum value of 15 recommended in the last section. The reason for this is that the inclusion of 20 orders is quite justifiable for preliminary work, where one may merely want to detect any gross errors; but for final accurate work, the strips should not be used much above the index 15. If higher indices than this have to be included, then the  $6^\circ$  strips are not adequate.

In fig. 90(i) only one quarter of the complete function is included. This modification is possible because any cosine or sine curve can be

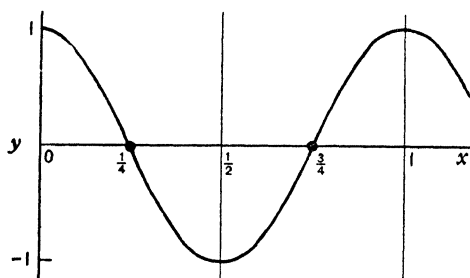


FIG. 90 (ii). Curve  $y = \cos 2\pi x$ , showing lines of symmetry at  $x=0, \frac{1}{2}, 1$  and points of antisymmetry at  $x=\frac{1}{4}, \frac{3}{4}$

The function is said to be symmetrical about the value  $x=\frac{1}{2}$  and anti-symmetrical about the values  $x=\frac{1}{4}, x=\frac{3}{4}$ . These relationships hold for all the curves  $y = \cos 2\pi hx$  for which  $h$  is odd; the relationship

built up by repetition of the first quadrant by either inversion about a point or reflexion across a line; for example, the curve  $y = \cos 2\pi x$  can be derived from the first quadrant by inversion about the point  $(\frac{1}{4}, 0)$ , reflexion across the line  $x=\frac{1}{2}$ , and inversion about the point  $(\frac{3}{4}, 0)$  (fig. 90 (ii)).

for the curves for even values of  $h$  and for the two corresponding sine curves can be easily derived.

Thus to derive the complete cycle from any one cosine strip with odd index, the numbers on the strip are first read off to give the values for  $x=0$  to  $x=\frac{1}{4}$ ; these numbers are then read off in the reverse direction with the signs changed for  $x=\frac{1}{4}$  to  $\frac{1}{2}$ ; they are read in the original direction, again with changed signs, for  $x=\frac{1}{2}$  to  $\frac{3}{4}$ ; and finally they are read in the reverse direction, with the signs changed back to their original values, for  $x=\frac{3}{4}$  to 1. Since these rules apply to all the terms with  $h$  odd, they also apply to their sum. It is therefore worth while separating the cosine terms with even index from those with odd index; the sum of the even terms is symmetrical about  $x=\frac{1}{4}$  and the sum of the odd terms is anti-symmetrical about  $x=\frac{1}{4}$ , and so the sum up to  $x=\frac{1}{2}$  can be obtained by adding the corresponding sums up to  $x=\frac{1}{4}$ , and subtracting them to obtain the sums up to  $x=\frac{3}{4}$ . This process is shown in table 92. The sums of sine terms are obtained by making use of the symmetry of the sine curve; a set of summations is shown in table 93.

There can be no doubt about the operation of the symmetrical and anti-symmetrical relations; at a point where a function is symmetrical the ordinate is equal to the amplitude (positive or negative), and where it is anti-symmetrical the ordinate is equal to zero.

As we have seen, the strips are useful only for crystals whose cell edges do not greatly exceed  $10\text{\AA}$  in length. For larger unit cells, finer subdivision is required, and for this reason a new version of the strips has been produced by Beevers (1952a). In these strips the interval of division is  $3^\circ$ , and therefore twice as many ordinates appear. In order that the strips should not be unmanageably long, the even ordinates are printed on one side and the odd ordinates on the other, and so only the same number of figures has to be accommodated in a given length; on the other hand, a separate strip has to be printed for negative amplitudes, so that, for a given index, twice as many strips are required. It will be noted that the even sides show exactly the same quantities as the  $6^\circ$  strips.

Since the interval of division is halved, the strips can be used for rough work up to indices of 40. For economy, however, strips are provided only up to 30, and they can be extended beyond this value by the following artifice: for cosines, the even ordinates present the same values for indices  $h$  and  $60-h$ , and the odd ordinates for these two indices differ only in sign. Thus, if we wish to include, say, a curve with index 31, we choose the corresponding amplitude with index 29, take the given values on the even side of the strip, and values with the signs changed on the odd side of the strip. For sines, the rules are reversed: for even ordinates of index  $h$ , the signs of the numbers on the strip for  $60-h$  are reversed, and for the odd ordinates the signs are unchanged.

TABLE 92

Preliminary summations  
 Evaluation of  $\sum_k 2A_1 \cos 2\pi ky$ , for  $h=3$

		$y$ (60ths)															
		0	1	2	3	4	5	6	7	8	9	10	11	12	13	14	15
56 C	2	56	55	51	45	37	28	17	6	6	17	28	37	45	51	55	56 (0)
36 C	4	36	33	24	11	4	18	29	35	35	29	18	4	11	24	33	36 (36)
		20	22	27	34	41	46	46	41	29	12	10	33	56	75	88	92 (36)
80 C	1	80	80	78	76	73	69	65	59	54	47	40	33	25	17	8	0 (804)
88 C	3	88	84	71	52	27	0	27	52	71	84	88	84	71	52	27	0 (234)
24 C	5	24	21	12	0	12	21	24	21	12	0	12	21	24	21	12	0 (57)
76 C	7	76	56	8	45	74	66	23	31	69	72	38	16	61	76	51	0 (62)
14 C	9	14	8	4	13	11	0	11	13	4	8	14	8	4	13	11	0 (20)
38 C	11	38	15	25	36	4	33	31	8	37	22	19	38	12	28	35	0 (9)
		320	264	140	34	1	15	33	22	7	5	7	16	67	105	82	0 (576)
Sum		300	242	113	0	42	31	13	19	22	7	17	17	11	30	6	92
Differ- ence		340	286	167	68	40	61	79	63	36	17	3	49	122	180	170	
		30	29	28	27	26	25	24	23	22	21	20	19	18	17	16	15
		$y$ (60ths)															

Two other important modifications are also introduced in the strips. First, for work in which two-figure accuracy is thought to be insufficient, strips of amplitude 100, 200, etc., are included; thus when three-figure quantities arise, they can be obtained by the combination of two strips. This means that the work of addition will be slowed down somewhat, since extra strips are introduced, and also the errors are bigger than if a single strip were used, since the rounding-off errors in the two may combine. It is doubtful, however, whether this latter consideration is likely to be significant, since the strips should give results accurate to about 0.2 per cent.

The other modification is a means for checking the additions. The usual method of checking is to repeat each addition, but it is surprising how easily an error can be repeated. An entirely independent check is preferable, and this is provided by the total of the figures on each strip printed in parentheses at the right-hand end; the sum of these quantities should then be equal to the sum of the totals of the individual

TABLE 93

Evaluation of  $\sum_k 2A_2 \sin 2\pi ky$ , for  $h=3$ 

	$y$ (60ths)																
	0	1	2	3	4	5	6	7	8	9	10	11	12	13	14	15	
4 S 1	0	0	$\bar{1}$	$\bar{1}$	$\bar{2}$	$\bar{2}$	$\bar{2}$	$\bar{3}$	$\bar{3}$	$\bar{3}$	$\bar{3}$	$\bar{4}$	$\bar{4}$	$\bar{4}$	$\bar{4}$	(40)	
16 S 3	0	5	9	$\bar{13}$	$\bar{15}$	$\bar{16}$	$\bar{15}$	$\bar{13}$	9	5	0	5	9	13	15	16	(42)
24 S 5	0	12	$\bar{21}$	24	$\bar{21}$	$\bar{12}$	0	12	21	24	21	12	0	12	$\bar{21}$	$\bar{24}$	(57)
14 S 9	0	11	13	4	8	$\bar{14}$	8	4	13	11	0	$\bar{11}$	$\bar{13}$	4	8	14	(20)
10 S 11	0	9	7	3	10	5	$\bar{6}$	$\bar{10}$	2	8	9	$\bar{1}$	$\bar{10}$	7	4	10	(3)
	0	$\bar{15}$	25	$\bar{31}$	36	$\bar{39}$	$\bar{31}$	$\bar{10}$	20	35	27	1	18	$\bar{14}$	2	12	(122)
28 S 2	0	6	11	16	21	24	27	28	28	27	24	21	16	11	6	0	(266)
4 S 4	0	2	3	4	4	3	2	1	$\bar{1}$	$\bar{2}$	$\bar{3}$	$\bar{4}$	$\bar{4}$	$\bar{3}$	$\bar{2}$	0	(0)
	0	8	14	20	25	27	29	29	27	25	21	17	12	8	4	0	(266)
Sum	0	$\bar{7}$	$\bar{9}$	11	$\bar{11}$	$\bar{12}$	$\bar{2}$	19	47	60	48	18	$\bar{6}$	$\bar{6}$	6	12	
Difference	0	23	39	$\bar{51}$	61	$\bar{66}$	$\bar{60}$	39	7	10	6	$\bar{16}$	$\bar{30}$	$\bar{22}$	2		
	30	29	28	27	26	25	24	23	22	21	20	19	18	17	16	15	
$y$ (60ths)																	

Note that the numbers in these tables are derived either from the  $6^\circ$  strips or from the even sides (denoted by CE or SE) of the  $3^\circ$  strips. For division into  $12^\circ$ , either alternate columns only are added, or the indices are doubled.

columns. This means of checking is shown in tables 92 and 93. A reliable computer should find that this device saves a considerable time, as each column need be added only once. If, however, mistakes are frequent, the device will add considerably to the labour since, although it indicates mistakes, it gives no hint of their location. For this reason, it is better not to add a large number of strips at once, unless an adding machine is used; about ten is ideal.

3.2. *Robertson's strips.* An objection to the original Beevers-Lipson strips is that they could be used only to two significant figures. They could, of course, have contained three significant figures, but this would have been at variance with the intention of the designers; the essential purpose of the strips was to produce a *rapid* method of summation, and three-figure working would have militated against this. Moreover, it is doubtful whether, in most ordinary work, the accuracy

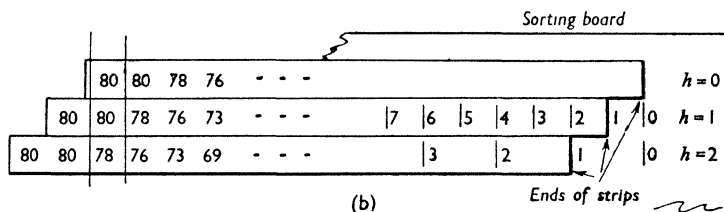


of determination of structure amplitudes is consistently much better than 5 per cent, and for data of this accuracy, two-figure working should be quite adequate.

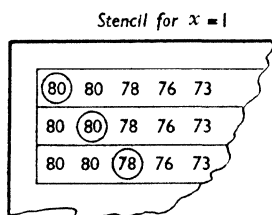
For exceptional work, however, it is possible that two-figure accuracy is not adequate, and then three figures may be introduced either by the device described in the last section, or by the introduction of strips for every unit up to 1000. As we have seen, the former is quite practicable, but the latter increases to an impossibly large value the number of strips that have to be available.

80	C 0	80	80	80	80	80	80	80	80	80	80	80	80	80	80	80	80	80
80	C 1	80	80	78	76	73	69	65	59	54	47	40	33	25	17	8	0	
80	C 2	80	78	73	65	54	40	25	8	$\bar{8}$	$\bar{25}$	$\bar{40}$	$\bar{54}$	$\bar{65}$	$\bar{73}$	$\bar{78}$	$\bar{80}$	

(a)



(b)



(c)

FIG. 95. Relationship between three methods of Fourier summation: (a) shows three Beavers-Lipson strips; (b) shows dispositions of Robertson's strips to give column shown between vertical lines in (a); (c) shows same column extracted by Patterson-Tunell stencils

Robertson (1936a) has adopted a completely different method. In his method there are strips for unit index only, and the ordinates for all other indices are obtained from this one, by appropriate translation. To explain this process, we may consider three Beavers-Lipson cosine strips, of the same amplitude, for  $h=0$ ,  $h=1$  and  $h=2$  (fig. 95a); it will be noted that the numbers in successive columns in the strip for  $h=2$  appear in alternate columns for  $h=1$ , and therefore we could obtain the successive values required by moving the strip for  $h=1$  one place

to the left, and the strip for  $h=2$  two places to the left, after each addition (fig. 95*b*). For higher indices the movements are made appropriately, and obviously, when the right-hand side of the strip has been reached, the strip must be moved correspondingly to the right, perhaps with a change of sign.

Robertson's device therefore consists of a set of strips for unit index, with amplitudes from 1 to 1000, and a board on which are marked the positions to which the strips must be moved to simulate the different indices. Part of the board is shown in fig. 95*b*) and the positions to which the strips have to be moved to represent the first three columns of the strips in fig. 95*a*) are shown.

The objection to this method of Fourier summation is that an extra operation is added after the addition of each column, and, although Robertson (1936*b*) claims that this is partly offset by the greater ease of selection from the smaller number of strips, the strips in the boxes designed by Beevers and Lipson make the selection extremely simple even with the large numbers involved. The individual movements necessary in Robertson's method increase the possibility of errors, and checking by the method introduced by Beevers is impossible.

The tedium of moving the strips has been largely overcome by a method devised by Robertson (1948*a*). For this device the strips, which have a subdivision of  $3^\circ$ , are arranged vertically, with horizontal figures; the required movements are thus vertical ones, and so can be produced by gravity, in the following way. In place of each set of positions shown in fig. 95*b*) there is a template cut appropriately. The strips are mounted in a container that can be rotated about a vertical axis, and one rotation causes the strips to fall against one end of the container and then to fall back against the steps of the template. The numbers to be added then appear in a horizontal row. Another turn repeats the operation, and in addition so moves the strips that they fall on to the next set of steps of the templates. Thus the movements of the strips are made completely automatic.

**3.3. Patterson-Tunell stencils.** A simpler method of overcoming the disadvantage of having to move the individual strips has been suggested by Patterson and Tunell (1942), who make use of a set of stencils which uncover only those numbers that have to be added. As in Robertson's method, strips of required amplitude have to be selected and over the set of strips is placed a card with a set of holes corresponding to a particular value of  $x$ . Thus, for  $x=0$  the holes are so disposed that they uncover the numbers in the first column; for  $x=1$ , they uncover the first number on the first strip, the second number on the second strip, and so on. Part of the stencil is shown in fig. 95*c*). Thus the movements of the individual strips are replaced by the single operation of placing a stencil over the set of strips and this can be accomplished quite rapidly.



There are, however, some complications. When negative amplitudes occur they have to be indicated in some way, and Beevers and Lipson have chosen the usual 'bar' notation. This, however, is not possible with the Robertson and the Patterson-Tunell methods, because, as explained in section 4.3.1, some of the numbers have to be reversed in sign again to represent different parts of the curves. Patterson and Tunell thus suggest the use of coloured strips to represent negative values and coloured rings round stencil holes to represent change of sign: if a number on a white card is surrounded by a coloured ring, it is negative, and if a number on a coloured card is not surrounded by a coloured ring, it is negative; but a number on a coloured card surrounded by a coloured ring is positive.

These complexities are obviously not desirable. Patterson and Tunell consider that the extra number of strips used by Beevers and Lipson may be the cause of error; for example, a strip of the wrong index may be abstracted from the box. But their method of cure may easily introduce greater possibilities of error: not only are the numbers inconveniently arranged for adding, but some mental agility has to be exerted to prevent errors in signs. Robertson (1948*b*) has made a useful contribution by the introduction of sign indicators which are placed at the tops of his strips, which, as explained in the last section, are vertical. A set of holes across the top of the stencils uncovers either the white or coloured parts of the indicators, according to the sign of the quantity on the strip; thus there is now only one indication of negative quantities and one indication of positive quantities.

The main objection to the stencil method as modified by Robertson is that the sign indication may be far removed from the number associated with it, and thus it is necessary to take care that the wrong signs are not used. In addition the sign indicators may easily be displaced when the stencils are changed.

*3.4. Punched-card methods.* The most rapid and accurate methods of Fourier summation are those based upon devices known as punched-card machines. There are two types of punched-card machines, the American (IBM) and the British (BTM or Hollerith). Both use the same principle of expressing the data in the form of holes in cards. The punched cards are passed between a metal roller and a series of wire brushes which can make electrical contact only through the holes in the cards. The circuit completed through a hole in a particular position on a card depends, except in the simplest machines, on the distribution of plugs in a control panel. Since these plug-boards are detachable, it is possible, by wiring a number of them in advance, to switch the machines rapidly from one task to another. The card itself has eighty vertical columns, in any one of which a hole to indicate a number between 0 and 9 can be punched. In addition, holes can be punched at two levels above those shown on the printed card, as

indicated in fig. 98. These 'overpunches' are mainly used to distinguish and sort out different classes of cards. For the purpose of computation

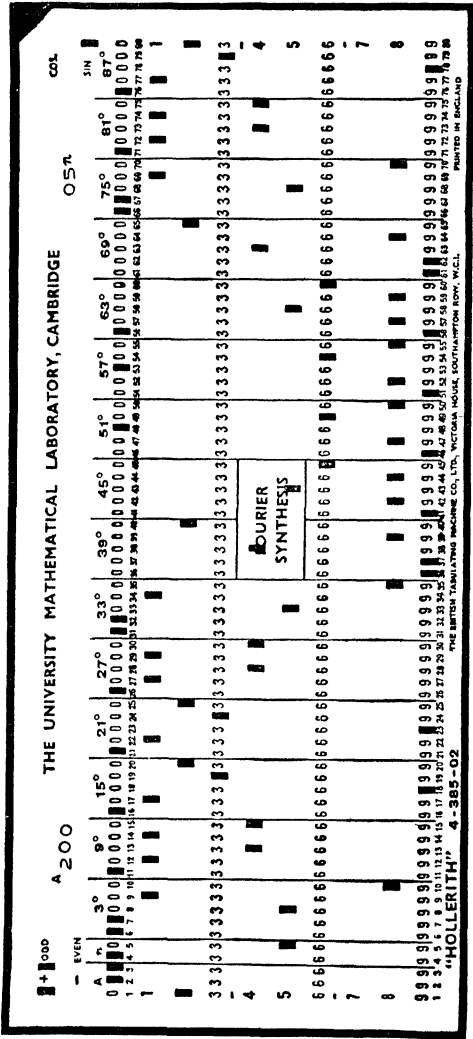


Fig. 98. A typical card (Hodgson, Clews and Cochran, 1949)

the eighty columns are regarded as divided into a number of groups or *fields*. Those in an *indicative* field give operational instructions to the machine, while those in an *additive* field represent the numbers on which

arithmetical operations are performed. The commonest items of Hollerith equipment are:

- (1) Key punch, for hand punching of holes in the card.
- (2) Sorter, which sorts the cards according to the number in a particular column.
- (3) Tabulator, which is essentially an adding machine with printing mechanism attached.
- (4) Reproducing punch, which duplicates existing cards or, when coupled to the tabulator, punches totals or sub-totals into a new set of cards.
- (5) Multiplying punches.
- (6) Collators.

Non-technical accounts of punched-card equipment have been given by Cox and Jeffrey (1949), Eckert (1940), and Comrie, Hey and Hudson (1937). The main difference between American and British tabulators is that the former are capable of direct subtraction of negative numbers; the latter subtract by adding complements. For example,  $-325.4$  would be represented by  $9674.5$ , which requires five columns.

The application of punched-card machines to crystal-structure calculations has been described by Shaffer, Schomaker and Pauling (1946), Cox, Gross and Jeffrey (1947, 1949), Hodgson, Clews and Cochran (1949), Donohue and Schomaker (1949) and Grems and Kasper (1949). We shall limit our description to that of a very simple method which requires only a tabulator and a set of cards which are used over and over again. It is essentially a mechanization of the Beevers-Lipson strip method (section 4.3.1). The cards carry values of the functions

$$A_{\sin}^{\cos} n(2m)3^{\circ} \quad \text{and} \quad A_{\sin}^{\cos} n(2m-1)3^{\circ}$$

for  $A = \pm 1, 2, \dots 5, 10, 20, \dots 50, 100, 200, \dots 500;$   
 $n = 0, 1, 2, \dots 30 \quad \text{and} \quad m = 1, 2, \dots 15.$

Different classes of cards are distinguished by overpunching for sorting and checking, and by printed information for visual inspection (fig. 98). The *master* pack contains 8 cards for every combination of  $A$  with  $n$  (cosine and sine, positive and negative amplitude, first entry at  $6^{\circ}$  and  $3^{\circ}$  respectively). The card shown in the figure, for example, carries values of  $+200 \sin 5 \times 3^{\circ}$ ,  $+200 \sin 5 \times 9^{\circ}$ , ... in successive fields. The working pack contains from 5 to 15 duplicates of each card in the master pack, the number of duplicates depending on the amplitude and wave-number of the card concerned. Cosine and sine cards, cards of odd and of even wave-numbers and cards which give the function at  $6^{\circ}, \dots 12^{\circ}, \dots 90^{\circ}$  and at  $3^{\circ}, 9^{\circ}, \dots 87^{\circ}$ , are filed in separate boxes. Cards differing only in the sign of the amplitude are filed next to one another, the card of negative amplitude being distinguished by a red stripe.

Another version of this method makes it possible to dispense with the cards of negative amplitude; each card is punched so that when it is passed into the tabulator upside down all numbers are read as their complements.

A two-dimensional or three-dimensional synthesis is evaluated as a series of one-dimensional syntheses, as in the Beevers-Lipson method. The procedure for evaluating a number of one-dimensional syntheses, each of the form

$$f(x) = \sum_n C_e \cos 2nx + C_o \cos (2n+1)x + S_o \sin (2n+1)x + S_e \sin 2nx$$

is as follows. If the function is to be evaluated at an interval of  $6^\circ$ , starting at  $0^\circ$ , the appropriate cards are drawn from the four filing boxes by hand and are arranged in the order:

Cosine cards of even wave number, in order of increasing wave number, | .

Cosine cards of odd wave number, in order of increasing wave number, | .

Sine cards of odd wave number, in order of increasing wave number, | .

Sine cards of even wave number, in order of increasing wave number, || .

A single vertical line denotes a blank card which enables the four classes of cards to be easily separated again. Double vertical lines represent *control* cards which round off the total by adding 0.5, cause the tabulator to print totals for the five fields being added, and clear the counters for the passage of the next group of cards. The figure to the right of the decimal point is not printed. This method gives the value of  $f(x)$  only as far as  $x = \pi/2$ . If a reproducing punch is not available the range can be extended to  $x = 2\pi$  only by rather a clumsy procedure: as each card is taken from the filing box, the corresponding card of opposite sign in amplitude is drawn at the same time and put in a separate pile. Corresponding to the set of cards of amplitude  $C_e$ , there will now be a set whose amplitudes are  $-C_e$ . Initially the cards  $C_e|C_o|S_o|S_e||$  were passed through the tabulator; now they are re-arranged and passed through in the order  $C_e|-C_o|S_o|-S_e||$ , and the totals represent values of  $f(\pi-x)$ . Values of  $f(\pi+x)$  and  $f(-x)$  are obtained similarly. If a reproducing punch is available, sub-totals of all cosine cards of even wave-number, etc., are punched into a new card, and the summing and differencing is done with these cards. Even the longer method is definitely faster than hand calculation, and systematic checks are more easily devised.

Better methods are described in the literature, but it is likely that the investigator will have to devise a method which will work with the apparatus available to him; the method we have described requires a minimum of apparatus.

Structure-factor calculation by evaluation of

$$\sum f_j \cos 2\pi(hx_j + ky_j + lz_j),$$

or a similar expression, cannot be done with simple equipment. Donohue and Schomaker (1949) have described a method which requires a multiplying punch. When a punched-card method of evaluating Fourier series has been devised, however, it can be used to calculate structure factors by the sampling method (section 3.2.8), and the simple method described above has been found to be reasonably efficient.

3.5. *Summary.* It will be seen that several methods of summation are possible, and there is little doubt that personal preference plays a large part in the choice made by any particular individual. Nevertheless there are some points of guidance that can be given.

For three-dimensional work of reasonable complexity there is little doubt that punched-card methods are almost a necessity. If a machine is not available, it is necessary to have work done by a computing service, which must, of course, have the necessary cards (corresponding to the strips of the other methods) already available. For two-dimensional work it is generally agreed that the labour of arranging the cards makes the use of punched-card machines less profitable, but even so they are worth using if they are available.

For two-dimensional work, one has the choice of the Beevers-Lipson strips, Robertson's strips with mechanical sorter, and the Patterson-Tunnell stencil method. The first method has the advantage that it requires the least number of operations, and if the additions are to be done mentally—for many people the quickest method of addition—the arrangement of figures is the best. In addition it is possible to check the additions. If adding machines are to be used, the stencil method offers the advantages of a smaller number of strips and a slightly better accuracy, but at the expense of a rather less simple sign indication. There can be little doubt that the Robertson mechanical sorter is considerably more efficient than the stencils, but it needs to be specially constructed. In general, therefore, one may say that the Beevers-Lipson strips are quite satisfactory for practically all work, but that if extra accuracy is required without the use of extra strips, the stencil method or the automatic sorter should be used.

3.6. *Strip methods of computing structure factors.* In section 3.2.8 it was pointed out that the formulae for the calculation of structure factors and of electron densities are essentially similar. In deriving values of electron density, however, we can choose the values of  $x$ ,  $y$  and  $z$  at which we wish to perform the summation, whereas in deriving structure factors our methods must accommodate themselves to any values that may occur. Thus there is an essential difference between

the two operations, and the methods of performing Fourier summations cannot be used for structure-factor calculation without some modification.

The simplest modification is to express the atomic positions as multiples, in angular measure, of  $3^\circ$ ; then no parameter will be in error of more than  $1\frac{1}{2}^\circ$ , or  $1/240$ th of the cell edge. We then set up an array similar to the set of coefficients used for Fourier synthesis, but whose indices are now the multiples of  $3^\circ$  that express the atomic positions, and whose amplitudes are the atomic numbers of the atoms. The Fourier synthesis of this set of coefficients is then the set of structure factors given by a structure containing point atoms. These values may be multiplied by the standard  $f$ -curve (section 3.2.5) to give quantities comparable with those determined by experiment (Beever and Lipson, 1952).

The limitation of the accuracy of the atomic positions is unsatisfactory: an error of  $1\frac{1}{2}^\circ$  may produce, in the 20th order, an error of half the total possible contribution of an atom. Robertson (1936*b*) has pointed out how this difficulty may be overcome if a new set of sorting boards is made for his Fourier strips (section 4.3.2). A strip of amplitude proportional to the atomic number represents each atom, and this strip is moved along to represent change of index. If the atom had zero  $x$  co-ordinate, it would not be necessary to move the strip at all, since  $hx$  is always zero, and if the atom had an  $x$  co-ordinate of  $3^\circ$ , each successive place on the strip would represent successive contributions to the orders 0, 1, 2, 3, ... . But if the  $x$  co-ordinates were  $1^\circ$ , the strip may be kept stationary to represent  $h=0$  and 1, to the first place to represent  $h=2$ , 3 and 4, to the second place to represent  $h=5$ , 6 and 7, and so on. Thus errors of  $1^\circ$  are still introduced, but they do not increase with index, and so the final errors are never serious. The only difficulty is that a new sorting board, three times as complicated as the one for Fourier synthesis, is needed. Since, however, one needs only relatively few values of the parameters for any one set of calculation, the sorting-board strips may be made separately and mounted as required.

*3.7. General application of Fourier methods to computation of structure factors.* The defect of the methods described in the previous section is that the atoms have to be assumed to be points, and that the results have therefore to be finally modified by the standard scattering-factor curve; this is unsatisfactory if atoms of widely differing atomic number are concerned. This difficulty can be overcome by representing each atom by a complete set of electron-density values at specific points, which can be taken as multiples of  $3^\circ$ . The specific values may be obtained from atoms in known crystal structures, and the Fourier synthesis then gives the set of structure factors directly, corrected for the variation of electron density within the various atoms, different as

these may be. Full details of the method are described by Sayre (1951).

It will be noted that the Fourier method can be used directly only if the crystal has a centre of symmetry; otherwise the coefficients for the points  $x, y, z$  and  $\bar{x}, \bar{y}, \bar{z}$  are not equal. This difficulty may be overcome by evaluating the real and imaginary parts of the structure factors separately; to determine the former we add to the structure another one related to it by a centre of symmetry, and to determine the latter we add an anti-symmetrically related structure, that is, with negative electron densities.

In addition to taking account of different electron-density distributions in atoms, the method allows the introduction of other departures from the ideal simplicity of the spherical atom. Asymmetric distributions or electron contents in bonds may be introduced, processes which are not possible with any of the methods so far described. Thus the method is of fundamental importance, and may become of even greater importance as the accuracy of the measurement of intensities increases, and methods of Fourier synthesis become simpler and more rapid.

There is, however, a theoretical difficulty which is discussed by Sayre. By taking, as a basis for the calculation, the electron densities at regularly arranged points, a spurious regularity is inserted and a systematic error is introduced; we have replaced a continuous function by a set of point scatterers and so the diffraction pattern consists of sets of spectra instead of one set only. For example, if the unit cell is sampled at  $n$  points spaced in one dimension, the  $n$ th order of diffraction would be equal in amplitude to the zero order, and in general the  $q$ th order would be equal to the  $(n \pm q)$ th. Thus the calculation of any structure factor  $q$  will include also the  $(n - q)$ th from the first set of spectra, the  $(2n - q)$ th from the second set, and so on.

To overcome this difficulty it is necessary to ensure that the various sets of spectra do not overlap—that is, for the highest index  $q$  observed, the  $(n - q)$ th and higher orders should be negligible. In other words  $n$  must be made so large that the sets of orders are well spaced from each other. If, for example, we wish to deal with 15 orders,  $n$  must be made much greater than 30, for if it were only 30, the 15th order would be doubled. To allow a margin of safety, it would be advisable to make  $n$  about 45, and so we arrive at the general rule that, if we wish to calculate structure factors in this way, the number of points at which the electron density should be sampled in any one direction should be about three times the highest index observed in that direction. This rule is similar to that deduced for the subdivision of cell edges for Fourier synthesis (section 4.2.6); the two matters are, of course, closely related.

**3.8. Computation of Fourier transforms.** The Fourier transform of a single unit of pattern can be derived by means of methods that are essentially the same as those described in the last section. In fact, of

course, the weighted reciprocal lattice, as explained in section 1.3.3, is the Fourier transform of the single unit, evaluated at specific points. The reciprocal lattice is, however, a very poor representation, because the points of evaluation are too widely spaced; this must be so if the unit has the same order of magnitude as the spacings of the crystal, and in order to evaluate the Fourier transform in reasonable detail it is necessary to postulate a hypothetical crystal in which the spacings are several times as large as the dimensions of the unit: then the reciprocal lattice—the sampling mesh—is much finer.

Obviously a great deal of work is entailed in this calculation. If the sampling mesh is three times as fine as the reciprocal lattice, the amount of work involved in the calculation of a two-dimensional transform is nine times as great as for the calculation of the reciprocal lattice, and if the three-dimensional transform is required the work is 27 times as great. On the other hand, for some of the purposes for which the transform is required, only the central portion of the transform is needed, and so the work of evaluation can be reduced.

#### 4. REPRESENTATION OF RESULTS

4.1. *Plotting of contours.* The methods of Fourier summation so far described give values of the electron density at specific points in the unit cell, and, although some of the earlier papers expressed the results in this way, it is now generally agreed that the results expressed as a set of contours of constant electron density are much more useful.

We have therefore to consider ways of deriving these contours from the numerical data. Two ways are possible—drawing the contours between the numbers by subjective judgment, and obtaining the positions of specific values of electron density by graphical interpolation. The former method is much more rapid, and is certainly good enough for much work, particularly in the preliminary stages of a structure determination. If accuracy is required, however, contours should not be derived by subjective methods. Curves should be drawn of the values of electron density along the rows of points for which the calculations have been performed, and the co-ordinates at which the electron density attains the values to be plotted obtained by interpolation.

The smoothness of the contours produced by any method is to some extent a verification of the correctness of the computations, for if any variations are found which are on a finer scale than the limit of resolution, they must be erroneous. Moreover, some Fourier diagrams show unjustifiable ripples in the contours; these are almost certainly introduced by assuming too high an accuracy in the summations: the best *smooth* curve should always be drawn between the points, in the way accepted for other forms of graphical representation.



The main reason for accurate drawing of contours is the determination of atomic positions. As described in Chapter 9, however, there are other, more accurate, ways of obtaining these positions, and the care taken in careful drawing of contours is often largely wasted. Even when accuracy is required, only the regions near the peak positions need be carefully drawn. The justification for drawing the lower contours accurately is that they may show unexpected detail, such as hydrogen atoms (Morrison, Binnie and Robertson, 1948) or departures of the atoms from spherical form.

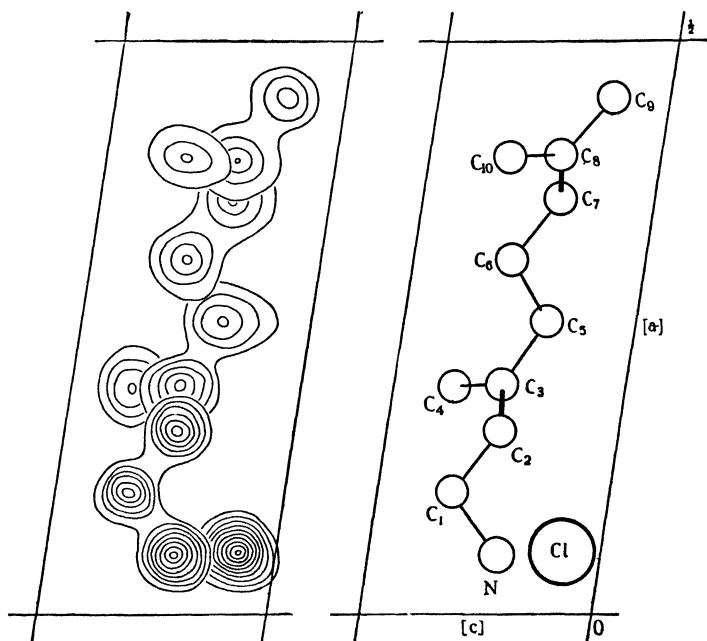


Fig. 105. Representation of three-dimensional electron density in geranylamine hydrochloride. The molecule is shown for comparison (Jeffrey, 1945)

In three dimensions, further problems arise. Obviously, in the two dimensions available, exact representation is not possible, and the usual procedure is to extract important parts of certain projections and to place them in juxtaposition to show as graphically as possible the relative positions of the various atoms in the molecule; an example, due to Jeffrey (1945), is shown in fig. 105.

In drawing a two-dimensional projection, it must be remembered that if the direction of projection is parallel to a crystal axis, it is not

necessarily perpendicular to a face of the unit cell. Thus the parallelogram that limits the area of the projection may not have the shape of the face of the unit cell; the shape is that of the projection of this face on a plane perpendicular to the direction of projection. If the direction of projection is markedly oblique to the face of the unit cell, a noticeable distortion of the atomic shapes will be produced if the wrong area of projection is used.

In presenting the results for publication, it is only necessary to draw the asymmetric part of the projection, since the other parts can be derived by the operations of symmetry. It is helpful, however, if these operations are indicated by the standard symbols (International Tables, 1952, pp. 49, 50) so that the reader can visualize clearly and unambiguously the relationships of the various atomic peaks to each other.

**4.2. *Electron counts.*** The complete electron-density results have been greatly used for finding atomic positions, but it has been largely forgotten that they contain other information as well—the numbers of electrons contained in the atoms. The earlier papers usually quoted such results, but they are not now often given. This is rather unfortunate, because the correctness of the numbers of electrons in each atom is as much a part of the proof of the correctness of a structure as are the relative positions of the atoms.

In order to derive these electron contents, it is necessary to integrate the electron density over the whole atom, and it is first necessary to decide where the ‘boundary’ of the atom is to be drawn. In three dimensions this is easy; each atom should be well resolved from its neighbours if sufficient orders of diffraction have been used, and it is therefore possible to construct a spherical surface around the atom over which the electron density is, on the average, zero. The total of the electron densities at the points within this sphere, multiplied by the volume of the unit of subdivision of the unit cell, then gives the total number of electrons within the atom.

For two dimensions similar methods may be used for an atom which is perfectly resolved from its neighbours; the total of electron densities at the various points must now be multiplied by the area of the unit of the mesh into which the projection of the unit cell is divided. When the atoms are not resolved, however, the method must be modified. For example, one may assume that the atom is spherical, and so deduce the electron densities in the region where the atom abuts on the other, deriving the electron count from the values so deduced. This is not quite so arbitrary as it sounds; since each atom can be treated separately the fact that the total of the separate electron densities at any point adds up to the calculated value can be confirmed, or, if there are any discrepancies, either the values deduced can be revised or some deduction made from them.



# PLATE IV

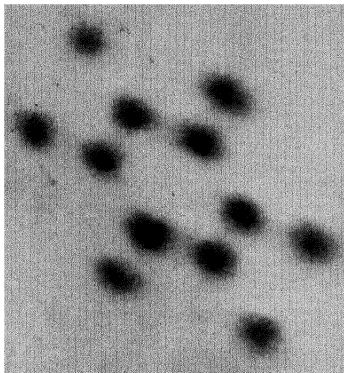


FIG. 107 (i). Optical synthesis of hexamethylbenzene, produced by means of Huggins masks

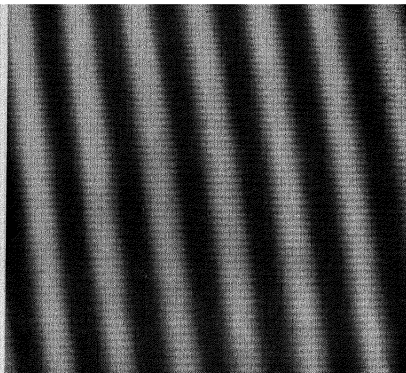


FIG. 107 (ii). Set of fringes used in Pepinsky's machine. Each horizontal line is modulated by a sine wave of appropriate wavelength, and successive lines have appropriate shifts of phase to produce the sloping fringes shown. An extra modulation of 60 c.p.s. is also superimposed to make the lines stand out; in practice the fringes appear perfectly continuous

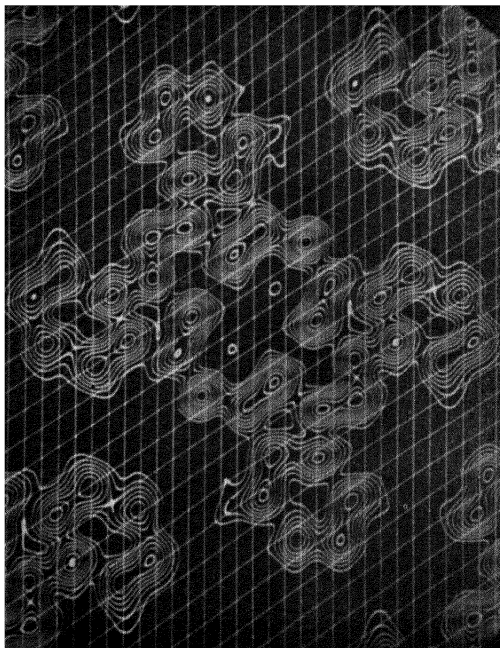


FIG. 107 (iii). Electron-density projection of phthalocyanine

## 5. OPTICAL METHODS OF FOURIER SYNTHESIS

5.1. *Bragg's photographic method.* We have seen in section 1.4.3 that the process of Fourier summation is essentially the adding of sets of fringes. W. L. Bragg (1929*b*) suggested that, for two dimensions, the process can be carried out photographically and showed (Volume I, p. 229) the successful application of this idea to three projections of diopside. Since it is not possible to produce negative values, the fringes were of the form  $1 + \cos 2\pi(hx + ky)$ , and these were projected on to a sheet of photographic paper on which the unit cell was drawn; for different reflexions the indices were controlled by the magnification and the orientation, the signs (the structure is centrosymmetrical) by placing either a maximum or a minimum at the origin, and the amplitudes by the exposure.

The result is a representation, with a magnification of about  $10^8$ , of what would be seen by means of an 'X-ray microscope' if the eye were sensitive to X-rays. The image is, of course, not a true one since the atomic peaks appear on a background that is much too high, but by suitable photographic processing the method can be made to produce striking results, as shown by the examples in Volume I. The method has not, however, been widely adopted, partly because it yields only qualitative results, and partly because it requires a great deal of care to avoid mistakes, since four quantities have to be controlled for every reflexion.

A more manageable procedure has been adopted by Huggins (1944), who produced, on 35 mm. film, sets of masks representing the fringes for indices up to ten, on the basis of a square unit cell. Each mask contains fringes with the right spacing and orientation, and there are separate masks for positive and negative signs; the exposure for each mask is made proportional to the structure amplitude. This procedure is quite rapid, and a quite extensive two-dimensional synthesis can be completed in about two hours; an example is shown in fig. 107(i).

The qualitative nature of the results is however an important disadvantage, and has been overcome in a device which promises to be the most important that has yet been constructed for assisting in the solution of crystallographic problems. The device is that described by Pepinsky (1947). The beam in a cathode-ray tube is made to trace out one of the sets of fringes, as shown in fig. 107(ii). Any sets of fringes up to indices of 20 can be produced in this way, and their amplitudes suitably controlled; by producing them simultaneously the Fourier synthesis would appear in form similar to that given by the method of Bragg and Huggins. It is, however, possible to present the result in the form of contours, a typical example being shown in fig. 107(iii).

For speed, this device would appear to have reached the acme of perfection; the time taken for a synthesis is effectively only the time

taken to set the amplitude controls. The device can deal with complex coefficients, can represent non-orthogonal unit cells, can give sections of three-dimensional syntheses, and can deal with indices up to 20. The only disadvantages would appear to be its cost and its complexity.

**5.2. The X-ray microscope.** The methods described in the previous section, effective though they have become in the hands of the electronicists, are essentially an artificial and cumbersome way of doing what waves can do much more elegantly themselves if the right conditions are presented to them—that is, if they are passed through an apparatus that causes them to interfere in the way described in section 1.4.3. W. L. Bragg has shown that it is possible, in certain circumstances, for the X-ray data to be simulated by a set of holes through which light can be passed, the transmitted light then being brought to a focus to give the required image.

The process may be described in the following way. We have seen that each Fourier component is, in two dimensions, a set of fringes. Such fringes can be produced by the interference of light passing through two small holes; the spacing of the fringes is inversely proportional to the distance between the holes, the fringes are perpendicular to the line joining the holes, and the intensity is proportional to the area of the holes. Consideration of the description of the reciprocal lattice (section 1.2.3) shows that the set of holes required to produce the image of a given crystal structure is represented by the reciprocal lattice of the crystal. The mask of holes

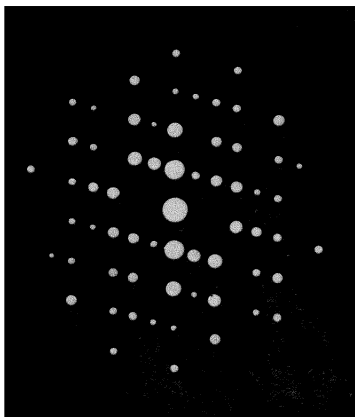


FIG. 108. Mask representing the  $h0l$  reciprocal lattice section of diopside (Bragg, 1939)

for diopside (Bragg, 1939) is shown in fig. 108.

To observe the diffraction pattern of the mask, we can use the apparatus (Bragg and Lipson, 1943) shown in fig. 236. Parallel light falls on the mask, and the transmitted light is brought to a focus in the focal plane of the second lens, where an image of the structure should appear. The result for the mask shown in fig. 108 is shown in fig. 109(i); in fig. 109(iv) the corresponding projection is shown and it will be seen that there is close correspondence.

There is, however, a difficulty that has so far prevented any general use of the method; there is no simple way of introducing phase shifts,



# PLATE V

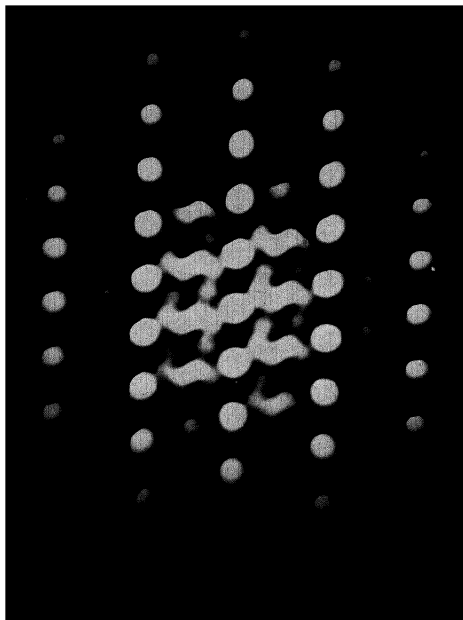


FIG. 109 (i). Optical synthesis of diopside obtained from mask shown in figure 108 with representation of projection of structure for comparison (fig. 109 (iv)) (Bragg, 1939)

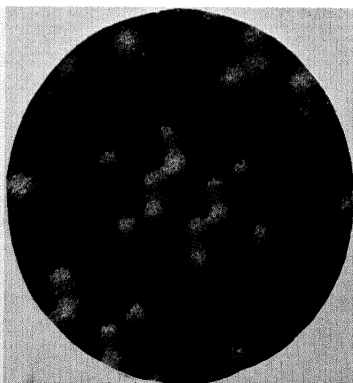
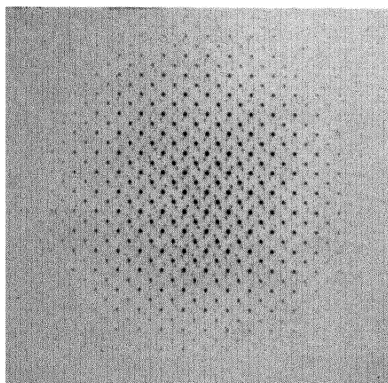


FIG. 109 (ii). Optical synthesis of marcasite,  $\text{FeS}_2$  (Buerger, 1951)

FIG. 109 (iii). Optical synthesis of hexamethyl benzene (Hanson, 1952)



and so the method can be used only if all the phases are zero. This is so if the structure has a heavy atom at the origin, and for diopside,  $\text{CaMg}(\text{SiO}_3)_2$ , this condition applies because calcium and magnesium atoms overlap exactly in the projection shown in fig. 109(iv).

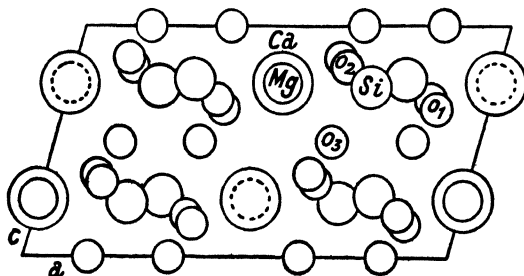


FIG. 109(iv). Representation of projection of structure of diopside on (010)  
(Compare fig. 109(i))

Two methods have been successfully used for introducing the phase shifts required for more general crystal projections. Buerger (1951) places over each reciprocal-lattice hole a mica plate so tilted as to produce the appropriate increase in the optical path of the light passing through it; in order that the paths of the light passing through all the holes shall be accurately comparable, the mica plates are cut from the same uniform cleavage sheet. Buerger's results for marcasite,  $\text{FeS}_2$ , are shown in fig. 109(ii).

The second method, described by Hanson, Taylor and Lipson (1951), also uses mica plates cut from a uniform sheet. The reciprocal lattice, however, is represented by a set of equal holes, which are placed between crossed Nicols in the diffraction spectroscopy (Hughes and Taylor, 1953) shown in fig. 236. Each mica plate has two positions of extinction, which are such that when they lie in the plane of polarization of the polarizer and analyser, no light is transmitted; but when the mica plate is rotated in its own plane through an angle  $\phi$ , the amplitude of the transmitted light is proportional to  $\sin 2\phi$ . Thus the intensities associated with the different reciprocal lattice points can be simulated by different values of  $\phi$ . Different signs for the structure factors can be simulated by rotating the mica plate either clockwise or anticlockwise.

An image of the (010) projection of the structure of hexamethylbenzene is shown in fig. 109(iii), and Hanson and Lipson (1952*b*) have suggested how the device could be used for the trial-and-error method of sign determination for centrosymmetrical projections (section 7.3.1). It cannot be used for other projections, but since optical methods are not likely to achieve a high degree of accuracy, their application to non-centrosymmetrical projections would not appear to be particularly fruitful.

## CHAPTER 5

### TRIAL-AND-ERROR METHODS

#### 1. INTRODUCTION

It has been shown in Chapter 1 that the process of crystal-structure determination cannot in general be direct, because, in the process of recording the diffraction pattern of a crystal, knowledge of the relative phases of the various diffracted beams is lost. Consequently we know only the amplitudes, and we are thus confronted with the problem of finding the structure from these alone. Although this information is incomplete, it is almost always sufficient because other information is also available—that the crystal structure contains discrete atoms which behave approximately as spherically symmetrical regions of electron density, and that there are no regions of negative electron density. Thus, although there is an infinity of distributions of electron density—positive and negative—that would diffract X-rays in the way observed, there is usually only one that can be interpreted as a collection of atoms.

The problem that has to be solved, therefore, is the derivation of this unique solution for a given collection of structure amplitudes, and usually the only method available is to postulate an atomic arrangement that conforms with the space-group symmetry, and to find, by calculation or otherwise, what structure amplitudes it would give for certain reflexions: if these amplitudes agree roughly with those observed, then the postulation is probably correct, and can be proved to be so by continuing the calculations for other reflexions; but if there are some violent disagreements, then the postulation is wrong, and another must be tried. This process is, for obvious reasons, known as ‘trial and error’.

Naturally, a great deal of experience is necessary to use the method effectively. While an incorrect structure will give recognizably incorrect results, an approximation to the right structure will give only approximately correct results and so may easily be dismissed as wrong. It is important, therefore, to recognize when agreement between calculated and observed structure amplitudes is possibly acceptable, and in this recognition lies the whole art of the method. There are no golden rules for success; almost everything depends upon individual experience, and perhaps even intuition, in recognizing what possibilities to dismiss and what possibilities to proceed with.

Because of this lack of certainty in the method, it is important to make use of any hints, however slight, that might be gained about the positions of the atoms in the unit cell. Such hints may be given by

experience from other crystals, by the physical and chemical properties of the compound, or by the X-ray intensities themselves. This chapter is chiefly concerned with summarizing—as far as they can be summarized—the general principles of the use of these devices.

## 2. SPATIAL CONSIDERATIONS

2.1. *Atomic radii.* The most important information that has been gained from crystal structures that have been determined is that of atomic sizes, and this information can, in its turn, be used in devising possible configurations of atoms in unknown structures. It is, of course, not to be expected that atoms behave as solid balls, but, nevertheless, it is found that, within narrow limits, a radius can be assigned to each different atom in crystals of similar nature.

This last qualification is important. The distance between two atoms depends upon the type of force between them; for example, the force between two metal atoms in an alloy is very different from that between one of these atoms and an acid radical in an inorganic salt. Fortunately, the number of essentially different forces is quite small, and attention may be confined to the two types, ionic and homopolar or metallic (Volume I, pp. 114 and 119). Tables of the two atomic radii for the different atoms are given in Appendix II.

The forces between an atom and its neighbours may be different in different directions, and thus we may find that no effective value of atomic radius can be found. This is so, for example, in the metals zinc and cadmium, which behave, when unalloyed, as though composed of atoms with the shapes of elongated ellipsoids of revolution; in alloys, however, all atoms seem to adopt fairly accurately the radii shown in the appendix. In organic crystals, the behaviour of the atoms is much more consistent; the forces between the atoms in a molecule are much stronger than the forces—the van der Waals forces—between atoms in different molecules, and thus atoms must be considered as having much larger radii when these latter forces are concerned. The distances between carbon atoms in adjacent molecules are about 3.4–3.8 Å, whereas the homopolar diameter for carbon is only about 1.4 Å.

The data in the tables of atomic radii must not be taken as precise; in view of the nature of atomic structure it would be surprising if the radii of the atoms were accurately invariant. In using the data, therefore, some latitude should be allowed; 0.2–0.3 Å is a possible variation. Goldschmidt (1929) has shown how these variations can be partly accounted for by differences in co-ordination—that is, by differences in environment—but since, in attempting to derive an unknown structure the co-ordination of certain atoms may not be known with certainty, it is preferable to accept a vagueness in the atomic radii that will allow for this uncertainty.

While we know that the final structure evolved for a crystal must have acceptable atomic radii, we are more concerned here with methods of making use of these radii in postulating structures for trial. It must be admitted that atomic radii are not often of great use in themselves, but nevertheless fairly complicated problems have arisen which have been almost completely solved by packing considerations alone.

Cyanite, for example, was solved in this way by Taylor and Jackson (1928). The unit cell has dimensions  $a=7.09$ ,  $b=7.72$ ,  $c=5.56$  Å,  $\alpha=90^\circ 05'$ ,  $\beta=101^\circ 02'$ ,  $\gamma=105^\circ 44'$ , and contains  $4(\text{Al}_2\text{SiO}_5)$ ; thus, since the crystal is centrosymmetrical, forty-eight parameters are needed to define the atomic positions unless some of the atoms are in special positions; this number of parameters would even now be regarded as presenting a formidable problem. The clue to the structure, however, was given by the packing of the oxygen atoms. Appendix II shows that the oxygen atoms, with radii of 1.35 Å, are much larger than the aluminium atoms (0.55 Å) and the silicon atoms (0.4 Å), and thus, as far as space is concerned, to a first approximation these latter atoms may be neglected.

With this assumption, calculation shows that each oxygen atom occupies a volume of  $13.6 \text{ Å}^3$ . Now the volume occupied by an atom of radius  $r$  in a close-packed structure is  $4\sqrt{2}r^3$ ; this can be seen by noting that the unit cell of the cubic close-packed structure contains four atoms and has a cell dimension of  $2\sqrt{2}r$ . For a close-packed structure of atoms of radius 1.35 Å, the volume per atom would be 13.9 Å<sup>3</sup>, and this is so close to the value deduced for the oxygen atoms in cyanite that these atoms must be approximately close-packed.

There are, however, many close-packed structures, ranging from cubic to hexagonal (Volume I, p. 144), and it is necessary to find in which one a unit cell of the observed dimensions can be found. The dimensions themselves give some help;  $c$  ( $=5.56$  Å) is equal to two atomic diameters, which is a repeat distance found in all close-packed structures, but  $b$  ( $=7.72$  Å) is equal to  $4\sqrt{2}r$ , a distance that occurs most frequently in the cubic close-packed structure. Closer inspection of this structure shows that it is possible to choose a unit cell defined by the vectors  $-\frac{3}{2}\mathbf{a} + \mathbf{b} - \frac{1}{2}\mathbf{c}$ ,  $2\mathbf{c}$  and  $\mathbf{a} + \mathbf{b}$ , where  $\mathbf{a}$ ,  $\mathbf{b}$  and  $\mathbf{c}$  are the vectors defining the edges of the cubic unit cell. Since the magnitudes of these vectors are  $2.7\sqrt{2} \text{ Å} = 3.82 \text{ Å}$ , the edges of the chosen unit cell are  $\sqrt{14} \times 1.91 \text{ Å}$  (7.15 Å),  $4 \times 1.91 \text{ Å}$  (7.64 Å) and  $2\sqrt{2} \times 1.91 \text{ Å}$  (5.40 Å), in close agreement with those observed. The cosines of the inter-axial angles are 0,  $-1/\sqrt{28}$ , and  $-1/\sqrt{14}$ , which give  $\alpha=90^\circ$ ,  $\beta=100.9^\circ$  and  $\gamma=105.5^\circ$ , also in good agreement with the observed angles.

Thus the chosen unit cell needs but little distortion to give the dimensions found experimentally, and so, if the reasoning is correct, the positions of the oxygen atoms may be taken as approximating to the positions of the atoms in the underlying close-packed structure.

The positions of the aluminium and silicon atoms, however, have still to be found before the structure can be proved to be correct, and to find these positions other considerations have to be used.

**2.2. Grouping of atoms.** Knowledge of other silicate structures provides important clues. Silicon atoms are always linked to four oxygen atoms, and hence only the tetrahedral interstices in the close-packed grouping of oxygen atoms need be tried; aluminium, on the other hand, tends to occupy octahedral interstices, although it can sometimes replace silicon in tetrahedral interstices. Since there are fewer octahedral than tetrahedral interstices in the structure, the aluminium atoms may be placed first, and the silicon atoms then distributed reasonably uniformly in the tetrahedral spaces available. Some trial placings are, of course, necessary, but the number of possibilities, at least for the aluminium atoms, is not large.

A diagram of the complete structure, showing also its relation to the underlying face-centred cubic arrangement of oxygen atoms, is shown in fig. 113.

Such information is usually available about inorganic structures, since the dimensions of many ions are now known (Wells, 1950). For example, the  $\text{SO}_4$  group consists of a sulphur atom at the centre of a tetrahedron of oxygen atoms of radius  $1.25 \text{ \AA}$ ; thus in sulphates, the  $\text{SO}_4$  group can be treated as a single unit with six parameters—three translational and three rotational—instead of the fifteen that would be needed if the atoms were treated as independent.

In addition to this knowledge of the shapes of ions, much is known of the functions of other units, such as molecules of water and ammonia (Jensen, 1948). In the simplest cases, water molecules form symmetrical complexes around the cations—tetrahedral if the cation is small and octahedral if it is rather larger—and thus such complexes may also be treated as units in the structure. The assumption is not always correct— $\text{SrCl}_2 \cdot 6\text{H}_2\text{O}$ , for example, does not contain a complex  $\text{Sr} \cdot 6\text{H}_2\text{O}$  (Jensen, 1940)—but it is often worth trying.

These principles are usually not sufficient for dealing with all the

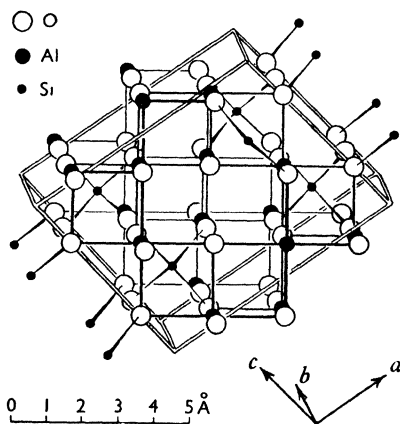


FIG. 113. Unit cell of cyanite (double lines showing relationship to cubic structure)

atoms in a structure. For example,  $\text{NiSO}_4 \cdot 7\text{H}_2\text{O}$  (Beevers and Schwartz, 1935) has to be treated as though it were composed of  $\text{SO}_4$  groups,  $\text{Ni} \cdot 6\text{H}_2\text{O}$  groups, and single  $\text{H}_2\text{O}$  molecules; the total number of parameters needed to specify the dispositions of these units is 15, a number too great to be handled by spatial methods alone, particularly since the space group, No. 18,  $\text{P2}_1\text{2}_1\text{2}_1$ , gives no help in limiting the atomic positions.

In organic structures, the scope for spatial methods is much wider, since a great deal is often known about the relative positions of the atoms in the molecules. Often, the complete stereochemistry of the molecule is known; it is then possible to make models and to fit these together in the unit cell with the space-group symmetry so that approximately correct van der Waals' distances occur between the separate molecules. As emphasized in the previous section, these distances must not be accepted precisely; although generally over 3 Å, they may be less, when they are usually attributed to the presence of hydrogen bonds (Bernal and Megaw, 1935). Thus a certain amount of uncertainty should be allowed for in the models used.

In order to make the best use of the available data, the models of the molecules should take up approximately the space corresponding to the van der Waals' radii of the atoms. Since these radii are greater than the covalent radii, the balls representing the atoms have to be cut off by planes at distances from the centres corresponding to these covalent radii. Thus one atom may have to be represented by a different model according to its state of combination. A carbon atom in a

$\text{CH}_3$  group, for example, may be represented by a sphere cut off by a single plane, corresponding to the single bond with which it is joined to the rest of the molecule, whereas the carbon atom in diamond has to be represented by a sphere cut off by four tetrahedrally disposed planes. Fig. 114 shows a diagram of a model of an organic molecule made in this way. Components for making these models, coloured according to a code given in Appendix IX, are obtainable commercially.

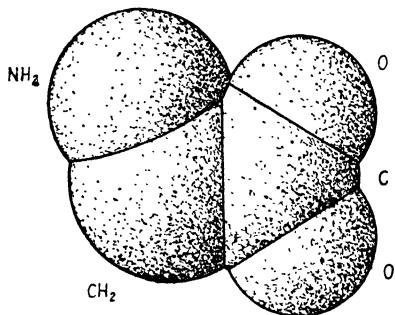


FIG. 114. Representation of molecule of glycine,  $\text{NH}_2 \cdot \text{CH}_2 \cdot \text{COOH}$  (Bunn, 1945)

coloured according to a code given in Appendix IX, are obtainable commercially.

While such models are excellent for finding possible modes of fitting of molecules in the unit cell, they are less useful in giving the structural parameters, since the centres of the balls cannot easily be located. For this purpose a completely different type of model is

wired; the molecule is made in the form of a wire skeleton, the components of which represent the interatomic bonds. Atom centres, in general, be at junctions of wires or at bends, and can be located by casting a shadow of the model from a distant source of light on to a drawing of the unit cell, or by other methods (Hughes, Phillips, Rogers and Wilson, 1949; Low and Waldram, 1949). Such shadows give the parameters of the atoms with an accuracy sufficient for calculating values of the structure factors of low-order reflexions.

*Use of symmetry elements.* In section 5.2.2 it was pointed out that substances such as  $\text{SO}_4$  have characteristic shapes that do not vary from molecule to molecule in the crystal. These shapes are often symmetrical, and the relations between the symmetry of the ion and the symmetry of the space group sometimes impose severe limitations on the possible positions of ions. For example, in section 2.7.1, it was seen that in potassium alum,  $\text{KAl(SO}_4)_2 \cdot 12\text{H}_2\text{O}$ , the potassium and aluminium atoms lie on centres of symmetry, and the sulphur atoms lie on three-fold axes. Even without the evidence that all the centres of symmetry are already occupied, a deduction could have been made that the sulphur atoms do not occupy these positions, because the  $\text{SO}_4$  group has no centre of symmetry. The data on point symmetry in the International Tables (1952) (see Appendix V) can be very helpful in giving quickly the symmetries of the various positions in a space group, although, of course, this information can be readily derived from the space-group diagram itself. If we make the assumption that the aluminium atoms form the centres of octahedral co-ordination groups of water molecules, the following facts emerge from a study of the space group No. 205,  $\text{Fd}\bar{3}m$ : first, the  $\text{Al} \cdot 6\text{H}_2\text{O}$  groups lie on centres of symmetry on three-fold axes, and would therefore be fixed by only one parameter (corresponding to rotation about the three-fold axes); secondly, the potassium atoms are completely fixed, on centres of symmetry; thirdly, the  $\text{SO}_4$  groups lie on three-fold axes, and so, in addition to the lack of knowledge of the direction in which the groups are pointing along the three-fold axes, two parameters, one translational and one rotational, are required to specify their complete dispositions. The remaining water molecules have to be treated separately as occupying a set of equivalent points, and so three parameters are involved. Thus the structure can be specified by only six parameters, a number that would not be too large to handle, in view of the other facts that are now known of the functions of water of crystallization (Jensen, 1948). That the structure was not so worked out (Cork, 1927) was due both to lack of this knowledge and to the misleading information obtained by other methods.

Important information about the location of molecules in an organic crystal can often be obtained in a similar way. For example, durene (Robertson, 1933*b*) belongs to the space group No. 14,  $\text{P2}_1/a$ , and has

a unit cell which contains two molecules. These two molecules cannot be placed in general positions, which are four-fold, and therefore we can deduce immediately that they are distributed around special positions. The only special positions in this space group are centres of symmetry, and thus the centres of the molecules are completely fixed. It may appear at first sight that the space-group data allow of four possibilities, but, for reasons similar to those mentioned in section 2.7.1, it does not matter which centres are chosen.

The reasoning proved incidentally that the durene molecule was centrosymmetrical. This was known initially and therefore the deduction was not in itself of great importance. Sometimes, however, such deductions, even without complete structure determination, can give useful information about the stereochemistry of a molecule. For example, metatolidine dihydrochloride (Fowweather and Hargreaves, 1950) is monoclinic with space group either No. 5,  $I2$  or No. 8,  $Im$ ; it cannot be No. 12,  $I2/m$  because the crystals are pyroelectric (section 5.3.1). The unit cell contains two molecules, and, therefore, since the general equivalent positions are four-fold, the molecules must lie in special positions. A schematic form of the molecule is shown in

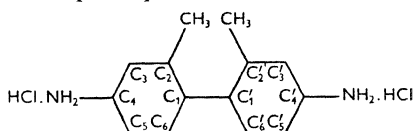


FIG. 116. Schematic form of molecule of metatolidine dihydrochloride (Fowweather and Hargreaves, 1950)

fig. 116, and it will be seen that it may have either a two-fold axis or a mirror plane of symmetry; the latter would demand that a plane of symmetry in the space group should coincide either with the plane of the molecule or with a

plane perpendicular to this and to the length of the molecule. Neither of these possibilities can occur, since the molecule is too long to be accommodated in these orientations in the unit cell. Thus the molecule must have a two-fold axis, in agreement with the conclusion reached in section 2.4.5.

If the unit cell contains a number of molecules sufficient to occupy general positions in the space group, it does not follow that these molecules do not occupy special positions. For example, in stilbene (Robertson and Woodward, 1937*a*) it is found that the four molecules in the unit cell divide into two non-equivalent sets both situated on centres of symmetry. This type of occurrence, though unusual, is by no means unknown, and its possibility should always be borne in mind (Bunn, 1945, p. 249).

These considerations do not normally apply to screw axes and glide planes, since these symmetry elements do not lead to special positions; or, to look at the matter in another light, molecules cannot possess screw axes or glide planes because these symmetry operations would lead to molecules of infinite size. This distinction, however, is not so clear for high polymers, in which the molecule is made of the same unit



indefinitely repeated; such molecules *can* possess screw axes and glide planes. Bunn and Garner (1942) have shown, for example, that rubber hydrochloride has molecules distributed on glide planes of symmetry. Such structures can be quickly solved if it is noted that the distance of translation involved in the symmetry operation is equal to a possible repeat distance in the molecule.

Symmetry elements are not only of importance in dealing with atoms in special positions or with groups of atoms with known symmetry; they can also indicate regions in the unit cell in which atoms cannot be placed. No atom can be at a distance less than its radius from a centre of symmetry, a rotation axis or a mirror plane (unless, of course, it lies *on* the symmetry element) because then it would overlap with a symmetrically related atom. The most productive use made of this principle is undoubtedly the determination of the structure of beryl (Bragg and West, 1926); the space group of this structure is No. 192,  $P6/mcc$ , and the unit cell, which has  $a=9.17$  Å,  $c=9.21$  Å, contains  $\text{Be}_6\text{Al}_4\text{Si}_{12}\text{O}_{36}$ . Reference to the space-group data shows that there are so many special positions in the space group that it is unlikely that a systematic survey of the various possibilities would be feasible. Neither can the structure be tackled in the same way as cyanite (section 5.2.1), because the volume associated with each oxygen atom is  $18.6$  Å<sup>3</sup> and so the arrangement of oxygen atoms is by no means close-packed.

The space-group, however, contains planes of symmetry perpendicular to the six-fold axes, interleaved by systems of two-fold axes distant  $2.3$  Å from them. Since the diameters of the oxygen atoms are  $2.7$  Å, and twenty-four of them have to avoid both the planes of symmetry and the two-fold axes, it can readily be appreciated that the possible positions of the atoms are severely limited; in fact, the 24 atoms in general positions are completely fixed, as described in Volume I, and once these positions are determined the positions of the other 12 atoms are immediately indicated. Considerations of the co-ordination of the remaining atoms allows their positions to be found quite quickly.

It will be seen that, in this structure determination, the opposite principle from the usual one was adopted; the positions of the atoms in general positions were found first, and those in special positions followed. Possibilities such as this should always be borne in mind. While this book is concerned mainly with the laying-down of general principles and methods of procedure, the possibility is always present that, in any particular problem, an unorthodox approach may yield rich dividends; indeed, in one sense, this book aims at being a chronicle of new approaches to the same problem, the intention being to encourage rather than to discourage the introduction of still more new ideas in the future.

**2.4. Pauling's rules.** Packing of atoms, although highly important, is not the only factor in deciding crystal structures and Pauling (1929)

has formulated others that enter into consideration. Most of these apply to silicates only, but one is of general importance and can sometimes be used to eliminate certain possibilities of atomic positions in the initial stages of determination of a crystal structure.

This rule is based upon the general principle that high concentration of electric charge is unlikely in a crystal structure and that ions or co-ordination groups of similar charge therefore tend to distribute themselves as uniformly as possible in the space available, producing alternations of positive and negative ions. This rule is so general that its application is not usually of any great importance, but there are occasions when it can help to dismiss some atomic arrangements which are spatially permissible. For example, in the preliminary survey of the possible atomic positions in the structure of analcite (section 2.7.4), Taylor (1930) points out that the allocation of the sodium and aluminium atoms to the 16-fold sites would be very unlikely; if they were so disposed it would mean that all the positive ions would be placed close together along the three-fold axes, and this would violate Pauling's rule that similar ions should be distributed as evenly as possible over the structure.

### 3. EVIDENCE FROM PHYSICAL PROPERTIES

3.1. *Detection of centrosymmetry.* It has been pointed out in section 2.4.2 that, because of Friedel's law, the presence or absence of a centre of symmetry cannot be deduced directly from the symmetry of the X-ray diffraction pattern of a crystal. The deduction may sometimes be made indirectly by the statistical methods introduced by Wilson (section 2.4.5) or by the detection of both a glide plane and screw axis as in the space group No. 14,  $P2_1/c$ . But often there is an ambiguity in space-group determination which can only be removed if direct evidence of the presence or absence of centrosymmetry can be obtained.

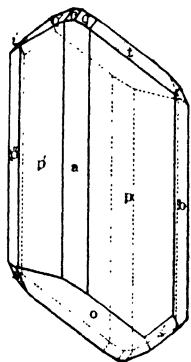


FIG. 118. Drawing of ideal crystal of  $\text{CuSO}_4 \cdot 5\text{H}_2\text{O}$

The classical approach to the problem was based upon the study of external morphology; a large number of small crystals, grown under carefully controlled conditions, were measured, and if pole figures of the distribution of face normals showed that each face was accompanied by a parallel face on the other side of the crystal, the presence of a centre of symmetry could be safely inferred. Tutton (1922) in this way showed that  $\text{CuSO}_4 \cdot 5\text{H}_2\text{O}$  had a centre of symmetry. Fig. 118 shows an idealized drawing of a crystal of this substance, and fig. 119 shows a pole-figure of the face normals (Phillips, 1946).

The method, however, has its drawbacks. It is not always easy to

obtain perfect crystals, and accidents of growth may obscure the true symmetry. Moreover, unless faces of a general form are exhibited,

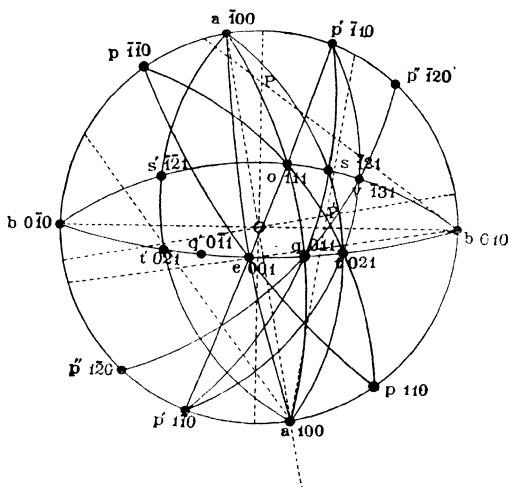


FIG. 119. Stereogram of faces marked on Fig. 118. Not all faces are marked, and the complete symmetry is shown only by the zone round the circumference

the symmetry of the crystal may be higher than the symmetry of the underlying structure; for example, most alum crystals show the forms  $\{100\}$ ,  $\{110\}$  and  $\{111\}$  and appear to have the symmetry  $m3m$ , whereas the true symmetry is  $m3$ . Many crystals cannot be grown with recognizable faces at all, or grow with insufficient faces for any reliable deductions to be made; for such crystals direct tests for centrosymmetry can be very valuable.

Such tests are based upon the detection of some physical property that can exist only in non-centrosymmetrical crystals, and therefore can prove only the absence of centrosymmetry; if no effect is shown it may merely be too small to be detected. This qualification applies to the methods to be described in this section.

One property that may be used is optical activity (Henry, Lipson and Wooster, 1951) but the difficulty of detecting this property in crystals has prevented its frequent use. Much more popular are the effects of pyroelectricity and piezoelectricity, which can be detected even in polycrystalline masses. Strong pyroelectricity can be detected by relatively simple methods (Maurice, 1930; Martin, 1931; Robertson, 1935a), but in general it is better to use a more sensitive apparatus such as that described by Wood and McCale (1940), since even a slight effect is sufficient to show the absence of centrosymmetry.

Piezoelectric evidence may be used in a similar manner. As Wooster

(1938) points out, however, there is one crystal class, 432, which, although non-centrosymmetrical, cannot show the piezoelectric effect. The crystal classes that can show the various effects are shown in a table drawn up by Henry, Lipson and Wooster (1951, p. 161), which also appears in a slightly rearranged form in International Tables (1952, p. 42).

An example of the application of the pyroelectric effect has already been mentioned in section 5.2.3; Fowweather and Hargreaves (1950) showed that the compound metatolidine dihydrochloride is pyroelectric, and therefore could not belong to the crystal class  $2/m$ , but must have either of the symmetries 2 or  $m$  separately.

*3.2. Optical and magnetic data.* The piezoelectric and pyroelectric effects can help to decide that a crystal does not possess a centre of symmetry, but they have not so far been used to find the positions of the atoms in a crystal structure. For this purpose we must make use of those physical properties which have been found to depend upon atomic arrangement, and the two most important properties so far used are refractivity and magnetic susceptibility.

The relationship between refractive indices and crystal structure has been firmly established by the work of Wasastjerna (1923); and Bragg (1924) has shown that it is possible to calculate the principal refractive indices of calcite from a knowledge of its structure. The problem that we are concerned with, however, is the opposite one—how to deduce, from the observed refractive indices, possible atomic arrangements; this problem is far more difficult and only in special circumstances can useful information be obtained.

Cyanite (section 5.2.1) provides a simple example. This crystal is pseudo-cubic, and the refractive index is high, 1.720. Bragg (1930) has pointed out that this value is associated with a packing of the oxygen ions in positions which correspond to close packing, and this evidence was used by Taylor and Jackson (1928) in the initial stages of the investigation of the structure of this compound. In general, however, one would not expect to gain much information from a knowledge of the refractive index of a cubic crystal, because it is independent of direction in the crystal.

For other crystal systems, however, the refractive index may not be constant, and its variation with direction may give some indication about the dispositions of certain atoms and ions in crystals. This subject is discussed by Bunn (1945), who gives the following rules:

(1) If a structure is composed of plate-like molecules approximately parallel to each other, then the refractive index for vibrations perpendicular to the plates is lower than in other directions.

(2) If a structure is composed of needle-like molecules approximately parallel to each other, the refractive index for vibrations parallel to the needles is higher than in other directions.

(3) If the crystal is composed of plate-like molecules which are far from parallel, but which have one direction in their planes in common, the refractive index for vibrations parallel to this direction is higher than in other directions, but the difference is less marked than for the second class of crystals.

These rules indicate the weakness of the method; it can be applied only if the crystals are optically very anisotropic. If there are no great differences between the principal refractive indices then the structure may be composed of approximately spherical molecules, or of plate-like or needle-like molecules which are far from parallel to each other. Of course, if the stereochemistry of the molecule is known, such information may be useful, but in general optical methods are more important when the anisotropy is pronounced.

Optical methods were used in this way in the investigation of melamine (Wood and Williams, 1940). The principal refractive indices are  $\alpha = 1.487$ ,  $\beta = 1.846$ ,  $\gamma = 1.879$ ; that is,  $\beta$  and  $\gamma$  are approximately equal and  $\alpha$  is much smaller; thus, from the rules stated above, the structure would be expected to contain plate-like molecules whose planes are approximately perpendicular to the direction of  $\alpha$ . This was found to be so by Hughes (1941).

Many other examples could be given of the part played by such optical measurements in structure determination and in many laboratories it is customary to begin the study of transparent crystals by optical examination, for obtaining information both about the symmetry (Hartshorne and Stuart, 1950) and about possible molecular dispositions. It is, however, important to realize the limitations of the method. Not only is it of little use for crystals that do not show pronounced anisotropy, but also, for inorganic crystals particularly, the results are complicated by the interactions of neighbouring groups of atoms which cannot be neglected in comparison with the interactions of the atoms in single groups.

This latter defect does not apply in so marked a degree to the magnetic method; the paramagnetic or diamagnetic susceptibility of a crystal depends much more simply on the crystal structure than does the refractive index, and thus one would expect to be able to make more precise deductions from such magnetic measurements (Lonsdale and Krishnan, 1936). The reason why the magnetic method has not been used as frequently as the optical is that it requires more specialized apparatus than the microscopes and immersion liquids that can be used for the optical method. It would certainly appear that the method deserves more attention than it has had in the past.

It would have been possible, for example, for the structure of  $\text{CuSO}_4 \cdot 5\text{H}_2\text{O}$  (Beevers and Lipson, 1934) to have been completed without recourse to Fourier methods (section 7.3.3) if measurements of its paramagnetic susceptibility had been taken into account. From measurements of the variation with temperature of the susceptibility of

powdered crystals, Jordahl (1934) had been able to deduce that, although the crystals were triclinic, the environments of the copper atoms must have approximately cubic symmetry. Moreover, Krishnan and Mookherji (1936, 1937, 1938) had found that single crystals were magnetically almost uniaxial, the axis being inclined at  $156^\circ$ ,  $65^\circ$  and  $52^\circ$  to the  $a$ ,  $b$  and  $c$  axes of the crystal. Now the most likely configuration of oxygen atoms around the copper atoms is octahedral; the copper atom is too large for a tetrahedral arrangement to be possible, and it would not be possible for three oxygens of the  $\text{SO}_4$  group to form, with the five water molecules, an eight-fold arrangement. If this argument is accepted, Krishnan and Mookherji's data give the orientations of the two octahedra, and there can be little doubt that the structure would have been solved much more quickly than it was had this information been available at the time the structure determination was carried out.

**3.3. Morphology and cleavage.** The external form of a crystal grown under ideal conditions should be that with minimum surface energy (Wells, 1946), and, since the surface energy of each face should be related to the internal structure, it might be expected that a careful study of the morphology of the crystals of a compound would give some indication of the internal structure. This problem has been given a great deal of attention by Donnay (1939), who has shown that it is often possible, by observing the frequency of occurrence of different faces on a large number of crystals of a compound, to deduce the space group. On the other hand, there are some outstanding exceptions to the rules (Donnay and Harker, 1937), and it would be unwise to place reliance upon results obtained in this way; moreover, the amount of work entailed in making the necessary goniometric measurements on a large number of crystals is so great that it would appear to be much simpler to deduce space groups in the manner described in Chapter 2.

It is still more difficult to make any deductions about atomic distributions from the occurrence of faces, although some general rules are given by Bunn (1945, p. 278). Of rather more utility is the information given by cleavage, which in some crystals is very pronounced. Mica (Jackson and West, 1930) is the most outstanding example, the cleavage indicating a distribution of alkali atoms in (001) planes. Such information proved to be of use in the determination of the structure of sodium sesquicarbonate, which has perfect cleavage parallel to (100) and good cleavage parallel to  $(10\bar{1})$  (Brown, Peiser and Turner-Jones, 1949); by analogy with mica, one would expect the sodium atoms to be grouped in planes parallel to these planes and fig. 123 shows that this is so.

Cleavage considerations, however, are rarely so helpful, but the evidence is so simply obtained that, if it exists, it is worth while bearing in mind in the initial stages of a structure determination.

3.4. *Infra-red absorption.* The disadvantage of the use of optical data—that it is difficult to separate intramolecular and intermolecular effects

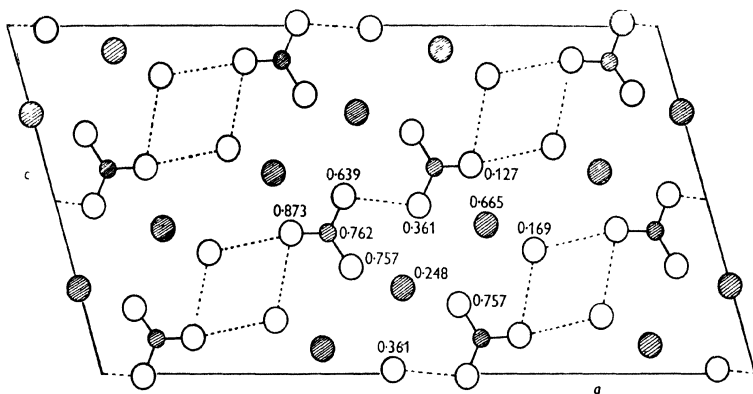


FIG. 123. Representation of structure of sodium sesquicarbonate  $\text{Na}_2\text{CO}_3 \cdot \text{NaHCO}_3 \cdot 2\text{H}_2\text{O}$ , showing distribution of sodium atoms (large shaded circles), in 100 and 101 planes (Brown, Peiser and Turner-Jones, 1949)

—can be largely overcome by the use of infra-red radiation. On the other hand, the use of this radiation requires special apparatus and large crystals and so has not been very extensive, but some results published by Crookes (1947) and Brown and Corbridge (1948) suggest that the method can be very useful indeed.

The basis of the method is the measurement of the absorption of infra-red radiation as a function of the direction of plane of polarization with respect to the crystal. For visible light such absorption is normally a property of the atomic arrangement as a whole, but for the lower quantum energies of infra-red radiation it is possible to identify the absorption of a particular band of wave-lengths with the presence of a particular detail of structure in the molecule such as a bond of a given nature; the absorption of this bond is greatest when the plane of vibration is parallel to its length. If the particular bonds are all parallel there should be a great variation of absorption with the plane of polarization, and the plane of maximum absorption gives the plane of the bonds; if the bonds are not all parallel, it should be possible to deduce their inclination to the plane of polarization of maximum absorption.

By considering different absorption bands, Brown and Corbridge (1948) were able to obtain information about the orientation of certain bonds in the acetanilide structure, which, supplemented by optical and cleavage data, enabled the complete structure to be so accurately postulated that only little refinement by X-ray methods was required.

3.5. *Thermal vibrations.* The theory outlined in Chapter 1 assumes that a crystal consists of a unit arrangement of atoms that is repeated regularly in three dimensions. The unit does not necessarily consist of stationary atoms, but any movements, which are due to temperature, can be considered as spherically symmetrical about the mean positions of the atoms, the total effect being to make the atoms occupy a larger volume than they would if they were at rest (section 1.2.5).

This method of treatment is not completely adequate; to X-rays, with a frequency of about  $10^{18}$  per sec., the atoms, which are vibrating with a frequency of about  $10^{13}$  per sec., would appear to be stationary and displaced from their mean positions. Even so, these displacements would not introduce any modification in Debye's formula for the effect of temperature on X-ray intensities if the displacements of neighbouring atoms were unconnected. This is not so, however; if at any moment a particular atom is displaced in a particular direction, its neighbours will tend to be displaced in the same direction, and this similarity of displacement leads to additional X-ray diffraction effects.

The theoretical basis underlying these effects is as follows. We have seen in Chapter 1 that a perfect crystal scatters X-rays appreciably only when the three Laue equations (section 1.2.1) are satisfied. The displacements just considered may be regarded as imperfections in the lattice, so that the Laue equations are somewhat relaxed, and X-rays are therefore scattered even when the Laue equations are not accurately obeyed; in reciprocal space, we may regard each reciprocal-lattice point as surrounded by a diffuse region (Lonsdale, 1942*a*, *b*), and these regions are manifested by the appearance of diffuse spots on X-ray photographs.

If the vibrations of every atom were spherically symmetrical, the diffuse regions around each reciprocal-lattice point would also be spherically symmetrical. In crystals containing groups of atoms that are bound together much more tightly than the groups themselves are bound together—in other words, in which molecules exist—the vibrations will not be spherically symmetrical, and some information about the way in which the atoms are arranged may be obtained from a study of the diffuse reflexions.

Particularly is this true of planar molecules; in these, atoms vibrate much more easily perpendicularly to the plane of the molecule than they do in the plane, and this is shown by intense diffuse reflexions which are approximately equally extensive in every direction parallel to the plane of the molecule. On the other hand, structures that are essentially chain-like give fine streaks associated with planes which are approximately perpendicular to the chain length.

Both of these principles are illustrated by the structure of sorbic acid (Lonsdale, Robertson and Woodward, 1941), for which both types of diffuse reflexion appear. These can be associated with certain molecular



features and played some part in enabling the crystal structure to be determined.

#### 4. DIRECT METHODS OF SOLUTION

4.1. *Crystals with few parameters.* Whatever the methods used for deriving a crystal structure, the final proof of its correctness must lie in the agreement between calculated and observed intensities. It is tempting, therefore, to try to dispense with the various preliminaries already discussed, and to produce, from the intensities themselves, a structure that has this necessary property. Many attempts have been made to solve this problem, but no method of general application has yet been evolved, and direct methods can only be applied to fairly simple structures.

For instance, if a structure is based on only one variable parameter, all the intensities can be calculated as a function of this parameter, and it is not difficult to find the value that gives the observed intensities. Graphical methods provide the best way of finding the correct solution, as shown in fig. 126, which is taken from a paper by Bradley and Lu (1937).

The material is  $\text{Cr}_2\text{Al}$ , which was found from powder photographs to be tetragonal, with  $a = 3.00 \text{ \AA}$  and  $c = 8.63 \text{ \AA}$ . This unit cell contains two Al and four Cr atoms. Since the only systematic absences observed were those of reflexions with  $h + k + l$  odd, the lattice was established as body-centred, but several space groups were possible; that of highest symmetry, No. 139,  $I4/mmm$ , was tried first and, since an acceptable structure based on this was found, there was no need to try those of lower symmetry (compare section 2.4.2).

In the space group  $I4/mmm$ , there are two sets of two-fold positions, (a)  $0, 0, 0$  and  $\frac{1}{2}, \frac{1}{2}, \frac{1}{2}$ , and (b)  $0, 0, \frac{1}{2}$  and  $\frac{1}{2}, \frac{1}{2}, 0$ ; as explained in section 2.7.1, either of these sets can be chosen, and it is simpler to choose (a). There are three sets of four-fold positions, (c)  $0 \frac{1}{2} 0, \frac{1}{2} 0 0, \frac{1}{2} 0 \frac{1}{2}$  and  $0 \frac{1}{2} \frac{1}{2}$ ; (d)  $0 \frac{1}{2} \frac{1}{4}, \frac{1}{2} 0 \frac{1}{4}, \frac{1}{2} 0 \frac{3}{4}$  and  $0 \frac{1}{2} \frac{3}{4}$ ; and (e)  $0 0 z, 0 0 \bar{z}, \frac{1}{2}, \frac{1}{2}, \frac{1}{2} + z$ , and  $\frac{1}{2}, \frac{1}{2}, \frac{1}{2} - z$ . Both (c) and (d) can be immediately rejected; they give unacceptable distances [e.g.  $2.1 \text{ \AA}$  between the chromium atoms (see Appendix II)] and the calculated intensities do not agree with the observed. For example, (c) would give a strong 002 reflexion, and (d) would give a strong 004 reflexion, whereas neither of these is observed. The positions (e), however, are not so easily dealt with, since a variable parameter, which Bradley and Lu call  $u$ , is involved.

The formula for the structure factor for the reflexions with  $h + k + l$  even is

$$F = 2f_{\text{Al}} + 4f_{\text{Cr}} \cos 2\pi u.$$

From this it can be seen that all reflexions with the same index  $l$  should have the same value of  $F$  when allowance is made for changes in scattering factor. As far as lack of resolution of certain powder lines

would allow, it was observed that reflexions with  $l$  equal to a multiple of 3 were strong, those with  $l$  equal to 1 or 4 were zero, and those with other values of  $l$  were of intermediate intensities. These facts suggested that  $u$  was near  $\frac{1}{3}$ , and fig. 126 shows how  $F$  varies with  $u$  for

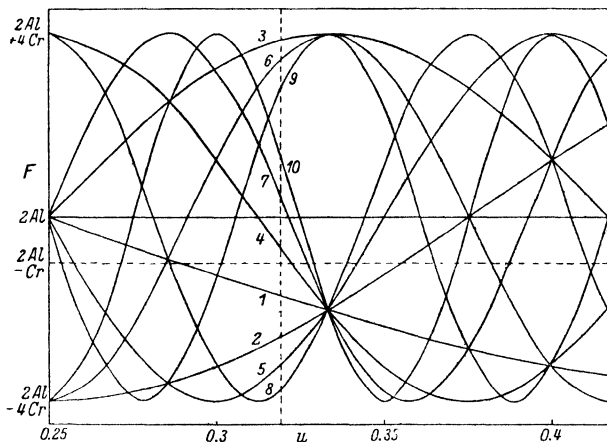


FIG. 126. Determination of parameter in  $\text{Cr}_2\text{Al}$  (Bradley and Lu, 1937)

different values of  $l$  over a range of values of  $u$  near to  $\frac{1}{3}$ , the scattering factors of the two atoms being taken as equal to their atomic numbers (13 for Al and 24 for Cr).

The horizontal dotted line corresponds to zero value for  $F$ , and it will be noted that only near 0.32 are the curves for  $l=1$  and 4 near to zero. Slightly larger values would be possible, but then the intensities of reflexions with  $l=8$  would become too weak, and, taking as much evidence as possible into consideration, Bradley and Lu decided upon the value of 0.319, shown by the vertical dotted line in the diagram.

While this type of method was devised for dealing with structures depending upon only one parameter, it can be applied to structures depending upon more than one parameter if the space group is such that certain intensities depend upon one parameter only. For example, marcasite  $\text{FeS}_2$  belongs to the space group No. 58,  $Pmnn$ , and the unit cell contains two iron atoms and four sulphur atoms (Buerger, 1931). The two iron atoms must be placed on centres of symmetry, and so do not introduce any variable parameters, but the sulphur atoms may be on either two-fold axes or mirror planes; consideration of certain absent reflexions such as 020 and 004 eliminates the possibility of any positions on the two-fold axes, and therefore the mirror planes, involving two variable parameters, must be chosen.

With appropriate choice of origin, the structure-factor formulae are

$$F(hkl) = 2f_{\text{Fe}} + 4f_{\text{S}} \cos 2\pi ky \cos 2\pi lz$$

when  $h + k + l$  is even,

and

$$F(hkl) = -4f_{\text{S}} \sin 2\pi ky \sin 2\pi lz$$

when  $h + k + l$  is odd.

For reflexions with  $l$  equal to zero, the first expression becomes independent of  $z$ , and the second becomes zero; thus the value of  $y$  can be found from the  $hk0$  reflexions by some such method as that described for  $\text{Cr}_2\text{Al}$ . In a similar way the value of  $z$  can be found from the reflexions  $h0l$ . It will be noted, however, that only reflexions with  $h + k + l$  even are used, and for this reason, and also because only the cosine function is involved, the method is unable to distinguish between values such as  $y$ ,  $\bar{y}$ ,  $\frac{1}{2} + y$ , and  $\frac{1}{2} - y$ ; the small number of possibilities can nevertheless soon be reduced to the one tenable result by making use of the general reflexions with no zero indices.

**4.2. Crystals with many parameters.** When more than three parameters are involved, graphical methods cannot easily be applied and analytical methods have to be used. Formally, the problem can be quite simply stated; we have a number of equations relating a number of variables, and so long as the former number is greater than the latter, the derivation of a unique solution should be possible. In practice, the problem is so difficult that no general method of solution has yet been found; thus, although the subject is important, we shall not deal with it here as it has not played a major role in any crystal-structure determination.

## 5. INDIRECT METHODS OF SOLUTION

**5.1. Importance of indirect methods.** Since direct methods of determining crystal structures would appear to be impracticable, other types of approach have to be resorted to, and the following sections contain what is hoped is a reasonably useful summary of these approaches. One can hardly claim more than this; almost every crystal provides different problems, and hence gives different opportunities for exercise of ingenuity and introduction of new methods. For this reason, the following sections are among the most important in this book. They introduce the various ways that have been used in trying to extract information about a crystal from the way in which it diffracts X-rays, and the use of the word 'indirect' should not be taken as implying any vagueness in the results finally obtained.

**5.2. General survey of intensities.** To begin with, a general survey of intensities, either over the whole reciprocal lattice or over isolated zones, can sometimes be rewarding. Particularly striking examples are

given by the work of Bradley and his collaborators in determining the structures of certain alloys from powder photographs. Despite its obvious disadvantages, the powder method does provide an overall view of the diffraction pattern, and the powder photographs of these alloys show obvious relationships to those of the simple structure with atoms at positions  $(0, 0, 0)$  and  $(\frac{1}{2}, \frac{1}{2}, \frac{1}{2})$ . The similarity implies that the structure approximates to that of the body-centred cube, but that differences in scattering factor and slight displacements of the atoms cause the unit cell to contain an integral number of the body-centred cubes; thus extra lines may appear, and the original lines from the body-centred cubic structure split into several components. The structure of  $\text{Cr}_2\text{Al}$  (section 5.4.1) is an example and would have been worked out by such methods if the direct approach had not proved so fruitful.

The first example, and that which provided the chief inspiration for the work that followed, is given by the alloy  $\text{Cu}_5\text{Zn}_8$ ,  $\gamma$  brass (Bradley and Thewlis, 1926), which is cubic with 52 atoms in the unit cell. Analysis of the powder photograph shows that the structure is based upon a body-centred lattice, but no information is given about the symmetry since the reflexions  $hkl$  and  $khl$  overlap. Westgren and Phragmen (1925) had obtained some information from Laue photographs of single crystals, and they deduced that the space group was either No. 211,  $I432$ ; No. 217,  $I\bar{4}3m$ ; or No. 229,  $Im\bar{3}m$ .

The cell dimension,  $8.85 \text{ \AA}$ , is approximately three times the cell dimension of  $\alpha$  iron, which has the body-centred cubic structure with an atomic radius about the same as that of copper and zinc. We may therefore assume that the structure of  $\text{Cu}_5\text{Zn}_8$  is based upon a unit cell that contains  $3^3$  body-centred cubes. There are, however, 54 atoms in this collection of unit cells, and the unit cell of  $\text{Cu}_5\text{Zn}_8$  contains only 52 atoms; two atoms must be removed. The only possible ones are those at  $(0, 0, 0)$  and  $(\frac{1}{2}, \frac{1}{2}, \frac{1}{2})$  in the new unit cell, since the removal of these still leaves the lattice body-centred cubic.

The removal of these two atoms, however, leaves 'holes' in the structure, and from consideration of atomic radii Bradley and Thewlis were able to postulate reasonable changes of atomic positions that would tend to fill in these holes. The atomic positions so chosen gave rough agreement with the observed intensities, and the agreement was improved by some further small changes. In this way the complete structure, involving five variable parameters, was determined.

Evidence leading to this type of approach can sometimes be more easily obtained from single-crystal photographs. For example, it may be observed that the odd layer lines on an oscillation photograph are weaker than the even layer lines. This may be taken to infer that the cell dimension about which the crystal is rotating is approximately halved; in other words, the two halves of the unit cell contain approximately similar contents, similarly situated. An illustration is given by the structure of thiophthen,  $\text{C}_6\text{H}_4\text{S}_2$ , which was worked out by Cox,

Gillott and Jeffrey (1949). It was found that oscillation photographs with  $[100]$  as axis showed odd layer lines that are much weaker than the even layer lines, and this fact was of value in determining the final structure, a projection of which on the  $(001)$  plane is shown in fig. 129(i).

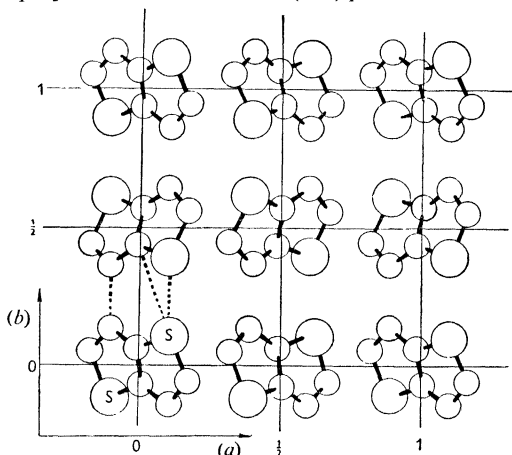


FIG. 129 (i). Projection of structure of thiophene on  $(001)$ , showing similarity of contents of unit cell at levels 0 and  $b/2$  (Cox, Gillott and Jeffrey, 1949)

It will be noted that in this projection the molecule repeats approximately at intervals of  $b/2$ , as deduced from the general weakness of reflexions with  $k$  odd. If it repeated accurately, the reflexions with  $k$  odd would be absent; this is so, for the projection, at intervals of  $a/2$ , and thus reflexions  $hk0$  with  $h$  odd are completely absent, but this is merely one of the characteristics of the space group, No. 61,  $Pbca$ , of the crystal.

Such information is not always obtainable by direct inspection of X-ray photographs, as the general relationships that may exist may not be simply dependent upon the indices. A rather more complicated dependence is shown by

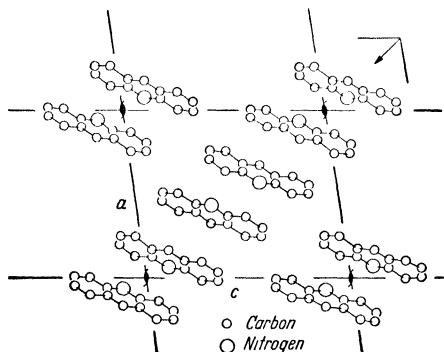


FIG. 129 (ii). Arrangement of molecules in  $(010)$  projection of acridine III (Phillips, 1950)

acridine (Phillips, 1950), which gives strong reflexions  $h0l$  only when  $h + l$  is divisible by four; this is explained by the existence of two molecules

whose projections on the (010) plane are approximately similar and separated by a distance of  $\frac{1}{4}(\mathbf{a} + \mathbf{c})$ . Fig. 129(ii) shows that the projection has this feature, the two molecules being different only in the interchange of the positions of a nitrogen and a carbon atom.

This illustration is still not very complicated, but it brings out the point that such general trends are worth searching for by drawing a representation of the weighted reciprocal lattice. It is also important to find whether any general relations found in two dimensions are continued in the three dimensions of the complete reciprocal lattice; if they are, then the molecules concerned must be approximately similarly oriented, but, if not, the similar orientations apply only to their projections on to the corresponding plane in real space.

If a heavy atom is present, any relationships found may be unduly dependent upon the position of this atom, and, in fact, the sulphur atoms in thiophthen are to some extent responsible for the weakness of the reflexions with  $k$  odd, even without the assistance of the carbon atoms. Consequently, under these circumstances, information about the lighter atoms is less precise, and may even be quite valueless. For example, general trends were found in the intensities of the reflexions from  $\text{CuSO}_4 \cdot 5\text{H}_2\text{O}$  (section 5.3.2) which gave the positions of the copper and sulphur atoms, but which gave no direct information about the positions of the oxygen atoms.

A section of the reciprocal lattice of this crystal is shown in table 85, and, in general, it will be seen that the reflexions with  $h+k$  even are stronger than those with  $h+k$  odd. This tendency is more pronounced at high angles than at low angles, suggesting that it is not due to approximate equality of the two parts of the unit cell separated by  $\frac{1}{2}\mathbf{a} + \frac{1}{2}\mathbf{b}$ ; if this were so, the tendency would be less pronounced at high angles, since any small variations in parameters would have greater effect there. The tendency indicates strongly certain relationships between the parameters of the copper and sulphur atoms, since the oxygen atoms have relatively higher scattering factors at the lower angles, and so become more nearly negligible as the angle increases.

The extra strength of the reflexions with  $h+k$  even is shown also by the  $hkl$  reflexions, and so there would appear to be a tendency towards C-face centring. There are three ways in which this can arise: the copper atoms, of which there are two in the unit cell, may occupy the positions  $(0, 0, 0)$  and  $(\frac{1}{2}, \frac{1}{2}, 0)$ , which are special positions in the space group No. 2,  $P\bar{1}$ ; the copper atoms may occupy the positions  $(\frac{1}{4}, \frac{1}{4}, 0)$  and  $(\frac{3}{4}, \frac{3}{4}, 0)$ , which are general positions; or the copper atoms may occupy positions  $(x, y, z)$  and  $(\bar{x}, \bar{y}, \bar{z})$ , and the sulphur atoms occupy the positions  $(\frac{1}{2} + x, \frac{1}{2} + y, z)$  and  $(\frac{1}{2} - x, \frac{1}{2} - y, \bar{z})$ . The two former possibilities correspond to a C-face centred arrangement of the copper atoms, and the last corresponds to a C-face centring of the copper atoms by the sulphur atoms.

The second possibility is unlikely. Although the atoms are in

general positions, the parameters would have to approximate very closely indeed to the particular values  $\frac{1}{4}$ ,  $\frac{1}{4}$  in order to account for the observed trend; the other two possibilities are more likely, and we shall confine our attention to them. If the first explanation is accepted, another general trend can be made use of: the intensities  $hk0$  with  $h+k$  even tend to be independent of  $h$  for a given value of  $k$ ; for example, when  $h+k$  is even, the spots with  $k=2, 5, 9$  and  $12$  tend to be weak or absent, and those with  $k=3, 4, 7$  and  $10$  tend to be strong. These facts would be explained if the  $x$  parameter of the sulphur atoms were zero, so that the index  $h$  did not enter the expression for the structure factor, and the  $y$  parameter had a value of  $0.29$ . (This value can be found by some such method as that described in section 5.4.1.) Thus we may say that the following arrangement of copper and sulphur atoms explains the general tendencies in the intensities:

Cu atoms in special positions  $(0, 0, 0)$  and  $(\frac{1}{2}, \frac{1}{2}, 0)$ ,

S atoms in general positions  $(0, 0.29, z)$ ,

where  $z$  is as yet undetermined.

We still have to consider the third possibility—that the sulphur atoms form a face-centred arrangement with the copper atoms. The structure-factor formulae are then

$$(f_{\text{Cu}} + f_{\text{S}}) \cos 2\pi(hx + ky + lz), \text{ when } h+k \text{ is even,}$$

$$\text{and } (f_{\text{Cu}} - f_{\text{S}}) \cos 2\pi(hx + ky + lz), \text{ when } h+k \text{ is odd.}$$

These formulae show immediately that the reflexions with  $h+k$  even should in general be stronger than those with  $h+k$  odd, and the second observation—that the  $hk0$  intensities tend to be independent of  $h$ —can again be explained by making  $x=0$ . Methods similar to those described in section 5.4.1, applied to the  $hk0$  reflexions, then lead to a value of  $y$  of  $0.14$ ; thus the general trends in the  $hk0$  reflexions can also be explained by the following arrangement of copper and sulphur atoms:

Cu atoms at  $0.00, 0.14, z$ ,

S atoms at  $0.50, 0.64, z$ .

Detailed calculations show that these positions give about as good a general agreement with observed intensities as the former positions give, and thus we cannot, on the basis of these intensities alone, distinguish between them. The only two procedures possible for distinguishing between them are, first, to see if either leads to a complete structure that is spatially possible (section 5.2.1) or, secondly, to try to find additional experimental evidence. The former proved to be too difficult to carry out, since little was known about the functions of the water molecules (sections 5.2.2 and 5.3.2), and evidence from the comparison of the reflexions with those from  $\text{CuSeO}_4 \cdot 5\text{H}_2\text{O}$  was used, as described later in section 5.5.7.

A more general application of these methods has been described by Vand (1951). A section of the reciprocal lattice of trilaaurin is given in fig. 132; it shows some outstandingly strong spots arranged in a

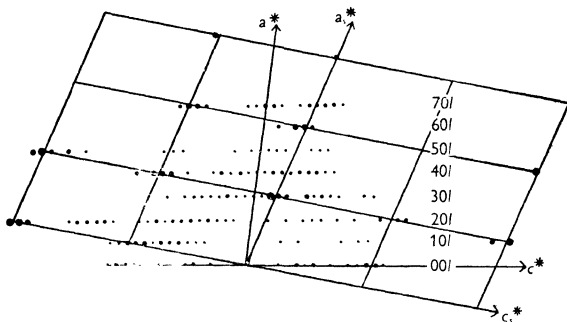


FIG. 132. Reciprocal-lattice section of trilaaurin, showing arrangement of stronger reflexions on coarse mesh with axes along  $a_s^*$  and  $c_s^*$  (Vand and Bell, 1951)

regular way, and, if all other spots were neglected, a reciprocal lattice with a much coarser mesh is left (Vand and Bell, 1951). This corresponds, in the crystal, to a unit cell containing only two atoms, and so we may deduce that the crystal structure is built up of these 'sub-units' repeated approximately regularly in the unit cell.

To summarize, it may be said that, although a general survey of intensities may not be informative, the method is so simple to try that it is worth considering as a first step; if no help is given, not much time will have been lost, but if some regularity can be noticed, a great deal of time may be saved. The subject will be discussed again in Chapter 7, when it assumes a greater importance in connexion with the Fourier-transform method.

**5.3. Importance of absolute intensities.** The methods so far described have been based on the observation of relative intensities, and, where these methods produce tangible results, they are of considerable value. But, obviously, if in addition we know the absolute values of the structure amplitudes, we have information of much greater significance; we may know not only that a reflexion is much stronger than any others, but that it is so strong that practically all the atoms must scatter in phase to produce it. The importance of knowledge of absolute intensities in crystal-structure determination was pointed out by Bragg and West (1928), who showed how such considerations had led to the derivation of the crystal structures of some minerals such as diopside (Warren and Bragg, 1928).

For some time after this paper by Bragg and West was published, their insistence on the importance of absolute intensities was largely



ignored and almost all published work was based upon relative intensities. This, of course, is understandable; if it is possible to determine a structure on the basis of relative intensities it is not worth while spending effort on absolute measurements. But as more complicated problems have arisen, new methods of solution have had to be found, and, as will be explained in Chapter 8, some of these methods depend critically upon knowledge of absolute values of structure amplitudes. Thus the importance of absolute measurements is now fully realized, and therefore, although this book is not concerned with experimental methods in general, it is thought worth while to include here some discussion of the various methods of making these absolute measurements.

The simplest experimental method involves the comparison of the intensities of the spots on an X-ray photograph with those from a standard crystal that gives reflexions of known absolute intensity. Robertson (1933*b*) has made great use of this method. Wooster and Martin (1936) describe a two-crystal Weissenberg goniometer which allows the two sets of reflexions to be recorded upon the same film so that no errors are introduced by any differences in photographic processing or in the properties of X-ray films.

The method appears to work well if both crystals are small enough to give negligible absorption of the incident X-ray beam; if we take 5 per cent as the largest allowable absorption, the value of  $\mu t$ , where  $\mu$  is the linear absorption coefficient and  $t$  is the mean thickness, must be about 0.05.

This condition is difficult to satisfy except for crystals with light atoms only. For example, naphthalene (Abrahams, Robertson and White, 1949) has  $\mu = 6.05 \text{ cm.}^{-1}$  and therefore crystals about 0.1 mm. in size satisfy the condition for negligible absorption, but for aniline hydrochloride (Brown, 1949)  $\mu = 40 \text{ cm.}^{-1}$  and crystals about 0.01 mm. in size would be necessary. Also, in crystals of high absorption another difficulty presents itself: if the crystal is not spherical—or cylindrical if only a zone of reflexions is to be considered—the absorption correction will vary even for reflexions at the same angle. Beevers and Hughes (1941) have overcome this difficulty by turning crystals to the required cylindrical shape, and then applying the corrections calculated by Bradley (1935*a*). More general graphical methods that apply for any known cross-section are described by Albrecht (1939) and Howells (1950).

Another method of eliminating the absorption error is described by Bragg and West (1928). A thin slip of the crystal is cut with its normal parallel to the zone axis considered, the thickness  $t$  being approximately equal to  $1/\mu$  as then the maximum intensity of reflexion is obtained. All the reflexions are then given by planes which are perpendicular to the surfaces of the crystal slip, and the paths of all rays contributing to a reflexion with Bragg angle  $\theta$  are equal to  $t \sec \theta$ .

Thus the absorption correction for each reflexion can be easily calculated. Bragg and West used an ionization spectrometer, and compared the integrated reflexions from the crystal with the 200 reflexion from a standard crystal of rock salt. Because crystal slips of several square millimetres are required the method has not become very popular.

A further difficulty is also discussed by Bragg and West; the strongest reflexions may be greatly reduced by extinction (Volume II, p. 49), and no satisfactory method has yet been proposed for eliminating this effect. Because of this difficulty, there is a tendency to ignore extinction, and it remains the largest factor that stands in the way of making a completely satisfactory set of absolute measurements of the intensities of reflexion from a crystal.

Experimental methods, although they are most direct, are not completely essential for deriving absolute measurements; a complete set of relative measurements contains within itself its own absolute standard. For a given content of a unit cell, any arbitrary arrangement of atoms would give a set of reflexions of the same average value, and this average value would be equal to the average value of the observed intensities.

This, of course, would be a cumbersome method of procedure, and, moreover, would be inaccurate unless the temperature factor (section 1.2.5) were known in advance. If the temperature factor is not known the average of the calculated intensities will exceed the average of the observed intensities by an amount that increases with  $\theta$ , and Wilson (1942) has shown how this difficulty can be overcome. Harker (1948) has devised an essentially similar method.

Equation 10.3 states that

$$F(hkl) = \sum_n f_n \exp \{2\pi i(hx_n + ky_n + lz_n)\}$$

and therefore

$$F^*(hkl) = \sum_n f_n \exp \{-2\pi i(hx_n + ky_n + lz_n)\},$$

where  $F^*$  is the complex conjugate of  $F$ . Thus

$$|F(hkl)|^2 = \sum_n f_n \exp \{2\pi i(hx_n + ky_n + lz_n)\} \\ \times \sum_n f_n \exp \{-2\pi i(hx_n + ky_n + lz_n)\}.$$

This may be written as

$$|F(hkl)|^2 = \sum_n f_n^2 + \sum_{n \neq m} f_n f_m \exp \{2\pi i[h(x_n - x_m) + k(y_n - y_m) + l(z_n - z_m)]\} \quad (134)$$

The first part of the summation, having only positive terms, will be large, whereas the second part, having terms which are as likely to be negative as positive, will have a most probable value of zero. Thus

if values of  $|F(hkl)|^2$ , which we may call the ideal intensity  $I(hkl)$ , are averaged over a large number of reflexions, we should expect that

$$\overline{I(hkl)} = \sum_n f_n^2, \quad (135)$$

where the superior bar represents the average value.

The difficulty that has just been mentioned concerning the lack of knowledge of the temperature factor can be overcome by dividing the reflexions into groups lying between certain values of  $\sin^2 \theta$ . The mean value of the observed intensities,  $I'(hkl)$ , may be evaluated over each range, and the constant  $c$  found which makes the average equal to the sum of the squares of the scattering factors; theoretical scattering factors should be used. This constant  $c$  will be found to increase as the reflexions with higher values of  $\theta$  are included, and if  $\log c$  is plotted against the mean value of  $\sin^2 \theta$  for each range of reflexions, a linear relationship should be found, the intercept at  $\sin \theta = 0$  being the value of  $c$  required.

The method works best for more complicated crystals, and is unsatisfactory if there are atoms in special positions; this probably accounts for the lack of agreement obtained by Wilson for the alums and  $\text{CuSO}_4 \cdot 5\text{H}_2\text{O}$ , both of which have atoms in special positions. Moreover, another difficulty also exists, in that these two examples were for single zones of reflexions, whereas the theory strictly applies only when all possible reflexions are considered. This is so because of the requirement that the second part of the summation in equation 134 should be zero; this will not be so if, for any one pair of atoms, the quantity  $[h(x_n - x_m) + k(y_n - y_m) + l(z_n - z_m)]$  remains near zero for all values of  $h$ ,  $k$  and  $l$ . In three dimensions, this difficulty should not arise, because no pair of atoms can be closer together than the sum of their radii, and thus one of the components  $x_n - x_m$ ,  $y_n - y_m$  or  $z_n - z_m$  must be reasonably large. But in projections on to planes, it is possible that the co-ordinates of two atoms may almost coincide, and thus the theory will not hold for them.

By comparison with equation 10.3, it can be seen that the quantity  $2\pi[h(x_n - x_m) + k(y_n - y_m) + l(z_n - z_m)]$  represents the phase difference between the X-rays scattered by the two atoms concerned, and the requirement that the second summation in equation 134 should be zero is equivalent to the requirement that this phase difference shall at least have values uniformly distributed between 0 and  $\pi$ . This, in turn, means that the distance between any two atoms shall be greater than half the minimum spacing of the reflexions considered. As already stated, this requirement is easily satisfied for most structures, but may not be so for projections on to planes; the tendency for such projections is for the reflexions to be rather stronger than the simple theory would demand. Nevertheless, projections play such a large part in structure determination that it is usually worth while applying the method to zones of intensities.

The process can be illustrated by means of the data for metatolidine dihydrochloride, already given in table 38. Table 136 shows the various steps needed in the deduction of the conversion constant, and fig. 136

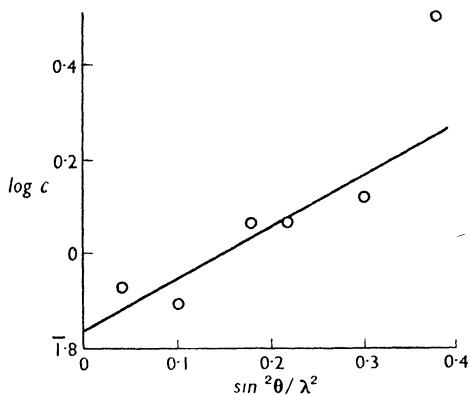


FIG. 136. Determination of absolute values of structure amplitudes of metatolidine dihydrochloride

shows the graph from which the final value of  $\log c$  is deduced. (The point representing the outermost range of reflexions must obviously be ignored.)

TABLE 136

$\sin^2 \theta / \lambda^2$	$\langle I \rangle$	$\Sigma f_n^2$	$c$	$\log c$
0.04	875	748	0.85	$\bar{1}.929$
0.10	612	475	0.78	$\bar{1}.892$
0.18	315	358	1.16	0.064
0.24	263	309	1.17	0.068
0.30	204	270	1.32	0.121
0.38	77	244	3.17	0.501

The value of  $\log c$  extrapolated to  $\sin^2 \theta / \lambda^2 = 0$  is  $\bar{1}.84$ , giving a value of  $c$  of 0.70. Since the data in table 38 were already on an absolute scale, the value should have been unity, and this degree of error is typical of the method; the error is less than it appears, for it corresponds to only 16 per cent in structure amplitudes.

Other suggestions, based essentially on the same general principles, have also been made. Kasper, Lucht and Harker (1950), for example, have tried equating to zero the minima in a three-dimensional Patterson synthesis computed without the zero-order term; they assumed that these minima corresponded to complete absence of interatomic peaks. The results, however, turned out to be unreliable, and they found that the method just described was more successful.

The choice of method of placing intensities on an absolute scale in any particular problem depends upon a number of considerations. If the crystal contains no atoms heavier than nitrogen, its absorption coefficient will be small, and direct comparison with a standard low-absorption crystal may be used. If the required apparatus is not available, Wilson's method may be used, on the understanding that it is most successful if three-dimensional data are used, and that it tends to give too high a value for the  $F$ 's from two-dimensional data.

**5.4. Information from outstanding reflexions.** In section 5.5.2 examples were given of structural information derived from general relationships between intensities. Sometimes it is possible to gain important information from only a few intensities if these are outstandingly large, since there are comparatively few ways in which the atoms can be placed to scatter in phase for a given reflexion, whereas there are many ways in which approximately zero scattering can be produced.

For crystals containing planar molecules, the main clue to the structure may be contained in only one reflexion; if a reflexion is found with a structure amplitude near the maximum possible it may be deduced that the molecules are nearly parallel to the crystallographic planes giving this reflexion. The degree of parallelism can be inferred from the strength of the higher orders of reflexion from these planes, since, if all the atoms lay exactly in the planes, the higher orders would also be outstandingly strong amongst reflexions of about the same Bragg angle. This type of deduction may often be made by considering relative intensities only, since, if a reflexion is much stronger than its fellows, it is likely to be significant; but if the intensities are known in absolute measure the deductions are so much the more reliable.

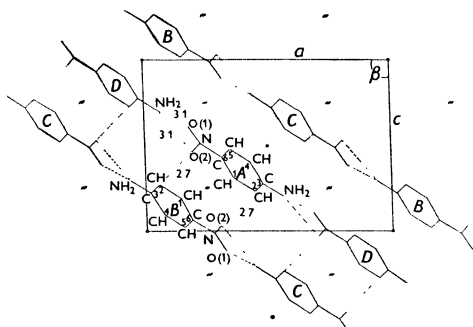


FIG. 137. Arrangement of molecules of para-nitroaniline in the (020) planes. The molecules are arranged in layers *A-D-A-D-*, and *B-C-B-C-*, the broken lines representing hydrogen bonds (Abrahams and Robertson, 1948)

Abrahams and Robertson (1948) made use of considerations of this sort in the determination of the structure of para-nitroaniline,

$\text{NO}_2 \cdot \text{C}_4\text{H}_4 \cdot \text{NH}_2$ . They found that the reflexion 202 had a structure amplitude of 119, compared with a maximum possible of 149. They therefore deduced that the molecules lay approximately in the (202) planes, in agreement with the pronounced cleavage of the crystal on the (101) planes. A structure based on these principles was found and is shown in projection in fig. 137. The projection has been verified by Donohue & Trueblood (1956) who have however found that the structure described in Fig. 137 is incorrect.

While such information concerning the general disposition of molecules in a crystal can only be expected to result from consideration of low-order reflexions, the combined information given by *several* outstandingly strong high-order reflexions has sometimes been found to give the structure in almost complete detail. Although one such reflexion by itself would allow of many possibilities for the atomic positions, because of the largeness of the indices, the combination of the information from several reflexions may be quite conclusive.

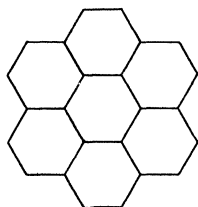


FIG. 138. Representation of the molecule of coronene

One of the earliest applications of this method is the determination of the structure of hexamethylbenzene (Lonsdale, 1929); a more recent example is given by coronene (Robertson and White, 1945). The molecule of coronene (fig. 138) is, to a first approximation, planar and composed of regular hexagons. Among the reflexions,  $1600$ ,  $160\bar{1}$ ,  $140\bar{8}$ ,  $100\bar{3}$ ,  $602$ ,  $40\bar{5}$ , and  $207$  are found to be outstanding, and fig. 139 shows the traces of the planes in which the atoms should lie in order that they should scatter in phase for each of these reflexions. The molecule can be fitted on to the intersections of these traces in only one way. This type of deduction is a special case of the use of Fourier transforms, which will be referred to in more detail in Chapter 7.

**5.5. Structure-factor graphs.** For non-planar molecules it is unlikely that such methods will be productive, and more general methods are required. The problem is to decide quickly and reliably the approximate values of certain selected structure factors given by a proposed structure: speed is necessary because many structures may have to be tried before the correct one is arrived at; reliability—not to be confused with accuracy—is necessary in order that the correct structure should not be missed by a single chance mistake.

The structure-factor graphs (section 3.3.2), although they were first proposed as a help in dealing with structures of high symmetry, have been found to be of considerable help in dealing with the initial stages of determination of structures of quite low symmetry. For this purpose the graphs need be drawn only roughly, since high accuracy is not

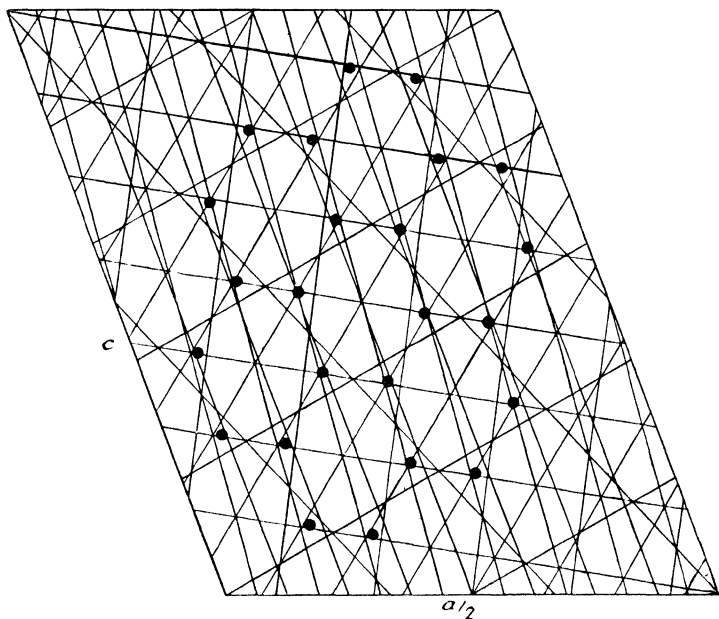


FIG. 139. Traces, on the (010) projection of coronene, of planes giving prominent x-ray reflexions. The superposition of the atoms in the molecule is also shown (Robertson and White, 1945)

required; with practice, even with only a few contours drawn, it is soon found possible to estimate the contribution of any one atom to a particular reflexion with an error of less than 10 per cent. It is, however, important that the regions of similar sign should be clearly labelled, as a misreading of a sign might lead to non-recognition of a correct structure.

Instead of rough structure-factor graphs drawn to scale, it is possible to use more accurate ones drawn on a square mesh, since these may be used for different structures and so are worth preparing in fair detail.

Structure-factor graphs were used with some success in the determination of the structure of penicillin (Crowfoot, Bunn, Rogers-Low and Turner-Jones, 1949). At first, graphs based upon a square unit cell were used, but since this involved considerable distortion of the projection of the molecule, most of the work was performed with graphs drawn to scale, with only the zero lines drawn in; these were used both as a rapid method for the determination of the signs of particular reflexions and for indication of atomic movements which would improve the intensity agreement.

5.6. *The fly's eye.* The limitations of the structure-factor graphs are that only relatively few reflexions can be considered at once, and that even these represent a tax upon the capabilities of the operator. It would be much better if some method existed whereby all the reflexions in a reciprocal-lattice section could be considered simultaneously, even if the method gave only qualitative estimations of the intensities.

The fly's eye (section 3.4.1) provides such a method. The mode of use can best be described by means of an actual example. Fig. 140(a) shows one of the attempts made by C. W. Bunn (Crowfoot et al., 1948) at the determination of the structure of sodium benzyl penicillin, together with the diffraction pattern (fig. 140(b)). It can be seen that this diffraction pattern shows some degree of correspondence with the observed structure amplitudes, which are given below each spot, and this was actually the first derivation of the approximate structure of the crystal. That the method will work with structures as complicated as this is strong evidence of its power. No claim is made that it will lead to accurate structures, and other methods were brought into play in the determination of the penicillin structure; but the fly's eye certainly helped to overcome the initial obstacles.

5.7. *Changes in scattering factors.* The methods of structure determination based upon intensities will, in general, give either the complete structure or nothing at all; it is not usually possible to determine one particular feature of a structure unless all the others are determined also. This is not so if a heavy atom is present, since, as we have seen in section 5.5.2, such an atom may be placed without knowledge of the positions of the others; but when the atoms are all approximately of equal weight, then none of the methods so far described can lead to information about only one atom in particular.

Such information would be obtainable, however, if it were possible to vary the scattering factor of a particular atom, and to note the corresponding changes in the intensities of the X-ray reflexions. In certain special cases it is possible to do this: the scattering factor of an atom may be effectively changed by replacing it by another of different atomic weight, or it may be varied by changing the wave-length of the X-rays, or by using other radiations such as electrons or neutron beams. None of these methods, however, is likely to be of general application, but they are sometimes worth considering.

The replacement method is possible if a pair of isomorphous compounds can be obtained. Isomorphism is indicated by a similarity of unit-cell dimensions of two compounds which are chemically similar; for example, the crystallographic constants of  $\text{CuSO}_4 \cdot 5\text{H}_2\text{O}$  and  $\text{CuSeO}_4 \cdot 5\text{H}_2\text{O}$  are given in table 141 (Groth, 1908). When such isomorphism occurs, it follows that the atomic positions in the two compounds are almost exactly the same.

The replacement of the sulphur in  $\text{CuSO}_4 \cdot 5\text{H}_2\text{O}$  by selenium decided



# PLATE VI

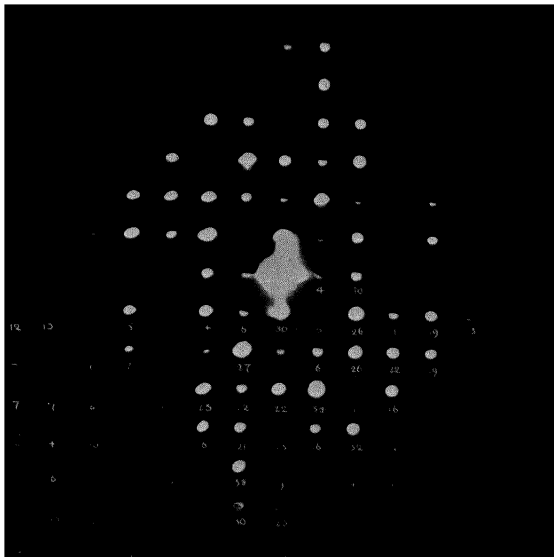
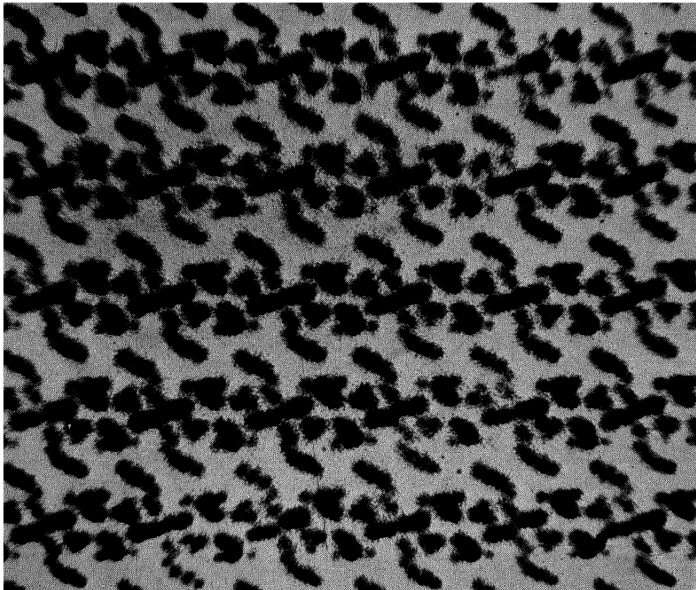


FIG. 140 (a). *Above*: Section of 'fly's eye' pattern representing trial structure of sodium benzylpenicillin. (b) *Below*: Diffraction pattern of above showing considerable agreement with observed structure factors (Crowfoot et al., 1949) *p.* 140



TABLE 141

	$a : b$	$c : b$	$\alpha$	$\beta$	$\gamma$
$\text{CuSO}_4 \cdot 5\text{H}_2\text{O}$	0.5721	0.5554	$82^\circ 05'$	$107^\circ 08'$	$102^\circ 41'$
$\text{CuSeO}_4 \cdot 5\text{H}_2\text{O}$	0.5675	0.5551	$81^\circ 58'$	$106^\circ 34'$	$103^\circ 11'$

the location of both the copper and the sulphur atoms. As shown in section 5.5.2, it was not found possible to decide directly whether the approximate face-centring shown by the intensities was due to the copper atoms alone or to the relative positions of the copper and sulphur atoms; if the copper atoms had a C-face-centred arrangement they would not contribute to the reflexions with  $h+k$  odd, whereas if the sulphur atoms formed a C-face-centred arrangement with the copper atoms, the total contribution of these atoms to those reflexions would depend upon the difference between the scattering factors of copper and sulphur. If, then, the sulphur were replaced by selenium, the reflexions with  $h+k$  odd would be expected to increase in intensity, since they would be largely due to these atoms if the copper atoms had the centred arrangement; whereas, if the copper atoms oppose the selenium atoms, the intensities of the reflexions with  $h+k$  odd would decrease, since the atomic numbers of these atoms are approximately equal.

It was found (Beevers and Lipson, 1934) that with  $\text{CuSeO}_4 \cdot 5\text{H}_2\text{O}$  the reflexions with  $h+k$  odd were relatively stronger than with  $\text{CuSO}_4 \cdot 5\text{H}_2\text{O}$ , thus proving that the copper atoms were at  $(0, 0, 0)$  and  $(\frac{1}{2}, \frac{1}{2}, 0)$ , and the sulphur atoms in general positions. It would have been possible to decide on the parameters of the sulphur atoms from the comparison of intensities of reflexions from the two compounds, but as shown in section 5.5.2, this was not necessary.

When the isomorphous-replacement method cannot be applied, the other methods of changing scattering factors have to be explored. The variation with wave-length (Compton and Allison, 1935, p. 298; Henry, Lipson and Wooster, 1951, p. 208) occurs only when one possible wave-length is near the absorption edge of the scattering atom, and so is available only for particular atoms. The effect occurs when the quantum of energy of the incident rays is near to that required to eject the K electrons, for example, and then the K electrons scatter with a difference of phase with respect to the rest of the electrons in the atom. If the two K electrons scatter with a phase difference of exactly  $\pi$ , the scattering factor is reduced by 4 units, and, since the K electrons occupy the innermost orbits, this reduction is almost independent of angle of scattering; thus for moderately heavy atoms the change of scattering factor can be quite appreciable, particularly at high angles.

The difficulty of application, however, lies in the small number of elements for which it can be used, because the number of elements that can be made into targets for X-ray tubes is small; the elements vanadium (23) to zinc (30) and some of the heavier elements such as zirconium (40), molybdenum (42), and silver (47) have been used. The range of K radiations given by the first series of elements gives the largest depression of scattering factor for elements of atomic number less by unity than the atomic number of the target element; thus  $\text{ZnK}\alpha$  depresses the scattering factor of copper by about 4 units (Jones and Sykes, 1937).

One of the first recorded uses of the depression of scattering factors is the determination of the structure of the Heusler alloys  $\text{Cu}_2\text{MnAl}$  (Bradley and Rodgers, 1934). Powder photographs showed that the alloy had a structure typified by  $\text{Fe}_3\text{Al}$  (Bradley and Jay, 1932), but because the atomic numbers of copper (29) and manganese (25) are nearly equal it is not easily possible to determine whether these atoms are arranged at random, or are distributed in an orderly way; both types of arrangement are possible in metal structures, in which many examples are known of crystallographically equivalent positions occupied by atoms of different kinds.

The powder photographs show two types of reflexions—the main reflexions, whose structure factors depend upon the sum of the scattering factors of the atoms, and superlattice lines; the structure factors of the superlattice reflexions can be further subdivided into those with even indices and those with odd indices. The relative intensities of these two sets of reflexions are critically dependent upon the relative scattering factors, and by taking powder photographs with  $\text{FeK}\alpha$  and  $\text{CuK}\alpha$  radiations, Bradley and Rodgers were able to show that the copper and manganese atoms must also be ordered. The wave-length of  $\text{FeK}\alpha$  radiation is  $1.934 \text{ \AA}$ , and the K absorption edge of manganese is at  $1.906 \text{ \AA}$ ; the ratio is 1.015, which gives a depression of the scattering factor of manganese of almost 4 units, leaving the scattering factors of copper and aluminium almost unchanged.

This illustration can hardly be regarded as typical, its success resulting from the simplicity of the structure; each atom gives its maximum contribution to the structure factors. There is, however, no reason why it should not be applied to other structures for which suitable radiations can be found, but so far there does not appear to be any example of a structure worked out in this way.

An unusual application of the effect has, however, been made by Peerdeman, van Bommel and Bijvoet (1951), who have used the phase change on scattering to deduce the *absolute* configuration of atoms in a crystal structure; normally, X-ray data cannot distinguish between an arrangement and its mirror image. The authors took photographs, with  $\text{ZrK}\alpha$  radiation, of sodium rubidium tartrate; since the wave-length of  $\text{ZrK}\alpha$  is  $0.788 \text{ \AA}$ , and the absorption edge of rubidium is at

0.816 Å, ZrK $\alpha$  radiation can excite the K electrons in the Rb atoms. It is shown in Volume II (p. 160) that under these circumstances the radiation scattered by the K electrons is not in phase with that scattered by the other electrons, and that the contribution of the K electrons to the scattering factor can therefore be represented by real and imaginary parts,  $f'$  and  $f''$  respectively. Now, for a non-centrosymmetrical structure the imaginary parts of  $F(hkl)$  and  $F(\bar{h}\bar{k}\bar{l})$  are equal and opposite, and thus if  $f''$  adds to one it will subtract from the other. Therefore the intensities of the reflexions  $hkl$  and  $\bar{h}\bar{k}\bar{l}$  will be different, and, making use of the table on p. 608 of Volume II, Peerdeman, van Bommel and Bijvoet were able to find the absolute configuration of the atoms in the tartrate ion.

The advantage of using electron waves lies in the fact that the variation with atomic number of the scattering of electrons by atoms is different from that of the scattering of X-rays; electrons are scattered by the potential field and not by the electron density (Volume I, p. 245). Fourier methods have been used to derive the potential field in crystals from the measured electron-beam intensities, with the signs of the Fourier coefficients determined by calculation as in X-ray work (Pinsker, 1949; Weinstein, 1954).

Theory predicts an intensity of electron reflection proportional to  $|F|^2$  only for very thin crystals. Pinsker (1949) concludes that the limiting thickness is about 500 Å under normal experimental conditions. For thick crystals the intensity is proportional to  $|F|$  but a modification is caused by interaction of the diffracted beams with the lattice and with one another (see also p. 30). Forbidden reflections may attain considerable intensity in this way, and the general effect is to even out the intensities. A similar effect is produced when a mosaic specimen consists of thin regions which scatter independently. Although corrections can be made, it is almost essential to use a crystal so thin that the effects of dynamic interaction and secondary diffraction are not important. Most of the single-crystal patterns recorded are therefore of little use for structure analysis.

In the diffraction of neutrons by crystals, the scattering lengths of atoms show no simple relation to atomic number (Bacon, 1955). (Scattering length  $b$  is analogous to atomic scattering factor  $f$  multiplied by  $\frac{e^2}{mc^2}$  and  $4\pi b^2$  is defined as the 'scattering cross section'). Certain elements, for example hydrogen, scatter radiation *in phase* with the incident beam, although the majority scatter with a 180° change of phase, as for X-rays. The predominant interaction of neutrons is with the nucleus but for certain elements (transition metals, rare earths) there is an additional magnetic interaction with the outer electrons. In principle, therefore, neutron-diffraction measurements may be used to derive maps of nuclear density, and in general such maps will show both positive and negative peaks. The hydrogen peaks are comparable in

magnitude with those due to heavy elements, and one of the chief applications of neutron crystallography is the location of hydrogen atoms in crystals (Bacon, 1955). Neutron diffraction can also be used to distinguish elements of nearly the same atomic number, for example Mg and Al whose  $b$ -values are  $+0.52$  and  $+0.35$  ( $\times 10^{-12}$ ) cm. respectively. When the intensity due to magnetic scattering can be separated from that due to nuclear scattering—and this is sometimes possible in practice—the magnetic electron distribution may be derived (Shull, Strauser and Wollan, 1951 ; Shull and Smart, 1949).

The experimental difficulties in neutron diffraction are greater than in X-ray diffraction. As yet only comparatively weak neutron beams are available, and the consequent use of large single crystals means that special care has to be taken to avoid errors caused by secondary extinction (Bacon and Lowde, 1948). Unless a crystal is composed of elements each of one isotope having zero spin, there will be a background of incoherent radiation from 'spin-incoherence' and isotope disorder. The spin-incoherent scattering from hydrogenous materials is particularly troublesome, and for this reason neutron diffraction experiments are often performed on crystals which contain deuterium in place of hydrogen (Rundle, Shull and Wollan, 1952).

## 6. PROOF OF CORRECTNESS OF STRUCTURES

6.1. *General considerations.* In view of the absence of general methods for structure determination, and dependence upon methods that are sometimes not classifiable as purely 'objective', the questions may well be asked 'Can we be sure that the structure arrived at in any particular instance is the only possible solution? May there not be others which would satisfy the X-ray data equally well?'

Obviously, no categorical answer can be given to these questions; no proof can be given that there are not two or more arrangements of atoms that would give effectively the same X-ray intensities. But general considerations suggest that it is unlikely. Those who have occupied themselves with structure determination know full well how an incorrect structure manifests itself by lack of agreement between calculated and observed intensities, and how, after many trials and tribulations, a set of atomic positions is found for which an appreciable measure of agreement is obtained. This agreement is improved by small changes, until, when a certain amount of change has been carried out, the calculated structure amplitudes agree in a remarkable way with the observed. One who has been through this process will need no convincing that the structure found is the only one that satisfies the X-ray data!

To those who are unconvinced by these arguments, one can only point out the unlikelihood that, if an approximate structure were

wrong, continued work on it would improve the agreement between calculated and observed intensities, finally producing a structure that was plausible, not only in the numbers and types of atoms (which have been assumed anyway) but also in distances of approach and in configuration. So long as one can rely upon the scientific integrity of the individual, there is little chance of an incorrect structure being produced—in fact, less chance than there is of mistakes in other types of scientific work, since there are usually so many experimental facts which must be satisfactorily accounted for.

6.2. *Homometric structures.* This attitude was rather upset by the discovery by Patterson (1944) of certain one-dimensional arrangements of atoms that gave identical sets of interatomic vectors, and thus must give the same X-ray intensities; he called such structures ‘homometric’. The number of homometric pairs found was quite large, and since no systematic method of deducing them was found, the suspicion was always present that there might be many more. Furthermore, there are still more pairs of homometric structures in two and three dimensions (section 6.3.4), and these are much more important, since no one relies only upon one-dimensional data as evidence in support of a given structure.

The question has been discussed by Robertson (1945), who decided that, in practice, the chance of finding homometric pairs in two and three dimensions was less, and not greater, than the chance of finding them in one dimension, and that the chance decreases with the complexity of the molecule; moreover, even if a pair were discovered, it is unlikely that both would represent structures that were chemically possible. He therefore concluded that if a structure is proposed that gives reasonable dispositions of atoms and satisfactory agreement between calculated and observed intensities, it is almost certainly correct.

6.3. *Measurement of structure-amplitude agreement.* It may then be asked ‘What is meant by satisfactory agreement between calculated and observed intensities?’, and much thought has been given to this question. Perfect agreement is never obtained, and the only basis for deciding what extent of disagreement is allowable is an empirical one; certain well-established structures give certain standards of agreement and we therefore expect that any new structures should give about the same.

First of all, therefore, we must decide what quantities to use. Ideally, the intensities should be calculated and compared with those observed, since it is always better to compare theoretical results with direct physical data rather than with deductions from them. On the other hand, tables of structure amplitudes and structure factors are of use to other workers in the same field, and thus it is usual for such tables

to appear in papers on crystal-structure determination; the observed structure amplitudes are represented by numbers, and the calculated structure factors by numbers with signs (for centrosymmetrical structures) or with phase angles (for non-centrosymmetrical structures).

It must be remembered, however, that structure factors involve the square roots of the intensities, and consequently any percentage errors in intensities will be halved in the structure factors; thus the agreement between structure amplitudes appears much better than the agreement between intensities, and this fact should always be allowed for. For example, if we decide to accept no discrepancy greater than 100 per cent in all moderate or stronger intensities, the limit of the discrepancy in structure-amplitude agreement should be about 40 per cent.

It has been found useful to express the overall agreement in terms of the mean discrepancy—the so-called ‘residual’,

$$R = \frac{\sum |F_o| - |F_c|}{\sum |F_o|},$$

where  $|F_o|$  and  $|F_c|$  are the moduli of the observed and calculated structure factors, and the summation is taken over all the reflexions (Booth, 1945*b*). Values of  $R$  can be a useful guide in deciding whether any particular change in parameters has produced any improvement in the agreement, but there is a tendency to use it for much more than this. Perhaps the most serious possibility is that  $R$  may hide some grave discrepancy; a few poor agreements may not increase the value of  $R$  greatly, but they may nevertheless prove that the structure is unacceptable.

In addition, there is a tendency to use the residual as quantity for comparison of the accuracy of the determination of different crystal structures. This also is to be deplored. A complicated crystal structure may give a large number of very weak reflexions, for which the discrepancies may be much greater than 40 per cent; the residual will then be rather large compared with that given by a much simpler structure, but the correctness is not thereby disproved. On the other hand, if the structure contains a single set of heavy atoms, the agreement should be rather better than usual. To take an extreme case, fairly good agreement may result from the heavy atoms alone, and the residual may not change much on insertion of the other atoms. To prove the correctness of the positions of these atoms, it would be necessary to show that the residual decreased when their contributions to the structure factors were inserted.

We must therefore be careful not to read too much from the actual value of the residual; there is no particular figure that must be reached before a structure becomes acceptable, nor does the attainment of a particular figure necessarily prove that the structure is correct. Jaeger, Terpstra and Westenbrink (1927) produced a tetragonal structure for gallium that gave quite good intensity agreement, but Bradley (1935*b*)



showed that, for a structure of that simplicity, the agreement was not good enough, and produced an orthorhombic structure that gave better agreement.

The only valid basis for the assessment of the correctness (as distinct from the accuracy) of a structure lies in the agreement for individual reflexions. It is difficult to lay down precise standards, since the nature of the agreement to be expected varies with the magnitude of the structure amplitude. For reflexions which are reasonably strong, and thus reliably estimated, one should expect that calculated and observed values should agree to within 40 per cent, most of them, of course, being much better than this; but for reflexions that are vanishingly small, one would expect the calculated structure amplitudes to be not more than two or three times the minimum that can be observed.

In deriving the value of  $R$ , the reflexions which are of vanishingly small structure amplitude are sometimes omitted; because the values of  $F_o$  cannot be quantitatively estimated it is not possible to assess accurately the value of the difference  $F_o - F_c$ . This is hardly satisfactory: to assess the agreement without taking into account the vanishingly small intensities means that an important part of the information is not utilized; moreover, a poor agreement does not influence the value of the residual  $R$ . This matter is discussed by Smare (1948), who gives a value of 0.16 for  $R$  when all the vanishingly small reflexions from a particular crystal (2,2'-dichlorobenzidine) are omitted. If the vanishingly small reflexions are taken as having structure amplitudes which are precisely zero,  $R$  becomes 0.32. Smare suggests that these structure amplitudes should be taken as half the minimum value that it has been found possible to observe at the corresponding angle, and on this basis the value of  $R$  became 0.24. This would seem to be a reasonable procedure. But, whatever procedure is used, it should be clearly stated when the value of  $R$  is given.

Another question that may be asked is 'What value of the residual is necessary in order to demonstrate that a proposed structure is substantially correct, and is worth proceeding with?' This again cannot be answered without qualification, but some results derived by Wilson (1950*b*) and discussed by Phillips, Rogers and Wilson (1950), provide a clue. Wilson shows that if a completely wrong structure, composed of atoms of about equal weight, is postulated, the most probable value for the residual is 0.83 for a centrosymmetrical structure and 0.59 for a non-centrosymmetrical structure; values near to these therefore indicate that the proposed structure is quite wrong. What values, then, are significant? To be on the safe side, about 0.5 and 0.4 for centrosymmetrical and non-centrosymmetrical structures respectively should be demanded. (It is not impossible that even these figures can be exceeded; for example, Furberg (1950) improved the value of  $R$  for cytidine from 0.60 down to 0.17.)

These values may indicate that the structure is substantially correct,

but that comparatively large movements of the atoms are necessary; this, of course, is what one hopes. But it may merely indicate that several of the atoms are in the correct relative positions but are incorrectly placed in the unit cell; some of the interatomic vectors (section 1.3.2) will thus be correct, and so some measure of intensity agreement will be obtained. It will, however, be found to be impossible to obtain satisfactory agreement for all the reflexions. This apparently was the difficulty in which Dunitz and Robertson (1947) found themselves in the determination of the structure of diacetylenedicarboxylic acid dihydrate. The crystal is centrosymmetrical, and the four molecules in the unit cell must lie on special positions—either two-fold axes or centres of symmetry. The latter seemed more likely, and a structure was devised which had a residual of 0.30, but it was found to be impossible to reduce this further. Another structure based upon the two-fold axes was then tried, and this was more successful; the residual was reduced to less than 0.20, a satisfactory value.

It is probably true to say that, when the agreement for a structure is good but cannot be improved, and a new structure has to be tried, the earlier work is not entirely wasted. Some of the features of the earlier structure must exist in the true one, and it is a test of the ingenuity of the investigator to find a new possibility in which some of these features can be incorporated.

**6.4. Causes of discrepancies.** To the uninitiated it may seem that the latitude allowed is extremely large; acceptance of errors of the order of 20 per cent is happily rare in scientific work. There are, however, several reasons why rather low standards have to be accepted.

First, the accuracy of measurement is not high. Considerable precautions have to be taken if reasonable accuracy is to be attained, and, as we have seen in section 5.5.3, corrections for such effects as absorption and extinction are not easily made. Moreover, for even moderately complicated crystals, fairly large numbers of reflexions have to be taken into account, and it is standard practice in most laboratories for intensities to be estimated visually. In general, an accuracy of not much better than 5–10 per cent in individual structure amplitudes can be claimed.

Even this figure is much less than the usual values of residuals found. This is explained by imperfections in the calculations, for in order to carry out the calculation of structure factors certain assumptions have to be made that are not necessarily true. For example, it is customary to neglect any hydrogen atoms that may be present, on the grounds that each is small, and that they are unlikely to combine in their scattering for any particular reflexion. This is usually true, but when a large number of reflexions is calculated, it is certain that the scatterings will combine for some of them, and for these reflexions discrepancies will result. Morrison, Binnie and Robertson (1948) have

shown that it is possible to improve considerably the agreement for certain crystals when plausible positions for the hydrogen atoms are chosen.

Further discrepancies can be caused by the adoption of particular scattering-factor curves. Strictly, special curves should be devised for each crystal, but errors due to this cause would not seem to be important. More serious is the possibility of anisotropic  $f$ -curves, due, for example, to anisotropic temperature movements. A still further possibility lies in the effects of those electrons which form the bonding agents between the atoms; it is difficult to allow for the effect of these electrons on the structure factors by any means other than the Fourier-transform method (section 4.3.7), and so they are usually ignored.

It will therefore be seen that accurate agreement between observed and calculated intensities is unlikely, even in the most favourable circumstances. What is surprising is that, with this poor agreement, it is still possible to find atomic positions with remarkable accuracy, and, still further, that the lack of agreement can in itself be a source of important information. This subject is discussed in more detail in Chapter 9.

## CHAPTER 6

### THE USE OF THE PATTERSON FUNCTION

#### 1. INTRODUCTION

The development of the ideas which led to the discovery of the function now known by his name has been traced back by Patterson to a paper by Zernike and Prins (1927), in which it was shown that the radial distribution of atoms surrounding any given atom of a liquid could be determined by application of Fourier integral analysis to the experimental X-ray diffraction pattern of the liquid. The method was successfully applied in practice by Debye and Mencke (1931) to determine the distribution of atoms in liquid mercury. Warren and Gingrich (1934) pointed out that the same method could be used to determine the radial distribution of atoms in a solid, given only the distribution of intensity in the X-ray powder pattern of the solid. The relevant formula is

$$P(r) = \int_0^\infty 4\pi S^2 i(S) \frac{\sin 2\pi r S}{2\pi r S} dS, \quad (150)$$

where  $4\pi r^2 P(r) dr$  is the number of centres of atoms in a shell of radius  $r$  and thickness  $dr$  drawn about the centre of any one atom,  $S = \frac{2 \sin \theta}{\lambda}$ , and  $i(S)$  can be obtained directly from the measured X-ray intensity.

Warren and Gingrich also drew attention to the fact that while the applicability of the Fourier-series method to a crystal is limited because only the magnitudes and not the phases of the coefficients can be measured, an important feature of the above formula is that it involves intensity, not amplitude. Instead of the arrangement of atoms, however, only the radial distribution of atoms about any one atom is obtained. The method was applied to show that in rhombic sulphur each atom has two nearest neighbours at a distance of about 2.35 Å, next nearest neighbours being more than 3.25 Å away. The structure therefore consists of long chains, or chains forming closed rings. The second possibility was regarded as the more probable, and has since been confirmed.

Patterson realized that there must exist a corresponding Fourier relation connecting the distances between atoms, as they occur in the ordered array of a single crystal, with the intensities of the X-ray reflexions. The derivation of this relation has already been given in Chapter 1, and follows closely that given by Patterson (1934, 1935a).

## 2. GENERAL CONSIDERATIONS

2.1. *Meaning of the Patterson Function.* We have already seen in Chapter 1 that the Patterson function of an electron-density distribution

$$\rho(x, y, z) = \frac{1}{V} \sum_h \sum_k \sum_l F(hkl) \exp [-2\pi i(hx + ky + lz)]$$

is defined as

$$P(u, v, w) = \int_0^1 \int_0^1 \int_0^1 \rho(x, y, z) \rho(x+u, y+v, z+w) V dx dy dz, \quad (151.1)$$

and can be represented by the Fourier series

$$P(u, v, w) = \frac{1}{V} \sum_h \sum_k \sum_l |F(hkl)|^2 \exp [-2\pi i(hu + kv + lw)]. \quad (151.2)$$

The physical interpretation of this function in terms of interatomic vectors was also mentioned earlier. We now consider some of the properties of this function from a more analytical point of view.

We define

$\mathbf{r} = x\mathbf{a} + y\mathbf{b} + z\mathbf{c}$  as a vector in the crystal,  
and  $\mathbf{H} = h\mathbf{a}^* + k\mathbf{b}^* + l\mathbf{c}^*$  as a vector to a reciprocal-lattice point.

Consequently  $\mathbf{H} \cdot \mathbf{r} = hx + ky + lz$  (compare eqn. 10.3). We now proceed to show that, just as a crystal may be regarded as built up from  $N$  atoms, each of which is repeated on an infinite lattice, so the Patterson function consists of  $N^2$  'Patterson peaks' repeated in the same way. For the crystal itself, we have the relation

$$F(\mathbf{H}) = \sum_{n=1}^N f_n(\mathbf{H}) \exp [2\pi i \mathbf{H} \cdot \mathbf{r}_n], \quad (151.3)$$

giving the structure factor in terms of the positions and scattering factors of the  $N$  atoms in the unit cell. If the  $n$ th atom is spherically symmetric,  $f_n$  is a function of  $S$  only. In the same notation,

$$\rho(\mathbf{r}) = \frac{1}{V} \sum_{\mathbf{H}} F(\mathbf{H}) \exp [-2\pi i \mathbf{H} \cdot \mathbf{r}]. \quad (151.4)$$

Substituting from (151.3) in (151.4), and changing the order of summation,

$$\rho(\mathbf{r}) = \sum_{n=1}^N \left\{ \frac{1}{V} \sum_{\mathbf{H}} f_n(\mathbf{H}) \exp [-2\pi i \mathbf{H} \cdot (\mathbf{r} - \mathbf{r}_n)] \right\}, \quad (151.5)$$

or

$$\rho(\mathbf{r}) = \sum_{n=1}^N \rho_n(\mathbf{r} - \mathbf{r}_n), \quad (151.6)$$

where

$$\rho_n(\mathbf{r}) = \frac{1}{V} \sum_{\mathbf{H}} f_n(\mathbf{H}) \exp [-2\pi i \mathbf{H} \cdot \mathbf{r}]. \quad (151.7)$$

Equation 151.6 brings out the point that the periodic distribution  $\rho(\mathbf{r})$  is a superposition of  $N$  periodic distributions, of which the  $n$ th is given by equation 151.7.

The Patterson function can be considered in the same way. We begin with the fact that, corresponding to (151.3),

$$\begin{aligned} |F(\mathbf{H})|^2 &= \left( \sum_{n=1}^N f_n(\mathbf{H}) \exp [2\pi i \mathbf{H} \cdot \mathbf{r}_n] \right) \left( \sum_{n=1}^N f_n(\mathbf{H}) \exp [-2\pi i \mathbf{H} \cdot \mathbf{r}_n] \right) \\ &= \sum_{n, m=1}^N f_n(\mathbf{H}) f_m(\mathbf{H}) \exp [2\pi i \mathbf{H} \cdot (\mathbf{r}_n - \mathbf{r}_m)]. \end{aligned} \quad (152.1)$$

We then substitute this value of  $|F(\mathbf{H})|^2$  in the equation for the Patterson function, which in the present notation is

$$P(\mathbf{r}) = \frac{1}{V} \sum_{\mathbf{H}} |F(\mathbf{H})|^2 \exp [-2\pi i \mathbf{H} \cdot \mathbf{r}],$$

obtaining in the same way as before

$$P(\mathbf{r}) = \sum_{n, m=1}^N P_{nm} \{ \mathbf{r} - (\mathbf{r}_n - \mathbf{r}_m) \}, \quad (152.2)$$

where

$$P_{nm}(\mathbf{r}) = \frac{1}{V} \sum_{\mathbf{H}} f_n(\mathbf{H}) f_m(\mathbf{H}) \exp [-2\pi i \mathbf{H} \cdot \mathbf{r}]. \quad (152.3)$$

$P_{nm}(\mathbf{r})$  is a periodic function, representing a single Patterson peak repeated on a lattice. The form of a Patterson peak, not repeated on a lattice, can be calculated from the integral corresponding to (152.3), which, when  $f_n$  and  $f_m$  are functions of  $S$  only, reduces to

$$P'_{nm}(r) = \int_0^\infty 4\pi S^2 f_n(S) f_m(S) \frac{\sin 2\pi r S}{2\pi r S} dS. \quad (152.4)$$

$P'_{nm}$ , when repeated by the lattice translations  $\mathbf{a}$ ,  $\mathbf{b}$ ,  $\mathbf{c}$ , produces  $P_{nm}$ . In practice, lattice translations are usually considerably greater than the distance within which a Patterson peak falls to zero. In such circumstances, repetition of  $P'_{nm}$  on a lattice does not result in overlap of adjacent peaks, which consequently retain their spherically-symmetric shape. Either equation 152.3 or equation 152.4 can therefore be used to calculate the shape of an individual Patterson peak, but it must be remembered that in calculating the shape of a peak in a Patterson function derived from a terminated Fourier series, the upper limit of the integral 152.4 has to be taken as  $S_0$ , the radius of the sphere in reciprocal space containing those reciprocal-lattice points  $\mathbf{H}$  for which  $|F(\mathbf{H})|^2$  is included in the series.

We also see from equation 152.2 that the Patterson function contains as many peaks as there are values of  $nm$ , which is  $N^2$ . Of these,  $N$  coincide at the origin (those for which  $n = m$ ), and  $\frac{1}{2}N(N-1)$  are related to the remaining  $\frac{1}{2}N(N-1)$  by a centre of symmetry. For every pair

of atoms at points  $\mathbf{r}_n$  and  $\mathbf{r}_m$  there is a Patterson peak at  $\mathbf{r}_n - \mathbf{r}_m$ . This does not necessarily mean that  $P(\mathbf{r})$  will pass through a maximum at that point, as neighbouring peaks may overlap.

The weight of the  $n$ th atom we shall define as  $\int_V \rho_n(\mathbf{r}) dV$ , where the integration is over one unit cell. The value of this integral is clearly the atomic number of the atom,  $Z_n$ . In the same way, the weight of the  $nm$ th Patterson peak is  $\int_V P_{nm}(\mathbf{r}) dV$ , which can be shown to be equal to  $Z_n Z_m$ . The weight of this peak should not be confused with its height, which is given by

$$P_{nm}(0) = \frac{1}{V} \sum_{\mathbf{H}} f_n(\mathbf{H}) f_m(\mathbf{H}) = \int_V \rho_n(\mathbf{r}) \rho_m(\mathbf{r}) dV. \quad (153.1)$$

$P_{nm}(0)$  is proportional to  $Z_n Z_m$  only to the extent that the electron distributions (or atomic scattering factors) of all atoms are the same, apart from a factor proportional to  $Z$ . This is true to a fair approximation, and to a good approximation when the atoms concerned do not differ greatly in atomic number.

Multiple peaks may occur in the Patterson function, apart from purely chance coincidences. For instance, when a structure is centrosymmetric, only  $\frac{1}{2}N$  of the peaks can be single (section 2.4.5). Patterson (1935*b*) has tabulated the coordinates, weights and multiplicities of peaks of the Patterson function corresponding to two-dimensional structures having the symmetry of each of the 17 plane groups. Each structure was taken to consist of two atoms in general positions, together with the atoms at equivalent points.

If we now make the assumption that the scattering factor of an atom can be taken to be

$$f_n = \hat{f} Z_n,$$

where  $\hat{f}$  is the same for all atoms (section 3.2.5),  $F(\mathbf{H})/\hat{f}$  represents the structure factor of a set of point atoms, occupying the same sites as the atoms whose structure factor is  $F(\mathbf{H})$ . This distribution of points, of which the  $n$ th has weight  $Z_n$  and is situated at  $\mathbf{r}_n$ , can be represented by a Fourier series,

$$\rho_s(\mathbf{r}) = \frac{1}{V} \sum_{\mathbf{H}} \frac{F(\mathbf{H})}{\hat{f}} \exp[-2\pi i \mathbf{H} \cdot \mathbf{r}], \quad (153.2)$$

while the corresponding Patterson function is given by

$$P_s(\mathbf{r}) = \frac{1}{V} \sum_{\mathbf{H}} \frac{|F(\mathbf{H})|^2}{\hat{f}^2} \exp[-2\pi i \mathbf{H} \cdot \mathbf{r}]. \quad (153.3)$$

It is not difficult to show that the latter consists of a set of points of weight  $Z_n Z_m$  occurring at  $(\mathbf{r}_n - \mathbf{r}_m)$ . The points  $\mathbf{r}_n$  may be called the

fundamental set, and the points  $(\mathbf{r}_n - \mathbf{r}_m)$  the vector set. They may also be said to be located in fundamental space and vector space respectively. We shall call  $\rho_s$  and  $P_s$  the weighted fundamental set and weighted vector set respectively.

**2.2. Symmetry in vector space.** The electron density, or the fundamental set, will usually possess symmetry—that of one of the 230 space groups in fact. The corresponding Patterson function, or the vector set, will not necessarily have the same symmetry. For instance, we have already seen that all Patterson functions have a centre of symmetry. In this connection it will be sufficient to discuss the relation between the symmetry of a fundamental set and that of the corresponding vector set. The fundamental set will consist of a number of points together with the equivalent points related to these by the symmetry of the fundamental set, which we denote by the symbol  $\mathcal{F}$ . Imagine every pair of points to be joined by a vector, to give a set of vectors in fundamental space, and therefore related by the symmetry  $\mathcal{F}$ . Now in vector space imagine a vector drawn from the origin to every point of the vector set. These vectors are related by the symmetry of the vector set, which we denote by the symbol  $\mathcal{V}$ , and are identical in number and orientation with those in fundamental space. They differ from the latter only in the fact that they radiate from a common origin. This corresponds merely to a removal of the translations which separate the ends of the vectors in fundamental space. It follows that the points at the ends of the vectors in vector space, namely the points of the vector set, are related by the ‘translation-free residue’ of the symmetry element which related vectors, and points, in fundamental space. For example, if  $\mathcal{F}$  contained a two-fold screw axis,  $\mathcal{V}$  will contain a parallel two-fold axis through the origin. To derive  $\mathcal{V}$  from  $\mathcal{F}$  we therefore substitute at the origin (and at all other lattice points of vector space) the translation-free residue of each generating symmetry element in  $\mathcal{F}$ , complete the group by forming the products of the operations of these elements with the lattice, and add a centre of symmetry at the origin if one is not already present. For example, if  $\mathcal{F}$  is  $P1$ ,  $P2_1/c$  or  $Pbca$ ,  $\mathcal{V}$  is  $P\bar{1}$ ,  $P2/m$  or  $Pmmm$  respectively. The possible symmetry of a vector set is therefore more restricted than that of a fundamental set; a vector set can in fact have the symmetry of one of only 24 space groups. These have been listed by Buerger (1950a). In two dimensions, the plane group of a vector set can be obtained simply by adding a centre of symmetry to the plane group of the corresponding fundamental set.

This discussion of symmetry brings us to another property of the Patterson function which is worthy of note. The one-dimensional Patterson function, for example, is given by

$$P(u) = \int_0^1 \rho(x)\rho(x+u)dx = \frac{1}{a} \sum_h |F(h)|^2 \exp[-2\pi i h u].$$



There is a second function closely related to  $P(u)$  which we define as

$$Q(u) = \int_0^1 \rho(x)\rho(u-x)dx = \int_0^1 \rho(\tfrac{1}{2}u+x)\rho(\tfrac{1}{2}u-x)dx. \quad (155.1)$$

The Fourier-series representation of  $Q(u)$  can be shown to be

$$Q(u) = \frac{1}{a} \sum_h F^2(h) \exp[-2\pi i h u]. \quad (155.2)$$

Mathematically expressed,  $Q(u)$  is the convolution of the electron density with itself, while  $P(u)$  is the convolution of the electron density with itself inverted in the origin. The function  $Q(u)$ , which involves  $F^2(h)$  instead of  $|F(h)|^2$ , can be given a physical interpretation. For a given value of  $u$ , the integral 155.1 measures the extent to which the electron density overlaps itself when inverted in a centre of symmetry at  $\frac{1}{2}u$ .  $Q(u)$  is therefore a measure of the degree to which  $\rho(x)$  approximates to centrosymmetry about a point at  $\frac{1}{2}u$ , or  $\frac{1}{2} + \frac{1}{2}u$ . If an atom at  $\frac{1}{2}u - x$  has a counterpart at or near  $\frac{1}{2}u + x$ , there will be a contribution to the integral. If there is an atom at  $\frac{1}{2}u$  there will be a contribution, because the atom itself closely approximates centrosymmetry. The function  $Q(u)$  corresponding to a set of atoms therefore contains two types of peaks: (i) peaks of weight  $Z_n^2$  at  $2x_n$  and (ii) peaks of weight  $2Z_n Z_m$  at  $x_n - x_m$ . In general  $Q(u)$  cannot be calculated, since the values of  $F^2(h)$  cannot be measured experimentally. However when the crystal is centrosymmetric, there is no distinction between  $F^2(h)$  and  $|F(h)|^2$ , and  $Q(u) = P(u)$ . Similar results hold, of course, in two or in three dimensions. This suggests a second interpretation of the Patterson function of a centrosymmetric crystal; it can be looked on as a mapping of the centrosymmetric properties of the crystal. If the Patterson function is drawn to one-half its usual linear dimensions, a peak at the point  $\mathbf{r}$  is an indication that the crystal possesses 'some centrosymmetry' at  $\mathbf{r}$ . On this scale, the origin peak recurs at all points where the crystal is truly centrosymmetric. Patterson (1952) has recently generalized this result, and has shown how the Patterson function can be regarded as indicative of other symmetry elements in the crystal, and the extent to which the asymmetric unit itself possesses the various symmetry elements of the space group.

### 3. DERIVATION OF A CRYSTAL STRUCTURE FROM THE PATTERSON FUNCTION

**3.1. Information contained in the Patterson function.** We have seen that in principle the Patterson function gives the vector distance between every pair of atoms in a crystal. This in itself is valuable information to have when one is trying to solve a crystal structure, but Patterson (1935a), in one of the earliest papers on the subject, showed

that sometimes it was possible to determine all the main features of a crystal structure from its Patterson function. This proved to be so in the case of  $\text{KH}_2\text{PO}_4$ , where the interpretation was greatly simplified by the occurrence of potassium and phosphorus atoms in special positions in the projection of the structure on (001). In the other examples which Patterson considered ( $\text{C}_6\text{Cl}_6$  and  $\text{CuSO}_4 \cdot 5\text{H}_2\text{O}$ ) it was also possible to proceed directly from the Patterson function to at least the main features of the crystal structure. Quite complex structures, having no special features, and in which all atoms were of about the same weight, have since been solved from their two- or three-dimensional Patterson functions, with the help of a few extraneous items of information such as the expected distances between bonded atoms. Experience has shown, therefore, that in particular examples it is possible to make effective use of the Patterson function in determining a crystal structure and we shall consider some practical points of strategy in later sections. In this section, however, we are more concerned with the important theoretical question of whether it is possible, even in principle, to 'recover' the electron density from the Patterson function. We have seen that, given the electron density, it is always possible to calculate the Patterson function, but there was nothing in the derivation to indicate when, if ever, the process can be carried through in the reverse direction. This problem can be regarded as simply another formulation of the phase problem—is it possible to determine a crystal structure knowing the magnitudes, but not the phases, of the Fourier coefficients? The relations between structure factors discovered by Karle and Hauptmann (1950), Goedkoop (1950), and others, show that this question can now be answered in the affirmative. The possibility of practical application of these results will be considered in Chapter 8. Their existence suggests that it is not hopeless to look for a general solution involving the Patterson function.

An obvious objection to the possibility of recovering even a fundamental set from its vector set is that fundamental sets of different symmetries may have vector sets all of the same symmetry. For example,  $\mathcal{F}$  may be  $P222$  or  $Pmmm$ , but  $\mathcal{V}$  corresponding to both is  $Pmmm$ . Now neither space group results in systematically-absent X-ray reflexions, and consequently not even the symmetry of the fundamental set is determined by the X-ray data. There would therefore appear to be no hope of determining the arrangement of points in the fundamental set, since this includes the symmetry. This argument is weakened by the fact that Wilson and his collaborators have now shown that there is information in the X-ray data which will distinguish all but a very few pairs of space groups (section 2.4.5). Previous to this work, it had in fact been pointed out by Buerger (1946) that information about space-group symmetry  $\mathcal{F}$  is carried over into vector space in the form of concentrations of Patterson peaks on certain lines, or on certain planes, of the Patterson function (section 2.4.5). A study of this subject

by Buerger (1950a) has shown that all space groups, except the eleven enantiomorphous pairs, can be distinguished in their vector representations. In practice the statistical methods described in Chapter 2 provide a more certain and convenient method of determining space groups.

**3.2. The Harker section.** The first discovery of a relation between the Patterson function and the electron density was made by Harker (1936). Harker pointed out that in some cases much useful information is concentrated in certain planes of the three-dimensional Patterson function. These are in fact the same planes as were mentioned in the previous paragraph. For example, suppose a crystal to have a two-fold  $b$ -axis. Then for every atom at  $(x_j, y_j, z_j)$  in the crystal, there is a peak of weight  $Z_j^2$  in the Patterson function at  $(2x_j, 0, 2z_j)$  corresponding to a vector between two equivalent atoms. A section through the Patterson function in the plane  $y=0$  is given by

$$P(x0z) = \frac{1}{V} \sum_h \sum_l \left\{ \sum_k |F(hkl)|^2 \right\} \cos 2\pi(hx + lz),$$

or putting  $C(hl) = \sum_k |F(hkl)|^2$ ,

$$P(x0z) = \frac{1}{V} \sum_h \sum_l C(hl) \cos 2\pi(hx + lz). \quad (157)$$

(We have previously used  $(uvw)$  to represent the coordinates of a point in the Patterson function, but since the latter has the same unit cell as the crystal we may equally well use  $(xyz)$ .) The series 157 can generally be evaluated without too great a computational effort, but it does require the measurement of the intensities of general  $(hkl)$  reflexions. If the crystal has a two-fold screw axis, the plane in which vectors connecting symmetry-related atoms fall is the plane  $y = \frac{1}{2}$ , and this plane section through the Patterson function is given by 157 with

$$C(hl) = \sum_k (-1)^k |F(hkl)|^2.$$

Such a section is now usually referred to as a Harker section. Sometimes the symmetry results in vectors between equivalent atoms being concentrated on a line in vector space. For instance, if the crystal has a mirror plane perpendicular to  $b$ , the Harker section is the line  $0y0$ . Table 158 gives the Harker sections corresponding to various symmetry elements, as given by Harker (1936), and Buerger (1946).

At first sight it might appear that, for a structure having a two-fold axis for instance, the function  $P(x, 0, z)$  should give a projection of the structure down the  $b$ -axis, atoms being represented by Patterson peaks, and the scale of presentation being increased by a factor of two.

TABLE 158

Symmetry element parallel to $b$	Harker section
$2, 3, \bar{3}, 4, \bar{4}, 6, \bar{6}$ $6_1, 6_5$ $4_1, 4_3$ $3_1, 3_2, 6_2, 6_4$ $2_1, 4_2, 6_3$	$P(x0z)$ $P(x\frac{1}{2}z)$ $P(x\frac{1}{4}z)$ $P(x\frac{3}{4}z)$ $P(x\frac{1}{2}z)$
Perpendicular to $b$	
$m$ Glide $\frac{1}{2}a$ $„ \frac{1}{2}(a+c)$ $„ \frac{1}{4}(a+c)$ $„ \frac{1}{4}(3a+c)$	$P(0y0)$ $P(\frac{1}{2}y0)$ $P(\frac{1}{2}y\frac{1}{2})$ $P(\frac{1}{2}y\frac{1}{4})$ $P(\frac{3}{4}y\frac{1}{4})$

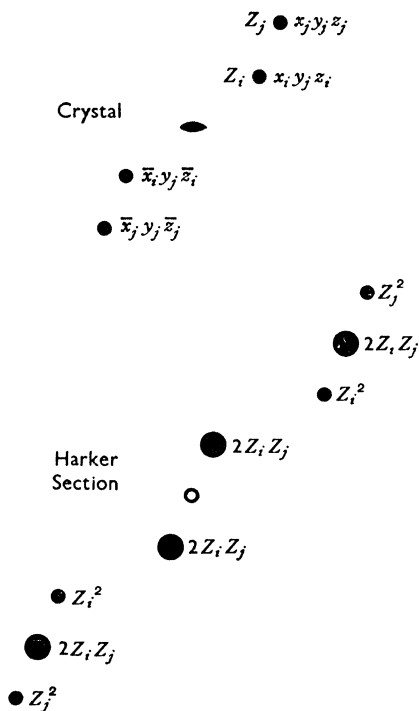


FIG. 158. Atoms related by a two-fold axis are necessarily at the same height. If by chance the unrelated atoms  $Z_i$  and  $Z_j$  are at the same height, peaks of weight  $2Z_i Z_j$  appear in the Harker section, as shown in the lower half of the diagram

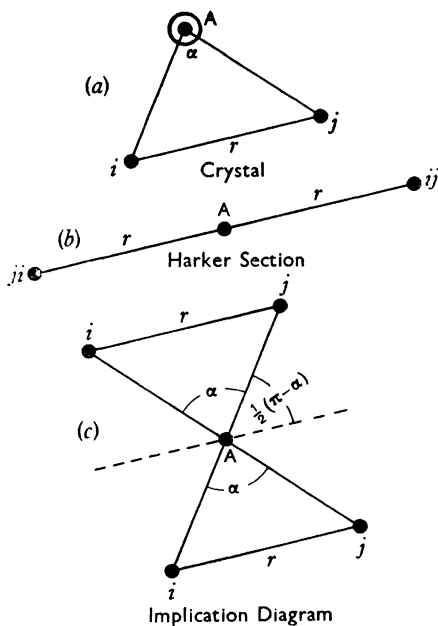


FIG. 159

There are two difficulties in the way of such an interpretation, however. The first, usually the less serious, is that there may be a pair of atoms  $i$  and  $j$ , not related by the two-fold axis, which by chance have the same  $y$ -coordinate. Each such pair results in peaks of weight  $2Z_iZ_j$  in the Harker section; these peaks do not represent atomic sites, but fall midway between points which do represent atomic sites (fig. 158). The more fundamental objection, however, is based on the fact that in this example an atom in any one of the four positions  $(x_j, y_j, z_j)$ ,  $(x_j, y_j, z_j + \frac{1}{2})$ ,  $(x_j + \frac{1}{2}, y_j, z_j)$  and  $(x_j + \frac{1}{2}, y_j, z_j + \frac{1}{2})$ , together with a symmetry-related atom, results in a Patterson peak at  $(2x_j, 0, 2z_j)$ . To any one peak of the Harker section there therefore correspond four possible atomic sites in the projection of the crystal.

**3.3. The implication diagram.** The ambiguities of interpretation of Harker sections can be brought out more clearly by transforming the coordinate system of the section to give what Buerger (1946) has called an 'implication diagram'. For the present we consider only the situation where atoms are related by  $n$ -fold axial symmetry elements, with or without symmetry planes parallel to the axes. Fig. 159a represents two atoms related by an  $n$ -fold axis, with  $\alpha = 2\pi/n$ . The

appropriate Harker section, fig. 159*b*, will contain two peaks *ij* and *ji* corresponding to vectors between these atoms. If now we wish to make the transformation in the reverse direction, we need only find two points in the crystal equidistant from the axis A, which subtend an angle  $\alpha$  at A, and are separated by a distance  $r$ . There are two solutions for this implication (fig. 159*c*), unless

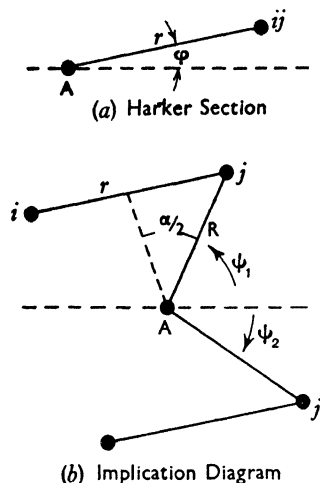
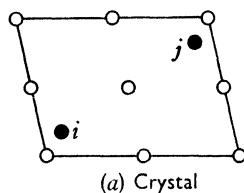


FIG. 160(i)

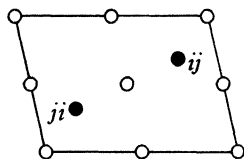
$\alpha = \pi$ , when the two coincide. If the polar coordinates of the peak in the Harker section are  $(r, \phi)$ , those of the corresponding two points in the implication diagram are  $(R, \psi_1)$  and  $(R, \psi_2)$ , where,

$$\left. \begin{aligned} R &= \frac{r}{2 \sin \alpha/2} = \frac{r}{2 \sin \pi/n} \\ \psi_1 &= \phi + \frac{1}{2}(\pi - \alpha) \text{ and } \psi_2 = \phi - \frac{1}{2}(\pi - \alpha). \end{aligned} \right\} (160)$$

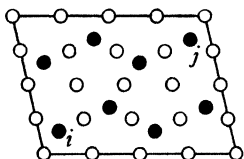
Fig. 160(i) makes clear the source of these relationships. The point  $(R, \psi_2)$  may be disregarded, as it is the point  $(R, \psi_1)$  for some other of the  $n$  points of a symmetrical set in the Harker section. An exception occurs for  $n=3$ , when the addition of a centre of symmetry results in the appearance of a six-fold axis in the Harker section and therefore in the implication diagram. Inspection of equations 160 and fig. 160(i) will reveal that every point on the Harker section transforms to a point on the implication diagram by a shrinkage of its radial polar coordinate and a rotation of its azimuth. The change of scale and rotation are constant for a given value of  $n$ , and are given in table 161.



(a) Crystal



(b) Harker Section



(c) Implication Diagram

FIG. 160(ii)

TABLE 161

## Transformation from Harker Section to Implication Diagram

$n$	2	3	4	6
Shrinkage Factor	$\frac{1}{2}$	$1/\sqrt{3}$	$1/\sqrt{2}$	1
Rotation	$0^\circ$	$30^\circ$	$45^\circ$	$60^\circ$ (or $0^\circ$ )

By considering the example  $n=2$  we can now see more clearly how the ambiguities in the interpretation of a Harker section arise. Fig. 160(ii)*a* shows one unit cell of a structure in projection, while 160(ii)*b* shows the corresponding Harker section. This is then reduced to one-half its former linear dimensions to give (say) the lower left-hand quarter of the implication diagram, 160(ii)*c*. Three neighbouring unit cells of the Harker section will cover the remaining three-quarters of the implication diagram of one unit cell. The implication diagram has a higher symmetry than the structure it represents, and contains in this case four times as many units as the original structure. We may say that the ambiguity factor is four. Fig. 162 shows the relations between the symmetry elements of the crystal, the Harker section and the implication diagram for the four possible values of  $n$ .

The value of the ambiguity factor can be seen to be  $M=4, 3, 2$  and  $1$  for  $n=2, 3, 4$  and  $6$  respectively. The net ambiguity is sometimes a submultiple of  $M$ ; for instance, if the structure is face-centred in projection the duplication of atoms in the implication diagram ceases to be an ambiguity, and the net ambiguity becomes  $M/q$ . Buerger (1948*b*) has shown that  $1/q$  is also the fraction of reflexions not systematically absent in the reciprocal-lattice plane parallel to the plane of the Harker section concerned, so the net ambiguity is easily predicted in any particular case.

A further complication in the implication diagram is the occurrence of 'satellite' peaks which do not correspond to atomic sites and are not related to atomic sites by the symmetry of the implication diagram. This is due to the fact that for certain axial symmetries, for example 4 or 6, there occurs in the same plane not only an atom related to the original atom by the first power of the symmetry operation, but also one or more additional atoms related to the original by higher powers of the same symmetry operation. Satellite peaks may also result from the presence of symmetry planes parallel to the symmetry axes, but for further details the original paper by Buerger (1946) should be consulted. This very complete study of the subject has shown that there are in fact five space groups (No. 169,  $P6_1$ ; No. 170,  $P6_5$ ; No. 178,  $P6_2$ ; No. 179,  $P6_3$ ; and No. 146,  $R3$ ) whose implication diagrams are free from satellite peaks (except for one at the origin in the case of  $R3$ ), and for which the ambiguity factor is unity. The implication diagram in such circumstances is therefore a map of the projected structure, apart from non-Harker peaks whose existence and possible

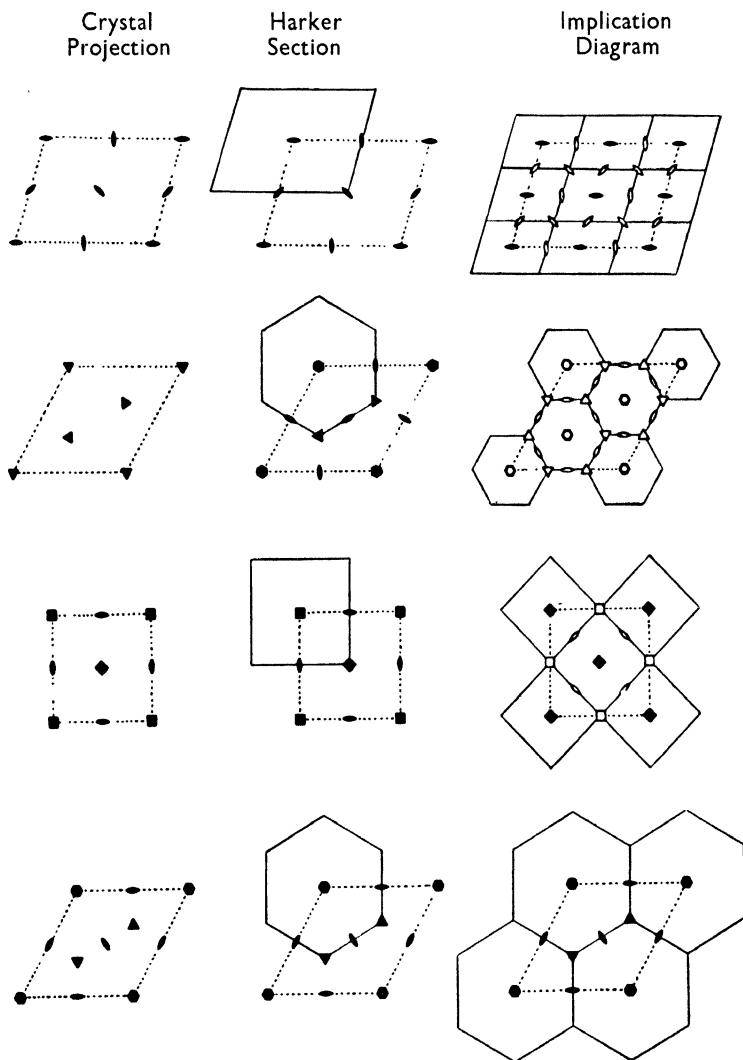


FIG. 162. Relations between the symmetry elements of the crystal, Harker section, and implication diagram for the four possible values of  $n$ . The outlines of the crystal cells are indicated by broken lines. The figure shows the domains (outlines in full lines) of the Harker section and their transfer to the implication diagram for each case. The locations of new symmetry in the implication diagram for the case of primitive cells are indicated by outlined symbols (Buerger, 1946)



distinguishing characteristics we have already noted (fig. 158). We may say that for these five space groups, the fundamental set (in projection) can be recovered from the implication diagram of the vector set. The implication method therefore constitutes in principle a limited solution of the phase problem, mainly of academic interest.

**3.4. Superposition methods.** An important paper on the relation between fundamental sets and vector sets was published by Wrinch (1939). It was shown that there exist methods by which the fundamental set, or sets, may be recovered from a vector set. Unlike the Harker-Buerger method, Wrinch's method makes use of all the points of the vector set. Because of the difficulty of illustrating geometrical relations in three dimensions we shall consider two-dimensional sets as examples. It should be emphasized at the outset that we are dealing with a procedure by which a fundamental set of *points* may be recovered from its vector set of *points*. In practice we have available not the vector set, but the Patterson function; the unravelling of the latter is bound to be more difficult and may be impossible. Like many other crystallographers who have discovered new methods of structure analysis, Wrinch optimistically considered the applicability of her method to the determination of the structures of crystalline proteins. In the ensuing controversy, Wrinch's important contribution to the theory of the interpretation of the Patterson function was lost sight of, and little attention was paid to it until parallel results were obtained ten years later, independently by Buerger (1950*b*, 1951), Beevers and Robertson (1950), Clastre and Gay (1950*a*, *b*), Garrido (1950*a*, *b*) and McLachlan (1951).

We consider first of all the vector set of two points, 1 and 2. It consists of four points, of which two coincide at the origin. The point 12 may be described as the image of point 2 in point 1, and 21 as the image of 1 in 2, etc. The vector set of three points is shown in fig. 164, and may be denoted by the symbol  $v(1 + 2 + 3)$ . We see by comparison with fig. 163 that  $v(1 + 2 + 3)$  consists of  $v(1 + 2)$ , plus  $v(3)$  (another point at the origin), plus the image of line 12 in 3, the image of 3 in line 12 and the image of 3 in line 21. Inspection of fig. 164*b* shows also that it can be described as a superposition of images of the triangle 123 in each of the points 1, 2 and 3. The centrosymmetrically-related (or *congruent*) triangle 1'2'3' also has  $v(1 + 2 + 3)$  as its vector set. Treating next the vector set of four coplanar points (fig. 165 (i)), we notice that it comprises  $v(1 + 2 + 3)$ , plus 44, plus the image of triangle 123 in 4, plus the image of 4 in each of the three points of this triangle. The congruent quadrilateral 1'2'3'4' has again the same vector set as 1234.

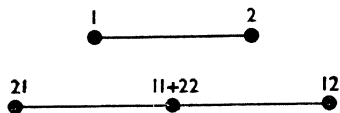


FIG. 163. Two points, and the vector set of two points

We now consider some of the ways in which  $1+2+3+4$  can be recovered from  $v(1+2+3+4)$ . First we select any point, say 12, and

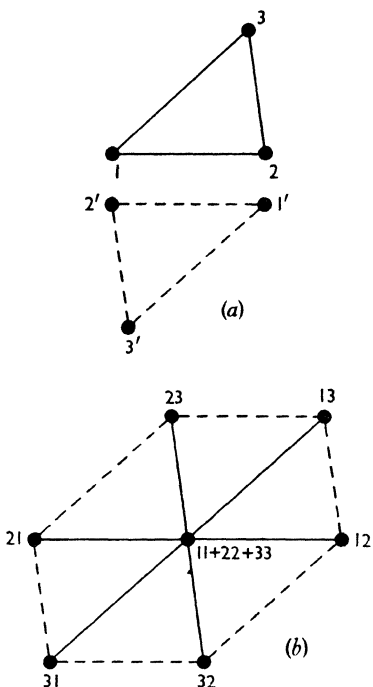


FIG. 164. (a) A fundamental set of three points. The three points of the congruent set are joined by dotted lines. (b) The vector set of this set of three points, or of its congruent set

join it to 0. We then draw in all lines parallel to this. These are 23-13, 24-14, 31-32 and 41-42. We now select arbitrarily any one of these lines which does not pass through the origin, say 31-32, and complete the triangle 0-31-32. We may now draw this triangle in fundamental space, as we recognise the points 13, 23, 21, 31, 32 and 12 as its vector set. We then examine the remaining lines 24-14 and 41-42 to see whether a point exists which, taken with the line, gives an image of this triangle. The point 43 is found to be in the correct relation to 41-42, so there must be a fourth point in fundamental space which bears the same relation to triangle 123 as the origin bears to triangle 41-42-43 of the vector set. This gives unambiguously the points 1234 in fundamental space. From triangle 0-23-13 we would have recovered the congruent quadrilateral 1'2'3'4'. This is Wrinch's method of extracting the fundamental set from the vector set.

A somewhat simpler method based on the same principles has been proposed by Buerger (1950*b*, 1951). Let us take any vector from the origin, say 0-12, and move it about in vector space. When the two ends of this vector simultaneously encounter points of the vector set, we record the coincidence by a cross at the centre of the line. This gives six points ABCDEF (fig. 165(i)(b)) which are in fact quadrilaterals 1234 and 1'2'3'4' superposed on a common line. This 'image-seeking' line has therefore resolved the vector set into the fundamental set, plus the congruent set. As the 'image-seeking function' we could use a triangle. This triangle must be one whose vector set is contained in the complete vector set, for example 0-13-23. We record the coincidences of the vertices of this triangle with points of the vector set by means of a circle at its centroid. This gives the points *abcd*, the centroids of the shaded triangles. They are the points of the fundamental set.

Other possible choices of triangle would have given the same set, or the congruent one.

Still another method is that due to Clastre and Gay (1950*a, b*). We make two drawings of the vector set, and lay the origin of one on any point of the other, say 21. Coincidences are then marked (circles in fig. 165(ii)). This gives us again the six points ABCDEF, which we may

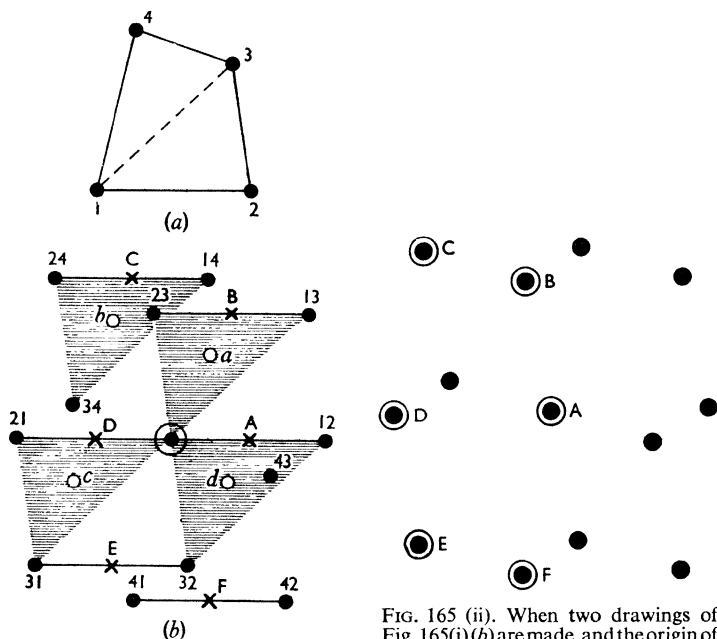


FIG. 165 (i). (a) A fundamental set of four points. (b) The vector set of this set of four points

FIG. 165 (ii). When two drawings of Fig. 165(i)(b) are made, and the origin of one transferred to the point 21 of the other, the coincidences which occur are denoted by rings in this figure

call the reduced vector set. The origin of one vector set is now transferred to some other point of the reduced vector set, say C. Coincidences are again marked, leaving only ABCD, identical with 1234. When the fundamental set is centrosymmetric, it can be recovered by a *single* superposition, provided that the origin of one vector set is transferred to one of the  $\frac{1}{2}N$  single points of the other vector set.

So far the discussion has been confined to non-periodic sets, but it is found that in order to solve a periodic vector set for its periodic fundamental set, it is sufficient to consider a unit cell of the periodic vector set which centrosymmetrically surrounds the origin. Points in this region are then treated just as if they belonged to a non-periodic set.

In the method of Beevers and Robertson (1950), the position of

certain atoms in the unit cell is assumed to be known. The coordinates of the heavier atoms can in practice often be found from the location of Patterson peaks which represent vectors between symmetry-related heavy atoms. As a very simple example, suppose the structure has a centre of symmetry as its only symmetry element, and has one atom per asymmetric unit which is much heavier than the others. The coordinates of this atom could then be fixed as  $(x_1y_1z_1)$  from the high Patterson peak at  $(2x_12y_12z_1)$ . In the method of Beevers and Robertson, the Patterson function is then set down with its origin at each of the known atomic positions  $(x_1y_1z_1)$  and  $(\bar{x}_1\bar{y}_1\bar{z}_1)$  in turn, to give a combined Patterson function

$$P_2(xyz) = P(x - x_1, y - y_1, z - z_1) + P(x + x_1, y + y_1, z + z_1). \quad (166.1)$$

In this function, the images of other atoms in each of the heavy atoms are brought into coincidence on atomic sites. Whether the latter can be recognized in practice depends on the relative weights of the atoms involved. Using a vector set of points, of course, the coordinates of a point of the fundamental set could be found by halving the coordinates  $(2x_j, 2y_j, 2z_j)$  of any *single* point in the vector set. Superposing the vector set on itself with origins at  $\pm(x_jy_jz_j)$  is then identical with the single-superposition method already mentioned.

$P_2(xyz)$  can be expressed as a Fourier series, which in this case is, from (166.1),

$$P_2(xyz) = \frac{2}{V} \sum_h \sum_k \sum_l [|F(hkl)|^2 \cos 2\pi(hx_1 + ky_1 + lz_1)] \cos 2\pi(hx + ky + lz). \quad (166.2)$$

In the general case of a non-centrosymmetric structure in which the positions of  $m$  atoms are known, a superposition of  $m$  identical Patterson functions with origins at the points  $(x_1y_1z_1)$ ,  $(x_2y_2z_2)$ , ...  $(x_my_mz_m)$  results, on addition, in a function

$$\begin{aligned} P_m(xyz) &= \sum_{j=1}^m P(x - x_j, y - y_j, z - z_j) \\ &= \frac{1}{V} \sum_h \sum_k \sum_l \{ |F(hkl)|^2 \sum_{j=1}^m \exp [2\pi i(hx_j + ky_j + lz_j)] \} \\ &\quad \exp [-2\pi i(hx + ky + lz)]. \end{aligned}$$

This is the 'mixed series' of McLachlan (1951). There are certain advantages in forming, instead of  $P_m(xyz)$ , the product function

$$\Pi_m(xyz) = \prod_{j=1}^m P(x - x_j, y - y_j, z - z_j),$$

or the minimum function  $M_m(xyz)$ , which is the lowest value of  $P(x - x_j, y - y_j, z - z_j)$  for any value of  $j$ . Relations between the electron density  $\rho(xyz)$  and either of  $\Pi_m(xyz)$  or  $M_m(xyz)$  do exist, but are

not entirely correct in the form in which they have been given (Buerger, 1950*c*, *d*).

We must now consider briefly some of the difficulties which may arise, even in principle, when an attempt is made to recover the point set from the vector set. These are more easily discussed in the terminology of the 'superposition' method than in that of the 'image-seeking' method, although, as we have seen, the two are really equivalent.

(i) On making a single superposition, two points of the vector sets may come into coincidence quite by accident to give a false atomic site. The latter is eliminated on making a second superposition of the vector set on the reduced vector set.

(ii) When the fundamental set lacks a centre of symmetry, we have seen that a single superposition produces two congruent fundamental sets. If the superposition is made with the origin of one vector set moved to a point of the other which is really  $p$  unresolved points, coincidences in the two vector sets will map out these two congruent sets  $p$  times in different relative positions. If a sufficient number of single points can be found, successive superpositions will eliminate all but one fundamental set.

(iii) Two or more non-congruent fundamental sets may have the same vector set, although not necessarily the same weighted vector set. Such fundamental sets have been called 'isovectorial' by Garrido. Three isovectorial sets are shown in fig. 167. Because of the different weighting in the vector sets, the three fundamental sets would not give the same values of  $|F|^2$ . All three can be derived from the vector set (fig. 167*d*), as has been shown by Wrinch (1939).

(iv) Different fundamental sets may not only be isovectorial, but even homometric, that is, give the same *weighted* vector set, and therefore the same values of  $|F|^2$  (section 5.6.2). The possible existence

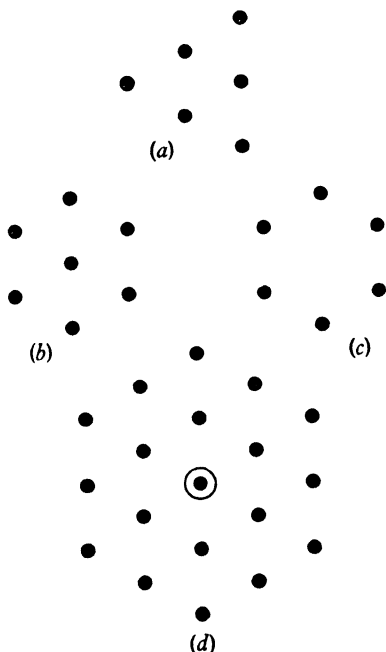


FIG. 167. *a*, *b*, *c* are three isovectorial fundamental sets. *d* is their common vector set

of non-congruent homometric structures first became evident from an investigation of the mineral bixbyite by Pauling and Shappell (1930). The space group of this crystal is No. 206,  $Ia\bar{3}$ , and a group of atoms occupy the special points  $24(d)$  of this space group. The positions of 24 atoms are fixed on allotting an  $x$ -coordinate to one of them, but it is found that the two values  $+x$  and  $-x$  of this parameter present two non-congruent arrangements of these atoms which are nevertheless homometric. The difficulty was overcome in this instance by showing that one arrangement of the atoms concerned allowed the remaining atoms of the structure to be fitted into the unit cell in a reasonable stereochemical configuration, while the other did not. The important theoretical point of the uniqueness of the solution obtained by X-ray analysis of a crystal structure was first raised by this observation. Patterson (1944) has discovered many pairs of one-dimensional homometric sets, and has shown that each such pair has its counterpart in two and in three dimensions. Whereas isovectorial sets may be either periodic or non-periodic it would appear that all homometric sets are periodic sets. We consider a set of  $N$  points per repeat distance  $a$  of a linear lattice, the  $j$ th point having a coordinate  $x_j$ . The discussion is facilitated by making the coordinate transformation

$$\phi_j = 2\pi \frac{x_j}{a},$$

so that a set of points on a line is replaced by points on the circumference of a circle. Homometric pairs can then be recognized more readily. An example is shown in fig. 168. For the structure shown in fig. 168*a*,

$$x_1 = 0 \quad x_2 = \frac{1}{8}a \quad x_3 = \frac{1}{2}a \quad x_4 = \frac{7}{8}a,$$

while for that shown in 168*b*,

$$x_1 = 0 \quad x_2 = \frac{1}{2}a \quad x_3 = \frac{5}{8}a \quad x_4 = \frac{7}{8}a.$$

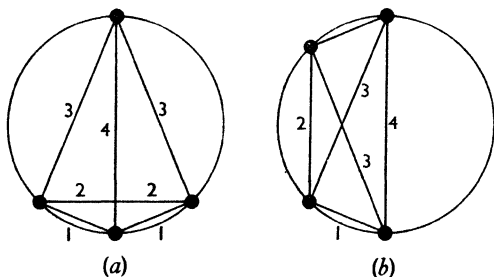


FIG. 168 *a, b*. Two one-dimensional homometric sets. A coordinate transformation has been made so that points repeated periodically on a straight line appear as points on the circumference of a circle.

The existence of this pair suggested to Patterson that further pairs of the same type might be found by arranging points on a circle at  $r$  of the  $n$  points of an inscribed regular polygon. Such sets Patterson calls *cyclotomic* sets. An examination of 2664 sets showed the existence among them of 390 homometric pairs, 7 sets of homometric triplets and 3 sets of homometric quadruplets. Non-cyclotomic homometric pairs were also discovered. Those shown in fig. 169 were obtained by generalization of the pair shown in fig. 168. The theory of this subject

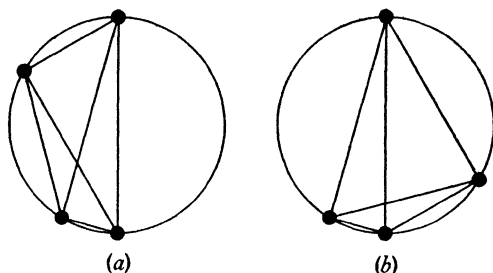


FIG. 169 *a, b*. Another homometric pair

is still in its infancy. Very little has been done to extend this study to two and three dimensions, although it has been shown that every one-dimensional homometric family has its counterpart in two- and three-dimensional periodic sets.

#### 4. POSSIBLE MODIFICATIONS OF THE PATTERSON FUNCTION

**4.1. The scale of the Patterson function.** The calculation of the Patterson function from the values of  $|F(hkl)|^2$  presents no special difficulties. It is always an easier calculation to make than a corresponding calculation of electron density, since all coefficients of the series representing the Patterson function are positive, and its higher symmetry means that it has generally to be evaluated over a smaller fraction of the unit cell. No further discussion of points already considered in Chapter 4 is therefore required.

When the Patterson function has been evaluated, it is often valuable to be able to attach a quantitative, and not merely a qualitative, significance to the numbers obtained. For instance, it is useful to know the shape of a single Patterson peak, and the height of a peak arising from two particular atoms, as one can then say whether a particular feature of the Patterson function is really a single peak, or whether, as is more probable in practice, it contains a number of unresolved Patterson peaks. The absolute scale of the Patterson function can be found with sufficient accuracy by Wilson's statistical method (section 5.5.3), which establishes both the scale of the  $|F|^2$ 's, and the value of the constant  $B$  in the equation

$$f_j = f_0 \exp \left[ -\frac{1}{4} B S_j^2 \right]. \quad (169)$$

The shape of a single Patterson peak arising from atoms  $i$  and  $j$  may be calculated from equation 152.3 in the form

$$P_{ij}(xyz) = \frac{1}{V} \sum_h \sum_k \sum_l f_i(hkl) f_j(hkl) \cos 2\pi(hx + ky + lz). \quad (170.1)$$

A line-section through this peak will give all we want, for instance

$$P_{ij}(x00) = \frac{1}{V} \sum_h \left\{ \sum_k \sum_l f_i(hkl) f_j(hkl) \right\} \cos 2\pi hx. \quad (170.2)$$

The tedious calculation of the coefficients of this one-dimensional series can be avoided in the following way. The product  $f_i f_j$ , as a function of  $S$  can always be approximated quite closely by

$$f_i f_j = Z_i Z_j \exp \left[ -\frac{\pi^2}{p} S^2 \right]. \quad (170.3)$$

With this assumption, it may be shown that

$$P_{ij}(x00) \simeq \frac{p}{\pi a} \sum_{h=-H}^{+H} \{ f_i f_j(h00) - f_i f_j(H00) \} \cos 2\pi hx. \quad (170.4)$$

$H$  represents the maximum value of  $h$  occurring inside the limiting sphere. This one-dimensional series is very easily evaluated. For two dimensions there is no corresponding simple result, but it is not difficult to evaluate directly

$$P_{ij}(x0) = \frac{1}{A} \sum_h \left\{ \sum_k f_i f_j(hk0) \right\} \cos 2\pi hx. \quad (170.5)$$

If equation 170.4 shows that a Patterson peak has fallen practically to zero in a distance of about  $1.4 \text{ \AA}$  (the minimum separation of atoms), and particularly when the atoms of the structure do not vary greatly in atomic number, a check is provided by the equation

$$\text{Height of Patterson peak } ij \simeq \text{Height of origin peak} \times \frac{Z_i Z_j}{\sum Z_j^2} \quad (170.6)$$

Equation 170.6 should be used with caution in a two-dimensional example, as the centre of the origin peak may be overlapped by adjacent peaks.

**4.2. The 'sharpened' Patterson function.** The theoretical considerations outlined in the previous section make it clear that the chances of interpretation of the Patterson function are greatest when individual peaks are resolved to the greatest possible extent. If the weighted vector set, in which each peak is replaced by a point, could be obtained, the determination of the crystal structure would be quite a simple matter. However the coefficients,  $|F|^2/\hat{f}^2$ , of the series representing the weighted vector set, are infinite in number, and cannot be measured



beyond some limiting value of  $S$ ,  $1.3 \text{ \AA}^{-1}$ , for instance when  $\text{CuK}\alpha$  radiation is used. By using radiation of shorter wave-length more coefficients may be obtained, but eventually the values of  $|F|^2$  must fall below the limit of experimental measurement. We note, however, that when the crystal is composed of spherically-symmetric atoms, the values of  $|F|^2$  may be multiplied by *any* function  $M(S)$ , and the Patterson function will still consist of spherically-symmetric peaks centred at the points of the vector set. These peaks may be modified to such an extent that the word 'peak' is scarcely appropriate any longer. For instance it would be quite possible to choose  $M(S)$  so that a section through a Patterson peak was as shown in fig. 171. Clearly this kind of

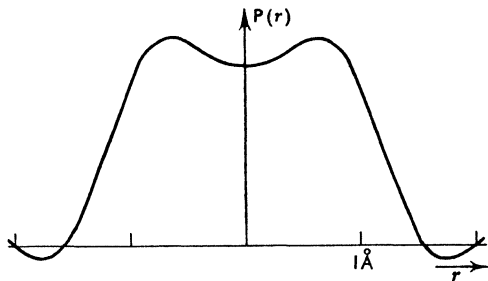


FIG. 171. An unsuitable modification of a Patterson peak

modification is not going to help in identifying individual vectors in the Patterson function. The best modification will be one which makes the central maximum of  $P_{ij}$  as sharp as possible, but does not introduce large subsidiary maxima and minima which will obscure or distort neighbouring peaks. Corresponding to the modified coefficients

$$|F_M|^2 = M(s)|F|^2,$$

we introduce modified atomic scattering factors

$$f_{Mj} = \sqrt{M(s)} f_j.$$

A single modified Patterson peak  $P'_{Mij}$  will then be the Fourier transform of  $f_{Mi}f_{Mj}$ , and its value when repeated by the lattice,  $P_{Mu}$ , can be calculated by replacing  $f_i f_j$  by  $f_{Mi} f_{Mj}$  in equation 170.2 or equation 170.5.

A possible modification was suggested by Patterson (1935a) and was used by him to increase the resolution of peaks in the two-dimensional Patterson function of  $\text{CuSO}_4 \cdot 5\text{H}_2\text{O}$ . This consists in taking

$$\sqrt{M(s)} = \sum_{j=1}^N Z_j / \sum_{j=1}^N f_{0j}.$$

We then have, using equation 169,

$$f_{Mj} \simeq Z_j \exp \left[ -\frac{1}{4} B S^2 \right],$$

the approximation again being closest when all atoms of the structure have about the same atomic number. This result is true only for

$S < S_0$ ; for  $S > S_0$  we must take  $f_{Mj} = 0$ . There is however no particular reason why the modification should be made so that the constant in the exponent is the actual temperature-factor parameter of the crystal, and we shall consider the shape of  $P_{Mij}$  for the general case,

$$f_{Mi} f_{Mj} = Z_i Z_j \exp \left[ -\frac{\pi^2}{p} S^2 \right] \quad (\text{for } S < S_0).$$

This corresponds to

$$M(S) = \left( \frac{1}{\hat{f}} \right)^2 \exp \left[ -\frac{\pi^2}{p} S^2 \right].$$

Only if  $f_{Mi} f_{Mj}$  has fallen to a small value, say  $0.01 Z_i Z_j$ , at  $S = S_0$ , can the shape of a single Patterson peak be taken to be the Fourier transform of  $f_{Mi} f_{Mj}$ , which is

$$P'_{Mij}(r) = Z_i Z_j \left( \frac{p}{\pi} \right)^{3/2} \exp [-pr^2] \text{ in three dimensions,}$$

and  $Z_i Z_j \left( \frac{p}{\pi} \right) \exp [-pr^2] \text{ in two dimensions.}$

If  $f_{Mi} f_{Mj}$  is appreciable at  $S = S_0$ , equation 170.4 can be used. In table 172a values of  $P_{Mij}(x00)$ , calculated from this equation, are given for a number of values of  $p$ , with  $S_0 = 1.3 \text{ \AA}^{-1}$ , the limit of  $\text{CuK}\alpha$  radiation;  $a$  was taken as  $10 \text{ \AA}$ , but the shape of  $P_{Mij}$  in the range considered is practically independent of  $a$ , provided the latter is not too small.

TABLE 172a

I $p$	II $\frac{f_{Mi} f_{Mj}(S_0)}{Z_i Z_j}$	III $\frac{P_{Mij}(000)}{Z_i Z_j}$	$P_{Mij}(x00) \div P_{Mij}(000) \text{ for } x =$											
			$\frac{0}{6}$	$\frac{1}{6}$	$\frac{2}{6}$	$\frac{3}{6}$	$\frac{4}{6}$	$\frac{5}{6}$	$\frac{6}{6}$	$\frac{7}{6}$	$\frac{8}{6}$	$\frac{9}{6}$	$\frac{10}{6}$	$\text{\AA}$
3.64	0.01	1.25	1.00	.90	.67	.41	.20	.08	.03	.00 <sub>7</sub>	.00 <sub>2</sub>	—	—	
4.77	0.03	1.74	1.00	.89	.63	.35	.14	.03 <sub>7</sub>	.01	.00 <sub>3</sub>	.00 <sub>2</sub>	.00 <sub>9</sub>	.00 <sub>9</sub>	
5.57	0.05	2.10	1.00	.88	.61	.30	.10	.01 <sub>5</sub>	.00 <sub>4</sub>	.01 <sub>0</sub>	.00 <sub>7</sub>	.00 <sub>3</sub>	.00 <sub>3</sub>	
7.25	0.10	3.00	1.00	.87	.56	.25	.04 <sub>5</sub>	0	.00 <sub>2</sub>	.01 <sub>6</sub>	.00 <sub>8</sub>	.00 <sub>6</sub>	.01	
10.4	0.20	3.85	1.00	.86	.52	.19	.00 <sub>9</sub>	.03	.00 <sub>3</sub>	.01 <sub>5</sub>	.00 <sub>2</sub>	.00 <sub>7</sub>	.00 <sub>7</sub>	
$\infty$	1.00	9.20	1.00	.83	.42	.07	.07 <sub>5</sub>	.05	.02	.03	0	.02	.01	

TABLE 172b

4.15	0.03	0.96	1.00	.82	.44	.10 <sub>6</sub>	.03 <sub>3</sub>	.05 <sub>3</sub>	.01 <sub>7</sub>	.00 <sub>7</sub>	.00 <sub>3</sub>	—	—	
4.15	0.03	0.82	1.00	.85	.51	.16	.03 <sub>7</sub>	.08 <sub>7</sub>	.04 <sub>6</sub>	.01	0	.01	.00 <sub>6</sub>	

The entry in column II of this table is approximately equal to the ratio of the average value of the modified coefficients  $|F_M|^2$  near  $S = S_0$ , to their average value near  $S = 0$ . A value of 1% to 3% for this quantity corresponds roughly to what is often obtained in practice, so the entries in the first two rows give an indication of the shape of a peak in an unmodified three-dimensional Patterson function. Again, the temperature factor  $\exp[-\frac{1}{2}BS^2]$  for many crystals has a value around 0.20 at  $S = 1.3 \text{ \AA}^{-1}$ , so the figures in the fifth row give an indication of the shape of the peak that would be obtained in this case on making the modification suggested by Patterson. The last row gives the shape of the peak when the coefficients have been modified so that they do not decrease at all with increasing  $S$ , that is,  $M(S) = (1/\hat{f})^2$ , and the modified coefficients are those that would be given by a set of point atoms—until  $S = S_0$  is reached when they fall at once to zero. In this case the central maximum of the Patterson peak is confined within a sphere of radius 0.55  $\text{\AA}$ , but the first minimum is fairly pronounced. The modification corresponding to the entries in row four has been found to be satisfactory in practice. It reduces the radius of a peak to about 0.7  $\text{\AA}$ , without introducing appreciable subsidiary maxima and minima.

Reliable experimental measurements must be available for the full benefit of the 'sharpening' of peaks to be obtained. The modification corresponding to  $p = 10.4$  (fifth row) may result in the multiplication of intensities near the limit of Cu radiation by a factor of 10 to 20. If a large proportion of these intensities are not observed experimentally, the series will be effectively terminated at a value of  $S$  less than the radius of the limiting sphere, and Patterson peaks will be broader, with larger subsidiary maxima and minima, than an application of equation 170.4 with  $H = \frac{2a}{\lambda}$  would indicate.

A modification suggested by Schomaker and Shoemaker (unpublished) consists in taking

$$M(S) = \left(\frac{1}{\hat{f}}\right)^2 S^2 \exp \left[ -\frac{\pi^2}{p} S^2 \right],$$

and therefore

$$f_{Mi} f_{Mj} \approx Z_i Z_j S^2 \exp \left[ -\frac{\pi^2}{p} S^2 \right].$$

If  $S_0^2 \exp \left[ -\frac{\pi^2}{p} S_0^2 \right]$  is very small, the shape of a single peak is given by

$$P'_{Mij}(r) = \left(\frac{p^5}{\pi^7}\right)^{\frac{1}{2}} \left(\frac{3}{2} - pr^2\right) \exp[-pr^2].$$

Values are given in the first row of table 172*b*, for  $p = 4.15$ . The radius of the central maximum is just over  $0.5 \text{ \AA}$ , and the negative trough is not too pronounced. When one takes account of the fact that the value of  $f_{M_i} f_{M_j}$  is not negligible at  $S = 1.3 \text{ \AA}^{-1}$  in this case, however, the situation is seen to be somewhat less favourable (last row of table 172*b*). This type of modification reduces greatly the influence of low-order terms on the Patterson function, which is advantageous when they are likely to be in error through extinction.

It is perhaps worth reminding the reader that these calculations refer to peaks in a three-dimensional Patterson function. In the two-dimensional function the height of a central maximum is somewhat smaller, and that of subsidiary maxima and minima, greater, relative to  $Z_i Z_j$ .

**4.3. Subtraction of certain peaks.** Another modification which can be made consists in the subtraction from the Patterson function of the peak at the origin, or any other peaks arising from atoms in known positions. From equation 153.3, the origin peak alone is given by

$$\sum_{j=1}^N P_{jj}(r) = \sum_{j=1}^N \left\{ \frac{1}{V} \sum_{\mathbf{H}} f_j^2(\mathbf{H}) \exp[-2\pi i \mathbf{H} \cdot \mathbf{r}] \right\}.$$

The series

$$\frac{1}{V} \sum_{\mathbf{H}} \left\{ |\mathbf{F}(\mathbf{H})|^2 - \sum_{j=1}^N f_j^2(\mathbf{H}) \right\} \exp[-2\pi i \mathbf{H} \cdot \mathbf{r}], \quad (174)$$

therefore represents the Patterson function without the origin peak. The coefficients of this series can be evaluated if measurements have been made on an absolute scale, and if the temperature factor of the atoms in the crystal is known. This is unlikely ever to be so in practice. It is true that scale and temperature factors can be established approximately by Wilson's method (sections 3.2.4 and 5.5.3), but the limitations of this method must be kept in mind. For instance, one cannot subtract the origin peak from a two-dimensional Patterson function, with scale and temperature factors established by Wilson's method, and hope to find another peak which in projection was completely obscured. This follows from the fact that we assume, in using Wilson's method, that

$$\sum_{j=1}^N f_j^2 = |\overline{\mathbf{F}}|^2.$$

The value of the modified Patterson function at the origin

$$\frac{1}{V} \sum_{\mathbf{H}} \{ |\mathbf{F}(\mathbf{H})|^2 - |\overline{\mathbf{F}}|^2 \},$$

is therefore bound to be zero. In a three-dimensional Patterson function, on the other hand, peaks representing vectors between nearest-neighbour atoms can always be resolved from the origin peak

in any case, if measurements extending to, say,  $S_0 = 1.3 \text{ \AA}^{-1}$  are available. There would therefore appear to be little to be gained by subtracting the origin peak.

**4.4. Generalized projections of the Patterson function.** As we have already seen, the Patterson function may be calculated in three dimensions, or we can more readily calculate its projection on a plane. It is also possible to project any section of the function on a plane. The Fourier-series formulation of the function in these various modifications may easily be derived by the processes already described in Chapter 4. In section 7.3.5 it will be shown that it is possible to calculate what is called a 'generalized' projection of the electron density. This can also be done for the Patterson function. For example, when there is a two-fold axis parallel to  $c$ ,

$$P_L(xy) = \int_0^1 P(xyz) \cos 2\pi Lz \, dz = \frac{1}{A} \sum_h \sum_k |F(hkL)|^2 \cos 2\pi(hx + ky),$$

is the  $L$ th generalized projection of  $P(xyz)$  on (001). Every Patterson peak appears in this projection, multiplied by a factor  $\cos 2\pi L(z_1 - z_2)$ ,  $z_1$  and  $z_2$  being the  $z$ -coordinates of the two corresponding atoms. The shape of a peak in a generalized projection can be calculated from equation 170.5, replacing  $f_i f_j(hk0)$  by  $f_i f_j(hkL)$ . Some examples of the use of these different modifications of the Patterson function will be considered in the next section.

## 5. PRACTICAL APPLICATIONS OF THE PATTERSON FUNCTION

The Patterson function of a crystal of even moderate complexity is generally very difficult to interpret in practice. The volume of the unit cell of a crystal is roughly proportional to  $N$ , the number of atoms it contains. The density of peaks in the Patterson function,  $N^2/V$ , therefore increases directly with the number of atoms, and for structures which have more than about ten atoms per unit cell there is little hope of recognizing individual peaks—a necessary preliminary to systematic application of any known direct methods. However one always has some knowledge of expected interatomic distances and additional items of information such as were discussed in Chapter 5, and one uses all these facts in trying to unravel the Patterson function.

**5.1. The heavy-atom method.** The only important practical case where the Patterson function can be used to solve a structure fairly directly is when the crystal contains a relatively small number of heavy atoms per unit cell. The Patterson peaks due to these atoms then stand out against a background of overlapping smaller peaks, and give immediately the coordinates of the heavy atoms. The remaining atoms can then be located by direct Fourier methods, as described in Chapter 7,

or the images of all other atoms in each of the heavy atoms can be brought into coincidence by the superposition method of Beevers and Robertson. An investigation of the structure of cholesteryl iodide by Carlisle and Crowfoot (1945) provides a good example of the first of these methods. The crystals are monoclinic, space group No. 4,  $P2_1$ , with

$$a = 12.5_7, b = 9.0_4, c = 21.8_9 \text{ \AA}, \beta = 149^\circ.$$

The Patterson function projected on (010) is shown in fig. 176(i). From

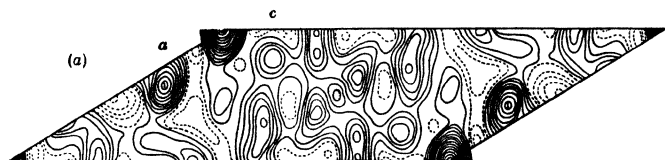


FIG. 176(i). Patterson function of cholesteryl iodide projected on (010). The large peaks represent vectors between iodine atoms (Carlisle and Crowfoot, 1945)

it the  $(xy)$  coordinates of an iodine atom can be measured as  $(0.217, 0.042)$ . The remaining atoms were then located as described in section 7.3.2.

One of the earliest applications of the Patterson function was to  $\text{CuSO}_4 \cdot 5\text{H}_2\text{O}$  (Patterson, 1935*a*). The structure of this compound

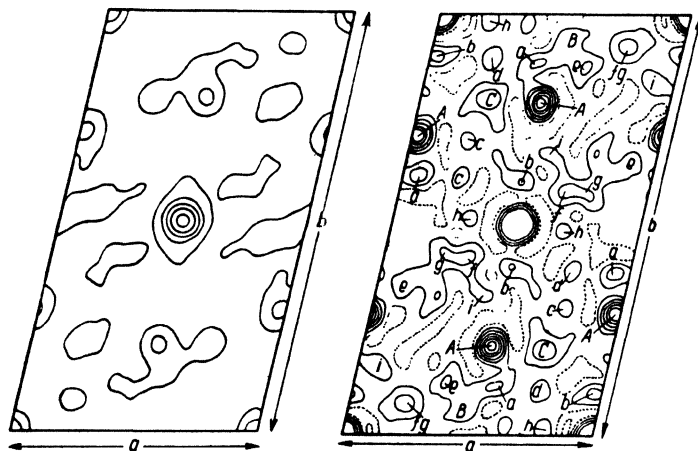


FIG. 176(ii). (a) Patterson function of  $\text{CuSO}_4 \cdot 5\text{H}_2\text{O}$  projected on (001) (Patterson 1935*a*). (b) The same function, with the coefficients of the Fourier series modified so as to produce greater resolution of peaks (Patterson, 1935*a*)

had been solved by Beevers and Lipson (1934) using Fourier methods, so that the Patterson function was used only as a check. The projection of this function on (001) is shown in Fig. 176(ii)a. The heavy peak at  $(\frac{1}{2}, \frac{1}{2})$  shows that some of the atoms occupy a centred lattice. If the Cu atoms were centred by the S atoms we would expect to find larger peaks elsewhere in the function which would correspond to Cu-Cu vectors. Their absence indicates that the Cu atoms occupy special positions of the plane lattice at (0, 0) and  $(\frac{1}{2}, \frac{1}{2})$ . The locations of the next highest peaks give the S coordinates as (·02, ·29)—or (·48, ·21), which corresponds merely to a change of origin. Patterson then calculated a modified function, with Fourier coefficients proportional to  $F^2(hk0)/(f_0)^2$ . The result is shown in fig. 176(ii)b. Many peaks which could not be distinguished in fig. 176(ii)a are now separately resolved. It is to be expected that the majority of these peaks will represent Cu-O vectors. If this is the case, two peaks should occur, at  $(x_j, y_j)$  and  $(\frac{1}{2} - x_j, \frac{1}{2} - y_j)$  respectively, for every atom at  $(x_j, y_j)$ . These two peaks are not symmetry-related in the Patterson function, and the occurrence of both serves as a check. Whether a particular pair corresponds to an atom at  $(x_j, y_j)$  or  $(\frac{1}{2} - x_j, \frac{1}{2} - y_j)$  cannot be decided; two alternative locations are therefore obtained for each atom—apart from the sulphur atom—for the choice of one of the alternative sites for the latter merely fixes the origin. Table 179 lists the coordinates  $xy$  of all peaks for which there is a corresponding peak at  $(\frac{1}{2} - x, \frac{1}{2} - y)$ . The choice between alternative coordinates cannot in this case be made from the Patterson function, since S-O peaks cannot be identified, but it will be seen from the table that in almost every case one of the alternatives agrees with the coordinates of an atom as determined by Beevers and Lipson. One atom is not represented, and another pair of peaks does not correspond to an atomic site. This is only what might have been expected when it is remembered that all S-O and O-O peaks have been neglected.

The two-fold ambiguity in the interpretation of the Patterson function of  $\text{CuSO}_4 \cdot 5\text{H}_2\text{O}$  arises from the fact that there are two Cu atoms per unit cell, and an image of every atom is formed in each of these heavy atoms.

Conditions which make it possible to interpret the Patterson function immediately in terms of the crystal structure occur in cysteinylglycine-sodium iodide (Dyer, 1951a). The unit cell is monoclinic, with  $a = 11 \cdot 1$ ,  $b = 5 \cdot 12$ ,  $c = 16 \cdot 0$  Å and  $\beta = 90^\circ 57'$ . The space group is No. 5,  $A2$ , and the unit cell contains  $4(\text{SH} \cdot \text{CH}_2 \cdot \text{CH}(\text{NH}_2) \cdot \text{CO} \cdot \text{NH} \cdot \text{CH}_2 \cdot \text{COOH}) + 2\text{NaI}$ . The iodine and sodium atoms must therefore occur in special positions on the diad axes. The unit cell in projection on (010) is halved in the  $c$ -direction, and contains only two organic molecules, plus one NaI. The plane group is  $p2$ , and the iodine atom can be taken to be at the origin. The plane group of the corresponding Patterson function in projection is also  $p2$ , and the images of all atoms

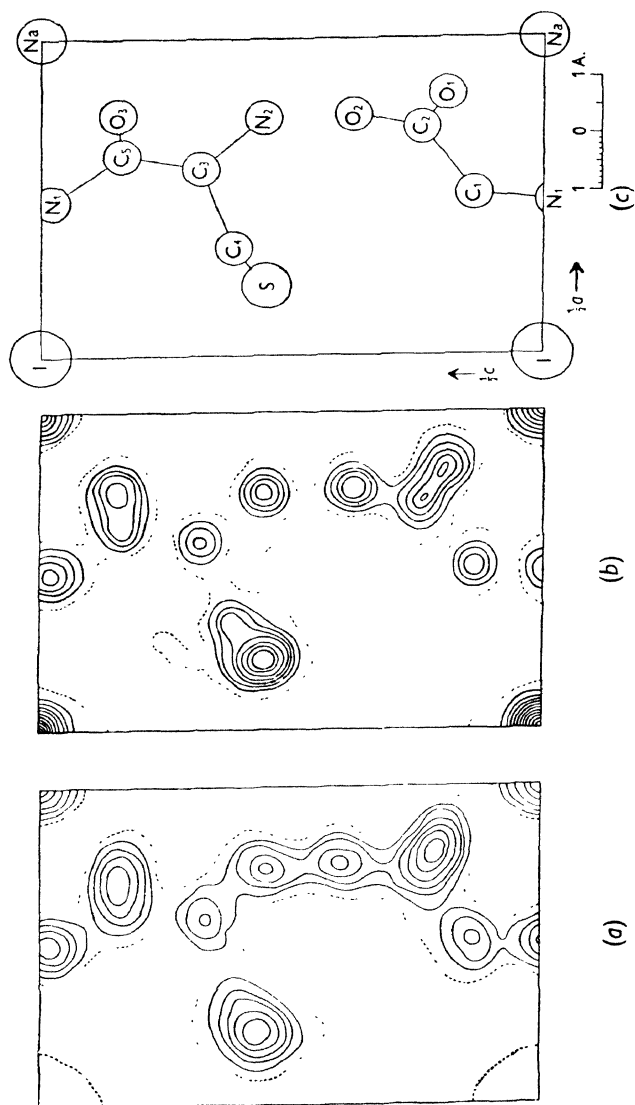


Fig. 178. (a) Projection of the Patterson function of cysteinylglycine sodium iodide on (010).  
 (b) Corresponding electron density map. (c) Key to (a) and (b) (Dyer, 1951a)



TABLE 179

Atom	Alternative coordinates from the Patterson function				Coordinates obtained from the electron-density map	
	$x$	$y$	$\frac{1}{2}-x$	$\frac{1}{2}-y$	$x$	$y$
Cu	0	0			0	0
Cu	0.50	0.50			0.50	0.50
S	0.02	0.29			0.01	0.29
O <sub>1</sub>	0.92	0.16	0.58	0.34	0.89	0.15
O <sub>2</sub>	0.21	0.30	0.29	0.20	0.24	0.31
O <sub>3</sub>	0.87	0.37	0.63	0.13	0.86	0.38
O <sub>4</sub>	—	—	—	—	0.02	0.30
(H <sub>2</sub> O) <sub>5</sub>	0.83	0.08	0.67	0.42	0.83	0.08
(H <sub>2</sub> O) <sub>6</sub>	0.26	0.11	0.24	0.39	0.29	0.11
(H <sub>2</sub> O) <sub>7</sub>	0.48	0.40	0.02	0.10	0.48	0.41
(H <sub>2</sub> O) <sub>8</sub>	0.76	0.43	0.74	0.07	0.76	0.42
(H <sub>2</sub> O) <sub>9</sub>	0.44	0.12	0.06	0.38	0.43	0.12
—	0.19	0.01	0.31	0.49	—	—

in the heavy iodine atom occur once only, and in the positions occupied by the corresponding atoms in the projection on (010). Apart from the difference in shape between Patterson peaks and atoms, and the occurrence of small peaks in the Patterson function in addition to those representing vectors between iodine and other atoms, the Patterson function may be expected to be identical with the corresponding electron-density projection. The close correspondence observed in practice is illustrated in figs. 178*a* and 178*b*.

This structure investigation also provides an example of how a generalized Patterson projection (section 6.4.4) can sometimes be used to give information about the third atomic coordinate, in this case  $y$ , which could not readily be obtained other than by calculating the Patterson function in three dimensions. The functions calculated in this case were

$$P_K(xz) = \frac{1}{A} \sum_h \sum_l |F(hKl)|^2 \cos 2\pi(hx + lz),$$

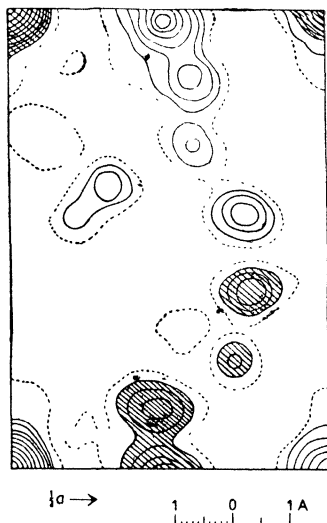


FIG. 179. The function  $P_1(xz)$  corresponding to  $P_0(xz)$  of Fig. 178*a* (Dyer, 1951*a*)

The functions calculated in this case were

with  $K=1$  and  $K=2$ . The function  $P_1(xz)$  is shown in fig. 179. Shaded areas represent negative regions. We have already seen that every peak in the projection  $P_0(xz)$  (fig. 178a) will occur with the same  $(xz)$  coordinates in  $P_1(xz)$ , slightly modified in shape as it is the two-dimensional Fourier transform of  $f_i f_j(h1l)$  instead of  $f_i f_j(h0l)$ , and multiplied by a factor  $\cos 2\pi(y_i - y_j)$ . As in  $P_0(xz)$ , we can neglect all peaks which do not involve the iodine atom; the height of the peak corresponding to atom  $j$  will therefore depend on  $\cos 2\pi y_j$ , since the  $y$ -coordinate of the iodine can be taken to be zero. The non-appearance in fig. 179 of the peaks corresponding to S, O<sub>1</sub> and O<sub>3</sub> (fig. 178c) shows at once that these atoms have  $y$ -coordinates close to  $y=0.25$  or  $0.75$ , and the fact that the peak at  $(0, \frac{1}{2})$  in fig. 179 is large and positive indicates that the sodium atom has about the same  $y$ -coordinate as the iodine. A misinterpretation of the Patterson function projected on (100) had previously placed the sodium atom at  $y=\frac{1}{2}$ . The  $y$ -coordinates of all atoms were eventually found with fair accuracy by comparing the relative heights of peaks in  $P_1(xz)$  and in  $P_2(xz)$ . This procedure does not distinguish between  $y$  and  $\bar{y}$ , but the information obtained was sufficient to enable the electron-density projection on (100) to be calculated, and refined in the usual way.

**5.2. Use of Harker sections.** We have seen that in certain circumstances a Harker section gives direct information about atomic coordinates, although usually with a certain ambiguity. An example is provided by Harker's (1936) investigation of proustite,  $\text{Ag}_3\text{AsS}_3$ . The hexagonal unit cell has dimensions  $a=10.74$ ,  $c=8.64$  Å, and the space group is No. 161,  $R3c$ . The true unit cell is rhombohedral, but for convenience the hexagonal unit cell was used. This space group provides the equivalent points

$$(2a) \quad (00z) \quad (0, 0, z + \tfrac{1}{2}),$$

$$\text{and} \quad (6b) \quad (xyz) \quad (\bar{y}, x-y, z) \quad (-x+y, \bar{x}, z), \\ (x, x-y, z + \tfrac{1}{2}) \quad (\bar{y}, \bar{x}, z + \tfrac{1}{2}) \quad (-x+y, y, z + \tfrac{1}{2}),$$

and positions derived from these by the operation of the rhombohedral lattice. The arsenic atoms are fixed in positions (2a) by symmetry, and  $z_{\text{As}}$  may be taken equal to zero. The silver and sulphur atoms are in general positions (6b). By subtracting coordinates of points related to one another by the glide plane perpendicular to  $y$ , it is found that  $P(xyz)$  will have peaks at  $(0, \pm(x-2y), \frac{1}{2})$ ,  $(0, \pm(-2x+y), \frac{1}{2})$  and  $(0, \pm(x+y), \frac{1}{2})$  for each kind of atom, silver or sulphur. The appropriate Harker section is therefore the line  $0, y, \frac{1}{2}$ .  $P(0y\frac{1}{2})$  is shown in fig. 181. The scale is arbitrary. The large peak at  $y=0$  represents an As-As vector and the peaks at  $y=\pm 0.17$ ,  $\pm 0.33$  and  $\pm 0.50$  must represent Ag-Ag vectors as silver is so much heavier than sulphur. Since we are dealing with only one atom and its equivalents, there is no ambiguity and we may take

$$(x+y)_{\text{Ag}} = \tfrac{1}{2}, \quad (2y-x)_{\text{Ag}} = \tfrac{1}{3} \quad \text{and} \quad (2x-y)_{\text{Ag}} = \tfrac{1}{6},$$

giving  $x_{\text{Ag}} \approx \frac{4}{18}$ ,  $y_{\text{Ag}} \approx \frac{5}{18}$ . Any other solution gives an equivalent point. The value of  $z_{\text{Ag}}$  was fixed by locating the As-Ag peak which occurs along the line  $(\frac{4}{18}, \frac{5}{18}, z)$ . The sulphur atoms were placed, to complete the structure, from the known bond lengths S-As = 2.25 and S-Ag = 2.40 Å.

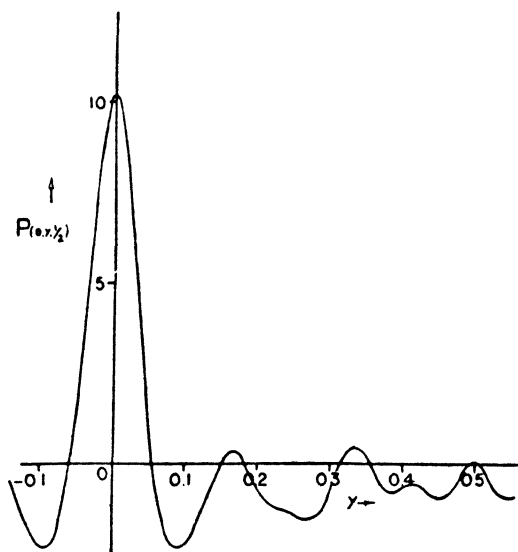


FIG. 181. The Harker section,  $x, y, \frac{1}{2}$  for the mineral proustite (Harker, 1936)

An interesting demonstration of the way in which it is sometimes possible to combine information from the projection of a Patterson function with that from a Harker section is provided by the work of Palin and Powell (1947), on an addition complex of quinol with sulphur dioxide. The chemical composition of the crystal investigated was  $3\text{C}_6\text{H}_4(\text{OH})_2 \cdot \text{SO}_2$ . The unit cell dimensions, referred to hexagonal axes, are  $a = 16.3$ ,  $c = 5.8$  Å, and the space group is either No. 148  $R\bar{3}$  (centrosymmetric) or No. 146  $R3$  (non-centrosymmetric). Tests for pyroelectricity and piezoelectricity gave no results; the space group  $R\bar{3}$  was therefore provisionally assumed and confirmed later by a special application of the Patterson function. Since there are nine molecules of quinol per unit cell, their centres must lie in special positions  $(\frac{1}{2}, 0, \frac{1}{2})$ ,  $(0, \frac{1}{2}, \frac{1}{2})$ ,  $(\frac{1}{2}, \frac{1}{2}, \frac{1}{2})$  with the equivalents at  $+(\frac{1}{3}, \frac{2}{3}, \frac{1}{3})$  and  $+(\frac{2}{3}, \frac{1}{3}, \frac{2}{3})$ . The asymmetric unit consists of half a quinol molecule. The non-centrosymmetric  $\text{SO}_2$  molecule cannot fit into the space group unless it is rotating, or takes up varied orientations in different

unit cells. The most probable arrangement would appear to be oxygen atoms at  $\pm(00z)$  with the sulphur atom moving in a circle of small radius around the  $c$ -axis at  $z=0$ . The structure could probably have been determined from the occurrence of this complex 'heavy atom' at the origin, by direct Fourier methods, but this was not attempted because of doubts about the space group. The Patterson projection on

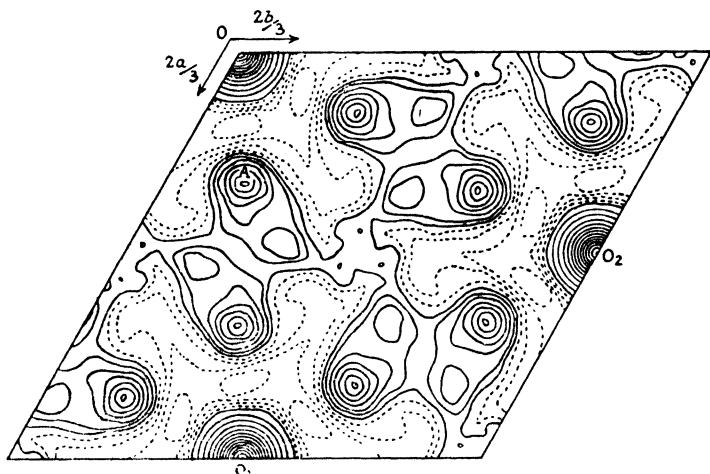


FIG. 182. (a) Patterson function of quinol-SO<sub>2</sub> projected on (001) (Palin and Powell, 1947)

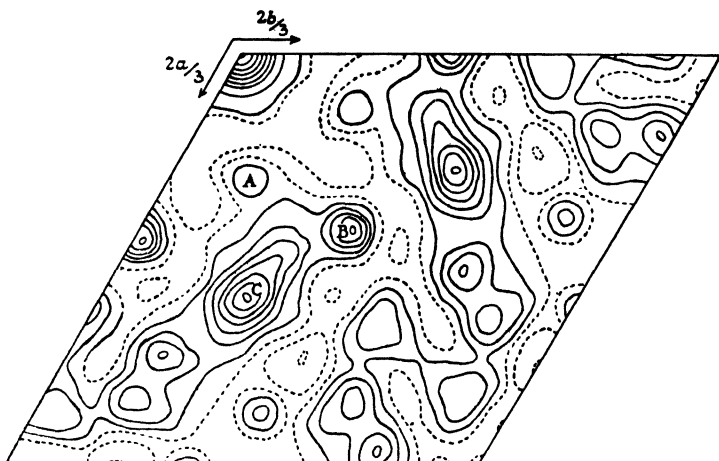


FIG. 182. (b) Harker section corresponding to the projection shown in Fig. 182 (a) (Palin and Powell, 1947)

001) and a corresponding Harker section at  $z=0$  were calculated (figs. 182*a* and 182*b*). Fig. 184 shows the sets of Patterson peaks to be

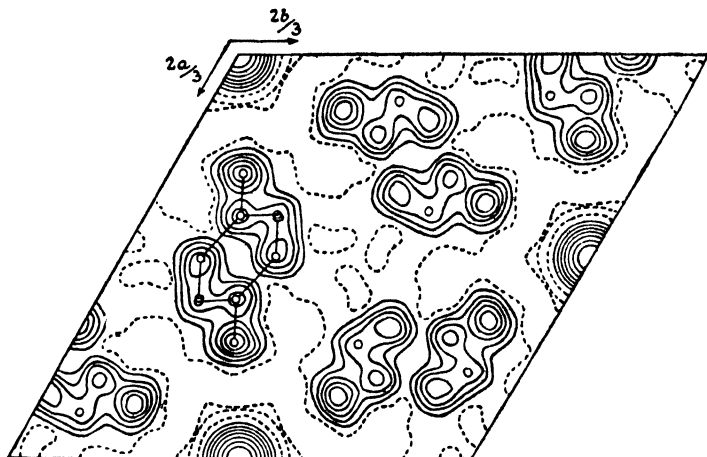


FIG. 183. Electron density in quinol-SO<sub>2</sub> projected on (001). The position of one quinol molecule is indicated (Palin and Powell, 1947)

expected in a projection on (001), and in the section, taking account only of a single atom near the origin, and those related to it by the symmetry  $R\bar{3}$  or  $R3$ , with and without the effect of a heavy atom at the origin. The comparatively great height of peak A in fig. 182*a* shows that the structure must have a heavy atom on the three-fold axis, as in (b), (d) or (e) of fig. 184. In the Harker section, fig. 182*b*, there are peaks A of an inner hexagon as required for (a), (b), (c) or (d), and also peaks B and C which can be explained only by arrangement (e). If the rotating SO<sub>2</sub> molecule is at (000), the hexagon of atoms must be at  $z = \frac{1}{2}$  because the relatively low height of A in fig. 182*b* shows that the SO<sub>2</sub> and the atoms concerned are not at the same level. The heights of B and C are certain to be enhanced by accidental overlapping of other peaks. The most satisfactory interpretation was found to be that the structure consists of quinol molecules arranged so that each oxygen atom lies on one corner of a hexagon round the trigonal axis, with a benzene ring connecting pairs of oxygen atoms which lie near different axes. An electron-density projection calculated on this basis is shown in fig. 183. The resemblance between figs. 182*a* and 183 is quite striking. This is in fact another example where the images of each quinol molecule in the heavy atom (rotating SO<sub>2</sub> molecule) provide the major contribution to the Patterson function, and occur in the positions occupied by the molecules themselves.

Harker sections have not found much application in structures composed of atoms of about the same atomic number. Even when the

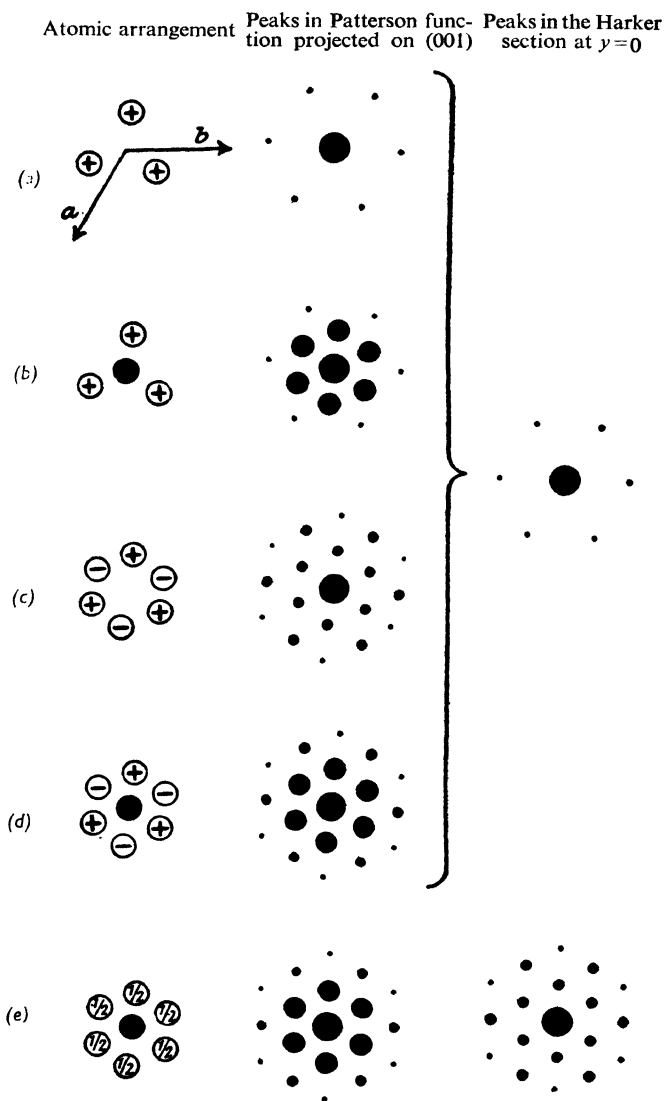


FIG. 184. Possible arrangements of atoms, and corresponding Patterson peaks, for quinol- $\text{SO}_2$ . The peaks have heights indicated qualitatively by their areas. The experimental Patterson functions of Figs. 182*a* and 182*b* agree best with arrangement (e), although certain peaks of the experimental Patterson functions are greatly enhanced by chance coincidences (Palin and Powell, 1947)

ambiguity factor is one or two—and it is most commonly four—difficulties arise because of the occurrence of non-Harker peaks. When something of the molecular shape and probable orientation is already known, the occurrence of non-Harker peaks may be a decided advantage, as is shown by the work of Stern and Beevers (1950) on tartaric acid. Crystals of the optically active form of tartaric acid are monoclinic, with  $a = 7.7_2$ ,  $b = 6.0_0$ ,  $c = 6.2_0$  Å and  $\beta = 100^\circ 10'$ . The space group is No. 4,  $P2_1$ . In attempting to solve the crystal structure, sections of the three-dimensional Patterson function at  $y=0$  (fig. 185(i)) and  $y=\frac{1}{2}$

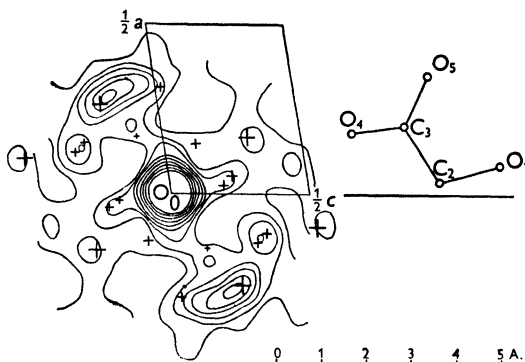


FIG. 185 (i). Orientation of one of the C.OH.CO<sub>2</sub>H groups of the tartaric acid molecule compared with the central region of the  $y=0$  Patterson section. Peaks due to atoms in this group are marked by crosses in the Patterson section, the sizes of the crosses indicating the relative weights of the peaks (Stern and Beevers, 1950)

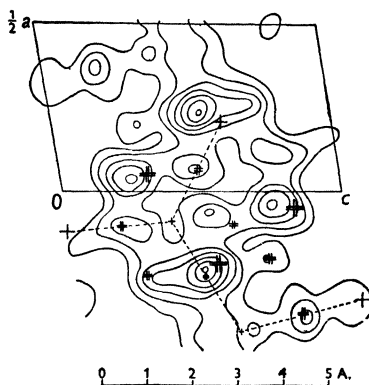


FIG. 185 (ii). Patterson section at  $y=\frac{1}{2}$ , together with the peaks at  $y=\frac{1}{2}$  due to  $C_2O_1C_3O_4O_5$ , marked by crosses as in Fig. 185(i), double crosses indicating double-weight peaks. To estimate the quality of the agreement all crosses should be imagined as plotted on the asymmetric unit of the Patterson section (Stern and Beevers, 1950)

(fig. 185(ii)) were calculated. We have seen that every atom at  $(x, z)$  should result in a peak in the section  $y = \frac{1}{2}$  at  $(2x, 2z)$ , and the ambiguity factor in this case is 4. Attempts to identify the Harker peaks in  $P(x, \frac{1}{2}, z)$  proved fruitless. The reason for this can be seen on examining the section  $y=0$ . This latter strongly suggests that one of the  $=\text{C.OH}$ .  $\text{COOH}$  groups of the molecule lies in a plane perpendicular to the  $b$ -axis. The group in its correct orientation, together with the peaks produced by it in  $P(x0z)$ , is shown in fig. 185(i)a. The five atoms having the same  $y$ -coordinates should produce in the Harker section  $P(x, \frac{1}{2}, z)$ , in addition to five Harker peaks, ten double peaks, each of which falls midway between two single Harker peaks (section 6.3.2). These multiple peaks will account for the main features of the Harker section. When the correct relative positions of these 15 peaks were drawn out, it was found that they could be fitted to  $P(x, \frac{1}{2}, z)$  in only one way, which is shown in fig. 185(ii). This fixed the position of the  $=\text{C.OH}$ .  $\text{COOH}$  group in the unit cell. The section  $P(x, \frac{1}{2}, z)$  of the Patterson function was used to give information about the configuration of the other half of the molecule, and the structure determination was completed by calculating Fourier syntheses of the electron density.

The limited success obtained in investigations of crystals of moderate complexity by means of Harker sections probably explains why the implication diagram has been used even less frequently. The real value of the latter lies in the way it demonstrates the fundamental difficulties of this approach to the problem.

**5.3. Use of superposition methods.** We have seen that superposition methods are not likely to be successful unless individual Patterson peaks can be identified. This will most commonly be the case when the structure contains one, or a few, heavy atoms, as for example strychnine hydrogen bromide, investigated by Robertson and Beevers (1951). This compound has space group No. 19,  $P2_12_12_1$ , for which the equivalent points are

$$(xyz), (\frac{1}{2} - x, \bar{y}, \frac{1}{2} + z), (\frac{1}{2} + x, \frac{1}{2} - y, z) \text{ and } (\bar{x}, \frac{1}{2} + y, \frac{1}{2} - z).$$

The space group of the Patterson function is No. 47,  $Pmmm$ , one atom and its equivalents producing peaks in  $P(xyz)$  at the points  $(\frac{1}{2} + 2x, 2y, \frac{1}{2})$ ,  $(\frac{1}{2}, \frac{1}{2} + 2y, 2z)$ ,  $(2x, \frac{1}{2}, \frac{1}{2} + 2z)$ , and symmetry-related points. In the case of strychnine-HBr the peaks corresponding to Br-Br vectors could easily be recognized in the function  $P(xyz)$ , and the coordinates of the four bromine atoms were therefore determined. Values of the Patterson function had been calculated on a lattice of points with spacings  $a/15, b/15, c/60$ . These numbers were written out four times, with the origin of the Patterson function transferred to each of the four bromine positions. The coincidence of three or four comparatively large numbers



at a particular point then indicated the presence of an atom near that point. This gave clear evidence of the approximate positions of the 27 carbon, nitrogen and oxygen atoms of the organic molecule. Robertson (1951) has shown that a similar procedure might have been helpful in the investigation of the structure of rubidium benzyl penicillin. In this case the reduced Patterson function, formed by adding four Patterson functions with their origins transferred to the known sites of the rubidium atoms, has planes of symmetry at  $z=0$  and  $z=\frac{1}{2}$ . The structure itself does not possess these symmetry planes—the space group is No. 19,  $P2_12_12_1$ ; they arise from the fact that the rubidium atoms occur in pairs at  $z=0$  and  $z=\frac{1}{2}$ . There is therefore a two-fold ambiguity in the interpretation of the reduced Patterson function, the coincidence of Patterson peaks at  $(xyz)$  and again at  $(xy\bar{z})$  corresponds to an atom in only one of these positions. In fact the symmetry of the reduced Patterson function is always the same as that of the approximation to the electron density that is obtained when the phase angles are calculated from the known positions of the heavy atoms alone.

When all the atoms of a structure are of about the same atomic number, and the number of atoms is not so small that individual peaks are resolved in the Patterson function, the superposition method may lead to a false structure which is, however, nearly isovectorial with the correct structure, and therefore gives structure factors which show some agreement with observed values. An example is provided by the investigation of  $\text{NaOH} \cdot 4\text{H}_2\text{O}$  by Hemily (1952). Crystals of this substance belong to the space group No. 12,  $C2/m$ , with  $a=15.4_9$ ,  $b=4.0_4$ ,  $c=9.4_6$  Å and  $\beta=117^\circ 16'$ . The atoms are confined to the two planes  $y=0$  and  $y=\frac{1}{2}$ , and since the  $b$ -axis is very short this should be a favourable case for utilizing the Patterson function in projection on (010). There are



FIG. 187. Patterson function of  $\text{NaOH} \cdot 4\text{H}_2\text{O}$ , projected on (010)

1.11 peaks per Å<sup>2</sup>, so one scarcely expects to find isolated peaks in this projection, which is shown in fig. 187. The average height of a Patterson peak was determined approximately by dividing the origin peak by the number of atoms; this showed that peaks can

occur only within areas bounded by the first solid line of fig. 187. A modified function was constructed which had the value unity wherever the Patterson function was higher than the height of a single peak, but was zero elsewhere. In other words it was simply the function shown in fig. 187, with only the first solid line as an indication of its value. From this modified projection of the Patterson function, several reduced functions were made. This was done by choosing a well-defined peak in one modified function and transferring the origin of another to this peak. Non-zero regions common to both then represented possible atomic sites. A series of superpositions using different peaks as starting points appeared to indicate clearly an ensemble of atomic coordinates. The agreement between  $F_o$  and  $F_c$  was satisfactory. After several successive approximations, the electron density map shown in fig. 188*a* was obtained. Irregularities of magnitude

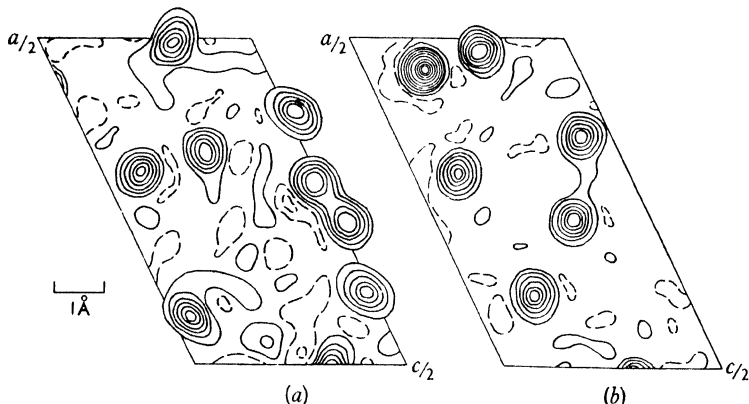


FIG. 188. (a) incorrect and (b) correct electron density maps of  $\text{NaOH} \cdot 4\text{H}_2\text{O}$ . Contours are drawn at an interval of  $2e/\text{\AA}^2$ , the zero contour is broken

about one-fifth the density at the centre of an atom are apparent in this projection, and further calculation did not lead to any improvement. Furthermore the agreement between  $F_o$  and  $F_c$  was not as good as it should be for a finished structure. Following this impasse, a three-dimensional Patterson function was calculated, or rather, since all atoms are contained in two crystallographically-equivalent planes, it was sufficient to calculate a section of this function, shown in fig. 189.

Special consideration was given to

- (1) Determination of the absolute scale by Wilson's method.
- (2) Modification of the function to obtain sharp peaks.
- (3) Subtraction of the origin peak.
- (4) Calculation of the exact form of the Patterson peak corresponding to any pair of atoms.

The heights of an Na-Na single peak, or an Na-O double peak are approximately the same, and such peaks can occur only inside the area bounded by the first solid line ( $300e^2/\text{\AA}^2$ ). This information was

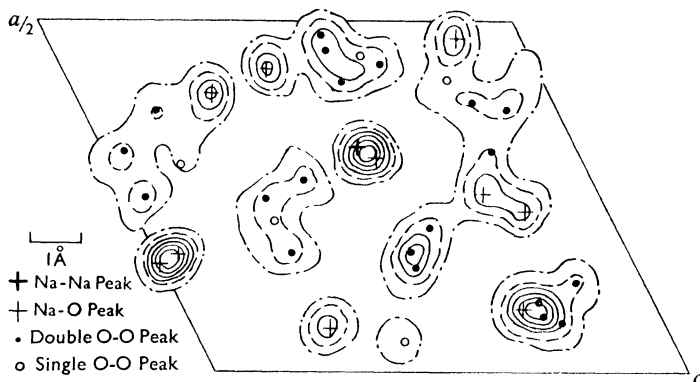


FIG. 189. Section in the plane  $y=0$  of the Patterson function of  $\text{NaOH}\cdot 4\text{H}_2\text{O}$ . Contours at  $100e^2/\text{\AA}^2$ .

sufficient to lead to the structure determination. Double O-O peaks lie within the broken line ( $200e^2/\text{\AA}^2$ ), and single O-O peaks within the remaining line of fig. 189. The positions of Patterson peaks as predicted by the final structure are indicated by the labelled crosses and dots of fig. 189. The true structure is shown by the electron-density projection of fig. 188*b*, and is very different from that determined by the superposition method.

**5.4. Use of known interatomic distances.** Particularly in the investigation of organic compounds, a good deal is known in advance about the distances between atoms in the same molecule, and the probable separation of atoms in different molecules can usually be predicted within fairly narrow limits. Good use of this information can sometimes be made in interpreting the Patterson function. An investigation of the structure of salicylic acid (Cochran, 1951*c*) provides a simple example. The space group of the crystals is No. 14,  $P2_1/a$ , with  $a=11.5$ ,  $b=11.2$ ,  $c=4.90$  Å and  $\beta=91^\circ$ . The positions of the atoms in one molecule are as shown in fig. 190(i)*a*, and the corresponding weighted vector set is shown in fig. 190(i)*b*. Only points within  $2.8$  Å of the origin have been considered, and the heights of CC, CO and OO Patterson peaks are assumed to be in the ratio 36:48:64. Because of the shortness of the  $c$ -axis, one would expect atoms belonging to different molecules to be separated by at least  $2.6$  Å in projection on (001). The distribution of peaks near the origin of the Patterson function projected on

(001) should therefore correspond to that shown in fig. 190(i)*b*. There will be two overlapping sets of vectors as there are two pairs of non-parallel molecules per unit cell (in other words the symmetry of the

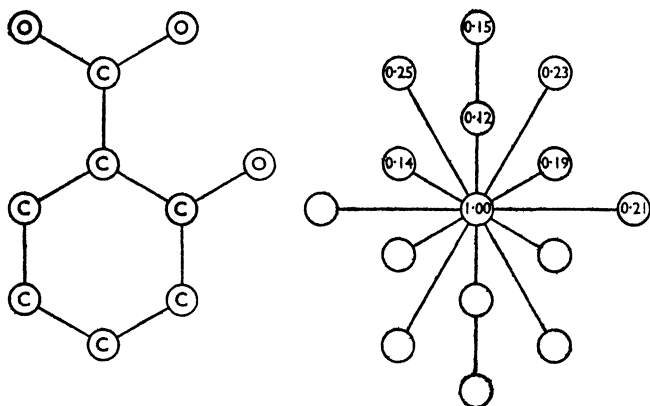


FIG. 190 (i). (a) A molecule of salicylic acid. (b) The relative positions and weights of peaks which will occur near the origin of the Patterson function of salicylic acid

Patterson function in projection is *pm̄m̄*), and the molecule is likely to be tilted so that in projection the peaks will not appear exactly in the relative positions shown in fig. 190(i)*b*. The appropriate region of the

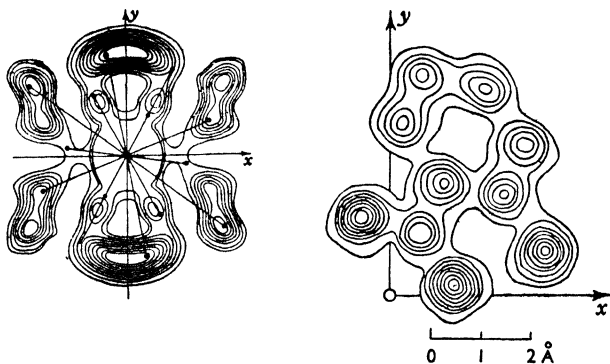


FIG. 190 (ii). (a) Peaks near the origin in the experimental Patterson function of salicylic acid projected on (001). Contours in the origin peak are omitted. (b) A single molecule of salicylic acid projected on (001), for comparison with (a)

experimentally-derived Patterson function is shown in fig. 190(ii)*a*. The coefficients of the  $F^2$ -series have been modified so that the shape of a peak is approximately as given in table 172*a*, row 4. It will be seen that

a satisfactory fit of the vector set of one molecule on the projected Patterson function can be obtained in two ways, corresponding to the fact that the vector set shown in fig. 190(i)b has a vertical plane of symmetry to within the limits of error to be expected in the Patterson function. The correct choice of orientation, and the approximate position of the molecule in the unit cell, were then found with the help of the structure-factor graphs of a few relatively strong reflexions.

Somewhat similar considerations were used by Hughes and Moore (1949) in an investigation of the crystal structure of  $\beta$ -glycylglycine. In this example the space group is No. 15,  $A2/a$ , and the unit-cell dimensions are  $a = 17.8_{\text{b}}$ ,  $b = 4.6_2$ ,  $c = 17.0_6$  Å,  $\beta = 125^\circ 10'$ . The Patterson function projected on (010) is shown in fig. 191. The smaller dotted

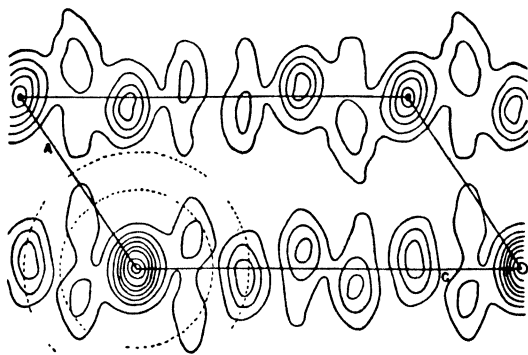


FIG. 191. Patterson function of  $\beta$ -glycylglycine projected on (010). One eighth of a cell from 0 to  $\frac{1}{8}c$  and from 0 to  $\frac{1}{4}a$  is shown and comprises the unique area (Hughes and Moore, 1949)

circle about the origin shows the area outside which all peaks which correspond to vectors between hydrogen-bonded atoms must lie, while peaks corresponding to vectors between atoms separated by the van der Waals distance must lie outside the larger circle. The distribution of peaks along the lines  $x=0$  and  $x=\frac{1}{2}$ , together with the optical properties of the crystal, suggest that the length of the molecule (shown in fig. 192) lies along the  $c$ -axis, and indeed one can see in the arrangement of peaks along  $x=0$  the suggestion of an extended zig-zag chain molecule. It therefore appears fairly certain that all the peaks along  $x=0$  represent vectors between atoms of one molecule. The length of the  $b$ -axis and the optical properties of the crystals suggest that the plane of the molecule is inclined at about  $45^\circ$  to (010). Trials were therefore made with an extended planar model of the molecule (fig. 192), tilted at  $45^\circ$  to (010). From the projection of the model in (010), the pattern of peaks along  $x=0$  was calculated and showed a reasonable fit with the observed Patterson function. A second possible

model failed to pass this test. The array of peaks to be expected between two molecules related by a centre of symmetry, which is the only

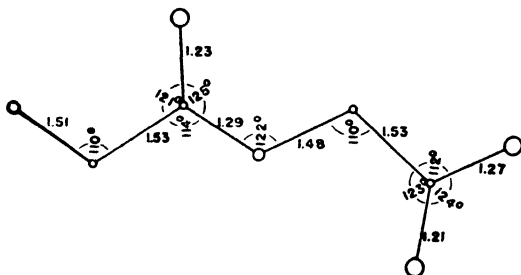
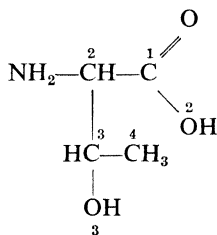


FIG. 192. A molecule of  $\beta$ -glycylglycine. Small circles represent carbons, intermediate circles nitrogens and large circles, oxygens (Hughes and Moore, 1949)

symmetry element in the  $b$ -axis projection of the space group  $A2/a$ , was plotted in duplicate on two sheets of tracing paper and these were superimposed with correct orientation on fig. 191. They were then moved about in such a way as to maintain the centres of symmetry in the Patterson function at  $(\frac{1}{4}, 0)$  and  $(\frac{1}{4}, \frac{1}{4})$ , and an arrangement was found which accounted for the peaks along  $x = \frac{1}{4}$ . The structure found in this way proved to be substantially correct.

In the examples considered so far, it proved possible to interpret the Patterson function in projection. For more complex structures there is little hope of success unless the three-dimensional Patterson function is used. Shoemaker, Donohue, Schomaker and Corey (1950) made extensive use of the three-dimensional Patterson function of  $l$ -threonine in determining its crystal structure. Crystals of threonine have the space group No. 19,  $P2_12_12_1$ , with  $a = 13.6$ ,  $b = 7.7_4$  and  $c = 5.14$  Å. The molecular formula is:—



The three-dimensional Patterson function was calculated by means of punched-card machines (section 4.3.4), the coefficients of the series being modified in the way suggested by Schomaker and Shoemaker (see section 6.4.2). The Harker sections could not be interpreted

because of the large number of non-Harker peaks, and it did not prove possible to find the molecular orientation from a study of the peaks near the origin as they were mostly unresolved. A well-resolved peak was found in the section  $y=0$  at a distance of  $2.25 \text{ \AA}$  from the origin. This is exactly the distance to be expected between the two oxygen atoms of the carboxyl group, and no other pair of atoms can be expected to have this separation. It was concluded that this peak represented the vector  $O_1-O_2$ . The positions of these two atoms in the unit cell were found by studying the Harker sections at  $x=\frac{1}{2}$ ,  $y=\frac{1}{2}$  and  $z=\frac{1}{2}$ . For a structure of this complexity it is difficult to correlate unambiguously, on the three Harker sections, the Harker peaks due to one atom, in spite of the restrictions imposed by symmetry on their coordinates; but once the relative positions of two atoms were known, it proved possible to identify the six Harker peaks corresponding to  $O_1$  and  $O_2$ , and three additional non-Harker peaks were also found in the predicted places. In the section  $y=0$  two other peaks were observed, separated by a vector equal to the  $O_1O_2$  vector. This suggests that, in Wrinch's terminology, this pair is the image of  $O_1O_2$  in some third atom, which is thereby located relative to  $O_1$  and  $O_2$ . This was proved by the success with which peaks were found in positions required by vectors between this new atom and all those already located ( $O_1$ ,  $O_2$  and symmetry-related atoms). A fourth atom was found in approximately the same way, and from its position it was identified as  $C_2$ . The third atom could be identified as  $C_3$  or N, with the former choice best satisfying stereochemical requirements. It is probable that the remaining atoms could now have been located by the Patterson-superposition or vector-coincidence method, but this method had not been developed at the time of the investigation of threonine. The remaining possibilities were in fact tested by trial-and-error procedures, using a model of the molecule and structure-factor graphs. Some features of the Patterson function of threonine are shown in fig. 194(i).

*5.5. Use of the Patterson functions of related compounds.* A comparison of the Patterson functions of two substances may, in favourable circumstances, show the structural relation between them. A good example is provided by Dyer's (1951*b*) work on the structures of two peptide derivatives, diglycylglycine ethyl ester hydrochloride and triglycylglycine ethyl ester hydrochloride. The unit-cell dimensions and space group of these compounds are shown below.

Short formula	<i>a</i>	<i>b</i>	<i>c</i>	Space Group
$G_3 \cdot Et.HCl$	8.95	9.12	$31.8_s \text{ \AA}$	No. 61, <i>Pcab</i>
$G_4 \cdot Et.HCl$	8.7	8.9	$36.5 \text{ \AA}$	No. 61, <i>Pcab</i>

The structure of the compound  $G_3 \cdot Et.HCl$  had already been determined by the isomorphous-replacement method (section 7.3.3). The structural formula and electron density in projection on (100) of this compound are given on p. 195. The change in length of the *c*-axis

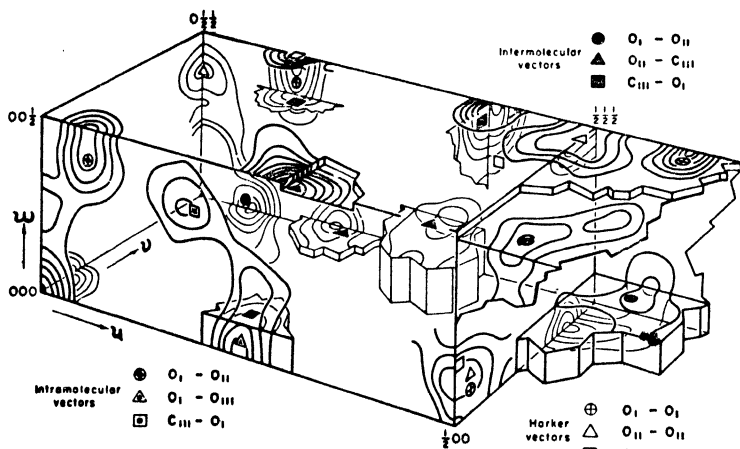


FIG. 194 (i). A representation of three-dimensional Patterson function of threonine. Since the Patterson function has symmetry  $Pmmm$ , only one octant of the Patterson unit cell is shown. Only the peaks which correspond to interactions among the atoms  $O_1O_2$  and  $C_8$  are shown; other peaks were omitted for clarity (Shoemaker, Donohue, Schomaker and Corey, 1950)

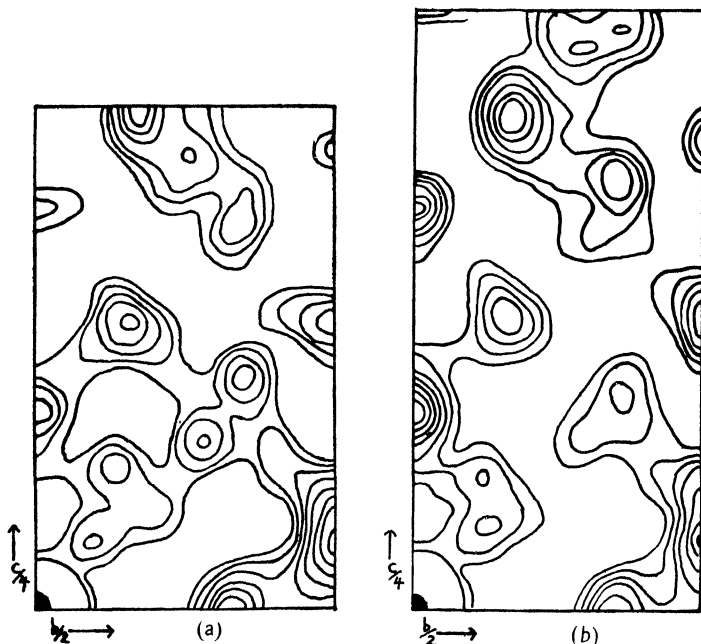


FIG. 194 (ii). The Patterson functions, projected on (001), of (a)  $G_3$ .Et HCl and of (b)  $G_4$ .Et.HCl



from one compound to the other, and the closeness of the other two dimensions in both compounds, suggested that the structures were essentially the same, the greater length of the  $c$ -axis of  $G_4 \cdot Et.HCl$  being accounted for by the extra glycine residue per molecule. This assumption received strong support from a comparison of the projections on (100) of the Patterson functions of the two compounds, shown in figs. 194(ii)*a* and *b*. These showed clearly that the majority of atoms occupy the same relative positions in the two compounds, and enabled the correct structure for  $G_4 \cdot Et.HCl$  to be postulated, and verified without much difficulty. Corresponding electron-density projections are shown in figs. 195*a* and *b*.

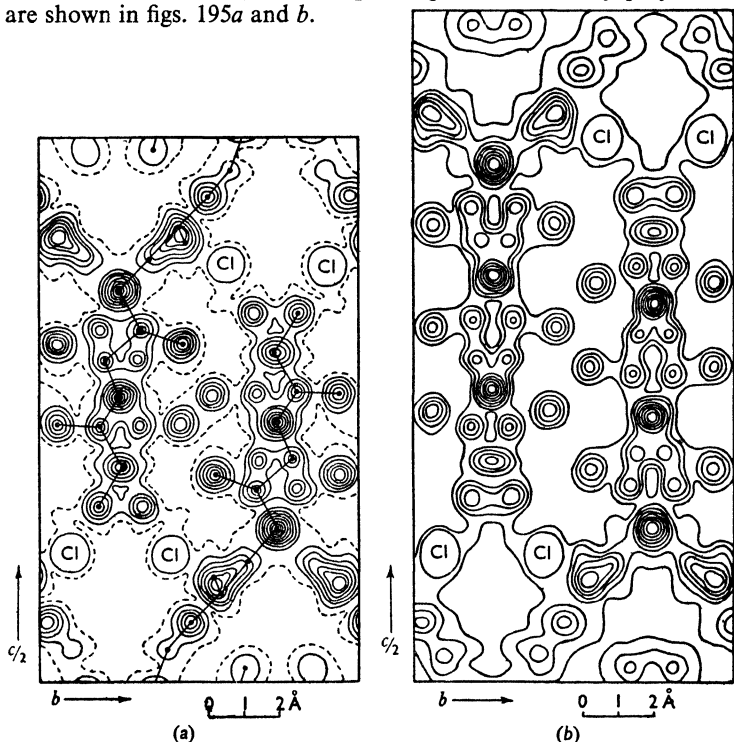


FIG. 195. The electron densities, projected on (100), of (a)  $G_4 \cdot Et.HCl$  and of (b)  $G_4 \cdot Et.HCl$

Molecules of horse methaemoglobin and human oxyhaemoglobin crystallize in ways which do not indicate any close structural resemblances. The unit cell dimensions in Å and space groups of these two proteins are as follows:

	<i>a</i>	<i>b</i>	<i>c</i>	$\beta$	Space Group
Horse methaemoglobin	109	63.2	54.4	111°	No. 5, C2
Human oxyhaemoglobin	62.5	83.2	52.8	98°	No. 4, P2 <sub>1</sub>

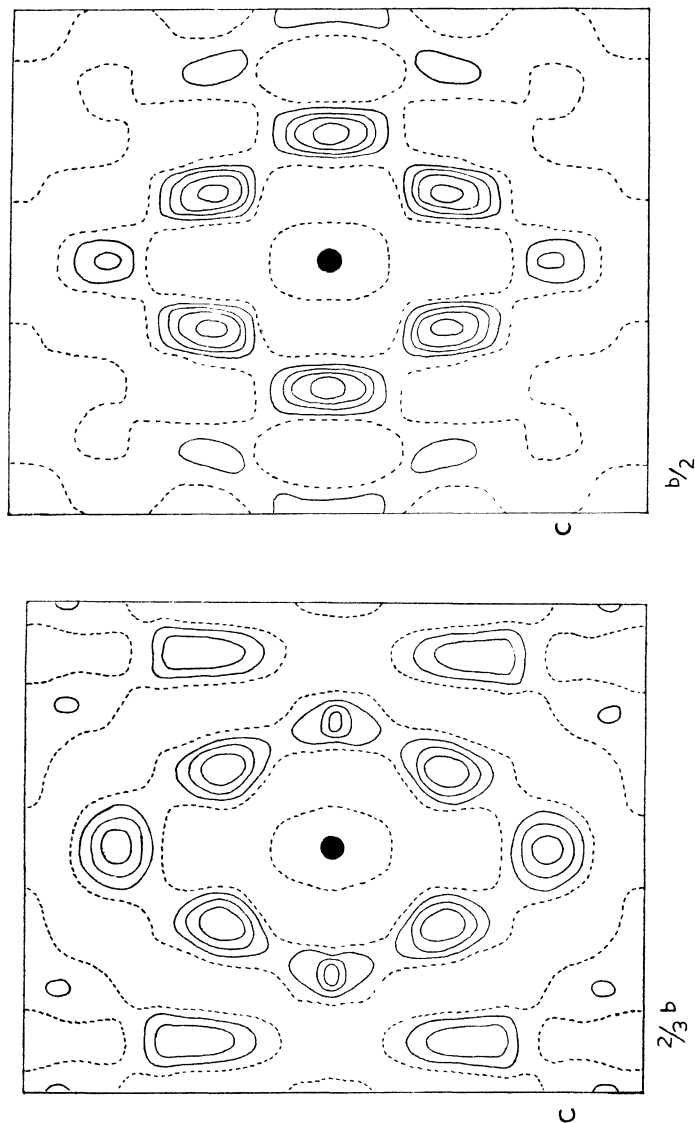


FIG. 196 *a, b*. The arrangement of peaks near the origin of the Patterson functions of (*a*) horse methaemoglobin and of (*b*) human oxyhaemoglobin

The Patterson function of the first of these compounds, projected on a plane perpendicular to the  $a$ -axis, is shown in fig. 196*a* (Boyes-Watson, Davidson and Perutz, 1947). The peaks at distances of about 10.6 Å from the origin are believed to represent vectors between polypeptide chains which are seen end-on in this projection. Exactly the same arrangement of peaks in the projection of the Patterson function of the second protein on a plane perpendicular to the  $a$ -axis can be seen in fig. 196*b*. Although details of the structures of these two proteins are not known, they clearly possess certain general features in common.

6. *Summary.* The distribution of electrons in a crystal can be represented by a Fourier series, whose coefficients are in general complex numbers,  $F(hkl)$ . The function whose Fourier coefficients are the corresponding  $|F(hkl)|^2$ 's is called the Patterson function. Its relation to the crystal structure is most readily understood by supposing the unit cell of the crystal to contain *point* atoms, of which the  $j$ th occurs at the point  $\mathbf{r}_j$  and has weight  $Z_j$ . The Patterson function is then finite only at the points  $\mathbf{r}_i - \mathbf{r}_j$ , where peaks of weight  $Z_i Z_j$  occur; that is, peaks of the Patterson function represent vectors between atoms, and there is one Patterson peak for every pair of atoms in the unit cell. The points  $\mathbf{r}_j$  may be called the fundamental set, and the points  $\mathbf{r}_i - \mathbf{r}_j$  the vector set. The set of point atoms would then be a weighted point set, and its Patterson function a weighted vector set. When the atoms of the structure are spherically symmetric but of finite extent, the peaks of the Patterson function are also spherically symmetric and approximately twice as broad as the atomic peaks. When the number of atoms per unit cell is  $N$ , the number of vectors and therefore of Patterson peaks is  $N^2$ , and these occupy the same unit cell volume. When the crystal is symmetrical, a number of Patterson peaks will occur in coincidence, but in all circumstances, unless  $N$  is very small, Patterson peaks will coincide by chance, and few or no peaks will be separately resolved and identifiable in most practical instances. The sharpness of the peaks, and therefore the degree of resolution of the Patterson function, can be increased by an appropriate modification of the Fourier coefficients, but in practice the Fourier series cannot be extended far enough to produce anything approaching the weighted vector set, which is the ideal limiting case.

Since in principle a crystal structure can be determined from the magnitudes of its Fourier coefficients alone, one might expect that it could also be determined from its Patterson function. Harker showed that for a crystal containing certain symmetry elements, a section along a line or in a plane through the three-dimensional Patterson function is related to a projection of the crystal structure on this line or plane. The peaks which occur in this 'Harker section' correspond to vectors between equivalent atoms of the structure. This work was given a firmer theoretical basis by Buerger, who showed that a

transformation of coordinates of the Harker section, to produce what was called an implication diagram, made the structural and symmetry relations between the section through the Patterson function and the corresponding electron-density projection much clearer. In the great majority of cases the symmetry of the implication diagram is higher than that of the corresponding projection, although for a few space groups they are the same. The practical application of these results is limited by the higher symmetry of the Harker section, and the fact that peaks may occur in the Harker section which do not represent vectors between symmetry-related atoms. In crystal-structure analysis the Harker section is generally used in conjunction with other information, such as the expected shape of a molecule.

Wrinch was the first to show that a fundamental set of points could be recovered completely from its vector set of points. In some cases the method showed that more than one fundamental set may correspond to a given vector set. Such fundamental sets are called 'isovectorial'. It is possible for two or more fundamental sets to have the same weighted vector set; the corresponding crystal structures would give the same X-ray diffraction pattern, and Patterson has called them 'homometric'. A structure which has a homometric counterpart is not likely to occur in practice at all frequently. All methods for the systematic recovery of the crystal structure from its Patterson function depend on the possibility of recognising individual Patterson peaks. It is therefore always possible to recover a fundamental set of points from the corresponding vector set of points, but the Patterson function does not consist of a set of points. When the number of atoms in the unit cell is very small, so that individual peaks are separately resolved in the Patterson function, or when the structure contains a few relatively heavy atoms so that the peaks corresponding to vectors between these and other atoms stand out in the Patterson function, the latter can lead directly to the crystal structure. Also when the positions of a number of atoms are already known, those of the remainder may be found directly from the Patterson function.

In the practical use of the Patterson function in other circumstances one is always able to make use of additional items of information, such as the expected distances between atoms or the known configuration of a particular group of atoms. Trial-and-error methods based on inspection of the Patterson function are probably the most powerful methods of crystal structure analysis available at the present stage of development of the subject.

## CHAPTER 7

### FOURIER METHODS

#### 1. INTRODUCTION

Despite its usefulness, the Patterson synthesis does not provide a proof of the correctness of any but the simplest structures, and generally serves only as a guide. Fourier synthesis, which gives a direct image of the structure, is much more definite and, in some instances, provides a straightforward way of determining crystal structures. To sum a Fourier series, however, requires knowledge of the relative phases of the coefficients, and thus information in addition to the structure amplitudes is needed. Ways of obtaining this information form the subject of this present chapter.

One particularly important advantage of Fourier synthesis is that, for very many crystals, it need be carried out only in two dimensions, whereas the most successful uses of Patterson synthesis are three-dimensional (sections 6.5.2 and 6.5.4). Thus a great deal of preparational work, in the form of analysis of X-ray photographs, estimation of intensities, and correction for various factors, is avoided. For most crystals, Fourier methods can fix a structure unambiguously from a knowledge of only two or three principal zones of intensities.

Although the basic principles of the application of Fourier series to the representation of crystal structures had been pointed out by W. H. Bragg in 1915, practical use was not made of these principles until 1925, when Duane (1925) and Havighurst (1925) used them to derive, from the results of Bragg, James and Bosanquet (1922), the electronic distribution in the sodium and chlorine atoms in rock salt. It was not until 1929 that W. L. Bragg suggested that Fourier methods could be used in crystal-structure determination; he showed that clear representations of projections on to three planes of the structure of diopside,  $\text{CaMg}(\text{SiO}_3)_2$ , could be obtained, and showed that knowledge of the positions of the calcium and magnesium atoms was sufficient to determine the relative phases of the structure factors for one of these projections.

Despite this work, however, the Fourier method was for some time largely adopted as a method of 'refining' structures—that is, of obtaining the best possible atomic positions in structures which had been derived by trial-and-error methods (Booth, 1945*a*). This subject, in which the work of Robertson (1937) is particularly prominent, will be discussed in more detail in Chapter 9. The present chapter is concerned only with methods that have been used for determining atomic positions *ab initio*.

In this connexion, a distinction must be made between centrosymmetrical and non-centrosymmetrical structures. For the latter, the reflexions have relative phase angles which may assume any values between 0 and  $2\pi$ ; thus slight errors in any postulated atomic position will lead to slight errors in the phase angles as well as in the structure amplitudes, and Fourier syntheses computed with these values of phase angles will tend to reproduce the atomic positions from which they were derived. For centrosymmetrical structures, however, only the values 0 or  $\pi$  are possible for the phase angle, and if these values can be correctly allotted to the various structure factors, a Fourier synthesis should give a close approximation to the correct structure. In other words, it is possible to envisage absolute correctness in the phase angles of a centrosymmetrical structure, but not in those of a non-centrosymmetrical structure.

Some qualification of this statement must be made, however; where Fourier methods are applied to two-dimensional projections, it is necessary only that the projection shall be centrosymmetrical, and the structure as a whole may be non-centrosymmetrical (compare section 3.1.4). This state of affairs exists when the projections are perpendicular to two-fold, four-fold or six-fold axes of symmetry. For example, the space group No. 3,  $P2_1$  gives  $hkl$  reflexions whose phase angles are arbitrary, but the reflexions  $h0l$  must have relative phase angles of 0 or  $\pi$  since projections on the (010) plane are centrosymmetrical. The space group No. 19,  $P2_12_12_1$ , which is exceedingly common (Nowacki, 1942), is non-centrosymmetrical, but has three centrosymmetrical projections perpendicular to the screw axes; the structure of  $\text{NiSO}_4 \cdot 7\text{H}_2\text{O}$ , which has this space group, was determined by Beevers and Schwartz (1935) by means of the Fourier projection method.

Some practical difficulties arise in dealing with this type of space group. In the commonly accepted set up for  $P2_12_12_1$  (International Tables, p. 105) none of the screw axes passes through the origin, and consequently none of the projections has a centre of symmetry at the origin; the relative phase angles are then limited to 0 or  $\pi$  for certain reflexions only, the others being limited to  $\pi/2$  or  $3\pi/2$ . While in principle there is no difficulty in handling a Fourier series with these properties, in practice it is found to be rather confusing, and the common practice is therefore to treat each projection separately with the origin lying on the screw axis perpendicular to it. In plotting the results finally, the fact that the origins of the three different projections are not identical must be borne in mind, and it is best to shift all the projections so that they refer to the usual origin for the space group.

## 2. USES OF FOURIER SYNTHESIS

**2.1. Completion of partially known structures.** In general, when an approximation to a correct structure has been derived, the method of

Fourier refinement should lead to a more accurate result. If, however, there is some doubt about the stereochemistry, and the structure is still not accurately enough known, the Fourier method may not be adequate, since it necessarily involves the assumption that certain peaks in the Fourier synthesis correspond to certain atoms. For example, at one stage in the determination of the structure of sodium benzyl penicillin (Crowfoot et al., 1949), a certain peak was assumed to correspond to sulphur, whereas the structure as finally deduced showed that it corresponded to two unresolved carbon atoms.

In this work Bunn made use of an elegant device which showed quite clearly which details of the postulated structure were incorrect. The principle of this device is as follows. In accepting the signs for the structure factors given by a postulated structure we are biasing the Fourier synthesis towards the pattern of that structure, for if we adopted both the signs *and* the magnitudes of the structure factors we should reproduce the postulated structure completely. Since, however, we use the signs given by the postulated structure and the magnitudes given by the true structure, we obtain a compromise between the two. Thus it should be possible to decide which detail in the postulated structure is wrong by finding which atoms are least well represented in the Fourier synthesis.

In view, however, of the deficiencies that are inevitably present in any Fourier synthesis, it is not always easy to decide which atoms are least well represented, and it may be still less easy to decide what changes are suggested. Bunn therefore suggests plotting directly the difference between the syntheses given by the observed and calculated structure factors, a result that can be arrived at by using the differences between the observed and calculated structure factors,  $F_o$  and  $F_c$  respectively, as Fourier coefficients.

A difficulty exists, however, in carrying out this suggestion; the signs of the observed structure factors may not be known with any certainty. For example, if  $|F_o| = 24$  and  $F_c = +3$ , the value of  $F_o - F_c$  is  $+21$  if  $F_o = +24$ , and is  $-27$  if  $F_o = -24$ . If, however,  $|F_o| = 3$  and  $F_c = +24$ , the value of  $F_o - F_c$  is  $-21$  if  $F_o = +3$  and is  $-27$  if  $F_o = -3$ ; there is little difference between these two values, and the probability that  $F_o$  has the same sign as  $F_c$  is so high that the value of  $-21$  for  $F_o - F_c$  may be confidently used, with the knowledge that if the sign of  $F_o$  is wrong no great error will result. The terms for which  $F_o$  is small and  $F_c$  is large may thus be used as Fourier coefficients with values  $F_o - F_c$ .

The resulting synthesis is named by Bunn the 'error synthesis', and, as can be seen from the last paragraph, it makes particular use of the reflexions that are of negligible observed intensity—a rather rare procedure in Fourier methods. Strongly negative regions in the synthesis indicate that, in the postulated structure, too much scattering matter has been assumed there, and positive regions indicate that too little

TABLE 202

Comparison of some observed and calculated  $F$ 's for an incorrect structure of durene

$hkl$	$F_o$	$F_c$	$F_o - F_c$
001	38.5	7.6	—
202	5.5	15.5	10.0
20 $\bar{4}$	8.0	28.1	20.1
20 $\bar{5}$	0.0	7.5	7.5
400	9.0	0.0	—
402	2.5	8.9	6.4
40 $\bar{2}$	6.0	27.3	21.3
404	9.0	17.5	8.5
60 $\bar{1}$	1.5	15.6	14.1
60 $\bar{6}$	3.5	12.6	9.1

The value in the last column is obtained by assuming that  $F_o$  has the same sign as  $F_c$ .  
For 001 and 400, the sign of  $F_o$  is doubtful.

matter has been assumed; a steep gradient at an assumed atomic position implies that the atom has been incorrectly placed.

The method can best be illustrated by an example. In table 202 are given observed and calculated values of  $F(h0l)$  for certain reflexions from durene (Robertson, 1933*b*), together with values calculated for an incorrect structure. In this structure the molecules are so oriented that the atoms in the benzene rings have the same co-ordinates as in the correct structure; but one pair of  $\text{CH}_3$  groups is slightly displaced, and the other pair is completely wrong. (The impossibility of fitting the molecules into the unit cell in these orientations is ignored.) For brevity, only those terms showing pronounced disagreement are included in the table; in the complete table sufficient correspondence is found to indicate a certain measure of correctness.

Of the terms in the table, all but two (001 and 400) have large calculated values and small observed values, and these are used for the error synthesis. The result, shown in fig. 203, with the postulated atomic positions superposed, shows clearly that one pair of  $\text{CH}_3$  groups is completely misplaced; fig. 203 also shows that the other pair of  $\text{CH}_3$  groups is somewhat misplaced, and indicates the direction of movement which would improve the agreement. There is no definite suggestion of movement of any of the atoms in the benzene ring.

From this example it can be seen that the uses of the error synthesis are two-fold. First, it indicates which atoms are in the wrong places,



and gives some indication—which knowledge of interatomic distances and stereochemistry can usually supplement—where they should be moved to; and secondly, it indicates which atoms are only slightly

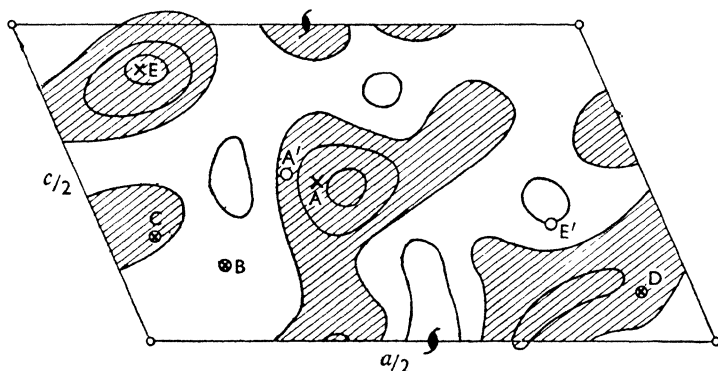


FIG. 203. Error synthesis for incorrect structure of durene. The negative areas are shaded. The assumed atomic positions are  $A$ ,  $B$ ,  $C$ ,  $D$  and  $E$ , and the fact that  $A$  and  $E$  lie in strongly negative regions suggests that their positions are incorrect. The correct positions are  $A'$  (which lies up a steep slope from  $A$ ) and  $E'$  (which is a completely different position from  $E$ , as suggested by the occurrence of a deep minimum at  $E$ )

displaced, and the directions in which they should be moved. If all the errors are of the second kind, then it is likely that practically all the signs of the structure factors will be known, and thus all the terms can be included in the error synthesis. The result, called the 'difference synthesis' (Cochran, 1951a), is of considerable use in improving the accuracy of atomic positions, and will be discussed in more detail in section 9.4.

Fig. 204 shows the error synthesis which helped in the determination of the structure of sodium benzyl penicillin. The postulated positions of the sodium atoms lie on gradients which indicate that some movement of these atoms is required. But the most striking indication is the strongly negative region around the position of the sulphur atom, flanked by two fairly large peaks; these details indicate that what was thought to be a sulphur atom was really two carbon atoms partly resolved. The synthesis hinted at other changes also, and altogether gave most useful evidence of the correct nature of the molecule.

**2.2. Determination of unknown structures.** As an aid to the determination of unknown structures, Fourier methods have proved invaluable, but there is no straightforward method by which they can be used generally. As already explained, the problem to be overcome is the determination of the relative phases of the diffracted beams, or, for centrosymmetrical crystals, the signs of the structure factors. Two

possible methods of approach suggest themselves: first, we may try to see whether the condition that crystals are composed of discrete atoms imposes any relationships between the structure factors, and so leads from their magnitudes to their signs; secondly, we may try to discover whether certain structural features give any indication of the signs. There would appear to be little hope of producing, by interference of the scattered X-ray beams, a direct image of the structure.

The first approach is naturally of importance in producing a logical proof of the uniqueness of a structure, but, in addition, it has led to several methods which have been successfully used for determining

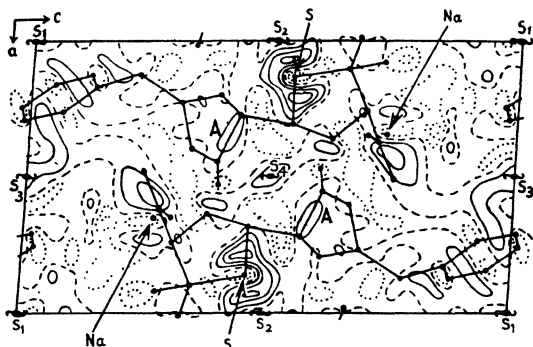


FIG. 204. Error synthesis used in the determination of the structure of sodium benzylpenicillin. The most striking feature is that which shows that the peak thought to be  $S$  is really two unresolved peaks. Also, the  $Na$  positions lie on steep gradients (Crowfoot et al., 1949)

new structures. Because of their importance, these methods will be described in Chapter 8, although it must be emphasized that they should always be explored before the methods described in this present chapter are brought into play.

### 3. METHODS OF DETERMINING RELATIVE PHASES OF STRUCTURE FACTORS

**3.1. Trials of different sign combinations.** It might be thought that a trial-and-error process of sign selection would be possible for centrosymmetrical crystals; since there are only two possibilities for each term, different combinations could be tried until one was found that gave an interpretable representation of the projection of the given structure. Errors in a few signs should not make a great difference, and so it should be possible to recognize when the correct structure was being approached. The difficulty, however, lies in the enormous number of combinations possible with even a few terms, and if any success is to be gained by such methods some degree of systematization must be introduced.

One useful fact is that not all the signs of the structure factors are absolute; some can be chosen arbitrarily. This arises from the number of different centres of symmetry that exist in the unit cell; in the (001) projection of space group  $P\bar{1}$ , for example, there are centres of symmetry at the points  $(0, 0, 0)$ ,  $(\frac{1}{2}, 0, 0)$ ,  $(0, \frac{1}{2}, 0)$  and  $(\frac{1}{2}, \frac{1}{2}, 0)$ , and any of these can be chosen as origin. A shift of origin from  $(0, 0, 0)$  to  $(\frac{1}{2}, 0, 0)$  merely corresponds to change of sign of all terms with  $h$  odd, and thus we can choose the positive sign for any *one* of these terms; once this term has been fixed, however, the other terms with  $h$  odd are fixed relatively to it: the terms with  $h$  even do not change at all. Similar considerations apply to the choice of sign for one term with  $k$  odd; the two possibilities correspond to origins at  $(000)$  and  $(0\frac{1}{2}0)$ .

We can make use of both these considerations simultaneously, if we choose as two arbitrary terms one with  $h$  odd and the other with  $k$  odd, making the structure factors both positive. These two signs must be correct for a structure referred to one of the points  $(0, 0, 0)$ ,  $(\frac{1}{2}, 0, 0)$ ,  $(0, \frac{1}{2}, 0)$  or  $(\frac{1}{2}, \frac{1}{2}, 0)$  as origin. If there are centres of symmetry at other points in a projection, then other possible choices of sign may be made, but it is impossible here to give the rules that would cover all contingencies. It is not difficult to decide from first principles on the rules for any particular projection.

The number of sign combinations is not greatly limited by these considerations, and, in general, it would be hopeless to consider dealing with all the terms in any reasonably complicated section of a reciprocal lattice. Some attempt must therefore be made to reduce the number that have to be considered, at any rate in the initial stages. Two possibilities suggest themselves: first, we may consider the largest terms first, choosing a small enough number to allow systematic consideration; and secondly, we may include only the terms within a small range of Bragg angle. The first method does not lend itself to systematic treatment, as even twelve terms, including two with arbitrary signs, would give over one thousand combinations; and it is doubtful whether twelve terms only would give a recognizable approximation to a moderately complicated structure.

The second method would appear to be more promising. The inclusion of only a small number of terms within a given range of Bragg angle would correspond to the decrease of the numerical aperture of an optical instrument (Bragg and West, 1930), and thus we should expect to see the structure with a lower degree of resolution, and so should have some idea of what to expect. An arbitrary cut-off at a given Bragg angle would however introduce unwanted diffraction effects, and it would probably be advisable to introduce an artificial temperature factor to eliminate these.

Not all combinations of sign are equally likely: for example, if a structure contains atoms of approximately equal weight, it is impossible for all the structure factors to be positive, since this would

imply an excessive concentration of electron density at the origin. Thus not all the thousand possibilities need be considered. In fact, the absence of a heavy atom at the origin demands that positive and negative structure factors should be present in about equal numbers, and such combinations of signs should therefore be tried. The existence of other centres of symmetry in structure projections suggests further limitations on the possible combinations of signs; thus it is impossible for all the structure factors with  $h$  even to be positive and all those with  $h$  odd to be negative, although this distribution would give approximately equal numbers of positive and negative signs. The number of combinations can thus be further reduced by eliminating such possibilities.

No success has yet been reported with methods such as these, although Hanson and Lipson (1952*b*) have shown that, by means of the optical method of Fourier synthesis described in section 4.5.2, the structure of hexamethylbenzene (Lonsdale, 1929) could have been derived in this way. Also, Boyes-Watson and Perutz (1943) have used computational methods to produce, with poor resolution, a representation of the projection of a protein molecule. This was possible because the crystal used gave very few reflexions, but as the number of reflexions that one wishes to include increases, so the computational work increases, and rapid methods of summation become more desirable. The apparatus designed by Pepinsky (1947) and mentioned in section 4.5.1, would appear to be admirably suited to this type of work; if this turns out to be so, the recording of the general rules given above will have been justified.

**3.2. 'Heavy-atom' method.** The failure of the sign-permutation method to produce a general solution to the problem of crystal-structure determination makes it necessary to consider whether less direct methods can be used. Direct determination of phase angles, for example by means of the double-reflexion phenomena described in section 2.4.4, does not appear to be promising (Lipscomb, 1949), but the indirect approach has been extraordinarily fruitful and most of the triumphs of the subject have been achieved in this way. Crystal structures with over a hundred variable parameters have been solved, and these would obviously have been far too difficult for the trial-and-error methods described in Chapter 5.

The term 'indirect' is applied to the methods in which the phase angles are inferred from certain structural features. The simplest of such features are atoms which have predominant scattering factors; their positions can be located fairly easily by Patterson methods (section 6.5.1), and thence the phase angles that would result from these atoms alone can be deduced. The assumption that these phase angles are those of the various reflexions should then give a Fourier synthesis which is a close approximation to the complete structure.

Formally, this result can be shown by writing the structure factor for a crystal with one heavy atom in the unit cell as

$$F(hkl) = f_H \exp 2\pi i(hx_H + ky_H + lz_H) + \sum_n f_n \exp 2\pi i(hx_n + ky_n + lz_n),$$

where  $f_H$  is the scattering factor of the heavy atom, whose parameters are  $x_H$ ,  $y_H$  and  $z_H$ . If  $f_H$  is much greater than  $f_n$ , then the first term will tend to be much greater than the second, since the summation, being due to several atoms, will usually be relatively small.

It is therefore unnecessary, and indeed inadvisable, that  $f_H$  should be greater than  $\sum f_n$ —that is, that the heavy atom should scatter more than all the other atoms together. If  $f_H$  is too large, the Fourier synthesis will tend to show only this atom, the lighter atoms being seen only with difficulty; at the best, their positions would be highly inaccurate. For example, Perutz and Weiss (1946) found that a projection of the structure of tribromo-trimethylphosphine-gold showed only the gold and bromine atoms, and the remaining features had to be inferred from spatial considerations. The work of Robertson and Woodward (1940) on platinum phthalocyanine, on the other hand, did show all the structural features expected, but the peaks representing the lighter atoms were much more distorted (fig. 209) than would be expected for a structure containing only light atoms.

As a rough guide, for successful use of the method the sum of the squares of the atomic numbers of the heavy atoms and of the light atoms should be approximately equal. This may be seen by considering equation 135,

$$\overline{I(hkl)} = \sum_j f_j^2,$$

which shows that, on the average, the contribution of any one atom to the diffracted intensity depends upon the square of its scattering factor. If we require that the average contribution of the heavy atoms should be about equal to the average contribution of the light atoms, the signs of about three-quarters of the structure factors will be correct; half will be correct because the two contributions have the same sign, and half of the remainder will be correct because the contributions of the light atoms are opposite in sign to, but less than, the contributions of the heavy atoms.

That the rule works well is indicated by some practical examples. For metatolidine dihydrochloride,  $C_{14}H_{18}N_2Cl_2$  (Fowweather and Hargreaves, 1950), the sum of the squares of the atomic numbers of the chlorine atoms is 578, and the sum of the squares of the atomic numbers of the carbon and nitrogen atoms is 602. For determining the structure of strychnine,  $C_{21}H_{22}N_2O_2$ , an element of atomic number near to 31 would be required; Robertson and Beevers (1950) made use of bromine (35) and Bokhoven, Schoone and Bijvoet (1948, 1949, 1951) made use of selenium (34).

The determination of the structure of phthalocyanine by Robertson and Woodward (1940) was the first direct application of the heavy-atom method. The molecular structure is shown in fig. 238*a*, and it will be seen that there is a large space at the centre of the molecule; into this space various metal atoms can be introduced. It has been shown already that platinum should be heavy enough to decide the phase angles of the reflexions, and this turned out to be so in a particularly simple way. The space group is No. 14,  $P2_1/a$ , and the unit cell contains two molecules; thus the molecules must have their centres on centres of symmetry and the platinum atoms must lie on these centres. The occupation of special positions by the heavy atoms, despite the advantage previously mentioned, can, however, lead to difficulties: usually, atoms in such positions do not contribute to certain reflexions, and thus do not help to fix the phases of the structure factors of these reflexions. In this space group, however, the  $h0l$  reflexions to which the platinum atoms do not contribute are those that are forbidden by the space group; thus a projection of the structure on to the (010) plane can be computed as though the crystal had one molecule in a cell with dimensions  $a/2$  and  $c$ , with a platinum atom at the origin—the most favourable circumstances for application of the heavy-atom method.

The structure factors of the  $h0l$  reflexions should all be positive, and the resulting Fourier synthesis is shown in fig. 209; it will be seen that all the details of the molecule are clearly shown. The molecule is tilted somewhat from the plane of projection, and so is foreshortened in one direction, but when this foreshortening is allowed for the molecular dimensions show good agreement with those found in other structures.

Results such as this can be obtained only if the experimental data are accurate. The electron density at the peak of the platinum atom is  $160e/A^2$ , whereas that at the peaks of the carbon atoms is only  $8e/A^2$ ; thus small errors in the structure amplitudes, which would affect the platinum atoms only slightly, would make much greater proportionate differences to the lighter atoms. It will be noted, as stated earlier in this section, that the carbon-atom peaks are rather distorted, and this effect must always exist to some extent if the heavy-atom method is used.

More general illustrations of the method are given by the determination of the structures of cholesteryl iodide (Carlisle and Crowfoot, 1945), calciferol (Crowfoot and Dunitz, 1948) and strychnine (Robertson and Beevers, 1950). The structure of calciferol was found by forming the compound calciferol-4-iodo-5-nitrobenzoate, which crystallizes in space group No. 19,  $P2_12_12_1$  with four molecules in the unit cell; 123 parameters are involved in the complete specification of the structure. The work on strychnine was carried out on the compound strychnine hydrobromide, which also crystallizes in the space group

$P2_12_1$  with four molecules in the unit cell; although rather fewer parameters—84—are involved, the difficulties were rather greater than

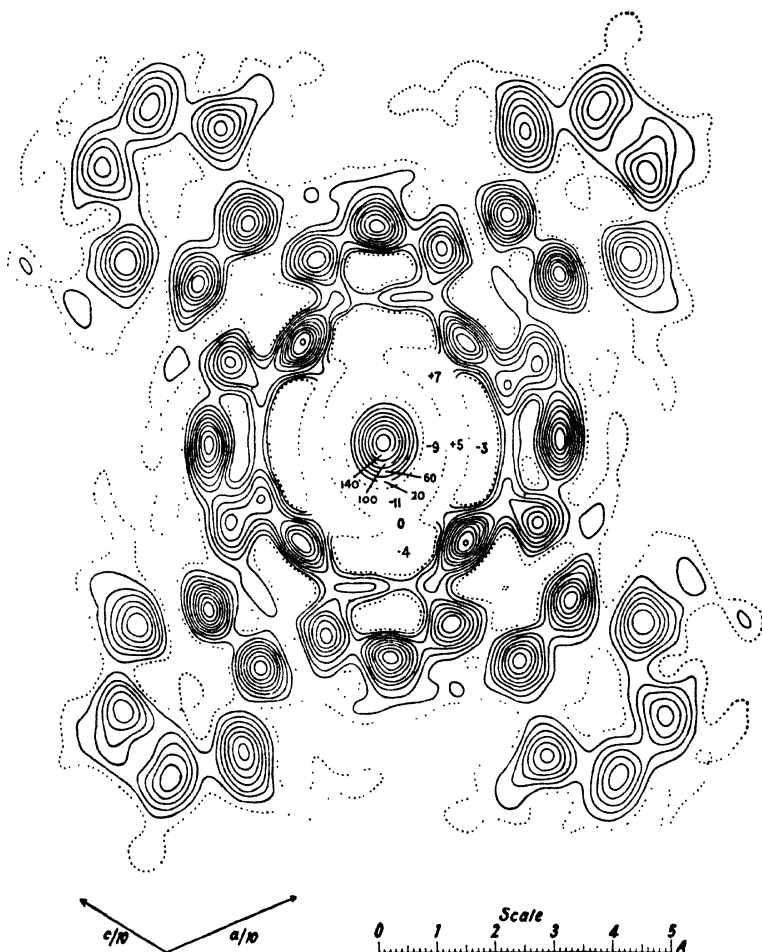


FIG. 209. Platinum phthalocyanine: (010) electron-density projection, with contours at intervals of  $1e/\text{\AA}^2$ , except in centre (Robertson and Woodward, 1940)

in the determination of the structure of the calciferol compound, because, at the outset of the work, much less was known of the molecular configuration.

Some points of general interest emerged from the work on cholesteryl iodide, which crystallizes in space group No. 4,  $P2_1$ ; the two molecules in the unit cell are in general positions. Although the space group is not centrosymmetrical, as explained in section 7.1 the structure factors of the  $h0l$  reflexions are all real, and the determination of the structure was largely based upon the (010) projection. The parameters of the iodine atoms were found by Patterson synthesis (section 6.5.1) and the signs of the structure factors given by these parameters were used to compute the electron-density projection shown in fig. 210. It will be noted that this projection is not particularly clear

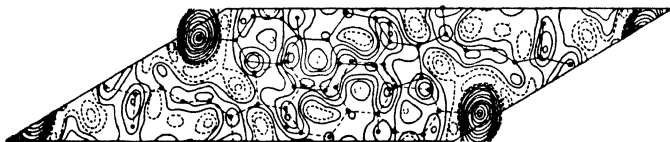


FIG. 210. Cholesteryl iodide: (010) Fourier synthesis with signs allotted to the coefficients according to the calculations from the iodine positions. The atomic positions suggested by the synthesis are also shown (Carlisle and Crowfoot, 1945)

and would not, by itself, be sufficient to establish the structure; stereochemical evidence had to be used to enable the projection to be interpreted, and the signs of the structure factors were recalculated with all the atoms taken into account. Finally, the parameters of the atoms suggested by the usual bond distances were used to establish the phase angles of the general reflexions  $hkl$ .

Here a fundamental difficulty arises. Since the space group contains only two-fold screw axes, the origin may be chosen arbitrarily at any point along one of these axes, and it is convenient to place it half-way between two iodine atoms; thus these two atoms (but no others) are exactly related by a centre of symmetry and the phase angles of their contributions to the structure factors are either 0 or  $\pi$ . If, however, these phase angles are used to compute the electron density, they cannot give the correct result, since they must inevitably give a centrosymmetrical structure, and the structure is not centrosymmetrical. Actually, the result obtained represents a superposition of two structures—the correct one and another related to it by a centre of symmetry half-way between the iodine atoms. In other words, of each pair of centrosymmetrically related peaks only one was correct, and careful choice, based on the knowledge of bond distances and stereochemistry, had to be made. Thus, although the structure determination was successful—a remarkable feat since eighty-four parameters were involved—prior knowledge of the main structural features was needed.

This was not so for  $\text{CuSO}_4 \cdot 5\text{H}_2\text{O}$  (Beevers and Lipson, 1934). The



establishment of this structure provided what is probably the first successful use of Fourier series in crystal-structure determination. The starting point was the knowledge of the positions of the copper and sulphur atoms (section 5.5.2). The copper atoms, being in the special positions  $(0, 0, 0)$  and  $(\frac{1}{2}, \frac{1}{2}, 0)$ , are not sufficient to establish enough signs to enable the Fourier method to be applied, although they contain nearly twenty-five per cent of the electron content; they do not contribute to those reflexions with  $h+k$  odd, and if these reflexions are omitted from the Fourier synthesis the correct projection would be combined with another related to it by a C-face-centring. It might have been possible to determine the structure from such a result, by means of methods similar to those used for cholesteryl iodide, but since the sulphur positions were known, the correct projection was found by making use of these positions to give the signs of the structure factors with  $h+k$  odd. It is interesting to note, however, that traces of the related projection are shown in the published result (fig. 211); the computations were made before systematic methods had been developed and, in order to economize in effort, the smaller structure factors were omitted; since there were more of these small ones with  $h+k$  odd than with  $h+k$  even, traces of face-centring remained, and are shown by a 'ghost' peak related to that of the sulphur atom.

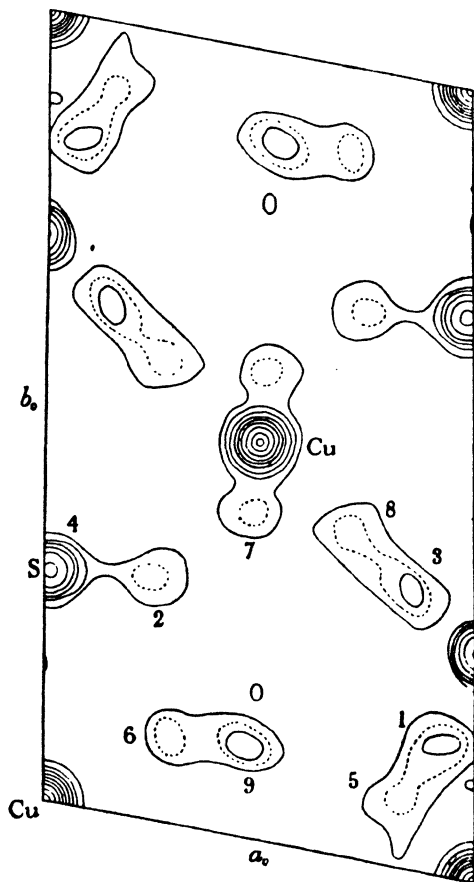


FIG. 211.  $\text{CuSO}_4 \cdot 5\text{H}_2\text{O}$ : (001) electron-density projection. The small peak near the water molecule 9 is a 'ghost' related to the peak S (Beevers and Lipson, 1934)

The indeterminacy of the phase angles of certain structure factors may arise in other problems, and is worth special consideration. It must occur when the heavy atoms are related by symmetry elements that are not present in the complete structure, since the phase angles given by the heavy atoms must give a structure that has this same symmetry. Although the effect will, in general, occur only when the heavy atoms are in special positions, as in  $\text{CuSO}_4 \cdot 5\text{H}_2\text{O}$ , this is not always so, as the experience with cholesteryl iodide shows. In rubidium benzyl penicillin, for example, the rubidium atoms have  $z=0$  (Crowfoot et al., 1949), and thus do not contribute to the  $h0l$  reflexions for which  $h+l$  is odd, nor to the  $0kl$  reflexions for which  $k$  is odd. If the structure factors with indeterminate signs were omitted, the projections showed too high a symmetry, and further application of the Fourier method was not possible because too little was known of the stereochemistry of the penicillin molecule.

It will thus be seen that the heavy-atom method, powerful as it has proved to be, is still not completely general. It is, of course, limited to those structures in which a heavy atom exists or into which one can be introduced, but also there may be many reflexions whose signs are not affected by the heavy atoms. Thus further evidence is greatly to be desired.

**3.3. Isomorphous replacement.** One method of obtaining this evidence is provided by comparing the X-ray intensities from a pair or a series of isomorphous compounds; we can then make use of the changes in structure amplitude when one atom is replaced by another, since, if the position of this atom is known, its contribution to a particular structure factor may determine the sign quite definitely. In effect, the method is similar to the heavy-atom method, since one of the replaceable atoms is usually much heavier than the other atoms in the structure, but it enables problems to be dealt with in which the replaceable atom contains much less than the proportion of the electron content that is required for the heavy-atom method. On the other hand, the changes in structure amplitude are difficult to interpret when variable phase angles are involved, and thus the isomorphous-replacement method is usually applied only to centrosymmetrical structures or projections; the heavy-atom method, as we have seen, is not confined to these cases.

One of the first attempts to make use of an isomorphous series was that of Cork (1927), who made extensive measurements of intensities from what is probably the best-known isomorphous series—the alums. This series is typified by the compound  $\text{KAl}(\text{SO}_4)_2 \cdot 12\text{H}_2\text{O}$ , the potassium being replaceable by certain monovalent atoms or radicals, the aluminium by other trivalent atoms, and the sulphur by selenium. Cork measured the intensities of reflexions of the types  $h00$ ,  $hh0$  and  $hhh$  from crystals containing ammonium, rubidium, caesium and thallium

in place of potassium, and chromium in place of aluminium, but the sulphur atom was left undisturbed. It has already been shown (section 2.7.1) that in the unit cell the metal atoms are fixed and that the sulphur atoms are situated on the three-fold axes; Cork's first problem therefore was to find the parameter of the sulphur atoms. Of the intensities measured, only the  $hhh$  reflexions can fix this uniquely, since neither the  $h00$  or the  $hh0$  reflexions can distinguish between parameters  $u$  and  $\frac{1}{2} - u$ , and thus Cork used these reflexions to compute the projection of the electron density on to the cube diagonal.

TABLE 213

Structure amplitudes of the  $hhh$  reflexions from various alums,  $R'Al(SO_4)_2 \cdot 12H_2O$

$hkl$	$NH_4(11)$	K(19)	Rb(37)	Tl(81)
111	86	38	29	113
222	0	19	79	195
333	111	125	158	236
444	25	6	55	125
555	24	49	64	131
666	86	86	122	164
777	53	34	0	18
888	0	16	22	56
999	25	0	0	25

Table 213 gives some of the measurements used, and it can be clearly seen how the structure factors change as the substitution proceeds. Thallium, of atomic number 81, is heavy enough to cause all the  $hhh$  reflexions to have positive structure factors, but as lighter atoms are substituted the value for 111, for example, decreases until for potassium it obviously becomes negative. The signs can all be fixed in this way, and the resulting Fourier syntheses are shown in fig. 214; only one half of the diagonal need be considered because the structure is centrosymmetrical. The synthesis shows clearly the peaks due to the metal atoms, and, in between them, a complex mass of sulphate ions and water molecules. (Actually caesium alum has a different structure from the other compounds used (Lipson, 1935), and the coincidence of its electron-density curve with the others is accidental. The data for caesium alum are not included in table 213.)

From these results it seems a reasonable guess that the sulphur atoms have a parameter of about 0.36, but Cork was not able to deduce a structure based on spatial considerations that gave acceptable agreement, and he had to abandon the determination. The reason for the impasse became apparent when measurements were made of the corresponding reflexions from potassium aluminium selenium alum

(Beevers and Lipson, 1935); these measurements are shown in table 214 and, if appropriate signs are allotted, the resultant Fourier synthesis

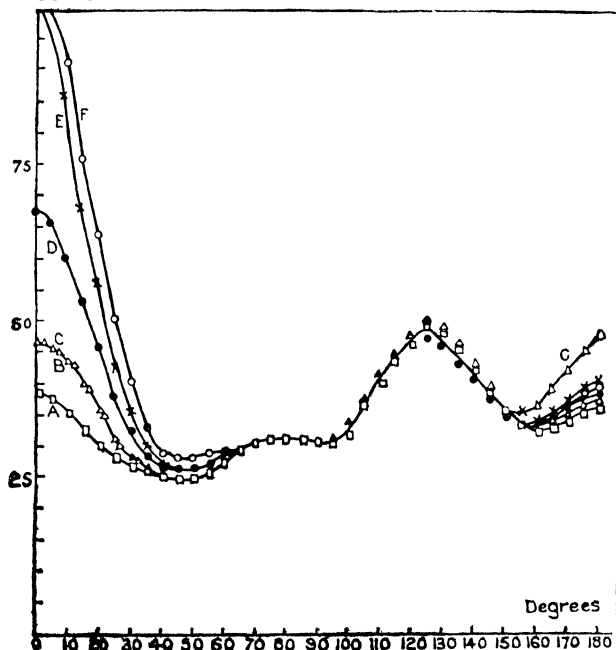


FIG. 214. Electron densities, in arbitrary units, between the (111) planes of various alums (Cork, 1927)

TABLE 214

Structure factors of  $hhh$  reflexions from  $\text{KAl}(\text{SO}_4)_2 \cdot 12\text{H}_2\text{O}$  and  $\text{KAl}(\text{SeO}_4)_2 \cdot 12\text{H}_2\text{O}$

Indices	111	222	333	444	555	666	777	888
Sulphate	$\overline{38}$	19	125	6	49	86	$\overline{34}$	16
Selenate	$\overline{48}$	$\overline{52}$	64	0	116	100	$\overline{16}$	0

The values for the selenate were given the same signs as for the sulphate (deduced from table 213); only for 222 did the assignment prove wrong. The incorrectness of the parameter 0.36 is evident from the decrease in structure amplitude of the reflexion 333.

(fig. 215) shows an increase of the peak at  $u=0.19$ , not that at 0.36. It was proved therefore that the apparently reasonable deduction that the sulphur lay in the high peak of fig. 214 was wrong, and that the much smaller peak at  $u=0.19$  was the correct one. This result indicates

the danger of relying only upon projections on to lines, as these can be deceptive because of the possibility of overlapping of several lighter atoms.

This difficulty was increased inadvertently by the adoption of an artificial temperature factor in the computation of the curves shown in fig. 214, as false detail due to the arbitrary termination of the series was feared; the curves shown in fig. 215 are derived from data that do

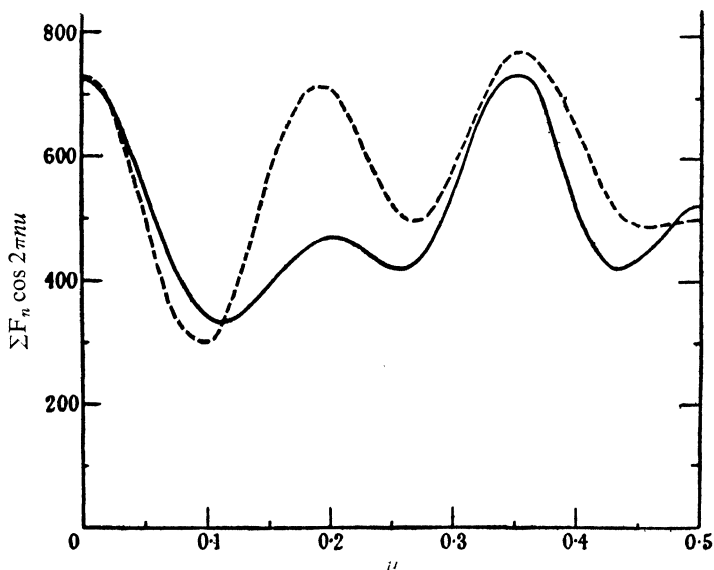


FIG. 215. Electron densities, in arbitrary units, between the (111) planes in  $\text{KAl}(\text{SO}_4)_2 \cdot 12\text{H}_2\text{O}$  (full line) and  $\text{KAl}(\text{SeO}_4)_2 \cdot 12\text{H}_2\text{O}$  (broken line). The enhancement of the peak at 0.20 shows that the S and Se parameters are in this vicinity (Beevers and Lipson, 1935)

not include this factor, and it will be seen that the sulphur peak is more pronounced: but whether this fact would have helped to locate the sulphur atoms is doubtful. This experience does, however, suggest that the adoption of an artificial temperature factor is rather dangerous; even if it is considered essential, the computations without the factor should also be carried out to see if any significant detail has been lost.

When the three heavy atoms had been located, the determination of the remaining atoms, by two-dimensional Fourier methods, was straightforward.

Despite its lack of complete success, Cork's work illustrates well the principles of the isomorphous-replacement method, and it also illustrates some of the difficulties that are met with when only a pair of compounds is available. Thus the change of sign for 111 on passing

from rubidium to potassium would not have been evident. Similar difficulties arose in the change from rubidium to potassium benzyl penicillin (Crowfoot et al., 1949); for example, the two structure amplitudes for the reflexion 004 were 7 and 5, but nevertheless there was a large contribution from the alkali atoms, since it ultimately turned out that the structure factors were +7 and -5.

Such difficulties can be avoided by a more general method introduced by Dr. A. Hargreaves and used by him to determine the structure of zinc paratoluene sulphonate (Hargreaves, 1946), by the comparison of the intensities of the reflexions with those from the corresponding magnesium salt. The method can be used when relative measurements only are available and, in fact, provides another, rather specialized, method of placing a set of structure amplitudes on an absolute basis (section 5.5.3); it depends upon knowledge of the difference on an absolute scale between the structure factors for the two compounds, and thus it can be applied only when the positions of the replaceable atoms are known.

The principle of the method can be described in terms of two isomorphous crystals of space group  $P\bar{1}$ , containing two equivalent replaceable atoms in the unit cell. Then, if  $F'_a$  and  $F'_b$  are the observed structure factors for the two crystals, on relative scales which are not necessarily the same,

$$c_a F'_a(hkl) = 2f_a \cos 2\pi(hx + ky + lz) + 2 \sum f_n \cos 2\pi(hx_n + ky_n + lz_n) \\ \text{and } c_b F'_b(hkl) = 2f_b \cos 2\pi(hx + ky + lz) + 2 \sum f_n \cos 2\pi(hx_n + ky_n + lz_n).$$

In these equations,  $c_a$  and  $c_b$  are the constants required to put the two sets of relative measurements on an absolute scale,  $f_a$  and  $f_b$  are the scattering factors of the two replaceable atoms, which have parameters  $(x, y, z)$  and the summations are taken over all the other atoms in the cell, which are supposed to have the same parameters in the two crystals. Thus, since the value of the summation is the same for the two crystals

$$c_a F'_a(hkl) - 2f_a \cos 2\pi(hx + ky + lz) \\ = c_b F'_b(hkl) - 2f_b \cos 2\pi(hx + ky + lz), \\ \text{or } c_a F'_a(hkl) - c_b F'_b(hkl) - 2(f_a - f_b) \cos 2\pi(hx + ky + lz) = 0. \quad (216.1)$$

The basis of the method is the graphical plotting of a relationship between the two sets of structure amplitudes, and in order to put this in its simplest form, we may rewrite equation 216.1 as

$$c_a \frac{F'_a(hkl)}{\cos 2\pi(hx + ky + lz)} - c_b \frac{F'_b(hkl)}{\cos 2\pi(hx + ky + lz)} - 2(f_a - f_b) = 0, \quad (216.2)$$

in which all the quantities are known except  $c_a$  and  $c_b$ . The quantity  $f_a - f_b$  is not, however, a constant, and although this fact could be allowed for by multiplying each equation by the appropriate factor to make  $f_a - f_b$  constant, this cannot be carried out unless the temperature

factor is known. Hargreaves found it simpler to consider only those reflexions within a small range of Bragg angle, for which the scattering factors can be considered as constant. Since the scattering factors of lighter atoms tend to fall off more rapidly than do those of heavier ones, the difference may tend to be reasonably constant.

Difficulties will be met for those reflexions for which  $\cos 2\pi(hx + ky + lz)$  is small, as then the quantities in equation 216.2 will be large and will not plot accurately; this corresponds, of course, to the fact that the signs of the structure factors cannot be determined from those reflexions for which the replaceable atoms have zero or only small contributions. In Hargreaves' work this difficulty did not arise, because the zinc and magnesium atoms lay in special positions at the origin of the projection (compare section 7.3.3); thus  $f_a - f_b$  was always a maximum—the most favourable case.

Values of the two sets of relative structure amplitudes for reflexions with  $\sin \theta < 0.25$  are given in table 217.

TABLE 217

Values of  $F(h0l)$  for Zn and Mg paratoluene sulphonate

<i>hkl</i>	200	400	600	800	101	301	501	701
$F'_a$	13.1	9.9	14.8	11.5	3.4	20.2	22.4	22.5
$F'_b$	5.3	2.5	12.1	10.5	6.3	9.0	11.1	11.5
<i>hkl</i>	$\bar{1}01$	301	501	701	002	202	402	$\bar{2}02$
$F'_a$	3.3	21.7	22.6	14.1	28.5	8.1	4.7	9.0
$F'_b$	5.9	10.9	12.4	7.1	15.8	8.1	—	9.5

A graph showing the relationship between these values is shown in fig. 218, and it will be seen that most of them lie reasonably well upon a straight line; some of them, however, appear to lie upon another parallel straight line, but this is so only because no account has been taken of the possibility of change of sign, and if five of the values are plotted with negative signs, as shown in fig. 218, all lie quite well upon the same straight line. Thus the signs of all the structure factors of the two crystals were established.

If a change of sign occurred on replacement, as was mentioned earlier in the penicillin work, the corresponding point would lie in the upper left-hand quadrant of fig. 218, and one example of such a point was found when reflexions at higher values of  $\theta$  were examined. Such values, however, are found only rarely, as both reflexions must be weak when the replacement of one atom is sufficient to change the sign. The intercepts of the straight line on the axes of the graph give the values of  $c_a$  and  $c_b$  required to put the measurements on an absolute basis. Thus when  $F'_b = 0$ ,  $F'_a = 5.4$ , and thus  $c_a = 2(f_a - f_b)/5.4$ . The

mean value of  $f_a - f_b$  over the range considered can be derived from tables of scattering factors, and so  $c_a$  can be derived. For zinc paratoluene sulphonate, there are two metal atoms in the true unit cell (as distinct from the unit cell of the projection), and thus if  $f_a - f_b$  is taken as 16, values of structure factors corresponding to the complete unit cell are obtained if  $c_a$  is taken as  $2 \times 16/5.4 = 5.9$ .

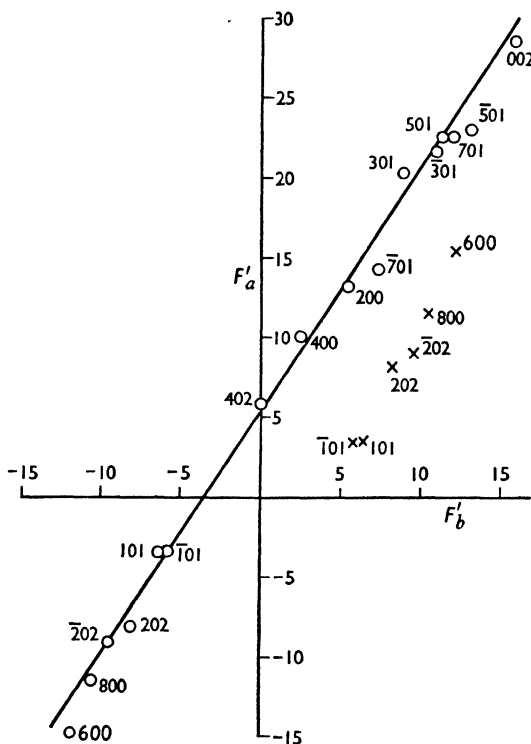


FIG. 218. Graphical relationship between structure amplitudes (on arbitrary scales) of reflexions from Zn and Mg paratoluene sulphonates. The points represented by crosses, when replotted with negative values, lie on the straight line through the other points

By these means, the signs of all the structure factors in the  $h0l$  zone were derived correctly, giving the projection of the structure shown in fig. 219. The methods are similar to those used by Robertson and Woodward (1937*b*) to find the signs of the  $h0l$  structure factors of phthalocyanine; these authors observed the changes that occurred when a nickel atom was placed in the molecule. They made use, however, of absolute values of the structure amplitudes, so that signs



could be allotted almost by inspection. Hargreaves' work is therefore more general.

The isomorphous-replacement method has proved to be extremely fruitful, perhaps its outstanding triumph being the determination of the structure of the strychnine molecule, which had baffled the chemist

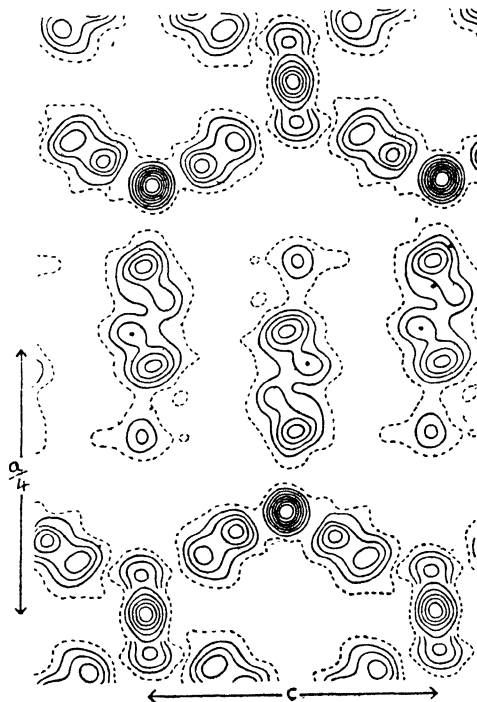


FIG. 219. Zinc paratoluene sulphonate: (010) electron-density projection (Hargreaves, 1946)

for some considerable time. Containing only carbon, nitrogen, oxygen and hydrogen atoms, the molecule itself cannot easily be dealt with by trial-and-error methods, and success was achieved by forming compounds with acid molecules. Bokhoven, Schoone and Bijvoet (1948, 1949, 1951) used compounds with sulphuric and selenic acid, and found a molecular structure in excellent agreement with that finally decided upon by chemical considerations (Robinson and Stephen, 1948).

This work gave rise to another interesting approach. The space group is No. 5,  $C2$ , so that the  $h0l$  reflexions have real structure factors, but all the others are complex. The calculation of the projection of the electron density upon the (010) plane, followed the general lines already described, the sulphur and selenium atoms, since they lie upon

the two-fold axes, being at the origin of the projection. With a molecule as complicated as strychnine, however, the details cannot be firmly established from one projection alone, and other projections had to be considered. For these projections the isomorphous-replacement method does not produce unique values for the phase angles.

This can be seen by drawing a diagram representing the vectors  $F_s$  and  $F_{se}$ , which are structure factors for the sulphate and selenate respectively. Now, since the space group C2 has no absolute origin, a sulphur atom may be taken as defining the origin, and consequently the contribution of the sulphur atoms will be the maximum possible for the real parts of the structure factors, and zero for the imaginary parts. Thus when sulphur is replaced by selenium, the real parts of the structure factors will be increased by an amount  $\Delta f$ —the difference between the scattering factors of selenium and sulphur—and the imaginary parts will be unchanged. These facts are represented in

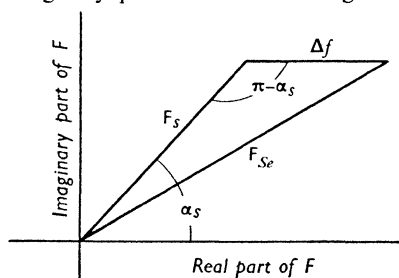


FIG. 220. Derivation of phase angles  $\alpha_s$  for strychnine sulphate

fig. 220, and it will be seen that if  $\alpha_s$  is the phase angle for the sulphate,

$$\cos \alpha_s = \frac{|F_{se}|^2 - |F_s|^2 - (\Delta f)^2}{2|F_s|\Delta f}.$$

Since all the quantities on the right-hand side are known,  $\alpha_s$  can be evaluated, but there is no indication of its sign.

The method of overcoming this difficulty was as follows.

Suppose we perform a summation with terms corresponding to both signs; that is, in addition to the term  $F(hk0) \cos \{2\pi(hx + ky) + \alpha(h, k)\}$  we include another,  $F(hk0) \cos \{2\pi(hx + ky) - \alpha(h, k)\}$ . The summation is then of the form

$$\sum_h \sum_k F(hk0) \cos \alpha(h, k) \cos 2\pi(hx + ky),$$

and, since this corresponds to a summation with real coefficients, the result is centrosymmetrical. Obviously, it corresponds to a superposition of the true structure on to its symmetrically related counterpart, and, as with the investigation of cholesteryl iodide, each atom is represented by a pair of peaks, one of which has to be discarded. The choice was made from knowledge of the projection on (010), and of interatomic distances.

**3.4. Comparison of related structures.** Methods similar to those involving isomorphous replacement can sometimes be applied to substances that are related to each other but which are not isomorphous. No general rules governing the application of these methods can be laid down, and recognition of opportunities of using them depends

to a considerable degree upon the intuition and background knowledge of the investigator; all that can be done at this stage is to provide examples for guidance of those who may wish to explore the possibilities of such methods.

One example is that given by Palin and Powell (1948). The two compounds concerned were molecular compounds of quinol with sulphur dioxide and with methanol. The structure of the former compound had already been determined (Palin and Powell, 1947), and was found to have the space group No. 148,  $R\bar{3}$ , whereas the latter had the space group No. 146,  $R3$ . Nevertheless, strong resemblances were found in the diffraction patterns of the two compounds, and, by assuming that both the  $\text{SO}_2$  molecules and the methanol molecules scatter as single units, signs for the  $hki0$  reflexions could be allotted for the methanol compound from knowledge of those for the  $\text{SO}_2$  compound; in this way a projection of the structure on to the basal plane was derived, and this showed the quinol molecules clearly, but indicated that the methanol molecules were fixed in holes in the structure, with their lengths parallel to the  $c$  axis.

A still more general example occurred in the determination of the structure of penicillin (Crowfoot et al., 1949), as here the comparison of the results for two partially known structures enabled both to be derived. The two structures were those of potassium benzyl penicillin which is orthorhombic, and sodium benzyl penicillin which is monoclinic; the isomorphous replacement of potassium by rubidium (section 5.5.7) had provided some degree of success in the structure determination of the former, and the fly's eye (section 5.5.6) had provided about the same degree of success in the latter: but neither structure could be improved to give the necessary agreement of calculated and observed intensities.

Comparison of projections of the two structures showed, however, that they had a great deal in common (fig. 222). By adopting the common features and rejecting the others, a new type of molecular configuration was found to fit fairly well, and refinement produced the correct structure.

The investigation is perhaps the most general that has so far been conducted. At the beginning little was known of the stereochemistry of the penicillin molecules, although enough was known to provide a start. In the later stages, however, the proposed chemical configurations tended to hinder progress, and the final success was due to the purely physical considerations just described. In the variety of methods used to determine the structure, this investigation stands supreme.

**3.5. Generalized crystal-structure projections.** Sometimes a crystal is found for which all the atoms are well resolved in one projection, making possible the assignment of, say,  $x$  and  $y$  coordinates, but for which there is no other clear projection. The evaluation of the electron

density in three dimensions, or of a projected section, would require the measurement of general ( $hkl$ ) structure factors, followed probably by much arduous calculation. Sometimes it may not be possible to avoid this, but unless very accurate coordinates are required a generalized projection or 'higher-layer-line synthesis' may be used to provide approximate  $z$ -coordinates, without requiring a great deal of experimental measurement or calculation.

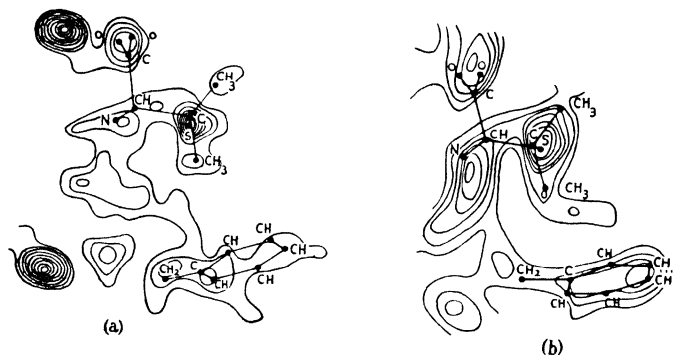


FIG. 222. Rubidium benzylpenicillin and sodium benzylpenicillin; comparison of approximate electron-density projections, showing similar groupings of atoms (Crowfoot et al., 1949)

The principle of the generalized projection may be made clear by considering first of all a crystal whose space group is No. 10,  $P112/m$ . The structure factor  $F(hk0)$  is given by

$$F(hk0) = 4 \sum_{n=1}^{N/4} f_n(hk0) \cos 2\pi(hx_n + ky_n), \quad (222.1)$$

where  $f_n(hk0)$  is the value of  $f_n$  for the reflexion  $hk0$ ; and the electron density projected on (001) is given by

$$\rho(x, y) = \frac{1}{A} \sum_h \sum_k F(hk0) \cos 2\pi(hx + ky). \quad (222.2)$$

The corresponding formula for a structure factor which belongs to the  $L$ th layer, is

$$F(hkL) = 4 \sum_{n=1}^{N/4} [f_n(hkL) \cos 2\pi Lz_n] \cos 2\pi(hx_n + ky_n). \quad (222.3)$$

The contribution of the  $n$ th atom to  $F(hkL)$  is the same as if this were an ( $hk0$ ) structure factor, but the atomic scattering factor had been changed from  $f_n(hk0)$  to  $f_n(hkL) \cos 2\pi Lz_n$ . By analogy with equations 10.3 and 12.3, the function

$$C_L(x, y) = \frac{1}{A} \sum_h \sum_k F(hkL) \cos 2\pi(hx + ky)$$

will contain projected 'atoms' at all the points  $(x_n, y_n)$ , the shape of each atom being such that its scattering factor at the point  $(hk)$  is  $f_n(hkL) \cos 2\pi Lz_n$ . This is a function of  $h$  and  $k$  only; if the real atom is spherically symmetric its 'generalized projection' will have circular symmetry. If the difference between  $f_n(hkL)$  and  $f_n(hk0)$  is small, to a good approximation  $C_L(xy)$  represents a projection of the structure on (001), with the electron density in the  $n$ th atom multiplied by  $\cos 2\pi Lz_n$ , a constant for that atom. In principle then, if the signs of the structure factors of one layer line are known, the value of  $\cos 2\pi Lz$  can readily be found for each atom. The lower the value of  $L$ , the less accurate will be each value of  $z_n$ , but the less will be the ambiguity of position, since there are  $L$  non-equivalent values of  $z_n$  which correspond to a given value of  $\cos 2\pi Lz_n$ . When the zero and  $L$ th layers are widely separated, the approximation  $f(hk0) = f(hkL)$  cannot be made, but the theory can easily be extended to make this assumption unnecessary.

The theory which follows is of general application. Corresponding to the electron density,

$$\rho(x, y, z) = \frac{1}{V} \sum_h \sum_k \sum_l F(hkl) \exp \{-2\pi i(hx + ky + lz)\},$$

we define the generalized projection of this distribution on a plane perpendicular to the  $c$ -axis as

$$\rho_L(x, y) = c \int_0^1 \rho(x, y, z) \exp [2\pi i Lz] dz. \quad (223.1)$$

Substituting for  $\rho(xyz)$  from 12.3 and using the fact that

$$\int_0^1 \exp [2\pi i(L-l)z] dz = 1 \quad \text{when } l=L \\ = 0 \quad \text{when } l \neq L,$$

we find that

$$\rho_L(x, y) = \frac{1}{A} \sum_h \sum_k F(hkL) \exp [-2\pi i(hx + ky)]. \quad (223.2)$$

If we let  $F(hkL) = A(hkL) + iB(hkL)$  as usual, and

$$\rho_L(x, y) = C_L(x, y) + iS_L(x, y), \quad (223.3)$$

we have from 223.2,

$$\left. \begin{aligned} C_L(x, y) &= \frac{1}{A} \sum_h \sum_k \{A(hkL) \cos 2\pi(hx + ky) + B(hkL) \sin 2\pi(hx + ky)\} \\ \text{and} \\ S_L(x, y) &= \frac{1}{A} \sum_h \sum_k \{B(hkL) \cos 2\pi(hx + ky) - A(hkL) \sin 2\pi(hx + ky)\}. \end{aligned} \right\} \quad (223.4)$$

These functions assume simpler forms when the structure possesses symmetry. For example, for space group No. 10,  $P2/m$ ,  $C_L(x, y) = \frac{1}{A} \sum_h \sum_k F(hkL) \cos 2\pi(hx + ky)$  as we have already seen, and  $S_L(xy) = 0$ .

We now make use of the fact that when the structure is composed of spherically-symmetric atoms,

$$F(hkL) = \sum_{n=1}^N f_n(hkL) \exp \{2\pi i(hx_n + ky_n + Lz_n)\}. \quad (224.1)$$

Substituting in equation 223.2 and using equation 223.3 we find

$$\left. \begin{aligned} C_L(x, y) &= \sum_{n=1}^N \sigma_{nL}(x - x_n, y - y_n) \cos 2\pi Lz_n \\ \text{and} \quad S_L(x, y) &= \sum_{n=1}^N \sigma_{nL}(x - x_n, y - y_n) \sin 2\pi Lz_n, \end{aligned} \right\} \quad (224.2)$$

$$\text{where} \quad \sigma_{nL}(x, y) = \frac{1}{A} \sum_h \sum_k f_n(hkL) \exp \{-2\pi i(hx + ky)\}. \quad (224.3)$$

These results express the fact that  $C_L(x, y)$ , for instance, can be built up by multiplying each  $\sigma_{nL}(x, y)$  by a factor  $\cos 2\pi Lz_n$  and centring it at the point  $(x_n, y_n)$ . The function  $\sigma_{nL}(x, y)$  corresponds to the electron distribution of the  $n$ th atom in an ordinary projection. It can readily be evaluated from equation 224.3, in which  $\exp \{-2\pi i(hx + ky)\}$  can be replaced by  $\cos 2\pi(hx + ky)$ , since  $f_n(hkL) = f_n(\bar{h}\bar{k}L)$ . In fact, since  $\sigma_{nL}(x, y)$  is circularly symmetric, it will be sufficient to evaluate

$$\sigma_{nL}(x, 0) = \frac{1}{A} \sum_h \left\{ \sum_k f_n(hkL) \right\} \cdot \cos 2\pi hx.$$

Comparison of the heights of the peaks in  $C_L(x, y)$  or  $S_L(x, y)$  with the corresponding  $\sigma_{nL}(x, y)$  then gives  $\cos 2\pi Lz_n$  or  $\sin 2\pi Lz_n$ .

It is clear that in practice only a very inaccurate value of  $z_n$  can be obtained if  $C_1(x, y)$  is being used, and  $z_n = 0$ , for instance. Nevertheless the generalized projection has been found to be useful in practical crystal-structure analysis, as the following example will show. Crystals of diglycylglycine ethyl ester hydrochloride and the corresponding hydrobromide are isomorphous (Dyer, 1951*b*). The unit-cell dimensions of the two compounds differ very little, and the space group is No. 61, *Pcab*. The projection of the electron density on (100), shown in fig. 225, was obtained by the isomorphous-replacement method (section 7.3.3). In this projection the unit cell is halved in the direction of the  $c$ -axis. Two molecules related by a glide plane at  $y = \frac{1}{4}$ , which appears as a plane of symmetry in projection, overlap in projection. In the diagram one molecule is distinguished by lines representing bonds, but at first, of course, there was no way of telling which atom belonged to which molecule. The projection on (010) does not resolve this ambiguity, and in any case this projection could not be obtained by the isomorphous-replacement method; the replaceable atom has an  $x$ -coordinate of zero and therefore does not contribute to one half of the  $F(h0l)$ 's. The difficulties were overcome by evaluating the function  $C_1(y, z)$ .

Since the structure is centrosymmetric, we have from equation 223.4,

$$C_1(y, z) = \frac{1}{A} \sum_k \sum_l F(1kl) \cos 2\pi(ky + lz). \quad (225.1)$$

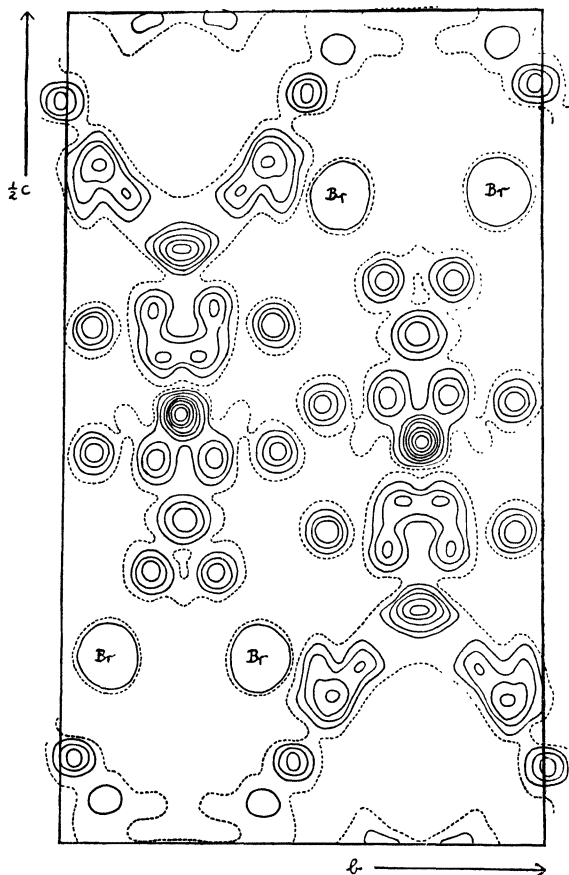


FIG. 225. Projection of electron density in diglycylglycine ethyl-ester hydrobromide on (100)

From the relations between  $F(1kl)$ ,  $F(1\bar{k}l)$ , etc., which are given by Lonsdale (1936) for this space group, we find

$$C(yz) = \frac{4}{A} \left\{ \sum_{k=1}^{\infty} \sum_{l=1}^{\infty} F(1kl) \cos 2\pi ky \cos 2\pi lz \right\} \quad k \text{ odd, } l \text{ odd} \\ - \frac{4}{A} \left\{ \sum_{k=2}^{\infty} \sum_{l=1}^{\infty} F(1kl) \sin 2\pi ky \sin 2\pi lz \right\} \quad k \text{ even, } l \text{ odd} \quad (225.2)$$

Only  $F(1kl)$ 's for which  $l$  is odd are involved, and their signs can be determined by the isomorphous-replacement method.  $C_1(y, z)$  was

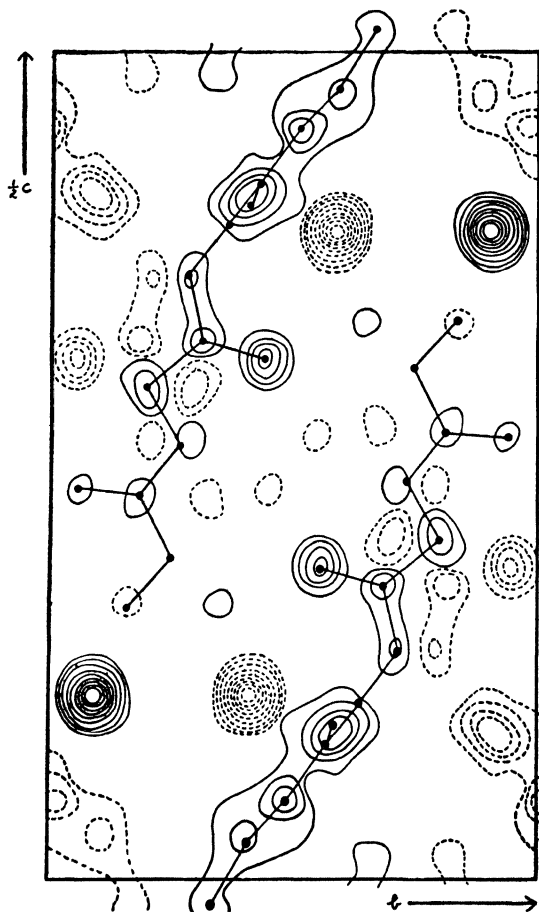


FIG. 226. Generalised projection of diglycylglycine ethyl-ester hydrobromide obtained from the structure factors  $F(1kl)$ . The separate molecules can be easily recognized from this projection although they overlap in Fig. 225

evaluated for the compound diglycylglycine ethyl ester hydrobromide; the result is shown in fig. 226. The plane of symmetry at  $y = \frac{1}{4}$  in fig. 225 is now replaced by a plane of antisymmetry. This follows from the fact that two atoms related by the glide plane at  $y = \frac{1}{4}$  have coordinates  $(xyz)$  and  $(\frac{1}{2} + x, \frac{1}{2} - y, z)$ . The heights of the corresponding peaks in  $C_1(y, z)$  therefore depend on  $\cos 2\pi x$  and  $\cos 2\pi(\frac{1}{2} + x)$ ; that is, they



are equal in magnitude but opposite in sign. A comparison of the heights of the peaks in fig. 225 with those in fig. 226 gave approximate  $x$ -coordinates for all the atoms. Two adjacent atoms  $p$  and  $q$  belonging to the same molecule will not differ greatly in their  $x$ -coordinates, so that  $\cos 2\pi x_p$  and  $\cos 2\pi x_q$  will have the same sign unless  $p$  and  $q$  lie on opposite sides of  $x = \frac{1}{4}$  or  $\frac{3}{4}$ . Adjacent peaks in fig. 226 which are both positive or both negative therefore represent atoms belonging to the same molecule. In this way, it was proved that the atoms of one molecule are as shown in fig. 226. More accurate  $x$ -coordinates were obtained by evaluating the function  $C_3(y, z)$ , and finally the signs of the  $F(h0l)$ 's were calculated from the  $x$ -coordinates obtained in this way; the projection on (010) was then evaluated and refined.

**3.6. Depression of scattering factors.** As in trial-and-error methods (section 5.5.7) use can also be made of the depression of scattering factors when wave-lengths near absorption edges are used. Fourier methods, however, allow a more systematic exploitation of the effect, although, of course, the same difficulties occur in the choice of scatterer and of diffracted radiation.

The general principle in the use of the effect is the same as that of isomorphous replacement, but instead of a comparison of the structure amplitudes from two isomorphous compounds, the comparison of the structure amplitudes from the same compound scattering two different radiations is made. The changes in scattering factor even with the most favourable choice of radiation are relatively small, and therefore success with the method is dependent upon high accuracy of the experimental measurements. Use of the method for determining the signs of structure factors has not yet been reported, but in view of the success obtained with it in trial-and-error methods (section 5.5.7), there would appear to be no reason why it should not be so used.

## 4. FOURIER-TRANSFORM METHODS

**4.1. Use of single transforms.** As explained in section 1.3.3, the process of crystal-structure determination is essentially the fitting of the reciprocal lattice on to the Fourier transform of the contents of the unit cell so that the modulus of the transform at each reciprocal-lattice point is equal to the structure amplitude of the corresponding X-ray reflexion. The calculation of structure factors is, in fact, the calculation of the Fourier transform at the reciprocal-lattice points, and, as shown in section 4.3.8, Fourier transforms can be evaluated in much the same way as structure factors.

In general, however, the use of Fourier transforms in the determination of crystal structures is not straightforward because the dispositions of the atoms in the unit cell are not known in advance; instead we may know only the more limited information of the dispositions of

the atoms with respect to each other in certain groups—chemical molecules for example—in the unit cell. The transform of each group may be evaluated, but the deduction of the relative positions of the groups is a matter of some difficulty and will be dealt with in the next section. In the present section we shall consider only those structures that contain one molecule in the unit cell, and for which, therefore, the Fourier-transform method is particularly suited.

Few crystals contain one molecule in the unit cell, however, and even for such crystals the evaluation of the Fourier transform would still be a rather arduous task; individual sections would have to be computed, and some method would have to be devised to represent the three-dimensional process of fitting the reciprocal lattice on the transform. These difficulties are great, and up to the present the method has been applied only to plane molecules, which have Fourier transforms with constant sections, and of which the section at any angle can be derived from the 'right section' as shown in fig. 228. In

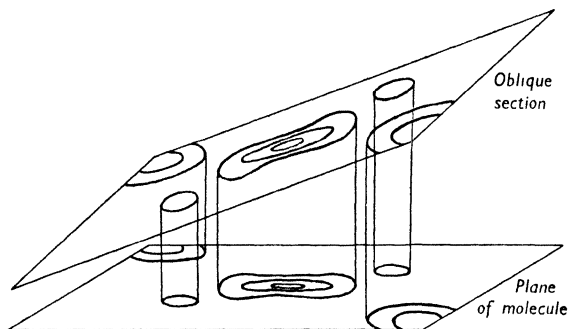


FIG. 228. Representation of three-dimensional transform of plane molecule containing point atoms, showing derivation of oblique section

addition, this process enables use to be made of crystals containing molecules that, because of the existence of glide planes, project as parallel units in the unit cell (section 7.3.2).

Under these conditions the method is easily applied, as shown by Knott (1940) for naphthalene. This molecule consists of two benzene rings sharing a common edge, and the two-dimensional Fourier transform is shown in fig. 229. In the calculation, point atoms are assumed; the true transform would have to be obtained by multiplying each ordinate by the corresponding value of the atomic scattering factor (section 3.2.5), but in the preliminary stages this can be allowed for mentally. The space group (Banerjee, 1930) is No. 14,  $P2_1/a$ , so that the projection of the structure on to the (010) planes shows two molecules similarly oriented and separated by  $a/2$ . Thus the problem is to 'match' the  $h0l$  section of the reciprocal lattice with the calculated Fourier transform. The best fit found by Knott is shown in fig. 229,

and the obliquity of the section that gives this fit is equal to the obliquity of the molecules in the unit cell; since the centres of the molecules are already known to be on centres of symmetry, the complete structure is thus derived.

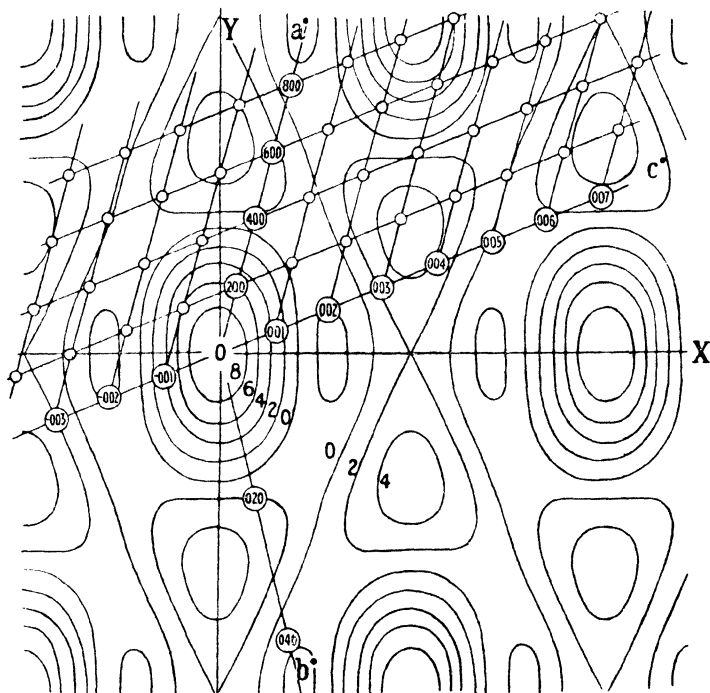


FIG. 229. Relation between the reciprocal lattice of naphthalene and the Fourier transform of the idealized molecule (cf. Fig. 237 (i)) (Knott, 1940)

This method has been applied successfully to the structure of flavan-throne (Stadler, 1953), which has a plane molecule of structure shown in fig. 230. Because the atoms in the idealized molecule all lie upon points of a hexagonal lattice the transform (fig. 230) is periodic, and thus only one unit cell need be calculated (Lipson and Taylor, 1951); this is a useful simplification in dealing with compounds such as flavan-throne and naphthalene. The  $h0l$  reciprocal-lattice section is shown in fig. 231 (i); the large values of the structure amplitudes of the reflexions  $8\ 0\ 7$ ,  $24\ 0\ 2$  and  $16\ 0\ 5$  make the fitting together of the two comparatively easy.

Transforms of molecules that consist mainly of parallel hexagons—such as condensed ring compounds—have one feature in common: the transforms are all based upon that of a single hexagon, which, of

course, has hexagonal symmetry. Thus they all tend to have hexagonal symmetry, and if only the strong peaks of the transform are taken into account, three different orientations of the molecules are possible. These strong peaks must therefore be taken only as a guide, and the three possible orientations tried to see which gives the best agreement with the minor features of the transform. This point will be discussed further in section 7.4.5.

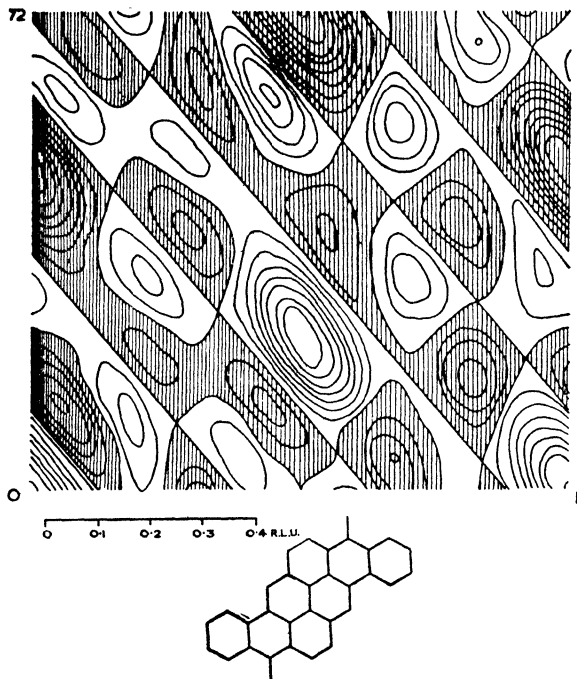


FIG. 230. Flavanthrone,  $C_{28}H_{12}O_3N_2$ : Fourier transform and molecular configuration (Stadler, 1953)

4.2. *Structures involving combinations of transforms.* When the molecules in the unit cell do not have similar projections on to one particular plane, the simple procedure just outlined cannot be carried out. The general problem of combination of transforms will be discussed in the next section, but Klug (1950) has shown that, even when a projection contains four differently oriented projections, the structure can be derived from the transform of a single molecule. The substance he investigated was triphenylene, of which the idealized molecule has the structure shown in fig. 231(ii); it will be seen that the molecule has no centre of symmetry, and moreover the space group is No. 19

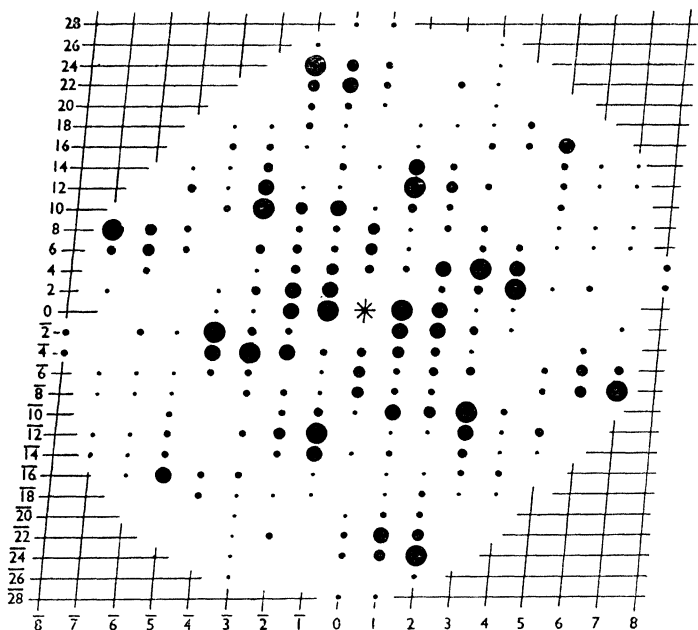


FIG. 231 (i). Weighted reciprocal lattice of flavanthrone (not on same scale as transform) (from data supplied by H. P. Stadler)

$P2_12_12_1$ , so that the crystal also has no centre of symmetry. Nevertheless, centrosymmetrical projections on to the faces of the unit cell occur, and Klug's work was mainly concerned with the projection on the plane (001). The reality of the structure factors  $F(hk0)$  does not, however, greatly simplify the problem; the transform of a single molecule is complex, and the real and imaginary parts have to be calculated separately. For triphenylene, these are shown in fig. 232.

For a non-centrosymmetrical molecule no absolute significance attaches to the real and imaginary parts of the transform; their forms depend upon the choice of origin, and the only absolute result is that obtained by adding the squares of the corresponding amplitudes of the two parts of the transform. It should also be noted that the real and imaginary parts of the transform need have no relationship to the real and imaginary parts of the structure factors, since, in general, the origin chosen for calculating the transform is not that of the unit cell. Thus it will be seen that the problem of

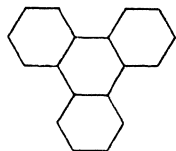


FIG. 231 (ii). Idealized form of molecule of triphenylene

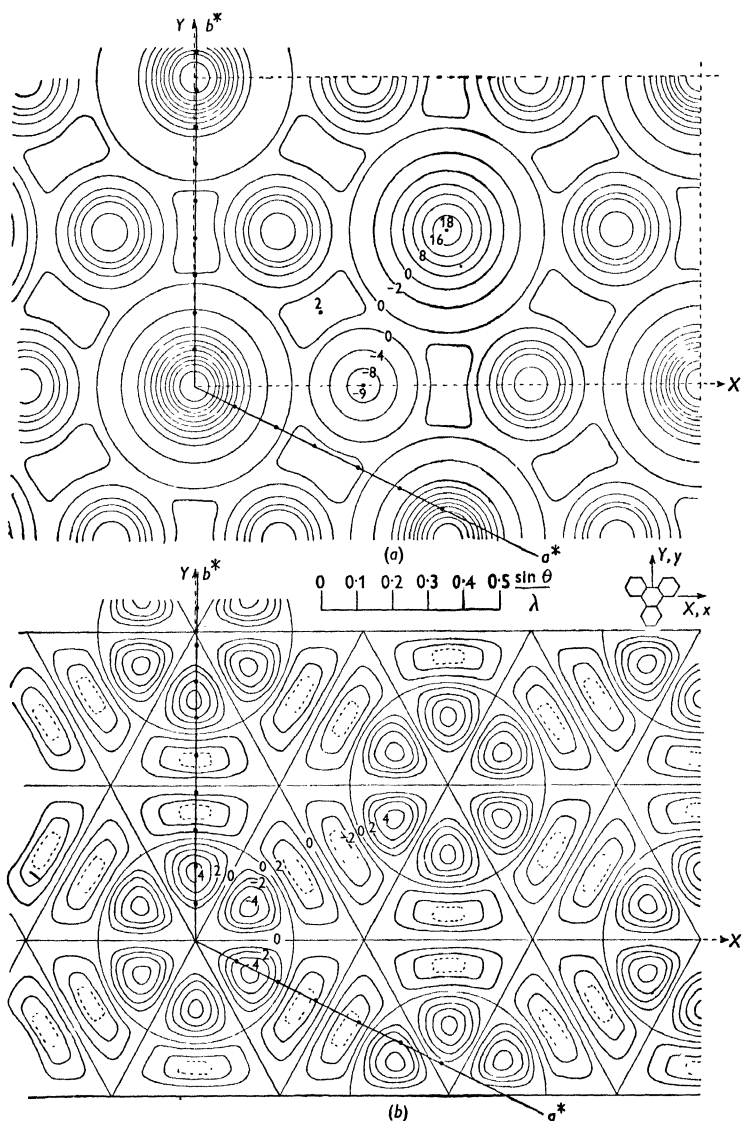


FIG. 232. Real and imaginary parts of Fourier transform of triphenylene molecule. The two straight lines which give the correct relative values of the structure amplitudes of the orders  $h00$  and  $oko$  are shown (Klug, 1950)

deciding the relative positions and orientations of the molecules in triphenylene is rather complicated.

Klug solved the difficulty by reducing the problem partly to one dimension; in the same way as projections on to planes may be much simpler to consider than the three-dimensional structure, so may projections on to lines be simpler still. In the space group  $P2_12_12_1$ , the molecules project, on to each cell edge, in pairs which are centrosymmetrically related and separated by half the length of the edge (accounting for the screw-axis space-group absences). The problem then reduces to finding two radial lines in the complete transform that give agreement for the strong reflexions; a strong reflexion must be associated with a strong part of the Fourier transform, but a weak reflexion may be associated either with a weak part or with the partial cancelling of the strong parts of two or more transforms.

The problem is still not simple, because changes in orientation and in scale—corresponding in tilt of the molecule from the (001) plane—must be considered simultaneously. Some properties of the transform were, however, found to be useful. The real part (fig. 232(a)) is almost circularly symmetrical near the origin, and so need not be considered in fixing possible orientations; the imaginary part provided the conclusive evidence, although some help in finding the correct fit was given by prior knowledge of orientation of the molecule from magnetic data (section 5.3.2). Fig. 232 shows the two lines that Klug found to correspond most clearly with the  $h00$  and  $0k0$  reflexions, and which gave a rough structure which was tested on more general reflexions, and was then refined by standard methods.

**4.3. Combination of Fourier transforms.** The use of special lines only within the transform seems, however, rather wasteful, and methods which make use of the complete transform would be aesthetically more pleasing and would probably lead to more definite results. The principles of the combination of the transforms of the several molecules in the unit cell are mathematically fairly simple and might well be applied to crystal-structure determination, but attempts to use them have so far not been very productive. In this present section, therefore, some of the more useful principles will be stated in order to serve, perhaps, as a basis for the more general application of the Fourier-transform method in the future.

To begin with, the nature of the transform must be appreciated. If the molecule has a centre of symmetry, the computation will be carried out with respect to that centre, and the transform will be everywhere real; but if the molecule has no centre of symmetry, there will in general be no absolute choice of origin, and thus the results obtained will depend upon the particular choice made. The transform will have real and imaginary parts, which must be evaluated separately, and the exact forms of these parts will differ if different origins are

chosen; but the sum of the squares of the moduli at any point will be invariant. These facts may be expressed mathematically as follows. The Fourier transform of a set of points, represented by vectors  $\mathbf{r}_n$  with respect to a chosen origin, is a function given at any point represented by a vector  $\mathbf{S}$  in reciprocal space, by the equation

$$G(\mathbf{S}) = \sum_{n=1}^N f_n \exp 2\pi i \mathbf{r}_n \cdot \mathbf{S}, \quad (234.1)$$

where  $f_n$  is the scattering factor associated with each point. If the vectors  $\mathbf{r}_n$  form a centrosymmetrical set, then

$$\begin{aligned} G(\mathbf{S}) &= \left\{ \sum_{n=1}^{N/2} f_n \exp (2\pi i \mathbf{r}_n \cdot \mathbf{S}) + \sum_{n=\frac{N}{2}+1}^N f_n \exp (-2\pi i \mathbf{r}_n \cdot \mathbf{S}) \right\} \\ &= 2 \sum_{n=1}^{N/2} f_n \cos 2\pi \mathbf{r}_n \cdot \mathbf{S}. \end{aligned} \quad (234.2)$$

For the purposes of computation this is expressed as

$$G(\mathbf{S}) = 2 \sum_{n=1}^{N/2} f_n \cos 2\pi(hx + ky + lz), \quad (234.3)$$

where  $x$ ,  $y$  and  $z$  have the usual meaning (section 1.2.6) with respect to any arbitrary axes, but  $h$ ,  $k$  and  $l$  may assume any values, integral or non-integral. If the vectors  $\mathbf{r}_n$  do not form a centrosymmetrical set, then  $G$  must be resolved into real and imaginary parts, say  $C + iD$ , exactly as for the structure-factor equation (II.1).

The simplest rule for combination of transforms is that which obtains when the transforms are computed with respect to the same origin; the sum of the real parts gives the real part of the complete transform, and the sum of the imaginary parts gives the imaginary part. A particularly important case is that which results when two molecules are related by a centre of symmetry; then the real part of the complete transform is double the real part of each separate transform, and the imaginary parts, being equal and opposite, cancel. This result is difficult to use directly, because the position of the centre of symmetry with respect to each molecule is not known in advance; but the fact that the modulus of the complete transform must never be greater than twice that of the separate transform at the same point may be important: a strong reflexion must always be associated with a large modulus of the Fourier transform, but weak reflexions are not necessarily associated with small moduli.

This rule of combination of two Fourier transforms is sometimes summarized in the statement that the addition of the separate transforms is governed by a 'fringe function' which depends upon the distance apart of the two units, being of smaller wave-length as the distance increases. This 'fringe function' arises as a direct result of the translation of one of the units from the centre of symmetry. Suppose



the translation vector is  $\mathbf{r}$ ; then the transform  $G$  of the set of points becomes

$$\begin{aligned} G_{\mathbf{r}} &= \sum_{n=1}^N f_n \exp 2\pi i(\mathbf{r}_n - \mathbf{r}) \cdot \mathbf{S} \\ &= \sum f_n \exp 2\pi i \mathbf{r}_n \cdot \mathbf{S} \exp \{-2\pi i \mathbf{r} \cdot \mathbf{S}\} \\ &= G_0 \exp \{-2\pi i \mathbf{r} \cdot \mathbf{S}\} \end{aligned} \quad (235.1)$$

where  $G_0$  is the transform of the set of points with respect to the original origin. The function  $\exp 2\pi i \mathbf{r} \cdot \mathbf{S}$  is the fringe function. (One can regard the structure-factor equation as the sum of the transforms of the various atoms, each carrying its own fringe function.) Now, if another centrosymmetrically-related set of points is added at a distance  $-\mathbf{r}$  from the new origin, then

$$G_{-\mathbf{r}} = G_0^* \exp 2\pi i \mathbf{r} \cdot \mathbf{S}, \quad (235.2)$$

where  $G_0^*$  is the complex conjugate of  $G_0$ . Thus the total transform is given by

$$G = G_{\mathbf{r}} + G_{-\mathbf{r}} = G_0 \exp \{2\pi i \mathbf{r} \cdot \mathbf{S}\} + G_0^* \exp \{-2\pi i \mathbf{r} \cdot \mathbf{S}\}. \quad (235.3)$$

The modulus of  $G$  can thus never be greater than  $2|G_0|$ .

A particularly simple result arises when the set of points  $\mathbf{r}_n$  is itself centrosymmetrical;  $G_0$  is then real and is equal to  $G_0^*$ , and thus

$$\begin{aligned} G &= G_0 [\exp \{2\pi i \mathbf{r} \cdot \mathbf{S}\} + \exp \{-2\pi i \mathbf{r} \cdot \mathbf{S}\}] \\ &= 2G_0 \cos 2\pi \mathbf{r} \cdot \mathbf{S}. \end{aligned} \quad (235.4)$$

Thus the fringe function is also real, and results in zeros along equally spaced straight lines in the transform. These lines can be seen, for example, in the transform of the idealized flavanthrone molecule, which can be regarded (fig. 235) as composed of two centrosymmetrical parts.

More complicated results arise when the molecules are related by symmetry elements other than centres of symmetry. If, for example, two molecules are related by a plane of symmetry, their complete transforms will also be related by a plane of symmetry, and, if the computations are made with respect to a point in the plane, the real and imaginary parts separately are also related in this way. The combination is made by superposing the two transforms and adding the moduli vectorially according to a fringe function which may be complex and which gives the phase angle between the two moduli at any point.

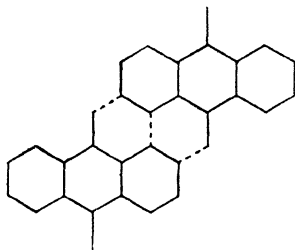


FIG. 235. Molecule of flavanthrone (cf. Fig. 230) considered as composed of two similar and parallel centrosymmetrical parts

This process is more difficult to envisage than the combination of two centrosymmetrically-related transforms, but there is no reason to suppose that it would be too difficult to apply in practice.

Further rules could be stated for symmetry elements involving translations; they are very similar to the rules governing the scattering of atoms at equivalent points in the various space groups. Until some examples can be given, however, it is not possible to cover the bare bones of the theory with the flesh of numerical results. The nearest approach to application is that of Waser and Lu (1944) on the structure of biphenylene, which has six molecules in the unit cell; this would, at first sight, appear to be unusually complicated, since four of the

molecules were in general positions and two in special positions, but, in fact, the analysis was greatly simplified by the discovery that all the reflexions for which  $h$  was not divisible by three were either weak or absent.

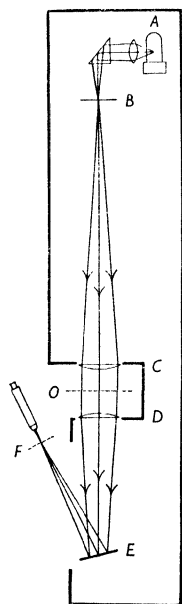


FIG. 236. Diffraction spectroscope.  $A$  is the light source,  $B$  is the pinhole,  $C$  and  $D$  are the lenses, and  $E$  is an optically flat mirror; the diffraction pattern of an object at  $O$  is seen in the plane  $F$  (Taylor, Hinde and Lipson, 1951)

4.4. *Use of optically-derived transforms.* It will be seen that more general use of Fourier transforms in crystal-structure analysis is hindered by a number of difficulties both practical and theoretical. The computations can be arduous, even when, as for plane molecules, only two dimensions are involved; and the theoretical complications of combining transforms might well deter those who are considering the use of the method, in view of the possibility that their calculations will be of no avail. Some rapid method of deriving transforms is therefore desirable, and such a method is provided by the optical apparatus described by Bragg (1939) and developed by Hughes and Taylor (1953), or by that described by Berry (1950).

In these methods only two-dimensional sections can be derived. The projection of the molecule on to any desired plane is represented by a set of holes in a mask (fig. 237(i)a), and the Fraunhofer diffraction pattern is then effectively the Fourier transform desired; the apparatus shown in fig. 236 (Taylor, Hinde and Lipson, 1951) has been used to produce these diffraction patterns required in the determination of the crystal structures of several organic compounds (Hanson, Lipson and Taylor, 1953). As an example the diffraction pattern of the naphthalene molecule is shown in fig. 237(i)b, and this may be compared with the calculated transform shown in fig. 237(iii). It must be



# PLATE VII

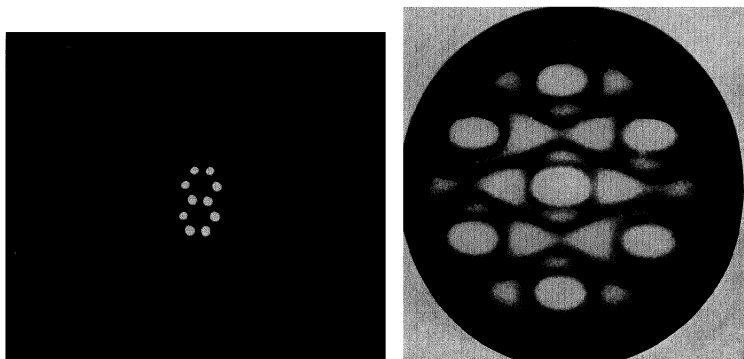


FIG. 237 (i). (a) Mask representing naphthalene molecule. (b) Diffraction pattern of mask (Lipson and Taylor, 1951)

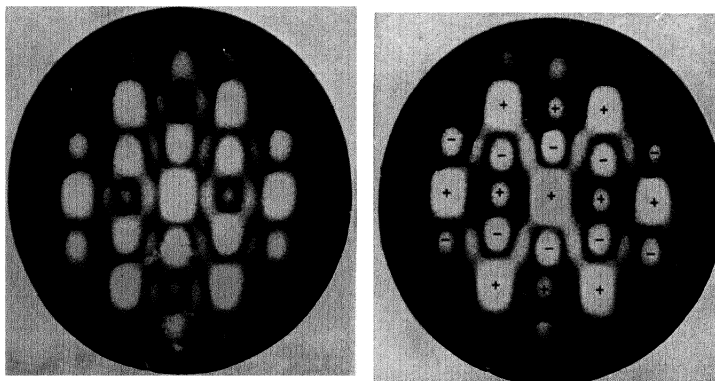


FIG. 237 (ii). Diffraction pattern of (left) mask representing durene molecule, (right) the same mask with an extra hole at the centre. Note the enhancement of the positive regions (Lipson and Taylor, 1951)

noted that the intensity of the light at any point of the diffraction pattern is proportional to the square of the modulus of the transform at the corresponding point, and thus positive and negative regions in fig. 237(iii) are indistinguishable in fig. 237(i)b. In order to make the distinction, an extra hole may be added at the centre of symmetry, and this will enhance the positive regions and depress the negative ones (fig. 237(ii)).

A further difference between the diffraction pattern and the Fourier transform will be noted; the general level of intensity of the former decreases with angle, whereas that of the latter does not. This difference arises because the transform is calculated for point atoms, whereas the holes in the diffracting mask have necessarily to be of finite size, and so the intensity at any point of the diffraction pattern is governed also by the transform of a single hole. This is not a disadvantage; by making the diameters of the holes correspond to about  $0.8 \text{ \AA}$  the variation of scattering factor with angle can be roughly simulated, and this helps in comparing the weighted reciprocal-lattice sections with the diffraction patterns.

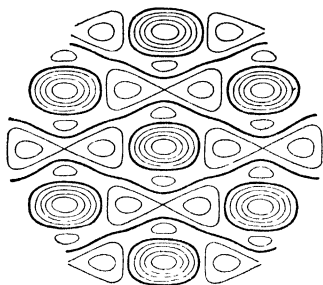


FIG. 237(iii). Calculated Fourier transform, for comparison with fig. 237(i)b (Lipson and Taylor, 1951)

Since the optical method is extremely rapid, it may be used to obtain the diffraction patterns of possible arrangements of the atoms in the unit cell of a structure, and these diffraction patterns can then be superimposed upon the reciprocal lattice directly, to see if any agreement is obtained with the observed intensities. An example of the use of the optical device in this way, to check the projection of the structure of naphthalene on the (100) plane is shown in fig. 74.3. Used in this way, the method is exactly similar to the 'fly's eye' method (section 5.5.6). It has, however, two advantages over the fly's eye: it is more rapid, since the diffraction pattern of the mask can be viewed directly, without the interposition of photographic processes; and if agreement is not obtained, knowledge of the features of the diffraction pattern may suggest ways in which the agreement can be improved.

This use of optical methods is not, however, very elegant, and a procedure for deriving a complete structure from the diffraction pattern of a single molecule would be much more valuable. The problems involved are, of course, exactly the same as those involved in the use of calculated transforms, but the optical method, being quicker, allows more complicated molecules to be dealt with. For example, the structure of phthalocyanine (section 7.3.2) can be derived directly by considering the projection on the (010) plane (Taylor and Lipson, 1951), and since this derivation brings out certain general principles,

it is worth while considering in some detail, as shown in figs. 238 *a-f*,

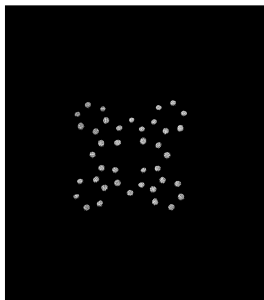
The configuration of the molecule is shown in fig. 238*a*, and the diffraction pattern of the mask corresponding to this is shown in fig. 238*b*. Some general features of this diffraction pattern will be noted: it has necessarily four-fold symmetry, and it has a strong peak at the origin; around the origin is a group of relatively strong peaks surrounded by a region of small intensity; then there is a square-shaped arrangement of stronger peaks, followed by a less pronounced weaker region, and then a partial ring of stronger peaks near the limit of the observed X-ray diffraction pattern.

To determine the orientation of the molecules in the unit cell, it is necessary to compare this diffraction pattern with the  $h0l$  section of the weighted reciprocal lattice; this is shown in fig. 238*c*. Features similar to those just described can be immediately seen, but there are some discrepancies: the strong peaks near the origin are surrounded by a weaker region, but following this is an elliptical arrangement of spots, rather than a square one. This difference can easily be accounted for; a tilt of the molecule with respect to the (010) plane would distort the square, and since the X-ray diffraction pattern is observed only at discrete points, the precise form of the optical diffraction pattern would not be expected to be faithfully reproduced.

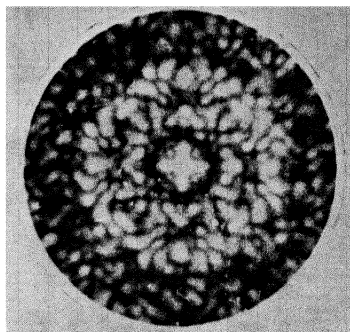
From the ratio of the axes of the elliptical pattern of spots shown in fig. 238*c*, the tilt of the molecule with respect to the (010) plane can be immediately deduced, and on the basis of this it is fairly easy to make the finer detail of the two diffraction patterns agree. A new mask (fig. 238*d*) is made corresponding to the angle of tilt deduced, and fig. 238*f* shows the main features of the optical diffraction pattern (fig. 238*e*) superimposed upon the reciprocal-lattice section in the relative orientation finally adopted. In this way a fairly good approximation to the structure was obtained extremely quickly, whereas the calculation of the Fourier transform would have occupied some considerable time.

**4.5. Recognition of features of molecules.** One of the difficulties in applying the Fourier-transform method is that, since the unit-cell contents occupy about the same volume as the unit cell itself, the 'texture' (the mean distance between lines of zero intensity) of the transform is about the same as the 'mesh' of the reciprocal lattice. This is another way of stating that there is no relation between the signs of successive structure factors, and therefore we cannot detect groups of reflexions that correspond to peaks in the Fourier transform. For small molecules such groups may exist, because the overall size of each molecule—the distance between extreme atomic centres—may be much smaller than the size of the unit cell; thus, for naphthalene, it will be seen from fig. 229 that several reciprocal-lattice points lie in

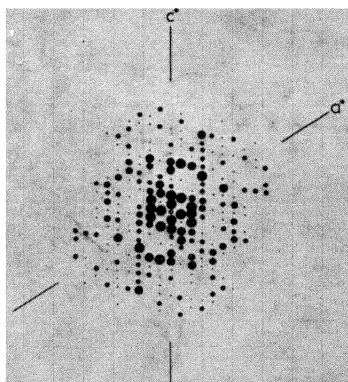
# PLATE VIII



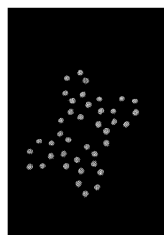
(a)



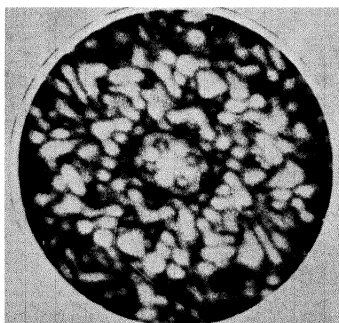
(b)



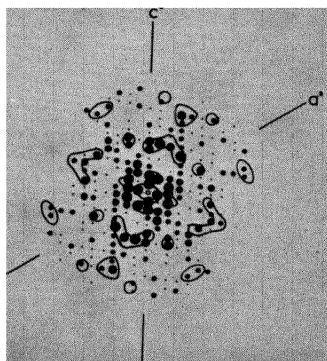
(c)



(d)



(e)



(f)

FIG. 238. (a) Mask representing molecule of phthalocyanine; (b) Diffraction pattern of (a); (c) Weighted *hol* reciprocal-lattice section; (d) Mask representing tilted molecule; (e) Diffraction pattern of (d); (f) As (c) with main features of (e) superimposed (Taylor and Lipson, 1951)





each region of the transform. For the much bigger molecule of phthalocyanine (fig. 238(a)) this is not so.

If a molecule is considered as a combination of separate features, some advantage may be taken of the groupings of reflexions in the reciprocal lattice, since each feature must be smaller than the molecule as a whole. The transform of the whole molecule can be regarded as the vector sum of the transforms of the separate parts, and the mesh of the reciprocal lattice should be finer than the texture of the separate transforms, though not finer than that of the combined transform. On the other hand, the transforms may so combine with each other that there is little trace of each separate one, but there may be enough trace left for the structural feature to be recognized from the weighted reciprocal lattice.

For example, the outlines of the positive regions of the Fourier transform of a hexagonal set of points (Knott, 1940) are shown in fig. 239(i) superimposed on the  $h0l$  section of the reciprocal lattice of coronene (Robertson and White, 1945), and the fineness of the mesh is apparent. Because the molecule consists of parallel hexagons, the weighted reciprocal-lattice section (fig. 239(ii)) shows clearly the hexagonal symmetry of the transform, distorted because of the tilt of the molecule. Since the molecules are located on centres of symmetry

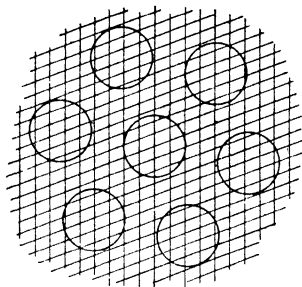


FIG. 239(i). Section  $h0l$  of reciprocal lattice of coronene, with zero contours of transform of benzene hexagon superimposed

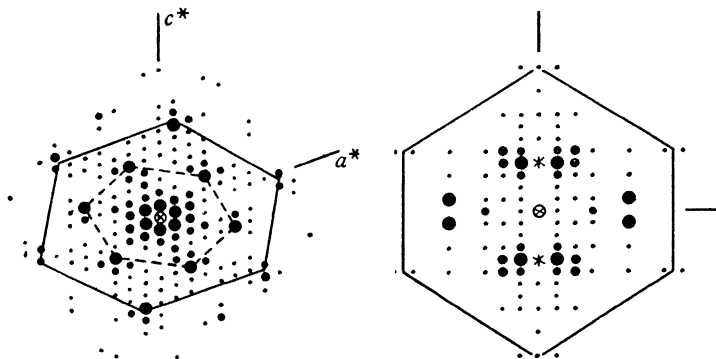


FIG. 239 (ii). Weighted reciprocal-lattice section of coronene, showing distorted hexagonal arrangement of stronger reflexions. The inner arrangement of stronger reflexions (shown by broken lines) is due to the hexagonal symmetry of the molecule (fig. 138). (iii) Weighted reciprocal-lattice section ( $okl$ ) of metatolidine, showing hexagonal arrangement of reflexions at distances of  $0.8 \text{ \AA}^{-1}$  from the origin

these considerations lead directly to the structure, in a much more rapid way than the method described in section 5.5.4.

When the hexagon is only a small part of the molecule, its recognition is not so simple, but in favourable circumstances the method can still be applied. Fig. 239(iii) shows the  $0kl$  section of the reciprocal lattice of metatolidine, the circle indicating the distances of the six outer peaks of the benzene transform. There are six relatively strong

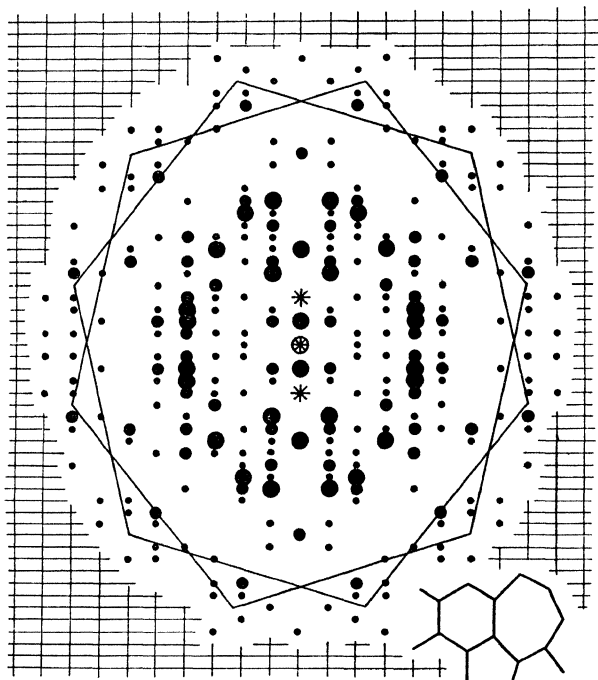


FIG. 240. Representation of weighted reciprocal-lattice section of purpurogallin molecule (inset). The two hexagons join the approximate centres of groups of spots about  $0.8 \text{ \AA}^{-1}$  from the origin; the transformations of these hexagons into real space give the projections of the hexagons in the molecules in their correct orientations

reflexions near to this ring, suggesting that one of the hexagons in the molecule is parallel to the (100) plane; this agrees with the deductions of Fowweather (1952). Considerations of this sort led to the determination of the structure of purpurogallin, of which the  $hk0$  section of the weighted reciprocal lattice is shown in fig. 240 (Taylor, 1952).

There would seem to be a great deal of scope in this approach to crystal-structure determination, once a collection of transforms of frequently occurring structural features has been made, and it may be

that this approach will ultimately prove to be the most fruitful of the Fourier-transform methods.

*4.6. Experimental observation of Fourier transforms.* The previous sections have shown clearly that the major difficulty that stands in the way of a general application of Fourier-transform theory is that the transform is observed only at well-separated points, and that only for very simple molecules can even an approximation to the complete transform be deduced from X-ray data. If it were possible, however, to observe the scattering of X-rays at points other than the reciprocal-lattice points, information about the complete transform might be obtained, and this would give considerable help in the structure determination. Several attempts have been made to explore this possibility, but none has so far led to any great success.

The most detailed work is that of Boyes-Watson and Perutz (1943), Boyes-Watson, Davidson and Perutz (1947), and Bragg, Howells and Perutz (1952), who made use of the variation of the unit cell of crystals of horse methaemoglobin as the degree of hydration was changed; as the unit cell changes, the reciprocal lattice changes also, and each reciprocal-lattice point can be regarded as exploring a finite length of the Fourier transform. Combination of the information provided by all the reciprocal-lattice points might be expected to give considerable information about the complete transform. For technical reasons connected with the changes in the unit cell and the crystal symmetry, it was, at first, thought possible to apply the method only to the 00/ reflexions, and thus only a projection of the electron density on to the *c*-axis could be deduced.

The observed values of  $|F|^2$  for the 00/ reflexions given at three different stages of shrinkage are plotted as ordinates in fig. 242*a*. It will be noted that the three 001 reflexions do not cover an extensive region, but as the angle of reflexion increases, the range covered is greater, so that at higher angles the complete range of angle is covered fairly thoroughly. It can be seen that it is possible to draw a rough envelope to these ordinates, and that this envelope reaches zero at certain points; we may assume that where these zeros occur the curve of *F* itself changes sign (fig. 242*b*), and thus if we assume that the 001 reflexions have positive sign (section 7.3.1) the signs of all the other terms follow. This solution, however, is not unique, since, as we have seen in section 7.3.1, the sign of a first-order reflexion cannot be used to determine the sign of a second order; but by trying out various possible sign combinations suggested by the existence of the zeros in fig. 242*a*, the results shown in fig. 242*b* seemed most promising. Bragg, Howells and Perutz have extended the method to two dimensions.

Until the complete structure is derived, it is difficult to assess the importance or validity of these results, as certain assumptions had to be made in their derivation. Thus it is necessary to assume that the

Fourier transform of the unit cell contents is independent of the degree of hydration, or, in other words, that the water molecules make no significant contribution to the scattering; this would be so if the

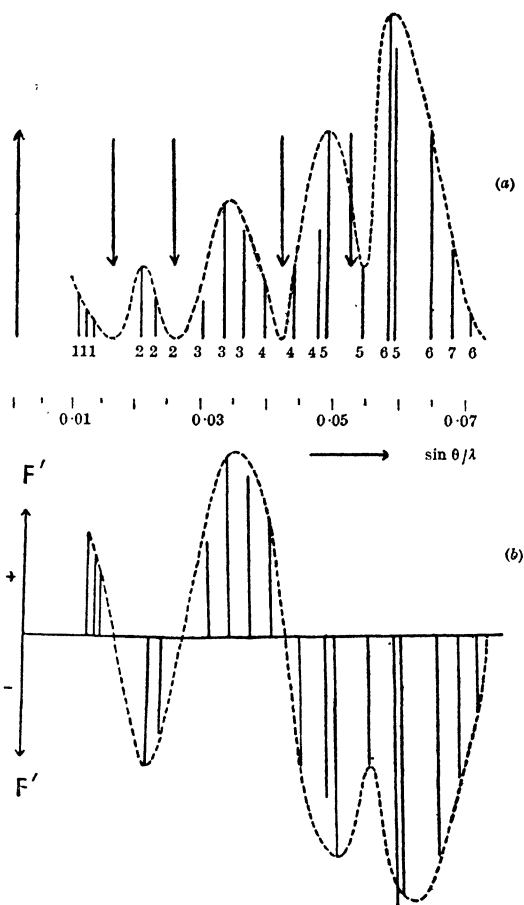


FIG. 242(a). Relative intensities of  $00l$  reflexions from horse methaemoglobin at different shrinkage stages, plotted along  $c$ . (b) Structure factors deduced from (a) (Boyes-Watson and Perutz, 1943)

water formed amorphous layers between the haemoglobin molecules, but the likelihood of this cannot be easily assessed. Since, in addition, there cannot be many crystals whose unit cells can so readily be changed, it would appear that this method of exploring the Fourier transform is not likely to be greatly used.



PLATE IX

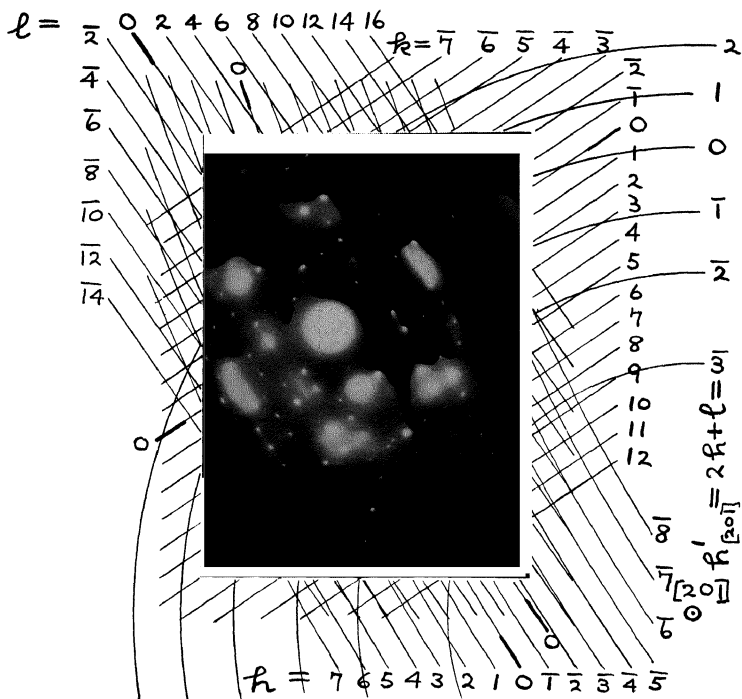


FIG. 243. Electron diffraction pattern of anthracene crystal, showing diffuse background. This diffuse background is complicated because the unit cell contains two molecules in different orientations (Charlesby, Finch and Wilman, 1939)

Booth (1946*d*) has suggested a more general approach, based upon the existence of diffuse reflexions (section 5.3.5) in X-ray diffraction patterns. These diffuse reflexions are evidence of departure from strict regularity in the crystal, and since, as we have seen in Chapter 1, it is this regularity that is responsible for the observation of the Fourier transform only at reciprocal lattice points, we might expect that the diffuse reflexions might allow the observation of the Fourier transform between the reciprocal-lattice points. Booth's specific suggestion is that, if two reflexions are joined by a diffuse streak, then the signs of their structure factors must be the same; such information, although unlikely to lead to complete structure determination, might certainly be of very great help.

Some thought must, however, be given to the underlying theory. For example, no absolute significance attaches to the signs of certain structure factors (section 7.3.1) because they depend upon choice of origin. For example, a choice of origin can always be made in which the reflexions 100 and 200 have opposite signs, whether they are joined by a diffuse streak or not. Stokes (1948) has pointed out that, if the crystal contains non-centrosymmetrical molecules arranged centrosymmetrically, the sign change can occur by a gradual change of relative phase angle from 0 to  $\pi$ , and the amplitude may not pass through zero. (The reciprocal lattice would then be such that it would 'sample' the Fourier transform only at those points where the phase angle was 0 or  $\pi$  exactly.) The method will therefore apply only to centrosymmetrical crystals (or projections) containing molecules (or projections of molecules) which lie upon centres of symmetry. For, although all centrosymmetrical patterns must have a unit which is centrosymmetrical, only if this unit is the molecule itself will it be expected to vibrate as a complete whole.

Even if the method were limited to this case, however, it would still be very useful, and the lack of success reported with it may be due to other reasons. It is unlikely that the molecules would vibrate in such a way that they would always remain parallel to themselves, and thus the observed transform would be formed by the superposition of transforms with slightly different orientations. These small differences might well be enough to mask the zeros upon which the success of the method depends.

The use of electrons instead of X-rays would appear to offer an additional line of attack. Because of the shortness of the exposures required for electron-diffraction photographs, the diffuse background to the reciprocal lattice can be brought out clearly, and, since only small angles of scattering are involved, the representation is undistorted. Charlesby, Finch and Wilman (1939) have shown electron diffraction patterns of anthracene in which the Bragg reflexions are superimposed upon a background which they claim to be the Fourier transform of the unit-cell contents (fig. 243). Although it is not very detailed, the

transform does show the orientation of the molecules in the crystal, and it is therefore possible that electron diffraction photographs of this type could be of considerable value in structure determination.

## 5. SUMMARY

Since so many different ways of using Fourier series are available, a summary of the conditions under which they are likely to be helpful is probably worth while.

First, trial-and-error methods of finding reasonable combinations of signs for centrosymmetrical projections are generally impracticable unless rapid methods of Fourier summation, such as those provided by Pepinsky's machine or by optical methods, are available. Even with such devices, the method is likely to be impracticable unless the structure is simple enough for about ten independent terms to give a recognizable representation.

For more complicated structures, attempts should be made to obtain a crystalline derivative containing a heavy atom; the Patterson method should give the parameters of this atom, and from these parameters the relative phases of most of the reflexions should follow. If the heavy atom is in special, or pseudo-special, positions, the relative phases of certain reflexions may be systematically indeterminate, but even with the omission of these reflexions, the Fourier series may still give considerable help in determining the complete structure.

If two isomorphous compounds can be obtained, still more powerful evidence is available—the change in the structure amplitude of each reflexion on passing from one compound to the other. This information enables signs of reflexions to be determined even when the contribution of the replaceable atom is opposed to that of the remaining atoms in the structure. In this respect the method is more powerful than the heavy-atom method, but it suffers in the same way from the defects that may arise when the replaceable atoms are in special positions. Nevertheless, these two methods have proved to be eminently successful, and have been responsible for most of the triumphs of crystal-structure determination.

The Fourier-transform method provides a completely different approach, and is most useful for crystals that contain atoms of about equal weight. In its complete form the method can be used only if the stereochemistry of the molecule is known, so that the molecular scattering factor can be evaluated. Even then, its application is difficult unless there is only one molecule in the unit cell, but this often is so for projections of monoclinic crystals that possess glide planes. Nevertheless, the method can be used for more complicated projections if the rules for the combination of Fourier transforms are utilized. Perhaps the greatest contribution of the method is that it offers a possibility of detecting the orientation of molecular features directly from



the X-ray data; in this way it is equivalent to the Patterson method, but the structural information is obtained without any calculation.

The labour of calculating Fourier transforms can be avoided by deriving them optically. For complicated molecules optically derived transforms may not be as detailed as calculated ones, but the rapidity of their derivation enables them to be used even when the chance of success is not high. Different orientations and relative dispositions of various parts of a molecule can be tried in rapid sequence, whereas the corresponding calculations would be prohibitive.

It will thus be seen that Fourier methods offer a wide variety of possible ways of determining crystal structures, and have been used successfully for solving many chemical problems.

## CHAPTER 8

### DIRECT METHODS

#### 1. INTRODUCTION

There are two ways in which we might hope to obtain a direct solution of a crystal-structure problem. The first would be to solve the equations

$$F(hkl) = \sum_{n=1}^N f_n \exp [2\pi i(hx_n + ky_n + lz_n)]$$

for the  $x_n$ ,  $y_n$  and  $z_n$ 's, thus avoiding all mention of Fourier series. This is not possible, even in principle, unless both the real and imaginary components of  $F$  are known. In principle, however, the equations

$$|F(hkl)|^2 = \sum_{n,m=1}^N f_n f_m \exp [2\pi i\{h(x_n - x_m) + k(y_n - y_m) + l(z_n - z_m)\}]$$

could be solved for the quantities  $x_n - x_m$ , etc., and from the latter the atomic coordinates could be deduced, as we saw in Chapter 6. Attempts to derive a general procedure for the solution of such equations have been made by Ott (1927) and by Avrami (1938), but have not met with sufficient success to exert any influence on the practice of crystal-structure analysis. Such methods may be classed with the Patterson function as 'direct-space methods'; they represent attempts to transfer into direct space one's knowledge of a distribution in reciprocal space—the values of the  $|F|^2$ 's.

The second class of direct methods may be described as 'reciprocal-space methods'; they depend on the fact that certain items of direct-space information of a completely general kind (for instance, that the electron density is always positive, or that it is a superposition of spherically-symmetric atoms of approximately the same shape) are of themselves sufficient to impose limitations on the reciprocal-space distribution, that is, on the magnitudes *and phases* of the structure factors. In some cases the restrictions are severe enough to determine the signs of all important structure factors, and this constitutes a solution of the crystal-structure problem. The fact that it is a reciprocal-space solution is unimportant, as it can be transferred to direct space by means of a Fourier synthesis. A general discussion of the limitations imposed on the  $F$ 's by the positivity of the electron density was first given by Karle and Hauptmann (1950). However, Harker and Kasper (1948) had already derived certain simple inequality relations between structure factors, which were in fact based on the positivity of the

electron density, although this point was not emphasized at the time. Later work by Goedkoop (1950) showed that the fact that the electron density is a superposition of atoms of approximately the same shape, results in certain equality relations between structure factors. A particular case of such relations had previously been considered by Banerjee (1933). Formally, Goedkoop's result constitutes a complete solution of the fundamental problem of crystal-structure analysis—how to derive the electron density from a knowledge of the moduli of the structure factors only—but so far the relations have been found to be too unwieldy to be of practical use.

Other equality relations between structure factors have been derived by Sayre (1952). They are based on the fact that if all atoms composing an electron distribution are equal, and completely resolved from one another, the operation of squaring the electron density gives a distribution which is still a superposition of equal spherically-symmetric 'atoms', centred on the same points as before. The relations between structure factors which hold when the above conditions are satisfied, as they are approximately in organic compounds, are unwieldy, but have proved to be of practical value. They have also led to the discovery of other less rigorous but more practically useful relations between the signs of structure factors.

## 2. DIRECT DETERMINATION OF ATOMIC COORDINATES

*2.1. The Ott-Avrami method.* The methods of Ott (1927) and of Avrami (1938) are very similar to one another, and we shall outline only the latter. Assuming that all atoms of a crystal structure have the same shape, we may take  $f_n = Z_n \hat{f}$ , as in previous chapters (section 3.2.5). We then have

$$\frac{F(hkl)}{f} = \sum_{n=1}^N Z_n \exp [2\pi i(hx_n + ky_n + lz_n)]. \quad (247.1)$$

It is possible to set up equations, dependent only on the values of  $F/\hat{f}$ , whose roots are the  $x_n$ ,  $y_n$  and  $z_n$ 's. Suppose it is the  $x_n$ 's which we wish to determine. Then, keeping  $k$  and  $l$  fixed, and setting

$$\frac{F(hkl)}{f} = A_h, \quad \exp [2\pi i x_n] = \alpha_n \quad \text{and} \quad Z_n \exp [2\pi i(ky_n + lz_n)] = d_n,$$

we have from (247.1)

$$A_h = \sum_{n=1}^N d_n \alpha_n^h. \quad (247.2)$$

We assume that the  $\alpha_n$ 's are the roots of an  $N$ th degree equation, which we write as

$$a_0 + a_1 \alpha + a_2 \alpha^2 + \dots + a_N \alpha^N = 0. \quad (247.3)$$

That is,  $a_0 + a_1\alpha_n + a_2\alpha_n^2 + \dots + a_N\alpha_n^N = 0$

for all values of  $n$ .

Multiplying throughout by  $d_n\alpha_n^p$ , we obtain

$$a_0d_n\alpha_n^p + a_1d_n\alpha_n^{p+1} + \dots + a_Nd_n\alpha_n^{p+N} = 0. \quad (248.1)$$

We now add together the equations which are obtained for each value of  $n$ , obtaining, with the help of equation 247.2,

$$a_0A_p + a_1A_{p+1} + a_2A_{p+2} + \dots + a_NA_{p+N} = 0.$$

This gives us a set of equations,

$$\begin{aligned} a_0 + a_1\alpha + a_2\alpha^2 + \dots + \alpha_N\alpha^N &= 0, \\ a_0A_p + a_1A_{p+1} + a_2A_{p+2} + \dots + a_NA_{p+N} &= 0, \\ \dots & \\ a_0A_{p+N-1} + a_1A_{p+N} + \dots + a_NA_{p+2N-1} &= 0, \end{aligned}$$

from which it follows that

$$\begin{vmatrix} 1 & \alpha & \alpha^2 & \dots & \alpha^N \\ A_p & A_{p+1} & A_{p+2} & \dots & A_{p+N} \\ \dots & \dots & \dots & \dots & \dots \\ A_{p+N-1} & A_{p+N} & A_{p+N+1} & \dots & A_{p+2N-1} \end{vmatrix} = 0. \quad (248.2)$$

This is an  $N$ th degree equation, whose roots are the  $N$  values of  $\alpha_n$ , but for  $N > 4$  the equation would be so difficult to solve that we need not pause to consider the other difficulties which prevent the practical application of this result to all but the simplest crystal-structure problems.

A similar equation may be derived whose roots are the values of  $\beta_{nm} = \exp [2\pi i(x_n - x_m)]$ , and which involves values of  $|F(hkl)|^2$ . The degree of this equation is  $\frac{1}{2}N(N-1)$ , and the minimum number of structure-factor moduli required is  $N(N-1)+1$ . Avrami applied equation 248.2 to determine the  $x$ - and  $y$ -coordinate parameters of the oxygen atoms in  $\text{KH}_2\text{PO}_4$ . The signs of a sufficient number of  $F$ 's were known from the known positions of the K and P atoms (West, 1930), and the equation led to oxygen parameters in good agreement with those which West obtained by Fourier methods. Avrami's method is of considerable academic interest, but of very limited practical application.

**2.2. The method of steepest descents.** A completely different approach to the problem of determining the atomic coordinates from the X-ray intensities has been suggested by Booth (1947a), who points out that a structure analysis really consists of two stages. In stage one, the arrangement of certain groups of atoms in the structure is often

known, or the structure of the asymmetric unit may even be known, if we are dealing with an organic compound. When this is so, it should be possible to proceed from arbitrary coordinates specifying the position and orientation of the molecule in the unit cell to coordinates which are correct for each atom, within the limits imposed by considering the molecule as a rigid unit of known structure. The second stage consists in the refinement of these coordinates and presents no major difficulties. The maximum number of parameters required to determine the structure is  $3m$ , where  $m$  is the number of atoms in the asymmetric unit. Six parameters, of which three are positional and three angular, are sufficient to determine the crystal structure if the relative coordinates of the atoms in the asymmetric unit are known.

We may introduce a quantity

$$R_2 = \sum (|F_o|^2 - |F_c|^2)^2$$

as a measure of the correctness of the parameters. The method of steepest descents is a method by which these parameters are systematically varied to produce a minimum value of  $R_2$ . We may imagine the value of  $R_2$  plotted in  $N$ -dimensional space, where  $N$  is now the number of parameters to be determined. Booth derived expressions which gave the way in which a point representing the parameters in this space had to be moved to minimize  $R_2$  most rapidly. The direction of movement is the direction of 'steepest descent' of the function  $R_2$ —hence the name. Will the direction of steepest descent lead to the lowest minimum of  $R_2$ , which we assume corresponds to the correct parameters, or merely to some subsidiary minimum? Contrary to Booth's original claim for the method, there can be no doubt that only in favourable circumstances will the lowest minimum be attained. This can be seen by transferring the problem from  $N$ -dimensional space, in which it is difficult to follow what is happening, to the vector space of the Patterson function. The Patterson function of the crystal structure is given by

$$P_o(xyz) = \frac{1}{V} \sum_{hkl} |F_o|^2 \cos 2\pi(hx + ky + lz),$$

while that of any postulated structure which might form a starting-point for the steepest-descent technique is

$$P_c(xyz) = \frac{1}{V} \sum_{hkl} |F_c|^2 \cos 2\pi(hx + ky + lz).$$

It follows that

$$R_2 = \sum_{hkl} (|F_o|^2 - |F_c|^2)^2 = V \int_V (P_o - P_c)^2 dV, \quad (249)$$

where  $\int_V$  denotes an integration over the unit-cell volume. From this result we see that  $R_2$  is a measure of the degree of resemblance

of the Patterson functions of the true and postulated structures. From this line of argument, it may be concluded that unless one begins with parameters which place all atoms within a distance about equal to an atomic diameter from their correct positions in the unit cell, the method of steepest descents cannot lead from arbitrary parameters to the correct ones. No successful application of the method to a complete structure determination has yet been reported, and Booth's success with the  $z$ -coordinates of oxalic acid (Booth, 1947*a*) was no doubt due to some chance resemblance between the random coordinates which he chose as a starting point, and the correct coordinates. The possibility of using the method to 'refine' atomic coordinates will be discussed in Chapter 9.

### 3. INEQUALITY RELATIONS BETWEEN STRUCTURE FACTORS

3.1. *Harker-Kasper inequalities.* The methods discussed in this section, and in section 8.3.4, lead not to the direct determination of atomic coordinates, but indirectly to the latter through direct determination of the phases, or signs, associated with the structure factors. We shall begin by considering the Harker-Kasper inequalities, since they are the simplest and most useful of the relations between structure factors.

The relation

$$\left| \int f g d\tau \right|^2 \leq \left( \int |f|^2 d\tau \right) \left( \int |g|^2 d\tau \right) \quad (250)$$

is known as Schwarz's inequality;  $f$  and  $g$  are *any* functions in a space of which  $d\tau$  is a volume element. We may apply this result to the expression for the structure factor in terms of  $\mathbf{H}$  and  $\mathbf{r}$  as defined in section 6.2.1,

$$F(\mathbf{H}) = \int \rho(\mathbf{r}) \exp [2\pi i \mathbf{H} \cdot \mathbf{r}] dV,$$

taking  $f = \rho^{\frac{1}{2}}$  and  $g = \rho^{\frac{1}{2}} \exp [2\pi i \mathbf{H} \cdot \mathbf{r}]$ .

Note that while  $f^2 = \rho$  by definition,  $|f|^2 = \rho$  only if the latter is always positive. Since this is true of the electron density in crystals,

$$|F(\mathbf{H})|^2 \leq \left\{ \int \rho(\mathbf{r}) dV \right\} \left\{ \int \rho(\mathbf{r}) |\exp [2\pi i \mathbf{H} \cdot \mathbf{r}]|^2 dV \right\}, \text{ from (250).}$$

Since  $|\exp [2\pi i \mathbf{H} \cdot \mathbf{r}]|^2 = 1$ , this reduces to  $|F(\mathbf{H})|^2 \leq \left[ \int \rho(\mathbf{r}) dV \right]^2$ , or

$|F(hkl)|^2 \leq F^2(000)$ , in the usual notation. This may seem an obvious result; if so it is only because X-ray crystallographers are accustomed to dealing with positive distributions. The result does not necessarily hold in neutron diffraction (section 5.5.7), for instance.

When the distribution  $\rho(\mathbf{r})$  possesses symmetry, Schwarz's inequality

can lead to more interesting results. For example, suppose the crystal has a centre of symmetry so that  $\rho(\mathbf{r}) = \rho(-\mathbf{r})$ . Then

$$F(\mathbf{H}) = \int \rho(\mathbf{r}) \cos 2\pi \mathbf{H} \cdot \mathbf{r} dV,$$

and by Schwarz's inequality,

$$F^2(\mathbf{H}) \leq \left[ \int \rho(\mathbf{r}) dV \right] \left[ \int \rho(\mathbf{r}) \cos^2 2\pi \mathbf{H} \cdot \mathbf{r} dV \right]$$

or 
$$F^2(\mathbf{H}) \leq F(0) \left[ \frac{1}{2} \int \rho(\mathbf{r}) (1 + \cos 4\pi \mathbf{H} \cdot \mathbf{r}) dV \right].$$

In the usual notation

$$F^2(hkl) \leq F(000) \left[ \frac{1}{2} F(000) + \frac{1}{2} F(2h, 2k, 2l) \right].$$

With  $u(hkl) = \frac{F(hkl)}{F(000)}$ , this result may be written

$$u^2(hkl) \leq \frac{1}{2} + \frac{1}{2} u(2h, 2k, 2l). \quad (251)$$

This inequality may be of use in finding the signs of certain structure factors. For instance, if  $u^2(hkl) > \frac{1}{2}$ ,  $u(2h, 2k, 2l)$  is positive, or if  $u^2(hkl)$  and  $u^2(2h, 2k, 2l)$  are both greater than 0.25, the same result must hold, and so on. It is not possible to prove  $u(2h, 2k, 2l)$  to be negative, however.

These results depend on the physical fact that the electron density in crystals is never a negative quantity. It is possible to make use of the fact that the density is approximately a superposition of spherically-symmetric atoms to obtain more powerful inequalities. We define the unitary structure factor for point atoms as

$$U(hkl) = \frac{F(hkl)}{\hat{f} F(000)} = \frac{u(hkl)}{\hat{f}}.$$

The quantity  $U$  plays the same role for point atoms as the quantity  $u$  does for actual atoms. In particular, since the  $U$ 's are unitary structure factors of a positive electron density, they must satisfy the Harker-Kasper inequalities, of which 251 is an example. The replacement of  $u$  by  $U$  provides stronger inequalities, indeed strong enough to be used in practice.

A simple derivation of the result 251, with  $U$  replacing  $u$ , can be given for the particular case where all  $N$  atoms of a structure are equal. We then have that

$$U(hkl) = \frac{1}{N} \sum_{n=1}^N \cos 2\pi(hx_n + ky_n + lz_n),$$

or 
$$U(\mathbf{H}) = \frac{1}{N} \sum_{n=1}^N \cos 2\pi \mathbf{H} \cdot \mathbf{r}_n,$$

in the more convenient notation.

Similarly

$$U(2H) = \frac{1}{N} \sum_{n=1}^N \cos 4\pi \mathbf{H} \cdot \mathbf{r}_n = \frac{1}{N} \sum_{n=1}^N (2 \cos^2 2\pi \mathbf{H} \cdot \mathbf{r}_n - 1).$$

Now the square of the sum of  $N$  numbers is never greater than  $N$  times the sum of the squares of these numbers, so that

$$\left( \sum_{n=1}^N \cos 2\pi \mathbf{H} \cdot \mathbf{r}_n \right)^2 \leq N \sum_{n=1}^N \cos^2 2\pi \mathbf{H} \cdot \mathbf{r}_n.$$

It follows that

$$U(2H) + 1 = \frac{2}{N} \sum_{n=1}^N \cos^2 2\pi \mathbf{H} \cdot \mathbf{r}_n \geq \frac{2}{N^2} \left( \sum_{n=1}^N \cos 2\pi \mathbf{H} \cdot \mathbf{r}_n \right)^2,$$

or  $U^2(\mathbf{H}) \leq \frac{1}{2} + \frac{1}{2}U(2H)$ , which is the same as equation 251, if  $u$  is replaced by  $U$ .

If the crystal has a two-fold axis, so that  $\rho(xyz) = \rho(\bar{x}y\bar{z})$ , a method similar to that which led to 251 for a centrosymmetric distribution of electrons, leads to

$$|u(hkl)|^2 \leq \frac{1}{2} + \frac{1}{2}u(2h, 0, 2l), \quad (252.1)$$

while if the crystal has a two-fold screw axis, the corresponding result is

$$|u(hkl)|^2 \leq \frac{1}{2} + \frac{1}{2}(-1)^k u(2h, 0, 2l). \quad (252.2)$$

While 251 and 252.1 can only be used to prove the sign of a particular  $u$  (or  $U$ ) to be positive, 252.2 may prove it either to be positive or negative. However, in all three instances the structure factor whose sign can be determined is one which has all its indices even. One can, however, obtain information about the signs of other structure factors in the following way.

Let

$$U(hkl) = \sum_{j=1}^N n_j \cos 2\pi(hx_j + ky_j + lz_j) = \sum_{j=1}^N n_j \cos \Theta_j, \quad (252.3)$$

where  $n_j = \frac{Z_j}{F(000)}$  is the fraction of the total number of electrons associated with the  $j$ th atom, and  $\Theta = 2\pi(hx + ky + lz)$ . Then

$$U(hkl) + U(h'k'l') = 2 \sum_{j=1}^N n_j \cos \frac{1}{2}(\Theta_j + \Theta'_j) \cos \frac{1}{2}(\Theta_j - \Theta'_j). \quad (252.4)$$

When dealing with the unitary structure factors of point atoms, it is convenient to use Cauchy's inequality, which states that

$$\left| \sum_{j=1}^N a_j b_j \right|^2 \leq \left( \sum_{j=1}^N |a_j|^2 \right) \left( \sum_{j=1}^N |b_j|^2 \right). \quad (252.5)$$



Applying this result to 252.4, with  $a_j = n_j^{\frac{1}{2}} \cos \frac{1}{2}(\Theta_j + \Theta'_j)$  and  $b_j = n_j^{\frac{1}{2}} \cos \frac{1}{2}(\Theta_j - \Theta'_j)$ , we find that

$$|U(hkl) + U(h'k'l')|^2 \leq \{1 + U(h+h', k+k', l+l')\} \{1 + U(h-h', k-k', l-l')\}. \quad (253.1)$$

A similar result holds for the difference of  $U(hkl)$  and  $U(h'k'l')$ , so that we may write 253.1 in the more general form,

$$|U(hkl) \pm U(h'k'l')|^2 \leq \{1 \pm U(h+h', k+k', l+l')\} \{1 \pm U(h-h', k-k', l-l')\}. \quad (253.2)$$

By taking  $a_j = n_j^{\frac{1}{2}}$  in equation 252.4, it may also be shown that

$$|U(hkl) \pm U(h'k'l')|^2 \leq 1 + \frac{1}{2}[U(2h, 2k, 2l) + U(2h', 2k', 2l')] \pm [U(h+h', k+k', l+l') + U(h-h', k-k', l-l')]. \quad (253.3)$$

Formulae 253.2 and 253.3 may often determine the sign of a particular  $U$  when the simpler inequalities give no result, and they may also be used to limit the signs of  $U$ 's for which  $h$ ,  $k$  and  $l$  are not all even.

Further inequalities can be derived when the crystal has more than one symmetry element. As an example, we consider a two-fold axis with a mirror plane normal to it, as in space group No. 10,  $P2/m$ . The simplified structure factor for this space group leads to

$$U(hkl) = 4 \sum_{j=1}^{N/4} n_j \cos 2\pi k y_j \cos 2\pi(hx_j + lz_j). \quad (253.4)$$

Cauchy's inequality can now be applied to this equation in more than one way, depending on the choice of  $a_j$ . The only rule to be observed is that  $a_j$  must be *real*, that is, we may take

$$a_j = n_j^{\frac{1}{2}},$$

$$a_j = n_j^{\frac{1}{2}} \cos 2\pi k y_j,$$

or

$$a_j = n_j^{\frac{1}{2}}(1 \pm \cos 2\pi k y_j)^{\frac{1}{2}},$$

but it is *not* permissible to take

$$a_j = n_j^{\frac{1}{2}}(\cos 2\pi k y_j)^{\frac{1}{2}}.$$

In this way the inequalities set out in table 254 may be derived.

These relations are more powerful than those which depend on the presence of a two-fold axis or a mirror plane separately. It should of course be noted that relations 251, 252.1, 253.2 and 253.3 still apply when the symmetry is  $P2/m$ , since they depend on symmetry elements present in this space group. The number of simple inequality relations increases with the space-group symmetry, those such as the first two of table 254 being particularly valuable in practice because of the small number of structure factors involved.

TABLE 254

Inequalities for space group No. 10,  $P2/m$ 

$$U^2(hkl) \leq \frac{1}{4}\{1 + U(0, 2k, 0) + U(2h, 0, 2l) + U(2h, 2k, 2l)\},$$

$$U^2(hkl) \leq \frac{1}{4}\{1 + U(0, 2k, 0)\}\{1 + U(2h, 0, 2l)\},$$

$$(U(h0l) \pm U(hkl))^2 \leq \frac{1}{2}(1 \pm U(0k0))$$

$$(1 + U(2h, 0, 2l) \pm [U(0k0) + U(2h, k, 2l)])$$

$$U(hkl) \pm U(h'k'l')^2 \leq \frac{1}{2}(1 \pm U(h+h', 0, l+l'))$$

$$(1 + U(0, 2k, 0) \pm [U(h-h', 0, l-l') + U(h-h', 2k, l-l')]),$$

$$(U(hkl) \pm U(h'k'l'))^2 \leq \frac{1}{4}\{2 + U(0, 2k, 0) + U(2h, 0, 2l) + U(2h, 2k, 2l)$$

$$+ U(0, 2k', 0) + U(2h', 0, 2l') + U(2h', 2k', 2l')$$

$$\pm 2[U(h-h', k-k', l-l') + U(h-h', k+k', l-l')$$

$$+ U(h+h', k-k', l+l') + U(h+h', k+k', l+l')\}.$$

The Harker-Kasper method of deriving the inequalities corresponding to any space-group symmetry may be summarized as follows. Write the formula for the structure factor as far as possible as a product involving cosines and sines. Consider this factor as the sum of the products of two quantities  $a_j$  and  $b_j$ , which can be chosen in any way provided that they are entirely real, and apply Cauchy's inequality, expanding the terms on the right-hand side of the inequality so that each represents a structure factor with indices different from the original one. A more elegant method has been given by MacGillavry (1950), but since its use requires a nodding acquaintance with group theory, it may not commend itself to everyone.

By utilizing certain other inequality theorems, Gillis (1948a) was able to derive additional relations between structure factors. For instance, since

$$\sum_{j=1}^N n_j |\cos \theta_j|^2 \geq \sum_{j=1}^N n_j |\cos \theta_j|^3,$$

$$|U(3h, 3k, 3l) + 3U(hkl)| \leq 2\{1 + U(2h, 2k, 2l)\}.$$

While these relations have not proved of great practical value, they may be useful in special circumstances. For more details, the original paper should be consulted.

**3.2. Practical application of Harker-Kasper inequalities.** The first step in applying inequalities is to derive the moduli of the unitary structure factors,  $U(hkl)$ , from the measured X-ray intensities, which will generally be on a relative scale, and involve an unknown temperature factor. Methods of establishing an approximately absolute scale have been described in section 5.5.3, and the  $U$ 's could be obtained from

absolute  $F$ 's derived in this way. It is simpler, however, to avoid the intermediate steps and make use of the fact that

$$\overline{U^2} = \sum_{j=1}^N n_j^2, \quad (255.1)$$

the result corresponding to equation 135. This quantity can be evaluated from the known  $n_j$  values. Then if  $I(hkl)$  represents the measured intensity of a particular reflexion and  $\bar{I}$  the average intensity of reflexions in that range of  $\sin \theta$ ,

$$\frac{U^2(hkl)}{\overline{U^2}} = \frac{I(hkl)}{\bar{I}},$$

and hence,

$$|U(hkl)| = \sqrt{I(hkl)} \left\{ \sum_{j=1}^N n_j^2 / \bar{I} \right\}^{\frac{1}{2}}. \quad (255.2)$$

Harker-Kasper inequalities cannot be used to limit usefully the phases of structure factors which have an imaginary component. Consequently in this section on practical applications, we shall consider only structure factors which are real, that is, which correspond to a centrosymmetric structure or projection of a structure. It is important to note that in such circumstances the signs of at least two structure factors can be chosen arbitrarily (section 7.3.1).

In the practical application of inequalities, as in so many other methods of crystal-structure analysis, there is no set procedure that should be followed. The following two general results are helpful, however:

(i) The indices of a term on the right-hand side of a Harker-Kasper inequality are the differences of the indices of terms appearing on the left-hand side, or of the indices of terms related by symmetry to those appearing on the left-hand side.

(ii) The sign of a term on the right-hand side can only be proved equal to the product of the signs of two terms, the difference of whose indices gives the indices of the term on the right-hand side.

These two results show that in general one should look for terms of large magnitude whose indices are related as in (i) above. The simplest way of doing this, when dealing with structure factors which have one index zero, is to draw out the corresponding reciprocal net, and insert on it at the appropriate points the magnitudes of all unitary-structure factors, marking in some way all for which  $|U|$  is greater than, say, 0.3. We shall assume that the only symmetry element present is a centre, as in Gillis' (1948*b*) application of inequalities to determine the crystal structure of oxalic acid. One looks first of all for structure factors satisfying the relation  $|U(2h, 0, 2l)| > 1 - 2U^2(h0l)$ , as  $U(2h, 0, 2l)$  is then certainly positive. In the example of oxalic acid, the sign of only one term was fixed in this way. One then looks for two unitary-structure factors of large magnitude which are separated by a vector

distance equal to the vector distance from the origin of another of large magnitude. For oxalic acid, the three terms  $|U(309)| = 0.66$ ,  $|U(202)| = 0.57$  and  $|U(1, 0, \bar{1}\bar{1})| = 0.88$  satisfy this condition, and are therefore all three involved in an inequality relation, in this case 253.2. The fourth term involved,  $U(507)$ , is also large ( $\pm 0.76$ ). Now relation (253.2) may be written

$$|U(309) + s(309)s(202)U(202)|^2 \leq \{1 + s(309)s(202)U(1, 0, 11)\} \\ \{1 + s(309)s(202)U(507)\},$$

where  $s(h0l)$  denotes the sign of  $U(h0l)$ . Writing the inequality in this way ensures that both terms of the left-hand side have the same sign, so that the value of the left-hand side is  $|(0.66 + 0.57)|^2 = 1.51$ . The inequality is satisfied only by taking  $(1 + 0.76)(1 + 0.88) = 3.32$  on the right-hand side. Hence  $s(1, 0, \bar{1}\bar{1}) = s(507) = s(309)s(202)$  (cf. theorem (ii) above). This illustrates the fact that inequalities give relations between the signs of structure factors more often than actual sign determinations. By successive applications of relation 253.2, Gillis was able to determine the signs of all but a few of the smaller structure factors in terms of  $s(0, 0, 10)$  and  $s(1, 0, 11)$ . The ambiguity in the signs of these two terms corresponds to four possible choices of origin, as mentioned above, and both may be taken as positive.\* Owing to a misunderstanding of this point, Gillis came to the erroneous conclusion that it is impossible to determine uniquely a crystal structure by application of inequalities, or indeed by any algebraic process.

Inequalities played an important part in the determination of the crystal structure of dekabborane,  $B_{10}H_{14}$ , by Kasper, Lucht and Harker (1950). General  $(hkl)$  structure factors had been measured, so that more extensive use of inequality relations could be made. The problem is unfortunately complicated by the fact that the structure is partially disordered, which causes certain reflexions to be diffuse. In applying inequalities, only the sharp reflexions, which would still be given by a structure having complete disorder of the type encountered, were used. The space group could then be taken as No. 58,  $Pnnm$ , with  $2B_{10}H_{14}$  per unit cell. First of all, the inequalities which depend on the presence of a single symmetry element were used. Of the several elements of symmetry associated with the space group, only the following yielded a definite sign determination:

From  $m$  at  $z = 0$ ,

$$U^2(hkl) \leq \frac{1}{2}\{1 + U(0, 0, 2l)\}, \quad (256.1)$$

and from  $n$  at  $y = \frac{1}{4}$ ,

$$U^2(hkl) \leq \frac{1}{2}\{1 + (-1)^{h+k+l} U(0, 2k, 0)\}. \quad (256.2)$$

\* Usually a structure factor whose indices are all even cannot arbitrarily be given a sign, but in this case the indexing corresponds to a non-primitive unit cell.

Results obtained from inequalities 256.1 and 256.2 are shown in table 257.

TABLE 257

<i>hkl</i>	$1 - 2U^2(hkl)$	$ U(0, 0, 2l) $ or $ U(0, 2k, 0) $	Conclusion
643	0.46	0.52	$s(006) = +1$
544	0.32	0.39	$s(080) = -1$
710	0.20	0.26	$s(020) = +1$
570	0.44		$U(0, 14, 0) > -0.44$
670	0.30		$U(0, 14, 0) < +0.30$

The last two entries of this table, while not establishing a sign, provide an interesting illustration of the limitations which may be placed on a structure factor whose indices lie outside the limiting sphere. Such information often proves to be of value when the term is involved in subsequent inequality relationships.

The next relations used were those which result from the combination of two symmetry elements. For instance, from  $n$  at  $x = \frac{1}{4}$  and  $m$  at  $z = 0$ ,

$$U^2(hkl) \leq \frac{1}{4}\{1 + U(0, 0, 2l)\}\{1 + (-1)^{h+k+l} U(2h, 0, 0)\}.$$

From four such relations, a number of further sign determinations were made. In a few cases one of the  $U$ 's appearing on the right-hand side lay outside the limiting sphere; the value  $\pm 1$  assigned to this unobserved  $U$  was that which made the magnitude of the right-hand side the greater, unless any limitation had been placed on the magnitude of this term by other inequalities.

Once a number of signs had been established in this way, it proved feasible to try the more complicated relations which utilize all the symmetry elements of the space group, although still involving only one  $U(hkl)$  on the left-hand side. At the conclusion of this stage, fifteen sign determinations had been made, all for terms having all indices even. Relation 253.2, which was used so extensively by Gillis, was the next to be applied. It depends on the presence of a single symmetry element, a centre, but two structure factors appear on the left-hand side. This enabled the signs of some fifteen  $U(hk0)$ 's to be determined, after two had been chosen arbitrarily. As the next step, inequalities which can be derived for this space group by adding two  $U$ 's which have one index zero and one in common were tried. For instance, when  $h + k$  is even,

$$|U(hk0) \pm U(h'k0)|^2 \leq \frac{1}{2}\{1 \pm U(h - h', 0, 0)\}\{1 + U(0, 2k, 0) \pm [U(h + h', 2k, 0) + U(h + h', 0, 0)]\}.$$

Finally, since many signs had by now been found, relations as complicated as the last one of table 254 could be used.

In all, the signs of 48  $U(hk0)$ 's, as well as those of a few others, were found from inequality relations. There are only 57 experimentally-observed  $F(hk0)$ 's, so that the 48 of known sign were adequate to give the projection of the structure on (001) with sufficient accuracy for the normal process of Fourier refinement to take over.

**3.3. The practical limitations of Harker-Kasper inequalities.** It is not to be expected that the Harker-Kasper inequalities will be powerful enough to be applied to any structure (Hughes, 1949a). The importance of the magnitudes of the unitary-structure factors for the successful application of inequalities is obvious, and Gillis states the position succinctly: 'The bigger the value of  $|U|$ , the bigger the difference between  $+U$  and  $-U$ , and so the better our prospects of being able to distinguish between the two analytically.' It is therefore of interest to consider how large, on the average, we may expect these quantities to be for crystals of varying complexity. In the following discussion, we shall assume for simplicity that the  $N$  atoms in a unit cell are all equal. We then have  $n_j = 1/N$ , and therefore

$$\overline{U^2} = \sum_{j=1}^N n_j^2 = \frac{1}{N}.$$

If the symmetry number, or number of equivalent points, is  $p$ , and the number of atoms in the asymmetric unit is  $m$ , then  $N = pm$ . (When one or two of the indices of  $U$  are zero, or otherwise systematically restricted, the value of  $\overline{U^2}$  may be greater by an integer than that given above. The reasons for this were outlined in section 2.4.5, but the fact is of minor importance in the present discussion.) It also follows from the reasoning of section 2.4.5 that when  $N$  is fairly large, values of  $U$  (or at least those corresponding to a centrosymmetric structure or structure projection) are distributed approximately according to the Gaussian law. Thus we may expect only about 10% of the  $U$ 's to exceed  $1.7/\sqrt{N}$ , and only one in a thousand to exceed  $3.3/\sqrt{N}$ . These predictions have been verified in a few practical examples (Hughes, 1949a).

We now consider the use of inequalities for sign determination in the light of these results. The simplest Harker-Kasper inequality can be written in the form

$$|U(hkl)|^2 \leq \frac{1}{p} [1 + \phi(U)],$$

where  $p$  is here the symmetry number, and  $\phi(U)$  is a function of  $U$ 's whose indices are related to  $hkl$  in a way that has already been mentioned (in section 8.3.2). We may write this result as

$$p|U(hkl)|^2 - 1 \leq \phi(U).$$

Now we have seen that  $\overline{U^2} = 1/pm$ , so that if  $m$ , the number of atoms in the asymmetric unit, is kept constant, the left-hand side of the

inequality will on the average be the same for all symmetries. The right-hand side is more difficult to discuss. Although the average size of each term varies as  $1/\sqrt{p}$ , the number of terms increases with  $p$ , and Hughes concludes that the average sum of the absolute magnitudes of the terms in  $\phi(U)$  increases with increasing  $p$ . Now in order to establish a sign for a given term on the right-hand side, it is necessary for it to be large enough to controvert the inequality even if all the other terms involved should happen to be of opposite sign; but merely to establish that all signs are not negative, it is only required that the sum of their absolute magnitudes exceed the inequality. We may therefore expect that as  $p$  increases, with  $m$  constant, it becomes easier to establish sign relationships between a number of  $U$ 's, but more difficult to establish an actual sign. Also as  $m$  increases there will be a smaller and smaller fraction of the  $U$ 's which can be given signs by the simple inequalities.

For oxalic acid dihydrate  $m=4$  and for dekabborane  $m=5$ . It seems clear that by the time  $m=9$  is reached, Harker-Kasper inequalities alone can provide very little information, except in unusual circumstances. Nevertheless, even when the  $U$ 's are too small to prove that a particular relation between the signs of certain structure factors is certainly true, their magnitudes may be sufficient to indicate that the relation is *probably* true, as we shall see in a later section. The method of Harker and Kasper is a useful adjunct to the whole body of other methods; it is certainly not destined to replace them, although the possibility of the discovery of some related or unrelated direct method which will do so cannot be ruled out.

**3.4. More general inequalities.** The results which we shall now consider have not yet proved of direct practical value in that they have not been used to solve the structure of any crystal. They are, however, of considerable interest, as they show all the restrictions that are placed on the structure factors by the fact that the electron density is everywhere either zero or positive. This outline of the subject is based on a paper by Karle and Hauptmann (1950). The restrictions placed on the coefficients of a Fourier series which represents a non-negative function were first investigated by Toeplitz (1911), and by Herglotz (1911), and the determinant relations between Fourier coefficients, which are given in this section, have been known to mathematicians as Herglotz's theorem. If we consider, for simplicity, a one-dimensional example, this theorem states that a necessary and sufficient condition

for  $\rho(x) = \frac{1}{a} \sum_{h=-\infty}^{+\infty} F(h) \exp[-2\pi i h x]$  to be non-negative is

$$D = \begin{vmatrix} F(0) & F(-\epsilon_1) & F(-\epsilon_2) & \dots & F(-\epsilon_n) \\ F(\epsilon_1) & F(0) & F(\epsilon_1 - \epsilon_2) & \dots & F(\epsilon_1 - \epsilon_n) \\ \cdot & \cdot & \cdot & \cdot & \cdot \\ F(\epsilon_n) & F(\epsilon_n - \epsilon_1) & F(\epsilon_n - \epsilon_2) & \dots & F(0) \end{vmatrix} \geq 0. \quad (259)$$

The indices  $\epsilon_1$  are different from each other, and from zero, but otherwise can have quite arbitrary positive and negative values. The rank of the determinant is not restricted in any way. For example, we have

$$\begin{vmatrix} F(0) & F(h) \\ F(\bar{h}) & F(0) \end{vmatrix} \geq 0 \text{ and } \begin{vmatrix} F(0) & F(\bar{5}) & F(2) \\ F(5) & F(0) & F(7) \\ F(\bar{2}) & F(\bar{7}) & F(0) \end{vmatrix} \geq 0, \text{ etc.}$$

By expanding the determinant  $D$ , and making use of the fact that certain other determinants of the expansion are also non-negative, Karle and Hauptman arrive at the result

$$\left| F(\epsilon_n) - \frac{\Delta'}{\Delta} \right| \leq \frac{\Delta_1^{\frac{1}{2}} \Delta_2^{\frac{1}{2}}}{\Delta}, \quad (260)$$

where  $\Delta$ ,  $\Delta'$ ,  $\Delta_1$  and  $\Delta_2$  are determinants of rank lower than the determinant  $D$ ;  $\Delta_1$  for instance is obtained from  $D$  by omission from the latter of the last row and last column. To express 260 in words, the coefficient  $F(\epsilon_n)$  lies within a circle in the complex plane whose centre is at  $\delta = \frac{\Delta'}{\Delta}$ , and whose radius is  $r = \frac{\Delta_1^{\frac{1}{2}} \Delta_2^{\frac{1}{2}}}{\Delta}$  (fig. 260). The vector  $F = A + iB$

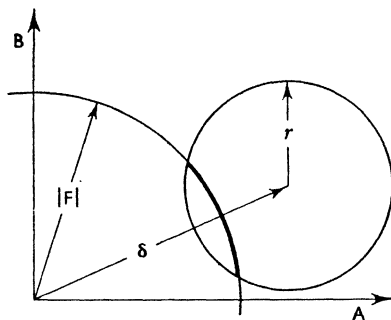


FIG. 260

representing  $F(\epsilon_n)$  in magnitude and phase must end somewhere in the circle. If the value of  $|F|$  is known, the phase angle is further limited, as  $F$  must then end somewhere on the heavy line. Generally speaking, the greater the rank of the determinant  $D$  (that is, the more structure factors known in magnitude and phase) the more closely will the magnitude and phase of an additional one be limited.

Inequalities of increasing complexity can be obtained from 259 and 260. As examples we give the first three:

(i)  $n=0$ . Then  $F(0) \geq 0$ , from 259.

(ii)  $n=1$ . Put  $\epsilon_1 = h$ , then  $\begin{vmatrix} F(0) & F(h) \\ F(h) & F(0) \end{vmatrix} \geq 0$ , or  $|F(h)| \leq F(0)$ .



We saw previously that this result could be derived from Schwarz's inequality.

(iii)  $n=2$ . Put  $\epsilon_1=h_1$ ,  $\epsilon_2=h_1+h_2$ . Then

$$\begin{vmatrix} F(0) & F(\bar{h}_1) & F(\bar{h}_1+\bar{h}_2) \\ F(h_1) & F(0) & F(\bar{h}_2) \\ F(h_1+h_2) & F(h_2) & F(0) \end{vmatrix} \geq 0 \text{ from 259.}$$

$$\text{or } \left| F(h_1+h_2) - \frac{F(h_1)F(h_2)}{F(0)} \right| \leq \frac{\left| \begin{vmatrix} F(0) & F(\bar{h}_1) \\ F(h_1) & F(0) \end{vmatrix} \right|^{\frac{1}{2}} \times \left| \begin{vmatrix} F(0) & F(\bar{h}_2) \\ F(h_2) & F(0) \end{vmatrix} \right|^{\frac{1}{2}}}{F(0)} \quad (261)$$

Symmetry considerations were not used to derive any of these general inequalities. If the origin is a centre of symmetry,  $F(h)=F(\bar{h})$ , and 261 becomes, for the special case,  $h=h_1=h_2$ .

$$\left| F(2h) - \frac{F^2(h)}{F(0)} \right| \leq \frac{F^2(0) - F^2(h)}{F(0)},$$

which requires

$$\left\{ \frac{F(h)}{F(0)} \right\}^2 \leq \frac{1}{2} + \frac{\frac{1}{2}F(2h)}{F(0)}.$$

This will be recognized as the first of the Harker-Kasper inequalities, applicable to a one-dimensional distribution. Extension of the general inequalities to a three-dimensional distribution presents no difficulties. The Harker-Kasper inequalities are special cases of these more general inequalities, and can be derived from them, but in practice the derivation is usually more troublesome than the derivation by means of Cauchy's inequality.

#### 4. EQUALITY RELATIONS BETWEEN STRUCTURE FACTORS

4.1. *Banerjee's equation, and its generalization.* Banerjee (1933) has shown that it is possible to extend the methods of Ott and Avrami (section 8.2.1) by developing equations which lead to relations between the structure factors alone, and not between structure factors and atomic coordinates.

The unitary structure factor for point atoms is given by

$$U(hkl) = \sum_{j=1}^N n_j \exp [2\pi i(hx_j + ky_j + lz_j)].$$

When all atoms are equal, this reduces to

$$N.U(hkl) = \sum_{j=1}^N \exp [2\pi i(hx_j + ky_j + lz_j)];$$

and hence

$$N.U(h00) = \sum_{j=1}^N \exp [2\pi i h x_j] = \sum_{j=1}^N \alpha_j^h.$$

For  $N.U(h00)$  we write  $U'(h)$ .

In discussing Avrami's method we saw that the  $\alpha$ 's must be the roots of an  $N$ th degree equation, which we now write in the form

$$\alpha^N + a_1\alpha^{N-1} + a_2\alpha^{N-2} + \dots + a_N = 0. \quad (262.1)$$

This equation may be regarded as an expansion of the equation

$$(\alpha - \alpha_1)(\alpha - \alpha_2)(\dots)(\alpha - \alpha_N) = 0, \quad (262.2)$$

which obviously has as its roots  $\alpha = \alpha_1$ ,  $\alpha = \alpha_2$ , etc. Comparing 262.1 and 262.2 we see that, for example,

$$-a_1 = \alpha_1 + \alpha_2 + \dots + \alpha_N = U'(1).$$

In fact, a series of relations of this kind exists. They are (Turnbull, 1944)

$$\left. \begin{aligned} U'(1) + a_1, &= 0 \\ U'(2) + a_1U'(1) + 2a_2, &= 0 \\ U'(N) + a_1U'(N-1) + \dots + a_{N-1}U'(1) + Na_N, &= 0 \end{aligned} \right\} \quad (262.3)$$

When the crystal has a centre of symmetry,  $x_j = -x_{N-j+1}$ . It follows that  $\alpha_j\alpha_{N-j+1} = 1$ . This result simplifies the equations. For example,  $a_N = \alpha_1\alpha_2 \dots \alpha_N = 1$ , since the products of all  $\alpha$ 's taken in pairs is unity. Similarly  $a_{N-1} = a_1$ , and in general  $a_{N-j} = a_j$ .

Now it follows from the equation 262.3 that

$$\begin{vmatrix} U'(1) & 1 & 0 & \dots & 0 \\ U'(2) & U'(1) & 2 & \dots & 0 \\ \cdot & \cdot & \cdot & \cdot & \cdot \\ U'(N) & U'(N-1) & U'(N-2) & \dots & N \end{vmatrix} = 0. \quad (262.4)$$

The rank of this determinant can be reduced from  $N+1$  to  $\frac{1}{2}N+1$  by making use of the result  $a_{N-j} = a_j$ , if the structure is centrosymmetric.

Banerjee (1933) tried out the method on the crystal structure of anthracene, using measurements of the  $(00l)$  structure factors made by Robertson (1933a).

TABLE 262

$l$	0	1	2	3	4	5	6	7	8	9	10
$U'(l)$	14	2.8	2.5	2.6	4.2	4.0	0	0	0	3.0	0

The structure is centrosymmetric with  $N=14$ , so the rank of the determinant is 8. On expansion of the determinant the following equation is obtained:

$$15 \cdot 5s_2s_4 - 11 \cdot 5s_1s_3s_4 - 11 \cdot 3s_1s_2s_5 + 5 \cdot 7s_2 - 3 \cdot 8s_2s_3 + 2 \cdot 8s_1s_5 + 2 \cdot 8s_3s_5 + 2 \cdot 5s_4 - 0 \cdot 5 - 0 \cdot 1s_1s_3 = 0. \quad (262.5)$$

In this equation the terms are introduced in decreasing order of magnitude, and  $s_l$  represents the sign of  $U'(l)$ . The sign of any one of the terms of odd index can be chosen arbitrarily. This leaves four signs

to determine, for which only sixteen combinations exist. By trial, Banerjee found three sets of signs which satisfied equation 262.5 closely. By testing them in another determinantal equation involving  $U'(9)$ , all but one were eliminated. Nevertheless, several other combinations of signs give fair agreement, and the method is obviously very dependent both upon the accuracy of measurement of the structure factors and knowledge of atomic scattering factors.

More general equality relations between structure factors can be obtained in similar fashion. We take

$$U(hkl) = \sum_{j=1}^N n_j \alpha_j^h \beta_j^k \gamma_j^l, \text{ where } \alpha_j^h = \exp [2\pi i h x_j], \text{ etc.}$$

As before, it follows that

$$\alpha_j^N + a_1 \alpha_j^{N-1} + \dots + a_N = 0 \text{ for } j=1, 2, \dots, N.$$

This may be written more concisely as

$$\sum_{a=0}^N a_{N-q} \alpha_j^q = 0.$$

We multiply each such relation by a factor  $n_j \alpha_j^h \beta_j^k \gamma_j^l$ , obtaining

$$\sum_{a=0}^N a_{N-q} n_j \alpha_j^{h+a} \beta_j^k \gamma_j^l = 0.$$

After summing over all values of  $j$  and writing the result in full we have

$$U(h+N, k, l) + a_1 U(h+N-1, k, l) + \dots + a_{N-1} U(h+1, k, l) + a_N U(hkl) = 0. \quad (263.1)$$

A similar equation was given by Banerjee (1933). Hughes (1949*b*) pointed out that equation 263.1 was still true when the atoms were not all equal. If one projection of a crystal structure has been dealt with satisfactorily, so that values of  $x_j$ , say, are known, the values of the  $a$ 's can then be calculated. Equation 263.1 then provides a check on the assignment of signs to other terms. Hughes (1949*b*) has shown that this result can sometimes be of practical value.

Similar equalities between structure factors can be obtained for any choice of  $(hkl)$ , and many forms of equation 263.1 can be obtained which involve different U's, but the same set of numbers  $a_{N-q}$ . If we now take any  $N+1$  of them, we have

$$\begin{aligned} &U(h_1+N, k_1, l_1) + a_1 U(h_1+N-1, k_1, l_1) + \dots + a_N U(h_1 k_1 l_1) = 0, \\ &U(h_2+N, k_2, l_2) + a_1 U(h_2+N-1, k_2, l_2) + \dots + a_N U(h_2 k_2 l_2) = 0 \end{aligned} \quad (263.2)$$

$$\begin{aligned} & \dots\dots\dots \\ & U(h_{N+1} + N, k_{N+1}, l_{N+1}) + a_1 U(h_{N+1} + N - 1, k_{N+1}, l_{N+1}) + \dots \\ & \qquad\qquad\qquad + a_N U(h_{N+1}, k_{N+1}, l_{N+1}) = 0 \end{aligned}$$

from which it is clear that the determinant formed by the  $U$ 's must vanish. The elements of each row of this determinant are  $N+1$  unitary structure factors along a reciprocal-lattice line in the  $[100]$  direction. Determinants corresponding to any other direction can be derived in the same way.

The above results may be stated concisely as follows: Let  $[U]$  be the  $(n+1) \times (n+1)$  dimensional matrix, of which the element in row  $p$ , column  $q$ , is  $U(\mathbf{H}_p - \mathbf{K}_q)$ . The symbol  $\mathbf{H}_p$  ( $p=0, 1, \dots, n$ ) represents *any* set of reciprocal-lattice vectors, and  $\mathbf{K}_q = q\mathbf{K}$  ( $q=0, 1, \dots, n$ ,  $\mathbf{K} \neq 0$ ). Then if  $n=N$ , the number of atoms in the unit cell, the determinant of  $[U]$  is zero.

In the determinant derived from equation 263.2, for example,

$$\mathbf{H}_p = h_p + N, k_p, l_p, \text{ while } \mathbf{K} = 1, 0, 0.$$

There is a certain lack of symmetry in the choice of the sets  $\mathbf{H}_p$  and  $\mathbf{K}_q$ , one being arbitrary and the other restricted to one reciprocal-lattice row. By a straightforward generalization of the procedure outlined above, Goedkoop (1952) showed that the determinant is zero for *any* choice of the sets  $\mathbf{H}_p$  and  $\mathbf{K}_q$ , provided only that the number of terms  $n+1$  in each set exceeds  $N+1$ . In the special case where  $\mathbf{H}_p = \mathbf{K}_p$  for every value of  $p$ , we have:

$$\text{element in row } p, \text{ column } q = U(\mathbf{H}_p - \mathbf{H}_q),$$

while

$$\text{element in row } q, \text{ column } p = U(\mathbf{H}_q - \mathbf{H}_p).$$

Now  $U(\mathbf{H}_p - \mathbf{H}_q)$  is the complex conjugate of  $U(\mathbf{H}_q - \mathbf{H}_p)$ , and when elements of a matrix are related in this way, the matrix is said to be *hermitian*. For such a matrix, it can be shown that the corresponding determinant has a positive value for  $n < N$ . This is in fact the Karle-Hauptmann result (equation 259).

Therefore all the restrictions placed on the structure factors of a structure which is composed of atoms all of the same shape can be summed up as follows: if  $\mathbf{H}_p$  and  $\mathbf{K}_q$  are any two sets of  $n+1$  different reciprocal-lattice vectors, the matrix  $[U]$  with elements  $U(\mathbf{H}_p - \mathbf{K}_q)$  has the properties

$$\det. [U] = 0 \text{ if } n \geq N$$

and

$$\det. [U] \geq 0 \text{ if } \mathbf{H}_p = \mathbf{K}_p \text{ for every } p, \text{ with no}$$

restriction on the value of  $n$ .

The possibility of making any practical application of these general determinantal equalities appears to be very slight. The smaller the number of independent terms in a determinant, the fewer the number of sign permutations that would have to be tried. In general the number of different structure factors will be  $(N+1)^2$ , the number of elements in the matrix  $[U]$ . A reduction may be made by proper choice of the sets  $\mathbf{H}_p$  and  $\mathbf{K}_q$ ; for instance, if the two are identical,

making  $[U]$  hermitian, all the diagonal elements are  $U(0)=1$ , and there are not more than  $\frac{1}{2}N(N+1)$  different structure factors. It is for this type of matrix that the inequalities hold. Again, if for the set  $H_p$  we take a row of  $N+1$  points,  $H_p=H_0+pH$ , and for  $K_q$  a similar row through the origin  $K_q=qH$ , then  $H_p-K_q=H_0+(p-q)H$ . All structure factors lie on one reciprocal-lattice row, and only  $2N+1$  are different. If  $H_0=0$  we obtain a further reduction to  $N$ . This occurred in Banerjee's application of equality relations, and we now see it to be the simplest one, as no further reduction in the number of independent structure factors can be made.

If the assumption of similar shape for all atoms (i.e.  $f_j=Z_j\hat{f}$ ) held rigorously, and the magnitudes of the structure factors were known with high accuracy, it would be sufficient to permute the signs in a single equality relation to determine the correct combination. In practice it appears unlikely that it will be possible to use the determinantal equalities to solve a crystal structure when the asymmetric unit contains more than three or four atoms, or unless there are other simplifying circumstances, as in the case of anthracene. For structures of this complexity there are many other methods which could be applied more easily. Perhaps the greatest importance of Goedkoop's results is that they show that the most stringent conditions imposed on the structure factors, by the mere fact that the structure is composed of atoms, are too complicated to be used, at least at the present time.

**4.2. Sayre's equation.** A special equality relation between structure factors exists when the structure is composed of identical atoms which are fully resolved from one another. When a function is periodic, its square is periodic, with the same unit cell, but has of course a different set of Fourier coefficients. The latter may however be derived from the coefficients of the original distribution. Corresponding to the result,

$$\rho(\mathbf{r}) = \frac{1}{V} \sum_{\mathbf{H}} F(\mathbf{H}) \exp [-2\pi i \mathbf{r} \cdot \mathbf{H}], \quad (265.1)$$

we may put

$$\rho^2(\mathbf{r}) = \frac{1}{V} \sum_{\mathbf{H}} G(\mathbf{H}) \exp [-2\pi i \mathbf{r} \cdot \mathbf{H}], \quad (265.2)$$

where the coefficients  $G(\mathbf{H})$  are at present unknown.

Now from equation 265.1,

$$\rho^2(\mathbf{r}) = \frac{1}{V^2} \sum_{\mathbf{H}'} \sum_{\mathbf{H}''} F(\mathbf{H}') F(\mathbf{H}'') \exp [-2\pi i \mathbf{r} \cdot (\mathbf{H}' + \mathbf{H}'')].$$

If all terms for which  $\mathbf{H}' + \mathbf{H}'' = \mathbf{H}$  are collected together, this becomes

$$\rho^2(\mathbf{r}) = \frac{1}{V^2} \sum_{\mathbf{H}} \left\{ \sum_{\mathbf{H}'} F(\mathbf{H}') F(\mathbf{H} - \mathbf{H}') \exp [-2\pi i \mathbf{r} \cdot \mathbf{H}] \right\}.$$

Comparison with equation 265.2 shows that

$$G(\mathbf{H}) = \frac{1}{V} \sum_{\mathbf{H}'} F(\mathbf{H}') F(\mathbf{H} - \mathbf{H}'). \quad (266.1)$$

This is a perfectly general equation, relating the Fourier coefficients of the square of a periodic function to those of the function itself. It may also be obtained directly from certain results in the theory of Fourier transforms which connect the operation of squaring in direct space with self-convolution in reciprocal space.

If we can now establish a relation between  $\rho(\mathbf{r})$  and  $\rho^2(\mathbf{r})$  in some other way, equation 266.1 may lead to a relation between structure factors. Consider a projection for which  $\rho(\mathbf{r})$  is composed of equal spherically-symmetric atoms which do not overlap one another. Then  $\rho^2(\mathbf{r})$  will also be composed of equal spherically-symmetric 'atoms', which have the same coordinates, but a more concentrated electron distribution than the real atoms of  $\rho(\mathbf{r})$ . If  $f$  is the atomic scattering factor of an atom, and  $g$  that of the corresponding 'squared atom',

$$F(\mathbf{H}) = \sum_{j=1}^N f \exp [2\pi i \mathbf{r}_j \cdot \mathbf{H}]$$

and 
$$G(\mathbf{H}) = \sum_{j=1}^N g \exp [2\pi i \mathbf{r}_j \cdot \mathbf{H}] = \frac{g}{f} F(\mathbf{H}).$$

Hence, using equation 266.1,

$$\frac{g}{f} F(\mathbf{H}) = \frac{1}{V} \sum_{\mathbf{H}'} F(\mathbf{H}') F(\mathbf{H} - \mathbf{H}'),$$

or in the more usual notation,

$$\frac{g}{f} F(hkl) = \frac{1}{V} \sum_h \sum_{k'} \sum_{l'} F(h'k'l') F(h-h', k-k', l-l'). \quad (266.2)$$

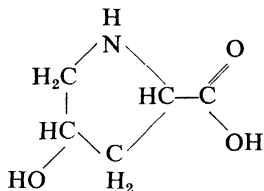
This equation was deduced by Sayre (1952).

A corresponding result, which holds when the atoms are equal, and are completely resolved in a projection on (001), is

$$\frac{g}{f} F(hk0) = \frac{1}{A} \sum_{h'} \sum_{k'} F(h'k'0) F(h-h', k-k', 0). \quad (266.3)$$

At first sight, the possibility of making any practical use of these equations appears to be slight. Any one structure factor is related to *all* others, or to all in one zone, so that even more are involved at the same time than in the determinantal equalities. This is in contrast to the Harker-Kasper inequalities which have the great advantage that one inequality relation involves only a very few structure factors and is quite independent of all the others. Nevertheless Sayre has shown convincingly that equation 266.3 is of practical value. He did this not

by testing a suggested procedure on a known crystal structure, but by using it to solve a problem to which he did not already know the answer. The crystal structure chosen for this test was that of hydroxyproline:—



The unit cell dimensions of this compound are  $a=5.0$ ,  $b=8.35$ ,  $c=14.1$  Å, and the space group is No. 19,  $P2_12_12_1$ . It appeared from the relative shortness of the  $a$ -axis that all atoms would be resolved in projection on (100), so that equation 266.3 should apply. In the practical use of this equation to establish sign relationships it is clearly advantageous to have as few terms appearing on the right-hand side as possible. This can be done in two ways: (a) by introducing a temperature factor to decrease the magnitudes of higher-order structure factors, and (b) by ignoring the smaller products on the assumption that they are likely to cancel out. In the investigation of hydroxyproline, the observed structure factors were first of all converted to those corresponding to point atoms by dividing them by  $\hat{f}$ , the scale having been established in the usual way. The values of  $\frac{|F_0|}{\hat{f}}$  were then multiplied by a factor

$$\exp \left[ -\frac{\pi^2}{p} S^2 \right], \text{ to give } |F| = \frac{|F_0|}{\hat{f}} \exp \left[ -\frac{\pi^2}{p} S^2 \right].$$

The structure factors  $F$  corresponded to a set of Gaussian atoms, in which the electron distribution is

$$\rho(\mathbf{r}) = Z \left( \frac{p}{\pi} \right) \exp [-p r^2],$$

and which have atomic scattering factors

$$f = Z \exp \left[ -\frac{\pi^2}{p} S^2 \right].$$

The corresponding 'squared atoms' have the scattering factor

$$g = Z^2 \left( \frac{p}{2\pi} \right) \exp \left[ -\frac{\pi^2}{2p} S^2 \right].$$

The value chosen for the constant  $p$  was  $2\pi$ . This represented a compromise between two conflicting requirements: too large a value for  $p$

makes the values of  $|F|$  fall off too slowly with increasing  $S$ , giving a large number of products on the right-hand side of each equation 266.3, while too small a value makes the electron density fall off too slowly with increasing  $r$ , so that the condition that atoms should be resolved is not satisfied. Finally the values of  $|F|$  were scaled to reduce  $F(000)$  from 280 to 18, since this gave  $F$ 's corresponding to atoms of density  $\rho(r) = \exp[-2\pi r^2]$ . (This step is not essential.) Values of  $|F(0kl)|$  and of  $\frac{g}{f}|F(0kl)|$  were now tabulated, the former being written out in full array, that is, in all four quadrants of the  $(0kl)$  reciprocal net, on both a sheet of paper and on a sheet of tracing cloth. By displacing the origin of the reciprocal net drawn on tracing cloth to the point  $(kl)$  of that drawn on paper, each structure factor  $F(k'l')$  came under another,  $F(k-k', l-l')$ , and all the products appearing in a particular equation were indicated. We may now write equation 266.3 in the form

$$A \frac{g}{f} F(kl) - 2F(00)F(kl) = \sum_{k'} \sum_{l'} F(k'l')F(k-k', l-l'),$$

where  $(k'l') = (00)$  is excluded from the products. For each  $(kl)$ , the value of  $\left(A \frac{g}{f} - 2F(00)\right)|F(kl)|$  was listed, together with that of each of the products  $F(k'l')F(k-k', l-l')$ , products of magnitude smaller than 4.0 on the scale  $F(00)=18$  being neglected. If, in any equation, a particular product  $F(k'l')F(k-k', l-l')$  is so large that all the other products, acting in opposition to it, could not add up to the expected total, it is clear that the sign of  $F(kl)$  must be equal to the product of the signs of  $F(k'l')$  and of  $F(k-k', l-l')$ , i.e.  $s(kl) = s(k'l')s(k-k', l-l')$ .

In the example we are considering, there were no individual products large enough to prove this result, although in a number of cases the contribution of a large product could only be outweighed by almost all others having the opposite sign, and this was considered to be very improbable. Examination of the equations for  $(kl) = (06)$ ,  $(20)$ ,  $(24)$ ,  $(2, 10)$ ,  $(44)$  and  $(4, 10)$  respectively, showed that each contained large products arising from others of these structure factors, and of the  $2^6 = 64$  possible sign combinations, only the eight satisfying

$$s(06) = s(2, 10)s(24) = s(4, 10)s(44)$$

and

$$s(20) = s(44)s(24) = s(4, 10)s(2, 10)$$

appeared at all likely. For a similar reason, it appeared probable that

$$s(14) = s(20)s(\bar{14}).$$

Since  $F(14) = -F(\bar{14})$  in this example, it follows that  $s(20) = -1$ . It then appeared probable from another equation that  $s(06) = +1$ . This eliminated all but two sign combinations for the six large structure factors mentioned above. Another method used was to 'develop' each



of the eight arrangements as far as possible; that is, the signs indicated in any of the eight arrangements were inserted throughout the equations, whereupon it became possible to draw conclusions about the signs of a few more terms. In principle, only the correct initial arrangement could be developed to the end without difficulty, any incorrect arrangement leading sooner or later to the situation where one equation requires the choice of a certain sign for a term, while another equation requires the opposite sign for this term. In the present example, because the basic postulates of the method were not fulfilled exactly, the equations could not be satisfied by any set of signs. It was evident that only the two arrangements already mentioned could admit of reasonably satisfactory development, and of these, one was to be preferred in that it allowed development to the point where 19 signs had been found. Beyond this point, contradictions became apparent, and although it was possible to determine 12 more signs with some certainty, by the time 53 signs had been determined, the inconsistencies were marked. Sayre did not attempt to carry the test further, but compared his results with those obtained by Zussman, who had determined the crystal structure by trial-and-error methods (Zussman, 1951). The comparison showed that of the 19 signs determined in the first stage, all were correct, of the next 12, one was incorrect, and of the last 22, 8 were incorrect. A Fourier synthesis involving only these 19 terms showed the molecule fairly clearly (fig. 269), and there is little doubt that the structure could have been refined from this point in the usual way. It is clear that hydroxyproline was not a favourable example to choose for a practical test of the squaring method, since when the atomic density function is taken as  $\exp. [-2\pi r^2]$ , two pairs of atoms overlap in projection to a considerable extent.

A somewhat different way in which Sayre's equation can be put to practical use is illustrated by the work of Cochran and Penfold (1952), described in the following section.

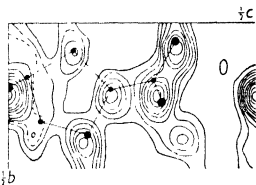


FIG. 269. An approximation to the projected electron density in hydroxyproline. The Fourier series contained only the 19 terms whose signs were determined by Sayre's equations. The correct atomic positions are indicated (Sayre, 1952).

**4.3. Sayre's equality and Harker-Kasper inequalities.** There is a close connection between Sayre's equation 266.2 and the results given by Karle-Hauptmann or Harker-Kasper inequalities. When the structure is centrosymmetric, 266.2 may be written

$$V \int F(hkl) = \sum_{h'} \sum_{k'} \sum_{l'} F(h'k'l') F(h+h', k+k', l+l').$$

Included among the products on the right-hand side there will be a term  $F(hkl)F(2h, 2k, 2l)$  which occurs for  $h=h', k=k', l=l'$ . We thus have

$$V \sum_f F(hkl) = F(hkl)F(2h, 2k, 2l) + \text{other terms.} \quad (270.1)$$

This suggests that when  $F(hkl)$  and  $F(2h, 2k, 2l)$  are both large, the sign of  $F(2h, 2k, 2l)$  may be positive to make  $F(hkl)F(2h, 2k, 2l)$  have the same sign as  $F(hkl)$ . Equation 270.1 does not usually prove that this is so, unless the signs and magnitudes of a sufficient number of terms which appear as products on the right-hand side of the equation are already known or are all relatively small. However, in similar circumstances the sign of  $F(2h, 2k, 2l)$  can often be proved to be positive from the inequality  $U^2(hkl) \leq \frac{1}{2} + \frac{1}{2} U(2h, 2k, 2l)$  without any knowledge of the signs or even of the magnitudes of any other structure factors.

More generally, Sayre's equation suggests that the result

$$s(hkl) = s(h'k'l')s(h+h', k+k', l+l') \quad (270.2)$$

is likely to be true if the corresponding three structure factors are large. As we saw in the previous section, Sayre made practical use of this fact. When inequalities give a relationship between the signs of three large structure factors, it is always as given by 270.2. This point has already been mentioned in section 8.3.2, and the example  $s(30\bar{9}) = s(202)s(50\bar{7})$ , taken from Gillis' investigation of oxalic acid, was given. A general proof has been given by Cochran (1952).

Experience has shown, however, that the result 270.2 holds very frequently when it is not required to do so by inequalities, and when the atoms are not all equal and resolved. Two theoretical explanations of this fact have been given; one by Cochran (1952) is based on Sayre's equation, and the other by Zachariasen (1952) is based on Harker-Kasper inequalities. The general conclusions reached are similar.

Let us consider the properties of the functions

$$\sigma(\mathbf{r}) = \frac{1}{V} \sum_{-\infty}^{+\infty} U(\mathbf{H}) \cos 2\pi \mathbf{H} \cdot \mathbf{r} \quad (270.3)$$

$$\text{and} \quad \sigma_p(\mathbf{r}) = \frac{1}{V} \sum_1^p U(\mathbf{H}) \cos 2\pi \mathbf{H} \cdot \mathbf{r}. \quad (270.4)$$

The first represents a distribution of point atoms, the weight of one atom being  $n_j = Z_j/F(0)$ , as in previous sections. The second is an approximation to this function, obtained by including in the Fourier series only  $p$  terms, which may have any indices but are chosen from among those having the largest values of  $|U|$ . It may readily be shown that this *partial* Fourier synthesis satisfies the condition

$$\sum_{j=1}^N n_j(\sigma_p)_j = \frac{1}{V} \sum_1^p U^2, \quad (270.5)$$

where  $(\sigma_p)_j$  is the value of  $\sigma_p$  at the centre of the  $j$ th atom. The approximation will be a recognizable representation of the crystal structure

if the value of  $\sigma_p$  at the centre of each atom is considerably greater than the average value of this function elsewhere, that is, if  $(\sigma_p)_j > \overline{\sigma_p}$ . An equivalent expression of this condition can be found, it is that

$\left\{ \sum_1^p U^2 \right\}^{\frac{1}{2}}$  should be greater than unity. This result shows, incidentally,

that for the more complex structures, for which the value of  $\overline{U^2}$  is small, a greater proportion of terms must be included in the series in order to give a reasonable picture of the structure. For simple structures having even a few very large unitary structure factors, the condition

$\left\{ \sum_1^p U^2 \right\}^{\frac{1}{2}} > 1$  may be satisfied when the series contains quite a

small number of independent terms, say  $t$ . The actual number of terms in the series will be  $p = tn$ , where  $n$  is the symmetry number, that is, the number of structure factors related by symmetry. The minimum value of  $n$  is 2, since we are excluding non-centrosymmetric structures from consideration. The condition can then be written  $\sqrt{nt} \overline{U} > 1$ , where  $\overline{U}$  is the R.M.S. value of the  $t$  unitary structure factors involved. This condition is already satisfied for  $n=4$ ,  $t=4$ ,  $\overline{U}=0.5$ , which are practical orders of magnitude. The fact that, with only a small number of terms in the series,  $\sigma_p$  may have values at atomic centres which are positive and greater than the average value of this function elsewhere, suggests that the correct choice of signs for the coefficients of the series 270.4 will generally be that which causes  $\sigma_p$  to make greater excursions in the positive than in the negative

direction. This condition can be imposed by requiring  $\int_V \sigma_p^3 dV$  to

have a maximum positive value. This result can also be expressed in terms of the  $U$ 's, by making use of a relation between the Fourier coefficients of  $\sigma_p$  and those of  $\sigma_p^2$ . This relation follows from equation 266.1. When the number of terms in the series is small, the condition is found to be  $s(\mathbf{H}) = s(\mathbf{H}')s(\mathbf{H} + \mathbf{H}')$ , which is identical with equation 270.2.

This approach to the problem suggests that this relation between the signs of any three structure factors can be expected to hold with increasing probability the more  $\sqrt{3n} \overline{U}$  exceeds unity. For unitary structure factors of a given magnitude, the relation is therefore more likely to be true the greater the symmetry number  $n$ . It is also more likely to be true (again for unitary structure factors of a given magnitude) if the structure contains one or more atoms of a relatively high

atomic number, since the condition that  $\int_V \sigma_p^3 dV$  should have a maximum positive value, which leads to equation 270.2, is necessarily satisfied to a greater extent when the structure contains a region of high electron density.

The way in which equation 270.2 can sometimes be used in conjunction

with Harker-Kasper inequalities and Sayre's equation, to determine a crystal structure directly from measured  $|F|$  values, is best illustrated by a practical example. Crystals of glutamine,  $C_5O_3N_2H_{10}$  have  $a = 16.0$ ,  $b = 7.8$  and  $c = 5.0$  Å, space group No. 19,  $P2_12_12_1$  (Cochran and Penfold, 1952). Trial-and-error methods, and inspection of the Patterson function projected on (001), failed to determine the crystal structure.

The signs of a few structure factors could be determined by Harker-Kasper inequalities. Those of three structure factors were determined as positive, two could be assumed to be positive, while those of the others were obtained in terms of  $s(620) = a$  and  $s(060) = b$ . The thirteen signs established in this way were, of course, consistent with equation 270.2. The considerations set out earlier in this section would lead us to expect this relation between the signs of three structure factors to hold with greatest probability when  $U > 1/\sqrt{12} \approx 0.3$ . For example, since  $U(120) = 0.30ab$ ,  $U(18, 2, 0) = 0.42a$  and  $|U(17, 4, 0)| = 0.30$ , we might expect  $s(17, 4, 0) = s(\bar{1}\bar{2}0)s(18, 2, 0) = -ab.a = -b$ . In the same way, it was found that probably  $s(16, 6, 0) = a$ ,  $s(470) = b$  and  $s(280) = +1$ . This gave a probable sign to 17 structure factors—almost all those for which  $|U| > 0.3$ , in fact. The signs of a number of structure factors with smaller values of  $|U|$  were established in much the same way, but generally the result was not regarded as reliable unless a few confirmations of sign were obtained. For example,

$$s(220) = s(060)s(280) = b \cdot +1,$$

and

$$s(220) = s(\bar{1}\bar{2}0)s(140) = -ab \cdot -a.$$

Both lead to  $s(220) = b$ . When the sign of a structure factor appeared to be established by a number of such checks, this term was used to establish further sign relationships. Greatest consistency with respect to equation 270.2 was obtained by taking  $a = -1$ , but the evidence was not strong. Eventually the signs of 35 structure factors were established, almost all involving  $a$  and  $b$  separately or together.

In the projection of this structure on (001), all atoms are approximately equal, and we may expect their centres to be separated by distances of about 1 Å. Sayre's equation may then be justifiably used in the modified form

$$U(hk0) = \alpha(\sin \theta) \sum_{h'} \sum_{k'} U(h'k'0)U(h+h', k+k', 0);$$

regarding  $\alpha(\sin \theta)$  simply as an unknown function whose value may be found in practice as explained later. The value of

$$T(hk0) = \sum_{h'} \sum_{k'} U(h'k'0)U(h+h', k+k', 0) \quad (272)$$

was now evaluated for all structure factors having  $|U(hk0)| > 0.1$ , and for a number of others. The only products appearing on the right-hand side of equation 272 were, of course, those involving the 35

structure factors whose signs had been established. The evaluation was made for each of the four possible sign combinations: (1)  $a = -1$ ,  $b = -1$ ; (2)  $a = +1$ ,  $b = +1$ ; (3)  $a = +1$ ,  $b = -1$ ; (4)  $a = -1$ ,  $b = +1$ . The reciprocal lattice was now divided into four regions by means of concentric circles with centres at the origin. The function  $\alpha$  was taken to be constant in any one of them, and given by  $\alpha = \frac{\sum |U(hk0)|}{\sum |T(hk0)|}$ ; the sum being over all terms for which  $T$  had been calculated in that particular region. Values of  $\alpha T$  and of  $U$  were now compared for each of the possibilities (1) to (4), and the value of  $\sum |U - \alpha T| / \sum |U|$  was found to be 0.45, 0.62, 0.60 and 0.65 in combinations (1), (2), (3) and (4) respectively. This showed that if any one of these were correct, it was certainly (1). For this choice of signs, there was sufficient agreement between values of  $\alpha T$  and of  $U$  for the signs of a further 30 structure factors to be taken as known, giving 65 known signs in all. (The number of  $(hk0)$  reflexions observed with copper  $K\alpha$  radiation, excluding those accidentally absent, was 134.) An attempt was next made to calculate the signs of still more structure factors by repeating the calculation of  $T(hk0)$ , making use of the additional terms which could now be included among the products  $U(hk0)U(h+h', k+k', 0)$ , but the new values of  $\alpha T$  did not agree better with values of  $U$  than those obtained using only 35 structure factors to form the products.

A Fourier synthesis was made using the 65 terms whose signs appeared reasonably certain; the result is shown in fig. 273. It showed

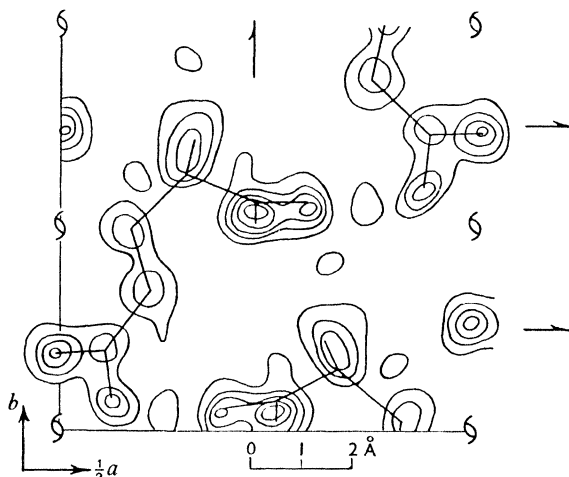


FIG. 273. An approximation to the projected electron density in glutamine. The Fourier series contained 65 terms whose signs were determined by a combination of three related methods. The computation of this projection was made on Pepinsky's machine (section 4.5.1) and the diagram is reproduced from a photograph of the contours on the presentation screen of this machine

clearly the approximate positions of all atoms in this projection. The structure was then refined by the usual methods. Now that the structure, in projection, was known, it became apparent that the signs of the smaller structure factors could not be calculated from Sayre's equation because the condition of equal resolved atoms was not satisfied—one carbon and one oxygen atom coincide in projection. Subsequent calculations showed that of the 65 signs established as described above, only 3 were incorrect. None of the 35 signs established by inequalities, or by the relation between the signs of three large structure factors, was incorrect.

Zachariasen's (1952) approach to this problem is based on the equality

$$\{|U(\mathbf{H})| + |U(\mathbf{H}')|\}^2 = 1 - D_{HH'} + s(\mathbf{H})s(\mathbf{H}')[U(\mathbf{H} + \mathbf{H}') + U(\mathbf{H} - \mathbf{H}')] + U(\mathbf{H} + \mathbf{H}')U(\mathbf{H} - \mathbf{H}'), \quad (274.1)$$

$$\text{where } D_{HH'} = 8 \sum_{j=1}^{N/2} \sum_{i=1}^{N/2} n_i n_j \left| \begin{array}{cc} \cos \pi(\mathbf{H} + \mathbf{H}') \cdot \mathbf{r}_j & \cos \pi(\mathbf{H} + \mathbf{H}') \cdot \mathbf{r}_i \\ \cos \pi(\mathbf{H} - \mathbf{H}') \cdot \mathbf{r}_j & \cos \pi(\mathbf{H} - \mathbf{H}') \cdot \mathbf{r}_i \end{array} \right|^2.$$

The Harker-Kasper inequality

$$\{|U(\mathbf{H})| + |U(\mathbf{H}')|\}^2 \leq \{1 + s(\mathbf{H})s(\mathbf{H}')U(\mathbf{H} + \mathbf{H}')\} \{1 + s(\mathbf{H}')s(\mathbf{H})U(\mathbf{H} - \mathbf{H}')\}$$

follows from the fact that  $D_{HH'} \geq 0$ . Zachariasen assumed that when the structure contains a large number of atoms,  $\overline{D_{HH'}} \simeq 1$ . This assumption is not correct in all circumstances, but when it is justified, equation 274.1 may be written as

$$\{|U(\mathbf{H})| + |U(\mathbf{H}')|\}^2 \simeq s(\mathbf{H})s(\mathbf{H}')\{U(\mathbf{H} + \mathbf{H}') + U(\mathbf{H} - \mathbf{H}')\} + U(\mathbf{H} + \mathbf{H}')U(\mathbf{H} - \mathbf{H}') \quad (274.2)$$

on the understanding that the equation is only statistically true. From this we may conclude that if  $|U(\mathbf{H})|$ ,  $|U(\mathbf{H}')|$  and  $|U(\mathbf{H} + \mathbf{H}')|$  are all large, it is probable that  $s(\mathbf{H})s(\mathbf{H}')U(\mathbf{H} + \mathbf{H}')$  is a positive quantity, that is, that  $s(\mathbf{H}) = s(\mathbf{H}')s(\mathbf{H} + \mathbf{H}')$ .

In equation 274.1, we replace  $\mathbf{H}'$  by  $\mathbf{H} + \mathbf{H}_1$ , and  $\mathbf{H}$  by  $\mathbf{H}_1$ . Let  $U(\mathbf{H})$  be a particular structure factor, and we stipulate that  $U(\mathbf{H}_1)$  and  $U(\mathbf{H} + \mathbf{H}_1)$  are to be pairs of large structure factors, defined as those for which  $|U| \geq 1.5(\overline{U^2})^{\frac{1}{2}}$ . We suppose that there are enough such pairs to justify the assumption  $\overline{D_{H_1, H+H_1}} = 1$ . Equation 274.1 may now be written

$$\frac{\{|U(\mathbf{H}_1)| + |U(\mathbf{H} + \mathbf{H}_1)|\}^2}{= s(\mathbf{H}_1)s(\mathbf{H} + \mathbf{H}_1)U(\mathbf{H}) + s(\mathbf{H}_1)s(\mathbf{H} + \mathbf{H}_1)U(\mathbf{H} + 2\mathbf{H}_1) + U(\mathbf{H})U(\mathbf{H} + 2\mathbf{H}_1)}. \quad (274.3)$$

The left-hand side of this equation is known from the observed data. Since  $U(\mathbf{H}_1)$  and  $U(\mathbf{H} + \mathbf{H}_1)$  are large structure factors, the value of

the left-hand side exceeds  $9\bar{U}^2$ , the probable value being about  $12\bar{U}^2$ . Some of the structure factors  $U(\mathbf{H}+2\mathbf{H}_1)$  occurring in the last two terms of equation 274.3 may correspond to reflexions outside the range of observation. It is possible, however, to set upper limits for the various terms of the right-hand side. For example

$$\overline{s(\mathbf{H}_1)s(\mathbf{H}+\mathbf{H}_1)U(\mathbf{H})} \leq |U(\mathbf{H})|.$$

Suppose that  $U(\mathbf{H})$  is a large structure factor. We may then take  $|U(\mathbf{H})| = 1.5(\bar{U}^2)^{\frac{1}{2}}$  and  $|\overline{U(\mathbf{H}+2\mathbf{H}_1)}| \simeq 0.7(\bar{U}^2)^{\frac{1}{2}}$ . Table 275 shows the value of the left-hand side of equation 274.3 compared with the estimated maximum values of the various terms of the right-hand side.

TABLE 275

Possible values of terms in equation (274.3)

	Value of L.H.S.	Maximum value of terms on R.H.S.		
$(\bar{U}^2)^{\frac{1}{2}}$	$12\bar{U}^2$	$1.5(\bar{U}^2)^{\frac{1}{2}}$	$0.7(\bar{U}^2)^{\frac{1}{2}}$	$\bar{U}^2$
0.20	0.48	0.30	0.14	0.04
0.15	0.27	0.23	0.11	0.02
0.10	0.12	0.15	0.07	0.01
0.07	0.06	0.11	0.05	0

On the basis of these figures, Zachariasen concludes that the first term on the right-hand side must be positive if  $(\bar{U}^2)^{\frac{1}{2}} > 0.07$ , that is, the equation  $s(\mathbf{H}) = s(\overline{s(\mathbf{H}_1)s(\mathbf{H}+\mathbf{H}_1)})$ , which is the statistical equivalent of equation 274.3, is reliable at least for  $(\bar{U}^2)^{\frac{1}{2}} > 0.07$ .

The practical application of Zachariasen's results is analogous to the utilization of Sayre's equation to determine the signs of additional structure factors when those of a few have been established, by inequalities or otherwise. The method was first applied to determine the structure of metaboric acid,  $\text{HBO}_2$ . For this compound,  $a=7.13$ ,  $b=8.85$ ,  $c=6.77$  Å and  $\beta=93.25^\circ$ . The space group is No. 14,  $\text{P2}_1/a$ , and the asymmetric unit consists of three molecules of  $\text{HBO}_2$ . The R.M.S. value of the unitary structure factors is  $(\bar{U}^2)^{\frac{1}{2}}=0.17$  and of the 1000 or so measured structure factors, 138 have  $|U| > 1.5(\bar{U}^2)^{\frac{1}{2}}=0.25$ . The signs of three structure factors were chosen arbitrarily as positive, and those of an additional 14 were determined by the inequality relation 253.2. When the signs of five further structure factors were expressed by symbols  $b, c, h, x, y$ , those of 18 more could be obtained in terms of these symbols. The signs of 40 structure factors were therefore determined in terms of five unknowns. Among these 40 there are five pairs of indices  $\mathbf{H}_1$  and  $\mathbf{H}+\mathbf{H}_1$  cor-

responding to  $\mathbf{H}=(154)$ . For each pair one finds  $s(\mathbf{H}_1)s(\mathbf{H}+\mathbf{H}_1)=+1$ . Hence  $s(154)=+1$ . Again, there are nine pairs of this type among the 40 structure factors corresponding to  $\mathbf{H}=(133)$ . For five of these,  $s(\mathbf{H}_1)s(\mathbf{H}+\mathbf{H}_1)=b$ , and for the remaining four,  $s(\mathbf{H}_1)s(\mathbf{H}+\mathbf{H}_1)=hb$ . Since the numerical value of  $s(\mathbf{H}_1)s(\mathbf{H}+\mathbf{H}_1)$  should certainly be nearer unity than zero for this class of structure factors, it follows that  $h=+1$ . The list of structure factors of known sign was gradually expanded in this way, until it included all for which  $|U(\mathbf{H})| \geq 0.25$ , and eventually all symbols were eliminated. The signs of a number of relatively small structure factors were also determined. For example, corresponding to  $\mathbf{H}=(001)$ , for which  $|U|=0.11$ , there are 21 pairs  $U(\mathbf{H}_1)$  and  $U(\mathbf{H}+\mathbf{H}_1)$  of large structure factors. The quantity  $s(\mathbf{H}_1)s(\mathbf{H}+\mathbf{H}_1)$ , averaged over these 21 pairs, has a value of  $-0.90$ , and hence  $s(001)=-1$ . When the signs of some 200 of the largest  $F$ 's had been determined, a three-dimensional Fourier synthesis was evaluated, and showed clearly the positions of all oxygen and boron atoms.



# CHAPTER 9

## THE ACCURACY OF A CRYSTAL STRUCTURE DETERMINATION

### 1. INTRODUCTION

In this final chapter we are concerned with crystal-structure analysis at the stage where the analyst has arrived, by one method or another, at atomic coordinates which are within say 0.1 Å of the truth. Often the interest of the work lies in determining the broad features of the crystal or molecular architecture, and these are already apparent at this stage. An increasing number of investigations are undertaken, however, whose object is to distinguish or identify chemical bonds which may differ in length by only a few hundredths of an Ångström. This is particularly true of work on organic compounds, where a satisfactory check on theories of molecular structure will be possible only when measured bond lengths can be relied on to within 0.01 Å. In such work, the process of finding a structure which is essentially correct becomes merely a necessary, although sometimes a very difficult, preliminary to the real task. In recent years, not much attention has been paid to the point that X-ray analysis provides a means of obtaining not only the lengths of bonds, but also the distribution of electrons in these bonds. This is mainly because the accuracy and methods of reduction of X-ray measurements have not been good enough to distinguish bonds except by their lengths, although in principle the electron distribution is more fundamental. The former, unlike the latter, can be determined completely by means other than Fourier synthesis, and we shall consider whether any of the analytical or semi-analytical methods that have been suggested for the location of atomic coordinates may lead to a more exact result than the orthodox  $F_0$  synthesis, defined as

$$\rho_0(xyz) = \frac{1}{V} \sum_{-H}^{+H} \sum_{-K}^{+K} \sum_{-L}^{+L} |F_0(hkl)| \cos 2\pi \left( \frac{hx}{a} + \frac{ky}{b} + \frac{lz}{c} - \alpha(hkl) \right). \quad (277)$$

The notation serves to emphasize the fact that the Fourier coefficients are measured experimentally, and are subject to at least random errors, and that the series often does not include all terms of appreciable magnitude. In this chapter we shall find it convenient to use  $x$  to denote a distance in the crystal measured in the  $a$ -direction, and not as this distance expressed as a fraction of  $a$ , as in previous chapters. The accuracy with which  $x_n$ , the  $x$ -coordinate of a particular atom, can be measured depends on the accuracy with which  $a$  can be measured. There is no difficulty in measuring unit-cell dimensions to 1 part in

1000, and this source of error is so small compared with others, and could so readily be reduced still further, that we are justified in neglecting it.

## 2. SOME METHODS OF OBTAINING ACCURATE ATOMIC COORDINATES

2.1. *The  $F_0$  synthesis.*  $F_0$  syntheses, both two- and three-dimensional, have been widely used for accurate molecular measurements; a good example of their use can be found in work on the structure of anthracene by Mathieson, Robertson and Sinclair (1950). This method has been fully described in previous chapters, and in the present connection the procedure may be summarized by saying that the electron density is evaluated at definite points on a lattice which generally has translations of  $1/60$  or  $1/120$  of the corresponding unit-cell edges. Points of maximum electron density are then found by graphical interpolation, or by calculation from the values of the electron density at a number of points near the maximum; a convenient table for this purpose has been published by Booth (1948, p. 64). As we shall see, greater accuracy is obtained by evaluating the electron density in three dimensions. In order to reduce the amount of calculation, it is usual to calculate only appropriate two-dimensional sections through the three-dimensional distribution of electrons. Caution is necessary in determining the coordinates of an atom from a section which does not pass very close to the atomic centre, since if the thermal motion of the atom is anisotropic, the coordinates of the point of maximum electron density in this section do not necessarily coincide with the corresponding atomic coordinates. Even when the atom is isotropic, due allowance must be made for the effect of non-orthogonality of the crystallographic axes, a point discussed in some detail by Parry and Pitt (1949).

Generally, of course, a number of successive  $F_0$  syntheses must be calculated since the initial coordinates, however obtained, are seldom sufficiently accurate to give correctly the sign or phase angle associated with each structure amplitude. The process of successive calculation of electron density and structure factors is often referred to as 'refinement' of a crystal structure. Refinement of three-dimensional electron distributions is not usually attempted because of the amount of calculation involved; where they have been used for accurate measurements the procedure has generally been to calculate the necessary signs or phase angles from atomic coordinates obtained by refinement of two-dimensional syntheses, and to evaluate the electron density in three dimensions once only. A notable exception is the work on the crystal structures of aminoacids by Pauling's school, for instance that on *l*-threonine by Shoemaker, Donohue, Schomaker and Corey (1950). As improved methods of calculation are introduced, such exceptions will no doubt become the rule.

2.2. *The Differential Fourier Synthesis.* A variant of the  $F_0$  synthesis was suggested by Booth (1946a). Instead of evaluating the electron density on a fixed lattice of points, one evaluates, at the points taken to be the atomic centres at this stage of refinement, the corresponding first differentials or slopes of the electron density in the directions of the crystallographic axes. For instance, assuming that the crystal has a centre of symmetry, equation 277 may be written

$$\rho_0 = \frac{1}{V} \sum_q F_0 \cos \Theta. \quad (279.1)$$

$\sum_q$  is used to indicate that the series contains only the  $q$  terms within the limiting sphere and

$$\Theta \equiv 2\pi \left( \frac{hx}{a} + \frac{ky}{b} + \frac{lz}{c} \right).$$

We then have

$$\frac{\partial \rho_0}{\partial x} = -\frac{2\pi}{aV} \sum_q hF_0 \sin \Theta.$$

The slope of the electron density in the  $x$ -direction at the point  $(x_n, y_n, z_n)$  is then

$$\left( \frac{\partial \rho_0}{\partial x} \right)_n = -\frac{2\pi}{aV} \sum_q hF_0 \sin \Theta_n.$$

The amounts by which the point of maximum electron density deviates from this point are then the solutions of the three equations

$$\left( \frac{\partial^2 \rho_0}{\partial x^2} \right)_n \Delta x_n + \left( \frac{\partial^2 \rho_0}{\partial x \partial y} \right)_n \Delta y_n + \left( \frac{\partial^2 \rho_0}{\partial x \partial z} \right)_n \Delta z_n + \left( \frac{\partial \rho_0}{\partial x} \right)_n = 0, \quad (279.2)$$

etc.

$\left( \frac{\partial^2 \rho_0}{\partial x^2} \right)_n$  is used to denote the second differential or curvature of the electron density at  $(x_n, y_n, z_n)$ , that is, near the centre of the  $n$ th atom. When the crystallographic axes are orthogonal, and the atoms spherically symmetric, these equations reduce to

$$\Delta x_n = - \left( \frac{\partial \rho_0}{\partial x} \right)_n / \left( \frac{\partial^2 \rho_0}{\partial x^2} \right)_n, \text{ etc.} \quad (279.3)$$

A useful result, first pointed out by Costain (1941) and developed by Booth (1946b) is that the electron density near the centre of an atom can be closely approximated by the relation

$$\rho = Z \left( \frac{p}{\pi} \right)^{3/2} \exp [-pr^2], \quad (279.4)$$

where  $\rho$  is the density at a distance  $r$  from the centre of the atom. As before,  $Z$  is the atomic number, and  $p$  is a constant which in this

case is best obtained from measurements on the electron-density map. These are used to give a graph of  $\log \rho$  against  $r^2$ . The value of  $p$  in practice is about 5.0, but depends of course on the temperature factor of the atom concerned, and the point at which the Fourier series for  $\rho_0$  is terminated. This approximation leads to

$$\left(\frac{\partial^2 \rho_0}{\partial x^2}\right)_n = 2pZ_n \left(\frac{p}{\pi}\right)^{3/2}, \quad \left(\frac{\partial^2 \rho_0}{\partial x \partial y}\right)_n = 2pZ_n \left(\frac{p}{\pi}\right)^{3/2} \cos \gamma, \text{ etc.,}$$

in the general case of a triclinic crystal. The amount of calculation involved is much reduced when this approximation is used. Equation 279.3 is derived on the assumption that the crystal has a centre of symmetry. Booth (1946c) also derived an analagous method for the simultaneous refinement of coordinates and phase angles, for use when the structure has no centre of symmetry. This procedure has since been shown by Cruickshank (1950a) to be unnecessary. The correct procedure consists in solving equations 279.2 with

$$\left(\frac{\partial \rho_0}{\partial x}\right)_n = -\frac{2\pi}{aV} \sum_q h|F_0| \sin(\Theta_n - \alpha), \text{ etc.,}$$

and then applying *twice* these corrections to the atomic coordinates. The factor is less than two if the structure does not have a centre of symmetry, but its projection on certain planes or lines is centrosymmetric (Shoemaker, Donohue, Schomaker and Corey, 1950). It is perhaps not sufficiently appreciated that this result also holds for  $F_0$  syntheses. For instance, if an atomic coordinate is taken as  $(x_n, y_n, z_n)$  in calculating phase angles, but the point of maximum electron density occurs at  $(x_n + \Delta x_n, \text{etc.})$  in the subsequent electron-density map, the process of refinement will be considerably speeded up by taking the centre of this atom to be at  $(x_n + 2\Delta x_n, \text{etc.})$  when phase angles are recalculated.

The differential synthesis does not give results which are free from the errors inherent in the  $F_0$  synthesis. Greater accuracy is obtained only in that the point of maximum electron density is precisely located without recourse to interpolation.

**2.3. The method of least squares.** The inherent errors of the  $F_0$  synthesis are, first, that the Fourier series can never be complete in practice, and secondly, that although the investigator is often well aware that some of the measured coefficients are more liable to be in error than others, there is no obvious way of decreasing the influence of the more inaccurate coefficients on the result. Alternative methods, free from these defects, have been suggested by Hughes (1941) and by Booth (1947a). These methods make greater use of our knowledge of the shapes of atoms than is made by the Fourier method.

The theory of errors predicts that if the errors in the measured  $F_0$ 's

follow the normal or Gaussian law, then the 'best' atomic parameters are those which result in a minimization of the quantity

$$R = \sum_u w_1(hkl)(|F_0(hkl)| - |F_c(hkl)|)^2,$$

where the weight  $w_1$  of a particular term should be taken inversely proportional to the square of the probable error of the corresponding  $F_0$ .  $\sum_u$  denotes a sum over all *independent* terms, or values of  $F_0$ .

It is often convenient to write  $R$  in the form

$$\sum_q w(hkl)(|F_0(hkl)| - |F_c(hkl)|)^2,$$

where the sum is taken over *all* terms which lie within the limiting sphere. The two expressions are equivalent if we take  $sw = w_1$ ,  $s$  being the multiplicity of a particular term.

Atomic parameters on which  $R$  depends include not only atomic coordinates, but all quantities which influence the value of the calculated structure factors, for instance the temperature factor. For the present we shall consider only the effect of changes in atomic coordinates. When the value of  $R$  is close to its minimum, systematic minimization can be accomplished as follows.

A small change  $\Delta x_n$  in the  $x$ -coordinate of the  $n$ th atom of a structure changes  $F_c$  by an amount

$$\frac{\partial F_c}{\partial x_n} \Delta x_n.$$

Changes to all coordinates simultaneously result in a change in  $F_c$  of amount

$$\Delta F_c = \sum_{n=1}^N \left( \frac{\partial F_c}{\partial x_n} \Delta x_n + \frac{\partial F_c}{\partial y_n} \Delta y_n + \frac{\partial F_c}{\partial z_n} \Delta z_n \right). \quad (28I)$$

The correct values of  $\Delta x_n$ , etc., are therefore those which most nearly equate  $\Delta F_c$  to  $F_0 - F_c$  for all the equations of this type which we can set up (corresponding to all the measured values of the  $F_0$ 's). For reasonably accurate results this number must be considerably greater than the number of independent coordinate corrections to be determined. The latter number is  $\frac{3}{2}N$  when the structure has a centre of symmetry as its only symmetry element. When this is so, equation 28I becomes

$$\Delta F_c = - \sum_{n=1}^{N/2} 4\pi f_n \left( \frac{h}{a} \Delta x_n + \frac{k}{b} \Delta y_n + \frac{l}{c} \Delta z_n \right) \sin 2\pi \left( \frac{hx_n}{a} + \frac{ky_n}{b} + \frac{lz_n}{c} \right).$$

The set of 'observational equations' must be reduced to a set of  $\frac{3}{2}N$  equations, called the 'normal equations'. The  $n$ th of these, for instance, is formed by multiplying both sides of each equation,  $\Delta F_c = F_0 - F_c$ ,

by  $w \frac{\partial F_c}{\partial x_n}$ , and then adding the  $q$  left-hand sides, and the  $q$  right-hand sides, to produce an equation:

$$\sum_q w \left\{ \left( \frac{\partial F_c}{\partial x_n} \right)^2 \Delta x_n + \frac{\partial F_c}{\partial x_n} \frac{\partial F_c}{\partial y_n} \Delta y_n + \frac{\partial F_c}{\partial x_n} \frac{\partial F_c}{\partial z_n} \Delta z_n + \sum_m \frac{\partial F_c}{\partial x_n} \left( \frac{\partial F_c}{\partial x_m} \Delta x_m + \frac{\partial F_c}{\partial y_m} \Delta y_m + \frac{\partial F_c}{\partial z_m} \Delta z_m \right) \right\} = \sum_q w (F_0 - F_c) \frac{\partial F_c}{\partial x_n}, \quad (282.1)$$

where  $\sum_m$  denotes a sum over all atoms except the  $n$ th.

The next normal equation is formed by multiplying throughout by  $w \frac{\partial F_c}{\partial x_{n+1}}$  before adding, and so on. The final result is a set of  $\frac{3}{2}N$  simultaneous equations which have to be solved for the  $\frac{3}{2}N$  unknowns,  $\Delta x_n, \Delta y_n, \Delta z_n$ , where  $n$  runs from 1 to  $\frac{1}{2}N$ . Successive applications of this procedure, which is known as the method of least squares, lead to atomic coordinates which minimize  $R$ . It will be clear from this account that even in a two-dimensional problem the full calculation could not very well be undertaken without the help of punched-card machines or similar equipment. If the atoms are well resolved from one another, however, it can be shown that quantities such as

$$\sum w \frac{\partial F_c}{\partial x_n} \frac{\partial F_c}{\partial x_m}$$

are likely to be very small compared with  $\sum_q w \left( \frac{\partial F_c}{\partial x_n} \right)^2$ . If the axes are orthogonal or nearly so,  $\sum_q w \frac{\partial F_c}{\partial x_n} \frac{\partial F_c}{\partial y_n}$ , etc., can also be neglected and equation 282.1 reduces to

$$\Delta x_n \sum_q w \left( \frac{\partial F_c}{\partial x_n} \right)^2 = \sum_q w (F_0 - F_c) \frac{\partial F_c}{\partial x_n}. \quad (282.2)$$

The quantities involved can now be evaluated with the help of a desk-calculating machine in a reasonable time.

A similar procedure may be used to minimize the function

$$R_2 = \sum_q w' (hkl) (|F_0(hkl)|^2 - |F_c(hkl)|^2)^2.$$

This was the function used by Shoemaker and his collaborators (1950) in applying the method. It has the disadvantage that a quantity such as  $\frac{\partial^2 |F_c|^2}{\partial x_n^2}$  will generally be more difficult to calculate numerically than  $\frac{\partial^2 F_c}{\partial x_n^2}$ . With the punched-card method of calculation used in the above case this was not so, and it was considered that  $R_2$  provided a more

convenient basis for assignment of weights  $w'$ . The results obtained by minimizing  $R_2$  will be almost identical with those obtained by minimizing  $R$ , provided that the respective weights  $w'$  and  $w$  are chosen so that  $w'|F_0|^2 = w$ .

Strict adherence to the rule that the weight of an observation should be taken inversely proportional to an external estimate of the standard deviation of the observation is not essential, since all reasonable systems of weighting lead to coordinates which differ by amounts small compared with the random errors of the final coordinates. When numerical calculations are being made, it is very convenient to give unit weight to all observations, except those of very intense reflections and accidentally absent reflections, which are given zero weight. The procedure in making the calculations will depend on the computational aids available. If a desk calculating machine is to be used the best procedure will be somewhat as follows. For the sake of definiteness we consider how the method would be applied to determine the best  $x$  and  $y$  coordinates from the values of the  $F_0(hk0)$ 's. The structure will be taken to have space group No. 19,  $P2_12_12_1$  with all atoms separated by at least 1 Å in projection on (001), except the  $i$ th and  $j$ th, which are closer together. It is supposed that the reflections have been measured to the limit given by Cu  $K\alpha$  radiation ( $\lambda = 1.54$  Å), and that more than say 75% of all reflections in this range were observed. Values of  $F_0$ ,  $F_c$  and  $F_0 - F_c$  are now tabulated for all reflections except those which are to be given zero weight, and values of  $\frac{\partial F_c}{\partial x_n}$  and  $\frac{\partial F_c}{\partial y_n}$  are tabulated for each reflection, and for each atom of the asymmetric unit. In this case, since

$$F_c = 4 \sum_{n=1}^{1N} f_n \cos 2\pi \frac{hx_n}{a} \cos 2\pi \frac{ky_n}{b},$$

$$\frac{\partial F_c}{\partial x_n} = -\frac{8\pi}{a} h f_n \sin 2\pi \frac{hx_n}{a} \cos 2\pi \frac{ky_n}{b},$$

for  $h+k$  even, with corresponding results when  $h+k$  is odd. (If certain reflections are to be given weights other than zero or unity,  $\sqrt{w_1}(F_0 - F_c)$ ,  $\sqrt{w_1} \frac{\partial F_c}{\partial x_n}$  and  $\sqrt{w_1} \frac{\partial F_c}{\partial y_n}$  are tabulated instead.) Values of  $\left(\frac{\partial F_c}{\partial x_n}\right)^2$  and of  $(F_0 - F_c) \frac{\partial F_c}{\partial x_n}$  are next tabulated, and finally each  $\Delta x_n$  is evaluated from

$$\Delta x_n = \sum_u (F_0 - F_c) \frac{\partial F_c}{\partial x_n} / \sum_u \left(\frac{\partial F_c}{\partial x_n}\right)^2,$$

and similarly for each  $\Delta y_n$ .

For the  $i$ th and  $j$ th atoms, for which the quantity  $\sum_u \frac{\partial F_c}{\partial x_i} \frac{\partial F_c}{\partial x_j}$  cannot be neglected compared with  $\sum_u \left(\frac{\partial F_c}{\partial x_i}\right)^2$ , the equations

$$\Delta x_i \sum_u \left(\frac{\partial F_c}{\partial x_i}\right)^2 + \Delta x_j \sum_u \frac{\partial F_c}{\partial x_i} \frac{\partial F_c}{\partial x_j} = \sum_u (F_0 - F_c) \frac{\partial F_c}{\partial x_i},$$

$$\Delta x_i \sum_u \frac{\partial F_c}{\partial x_i} \frac{\partial F_c}{\partial x_j} + \Delta x_j \sum_u \left(\frac{\partial F_c}{\partial x_j}\right)^2 = \sum_u (F_0 - F_c) \frac{\partial F_c}{\partial x_j}$$

must be used to obtain  $\Delta x_i$  and  $\Delta x_j$ , and similar equations for  $\Delta y_i$  and  $\Delta y_j$ .

When the coordinates have been corrected, values of  $F_c$  are re-calculated, and the process is repeated until the corrections obtained become very small. (In practical calculation it is obviously convenient to take the sums over independent terms only; hence the appearance of  $\sum_u$  and  $w_1$  in the above paragraph, as distinct from  $\sum_q$  and  $w$ , which are more convenient for theoretical considerations.)

**2.4. Steepest descents.** Structural parameters may also be refined by the method of steepest descents (section 8.2.2) introduced by Booth (1947*a*), and improved by Vand (1948*b*) and by Qurashi (1949). The expressions derived by Booth for the coordinate corrections  $\Delta x_n$ , based on this concept, were cumbersome and difficult to apply in practice. Qurashi showed that the rate of convergence to the minimum value of  $R$  depends markedly on the scales of representation for the atomic parameters, which as we have seen may involve quantities other than the positional coordinates. Transformations derived by Qurashi secure the optimum rate of convergence, and at the same time make all parameters mathematically equivalent. The application of these transformations leads to a simple formula for the corrections to atomic parameters which, for atomic coordinates, is identical with 282.2, whose derivation in terms of the method of least squares has already been discussed. A necessary condition for 282.2 to hold is that the reciprocal lattice points corresponding to the  $q$  different  $F_0$ 's should be fairly uniformly distributed throughout a sphere whose centre is the reciprocal-lattice origin. The two approaches to the problem of minimizing  $R$  as rapidly as possible are therefore closely related, although based on different concepts. We shall see later than the same ends can be achieved by means of a suitable Fourier synthesis which usually yields more information and is more convenient from a computational point of view than the analytical methods described above.

An exception to this rule must be made when intensities have been



measured from a powder photograph, when the experimental observations will in general be values, not of  $F_0^2$ , but of  $\sum_g F_g^2$ , the sum being over a group of reflections which are recorded as one line on the photograph. When this is so, a Fourier method cannot be used to refine atomic coordinates. Minimization of the function

$$R_g = \sum_u \left( \sum_g F_0^2 - \sum_g F_g^2 \right)^2.$$

may be accomplished, however, the symbol  $\sum_u$  now representing a sum over the  $u$  independent measurements. The simplified equation for  $\Delta x_n$  corresponding to (282.2) can be obtained from the latter by replacing each  $F_0$  and  $F_c$  by  $\sum_g F_0^2$  and  $\sum_g F_g^2$ . It should be noted, however, that if overlapping of lines reduces the number  $u$  of independent observations to the extent that this number is not much greater than the number of parameters to be determined, then the simple result cannot be used, and a more general result corresponding to equation 282.1 must take its place; that is, the method of least squares must be used without simplifying approximations.

### 3. ERRORS IN THE $F_0$ SYNTHESIS

**3.1. Errors of scale.** The scale of the  $F_0$ 's is obviously unimportant when the  $F_0$  synthesis is to be used only to determine atomic coordinates, but it is advisable to use absolute measurements when electron densities are required. The approximate scale of an electron-density map can always be determined by making use of our knowledge that the electron density is very nearly zero at all points which are more than about 1.5 Å from the centre of any atom, including hydrogen. Suppose, for example, that the electron density in projection is given by

$$\rho(xz) = \frac{F(000)}{A} + \frac{2}{A} \sum_{-H}^{+H} \sum_0^L F(h0l) \cos 2\pi \left( \frac{hx}{a} + \frac{lz}{c} \right),$$

but our measurements provide us only with values of  $KF$ , where the value of  $K$  is not known initially. We may, however, calculate

$$\rho'(xz) = \frac{2}{A} \sum_{-H}^{+H} \sum_0^L KF(h0l) \cos 2\pi \left( \frac{hx}{a} + \frac{lz}{c} \right),$$

and convert to values of  $\rho$  by the relationship

$$\rho = \frac{F(000)}{A} \left( \frac{\rho' - \rho'_{\text{zero}}}{-\rho'_{\text{zero}}} \right),$$

where  $\rho'_{\text{zero}}$  (a negative quantity) is the average value of  $\rho'$  over all the points where we consider the true value of  $\rho$  to be zero.

Any systematic error in the scale of the  $F_0$ 's which varies uniformly with  $S$  is unimportant, within limits, when only atomic coordinates are sought. This type of error occurs for instance if the intensity of equatorial-layer reflexions from a cylindrical specimen are not corrected for the absorption of X-rays in the specimen. The measured structure factors will be related to those corrected for absorption by the relation

$$F'_0 = \sqrt{A(S)} \cdot F_0,$$

where  $A(S)$  is an absorption factor. The use of the coefficients  $F_0$  in a synthesis would of course give a projection of the electron density; the use of the coefficients  $F'_0$  results in a projection which is modified so that the electron density of the  $n$ th atom corresponds to a scattering factor  $\sqrt{A(S)}f_n$  instead of  $f_n$ . Since this factor is isotropic if  $f_n$  is isotropic, the projection will still consist of a collection of circularly-symmetric atoms, grouped around the same points as in a synthesis whose coefficients are the  $F_0$ 's. Only the apparent distribution of electrons within the atoms is changed. If, however, the atoms are not completely resolved from one another, or if the series is terminated, coordinates derived from the  $F'_0$  synthesis will differ slightly from those derived from the  $F_0$  synthesis, if no corrections for overlap or series termination are made. An error of scale which varies systematically with  $S$  is very probably introduced when reflexions are recorded photographically and their intensities measured by eye comparison with a scale, since apart from absorption in the specimen, the divergence of the X-ray beam causes the reflexion to be recorded on a gradually-decreasing area as  $S$  increases, and also with most radiations the  $\alpha_1\alpha_2$  doublet is gradually resolved. It is fortunate that the resulting deviation of the  $F_0$ 's from the correct scale does not necessarily cause errors in derived atomic coordinates. Other systematic errors such as may arise from extinction, or absorption of the X-ray beam in a specimen of non-uniform cross-section, do of course result in errors in atomic coordinates as well as in electron density. Absorption corrections may be calculated, but it is difficult to correct for extinction, and the existence of the latter effect is likely to set the limit to the accuracy with which electron densities can be measured.

**3.2. Random errors of measurement.** Apart from the above-mentioned sources of inaccuracy, random errors will always be introduced because of the limitations of the measuring apparatus. As we have seen, errors in the unit-cell dimensions may be left out of account if a reasonably accurate method of measurement has been used. Before investigating the effect of random errors in the  $F_0$ 's it might be as well to recall two results from the theory of errors.

If some quantity  $x$  is measured  $n$  times, the error of each measurement is generally not known, but we can always find the deviation from the mean,

$$\delta x = x - \bar{x}.$$

The standard deviation of a single observation is then

$$\sigma(x) = \sqrt{\frac{\sum (\delta x)^2}{n-1}},$$

which is the same as the R.M.S. deviation when  $n$  is large. If the distribution of errors is Gaussian the probable error of an observation is  $0.6745\sigma$ , and errors greater than  $3\sigma$  occur with a frequency of only 1 in 1000, so that  $3\sigma$  is often called the maximum possible error.

The only other result we shall require is as follows. If

$$X = \lambda_1 x_1 + \lambda_2 x_2 + \dots = \sum_r \lambda_r x_r$$

$$\text{then } \sigma(X) = \left\{ \sum_r \left( \lambda_r \sigma(x_r) \right)^2 \right\}^{\frac{1}{2}}. \quad (287.1)$$

We can now apply these results to the case where the electron density is given by equation 279.1

$$\rho_0 = \frac{1}{V} \sum_q F_0 \cos \Theta.$$

As before,  $\sum_q$  indicates that the series contains  $q$  terms whose indices correspond to reciprocal-lattice points contained in a sphere of radius  $S_0$  whose centre is the reciprocal-lattice origin. The random error in  $\rho_0$  is then given by

$$\Delta \rho_0 = \frac{2}{V} \sum_{\frac{1}{2}q} \Delta F_0 \cos \Theta.$$

The limits of summation have been changed to emphasize the fact that  $\Delta F_0(hkl) = \Delta F_0(\bar{h}\bar{k}\bar{l})$ . It then follows from equation 287.1 that

$$\sigma(\rho_0) = \frac{2}{V} \left\{ \sum_{\frac{1}{2}q} \left( \sigma(F_0) \cos \Theta \right)^2 \right\}^{\frac{1}{2}}. \quad (287.2)$$

In order to simplify this result it is necessary to make some assumption about the dependence of  $\sigma(F_0)$  on the magnitude of  $F_0$ . The simplest, that  $\sigma(F_0)$  is the same for all  $F_0$ 's, large or small, leads to

$$\sigma(\rho_0) = \frac{2}{V} \sigma(F_0) \left\{ \frac{1}{2}q \right\}^{\frac{1}{2}} = \left\{ \frac{4\pi S_0^3}{3V} \right\}^{\frac{1}{2}} \sigma(F_0),$$

where we have made use of the results  $\overline{\cos^2 \Theta} = \frac{1}{2}$  and  $q = \frac{4}{3}\pi S_0^3 V$ . An assumption which is likely to be more nearly correct in practice is that  $\sigma(F_0) = K|F_0|$ , that is, that  $\sigma(F_0)$  is a constant percentage of  $|F_0|$ . On this assumption, equation 287.2 reduces to

$$\sigma(\rho_0) = \frac{2K}{V} \left\{ \sum_{\frac{1}{2}q} \frac{1}{2} F_0^2 \right\}^{\frac{1}{2}}.$$

Now from equation 279.1 it follows that

$$\overline{\rho_0^2} \equiv \int_V \rho_0^2 dV / \int_V dV = \frac{1}{V^2} \sum_q F_{0q}^2,$$

and hence

$$\sigma(\rho_0) = K(\overline{\rho_0^2})^{\frac{1}{2}}. \quad (288)$$

This rather neat result may be expressed as follows: if the  $F_0$ 's have a constant percentage standard deviation, the electron density at any point has a standard deviation which is the same percentage of the root mean square electron density, taken over the whole unit cell. This result can be taken a stage further by using the approximation that the electron density in the  $n$ th atom is given by equation 279.4.

Assuming the atoms are resolved, as they always are in a three-dimensional synthesis, we find from equation 279.4 that

$$\overline{\rho_0^2} = \left(\frac{p}{2\pi}\right)^{\frac{2}{3}} \left(\frac{1}{V} \sum_{n=1}^N Z_n^2\right).$$

It then follows from equation 288 that

$$\sigma(\rho_0) = K \left(\frac{p}{2\pi}\right)^{\frac{1}{3}} \left(\frac{1}{V} \sum_{n=1}^N Z_n^2\right)^{\frac{1}{2}}.$$

Similar calculations lead to formulae for  $\sigma(\rho_0)$  in a two-dimensional synthesis, and for  $\sigma(x_n)$  in both two- and three-dimensional syntheses,  $x_n$  as before being the  $x$ -coordinate of the  $n$ th atom. The results are set out in table 288.

TABLE 288

$\sigma(\rho_0)$  and  $\sigma(x_n)$  for a centrosymmetric three-dimensional synthesis

a	b
Assuming $\sigma(F_0)$ independent of $ F_0 $ ,	Assuming $\sigma(F_0) = K F_0 $ ,
$\sigma(\rho_0) = \left(\frac{4\pi S_0^3}{3V}\right)^{\frac{1}{2}} \sigma(F_0)$	$\sigma(\rho_0) = K\{\overline{\rho_0^2}\}^{\frac{1}{2}} = K \left(\frac{p}{2\pi}\right)^{\frac{1}{3}} \left(\frac{1}{V} \sum_{n=1}^N Z_n^2\right)^{\frac{1}{2}}$
$\sigma(x_n) = \left(\frac{4\pi S_0^3}{3V} \cdot \frac{\pi^5}{5p^5}\right)^{\frac{1}{2}} \frac{S_0}{Z_n} \sigma(F_0)$	$\sigma(x_n) = \frac{K}{\sqrt{2} Z_n} \left(\frac{\pi}{2p}\right)^{\frac{5}{6}} \left(\frac{1}{V} \sum_{n=1}^N Z_n^2\right)^{\frac{1}{2}}$

and for a centrosymmetric two-dimensional synthesis,

$\sigma(\rho_0) = \left(\frac{\pi S_0^2}{A}\right)^{\frac{1}{2}} \sigma(F_0)$	$\sigma(\rho_0) = K \left(\frac{p}{2\pi}\right)^{\frac{1}{2}} \left(\frac{1}{A} \sum_{n=1}^N Z_n^2\right)^{\frac{1}{2}}$
$\sigma(x_n) = \left(\frac{\pi S_0^2}{A} \cdot \frac{\pi^4}{4p^4}\right)^{\frac{1}{2}} \frac{S_0}{Z_n} \sigma(F_0)$	$\sigma(x_n) = \frac{K}{\sqrt{2} Z_n} \cdot \frac{\pi}{2p} \left(\frac{1}{A} \sum_{n=1}^N Z_n^2\right)^{\frac{1}{2}}$

The formulae for  $\sigma(x_n)$  were derived by Booth (1946*b*) and by Booth and Britten (1948). Small numerical discrepancies between their results and those given above are to be attributed mainly to the fact that

these authors derived their formulae for a non-centrosymmetric synthesis, although errors in phase angles were not taken into account.

In practice the true state of affairs is likely to lie somewhere between assumptions **a** and **b** (Table 288), in that small  $F_0$ 's will have nearly a constant standard deviation, about equal to the smallest detectable value of  $F_0$ , while large ones will have more nearly a constant percentage standard deviation. However, both sets of formulae lead to the same general conclusions. One unexpected result is that  $\sigma(\rho_0)$  is independent of the particular point of the unit cell considered, so that the standard deviation of the electron density at the centre of an atom is no greater than at a point where the expected value of the electron density is zero. (An exception occurs for special points such as the origin, for which the assumption  $\overline{\cos^2 \Theta} = \frac{1}{2}$  has to be replaced by  $\overline{\cos^2 \Theta} = 1$ .) We see also that when the crystal contains atoms of different atomic number, the standard deviation of the coordinate of a particular atom is inversely proportional to its atomic number. There is no reason to expect a greater standard deviation in say the  $x$ -direction than in any other, unless the atom has an anisotropic temperature factor. For the same accuracy of measurement of structure factors, a three-dimensional synthesis gives more accurate atomic coordinates than a two-dimensional one.

In order to find the order of magnitude of the standard deviations likely to occur in practice we may apply the above formulae to the case of dibenzyl, for which we find from data published by Robertson (1935*b*), Jeffrey (1947) and Cruickshank (1949*a*) that  $V = 540 \text{ \AA}^3$ ,  $A = 78 \text{ \AA}^2$  for the projection on (001),  $p = 3.35$  and  $S_0 = 1.07 \text{ \AA}^{-1}$ . A comparison of independent measurements made by Robertson and by Jeffrey gives  $\sigma(F_0) = 0.8$ , assuming  $\sigma(F_0)$  independent of  $|F_0|$ . If, on the other hand, we assume a constant percentage standard deviation, a figure of 10% is unlikely to be out by as much as a factor of two either way.

TABLE 289

$\sigma(\rho_0)$  and  $\sigma(x_n)$  for the three-dimensional Fourier synthesis of dibenzyl

<b>a</b>	<b>b</b>
Assuming $\sigma(F_0) = 0.8$ , $\sigma(\rho_0) = 0.08 \text{ e/\AA}^3$ $\sigma(x_n) = 5.3 \cdot 10^{-3} \text{ \AA}$	Assuming $\sigma(F_0) = 0.1 F_0 $ , $\sigma(\rho_0) = 0.09 \text{ e/\AA}^3$ $\sigma(x_n) = 6.2 \cdot 10^{-3} \text{ \AA}$
and for a two-dimensional synthesis,	
$\sigma(\rho_0) = 0.17 \text{ e/\AA}^2$ $\sigma(x_n) = 1.3 \cdot 10^{-2} \text{ \AA}$	$\sigma(\rho_0) = 0.26 \text{ e/\AA}^2$ $\sigma(x_n) = 2.0 \cdot 10^{-2} \text{ \AA}$

Although these figures apply to a particular example, very similar ones will be found in other cases where the same method of intensity

measurement—visual comparison with a scale—is used. This conclusion finds support from a more empirical study made by Robertson and White (1947), who investigated the effect of introducing known random errors, of magnitudes such as are likely to occur when the visual method is used, into the coefficients of a two-dimensional synthesis. The derivation of the standard deviation of an atomic position from the syntheses made with correct and incorrect  $F$ 's is complicated by the presence of series-termination errors, two different methods of reducing the results leading to values of 0.015 and 0.027 Å respectively. Substitution of the value  $\sigma(F_0)=0.7$  (derived from the known errors introduced) in the appropriate formula of table 288 with the appropriate values of the other constants gives a predicted positional standard deviation of 0.02 Å, in good agreement with the empirically-determined values.

Subject, therefore, to a large number of qualifications, we may conclude that when the  $F_0$ 's are derived from visual comparison, the standard deviation of an atomic coordinate, from three- and two-dimensional syntheses, is about  $5 \cdot 10^{-3}$  and  $1.5 \cdot 10^{-2}$  Å respectively. The corresponding standard deviations in electron density are about  $0.1e/\text{\AA}^3$  and  $0.2e/\text{\AA}^2$  respectively. These figures should not be regarded as giving more than the order of magnitude of the expected errors, but in any particular example a more accurate estimate may be obtained by application of the formulae of table 288. These general formulae suggest only two certain methods of reducing the value of  $\sigma(x_n)$ . The most effective is to increase the accuracy of the experimental measurements, when the accuracy of derived results will be increased in the same ratio. An extension of the synthesis from two dimensions to three reduces  $\sigma(x_n)$  by a factor numerically equal to about  $(V/A)^{\frac{1}{2}}$ .

In this section it has been assumed that in the final stages of refinement, atomic scattering factors are known with sufficient accuracy to give correctly the signs of all structure factors. In practice the magnitudes of coefficients inserted with incorrect signs are unlikely to be much greater than the value of  $\sigma(F_0)$ ; for such terms, the net result is equivalent to an increase in the value of  $\sigma(F_0)$  for small  $F_0$ 's. Except in the most accurate work the effect is not important.

In the case of a non-centrosymmetric synthesis, the phase angles  $\alpha$  which occur in the formula

$$\rho_0 = \frac{1}{V} \sum_q |F_0| \cos(\Theta - \alpha),$$

and are calculated from a postulated structure, will always be in error even when the scattering factors of the atoms in the real and postulated structures are identical. The reason for this is that the random errors of the coefficients cause errors in the derived atomic coordinates, and these in turn cause errors in calculated phase-angles.

The net result, as was shown by Cruickshank (1950*b*), is that the standard deviation of a coordinate derived from a non-centrosymmetric synthesis is twice that of one derived from an otherwise identical centrosymmetric synthesis. It is clear that errors in assumed atomic scattering factors, or, more precisely, in their ratios, will also cause errors in phase angles. No exact treatment of the effect of such errors has been given; general considerations suggest that although the electron density will be affected, the influence on atomic coordinates will be very small.

**3.3. Series-termination errors.** The way in which an electron distribution expressed in the form of a Fourier series is changed by the termination of the series when its coefficients are still appreciable can be seen from the following considerations. To any three-dimensional distribution  $\rho(\mathbf{r})$  there corresponds a function.

$$F(\mathbf{S}) = \int_V \rho(\mathbf{r}) \exp [2\pi i \mathbf{r} \cdot \mathbf{S}] dV, \quad (291.1)$$

which is called the Fourier transform (section 1.3.3) of  $\rho(\mathbf{r})$  and possesses the property expressed in the equation

$$\rho(\mathbf{r}) = \int_{V^*} F(\mathbf{S}) \exp [-2\pi i \mathbf{r} \cdot \mathbf{S}] dV^*. \quad (291.2)$$

Volume elements in space and in reciprocal space are represented by  $dV$  and  $dV^*$  respectively, and each integral is taken over the whole of the appropriate space. As has already been pointed out,  $F(\mathbf{S})$  may be regarded as a generalized structure factor which is a continuous function in reciprocal space. When the distribution  $\rho(\mathbf{r})$  is repeated at regular intervals by the translations of an infinite lattice,  $F(\mathbf{S})$  is observable only at the points of a corresponding reciprocal lattice, and the Fourier integral 291.2 is replaced by a Fourier series. Provided that the translations of the direct lattice are sufficiently great to contain the distribution  $\rho(\mathbf{r})$  within one unit cell, repetition on a lattice will have no effect on  $\rho(\mathbf{r})$ , and it may still be calculated from 291.2;  $\rho(\mathbf{r})$  might represent a single atom, for instance. The termination of the Fourier series will have the same effect on  $\rho(\mathbf{r})$  as integrating 291.2 over the region  $S < S_0$ , giving instead of  $\rho(\mathbf{r})$  the modified distribution

$$\begin{aligned} \rho'(\mathbf{r}) &= \int_{\text{sphere } S < S_0} F(\mathbf{S}) \exp [-2\pi i \mathbf{r} \cdot \mathbf{S}] dV^* \\ &= \int_{V^*} t(\mathbf{S}) F(\mathbf{S}) \exp [-2\pi i \mathbf{r} \cdot \mathbf{S}] dV^*, \end{aligned}$$

where

$$\begin{aligned} t(\mathbf{S}) &= 1 \text{ for } S < S_0, \\ &= 0 \text{ for } S > S_0. \end{aligned}$$

But by equation 291.1,

$$F(S) = \int_V \rho(\mathbf{r} + \mathbf{R}) \exp [2\pi i(\mathbf{r} + \mathbf{R}) \cdot \mathbf{S}] dV.$$

It follows that

$$\rho'(\mathbf{r}) = \int_{V^*} t(S) \left\{ \int_V \rho(\mathbf{r} + \mathbf{R}) \exp [2\pi i(\mathbf{r} + \mathbf{R}) \cdot \mathbf{S}] dV \right\} \exp [-2\pi i\mathbf{r} \cdot \mathbf{S}] dV^*,$$

or, changing the order of integration,

$$\rho'(\mathbf{r}) = \int_V \rho(\mathbf{r} + \mathbf{R}) \left\{ \int_{V^*} t(S) \exp [2\pi i\mathbf{R} \cdot \mathbf{S}] dV^* \right\} dV. \quad (292)$$

The expression within brackets on the right-hand side of equation 292 will be recognized as the Fourier transform of  $t(S)$ , and can be shown to be a function of  $\mathbf{R}$  only, given by

$$T_3(\mathbf{R}) = \frac{4}{3} \pi S_0^3 \cdot \frac{3(\sin 2\pi S_0 R - 2\pi S_0 R \cos 2\pi S_0 R)}{(2\pi S_0 R)^3}.$$

Hence, finally, the relation between  $\rho'(\mathbf{r})$  and  $\rho(\mathbf{r})$  is

$$\rho'(\mathbf{r}) = \int_V \rho(\mathbf{r} + \mathbf{R}) T_3(\mathbf{R}) dV.$$

Expressed in terms of Cartesian coordinates, with  $x, y, z$  and  $u, v, w$  the components in the  $a, b, c$  directions of  $\mathbf{r}$  and  $\mathbf{R}$  respectively,

$$\rho'(xyz) = \int_V \rho(x+u, y+v, z+w) T_3(\mathbf{R}) du dv dw,$$

where

$$\mathbf{R} = \mathbf{u} + \mathbf{v} + \mathbf{w}.$$

In the same way it may be shown that in the corresponding two- and one-dimensional cases,

$$\rho'(xy) = \int_A \rho(x+u, y+v) T_2(\mathbf{R}) du dv,$$

where

$$\mathbf{R} = \mathbf{u} + \mathbf{v}$$

and

$$\rho'(x) = \int_V \rho(x+u) T_1(u) du.$$

$T_2$  is the two-dimensional Fourier transform of a function which is unity inside a circle of radius  $S_0$ , and is zero elsewhere, being given by

$$T_2(\mathbf{R}) = \pi S_0^2 \frac{2J_1(2\pi S_0 R)}{2\pi S_0 R},$$

while

$$T_1(\mathbf{R}) = 2S_0 \frac{\sin 2\pi S_0 R}{2\pi S_0 R}$$



is the transform of a function which is unity from  $S = -S_0$  to  $+S_0$ , but zero elsewhere.

What these results mean physically can be illustrated by considering the expression for  $\rho'(x)$ . Given the distribution  $\rho(x)$  of fig. 293, the value

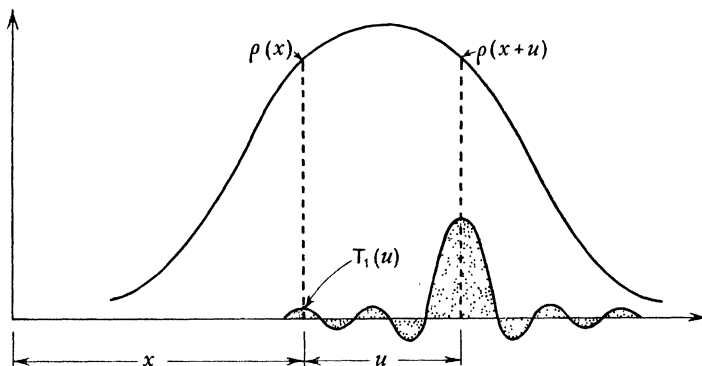


FIG. 293. When a one-dimensional Fourier series is terminated, the corresponding electron density in a line element  $du$  is spread out through

$$\text{multiplication by } T_1(u) = \frac{\sin 2\pi S_0 u}{\pi u}$$

of  $\rho'(x)$  is obtained by summing contributions from all points  $x+u$ , the contribution from a line element  $du$  at  $x+u$  being  $\rho(x+u)T_1(u)du$ . The electrons in every line element are spread out into the curve shown in fig. 293, and the net result is obtained by superposing all such curves. The distribution  $\rho'$  bears the same relation to  $\rho$  as an image in a microscope of limited resolving power bears to the object, in the two-dimensional case. Similarly, in three dimensions, the electrons in every volume element  $dudvdw$  at distance  $R$  from  $(xyz)$  are spread out through multiplication by  $T_3(R)$  and contribute to  $\rho'(xyz)$  an amount  $\rho(x+u, y+v, z+w)T_3(R)dudvdw$ .

The termination of the Fourier series may be said to 'scramble' the electron density; the scrambling is least when the functions  $T$  are 'sharpest'. The degree of sharpness depends only on the range of the series, that is, on the value of  $S_0$ .

We can now make use of these results to find the modified electron density corresponding to a spherically-symmetric atom whose density is  $\rho(r)$ . A rough, but convenient, approximation is to treat the atom as if all its electrons were concentrated at its centre. It is then clear from the treatment given above that  $\rho'(r)$  is directly proportional to  $T(r)$ . This approximation has been used by Bragg and West (1930) and by James (1948) to estimate the effect of series termination on two- and three-dimensional syntheses respectively. Although the approximation appears to be a crude one, the results obtained from it are not unsatisfactory. An exact result can be obtained for any

spherically-symmetric atom by a method suggested by Cruickshank (1949*a*). For an atom,

$$\rho(r) = \int_0^\infty 4\pi S^2 f(S) \frac{\sin 2\pi r S}{2\pi r S} dS,$$

where  $f(S)$  is the atomic scattering factor. Correspondingly,

$$\rho'(r) = \int_0^{S_0} 4\pi S^2 f(S) \frac{\sin 2\pi r S}{2\pi r S} dS,$$

and is also spherically symmetric.

Suppose the area under the  $f$ -curve of an atom (fig. 294) to be divided

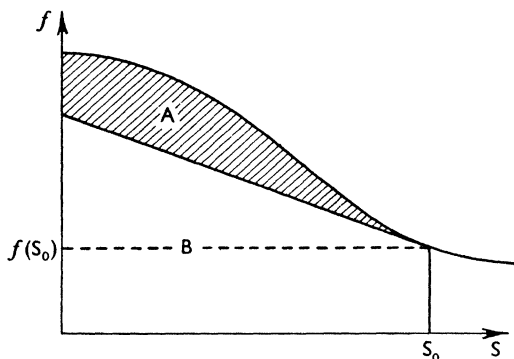


FIG. 294. Division of the area under the  $f$ -curve into two parts  $A$  and  $B$  by a straight line which is a tangent to the curve at  $S = S_0$ .

into two parts,  $A$  and  $B$ , by a line  $f_e(S) = a + bS$  which is a tangent to the  $f$ -curve at  $S = S_0$  so that  $f_0 \equiv f(S_0) = a + bS_0$ ,  $f_0' \equiv \left(\frac{df}{dS}\right)_{S=S_0} = b$ ;  $\rho'$  can then be considered as the sum of  $\rho'_A$  and  $\rho'_B$ , where

$$\begin{aligned} \rho'_B(r) &= \int_0^{S_0} (a + bS) 4\pi S^2 \frac{\sin 2\pi r S}{2\pi r S} dS \\ &= \cos 2\pi S_0 r \left( \frac{-S_0 f_0}{\pi r^2} + \frac{f_0'}{2\pi^3 r^4} \right) - \frac{f_0'}{2\pi^3 r^4} + \sin 2\pi S_0 r \left( \frac{f_0 + S_0 f_0'}{2\pi^2 r^3} \right) \end{aligned}$$

and

$$\rho'_A(r) = \int_0^{S_0} (f - f_e) 4\pi S^2 \frac{\sin 2\pi r S}{2\pi r S} dS,$$

which can be evaluated numerically. Cruickshank's calculations show that in a particular example  $\rho'_A$  falls to zero, without assuming negative values, in a distance of about 2 Å. In the unit cell of a crystal it would therefore overlap only nearest-neighbour atoms. Although the exact form of  $\rho'_A$  will depend on the form of the  $f$ -curve and the value of  $S_0$ , this result is likely to be generally true. There remains the effect of

$\rho'_B(r)$ , which is approximately periodic with wave-length  $1/S_0$ , and amplitude decreasing with  $r$ . For large values of  $r$ ,

$$\rho'_B(r) = -\frac{S_0 f_0}{\pi r^2} \cos 2\pi S_0 r.$$

This is also essentially the result given by the point-atom approximation, when the constant scattering factor of the point atom is taken as  $f_0$ , the scattering factor of the actual atom for  $S=S_0$ . The same method, applied to a two-dimensional example, for which

$$\rho'(r) = \int_0^{S_0} 2\pi S f(S) J_0(2\pi r S) dS,$$

leads to

$$\rho'_B(r) = \frac{aS_0}{r} J_1(2\pi S_0 r) + \frac{b}{4\pi^2 r^3} \int_0^{2\pi S_0 r} x^2 J_0(x) dx.$$

The maxima and minima of  $\rho'_B(r)$ , as defined above, are quite closely fitted by those of  $\frac{J_1(2\pi S_0 r)}{2\pi S_0 r}$ , which is proportional to the modified density corresponding to a point atom, so that again the point-atom approximation gives a reasonable result except for small values of  $r$ .

When the electron distribution consists of a group of spherically-symmetric atoms, the modified density given by a terminated Fourier series also consists of a group of spherically-symmetric distributions centred around the *same* points, so that it is not immediately obvious why the atomic coordinates given by a terminated series are inaccurate. The reason is that while  $\rho(r)$  for an individual atom will generally decrease to zero in a distance less than that between the centres of neighbouring atoms, this will not be true of  $\rho'(r)$ , and the point of maximum (modified) electron density of one atom will be slightly displaced by the superposition of the modified densities of all others;  $\rho'_A(r)$  of a given atom will at most overlap nearest neighbours only, but  $\rho'_B(r)$  will overlap all others, although its effect diminishes with increasing separation of the atomic centres.

If two atoms 1 and 2 (fig. 295) are situated a distance  $d$  apart, the effect of the first is to displace the point of maximum electron density of the second by

$$\Delta d = -\frac{\left(\frac{\partial \rho_1'}{\partial r}\right)_{r=d}}{C_2}.$$

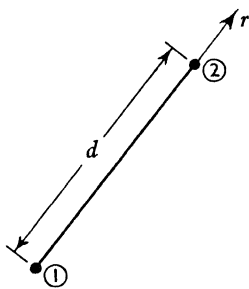


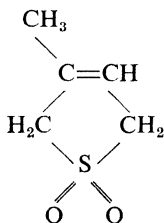
FIG. 295

$\rho'_1$  and  $\rho'_2$  are the modified electron densities of the first and second atom respectively, and  $C_2$  is the value of  $\frac{\partial^2 \rho'_2}{\partial r^2}$  at the centre of the second atom. For values of  $r$  greater than about 2 Å we can take  $\rho' = \rho'_B$ , and consequently

$$(\Delta d)_{\max} = \frac{2S_0^2 f_{01}}{C_2 r^2},$$

where  $f_{01}$  is the scattering factor of the first atom at  $S = S_0$ . The above results enable us to make an estimate of the importance of series-termination errors in practice. We see that the effect of one atom on the coordinates of another decreases rapidly with increasing separation of the atoms concerned, and that the coordinates of atoms of low atomic number in a structure are most affected by series termination, just as they are most affected by random errors in the coefficients. The presence in a structure of one atom of high atomic number will result in particularly large series-termination errors in the coordinates of other atoms, especially those which lie near the heavy atom. Series-termination errors are about the same in two-dimensional as in three-dimensional syntheses.

Taking dibenzyl as an example where the atoms are all of the same atomic number, but each peak is disturbed by the ripples from two or three others, the effect of terminating the series at  $S_0 = 1.07 \text{ Å}^{-1}$ , where  $f_0 = 0.32$  and  $f'_0 = 1.16$  for all atoms, would be to shorten a bond of length 1.54 Å by about 0.025 Å, while a benzene ring of side 1.385 Å would appear with each bond shortened by 0.01 Å. In dibenzyl, the combined effect of all other atoms is to change the maximum (modified) density in an atom of the benzene ring from 5.70  $e/\text{Å}^3$  to 6.00  $e/\text{Å}^3$ . A reinvestigation of the crystal structure of  $\beta$ -isoprene sulphone by Jeffrey (1951) showed that in this compound the mean coordinate error due to series termination was 0.02 Å, and the maximum 0.06 Å. These comparatively large errors are to be attributed mainly to the presence of a sulphur atom in the molecule:—



The standard deviation of the coordinate of a carbon atom, due to random errors of measurement, was only 0.016 Å, which emphasizes the relative importance of series termination errors. The discussion of series-termination errors, given above, is important from a theoretical

view, but fortunately simpler methods are available by means of which these systematic errors can be at least partially corrected. A well-known one is that first used by Bragg and West (1930). This consists of the introduction of a converging factor  $\phi(S)$ , which is chosen so as to reduce the coefficients at  $S=S_0$  to very small values. The modified density in a particular atom, as it appears when the coefficients  $\phi(S)F_0$  replace the coefficients  $F_0$  in the Fourier series, is related to the unmodified density by the equation.

$$\rho'(\mathbf{r}) = \int_V \rho(\mathbf{r} + \mathbf{R})\psi(\mathbf{R})dV,$$

where  $\psi(\mathbf{R})$  is the Fourier transform of  $\phi(S)$ . The form of the converging factor is usually taken to be

$$\phi(S) = \exp[-\alpha S^2];$$

its effect is then to modify the electron density in exactly the same way as it is modified by the temperature movement of the atoms, so that  $\phi$  is usually referred to as an artificial temperature factor. By choosing a sufficiently large value of  $\alpha$  ( $\sim 2$  in practice), series termination errors may be eliminated in the sense that each atom is no longer the centre of a modified density which extends over large distances. The overlapping of an atom by its nearest neighbours, to which reference has already been made, is however increased by the introduction of a converging factor, and a correction for this must be made, although it can scarcely be called a series-termination correction. Booth claims for this method that it is likely to reduce the effect of experimental errors. This will depend entirely on how the errors are distributed among the various  $F_0$ 's; for instance, if the  $F_0$ 's corresponding to large values of  $S$  have the largest standard deviations the introduction of a suitable converging factor will reduce the value of  $\sigma(x_n)$ . If, however, most of the coefficients are within the range for which the assumption  $\sigma(F_0) = K|F_0|$  is likely to be valid, the appropriate equation of table 288 predicts an increase in the value of  $\sigma(x_n)$  on decreasing the value of  $p$ , which is one of the effects of an artificial temperature factor.

A particularly simple method for the correction of atomic coordinates for the effect of series termination was suggested by Booth (1946*b*, 1947*b*). Corresponding to the  $F_0$  synthesis, an  $F_c$  synthesis is made using structure factors calculated from the coordinates given by the  $F_0$  synthesis, and assumed values of atomic scattering factors. The points of maximum electron density of the  $F_c$  synthesis will deviate by small amounts from the coordinates used to calculate the coefficients. These deviations, with reversed signs, are the corrections to the atomic coordinates. The accuracy of this method of correction, assuming that no errors are introduced by the method used to locate the points of maximum electron density, depends essentially on the

accuracy of the assumed atomic scattering factors, a point we shall discuss later. This method makes no correction to the electron density, but a way in which this can be done and coordinates corrected at the same time, was suggested by van Reijen (1942). This method consists in including, as Fourier coefficients, the values of  $F_c$  where experiment has not supplied the corresponding  $F_0$ 's. This gives for the electron density

$$\rho = \frac{1}{V} \sum_q F_0 \cos \Theta + \frac{1}{V} \sum_{q \neq q} F_c \cos \Theta,$$

where the notation indicates that  $q$  coefficients have been measured experimentally, and of the remainder all but  $Q - q$  are of negligible magnitude. This result may be rewritten as

$$\rho = \frac{1}{V} \sum_q (F_0 - F_c) \cos \Theta + \frac{1}{V} \sum_q F_c \cos \Theta,$$

or 
$$\rho = \frac{1}{V} \sum_q (F_0 - F_c) \cos \Theta + \rho_c^*,$$

where  $\rho_c^*$  is the electron distribution on which the calculated structure factors are based. Provided the actual and assumed atomic scattering factors coincide in the range  $S > S_0$ , this method will lead, apart from the effects of random errors in the  $F_0$ 's, to the correct atomic coordinates and electron distribution, when a sufficient number of successive syntheses have been calculated.

#### 4. THE USE OF THE $(F_0 - F_c)$ SYNTHESIS FOR ACCURATE STRUCTURE ANALYSIS

At the end of the last section we found that one method of correcting for series termination involved a synthesis whose coefficients were the values of  $(F_0 - F_c)$ . This synthesis has a number of properties which make it particularly useful in the final stages of a crystal-structure analysis. Its use in the earlier stages has already been described in Chapter 7. There is an unexpected connection between the results given by this synthesis and those obtained by minimization of  $R = \sum_q w(F_0 - F_c)^2$ , which we discussed earlier (Section 9.2.3). Let us consider the very similar function,

$$\phi_n = \sum_q \frac{1}{f_n} (F_0 - F_c)^2, \quad (298)$$

where  $f_n$  is, as before, the scattering factor of the  $n$ th atom. The coordinates which minimize  $\phi_n$  satisfy the conditions

$$\frac{\partial \phi_n}{\partial x_n} = \frac{\partial \phi_n}{\partial y_n} = \frac{\partial \phi_n}{\partial z_n} = 0.$$

That is, 
$$\sum_q \frac{1}{f_n} (F_0 - F_c) \frac{\partial F_c}{\partial x_n} = \dots = 0,$$
  
etc.

Now for a centrosymmetric structure,

$$F_c = 2 \sum_{n=1}^{N/2} f_n \cos \Theta_n,$$

$$\therefore \frac{\partial F_c}{\partial x_n} = -\frac{4\pi h}{a} f_n \sin \Theta_n,$$

and the condition  $\frac{\partial \phi_n}{\partial x_n} = 0$  becomes

$$-\frac{4\pi}{a} \sum_q h(F_0 - F_c) \sin \Theta_n = 0. \quad (299)$$

However, the function

$$D = \rho_0 - \rho_c = \frac{1}{V} \sum_q (F_0 - F_c) \cos \Theta$$

has a slope in the  $x$ -direction at the point  $(x_n, y_n, z_n)$  given by

$$\left( \frac{\partial D}{\partial x} \right)_n = -\frac{2\pi}{aV} \sum_q h(F_0 - F_c) \sin \Theta_n.$$

Comparison with equation 299 shows that the condition for  $\phi_n$  to be a minimum with respect to the coordinates of the  $n$ th atom is that  $\frac{\partial D}{\partial x}$ ,  $\frac{\partial D}{\partial y}$  and  $\frac{\partial D}{\partial z}$  should all vanish at  $(x_n, y_n, z_n)$ , the centre of this atom.

If the Fourier series is not terminated, the condition  $\left( \frac{\partial D}{\partial x} \right)_n = 0$  becomes  $\left( \frac{\partial \rho_0}{\partial x} \right)_n = 0$ , since it is clear that  $\left( \frac{\partial \rho_c}{\partial x} \right)_n = 0$  in these circumstances. In short, when the series is not terminated, taking the atomic coordinates of the  $n$ th atom at the corresponding point of maximum electron density of the  $F_0$  synthesis results in the minimization of  $\phi_n$ . We notice that this results in the minimization of a different function for each different kind of atom in the structure, but since the  $f$ -curves of all atoms are somewhat similar (section 3.2.5), the coordinates will not deviate significantly from those that would be obtained on minimizing

$$\phi = \sum_q \frac{1}{f} (F_0 - F_c)^2.$$

If the series is terminated, and contains only  $q$  of the  $Q$  terms of appreciable magnitude, taking the atomic coordinates as the points

of maximum electron density in  $\rho_0$  results in the minimization, not of

$$\sum_a \frac{1}{f} (F_0 - F_c)^2,$$

but of

$$\sum_a \frac{1}{f} (F_0 - F_c)^2 + \sum_{a-a} \frac{1}{f} F_c^2.$$

As we have seen, to minimize only the first term of this expression we must choose atomic coordinates which make the slope of  $D$  vanish at all atomic centres. The  $(F_0 - F_c)$  synthesis therefore leads to atomic coordinates which are exactly the same as would be given by the method of least squares, if in using the latter each observation were given the somewhat arbitrary weight  $w = \frac{1}{f}$ . It is not difficult to show

that the correcting methods of Booth and of van Reijen also lead to coordinates which minimize  $\phi$ ; the  $(F_0 - F_c)$  synthesis simply accomplishes this more conveniently.

When the slope of  $D$  is not zero at a point taken to be an atomic coordinate, the correction to this coordinate can be found as follows. We assume that in the neighbourhood of an atomic centre,  $\rho_0$  and  $\rho_c$  coincide in shape, but the points at which they reach a maximum differ by  $(\Delta x_n, 0, 0)$  (fig. 300). Simple geometrical considerations then show

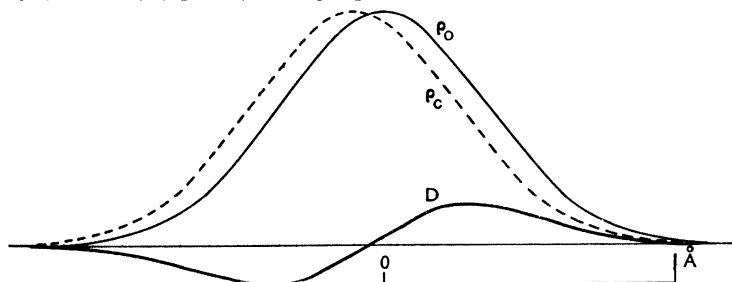


FIG. 300. A section through the projected electron density to show the appearance of  $D = \rho_0 - \rho_c$  when an atomic coordinate differs by  $0.1\text{\AA}$  from its correct value. The diagram represents an idealised situation in that the Fourier series from which the curves were obtained was not terminated, and the coefficients were free from experimental errors. This is true also of Figs. 302 and 303

that

$$\Delta x_n = - \left( \frac{\partial D}{\partial x} \right)_n \bigg/ \left( \frac{\partial^2 \rho_c}{\partial x^2} \right)_n. \quad (300)$$

From the definitions of  $D$ ,  $\rho_c$  and  $F_c$  it is readily shown that this result can also be written as

$$\Delta x_n = \frac{\sum_a \frac{1}{f_n} (F_0 - F_c) \frac{\partial F_c}{\partial x_n}}{\sum_n \frac{1}{f_n} \left( \frac{\partial F_c}{\partial x_n} \right)^2},$$



which is exactly the correction obtained by the method of least squares, or by Qurashi's modification of the method of steepest descents,

taking  $w = \frac{1}{f_n}$ .

In practice, equation 300 is best applied in the following way. On a two-dimensional ( $F_0 - F_c$ ) synthesis contours of constant  $D$  are drawn. The direction in which the  $n$ th atomic centre should be moved is perpendicular to the contour passing through this centre, and in the direction of increasing  $D$ . The magnitude of the correction is proportional to the gradient of  $D$  in this direction. In practice this is easily evaluated with sufficient accuracy from the separation of the contour lines of the ( $F_0 - F_c$ ) synthesis near the atomic centre. In equation 300,  $\left(\frac{\partial^2 \rho_c}{\partial x^2}\right)_n$  can be replaced by  $\left(\frac{\partial^2 \rho_0}{\partial x^2}\right)_n$ , which can be determined directly from the shape of the  $n$ th atom in the corresponding  $F_0$  synthesis. The approximation 279.4 again comes in useful here; by its use we find

$$\left(\frac{\partial^2 \rho_0}{\partial x^2}\right) = -2p\rho_0(x_n y_n z_n).$$

Hence finally we have the result that the centre of an atom should be moved a distance

$$\Delta r_n = \frac{\left(\frac{\partial D}{\partial r}\right)_n}{2p(\rho_0)_n},$$

where  $r$  denotes a distance measured in the direction in which  $D$  increases most rapidly. For example, if we find that at the centre of the  $n$ th atom, an  $F_0$  synthesis shows  $(\rho_0)_n = 10e/\text{\AA}^2$  and  $p = 5.0$ , while the ( $F_0 - F_c$ ) synthesis shows a slope of  $1.0e/\text{\AA}^3$  at this point, the centre of the atom should be moved by  $0.01 \text{ \AA}$  in the direction of maximum slope.

It would be difficult to apply this procedure in three dimensions. There it is likely to be more convenient to evaluate separately each of the quantities

$$\left(\frac{\partial D}{\partial x}\right)_n, \left(\frac{\partial D}{\partial y}\right)_n \text{ and } \left(\frac{\partial D}{\partial z}\right)_n$$

and apply equation 300 directly. If the crystallographic axes are not orthogonal, the corrections are the solutions of the equations

$$\left.\begin{aligned} \left(\frac{\partial^2 \rho_0}{\partial x^2}\right)_n \Delta x_n + \left(\frac{\partial^2 \rho_0}{\partial x \partial y}\right)_n \Delta y_n + \left(\frac{\partial^2 \rho_0}{\partial x \partial z}\right)_n \Delta z_n + \left(\frac{\partial D}{\partial x}\right)_n &= 0, \\ \text{etc.} \end{aligned}\right\}$$

It will be noticed that these are simply the equations 279.2 of Booth's differential Fourier method, with  $D$  replacing  $\rho_0$ .

When one or more successive corrections have reduced the values of  $\left(\frac{\partial D}{\partial x}\right)_n$ , etc., to zero at each atomic centre, the coordinates are free from series-termination errors, provided the values assumed for the  $f_n$ 's are correct. Cruickshank's discussion of the origin of series-termination errors, which has been outlined in section 9.3.3, shows, however, that if the true and assumed scattering factors have the same magnitude and slope at  $S=S_0$ , where the series is terminated,  $\rho_0$  and  $\rho_c$  will cancel one another in the  $(F_0 - F_c)$  synthesis except in the immediate neighbourhood of atomic centres. Only the coordinates of the nearest neighbours of the  $n$ th atom will be effected by assuming an incorrect value of  $f_n$  in the range  $S>S_0$ , provided that the values near  $S=S_0$  are correct. However, the  $(F_0 - F_c)$  synthesis does, to a considerable extent, show when incorrect values for  $f_n$  are being used. For instance, if the temperature-factor parameter  $B_n$  of an atom, defined by the equation

$$f_n = f_{0n} \exp \left[ -\frac{1}{4} B_n S^2 \right]$$

has been overestimated in magnitude,  $\rho_c$  in the neighbourhood of the  $n$ th atomic centre will be more diffuse than  $\rho_0$ , and  $D$  will exhibit the variation shown in fig. 302.

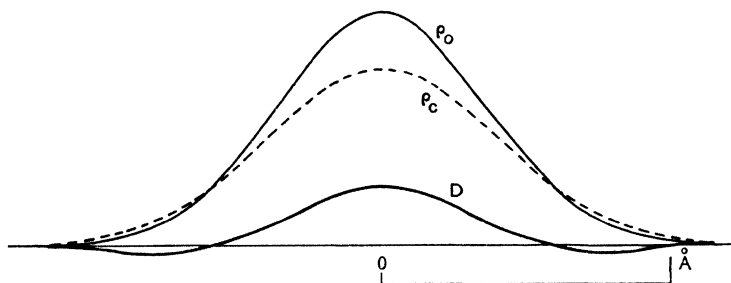


FIG. 302. A section through the projected electron density which shows the appearance of  $D = \rho_0 - \rho_c$  when the temperature factor parameter of an atom is incorrectly estimated

If the thermal vibration of an atom is anisotropic, but an isotropic scattering factor is assumed for this atom in the calculation of structure factors, contours of constant  $\rho_0$  and of constant  $\rho_c$  will be as shown in figs. 303(i) and 303(ii), while  $D$  will be as shown in fig. 304 (i).

More quantitative relationships have been given by Cochran (1951*a*). A reinvestigation of the crystal structure of adenine hydrochloride by Cochran (1951*b*) provides an example of the practical utilization of the properties of the  $(F_0 - F_c)$  synthesis. The projection of this crystal structure on (010) can be referred to a unit cell of dimensions  $a = 8.77 \text{ \AA}$ ,  $c = 9.73 \text{ \AA}$  and  $\beta = 114^\circ 15'$ , containing two molecules. Coordinates

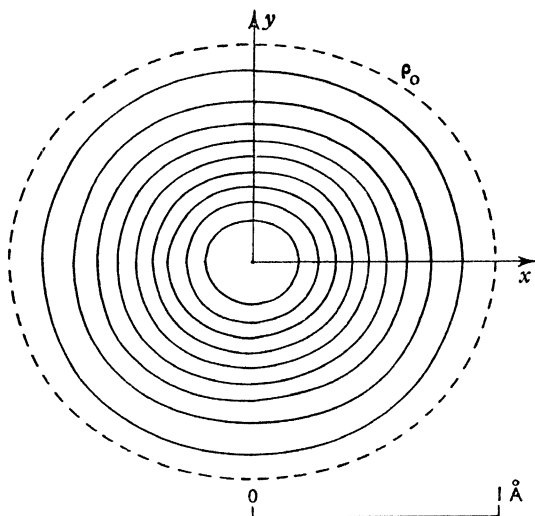


FIG. 303 (i). Contours of constant electron density in an atom whose thermal vibration is greater in the  $x$ - than in the  $y$ -direction

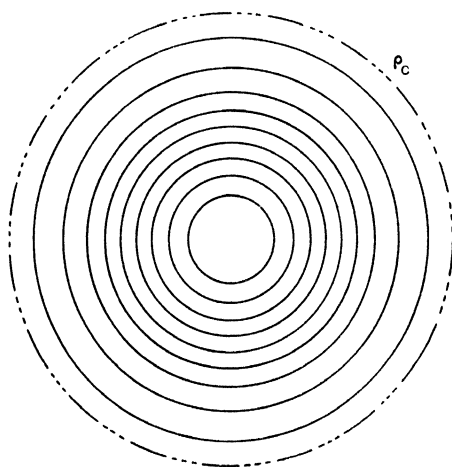


FIG. 303 (ii). Contours of constant electron density in an atom which has a corresponding isotropic thermal vibration. The contours may be taken to represent density increments of  $1e/\text{\AA}^2$ . The  $0.5e/\text{\AA}^2$  contour is dotted

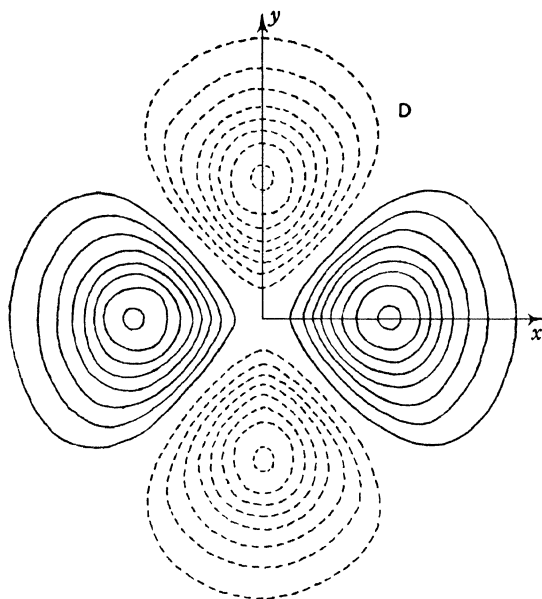


FIG. 304 (i). The difference of the electron densities shown in 303 (i) and 303 (ii). The contours represent density increments of  $0.05e/\text{\AA}^2$ . Contours are dotted where the function is negative

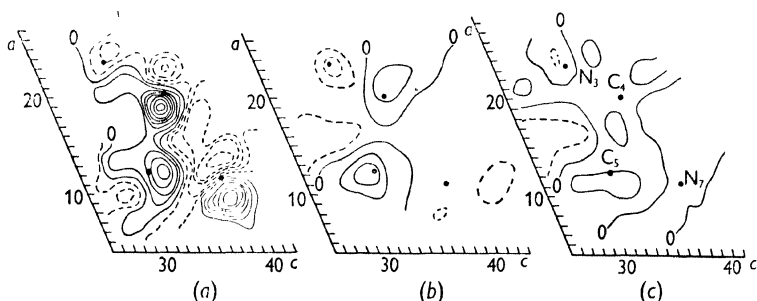


FIG. 304 (ii). (a) The appearance of  $D$  in a practical example. The atomic coordinates are indicated by dots. (b) The coordinates have now been corrected to eliminate the slope of  $D$  at atomic centres. (c) Temperature factor parameters have been chosen so as to make  $D$  approximately zero at the centre of each atom. Contours are drawn at an interval of  $0.25e/\text{\AA}^2$ , the zero contour is indicated by 0, and negative contours are dotted. Lines parallel to the  $a$  and  $c$  axes are subdivided into 60ths of  $a$  and  $c$  respectively (Cochran, 1951*b*)

were first obtained from photographically-recorded X-ray intensities, by means of an  $F_0$  synthesis. More accurate coefficients were subsequently obtained, and an  $(F_0 - F_c)$  synthesis calculated. The variation of  $D$  in the neighbourhood of certain atoms of the organic molecule is shown in fig. 304(ii)*a*. The centres of the atoms are indicated by dots, and all of them fall in regions where  $D$  has a large slope. Fig. 304(ii)*b* shows the fourth  $(F_0 - F_c)$  synthesis of a series, the coordinates having now been corrected to remove the slope of  $D$  at atomic centres. In fig. 304(ii)*c* the temperature-factor parameters have been adjusted to

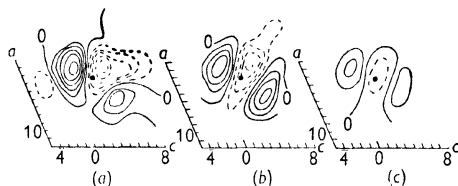


FIG. 305 (i). These diagrams show the gradual reduction of  $D$  in the neighbourhood of an atom as its coordinates and temperature factor parameters are corrected in a practical case. The shape of the function in (a) arises from a combination of the conditions illustrated in Figs. 300 and 304(i) (Cochran, 1951*b*)

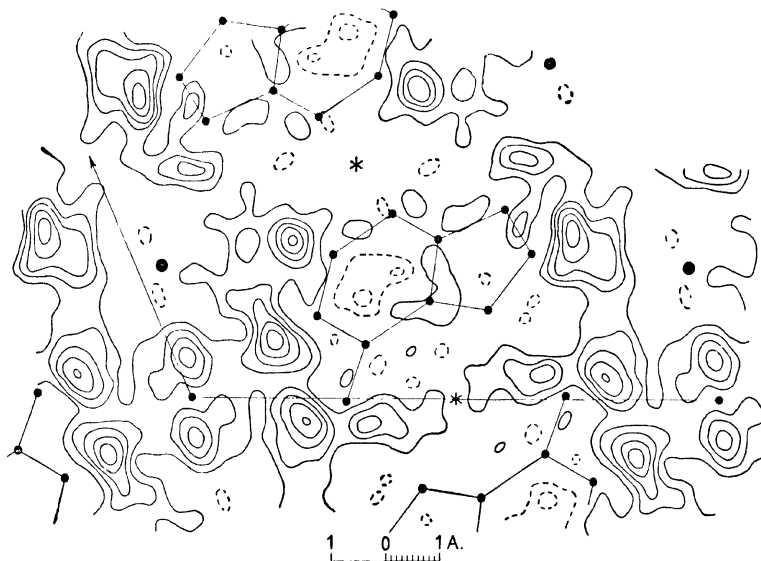


FIG. 305 (ii). Final  $(F_0 - F_c)$ —synthesis of adenine hydrochloride, showing the difference between the electron density projected on (010) and that calculated for isolated Cl, O, N and C atoms whose centres are indicated by dots. Contours are at 0.2, 0.4 ... 1.0  $e/\text{\AA}^2$ . The significant electron density maxima in this map are due to hydrogen atoms (Cochran, 1951*b*)

make  $D$  approximately zero at the centre of each atom. Fig. 305(i) shows the gradual reduction of  $D$  in the neighbourhood of the centre of the chlorine atom, as the coordinates and temperature-factor parameters are corrected. The final  $(F_0 - F_c)$  synthesis (the seventh) is shown in fig. 305(ii). All the significant electron-density maxima can be interpreted as hydrogen atoms. The latter were not detectable in the original  $F_0$  synthesis, because of series-termination errors, and the greater random errors of the photographically-recorded intensities.

Our lack of knowledge of the electron distribution in molecules compels us to use the scattering factors of individual isolated atoms for structure-factor calculations, and when atomic coordinates and temperature-factor parameters have been correctly chosen, the  $(F_0 - F_c)$  synthesis should show not only the positions of hydrogen atoms, but also the rearrangement of electrons consequent on chemical bonding. This application of the  $(F_0 - F_c)$  synthesis has recently been made by Brill (1950) to the case of diamond, but conclusive evidence on the extent of the electron redistribution in this and other compounds is not yet available. Since the electron density in a region near the nucleus of an atom will remain spherically symmetric when chemical bonds are formed, no difficulties arise in assuming that an atomic centre is a point of maximum electron density in an untruncated three-dimensional synthesis, but this is not necessarily true for a two-dimensional synthesis.

In principle the best atomic coordinates are not those which result in zero slope in the  $(F_0 - F_c)$  synthesis at atomic centres, and which therefore minimize  $\phi$ , but are those which result in a minimization of

$$R = \sum_q w(F_0 - F_c)^2,$$

with  $w$  correctly chosen for each observation. But just as  $\phi$  is associated with  $D$ , so is  $R$  associated with the function

$$D^1 = \frac{1}{V} \sum_q w f(F_0 - F_c) \cos \Theta,$$

for when  $R$  is a minimum,  $D^1$  has zero slope at atomic centres. The use of the function  $D^1$  to refine atomic coordinates is no different from the use of  $D$ , equation 300 for example being replaced by

$$\Delta x_n = - \left( \frac{\partial D^1}{\partial x} \right)_n / \left( \frac{\partial^2 \rho_c^1}{\partial x^2} \right)_n,$$

where

$$\rho_c^1 = \frac{1}{V} \sum_q w f F_c \cos \Theta.$$

In practice, however, the small improvement in the standard deviation of atomic coordinates which can be obtained by using the  $w f(F_0 - F_c)$  synthesis does not usually outweigh the other advantages of the

$(F_0 - F_c)$  synthesis, such as the ability of the latter to show electron density details which may be significant. When the agreement between calculated and observed structure factors is much worse for a few reflexions of comparatively great intensity than it is for all others, it is quite legitimate to give these observations zero weight by omitting the corresponding terms from the  $(F_0 - F_c)$  synthesis, on the grounds that the large deviations are probably caused by the effects of extinction. Whether terms corresponding to accidentally-absent reflexions should also be omitted will depend on the relative accuracy of such measurements. When intensities have been measured photographically, and particularly if a very small crystal or one containing only atoms of low atomic number has been used,  $\sigma(F_0)$  is likely to be larger when  $F_0 = 0$  than when  $F_0$  has a moderate value. Certainly if a large number of reflexions in the higher ranges of  $S$  are not observed experimentally the corresponding terms should be omitted from the  $(F_0 - F_c)$  synthesis. It must be remembered that when terms of the  $(F_0 - F_c)$  synthesis have been given reduced weight, one must be cautious in attaching significance to any electron-density detail which the synthesis may show.

## 5. THE ASSESSMENT OF THE ACCURACY OF A STRUCTURE DETERMINATION

Proper assessment of the limits of error of physical measurements is rightly emphasized by all teachers of the physical sciences, but the latter are themselves liable to be overoptimistic when discussing the accuracy of their own results. This has been particularly true of crystal-structure measurements of the kind we have been discussing in this chapter, mainly because there has been no accepted procedure by which the limits of error could be estimated. The standard deviations of electron density and atomic coordinates have been derived in section 9.3.2, but are given in terms of  $\sigma(F_0)$ , of which no very reliable estimate can generally be made in practice. It is clear that the agreement between calculated and observed structure factors is to some extent a measure of the accuracy of final results, and it has become customary to take

$$R_1 = \sum_q |F_0 - F_c| / \sum_q |F_0|$$

as a sort of 'reliability index'. It is an unsatisfactory index, however, in that we cannot say, for instance, that a particular value of  $R_1$  corresponds to a particular standard deviation of an atomic coordinate. A formula given by Booth (1945*b*) relates the value of

$$R_2 = \sum_q (F_0 - F_c)^2 / \sum_q F_0^2$$

to  $\sigma(x_n)$ , but is based on incorrect assumptions. Formulae for the

same purpose have been derived by Hughes and Lipscomb (1946) and by Cruickshank (1949*a*). Cruickshank's formulae are

$$\sigma(\rho_0) = \frac{1}{V} \left\{ \sum_q (F_0 - F_c)^2 \right\}^{\frac{1}{2}} \quad (308.1)$$

and 
$$\sigma(x_n) = \frac{2\pi \left\{ \sum_q h^2 (F_0 - F_c)^2 \right\}^{\frac{1}{2}}}{aVC_n}, \quad (308.2)$$

where  $C_n$  is the central curvature,  $\frac{\partial^2 \rho_c}{\partial x^2}$ , at the centre of the  $n$ th atom.

It may readily be shown that Cruickshank's equations 308.1 and 308.2 may be written

$$\sigma(\rho_0) = \{\bar{D}^2\}^{\frac{1}{2}} \quad (308.3)$$

and 
$$\sigma(x_n) = \left\{ \left( \frac{\partial \bar{D}}{\partial x} \right)^2 \right\}^{\frac{1}{2}} / C_n, \quad (308.4)$$

where  $D = \rho_0 - \rho_c$ , as before, and the averages are taken over the whole unit cell, or projected area of the unit cell. This is a more illuminating approach to the problem; clearly  $\sigma(\rho_0)$  is more likely to be found directly from a comparison of calculated and observed electron densities than by comparing corresponding sets of structure factors. This suggests that the final  $(F_0 - F_c)$  synthesis of a series can be used to assess the accuracy of the results obtained from it. This is indeed the case, and we may adopt one of two possible procedures to assess the standard deviation of the electron density. (a) We may take  $\sigma(\rho_0) = \{\bar{D}^2\}^{\frac{1}{2}}$  where the average is over the whole unit cell. The result obtained will be identical with that given by equation 308.1. The value of  $\sigma(\rho_0)$  obtained in this way is likely to be a slight overestimate, since no distinction is made between values of  $D$  which are due to experimental errors or residual series-termination errors, and those which are due to a real redistribution of electrons. (b) We may make use of the result mentioned in section 9.3.2, that  $\sigma(\rho_0)$  is approximately the same at all points of the unit cell (an assumption which is also implicit in Cruickshank's formula), and the fact that there is always a large number of points in the unit cell of a crystal for which the true value of  $\rho$ , and therefore of  $D$ , is zero. On these assumptions, we take  $\sigma(\rho_0) = \{\bar{D}^2\}^{\frac{1}{2}}$ , where the average is now taken only over points where the expected value of  $D$  is zero. The result obtained in this way may be a slight underestimate.

Corresponding procedures can be used to obtain  $\sigma(x_n)$ . As we have seen, any differences between  $\sigma(x_n)$ ,  $\sigma(y_n)$  and  $\sigma(z_n)$  are not significant, at least when the atom is spherically symmetric.

Formulae 308.1, 308.2, 308.3 and 308.4 require amendment in the following circumstances:



(a) If the structure does not have a centre of symmetry, each value of  $\sigma(\rho_0)$  or  $\sigma(x_n)$  given by the formulae must be increased by a factor of two (Cruickshank, 1950*b*). If the structure is not centrosymmetric, but certain of its projections on planes or on lines are centrosymmetric, the factor has some value intermediate between one and two (Shoemaker, Donohue, Schomaker and Corey, 1950).

(b) If the number  $v$  of unknown parameters is not much less than the number  $u$  of independent  $F_0$  values, each estimate of  $\sigma(x_n)$  should be increased by a factor  $\left\{ \frac{u}{u-v} \right\}^{\frac{1}{2}}$  (Cruickshank, 1949*b*).

(c) If certain terms have been given reduced weight the curvature  $C_n$  must be derived from an F synthesis in which the same terms are given the same reduced weight. For example, if any terms corresponding to reflections either inside or outside the limiting sphere have been omitted from the  $(F_0 - F_c)$  synthesis, the same terms should be omitted from the corresponding F synthesis from which the curvature is determined. It does not matter whether an  $F_0$  or an  $F_c$  synthesis is used for this purpose, provided that this rule is observed.

The standard deviation of the length of a bond between two atoms is given by the relation

$$\sigma^2(d_{12}) = \sigma^2(x_1) + \sigma^2(x_2),$$

or  $\sigma(d_{12}) = \sqrt{2}\sigma(x_1)$  when the atoms are the same. If the atoms are related by a mirror plane, or a centre of symmetry,

$$\sigma(d_{12}) = 2\sigma(x_1),$$

and other amendments must be made to deal, for example, with atoms in special positions.

The importance of applying proper significance tests before drawing conclusions from a comparison of two measurements both of which are subject to error, has been emphasized by Cruickshank, who considers the following example. A bond length A, standard deviation  $\sigma(A)$ , is determined as greater than a bond length B, standard deviation  $\sigma(B)$ , by an amount  $\delta l$ . Is there a real difference between A and B or not? Cruickshank suggests the adoption of the following numerical significance levels, where P is the probability that A could be at least  $\delta l$  greater than B by chance, and  $\sigma^2 = \sigma^2(A) + \sigma^2(B)$ .

If  $P \geq 5\%$ ,  $\delta l \leq 1.645\sigma$ , the difference is not significant.

If  $5\% > P > 1\%$ ,  $2.327\sigma > \delta l > 1.645\sigma$ , the difference is possibly significant.

If  $1\% > P > 0.1\%$ ,  $3.090\sigma > \delta l > 2.327\sigma$ , the difference is significant.

For instance, when all atoms concerned have  $\sigma(x) = 1.5 \times 10^{-2}$  Å, bond length differences of less than  $5 \times 10^{-2}$  Å are not significant. Undoubtedly a great deal of space in crystallographic papers has been devoted to the explanation of smaller differences when the standard deviation was larger than in this example. It is suggested

that X-ray crystallographers should estimate the standard deviations of their results, using numerically specified levels of significance in comparing them.

## 6. SUMMARY

The usual object of the X-ray analysis of a crystal is the measurement of the lengths of the bonds between certain atoms in the crystal; less frequently it is the measurement, with some accuracy, of the electron distribution in the crystal. Of these two problems the first is the more easily solved, because atoms in crystals are so nearly spherically symmetric, and their atomic scattering factors are known with reasonable accuracy. When so much is known in advance about the 'shape' of the atoms in the crystal concerned, accurate atomic coordinates can be derived from an accurate set of experimental measurements which is incomplete in that structure factors which cannot be measured because of the experimental arrangement, or whose magnitudes lie outside a certain range of values, are excluded. This is not true of measurements of the electron density, when a complete set of intensity measurements is required, at least in the range where the atomic scattering factors of the atoms concerned are not known with high accuracy.

The 'best' atomic coordinates are, according to the theory of errors, those which result in a minimization of the quantity

$$R = \sum_q w(F_0 - F_c)^2,$$

where the weight allotted to each observation depends on the accuracy with which it was made. If a particular structure factor has not been measured at all, or if the measurement is for some reason considered to be very inaccurate, the weight  $w$  is taken to be zero. Starting from approximate values, atomic coordinates may be varied systematically, so as to minimize  $R$ , by a number of methods which, although apparently quite different, are in fact closely related. The method of least squares leads, in certain circumstances, to results which are identical with those given by a modification of Booth's application of the method of steepest descents to this problem. Again, if we impose on the function

$$D^1 = \frac{1}{V} \sum_q (F_0 - F_c) w \hat{f} \cos \theta$$

the condition that its first derivative should be zero at points which coincide with the centres of atoms, the function  $R$  is minimized. The form of  $D^1$  at any stage of the approximation to the final coordinates can be used to minimize  $R$  systematically.

In practice use of the function

$$D = \frac{1}{V} \sum_q (F_0 - F_c) \cos \theta$$

is often to be preferred. Although it does not give the correct weight to each observation, it has the great advantage that, when a reasonably complete set of measurements has been made within a certain range, it may show not only when the assumed coordinate of an atom is incorrect, but also when the assumed value of the atomic scattering factor is incorrect. This function can be used, therefore, not only to derive accurate bond lengths, but also for accurate electron-density measurement. The standard deviations of results obtained from it are very easily estimated.



## APPENDICES

APPENDIX I

TABLES OF WAVE-LENGTHS

IN ÅNGSTRÖM UNITS

(from Acta Cryst. 1950, 3, 400)

Element	$K\alpha_1$	$K\alpha_2$	$K\alpha$ (wtd. mean)	$K\beta$
Cr	2·28962	2·29351	2·2909	2·08480
Mn	2·10175	2·10569	2·1031	1·91015
Fe	1·93597	1·93991	1·9373	1·75653
Co	1·78892	1·79278	1·7902	1·62075
Ni	1·65784	1·66169	1·6591	1·50010
Cu	1·54051	1·54433	1·5418	1·39217
Zn	1·43511	1·43894	1·4364	1·29522
Mo	0·70926	0·71354	0·7107	0·63225
Rh	0·61325	0·61761	0·6147	0·54559
Pd	0·58542	0·58980	0·5869	0·52052
Ag	0·55936	0·56378	0·5608	0·49701

## APPENDIX II RADII OF THE ELEMENTS

Element	Ionic Å	Covalent, Metallic Å	Element	Ionic Å	Covalent, Metallic Å
Ag	1.0	1.45	Mo	0.65	1.4
Al	0.55	1.3	N	1.5	0.7
As <sup>5+</sup>	0.6	} 31.	Na	0.95	1.9
As <sup>3-</sup>	2.0		Ni	0.7	1.2
Au	1.4	1.4	O	1.35	0.65
B	0.2	0.9	Os	0.65	1.3
Ba	1.35	2.2	P	2.0	1.1
Be	0.75	1.1	Pd		1.35
Bi <sup>3+</sup>	1.2	} 1.6	Pb <sup>4+</sup>	0.7	} 1.6
Bi <sup>3-</sup>	2.1		Pb <sup>2+</sup>	1.2	
Br	1.95	1.15	Pt	0.5	1.35
C		0.7	Rb	1.5	2.5
Ca	1.0	1.3	Rh	0.7	1.3
Ca(met.)		1.9	Ru	0.6	1.3
Cd	1.0	1.5			
Ce	1.0	1.8	S <sup>6+</sup>	0.3	} 1.05
Cl <sup>7+</sup>	0.3	} 1.0	S <sup>2-</sup>	1.85	
Cl <sup>1-</sup>	1.8		Sb <sup>3+</sup>	0.9	} 1.45
Co	0.7	1.25	Sb <sup>3-</sup>	2.1	
Cr	0.6	1.25	Sc	0.8	1.65
Cs	1.7	2.7	Se	1.9	1.25
Cu	0.6	1.25	Si	0.4	1.2
F	1.35	0.65	Sn <sup>4+</sup>	0.7	} 1.5
Fe	0.7	1.25	Sn <sup>2+</sup>	1.0	
Ga	0.6	1.3	Sr	1.15	2.15
Ge	0.6	1.3	Ta		1.45
H	1.3	0.3	Te <sup>4+</sup>	0.8	} 1.4
Hg	0.7	1.5	Te <sup>2-</sup>	2.1	
I	2.2	1.3	Th	1.1	1.8
In	0.9	0.5	Ti	0.7	1.4
Ir	0.65	1.3	Tl <sup>3+</sup>	1.0	} 1.8
K	1.3	2.3	Tl <sup>1+</sup>	1.5	
Li	0.6	1.6	U	1.05	1.45
Mg	0.7	1.5	V	0.6	1.35
Mn	0.65	1.4	W	0.7	1.4
			Zn	0.8	1.35
			Zr	0.8	1.6

Some other important values: Van der Waals' radius 1.7 Å; Hydrogen bond 2.75 Å when only C, N and O are involved.

These radii are not accurate, and are intended only to be used as a guide in the initial stages of a structure determination.

An extensive table of molecular dimensions and configurations is given by Allen & Sutton (1950).

## APPENDIX III

### TRANSFORMATION OF AXES AND ATOMIC PARAMETERS

We sometimes, as in section 2.2.1, wish to choose a new unit cell for a crystal, and to find the new values of parameters of the atoms. Suppose that the original axes are **a**, **b** and **c**, and that the new axes **a'**, **b'** and **c'** are related to them by the equations

$$\begin{aligned}\mathbf{a}' &= x_1\mathbf{a} + y_1\mathbf{b} + z_1\mathbf{c}, \\ \mathbf{b}' &= x_2\mathbf{a} + y_2\mathbf{b} + z_2\mathbf{c}, \\ \mathbf{c}' &= x_3\mathbf{a} + y_3\mathbf{b} + z_3\mathbf{c}.\end{aligned}$$

Then, if **r** is the vector to the point *xyz* in the old coordinates, which has parameters *x'y'z'* in the new coordinates,

$$\begin{aligned}\mathbf{r} &= x\mathbf{a} + y\mathbf{b} + z\mathbf{c} \\ &= x'\mathbf{a}' + y'\mathbf{b}' + z'\mathbf{c}' \\ &= x'(x_1\mathbf{a} + y_1\mathbf{b} + z_1\mathbf{c}) + y'(x_2\mathbf{a} + y_2\mathbf{b} + z_2\mathbf{c}) + z'(x_3\mathbf{a} + y_3\mathbf{b} + z_3\mathbf{c}),\end{aligned}$$

whence

$$\begin{aligned}x'x_1 + y'x_2 + z'x_3 &= x, \\ x'y_1 + y'y_2 + z'y_3 &= y, \\ x'z_1 + y'z_2 + z'z_3 &= z.\end{aligned}$$

The solutions of these equations are:

$$x' = \frac{\begin{vmatrix} x & x_2 & x_3 \\ y & y_2 & y_3 \\ z & z_2 & z_3 \end{vmatrix}}{\Delta}, \quad y' = \frac{\begin{vmatrix} x_1 & x & x_3 \\ y_1 & y & y_3 \\ z_1 & z & z_3 \end{vmatrix}}{\Delta}, \quad z' = \frac{\begin{vmatrix} x_1 & x_2 & x \\ y_1 & y_2 & y \\ z_1 & z_2 & z \end{vmatrix}}{\Delta},$$

where

$$\Delta = \begin{vmatrix} x_1 & x_2 & x_3 \\ y_1 & y_2 & y_3 \\ z_1 & z_2 & z_3 \end{vmatrix}.$$

These equations give the new parameters in terms of the old.

Thus, in the example quoted in section 2.2.1,

$$\Delta = \begin{vmatrix} -\frac{3}{2} & 0 & 1 \\ 1 & 0 & 1 \\ -\frac{1}{2} & 2 & 0 \end{vmatrix} = 5,$$



and so

$$x' = \frac{\begin{vmatrix} x & 0 & 1 \\ y & 0 & 1 \\ z & 2 & 0 \end{vmatrix}}{\Delta} = \frac{-2x+2y}{5},$$

$$y' = \frac{\begin{vmatrix} -\frac{3}{2} & x & 1 \\ 1 & y & 1 \\ -\frac{1}{2} & z & 0 \end{vmatrix}}{\Delta} = \frac{-x+y+5z}{10},$$

and

$$z' = \frac{\begin{vmatrix} -\frac{3}{2} & 0 & x \\ 1 & 0 & y \\ -\frac{1}{2} & 2 & z \end{vmatrix}}{\Delta} = \frac{2x+3y}{5}.$$

## APPENDIX IV

### ARRANGEMENT OF SPACE-GROUP DATA IN THE INTERNATIONAL TABLES (1935)

1. Space-group symbol in Schönflies and abbreviated Hermann-Mauguin notations.
2. Punktlagen—equivalent points (*a*), (*b*), (*c*), ... , in order of increasing multiplicity.
3. Punktsymmetrie—the symmetries of the various special positions.
4. Gitterkomplexe—the space group of each set of equivalent positions. For example, the positions (*a*) in space group No. 52  $D_{2h}^6$ ,  $Pnna$ , are 000;  $\frac{1}{2}00$ ;  $0\frac{1}{2}\frac{1}{2}$ ;  $\frac{1}{2}\frac{1}{2}\frac{1}{2}$ . These define a unit cell with *a* halved, and are the (*a*) positions in the space group No. 65,  $Cmmm$ .
5. Weitere Symmetrieelemente—the symmetry elements which do not lead to special positions.
6. Untergruppen (sub-groups)—the space groups which contain only part of the symmetry of the space group concerned.
7. Strukturfaktor—the general expressions for the A and B parts of the structure factor for one set of unit atoms in general positions.
8. Auslöschungen—systematic absences for the general positions and each set of special positions.
9. Diagrams of general positions and of symmetry elements, with the following convention of axes:

$$\begin{array}{c}
 b \\
 \hline
 a \mid c \text{ upwards}
 \end{array}$$

## APPENDIX V

### ARRANGEMENT OF SPACE-GROUP DATA IN THE INTERNATIONAL TABLES (1952)

1. Number of space group, Hermann-Mauguin symbol, and Schönflies symbol.
  2. Diagrams of general equivalent points and symmetry elements with the same convention of axes as in the 1935 tables.
  3. Position of the origin with respect to the symmetry elements.
  4. Coordinates of general and special equivalent positions, in order of decreasing multiplicity (i.e. general positions first). On the left-hand side are also given the multiplicity, the Wyckoff symbol for the set, and the symmetry of each set of coordinates; on the right-hand side are given the systematic absences.
- 

The formulae for structure factors and the electron densities are given in a separate part of the tables, arranged in the following way:

5. Number of space group, Hermann-Mauguin symbol and Schönflies symbol.
6. Position of the origin with respect to the symmetry elements.
7. General equivalent positions.
8. General expressions for the A and B parts of the structure factor, for one set of unit atoms in general positions.
9. General relationships between the structure factors, if any.
10. Structure-factor formulae for reflexions of different types (e.g.  $h+k$  even,  $h+k$  odd), together with relationships between the structure factors for each type of reflexion, if these relationships are not all the same (see (9)).
11. Electron-density formulae, the summations being given for the different types of reflexions (see (10)).

## APPENDIX VI

### STRUCTURE-FACTOR MACHINES AND DEVICES

1. *Graphical methods.* Bunn (1945, p. 270) has described a slide rule which gives  $\cos 2\pi(hx + ky + lz)$  in terms of  $hx + ky + lz$ . For fixed values of two indices, say  $h$  and  $k$ , the instrument can be rapidly adjusted to give values of  $\cos 2\pi(hx + ky + lz)$  for consecutive values of  $l$ , and so is of considerable value for use in conjunction with tabular methods (section 3.2.1). The slide rule has to be reset when the end is reached, and Hägg (1950) has described a circular form that does not suffer from this defect.

Hargreaves (1953) has devised an instrument that is based on the structure-factor graphs (section 3.3.2) and can be used for reflexions with one index zero. A chart having the form of a number of unit cells of the 100 structure-factor graph (both  $\cos 2\pi(x + y)$  and  $\cos 2\pi x \cos 2\pi y$  are available) is placed below two perpendicular sets of wires; each set has a uniform spacing, which can be varied. Each atom is dealt with separately: the spacings of the two sets of wires are so adjusted that they correspond to  $x$  and  $y$ , and thus the intersection of the  $h$ th wire of one set and the  $k$ th wire of the other will have co-ordinates  $hx$  and  $ky$ ; the value of the function at this point can then be read from the chart. This instrument is again particularly useful in conjunction with tabular methods.

The foregoing instruments, however, are of little use for dealing with individual reflexions. For this purpose, Vand (1948*a*) has described a device which makes use of the principles of graphical summation of vectors, and gives the value of the structure factor from a knowledge of the quantities  $hx + ky + lz$  for the various atoms; the necessity for deriving these quantities would however appear to slow down the operation somewhat.

An ingenious way of systematically deriving the required values of  $hx + ky + lz$  is described by Donnay (1949). The three parameters  $x$ ,  $y$  and  $z$  for one atom, and the three indices  $h$ ,  $k$ ,  $l$  are each combined into single expressions,

$$X = x \times 10^{-6} + y \times 10^{-3} + z,$$

$$H = h \times 10^6 + k \times 10^3 + l.$$

Then

$$HX = 10^6(hz) + 10^3(kz + hy) + (hx + ky + lz) \\ + 10^{-3}(ly + kx) + 10^{-6}(lx).$$

If  $x$ ,  $y$  and  $z$  are given to not more than three decimal places, these

five terms will not overlap appreciably, and so the middle term can be easily picked out. For example, if  $x=0.789$ ,  $y=0.456$  and  $z=0.123$ ,

$$X=0.123,455,789.$$

(Note that the sixth place is a 5, because  $X$  must have 6 in this position when expressed to six decimal places.)

For the 123 reflexion,  $H=1,002,003$ , and thus

$$HX=123703.070945367.$$

The required value is given by the three figures following the decimal point, 0.071. The correct value is 0.070.

Although this process looks cumbersome, it is well suited to the operation of a calculating machine.

2. *Planimeter-type machines.* If a wheel, in contact with a surface, is moved through a given distance, the axle will turn through an angle proportional to the distance. This property is the basis of a machine devised by Evans and Peiser (1942). In this machine the wheel has a fixed horizontal axis, and rests on a horizontal disc; if this latter rotates, the former rotates through an angle proportional to the distance of the point of contact from the centre of the horizontal disc and to the angle of rotation of the disc. This angular rotation can be made in multiples of one complete rotation, the multiples corresponding to an index, say  $h$ ; the position of the vertical wheel can be adjusted to correspond with a parameter,  $x$ . A similar set-up can be made to give values of  $ky$ , and the two combined to give  $hx+ky$ ; a simple mechanical contrivance then gives  $\cos 2\pi(hx+ky)$ , which can be read on a scale.

The device can thus give, without any limit, the values required for systematic calculation. By having one unit for each atom it would be possible for complete sets of structure factors to be derived, but, until such a machine has been constructed, the device must be considered only as an aid to computation.

Booth (1947c) has made use of a similar principle; a wheel has a horizontal axis, which is pivoted about a fixed point, so that the wheel can trace out a circular path with any given radius. If the circular path has a length proportional to  $\cos 2\pi(hx+ky+lz)$  and its radius is proportional to  $f$ , the angle through which the wheel moves is proportional to  $f \cos 2\pi(hx+ky+lz)$ . Thus the reflexions can be treated individually, as in Vand's method. A scale allows values of  $\cos 2\pi(hx+ky+lz)$  to be obtained directly by setting a pointer to the appropriate value of  $hx+ky+lz$ , but the necessity of deriving these values beforehand is still a drawback.

3. *Harmonic analysers.* Some thought has been given to the application of the principle of the Kelvin tide predictor to crystallographic

computations. The principle is quite simple; if a tape, fixed at one end, passes successively over a number of pulleys moving with simple harmonic motion, the free end will trace out the sum of the separate motions. Nevertheless, the construction of accurate tide predictors has proved to be extremely costly, and this fact has tended to discourage attempts to apply the principle to the construction of a cheap laboratory instrument.

Booth (1948, p. 76) has described such a machine, and Vand (1949*b*, 1950) has developed a rather simpler model, in which standard 'Meccano' parts are used except where accuracy is essential. The movements of the pulleys are produced by what Vand calls a 'multiplier bar'—a bar to which strings are attached, each representing an atomic parameter, say  $x$ . The bar is pivoted about a fixed point, and so movement of the bar produces a movement of a string proportional to the distance from the pivot of the point of attachment of the string. If values of, say,  $ky$  are initially set in the machine, the movement of the multiplier bar  $h$  times will add  $hx$  for each atom. The machine thus gives a set of structure factors for the expression  $\cos 2\pi(hx + ky)$ , in rows with constant  $h$ .

4. *Analogue machines.* The term 'analogue machine' is applied to machines in which the quantity to be measured is equated to some other type of physical quantity which is more conformable to instrument design. Cox (1939), for example, suggested representing scattering factors by condensers, and the cosine functions by electric potentials; the charge on each condenser would then be proportional to  $f \cos 2\pi(hx + ky)$ , for  $hk0$  reflexions, and the summation could be made by passing the total charge through a ballistic galvanometer.

Lipson and Taylor (1949) have suggested the use of the Huggins' masks (section 4.5.1) for producing the required cosine function for  $hk0$  reflexions, and photocells for representing the scattering factors; Woolfson (1951) has described a further development of this idea.

$x$ $(0 - \frac{1}{4})$	$\cos 2\pi x$	$x$ $(\frac{3}{4} - 1)$	$x$ $(\frac{1}{4} - \frac{1}{2})$	$\cos 2\pi x$	$x$ $(\frac{1}{2} - \frac{3}{4})$
0.000	1.000	1.000	0.250	0.000	0.750
0.005	1.000	0.995	0.255	<u>0.031</u>	0.745
0.010	0.998	0.990	0.260	<u>0.063</u>	0.740
0.015	0.996	0.985	0.265	<u>0.094</u>	0.735
0.020	0.992	0.980	0.270	<u>0.125</u>	0.730
0.025	0.988	0.975	0.275	<u>0.156</u>	0.725
0.030	0.982	0.970	0.280	<u>0.187</u>	0.720
0.035	0.976	0.965	0.285	<u>0.218</u>	0.715
0.040	0.969	0.960	0.290	<u>0.249</u>	0.710
0.045	0.960	0.955	0.295	<u>0.279</u>	0.705
0.050	0.951	0.950	0.300	<u>0.309</u>	0.700
0.055	0.941	0.945	0.305	<u>0.339</u>	0.695
0.060	0.930	0.940	0.310	<u>0.368</u>	0.690
0.065	0.918	0.935	0.315	<u>0.397</u>	0.685
0.070	0.905	0.930	0.320	<u>0.426</u>	0.680
0.075	0.891	0.925	0.325	<u>0.454</u>	0.675
0.080	0.876	0.920	0.330	<u>0.482</u>	0.670
0.085	0.861	0.915	0.335	<u>0.509</u>	0.665
0.090	0.844	0.910	0.340	<u>0.536</u>	0.660
0.095	0.827	0.905	0.345	<u>0.562</u>	0.655
0.100	0.809	0.900	0.350	<u>0.588</u>	0.650
0.105	0.790	0.895	0.355	<u>0.613</u>	0.645
0.110	0.770	0.890	0.360	<u>0.637</u>	0.640
0.115	0.750	0.885	0.365	<u>0.661</u>	0.635
0.120	0.729	0.880	0.370	<u>0.684</u>	0.630
0.125	0.707	0.875	0.375	<u>0.707</u>	0.625
0.130	0.684	0.870	0.380	<u>0.729</u>	0.620
0.135	0.661	0.865	0.385	<u>0.750</u>	0.615
0.140	0.637	0.860	0.390	<u>0.770</u>	0.610
0.145	0.613	0.855	0.395	<u>0.790</u>	0.605
0.150	0.588	0.850	0.400	<u>0.809</u>	0.600
0.155	0.562	0.845	0.405	<u>0.827</u>	0.595
0.160	0.536	0.840	0.410	<u>0.844</u>	0.590
0.165	0.509	0.835	0.415	<u>0.861</u>	0.585
0.170	0.482	0.830	0.420	<u>0.876</u>	0.580
0.175	0.454	0.825	0.425	<u>0.891</u>	0.575
0.180	0.426	0.820	0.430	<u>0.905</u>	0.570
0.185	0.397	0.815	0.435	<u>0.918</u>	0.565
0.190	0.368	0.810	0.440	<u>0.930</u>	0.560
0.195	0.339	0.805	0.445	<u>0.941</u>	0.555
0.200	0.309	0.800	0.450	<u>0.951</u>	0.550
0.205	0.279	0.795	0.455	<u>0.960</u>	0.545
0.210	0.249	0.790	0.460	<u>0.969</u>	0.540
0.215	0.218	0.785	0.465	<u>0.976</u>	0.535
0.220	0.187	0.780	0.470	<u>0.982</u>	0.530
0.225	0.156	0.775	0.475	<u>0.988</u>	0.525
0.230	0.125	0.770	0.480	<u>0.992</u>	0.520
0.235	0.094	0.765	0.485	<u>0.996</u>	0.515
0.240	0.063	0.760	0.490	<u>0.998</u>	0.510
0.245	0.031	0.755	0.495	<u>1.000</u>	0.505
0.250	0.000	0.750	0.500	<u>1.000</u>	0.500

$x$ (0— $\frac{1}{4}$ )	$\sin 2\pi x$	$x$ ( $\frac{1}{4}$ — $\frac{1}{2}$ )	$x$ ( $\frac{1}{2}$ — $\frac{3}{4}$ )	$\sin 2\pi x$	$x$ ( $\frac{3}{4}$ —1)
0.000	0.000	0.500	0.500	0.000	1.000
0.005	0.031	0.495	0.505	0.031	0.995
0.010	0.063	0.490	0.510	0.063	0.990
0.015	0.094	0.485	0.515	0.094	0.985
0.020	0.125	0.480	0.520	0.125	0.980
0.025	0.156	0.475	0.525	0.156	0.975
0.030	0.187	0.470	0.530	0.187	0.970
0.035	0.218	0.465	0.535	0.218	0.965
0.040	0.249	0.460	0.540	0.249	0.960
0.045	0.279	0.455	0.545	0.279	0.955
0.050	0.309	0.450	0.550	0.309	0.950
0.055	0.339	0.445	0.555	0.339	0.945
0.060	0.368	0.440	0.560	0.368	0.940
0.065	0.397	0.435	0.565	0.397	0.935
0.070	0.426	0.430	0.570	0.426	0.930
0.075	0.454	0.425	0.575	0.454	0.925
0.080	0.482	0.420	0.580	0.482	0.920
0.085	0.509	0.415	0.585	0.509	0.915
0.090	0.536	0.410	0.590	0.536	0.910
0.095	0.562	0.405	0.595	0.562	0.905
0.100	0.588	0.400	0.600	0.588	0.900
0.105	0.613	0.395	0.605	0.613	0.895
0.110	0.637	0.390	0.610	0.637	0.890
0.115	0.661	0.385	0.615	0.661	0.885
0.120	0.684	0.380	0.620	0.684	0.880
0.125	0.707	0.375	0.625	0.707	0.875
0.130	0.729	0.370	0.630	0.729	0.870
0.135	0.750	0.365	0.635	0.750	0.865
0.140	0.770	0.360	0.640	0.770	0.860
0.145	0.790	0.355	0.645	0.790	0.855
0.150	0.809	0.350	0.650	0.809	0.850
0.155	0.827	0.345	0.655	0.827	0.845
0.160	0.844	0.340	0.660	0.844	0.840
0.165	0.861	0.335	0.665	0.861	0.835
0.170	0.876	0.330	0.670	0.876	0.830
0.175	0.891	0.325	0.675	0.891	0.825
0.180	0.905	0.320	0.680	0.905	0.820
0.185	0.918	0.315	0.685	0.918	0.815
0.190	0.930	0.310	0.690	0.930	0.810
0.195	0.941	0.305	0.695	0.941	0.805
0.200	0.951	0.300	0.700	0.951	0.800
0.205	0.960	0.295	0.705	0.960	0.795
0.210	0.969	0.290	0.710	0.969	0.790
0.215	0.976	0.285	0.715	0.976	0.785
0.220	0.982	0.280	0.720	0.982	0.780
0.225	0.988	0.275	0.725	0.988	0.775
0.230	0.992	0.270	0.730	0.992	0.770
0.235	0.996	0.265	0.735	0.996	0.765
0.240	0.998	0.260	0.740	0.998	0.760
0.245	1.000	0.255	0.745	1.000	0.755
0.250	1.000	0.250	0.750	1.000	0.750



## APPENDIX VIII

### FOURIER MACHINES

1. *One-dimensional mechanical machines.* Most of the attempts at Fourier machines are essentially concerned with eliminating the computational work involved in processes such as those described in section 4.2.1; in other words, they are one-dimensional. The principle of Kelvin's tide predictor (Appendix VI) can be used (Booth, 1948), but no instrument of this type suitable for electron-density calculations has yet been constructed. Robertson (1932) has suggested making use of the principle of the transmission of hydraulic pressure, but no development of this idea has been reported.

Vand (1952) has described an application of the principle of moments, a set of weights being carried on rotatable arms whose motions are geared together; this device can give the electron density along a line in a projection, and this line can be made to cover the whole of a projection by employing the principle of the 'one-dimensional crystal' of Donnay and Donnay (1949). This principle makes use of the transformation of the unit cell of a crystal, as shown in two dimensions in fig. 325, to one which is long and thin. The calculation of the

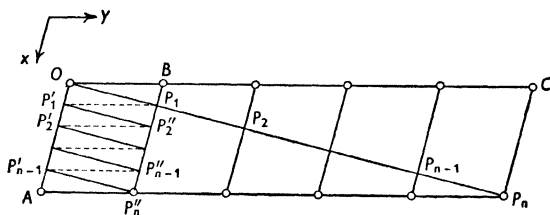


FIG. 325. Transformation of axes of unit cell from  $OA, OC$ , to  $OP_n, OC$ . The cell edge  $OP$  is then equivalent to a set of sloping lines,  $OP_1, P_1', P_2'' \dots$  in the original cell (Donnay and Donnay, 1949)

electron density along the long edge of this cell is then equivalent to the calculation along a set of sloping lines in the original cell. Bragg (1952) has described a modification of Vand's device.

Beevers (1952b) has constructed an instrument that makes use of the true planimeter principle; that is, the axis of the wheel is parallel to the surface on which the wheel rests, but can be inclined to the direction of relative motion of the wheel with the surface. This device is so simple that it is possible to have a set of them to represent different values of a coordinate; thus the equivalent of a complete strip can be dealt with in one operation, and the adding of a set of strips involves

only as many operations as there are strips. The machine would therefore seem to be particularly promising.

2. *One-dimensional electrical machines.* Beevers (1939) and MacEwan and Beevers (1942) have described an electrical machine that is based upon the two-figure strips (section 4.3.1); the change in number in any one column as the amplitude changes by unity is represented by an electrical impulse, which can be counted in the usual way. The difficulty of obtaining counters which can deal with positive and negative quantities seems to have held up the development of this idea.

Hägg and Laurent (1946) have made use of a machine in which the Fourier components are represented by electrical potentials provided by a specially constructed tapped potentiometer. Theappings are made to have values proportional to  $\cos 0^\circ$ ,  $\cos 6^\circ$ ,  $\cos 12^\circ$ , ...  $\cos 90^\circ$ , ...  $\cos 180^\circ$ , and the equivalent of different indices are obtained by connecting these potentials in different sequences; thus connexion to the first tapping only is equivalent to index 0, connexion to successiveappings is equivalent to index 1, connexion to alternateappings is equivalent to index 2, and so on. The different Fourier coefficients are obtained by means of calibrated potentiometers. The resulting potential differences are connected across accurately equal high resistances, and the total currents measured by a bridge circuit. Rymer and Butler (1944) have described an essentially similar machine. This type of instrument seems promising, but, unless elaborate precautions are taken, it would not appear to be of high accuracy.

3. *Two-dimensional machines.* The reduction of a set of two-dimensional summations to a number of one-dimensional sets must inevitably reduce the speed of operation. Several attempts have therefore been made to introduce each Fourier coefficient directly in two dimensions, the most successful being based upon the photographic method (section 4.5.1) of Bragg (1929*b*), as developed by Huggins (1941, 1944, 1945), Eller (1951), & Howell, Christensen & McLachlan (1951), culminating in the electronic machine of Pepinsky (1947). Bragg's interference method (section 4.5.2), as developed by Buerger (1941*a*, 1950*e*, *f*), Magnéli (1951), Hanson, Taylor and Lipson (1951), and Hanson and Lipson (1952*b*), also seems promising.

Of other methods suggested, that of Shimizu, Elsey and McLachlan (1950) seems most successful. Their machine is based upon types of electrical three-phase generators known as selsyns; these are geared together in a two-dimensional array controlled by twelve-point single-pole rotary switches. The positions of these switches correspond to the set of structure factors, which can thus be inserted directly, and the electron density is read on a voltmeter, point by point in the area of projection.

An earlier machine, devised by McLachlan and Champayne (1946), making use of sand deposited in waves, would appear to be too complicated to be successful.

APPENDIX IX

STANDARDIZATION OF  
CRYSTAL-STRUCTURE MODELS

(from J.Sci.Instr. 1947, 24, 249)

1. It is recommended that common atoms and ions be represented by spheres of the colours shown in table 328(i). Other elements may be represented by colours chosen at the discretion of the manufacturer; pink may be used for special purposes.

2. It is recommended that models should be built to one of the scales shown in table 328(ii). The scale of 2.5 cm. = 1 Å is that likely to be the most widely used; it is sufficiently large to allow the construction of robust yet not unwieldy models, it is that adopted in the German models well known in Great Britain and widely used in Continental laboratories, and the close approximation to 1 in. = 1 Å is likely to be a convenience in some applications. Models of simple structures should generally be 'exact' with all distances correct to within the equivalent of 0.1 Å. It may sometimes be necessary to build more complex models in an 'idealized' form, but this should be avoided if possible.

3. The material of the spheres is left to the discretion of the manufacturer, but it should be durable and free from secular changes in dimensions in order that the pins may be held securely and permanently. Similarly the method of colouring should be permanent.

4. The exact sizes of the spheres are also left to the manufacturer's discretion, but it is recommended that they should in no case exceed in diameter the equivalent of 1 Å and that preferably they should be somewhat smaller. Experience has shown that for models on the scale of 2.5 cm. = 1 Å spheres of diameter 2 cm. (say  $\frac{3}{4}$  in.) give an adequately 'open' model of pleasing appearance. It is not expected that it will generally be practicable to use spheres of different sizes in a single model, but if this is done the sizes should correspond in sequence, but not necessarily in exact scale, to the sizes of the atoms or ions.

5. The pins may be of any material and gauge adequate to give reasonable strength to the model. They should be firmly secured in each ball, should not bend readily, and should be protected against corrosion. Stainless steel wire of  $\frac{3}{32}$  in. diameter, hard-drawn and polished, has been found very suitable for models on the scale of 2.5 cm. = 1 Å.

6. The models should be so constructed that, as far as possible, only

TABLE 328 (i)  
Colours to represent atoms and ions

Atom or ion	Colour	Remarks
H	Cream	White acceptable.
C, Si	Black	—
O	Red	—
S	Yellow	—
N	Blue	Colour should approximate to No. 5 (Oxford blue) of British Standard Specification 381.
P	Purple	—
Halogens	Green	Where two or more of these elements are present they may be distinguished by different shades of green, the darker colours being used for the elements of higher atomic number.
OH	Blue-green	Colour should approximate to No. 2 (turquoise blue) of British Standard Specification 381.
H <sub>2</sub> O	Orange	—
Metals	Brown, Grey (or silver), Gold	Any of these acceptable for a single metal. In models containing two or more metals these colours should be used in order of increasing coordination number.

TABLE 328 (ii)

## Scale of models

For small models (e.g. for museum case display)	1 cm. = 1 Å.
For general purposes	2.5 cm. = 1 Å.
For large models (e.g. for lecture demonstrations)	5 cm. = 1 Å.

pins representing 'bonds' in the structure are used, except that pins outlining a unit cell may also be inserted.

7. All models should embrace at least one unit cell of the structure, and in addition sufficient adjacent cells to display the full coordination of all atoms within or in the faces of the chosen unit cell.

8. Models should be marked with a durably engraved label showing (a) the name of the structure, (b) its chemical composition, (c) the scale of the model, (d) if the model is 'idealized', a statement to that effect, (e) (in the case of complex structures) a literature reference to the original structure determination, and (f) (optionally) an explanation of the colour code.

## REFERENCES AND NAME INDEX

Abbe, E	-	-	-	-	-	-	18
Abrahams, S. C. & Robertson, J. M., 1948.	Acta Cryst.	<b>1</b> , 252	-	-	-	-	137
Abrahams, S. C., Robertson, J. M. & White, J. G., 1949.	Acta Cryst.	<b>2</b> , 238	-	-	-	-	133
Albrecht, G., 1939.	Rev. Sci. Instr.	<b>10</b> , 221	-	-	-	-	133
Allen, P. W. & Sutton, L. E., 1950.	Acta Cryst.	<b>3</b> , 46	-	-	-	-	315
Allison, S. K.	See Compton, A. H.	-	-	-	-	-	-
Avrami, M.	-	-	-	-	-	-	248, 261
Avrami, M., 1938.	Phys. Rev.	<b>54</b> , 300	-	-	-	-	246, 247
Babinet, J.	-	-	-	-	-	-	72
Bacon, G. E. 1955	Neutron Diffraction.	Oxford University Press	-	-	-	-	143
Banerjee, K.	-	-	-	-	-	-	265
Banerjee, K., 1930.	Nature	<b>125</b> , 456 ; Ind. J. Phys.	<b>4</b> , 557	-	-	-	228
Banerjee, K., 1933.	Proc. Roy. Soc. A.	<b>141</b> , 188	-	-	-	-	247, 261, 262, 263
Barth, T. F. W. & Posnjak, E. 1932.	Z. Krist.	<b>82</b> , 325	-	-	-	-	51
Beevers, C. A.	-	-	-	-	-	89 et seq., 99, 101, 166	-
Beevers, C. A. 1939.	Proc. Phys. Soc.	<b>51</b> , 660	-	-	-	-	89, 325
Beevers, C. A. 1952a.	Acta Cryst.	<b>5</b> , 670	-	-	-	-	91
Beevers, C. A., 1952b.	<i>Computing Methods and the Phase Problem in X-ray Crystal Analysis.</i>	State College, Pennsylvania : X-ray Crystal Analysis Laboratory	-	-	-	-	325
Beevers, C. A. & Hughes, W. 1941.	Proc. Roy. Soc. A.	<b>177</b> , 251	-	-	-	-	133
Beevers, C. A. & Lipson, H. 1932.	Z. Krist.	<b>82</b> , 297	-	-	-	-	28
Beevers, C. A. & Lipson, H. 1934.	Proc. Roy. Soc. A.	<b>146</b> , 570	-	-	-	-	60, 86, 121, 141, 177, 210, 211
Beevers, C. A. & Lipson, H. 1935.	Proc. Roy. Soc. A.	<b>148</b> , 664	-	-	-	-	214, 215
Beevers, C. A. & Lipson, H. 1938.	Proc. Phys. Soc.	<b>50</b> , 275	-	-	-	-	69, 71
Beevers, C. A. & Lipson, H. 1952.	Acta Cryst.	<b>5</b> , 673	-	-	-	-	102
Beevers, C. A. & Robertson, J. H. 1950.	Acta Cryst.	<b>3</b> , 164	-	-	-	-	163, 165
Beevers, C. A. & Schwartz, C. M. 1935.	Z. Krist.	<b>91</b> , 157	-	-	-	-	114, 200
Beevers, C. A.	See also Lipson, H., MacEwan, D., Robertson, J. H., Stern, F.	-	-	-	-	-	-
Bell, I. P.	See Vand, V.	-	-	-	-	-	-
Bernal, J. D., 1926.	Proc. Roy. Soc. A.	<b>113</b> , 117	-	-	-	-	31
Bernal, J. D. & Megaw, H. D., 1935.	Proc. Roy. Soc. A.	<b>151</b> , 384	-	-	-	-	114
Berry, C. R., 1950.	J. App. Phys.	<b>18</b> , 269	-	-	-	-	236
Bijvoet, J. M.	See Bokhoven, C., MacGillavry, C. H., Peerdeman, A. F.	-	-	-	-	-	-
Binnie, W. P.	See Morrison, J. D.	-	-	-	-	-	-
Bokhoven, C., Schoone, J. C. & Bijvoet, J. M., 1948.	Kon. Ned. Acad. Wet.	<b>51</b> , No. 8	-	-	-	-	207, 219
Bokhoven, C., Schoone, J. C. & Bijvoet, J. M., 1949.	Kon. Ned. Acad. Wet.	<b>52</b> , No. 2	-	-	-	-	207, 219
Bokhoven, C., Schoone, J. C. & Bijvoet, J. M., 1951.	Acta Cryst.	<b>4</b> , 275	-	-	-	-	207, 219
Bommel, A. J. van.	See Peerdeman, A. F.	-	-	-	-	-	-
Booth, A.D.	-	-	-	-	-	-	300, 301

- Booth, A. D., 1945a. *Nature*, **156**, 51 - - - 199
- Booth, A. D., 1945b. *Phil. Mag.* **36**, 609 - - - 146, 307
- Booth, A. D., 1945c. *Trans. Faraday Soc.* **41**, 434 - - - 80, 82
- Booth, A. D., 1946a. *Trans. Faraday Soc.* **42**, 444. - - - 279
- Booth, A. D., 1946b. *Proc. Roy. Soc. A.* **188**, 77 - - 279, 288, 297
- Booth, A. D., 1946c. *Trans. Faraday Soc.* **42**, 617 - - - 280
- Booth, A. D., 1946d. *Nature* **158**, 380 - - - 243
- Booth, A. D., 1947a. *Nature* **160**, 196 - - 248, 250, 280, 284
- Booth, A. D., 1947b. *Proc. Roy. Soc. A.* **190**, 482 - - - 297
- Booth, A. D., 1947c. *J. App. Phys.* **18**, 664 - - - 321
- Booth, A. D., 1948. *Fourier Technique in Organic Structure Analysis*.  
Cambridge : University Press - - - 278, 322, 325
- Booth, A. D. & Britten, K. H. V., 1948. *Proc. Roy. Soc. A.* **193**, 305 - 288
- Bosanquet, C. H. *See* Bragg, W. L.
- Boyes-Watson, J., Davidson, E. & Perutz, M. F., 1947. *Proc. Roy. Soc. A.*  
**191**, 83 - - - 197, 241
- Boyes-Watson, J. & Perutz, M. F., 1943. *Nature* **151**, 714 - 206, 241, 242
- Bradley, A. J., 1935a. *Proc. Phys. Soc.* **47**, 879 - - - 133
- Bradley, A. J., 1935b. *Z. Krist.* **91**, 302 - - - 146
- Bradley, A. J. & Jay, A. H., 1932. *Proc. Roy. Soc. A.* **136**, 210 - - 142
- Bradley, A. J. & Lu, S. S., 1937. *Z. Krist.* **96**, 20 - 29, 61, 125, 126
- Bradley, A. J. & Rodgers, J. W., 1934. *Proc. Roy. Soc. A.* **144**, 340 - 142
- Bradley, A. J. & Thewlis, J., 1926. *Proc. Roy. Soc. A.* **112**, 678 - 29, 128
- Bragg, W. H., 1915. *Phil. Trans. Roy. Soc.* **210**, 253 - - - 199
- Bragg, W. L. - - - 1 et seq.
- Bragg, W. L., 1913. *Proc. Camb. Phil. Soc.* **17**, 43 - - - 4
- Bragg, W. L., 1924. *Proc. Roy. Soc. A.* **105**, 370, 106, 346. - - 120
- Bragg, W. L., 1929a. *Proc. Roy. Soc. A.* **123**, 537 - - 79, 199
- Bragg, W. L., 1929b. *Z. Krist.* **70**, 483 - - - 107, 326
- Bragg, W. L., 1930. *Z. Krist.* **74**, 237 - - - 120
- Bragg, W. L., 1939. *Nature* **143**, 678 - - 20, 108, 236
- Bragg, W. L., 1944. *Nature* **154**, 69 - - 20, 71, 75
- Bragg, W. L., 1952. *Acta Cryst.* **5**, 474 - - - 325
- Bragg, W. L., Howells, E. R. & Perutz, M. F., 1952. *Acta Cryst.* **5**, 136 - 241
- Bragg, W. L., James, R. W. & Bosanquet, C. H., 1922. *Phil. Mag.* **44**, 433 199
- Bragg, W. L. & Lipson, H., 1936. *Z. Krist.* **95**, 323 - - 53, 66ff
- Bragg, W. L. & Lipson, H., 1943. *J. Sci. Instr.* **20**, 110 - 74, 108
- Bragg, W. L. & Stokes, A. R., 1945. *Nature* **156**, 332 - - 73
- Bragg, W. L. & West, J., 1926. *Proc. Roy. Soc. A.* **111**, 691 - - 117
- Bragg, W. L. & West, J., 1928. *Z. Krist.* **69**, 120 - - 132, 133
- Bragg, W. L. & West, J., 1930. *Phil. Mag.* **10**, 823 - 88, 205, 293, 297
- Bragg, W. L. *See also* Warren, B. E.
- Brill, R., 1950. *Acta Cryst.* **3**, 333 - - - 306
- Britten, K. H. V. *See* Booth, A. D.
- Brown, C. J., 1949. *Acta Cryst.* **2**, 228 - - - 133
- Brown, C. J. & Corbridge, D. E. C., 1948. *Nature* **162**, 72 - - 123
- Brown, C. J., Peiser, H. S. & Turner-Jones, A., 1949. *Acta Cryst.* **2**, 167 122, 123
- Buerger, M. J. - - - 33, 197
- Buerger, M. J., 1931. *Amer. Min.* **16**, 361 - - - 126
- Buerger, M. J., 1941a. *Proc. Nat. Acad. Sci.* **27**, 117 - - 326
- Buerger, M. J., 1941b. *Geol. Soc. Am. Special Papers No.* 53 - - 60

- Buerger, M. J., 1946. *J. App. Phys.* **17**, 579 - 32, 156, 157 159, 161, 162  
 Buerger, M. J., 1948. *Acta Cryst.* **1**, 259 - - - 161  
 Buerger, M. J., 1950a. *Acta Cryst.* **3**, 465 - - - 32, 154, 157  
 Buerger, M. J., 1950b. *Acta Cryst.* **3**, 87 - - - 163, 164  
 Buerger, M. J., 1950c, d. *Proc. Nat. Acad. Sci.*, **36**, 376 & **36**, 738 - 167  
 Buerger, M. J., 1950e. *Proc. Nat. Acad. Sci.*, **36**, 330 - - 326  
 Buerger, M. J., 1950f. *J. App. Phys.* **21**, 909 - - - 32  
 Buerger, M. J., 1950g. *Proc. Nat. Acad. Sci.* **36**, 324 - - 326  
 Buerger, M. J., 1951. *Acta Cryst.* **4**, 531 - - 109, 163, 164  
 Bunn, C. W. - - - 73, 201  
 Bunn, C. W., 1945. *Chemical Crystallography*. Oxford : University Press  
 - - 69, 70, 71, 114, 116, 120, 122, 320  
 Bunn, C. W. & Garner, E. V., 1942. *J. Chem. Soc.* 654 - 117  
 Bunn, C. W. *See also* Crowfoot, D.  
 Butler, C. C. *See* Rymer, T. B.
- Carlisle, C. H. & Crowfoot, D., 1945. *Proc. Roy. Soc. A.* **184**, 64 176, 208, 210  
 Cauchy, A. L. - - - 252, 254, 261  
 Champaygne, E. F. *See* McLachlan, D.  
 Charlesby, A., Finch, G. I. & Wilman, H., 1939. *Proc. Phys. Soc.* **51**, 479 243  
 Christensen, C. J. *See* Howell, B.  
 Chrobak, L., 1937. *Z. Krist.* **96**, 503 - - - 69  
 Clastre, J. & Gay, R., 1950a. *C. R. Acad. Sci., Paris.* **230**, 1976 - 163, 165  
 Clastre, J. & Gay, R., 1950b. *J. Phys. Radium* **11**, 75 - 163, 165  
 Clews, C. J. B. *See* Hodgson, M. L.  
 Cochran, W., 1951a. *Acta Cryst.* **4**, 408 - - 203, 302  
 Cochran, W., 1951b. *Acta Cryst.* **4**, 81 - - 302, 304, 305  
 Cochran, W., 1951c. *Acta Cryst.* **4**, 376 - - 189  
 Cochran, W., 1952. *Acta Cryst.* **5**, 65 - - 270  
 Cochran, W. & Penfold, B. R., 1952. *Acta Cryst.* **5**, 644 - 269, 272  
 Cochran, W. *See also* Hodgson, M. L.  
 Collin, R. L. & Lipscomb, W. N., 1949. *Acta Cryst.* **2**, 104 - - 32  
 Compton, A. H. & Allison, S. K., 1936. *X-rays in Theory and Experiment*.  
 New York : van Nostrand - - - 141  
 Comrie, L. J., Hey, G. B. & Hudson, H. G., 1937. *J. R. Statist. Soc. Suppl.*  
**4**, 210 - - - 99  
 Corbridge, D. E. C. *See* Brown, C. J.  
 Corey, R. B. *See* Schomaker, D.  
 Cork, J. M., 1927. *Phil. Mag.* **4**, 688 - - 115, 212, 214  
 Costain, W., 1941. *Ph.D. Thesis*, University of Birmingham - - 279  
 Cox, E. G., 1939. *Proc. Phys. Soc.* **51**, 666 - - 322  
 Cox, E. G., Gillott, R. J. J. H. & Jeffrey, G. A., 1949. *Acta Cryst.* **2**, 356 129  
 Cox, E. G., Gross, L. & Jeffrey, G. A., 1947. *Proc. Leeds Phil. Soc.* **5**, 1 - 99  
 Cox, E. G. Gross, L., & Jeffrey, G. A., 1949. *Acta Cryst.* **2**, 351 - 99  
 Cox, E. G. & Jeffrey, G. A., 1949. *Acta Cryst.* **2**, 341 - - 99  
 Crookes, D. A., 1947. *Nature* **160**, 17 - - 123  
 Crowfoot, D., Bunn, C. W., Rogers-Low, B. W. & Turner-Jones, A., 1949.  
*The X-ray Crystallographic Investigation of the Structure of Penicillin*.  
 Oxford : University Press - 73, 139, 140, 201, 204, 212, 216, 221, 222  
 Crowfoot, D. & Dunitz, J. D., 1948. *Nature* **162**, 608 - - 208  
 Crowfoot, D. *See also* Carlisle, C. H.

- Cruickshank, D. W. J. - - - - - 302, 308  
 Cruickshank, D. W. J., 1949a. *Acta Cryst.* **2**, 65 - - 289, 294, 308  
 Cruickshank, D. W. J., 1949b. *Acta Cryst.* **2**, 154 - - - 309  
 Cruickshank, D. W. J., 1950a. *Acta Cryst.* **3**, 10 - - - 280  
 Cruickshank, D. W. J., 1950b. *Acta Cryst.* **3**, 72 - - 291, 309  
  
 Davidson, E. *See* Boyes-Watson, J.  
 Davidson, W. L. *See* Shull, C. G.  
 Debye, P. - - - - - 124  
 Debye, P. & Mencke, H., 1931. *Ergebn. tech. Röntgenk.* **2**, 1 - - 150  
 Donnay, G. H., 1949. *Acta Cryst.* **2**, 370 - - - 320  
 Donnay, G. H. *See also* Donnay, J. D. H.  
 Donnay, J. D. H., 1939. *Amer. Min.* **24**, 184 - - 122  
 Donnay, J. D. H. & Donnay, G. H., 1949. *Acta Cryst.* **2**, 366 - - 325  
 Donnay, J. D. H. & Harker, D., 1937. *Amer. Min.* **22**, 446 - - 122  
 Donohue, J. & Schomaker, V., 1949. *Acta Cryst.* **2**, 344 - 99, 101  
 Donohue, J. & Trueblood, K. N., 1956. *Acta Cryst.* **9**, 960 - 138  
 Donohue, J. *See also* Shoemaker, D. P.  
 Drude, P., 1929. *Theory of Optics*. London : Longmans, Green - 72  
 Duane, W., 1925. *Proc. Nat. Acad. Sci.* **11**, 489 - - 199  
 Dunitz, J. D. & Robertson, J. M., 1947. *J. Chem. Soc.* 1145 - - 148  
 Dunitz, J. D. *See also* Crowfoot, D.  
 Dyer, H. B., 1951a. *Acta Cryst.* **4**, 42 - - 177, 178, 179  
 Dyer, H. B., 1951b. *Ph.D. Thesis*. University of Cambridge - 193, 224  
  
 Eckert, W. J., 1940. *Punched Card Methods in Scientific Computations*. New York : Thomas J. Watson Astronomical Computing Bureau, Columbia University - - 99  
 Edwards, O. S. & Lipson, H., 1942. *Proc. Roy. Soc. A* **180**, 268 - 50  
 Eller G., 1951. *Compt. rend.* **232**, 1122 ; **233**, 2333 - - 326  
 Elsey, P. J. *See* Shimizu, H.  
 Emde, F. *See* Jahnke, E.  
 Evans, R. C. & Peiser, H. S., 1942. *Proc. Phys. Soc.* **54**, 457 - - 321  
 Ewald, P. P., 1921. *Z. Krist.* **56**, 129 - - 31  
  
 Fermi, E. - - - - - 63  
 Finch, G. I. *See* Charlesby, A.  
 Fourier, J. B. J. - - - - - 1 et seq.  
 Fowweather, F., 1952. *Acta Cryst.* **5**, 820 - - 240  
 Fowweather, F. & Hargreaves, A., 1950. *Acta Cryst.* **3**, 81 37, 116, 120, 207  
 Fraunhofer, J. von - - - - - 236  
 Fricke, R. & Havestadt, L., 1928. *Z. Anorg. Chem.* **170**, 35 - 28  
 Friedel, G. - - - - - 28, 118  
 Furberg, S., 1950. *Acta Cryst.* **3**, 325 - - 147  
  
 Garrido, J. - - - - - 167  
 Garrido, J., 1950a, b. *C. R. Acad. Sci., Paris.* **230**, 1878 & **231**, 297 - 163  
 Garrido, J. *See also* Clastre, J.  
 Garner, E. V. *See* Bunn, C. W.  
 Gay, R. *See* Clastre, J.  
 Gillis, J. - - - - - 256, 257, 270



## REFERENCES AND NAME INDEX

333

- Gillis, J., 1948a. *Acta Cryst.* **1**, 76 - - - - 254  
 Gillis, J., 1948b. *Acta Cryst.* **1**, 174 - - - - 255  
 Gillott, R. J. J. H. *See* Cox, E. G.  
 Gingrich, N. S. *See* Warren, B. E.  
 Goedkoop, J. A. - - - - 265  
 Goedkoop, J. A., 1950. *Acta Cryst.* **3**, 374 - - 156, 247  
 Goedkoop, J. A., 1952. *Computing Methods and the Phase Problem in X-ray Crystal Analysis*. State College, Pennsylvania : X-ray Crystal Analysis Laboratory - - - - 264  
 Goldschmidt, V. M., 1929. *Geochemische Verteilungsgesetze der Elemente*, P VII - - - - 111  
 Goodwin, T. H. & Hardy, R., 1938. *Phil. Mag.* **25**, 1096 - - 82  
 Gremis, M. D. & Kasper, J. S., 1949. *Acta Cryst.* **2**, 347 - - 99  
 Gross, L. *See* Cox, E. G.  
 Groth, P., 1908. *Chemische Kristallographie* **2**. Leipzig ; Englemann - 140  
 Hägg, G., 1950. *Acta Cryst.* **3**, 315 - - - - 320  
 Hägg, G. & Laurent, T., 1946. *J. Sci. Instr.* **23**, 155 - - - 326  
 Hanson, A. W., 1952. *Nature* **170**, 580 - - - 109  
 Hanson, A. W. & Lipson, H., 1952a. *Acta Cryst.* **5**, 145 - - 73  
 Hanson, A. W. & Lipson, H., 1952b. *Acta Cryst.* **5**, 362 109, 206, 326  
 Hanson, A. W., Taylor, C. A. & Lipson, H., 1951. *Nature*. **168**, 160 109, 326  
 Hanson, A. W., Lipson, H. & Taylor, C. A., 1953. *Proc. Roy. Soc. A*. **218**, 371. - - - 236  
 Hardy, R. *See* Goodwin, T. H.  
 Hargreaves, A., 1946. *Nature* **158**, 620 - - - 216, 219  
 Hargreaves, A., 1953. (To be published.) - - - 320  
 Hargreaves, A. *See also* Fowweather, F.  
 Harker, D. - - - 159 et seq., 181 et seq., 250 et seq.  
 Harker, D., 1936. *J. Chem. Phys.* **4**, 381 - - - 157, 180, 181  
 Harker, D., 1948. *Amer. Min.* **33**, 764 - - - 134  
 Harker, D. & Kasper, J. S., 1948. *Acta Cryst.* **1**, 70 - - 63, 246  
 Harker, D. *See also* Donnay, J. D. H., Kasper, J. S.  
 Hartshorne, N. H. & Stuart, A., 1950. *Crystals and the Polarizing Microscope*. London : Arnold. - - - 28, 121  
 Hauptmann, H. - - - 260, 264, 269  
 Hauptmann, H. *See also* Karle, J.  
 Havestadt, L. *See* Fricke, R.  
 Havighurst, R. J., 1925. *Proc. Nat. Acad. Sci.* **11**, 502 - - - 199  
 Hemily, P. 1952. *C. R. Acad. Sci., Paris*. **234**, 2085 - - - 187  
 Henry, N. F. M., Lipson, H. & Wooster, W. A., 1951. *Interpretation of X-ray Diffraction Photographs*. London : MacMillan - - 119, 120, 141  
 Herglotz, G., 1911. *Ber. sachs. Ges. (Akad.) Wiss.* **63**, 501 - - 259  
 Hermann, C. - - - 26, 318, 319  
 Hey, G. B. *See* Comrie, L. J.  
 Hilton, H., 1906. *Mathematical Crystallography*. Oxford : University Press - - - 27  
 Hinde, R. M. *See* Taylor, C. A.  
 Hodgson, M. L., Clews, C. J. B. & Cochran, W., 1949. *Acta Cryst.* **2**, 113 98, 99  
 Howell, B., Christensen, C. J. & McLachlan, D., 1951. *Nature* **168**, 282 - 326  
 Howells, E. R., Phillips, D. C. & Rogers, D., 1949. *Research*, **2**, 338 - 37  
 Howells, E. R., Phillips, D. C. & Rogers, D., 1950. *Acta Cryst.* **3**, 210 - 35

Howells, E. R. *See also* Bragg, W. L.

Howells, R. G., 1950. <i>Acta Cryst.</i> <b>3</b> , 366	-	-	-	-	133
Huggins, M. L. -	-	-	-	-	322
Huggins, M. L., 1941. <i>J. Am. Chem. Soc.</i> <b>63</b> , 66	-	-	-	-	326
Huggins, M. L., 1944. <i>J. Chem. Phys.</i> <b>12</b> , 520	-	-	-	-	107, 326
Huggins, M. L., 1945. <i>Nature</i> <b>155</b> , 18	-	-	-	-	326
Hughes, E. W., 1941. <i>J. Am. Chem. Soc.</i> <b>63</b> , 1737	-	-	-	-	121, 280
Hughes, E. W., 1949a. <i>Acta Cryst.</i> <b>2</b> , 34	-	-	-	-	258
Hughes, E. W., 1949b. <i>Acta Cryst.</i> <b>2</b> , 37	-	-	-	-	263
Hughes, E. W. & Lipscomb, W. N., 1946. <i>J. Am. Chem. Soc.</i> <b>68</b> , 1970	-	-	-	-	308
Hughes, E. W. & Moore, W. J., 1949. <i>J. Am. Chem. Soc.</i> <b>71</b> , 2618	-	-	-	-	191, 192
Hughes, J. W., Phillips, D. C., Rogers, D. & Wilson, A. J. C., 1949. <i>Acta Cryst.</i> <b>2</b> , 420	-	-	-	-	115
Hughes, W. & Taylor, C. A., 1953. <i>J. Sci. Instr.</i> <b>30</b> , 105	-	-	-	-	109, 236
Hughes, W. <i>See</i> Beevers, C. A.					
Hulme, R., 1952. <i>Acta Cryst.</i> <b>5</b> , 144	-	-	-	-	73

International Tables, 1935

*Internationale Tabellen zur Bestimmung von Kristallstrukturen.* Berlin : Borntraeger - - - - 56, 318

International Tables, 1952

*International Tables for X-ray Crystallography.* Birmingham : Kynoch Press - - - - 23 et seq. 319

Jackson, W. W. & West, J., 1930. <i>Z. Krist.</i> <b>76</b> , 211	-	-	-	122
Jackson, W. W. <i>See</i> Taylor, W. H.				
Jaeger, F. M., Terpstra, P. & Westenbrink, H. G. K., 1927. <i>Z. Krist.</i> <b>66</b> , 195				146
Jahnke, E. & Emde, F., 1933. <i>Funktionen Tafeln mit Formerln und Kurven.</i> Leipzig : Teubner	-	-	-	36
James, R. W., 1948. <i>Acta Cryst.</i> <b>1</b> , 132	-	-	-	293
James, R. W. <i>See also</i> Bragg, W. L.				
Jay, A. H. <i>See</i> Bradley, A. J.				
Jeffrey, G. A., 1945. <i>Proc. Roy. Soc. A.</i> <b>183</b> , 388	-	-	-	105
Jeffrey, G. A., 1947. <i>Proc. Roy. Soc. A.</i> <b>188</b> , 222	-	-	-	289
Jeffrey, G. A., 1951. <i>Acta Cryst.</i> <b>4</b> , 58	-	-	-	296
Jeffrey, G. A. <i>See also</i> Cox, E. G.				
Jenkins, F. A. & White, H. E., 1951. <i>Fundamentals of Optics.</i> New York : McGraw-Hill	-	-	-	17
Jensen, A. T., 1940. <i>Kgl. D. Vid. Selsk. mat. fys. Medd.</i> <b>17</b> , No. 9				113
Jensen, A. T., 1948. <i>Krystallinske Salthydrater.</i> Copenhagen : Arnold Busck	-	-	-	113, 115
Jones, F. W. & Sykes, C., 1937. <i>Proc. Roy. Soc. A.</i> <b>161</b> , 440	-	-	-	142
Jordahl, O. M., 1934. <i>Phys. Rev.</i> <b>45</b> , 87	-	-	-	122
Karle, J.	-	-	-	260, 264, 269
Karle, J. & Hauptmann, H., 1950. <i>Acta Cryst.</i> <b>3</b> , 181	-	-	-	156, 246, 259
Kasper, J. S.	-	-	-	250 et seq.
Kasper, J. S., Lucht, C. M. & Harker, D., 1950. <i>Acta Cryst.</i> <b>3</b> , 436				136, 256
Kasper, J. S. <i>See also</i> Harker, D., Grems, M. D.				
Kästner, F., 1931. <i>Z. Krist.</i> <b>77</b> , 353	-	-	-	51
Kelvin, Lord	-	-	-	321, 325
Klug, A., 1950. <i>Acta Cryst.</i> <b>3</b> , 176-	-	-	-	230, 232

- Knott, G., 1940. *Proc. Phys. Soc.* **52**, 229 - - 75, 228, 229, 239  
 Krishnan, K. S. & Mookherji, A., 1936. *Phys. Rev.* **50**, 860 - - 122  
 Krishnan, K. S. & Mookherji, A., 1937. *Nature* **140**, 896 - - 122  
 Krishnan, K. S. & Mookherji, A., 1938. *Phys. Rev.* **54**, 533 & 841 - 122  
 Krishnan, K. S. *See also* Lonsdale, K.
- Laue, M. von - - - 4 et seq. 124, 128  
 Laurent, T. *See* Hägg, G.  
 Lipscomb, W. N., 1949. *Acta Cryst.* **2**, 193 - - - 206  
 Lipscomb, W. N. *See also* Collin, R. L., Hughes, E. W.  
 Lipson, H. - - - 89 et seq., 99, 101  
 Lipson, H., 1935. *Nature* **135**, 912 - - - 213  
 Lipson, H. & Beevers, C. A., 1936. *Proc. Phys. Soc.* **48**, 772 - - 90  
 Lipson, H. & Taylor, C. A., 1949. *Acta Cryst.* **2**, 130 - - 322  
 Lipson, H. & Taylor, C. A., 1951. *Acta Cryst.* **4**, 458 - - 75, 229, 237  
 Lipson, H. *See also* Beevers, C. A., Bragg, W. L., Edwards, O. S., Hanson, A. W., Henry, N. F. M., Taylor, C. A.  
 Lonsdale, K., 1929. *Proc. Roy. Soc. A.*, **123**, 494 - - 138, 206  
 Lonsdale, K., 1936. *Structure Factor Tables*. London : Bell 11, 56, 78, 225  
 Lonsdale, K., 1942a. *Phys. Soc. Rep. Prog. Phys.* **IX**, 256 - - 124  
 Lonsdale, K., 1942b. *Proc. Phys. Soc.* **54**, 314 - - 124  
 Lonsdale, K. & Krishnan, K. S., 1936. *Proc. Roy. Soc. A.* **156**, 597 - 121  
 Lonsdale, K., Robertson, J. M. & Woodward, I., 1941. *Proc. Roy. Soc. A.* **178**, 43 - - 124  
 Low, B. W. & Waldram, J. M., 1949. *J. Sci. Instr.* **26**, 311 - - 115  
 Lu, C. S. *See* Waser, J.  
 Lu, S. S. *See* Bradley, A. J.  
 Lucht, C. M. *See* Kasper, J. S.
- McCale, C. H. *See* Wood, R. G.  
 MacEwan, D. & Beevers, C. A., 1942. *J. Sci. Instr.* **19**, 150 - - 326  
 MacGillavry, C. H., 1950. *Acta Cryst.* **3**, 214 - - 254  
 MacGillavry, C. H., de Wilde, J. H. & Bijvoet, J. M., 1938. *Z. Krist.* **100**, 212 - - 49  
 McLachlan, D., 1951. *Proc. Nat. Acad. Sci.* **37**, 115 - - 163, 166  
 McLachlan, D. & Champayne, E. F., 1946. *J. App. Phys.* **17**, 1006 - 326  
 McLachlan, D. & Woolley, R. H., 1951. *Rev. Sci. Instr.* **22**, 423.  
 McLachlan, D. *See also* Howell, B., Shimizu, H.  
 Magnéli, A., 1951. *J. Sci. Instr.* **28**, 122 - - 326  
 Martin, A. J. P., 1931. *Min. Mag.* **22**, 519 - - 119  
 Martin, A. J. P. *See also* Wooster, W. A.  
 Mathieson, A. M., Robertson, J. M. & Sinclair, V. C., 1950. *Acta Cryst.* **3**, 245 & 251 - - 278  
 Mauguin, C. - - - 26, 318, 319  
 Maurice, M. E., 1930. *Proc. Camb. Phil. Soc.* **24**, 491 - - 119  
 Megaw, H. D. *See* Bernal, J. D.  
 Mencke, H. *See* Debye, P.  
 Miller, W. H. - - - - 4, 6  
 Mookherji, A. *See* Krishnan, K. S.  
 Moore, W. J. *See* Hughes, E. W.

- Morrison, J. D., Binnie, W. P. & Robertson, J. M., 1948. *Nature* **162**, 889  
105, 148
- Morton, G. A. *See* Shull, C. G.
- Náray Svabó, S. & Sasvari, K., 1938. *Z. Krist.* **99**, 27 - - - 58
- Nowacki, W., 1942. *Helv. Chim. Acta.* **25**, 863 - - - 200
- Ott, H. - - - - - 261
- Ott, H., 1927. *Z. Krist.* **66**, 136 - - - 246, 247
- Palin, D. E. & Powell, H. M., 1947. *J. Chem. Soc.* 208 181, 182, 183, 221
- Palin, D. E. & Powell, H. M., 1948. *J. Chem. Soc.* 571 - - 221
- Parry, G. S. & Pitt, G. J., 1949. *Acta Cryst.* **2**, 145 - - 278
- Patterson, A. L. - - - - 2, 12, 32, 101, 150 et seq.
- Patterson, A. L., 1934. *Phys. Rev.* **46**, 372 - - - 150
- Patterson, A. L., 1935a. *Z. Krist.* **90**, 517 - - 12, 150, 155, 171, 176
- Patterson, A. L., 1935b. *Z. Krist.* **90**, 543 - - 53, 153
- Patterson, A. L., 1944. *Phys. Rev.* **65**, 195 - - 145, 168
- Patterson, A. L., 1952. *Computing Methods and the Phase Problem in X-ray Crystal Analysis*. State College, Pennsylvania : X-ray Crystal Analysis Laboratory - - - 155
- Patterson, A. L. & Tunell, G., 1942. *Amer. Min.* **27**, 655 - - 96
- Pauling, L. - - - - - 118
- Pauling, L., 1929. *J. Am. Chem. Soc.* **51**, 1010 - - 117
- Pauling, L. & Shappell, M. D., 1930. *Z. Krist.* **75**, 128 - - 168
- Pauling, L. *See also* Shaffer, P. H.
- Peerdeman, A. F., van Bommel, A. J. & Bijvoet, J. M., 1951. *Kon. Nederl. Akad. Wet. B.* **54**, 16 - - 142
- Peiser, H. S. *See* Brown, C. J., Evans, R. C.
- Penfold, B. R. *See* Cochran, W.
- Pepinsky, R. - - - - - 244, 273
- Pepinsky, R., 1947. *J. App. Phys.* **18**, 601 - - 107, 206, 326
- Perutz, M. F. & Weiss, O., 1946. *J. Chem. Soc.* 438 - - 207
- Perutz, M. F. *See also* Boyes-Watson, J., Bragg, W. L.
- Phillips, D. C., 1950. *Research*, **3**, 578 - - 129
- Phillips, D. C., Rogers, D. & Wilson, A. J. C., 1950. *Acta Cryst.* **3**, 398 - 147
- Phillips, D. C. *See also* Howells, E. H., Hughes, J. W.
- Phillips, F. C., 1946. *Introduction to Crystallography*. London : Longmans, Green - - 23, 27, 28, 118
- Phragmen, G. *See* Westgren, A.
- Pinsker, Z. G. 1949 *Electron Diffraction*. Academy of Sciences of the U.S.S.R. - - 143
- Pitt, G. J. *See* Parry, G. S.
- Posnjak, E. *See* Barth, T. F. W.
- Powell, H. M. *See* Palin, D. E.
- Preston, G. D., 1944. *J. Sci. Instr.* **21**, 205 - - 16
- Prins, J. A. *See* Zernicke, F.
- Qurashi, M. M. - - - - - 301
- Qurashi, M. M., 1949. *Acta Cryst.* **2**, 404 - - 284
- Reijen, L. L. van - - - - - 300
- Reijen, L. L. van, 1942. *Physica IX*, **5**, 461 - - 298

- Renninger, M., 1937. *Z. Krist.* **97**, 107 - - - 30  
 Robertson, J. H. - - - - 166  
 Robertson, J. H., 1951. *Acta Cryst.* **4**, 63 - - - 187  
 Robertson, J. H. & Beevers, C. A., 1950. *Nature* **165**, 690 - 207, 208  
 Robertson, J. H. & Beevers, C. A., 1951. *Acta Cryst.* **4**, 270 - - 186  
 Robertson, J. H. *See also* Beevers, C. A.  
 Robertson, J. M. - - - - 93, 101  
 Robertson, J. M., 1932. *Phil. Mag.* **13**, 413 - - - 325  
 Robertson, J. M., 1933a. *Proc. Roy. Soc. A.* **140**, 79 - - - 262  
 Robertson, J. M., 1933b. *Proc. Roy. Soc. A.* **141**, 594 ; **142**, 659 115, 133, 202  
 Robertson, J. M., 1935a. *J. Chem. Soc.* 615 - - - 119  
 Robertson, J. M., 1935b. *Proc. Roy. Soc. A.* **150**, 348 - - - 289  
 Robertson, J. M., 1935c. *Proc. Roy. Soc. A.* **150**, 106 - - - 63  
 Robertson, J. M., 1936a. *Phil. Mag.* **21**, 176 - - - 95  
 Robertson, J. M., 1936b. *Nature* **138**, 683 - - - 96, 102  
 Robertson, J. M., 1937. *Phys. Soc. Rep. Prog. Phys.* **4**, 332 - - 199  
 Robertson, J. M., 1945. *Nature* **155**, 645 - - - 145  
 Robertson, J. M., 1948a. *J. Sci. Instr.* **25**, 216 - - - 96  
 Robertson, J. M., 1948b. *J. Sci. Instr.* **25**, 28 - - - 97  
 Robertson, J. M. & White, J. G., 1945. *J. Chem. Soc.* 607 - 138, 139, 239  
 Robertson, J. M. & White, J. G., 1947. *Proc. Roy. Soc. A.* **190**, 329 - 290  
 Robertson, J. M. & Woodward, I., 1937a. *Proc. Roy. Soc. A.* **154**, 187 - 116  
 Robertson, J. M. & Woodward, I., 1937b. *J. Chem. Soc.* 219 - - 218  
 Robertson, J. M. & Woodward, I., 1940. *J. Chem. Soc.* 36 207, 208, 209  
 Robertson, J. M. *See also* Abrahams, S. C., Lonsdale, K., Mathieson, A. M.,  
 Morrison, J. D., Dunitz, J. D.  
 Robinson, R., and Stephen, A. M., 1948. *Nature* **162**, 177 - - 219  
 Rodgers, J. W. *See* Bradley, A. J.  
 Rogers, D., 1950. *Acta Cryst.* **3**, 455 - - - 42  
 Rogers, D. *See also* Howells, E. H., Hughes, J. W., Phillips, D. C.  
 Rogers-Low, B. W. *See* Crowfoot, D.  
 Rundle, R. E., Shull, C. G. & Wollan, E. O., 1952. *Acta Cryst.* **5**, 22 - 143  
 Rymer, T. B. & Butler, C. C., 1944. *Phil. Mag.* **35**, 606 - - 326
- Sasvari, K. *See* Náray Szabó, S.  
 Sayre, D. M. - - - - 269, 270, 272, 274, 275  
 Sayre, D. M., 1951. *Acta Cryst.* **4**, 362 - - - 103  
 Sayre, D. M., 1952. *Acta Cryst.* **5**, 60 - - - 247, 266, 269  
 Schomaker, V. *See* Donohue, J., Shoemaker, D., Shaffer, P. H.  
 Schönflies, A. - - - - 318, 319  
 Schoone, J. C. *See* Bokhoven, C.  
 Schwartz, C. M. *See* Beevers, C. A.  
 Schwarz, H. A. - - - - 250, 251, 261  
 Shaffer, P. H., Schomaker, V. & Pauling, L., 1946. *J. Chem. Phys.* **14**, 648 99  
 Shappell, M. D. *See* Pauling, L.  
 Shimizu, H., Elsey, P. J. & McLachlan, D., 1950. *Rev. Sci. Instr.* **21**, 779 326  
 Shoemaker, D. P., Donohue, J., Schomaker, V. & Corey, R. B., 1950. *J. Am.*  
*Chem. Soc.* **72**, 2328 - - - 192, 194, 278, 280, 282, 309  
 Shull, C. G. & Smart, J. S., 1949. *Phys. Rev.* **76**, 1256 - - 144  
 Shull, C. G., Strauser, W. A., and Wollan, E. O., 1951. *Phys. Rev.* **83**, 333 - 144

- Shull, C. G. *See also* Rundle, R. E.  
 Siegel, S. *See* Shull, C. G.  
 Sinclair, V. C. *See* Mathieson, A. M.  
 Smare, D. L., 1948. *Acta Cryst.* **1**, 150 - - - 147  
 Smart, J. S. *See* Shull, C. G.  
 Stadler, H. P. - - - - 231  
 Stadler, H. P., 1953. *Acta Cryst.* **6**, 540 - - - 229, 230  
 Stephen, A. M. *See* Robinson, R.  
 Stern, F. & Beevers, C. A., 1950. *Acta Cryst.* **3**, 341 - - - 185  
 Stokes, A. R. - - - - 74  
 Stokes, A. R., 1946. *Proc. Phys. Soc.* **58**, 306 - - - 73  
 Stokes, A. R., 1948. *Nature* **161**, 679 - - - 243  
 Stokes, A. R. *See also* Bragg, W. L.  
 Stuart, A. *See* Hartshorne, N. H.  
 Sutton, L. E. *See* Allen, P. W.  
 Sykes, C. *See* Jones, F. W.
- Taylor, C. A., 1952. *Nature* **169**, 1086 - - - 240  
 Taylor, C. A., Hinde, R. M. & Lipson, H., 1951. *Acta Cryst.* **4**, 261 - 236  
 Taylor, C. A. & Lipson, H., 1951. *Nature* **167**, 809 - - 237  
 Taylor, C. A. *See also* Hanson, A. W., Hughes, W., Lipson, H.  
 Taylor, W. H., 1930. *Z. Krist.* **74**, 1 - - - 51, 118  
 Taylor, W. H. & Jackson, W. W., 1928. *Proc. Roy. Soc. A.* **119**, 132 112, 120  
 Terpstra, P. *See* Jaeger, F. M.  
 Thewlis, J. *See also* Bradley, A. J.  
 Thomas, W. - - - - 63  
 Toeplitz, O., 1911. *Math. Ann.* **70**, 351 - - - 259  
 Trueblood, K. N. *See* Donohue, J.  
 Tunell, G. - - - - 97, 101  
 Tunell, G. *See also* Patterson, A. L.  
 Turnbull, H. W., 1944. *Theory of Equations*. Edinburgh : Oliver & Boyd 262  
 Turner-Jones, A. *See* Crowfoot, D., Brown, C. J.  
 Tutton, A. E. H., 1922. *Crystallography and Practical Crystal Measurement*.  
 London : MacMillan - - - - 118
- Van der Waals, J. D. - - - - 111, 114, 315  
 Vand, V., 1948a. *J. Sci. Instr.* **25**, 352 - - - 320  
 Vand, V., 1948b. *Nature*, **161**, 600 - - - 284  
 Vand, V., 1949. *Nature* **163**, 169 - - - 322  
 Vand, V., 1950. *J. Sci. Instr.* **27**, 257 - - - 322, 325  
 Vand, V., 1951. *Acta Cryst.* **4**, 104 - - - 132  
 Vand, V., 1952. *J. Sci. Instr.* **29**, 118 - - - 325  
 Vand, V., & Bell, I. P., 1951. *Acta Cryst.* **4**, 465 - - - 132  
 Vos, P. J. G. de, 1948. *Acta Cryst.* **1**, 118 - - - 74
- Waldram, J. M. *See* Low, B. W.  
 Warren, B. E. & Bragg, W. L., 1928. *Z. Krist.* **69**, 168 - - - 132  
 Warren, B. E. & Gingrich, N. S., 1934. *Phys. Rev.* **46**, 368 - - - 150  
 Wasastjerna, J. A., 1923. *Soc. Sci. Fenn. I.* 37 - - - 120

## REFERENCES AND NAME INDEX

339

- Waser, J. & Lu, C. S., 1944. *J. Am. Chem. Soc.* **66**, 2035 - - 236
- Weinstein, B. K., 1954 *Travaux de l'Institut de Cristallographie. Communications au 3<sup>me</sup> Congres International de Cristallographie* - - 143
- Weiss, O. *See* Perutz, M. F.
- Weissenberg, K. - - - - 133
- Wells, A. F., 1946. *Phil. Mag.* **37**, 184, 217 & 605 - - 122
- Wells, A. F., 1950. *Structural Inorganic Chemistry*. Oxford : Clarendon Press - - 113
- West, J. - - - - 134
- West, J., 1930. *Z. Krist.* **74**, 306 - - 248
- West, J. *See also* Bragg, W. L., Jackson, W. W.
- Westenbrink, H. G. K. *See* Jaeger, F. M.
- Westgren, A. & Phragmen, G., 1925. *Phil. Mag.* **50**, 311 - - 128
- White, H. E. *See* Jenkins, F. A.
- White, J. G. *See* Abrahams, S. C., Robertson, J. M.
- Wilde, J. H. de. *See* MacGillavry, C. H.
- Williams, G. *See* Wood, R. G.
- Wilman, H. *See* Charlesby, A.
- Wilson, A. J. C. - - - 118, 135, 137, 156, 169, 174, 188
- Wilson, A. J. C., 1942. *Nature* **150**, 152 - - 61, 134
- Wilson, A. J. C., 1949. *Acta Cryst.* **2**, 318 - - 35
- Wilson, A. J. C., 1950a. *Acta Cryst.* **3**, 258 - - 39
- Wilson, A. J. C., 1950b. *Acta Cryst.* **3**, 397 - - 147
- Wilson, A. J. C. *See also* Hughes, J. W., Phillips, D. C.
- Wollan, E. O. *See* Rundle, R. E., Shull, C. G.
- Wood, R. G. & McCale, C. H., 1940. *J. Sci. Instr.* **17**, 225 - - 119
- Wood, R. G. & Williams, G., 1940. *Proc. Roy. Soc. A.* **177**, 144 - - 121
- Woodward, I. *See* Lonsdale, K., Robertson, J. M.
- Woolfson, M. M., 1951. *Acta Cryst.* **4**, 250 - - 322
- Woolley, R. H. *See* McLachlan, D.
- Wooster, W. A., 1938. *Crystal Physics*. Cambridge : University Press - - 119
- Wooster, W. A. & Martin, A. J. P., 1936. *Proc. Roy. Soc. A.* **155**, 150 - - 133
- Wooster, W. A. *See also* Henry, N. F. M.
- Wrinch, D. M. - - - - 164, 193, 198
- Wrinch, D. M., 1939. *Phil. Mag.* **27**, 98 - - 14, 163, 167
- Wrinch, D. M., 1946. *Fourier Transforms and Structure Factors*. Cambridge, Mass. : A.S.X.R.E.D. - - 15, 75
- Wyckoff, R. W. G. - - - - 319
- Zachariasen, W. H. - - - - 275
- Zachariasen, W. H., 1952. *Acta Cryst.* **5**, 68 - - 270, 274
- Zernicke, F. & Prins, J. A., 1927. *Z. Phys.* **41**, 184 - - 150
- Zussman, J., 1951. *Acta Cryst.* **4**, 72 & 493 - - 269





# SUBJECT INDEX

*Page numbers in bold type indicate section headings*

*For subjects which occur frequently (e.g. reciprocal lattice) only the more important references are given*

- ABBE's theory, **18 f**  
 absences, accidental, 29, 283, 307  
 —, systematic, **29, 57, 318 f**  
 absolute intensities, 12, **132 ff**, 216, 254 f, 285  
 — molecular configurations, 142 f  
 absorption, 40, 41, 133, 148, 286  
 — coefficient, 133  
 — edge, 141 f, 227  
 —, infra-red, **123**  
 accuracy of intensity measurements, 148, 289  
 — of atomic co-ordinates, 149, **277 ff**  
 — — —, assessment of, **307**  
 — — — by difference synthesis, **298, 308**  
 — — — by differential synthesis, **279**  
 — — — by Fourier synthesis, 105, **278 ff**  
 — — — by least squares, **280**  
 — — — by steepest descents, **284**  
 — of unit-cell dimensions, 277 f  
 acentric distribution of intensities, 37, 39  
 acetanilide, 123  
 acridine, 129  
 additive field (Hollerith), 98  
 adenine hydrochloride, 302 ff  
 agreement residual, 146  
 alpha doublet, 286  
 alums, 28, **47, 115, 119, 135, 212 ff**  
 ambiguity factor (of implication diagram), 161  
 aminoacids, 278  
 analcite, **51, 118**  
 analogue machines, **322**  
 aniline hydrochloride, 133  
 anthracene, 243 f, 262, 278  
 antiferromagnetism, 144  
 antisymmetry, 90, 103  
 artificial temperature factor, 215, 297  
 asymmetric unit, 155, 181, 249, 258, 265  
 — —, Fourier synthesis of, 106  
 atomic radii, **111, 315**  
 — scattering factor, **8, 60**  
 — — —, depression, 140, 142, 227  
 axes, transformation of, **316**  
 axis of rotation, 21  
  
 $B_{10}H_{14}$ , 256, 259  
 B.T.M. punched-card machine, 97  
 Babinet's theorem, 72  
 Banerjee's equation, **261**  
 barn (unit of neutron scattering), 143  
 Beavers-Lipson strips, **6°, 89 ff, 99, 101**  
 — — **3°, 91 ff**  
  
 benzene ring, 296  
 — —, Fourier transform of, 239  
 beryl, 117  
 beryllium sulphate, 28  
 beta-glycylglycine, 191  
 beta isoprene sulphone, 296  
 biaxial crystals, 28  
 biphenylene, 236  
 bixbyite, 168  
 body-centred lattice, 25, 32, 128  
 bond lengths (accuracy of), 277, 309  
 bounded projection, 80 f  
 Bragg's law, 1, **4 ff, 17**  
  
 CADMIUM, 111  
 calciferol, 208  
 Cauchy's inequality, 252  
 central row of reflexions, 39  
 centre of inversion, 22  
 centre of symmetry, 22, 28  
 — —, detection of, **118**  
 centred cell, 25, 29  
 centric distribution of intensities, 37  
 centrosymmetry, detection of, 28, 35, 40, **118**  
 cholesteryl iodide, 176, 208 ff, 220  
 cleavage, **122, 138**  
 close-packed structures, 112  
 cobalt, 50  
 collator (Hollerith), 99  
 colour code for models, 114, 327  
 combination of Fourier transforms, **230 ff, 233**  
 complexes, ionic, 113  
 computation of Fourier synthesis, **89 ff**  
 — — transforms, **103**  
 — of structure factors, **58 ff**  
 condensed-ring compounds, 229  
 congruent set of points, 163 f  
 contours (on electron-density maps), **104, 107**  
 control cards (Hollerith), 100  
 convolution, 155, 266  
 coronene, 138, 239  
 correctness of structures, **144 f**  
 cosine tables, **60, 323**  
 covalent bond, 114  
 $Cr_2Al$ , 61, 125 ff  
 cryolite, 58, 70  
 crystal class, **28 f**  
 — structure models, 114, **327 f**  
 — system, 27

- $\text{CuFe}_2\text{O}_4$ , 50  
 $\text{CuK}\alpha$  radiation, 88, 142, 171 f, 283  
 $\text{CuSO}_4 \cdot 5\text{H}_2\text{O}$ , 60, 85 ff, 118, 121, 130, 135,  
 140 f, 171, 176 f, 210 f  
 $\text{CuSeO}_4 \cdot 5\text{H}_2\text{O}$ , 140 f  
 curvature of electron-density function,  
 279 f, 308 f  
 cyanite, 112, 120  
 cyclotomic sets, 169  
 cysteinyl glycine sodium iodide, 177  
 cytidine, 147
- DEKABORANE**, 256, 259  
 depression of scattering factors, 141 f, 227  
 determinantal equalities, 262, 264  
 — inequalities, 259 f  
 deuterium, 143  
 diacetylene dicarboxylic acid, 148  
 diamagnetic susceptibility, 121  
 diamond, 306  
 dibenzyl, 289, 296  
 dichlorobenzidine, 147  
 difference synthesis, 203, 298, 308, 311  
 differential synthesis, 279, 301  
 diffraction of light, 2, 16, 72 f, 75  
 — effects in Fourier synthesis, 205  
 — grating, 1, 4, 16 ff, 72  
 — spectroscopy, 109, 236  
 diffuse reflexions, 9, 17, 124, 243  
 diglycylglycine ethyl ester hydrobromide,  
 224 ff  
 — — hydrochloride, 193 ff, 224 ff  
 diopside, 108, 132, 199  
 direct methods of structure analysis, 125 ff,  
 246 ff  
 distribution of intensities, 35 ff, 127 f, 258  
 Donnay-Harker law, 122  
 double reflexions, 30, 206  
 durene, 115, 202
- ELECTRON counts**, 106  
 — density, 11  
 — — maps, 104, 285  
 — diffraction, 143, 243  
 empirical scattering factors, 63  
 enantiomorphic equivalent points, 45  
 — space groups, 157  
 equality relationships between  $F$ 's, 261 ff  
 equivalent points, 23, 33, 42 ff, 54  
 error function, 36  
 — synthesis, 210 f  
 errors in Fourier synthesis, 285 ff  
 etch figures, 28  
 external symmetry, 21 ff  
 extinction, 134, 144, 148, 286, 307  
 —, optical, 109  
 extinctions, space-group, 29
- FACE-centred lattice**, 26 f, 31  
**f-curve**, 8, 16, 62 f, 149, 294  
 —, anisotropic, 149, 302  
 —, standard, 64, 102  
 $\text{Fe}_3\text{Al}$  142
- $\text{FeK}\alpha$  radiation, 142  
 figure fields (structure-factor graphs), 71  
 flavanthrone, 229 f, 235  
 fly's eye, 71 ff, 140, 221, 237  
 Fourier integral, 150  
 — machines, 325 f  
 — methods, 199 ff  
 — projections, 79 ff, 105 f, 200 ff  
 — —, generalized, 221  
 — series for electron density, 11, 76 ff  
 — — for calculation of structure factors,  
 65, 101 ff  
 — summations, 82 ff  
 — —, subdivision of cell, 88 f  
 — synthesis, electron counts from, 106  
 — —, one-dimensional, 80, 213 f  
 — —, optical, 108 f, 206, 244, 326  
 — —, photographic, 107, 326  
 — —, plotting contours of, 104, 107  
 — —, three-dimensional, 79, 80, 82 f, 105 f  
 — —, two-dimensional, 79 ff, 83 ff  
 — transform, 1, 2, 15, 18, 65, 74 f, 227 ff,  
 243 f, 291, 292  
 — — combination, 230 ff, 233  
 — —, computation of, 103, 234  
 — —, experimental observation of, 241 f  
 — — method for structure factors, 65,  
 74 f, 149  
 — —, optical, 75, 236 f, 245  
 — —, texture of, 238 f  
 Fraunhofer diffraction, 75, 236  
 Friedel's law, 28, 118  
 fringe function, 15, 234 f  
 fringes, diffraction, 19 f, 108  
 fundamental set, 154 ff, 163, 197  
 — space, 154 ff
- GALLIUM**, 146 f  
 gamma brass, 128  
 Gaussian atoms, 267, 279  
 — distribution of  $F$ 's, 258  
 — — of errors, 281, 287  
 general equivalent points, 9 f, 41, 42 ff,  
 47, 56, 318 f  
 generalized projections, 175, 179, 221 ff  
 geranylamine hydrochloride, 105  
 ghost peaks in Fourier synthesis, 211  
 glide plane, 24 ff  
 glutamine, 272  
 glycine, 114  
 glycylglycine,  $\beta$ , 191  
 graphical determination of parameters,  
 125 f  
 grating, diffraction, 1, 4, 16, 72
- HAEMOGLOBIN**, 195, 241 f  
 Harker-Kasper inequalities, 246, 250 ff,  
 269 f  
 — — —, applications, 254 ff  
 — — —, limitations, 258 f  
 — section, 157 ff, 180 ff, 193  
 harmonic analysers, 321

- heavy-atom method, 49, 140, 166, **175 f**,  
182, **206 ff**, 244  
Herglotz's theorem, 259  
Hermann-Mauguin symbols, 26, 46, 318,  
319  
hermitian matrix, 264 f  
Heusler alloys, 142  
hexachlorobenzene, 156  
hexamethylbenzene, 138, 206  
higher-layer-line synthesis, 221  
Hollerith machine, 97  
homometric structures, **145**, 167 ff, 198  
— sets, 167, 169, 198  
homopolar forces, 111  
horse methaemoglobin, 195, 241 f  
Huggins masks, 107 ff, 322  
human oxyhaemoglobin, 195  
hydrogen atoms, 105, 144, 148 f, 306  
— bond, 114, 315  
hydroxyproline, 267 ff
- I.B.M. punched-card machine, 97  
identical operation, 22  
image formation, **18 f**, 108, 204  
— -seeking function, 164  
implication diagram, **159 ff**, 186  
indicative field (Hollerith), 98  
indirect methods of structure determin-  
ation, 127 ff  
inequalities, 246, 250 ff  
infra-red absorption, **123**  
intensity statistics, **32**, 35 ff, 61, 118, 134 f,  
156, 169, 174, 188  
interatomic distances, 111 f, **189 f**, 210  
— forces, 111  
— vectors, 14, 33, 151 ff  
interaxial angles, 7  
interference of light, 20, 108  
interval of division of unit cell for Fourier  
synthesis, **88**  
inversion, 22, 90  
inversion axes, 22, 46  
ions, 113, 120  
ionization spectrometer, 134  
isomorphism, 50, 140 f  
isomorphous-replacement method, 140 f,  
193 f, **212 f**, 244  
isoprene sulphone,  $\beta$ , 296  
isotopes, 143  
isovectorial sets, 167 f, 187, 198
- K electrons, 141, 143  
Karle-Hauptmann inequalities, 259 ff  
key punch (Hollerith), 99
- LATTICE, **1**, **3**  
— constants, 3  
— parameters, 3  
— symmetry, **23**  
Laue groups, 28  
— photographs, 28, 128  
Laue's equations, 4 ff, 11, 15, 124  
layer lines, 27, 128 f
- least squares, **280 ff**, 300, 310  
limit of resolution, 88, 205  
limiting sphere, 152, 170, 257, 281
- MAGNESIUM paratoluene sulphonate, 216  
magnetic susceptibility, **120 f**, 233  
manganese, 143  
marcasite, 109, 126  
master pack (punched cards), 99  
Meccano, 322  
melamine, 121  
mercury, 150  
metaboric acid, 275  
metatolidine, 239 f  
— dihydrochloride, 36 ff, 62, 116, 120  
136, 207  
 $\text{MgAl}_2\text{O}_4$ , 50  
 $\text{MgFe}_2\text{O}_4$ , 51  
mica, 122  
— plates, 109  
Miller indices, 4 f  
minimum function, 166  
mirror plane, 22  
mixed series, 166  
 $\text{MnCr}_2\text{O}_4$ , 50  
models, crystal-structure, 114, **327 f**  
—, projection of, 114 f  
molybdenum target, 142  
monoclinic system, 23, 26, 53, 67  
morphology, 118 f, 122  
multiple peaks (Patterson), **153**  
multiplicity, 47, 50, 56, 281, 318, 319  
multiplier bar, 322  
multiplying punch (Hollerith), 99, 101
- NAPHTHALENE, 133, 228 f, 236 ff  
neutron diffraction, 143 f, 250  
nickel, 143  
nickel sulphate heptahydrate, 114, 200  
Nicol prism, 109  
non-equivalent symmetry elements, 42, 47  
— molecules, 116  
non-Harker peaks, 161 f, 185 f, 193  
non-orthogonal crystal axes, 278  
non-primitive lattices, **24 ff**  
normal equations, 281 f  
numerical aperture, 205
- OBLIQUE system, 53  
observational equations, 281  
one-dimensional crystal, 325  
optical activity, 119  
— Fourier synthesis, 108 ff, 206  
— properties of crystals, **120 f**, 191  
— transform, 75, 236 ff, 245  
order-disorder phenomena, 50, 144  
order of diffraction, 4, 17, 19  
origin, arbitrariness of, 177, 205, 210, 243,  
256  
origin peak, subtraction of, 174, 188  
orthogonal axes, 279, 282  
Ott-Avrami method, **247 f**, 261

outstanding reflexions, 137 f  
 oxalic acid, 250, 255 f, 259, 270

PACKING of atoms, 111 f, 120  
 para-diisocyanobenzene, 73  
 parallel sections of Fourier synthesis, 82  
 parameters, structural, 10, 21, 45  
 para-nitroaniline, 137 f  
 Patterson function, 2, 12 ff, 33, 150 ff  
 — —, generalized projections of, 175, 179 f  
 — —, shapes of peaks in, 170  
 — —, sharpened, 170 f  
 — —, subtraction of peaks from, 174, 188  
 — —, symmetry of, 154  
 — -Tunell stencils, 95, 96 f  
 Pauling's rules, 117  
 penicillin, 73, 139 f, 221 f  
 —, potassium benzyl, 216, 221 f  
 —, rubidium benzyl, 187, 212, 216, 221 f  
 —, sodium benzyl, 73, 140, 201, 203 f, 221 f  
 Pepinsky machine, 107, 206, 244, 326  
 peptides, 197  
 phase angle, 76, 200, 220, 290  
 phase change on scattering, 141 f  
 — of wave, 2, 11, 18, 109  
 phthlocyanine, 207 f, 218, 237 ff  
 —, nickel, 218  
 —, platinum, 207 f  
 physical optics, 1, 16 f  
 piezo electricity, 28, 119 f, 181  
 planar molecules, 124, 137 f, 228  
 plane groups, 52, 53, 153 f  
 plane of symmetry, 22  
 planimeter, 321, 325  
 plug board (Hollerith), 97  
 point atoms, 102, 197, 261, 295  
 — group, 23, 26  
 polarization, 8, 109, 123  
 polarizing microscope, 28  
 pole figure, 118  
 polymer structures, 116 f  
 polypeptide chain, 197  
 positivity of electron density, 246  
 potassium dihydrogen phosphate, 156, 248  
 — mercury chloride, 49  
 powder photographs, 128, 142, 285  
 primitive lattice, 24  
 probable error, 287  
 product function, 166  
 projected sections, 82  
 projection of electron density, 79, 82  
 proteins, 163, 195, 206  
 proustite, 180 f  
 punched-card machines, 97 ff, 192, 282  
 purpurogallin, 240  
 pyroelectricity, 28, 119, 181

QUINOL-methanol, 221  
 — sulphur dioxide, 181 ff, 221

R.M.S. deviation, 287  
 radial distribution, 150  
 random errors, 286

reciprocal lattice, 1, 6, 71 f  
 — —, weighted, 15 f, 73, 104, 130, 238 f  
 — space, 7, 124, 246, 291  
 rectangular system, 53  
 refinement of parameters, 199, 278 ff  
 reflexion of X-rays, 5  
 refractive index, 120  
 related structures, 193 ff, 220  
 reproducing punch (Hollerith), 99 f  
 residual (reliability index), 146, 307  
 resolving power, 88, 293  
 Robertson's strips, 93 ff  
 — —, mechanical sorter for, 96, 101  
 rock salt, 199  
 rotation axes, 21, 46, 52  
 rounding-off errors, 92  
 rubber hydrochloride, 117

SALICYLIC acid, 189  
 satellite peaks (on implication diagram), 161  
 Sayre's equation, 247, 265 ff, 272  
 scattering cross sections, 143  
 scattering factors, 8, 16, 18, 60 f, 73 f, 149,  
 — —, depression of, 141 f, 227  
 — —, empirical, 63  
 — —, unitary, 63, 251  
 Schwarz's inequality, 250, 261  
 Schönlies symbols, 318, 319  
 screw axis, 24 f  
 selsyn, 326  
 series-termination errors, 290, 291 ff  
 sign indicators for Fourier strips, 97  
 — combinations, 109, 204 ff, 244, 264, 268,  
 273  
 — relations between F's, 270 f  
 significance levels, 309  
 silicates, 113, 118  
 silver target, 142  
 sine tables, 60, 324  
 slide rule, 320  
 slit, diffraction pattern of, 17  
 sodium benzyl penicillin, 73, 140, 201, 203 f,  
 221 f  
 — hydride, 144  
 — hydroxide tetrahydrate, 187 f  
 — rubidium tartrate, 142  
 — sesquicarbonate, 122  
 sorbic acid, 124  
 sorting board for Fourier strips, 95 f, 102  
 space-group absences, 29, 57, 318 f  
 — — representations, 42 f  
 space groups, 26 f, 318, 319  
 — —, monoclinic, 26  
 — lattice, 3  
 spacing of lattice planes, 5  
 spatial considerations, 111, 213  
 special equivalent positions, 45 f, 56 f, 60,  
 135  
 — form of crystal, 28  
 sphere of reflexion, 31  
 spinel, 50  
 square system, 53

- standard crystal, for absolute intensities, 133 f  
 — deviation, 287 ff, 306 ff  
 — f-curve, 63 f, 102  
 statistical methods, 35 f, 61 f, 134 ff, 169, 174  
 steepest descents, 248 f, 284 f, 301, 310  
 stereochemistry, 114, 116, 121, 193, 210, 221  
 stereographic projection, 27  
 stilbene, 116  
 strontium chloride hexahydrate, 113  
 structural parameters, 10, 21, 45  
 — —, transformation of, 316  
 structure amplitude, 2, 11, 29, 35  
 — — agreement, 145  
 — factor, 2, 11 f, 29  
 — — calculation, 54 ff, 101 f  
 — — formulae, 54 ff, 318, 319  
 — — graphs, 65 ff, 138 f, 191, 193, 320  
 — — machines, 320  
 — —, unitary, 251, 261  
 strychnine hydrogen bromide, 186, 207 f,  
 — sulphate, 219  
 sub-cell, 67  
 — groups, 318  
 — units, 132  
 subdivision of unit cell for Fourier sum-  
 mations, 88  
 sulphur, 60, 150  
 superlattice, 142  
 superposition methods, 163 ff, 167, 186 ff  
 surface energy, 122  
 symmetry, 21, 77  
 — elements, 23, 26, 33, 36, 115, 318, 319  
 —, external, 21 ff  
 —, ionic, 115  
 symmetry, molecular, 115  
 — number, 271  
 — in vector space, 154  
 — of Fourier synthesis, 106  
 — operations, 21, 44  
 — —, two-dimensional, 52  
 systematic absences, 29 f, 35, 41, 47, 57,  
 233, 318, 319
- TABULATOR (Hollerith), 99 f  
 target, X-ray, 142  
 tartaric acid, 185  
 tartrate ion, 143  
 temperature factor, 9, 61 ff  
 — —, anisotropic, 278, 302 f  
 — —, artificial, 215, 267, 297  
 thermal vibrations, 9, 124  
 — —, anisotropic, 278, 302 f  
 thiophthen, 128 f  
 three-dimensional Fourier synthesis, 105  
 three-fold axes, 53, 69, 115
- threonine, 192 f, 278  
 tide predictor, 321 f, 325  
 transformation of axes, 112, 316  
 trial-and-error methods, 49, 75, 110 ff,  
 193, 199, 269  
 tribromo-trimethylphosphine gold, 207  
 triclinic system, 23  
 triglycylglycine ethyl ester hydrochloride,  
 193 ff  
 trilaurin, 132  
 triphenylene, 230 ff  
 two-dimensional symmetry operations, 52  
 — — systems, 52  
 two-fold axis, 23
- UNIAXIAL crystals, 28  
 unit cell, 2, 7, 9 f, 316  
 — — dimensions, 3, 277 f  
 Unit cell, projection of, 105 f  
 unitary scattering factors, 63, 153  
 — structure factor, 251, 261  
 unresolved peaks (Patterson), 14, 197
- VAN der Waals force, 111, 114, 191  
 — — radii, 114, 191, 315  
 vanadium target, 142  
 vector-coincidence method, 165 f, 186 f,  
 193  
 — set, 154, 156, 163, 197 f  
 — space, 154  
 visual estimations, 148, 286, 290
- WATER molecules, 49, 113, 115,  
 wave-lengths, X-ray, 7, 314  
 weighted reciprocal lattice, 15 f, 73, 104,  
 130, 238 f  
 — — — section, 237, 239 f  
 weighting of observations, 281, 283, 310 f  
 weights of Patterson peaks, 153  
 Weissenberg goniometer, 133  
 Wilson's statistical methods, 35, 61 f, 134 ff,  
 169, 174
- X-RAY goniometer, 88  
 — microscope, 108 f  
 — photographs, 27  
 — wave-lengths, 7, 314
- ZACHARIASEN's method, 274 ff  
 zero order of diffraction, 20, 72, 76 ff, 136  
 zinc, 111  
 — paratoluene sulphonate, 216 ff  
 zirconium target, 142  
 ZnK $\alpha$  radiation, 142  
 zone axis, 133  
 zones of reflexions, 36, 71, 127 f, 135











